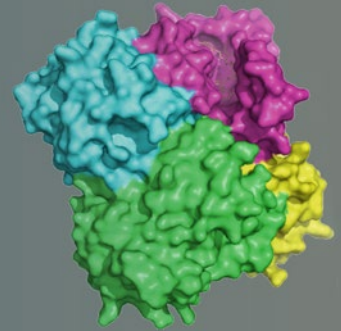


Methods in
Molecular Biology 1051

Springer Protocols



Jose M. Guisan *Editor*

Immobilization of Enzymes and Cells

Third Edition

 Humana Press

METHODS IN MOLECULAR BIOLOGY™

Series Editor
John M. Walker
School of Life Sciences
University of Hertfordshire
Hatfield, Hertfordshire, AL10 9AB, UK

For further volumes:
<http://www.springer.com/series/7651>

Immobilization of Enzymes and Cells

Third Edition

Edited by

Jose M. Guisan

Instituto de Catalisis y Petroleoquimica, CSIC, Madrid, Spain

 **Humana Press**

Editor

Jose M. Guisan
Instituto de Catalisis
y Petroleoquimica, CSIC
Madrid, Spain

ISSN 1064-3745 ISSN 1940-6029 (electronic)
ISBN 978-1-62703-549-1 ISBN 978-1-62703-550-7 (eBook)
DOI 10.1007/978-1-62703-550-7
Springer New York Heidelberg Dordrecht London

Library of Congress Control Number: 2013944230

© Springer Science+Business Media New York 2013

This work is subject to copyright. All rights are reserved by the Publisher, whether the whole or part of the material is concerned, specifically the rights of translation, reprinting, reuse of illustrations, recitation, broadcasting, reproduction on microfilms or in any other physical way, and transmission or information storage and retrieval, electronic adaptation, computer software, or by similar or dissimilar methodology now known or hereafter developed. Exempted from this legal reservation are brief excerpts in connection with reviews or scholarly analysis or material supplied specifically for the purpose of being entered and executed on a computer system, for exclusive use by the purchaser of the work. Duplication of this publication or parts thereof is permitted only under the provisions of the Copyright Law of the Publisher's location, in its current version, and permission for use must always be obtained from Springer. Permissions for use may be obtained through RightsLink at the Copyright Clearance Center. Violations are liable to prosecution under the respective Copyright Law.

The use of general descriptive names, registered names, trademarks, service marks, etc. in this publication does not imply, even in the absence of a specific statement, that such names are exempt from the relevant protective laws and regulations and therefore free for general use.

While the advice and information in this book are believed to be true and accurate at the date of publication, neither the authors nor the editors nor the publisher can accept any legal responsibility for any errors or omissions that may be made. The publisher makes no warranty, express or implied, with respect to the material contained herein.

Printed on acid-free paper

Humana Press is a brand of Springer
Springer is part of Springer Science+Business Media (www.springer.com)

Preface

Enzymes and whole cells are able to catalyze the most complex chemical processes under the most benign experimental and environmental conditions. In this way, enzymes and cells could be excellent catalysts for a much more sustainable chemical industry. However, enzymes and cells have also some limitations for nonbiological applications: fine chemistry, food chemistry, analysis, therapeutics, and so on. Enzymes and cells may be unstable, difficult to handle under nonconventional conditions, poorly selective towards synthetic substrates, etc. From this point of view, the transformation, from the laboratory to the industry, of chemical processes catalyzed by enzymes and cells may be one of the most complex and exciting goals in biotechnology.

For most of the industrial applications, enzymes and cells have to be immobilized, via very simple and cost-effective protocols, in order to be reused for very long periods of time. From this point of view, immobilization, simplicity, and stabilization have to be strongly related concepts. For the last 30 years a number of protocols for immobilization of cells and enzymes have been reported in scientific literature. However, only very few protocols are simple enough and only very few protocols are useful enough to greatly improve the functional properties of enzymes and cells: activity, stability, selectivity, etc.

The third edition of *Immobilization of Enzymes and Cells* intends to be an update as well as a complement of the two previous editions. This volume now includes the following aspects of old and new protocols for immobilization:

1. Very simple protocols for immobilization of enzymes and cells which could be very useful for application at industrial scale.
2. Immobilization protocols useful to greatly improve functional properties of enzymes and cells.

There is still a long and exciting way to develop very simple and very efficient protocols for the preparation, characterization, and utilization of immobilized enzymes and cells. This volume tries to show some very interesting results already obtained and, at the same time, it intends to persuade to the readers for working in a further development of even more important protocols of immobilization. Very likely, the development of excellent protocols for immobilization will promote a massive implementation of enzyme and cells as industrial biocatalysts. This implementation could be decisive for the development of a much more skilled and sustainable chemical industry: the cost-effective production of very complex and useful molecules under the mildest conditions.

Madrid, Spain

Jose M. Guisan

Contents

<i>Preface</i>	v
<i>Contributors</i>	ix
1 New Opportunities for Immobilization of Enzymes	1
<i>Jose M. Guisan</i>	
2 Immobilization of Enzymes: A Literature Survey	15
<i>Beatriz Brena, Paula González-Pombo, and Francisco Batista-Viera</i>	
3 Glutaraldehyde-Mediated Protein Immobilization	33
<i>Fernando López-Gallego, Jose M. Guisán, and Lorena Betancor</i>	
4 Immobilization of Enzymes on Monofunctional and Heterofunctional Epoxy-Activated Supports	43
<i>Cesar Mateo, Valeria Grazu, and Jose M. Guisan</i>	
5 Stabilization of Enzymes by Multipoint Covalent Immobilization on Supports Activated with Glyoxyl Groups	59
<i>Fernando López-Gallego, Gloria Fernandez-Lorente, Javier Rocha-Martin, Juan M. Bolivar, Cesar Mateo, and Jose M. Guisan</i>	
6 Oriented Covalent Immobilization of Enzymes on Heterofunctional-Glyoxyl Supports	73
<i>Cesar Mateo, Gloria Fernandez-Lorente, Javier Rocha-Martin, Juan M. Bolivar, and Jose M. Guisan</i>	
7 Reversible Covalent Immobilization of Enzymes via Disulfide Bonds	89
<i>Karen Ovsejevi, Carmen Manta, and Francisco Batista-Viera</i>	
8 Immobilization of <i>Candida rugosa</i> Lipase on Superparamagnetic Fe ₃ O ₄ Nanoparticles for Biocatalysis in Low-Water Media	117
<i>Joyeeta Mukherjee, Kusum Solanki, and Munishwar Nath Gupta</i>	
9 Immobilization of Enzymes by Bioaffinity Layering	129
<i>Veena Singh, Meryam Sardar, and Munishwar Nath Gupta</i>	
10 Immobilization of Enzymes on Magnetic Beads Through Affinity Interactions	139
<i>Audrey Sassolas, Akhtar Hayat, and Jean-Louis Marty</i>	
11 Tips for the Functionalization of Nanoparticles with Antibodies	149
<i>Ester Polo, Sara Puertas, María Moros, Pilar Batalla, José M. Guisán, Jesús M. de la Fuente, and Valeria Grazú</i>	
12 Design and Characterization of Functional Nanoparticles for Enhanced Bio-performance	165
<i>Pablo del Pino, Scott G. Mitchell, and Beatriz Pelaz</i>	

13	Immobilization of Enzymes on Ethynyl-Modified Electrodes via Click Chemistry	209
	<i>Akhtar Hayat, Audrey Sassolas, Amina Rhouati, and Jean-Louis Marty</i>	
14	Modification of Carbon Nanotube Electrodes with 1-Pyrenebutanoic Acid, Succinimidyl Ester for Enhanced Bioelectrocatalysis	217
	<i>Guinevere Strack, Robert Nichols, Plamen Atanassov, Heather R. Luckarift, and Glenn R. Johnson</i>	
15	Enzyme Immobilization by Entrapment Within a Gel Network	229
	<i>Audrey Sassolas, Akhtar Hayat, and Jean-Louis Marty</i>	
16	Practical Protocols for Lipase Immobilization via Sol–Gel Techniques	241
	<i>Manfred T. Reetz</i>	
17	Improving Lipase Activity by Immobilization and Post-immobilization Strategies	255
	<i>Jose M. Palomo, Marco Filice, Oscar Romero, and Jose M. Guisan</i>	
18	High Activity Preparations of Lipases and Proteases for Catalysis in Low Water Containing Organic Solvents and Ionic Liquids.	275
	<i>Ipsita Roy, Joyeeta Mukherjee, and Munishwar Nath Gupta</i>	
19	Biomedical Applications of Immobilized Enzymes: An Update	285
	<i>Marta Pastor, Amaia Esquisabel, and José Luis Pedraz</i>	
20	Immobilization of Whole Cells by Chemical Vapor Deposition of Silica	301
	<i>Susan R. Sizemore, Robert Nichols, Randi Tatum, Plamen Atanassov, Glenn R. Johnson, and Heather R. Luckarift</i>	
21	Encapsulation of Cells in Alginate Gels	313
	<i>Pello Sánchez, Rosa María Hernández, José Luis Pedraz, and Gorka Orive</i>	
22	Microalgal Immobilization Methods	327
	<i>Ignacio Moreno-Garrido</i>	
23	Therapeutic Applications of Encapsulated Cells	349
	<i>Argia Acarregui, Gorka Orive, José Luis Pedraz, and Rosa María Hernández</i>	
24	Whole Cell Entrapment Techniques	365
	<i>Jorge A. Trelles and Cintia W. Rivero</i>	
	<i>Index</i>	375

Contributors

- ARGIA ACARREGUI • *NanoBioCel Group, Laboratory of Pharmaceutics, School of Pharmacy, University of the Basque Country (UPV/EHU), Vitoria-Gasteiz, Spain*
- PLAMEN ATANASSOV • *Department of Chemical and Nuclear Engineering, Center for Emerging Energy Technologies, University of New Mexico, Albuquerque, NM, USA*
- PILAR BATALLA • *Department of Analytical Chemistry, Physical Chemistry and Chemical Engineering, Faculty of Chemistry, University of Alcalá, Madrid, Spain*
- FRANCISCO BATISTA-VIERA • *Cátedra de Bioquímica, Departamento de Biociencias, Facultad de Química, Universidad de la República, Montevideo, Uruguay*
- LORENA BETANCOR • *Laboratorio de Biotecnología, Facultad de Ingeniería, Universidad ORT Uruguay, Montevideo, Uruguay*
- JUAN M. BOLIVAR • *Institute of Catalysis, CSIC, CAMPUS UAM-Cantoblanco, Madrid, Spain*
- BEATRIZ BRENA • *Cátedra de Bioquímica, Departamento de Biociencias, Facultad de Química, Universidad de la República, Montevideo, Uruguay*
- AMAIA ESQUISABEL • *NanoBioCel Group, Laboratory of Pharmaceutics, School of Pharmacy, University of the Basque Country, Vitoria-Gasteiz, Spain; Networking Biomedical Research Center on Bioengineering, Biomaterials and Nanomedicine, CIBER-BBN, Vitoria-Gasteiz, Spain*
- GLORIA FERNANDEZ-LORENTE • *Instituto de Investigación en Ciencias de la Alimentación (CIAL) CSIC-UAM, Madrid, Spain*
- MARCO FILICE • *Institute of Catalysis, CSIC, CAMPUS UAM-Cantoblanco, Madrid, Spain*
- JESÚS M. DE LA FUENTE • *Nanotherapy and Nanodiagnostics Group (GN2), Instituto de Nanociencia de Aragón (INA), Universidad de Zaragoza, and Fundación ARAID, Zaragoza, Spain*
- PAULA GONZÁLEZ-POMBO • *Cátedra de Bioquímica, Departamento de Biociencias, Facultad de Química, Universidad de la República, Montevideo, Uruguay*
- VALERIA GRAZU • *Nanotherapy and Nanodiagnostics Group (GN2), Instituto de Nanociencia de Aragón, Universidad de Zaragoza, Zaragoza, Spain*
- JOSE M. GUISAN • *Instituto de Catalysis y Petroquímica, CSIC, Madrid, Spain*
- MUNISHWAR NATH GUPTA • *Department of Chemistry, Indian Institute of Technology Delhi, New Delhi, India*
- AKHTAR HAYAT • *IMAGES EA 4218, University of Perpignan, Perpignan Cedex, France*
- ROSA MARÍA HERNÁNDEZ • *NanoBioCel Group, Laboratory of Pharmaceutics, School of Pharmacy, University of the Basque Country (UPV/EHU), Vitoria-Gasteiz, Spain*
- GLENN R. JOHNSON • *Air Force Research Laboratory, Airbase Sciences, Tyndall AFB, FL, USA; Integration Innovation Inc (i3), Huntsville, AL, USA*
- FERNANDO LÓPEZ-GALLEGO • *Institute of Catalysis, CSIC, CAMPUS UAM-Cantoblanco, Madrid, Spain*

- HEATHER R. LUCKARIFT • *Universal Technology Corporation, Dayton, OH, USA; Airbase Sciences Branch, Air Force Research Laboratory, Tyndall Air Force Base, Panama city, FL, USA*
- CARMEN MANTA • *Cátedra de Bioquímica, Departamento de Biociencias, Facultad de Química, Universidad de la República, Montevideo, Uruguay*
- JEAN-LOUIS MARTY • *IMAGES EA 4218, University of Perpignan, Perpignan Cedex, France*
- CESAR MATEO • *Institute of Catalysis, CSIC, CAMPUS UAM-Cantoblanco, Madrid, Spain*
- SCOTT G. MITCHELL • *Nanotherapy and Nanodiagnosics Group (GN2), Campus Rio Ebro, Instituto de Nanociencia de Aragón, Universidad de Zaragoza, Zaragoza, Spain*
- IGNACIO MORENO-GARRIDO • *Department of Ecology and Coastal Management, Institute of Marine Sciences of Andalucía (ICMAN-CSIC), Cádiz, Spain*
- MARÍA MOROS • *Nanotherapy and Nanodiagnosics Group (GN2), Instituto de Nanociencia de Aragón (INA), Universidad de Zaragoza, Zaragoza, Spain*
- JOYEETA MUKHERJEE • *Department of Chemistry, Indian Institute of Technology Delhi, New Delhi, India*
- ROBERT NICHOLS • *Universal Technology Corporation, Dayton, OH, USA; Airbase Sciences Branch, Air Force Research Laboratory, Tyndall Air Force Base, Panama city, FL, USA*
- GORKA ORIVE • *NanoBioCel Group, Laboratory of Pharmaceutics, School of Pharmacy, University of the Basque Country (UPV/EHU), Vitoria-Gasteiz, Spain*
- KAREN OVSEJEVI • *Cátedra de Bioquímica, Departamento de Biociencias, Facultad de Química, Universidad de la República, Montevideo, Uruguay*
- JOSE M. PALOMO • *Institute of Catalysis, CSIC, CAMPUS UAM-Cantoblanco, Madrid, Spain*
- MARTA PASTOR • *NanoBioCel Group, Laboratory of Pharmaceutics, School of Pharmacy, University of the Basque Country, Vitoria-Gasteiz, Spain; Networking Biomedical Research Center on Bioengineering, Biomaterials and Nanomedicine, CIBER-BBN, Vitoria-Gasteiz, Spain*
- JOSÉ LUIS PEDRAZ • *NanoBioCel Group, Laboratory of Pharmaceutics, School of Pharmacy, University of the Basque Country (UPV/EHU), Vitoria-Gasteiz, Spain*
- BEATRIZ PELAZ • *Nanotherapy and Nanodiagnosics Group (GN2), Campus Rio Ebro, Instituto de Nanociencia de Aragón, Universidad de Zaragoza, Zaragoza, Spain*
- PABLO DEL PINO • *Nanotherapy and Nanodiagnosics Group (GN2), Campus Rio Ebro, Instituto de Nanociencia de Aragón, Universidad de Zaragoza, Zaragoza, Spain*
- ESTER POLO • *Nanotherapy and Nanodiagnosics Group (GN2), Instituto de Nanociencia de Aragón (INA), Universidad de Zaragoza, Zaragoza, Spain*
- SARA PUERTAS • *Nanotherapy and Nanodiagnosics Group (GN2), Instituto de Nanociencia de Aragón (INA), Universidad de Zaragoza, Zaragoza, Spain*
- MANFRED T. REETZ • *Max-Planck-Institut für Kohlenforschung, Mulheim an der Ruhr, Germany*
- AMINA RHOUBATI • *IMAGES EA 4218, University of Perpignan, Perpignan Cedex, France*
- CINTIA W. RIVERO • *Laboratorio de Investigaciones en Biotecnología Sustentable (LIBioS), Universidad Nacional de Quilmes, Bernal, Argentina*
- JAVIER ROCHA-MARTIN • *Institute of Catalysis, CSIC, CAMPUS UAM-Cantoblanco, Madrid, Spain*

- OSCAR ROMERO • *Institute of Catalysis, CSIC, CAMPUS UAM-Cantoblanco, Madrid, Spain*
- IPSITA ROY • *Department of Biotechnology, National Institute of Pharmaceutical Education and Research, Punjab, India*
- PELLO SÁNCHEZ • *NanoBioCel Group, Laboratory of Pharmaceutics, School of Pharmacy, University of the Basque Country, Vitoria-Gasteiz, Spain; Networking Biomedical Research Center on Bioengineering, Biomaterials and Nanomedicine, CIBER-BBN, Vitoria-Gasteiz, Spain*
- MERYAM SARDAR • *Department of Biosciences, Jamia Milia Islamia, New Delhi, India*
- AUDREY SASSOLAS • *IMAGES EA, University of Perpignan, Perpignan Cedex, France*
- VEENA SINGH • *Department of Chemistry, Indian Institute of Technology Delhi, New Delhi, India*
- SUSAN R. SIZEMORE • *Universal Technology Corporation, Dayton, OH, USA; Airbase Sciences Branch, Air Force Research Laboratory, Tyndall Air Force Base, Panama city, FL, USA*
- KUSUM SOLANKI • *Centre for Biotechnology and Interdisciplinary Studies, Rensselaer Polytechnic Institute, Troy, NY, USA*
- GUINEVERE STRACK • *Oak Ridge Institute for Science and Education, Oak Ridge, TN, USA; Airbase Sciences Branch, Air Force Research Laboratory, Tyndall Air Force Base, Panama city, FL, USA*
- RANDI TATUM • *Universal Technology Corporation, Dayton, OH, USA; Airbase Sciences Branch, Air Force Research Laboratory, Tyndall Air Force Base, Panama city, FL, USA*
- JORGE A. TRELLES • *Laboratorio de Investigaciones en Biotecnología Sustentable (LIBioS), Universidad Nacional de Quilmes, Bernal, Argentina*

Chapter 1

New Opportunities for Immobilization of Enzymes

Jose M. Guisan

Abstract

In this chapter, as a general introduction, we summarize our personal point of view on immobilization technique in order to prepare optimal and cost-effective biocatalysts. Special attention is paid to the improvement of enzyme properties via immobilization techniques. From the stabilization by multipoint covalent attachment to the generation of hydrophilic environments via post-immobilization techniques are here discussed. Immobilization techniques, a necessary tool to reuse enzyme, have to be simple and, if possible, may become a very powerful tool to greatly improve properties of every kind of enzymes: monomeric, multimeric, stable, labile, poorly selective, etc.

Key words Simple immobilization protocols, Immobilization as a technique for the improvement of enzyme properties

1 Advantages and Limitations of Enzymes as Industrial Catalysts

Because of their excellent functional properties (activity, selectivity, specificity), enzymes are able to catalyze the most complex chemical processes under the most benign experimental and environmental conditions [1]. Enzymes are able to catalyze, under very mild conditions, very fast modifications of a unique functional group (between several similar groups) existing in only one substrate in the presence of other very similar molecules. Therefore, enzymes may be excellent industrial catalysts in a number of areas of chemical industry: fine chemistry, food chemistry, analysis, etc.

However, enzymes have been modified, during biological evolution, to optimize their behavior in the framework of complex catalytic chains inside the living beings under stress and needing regulation. Obviously, enzymes have not been optimized in order to work inside industrial reactors. In this way, enzymes, in addition to their excellent catalytic properties, also have some characteristics that are not very suitable for industrial applications: they are soluble

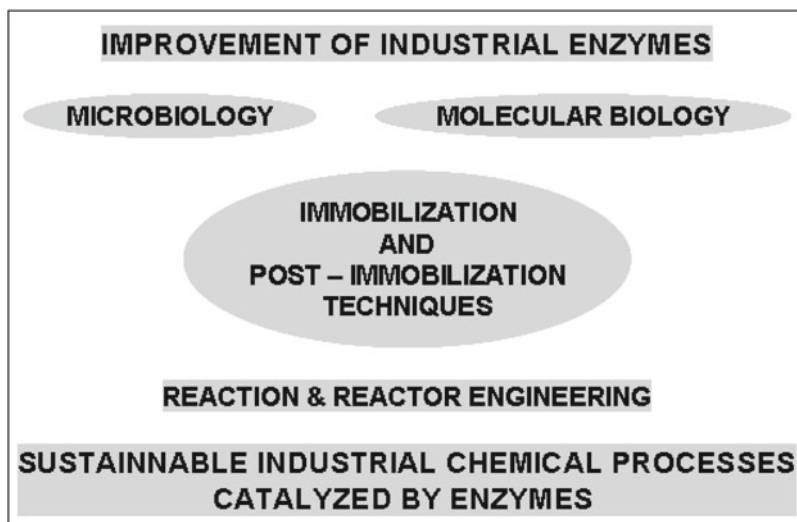


Fig. 1 Biological and chemical tools to improve the enzyme properties

catalysts; they are usually very unstable; they may be strongly inhibited by substrates and products; they work well only on natural substrates and under physiological conditions, etc.

In most cases, enzymes have to be greatly improved before their use in industrial processes. The engineering of enzymes, from biological to chemical industries, is one of the most exciting, complex and interdisciplinary goals of biotechnology. The large-scale implementation of enzymes as industrial catalysts requires a multidisciplinary utilization of very different techniques (Fig. 1): (a) the screening of enzymes with suitable properties [2], (b) the improvement of enzyme properties via techniques of molecular biology [3], (c) the improvement of enzyme properties via immobilization and post-immobilization techniques [4, 5], (d) the improvement of enzyme properties via reaction and reactor engineering [6–9], etc. Such a successful improvement of enzyme properties should be one of the key solutions for the development of a much more sustainable chemical industry able to synthesize very complex and useful compounds under very mild and cost-effective conditions.

2 Immobilized Enzymes as Catalysts of Industrial Chemical Processes

For technical and economical reasons most chemical processes catalyzed by enzymes require the reuse or the continuous use of the biocatalyst for a very long time [10, 11]. Under this perspective, immobilization of enzymes may be defined as any technique able to allow the reuse or continuous use of the biocatalysts.

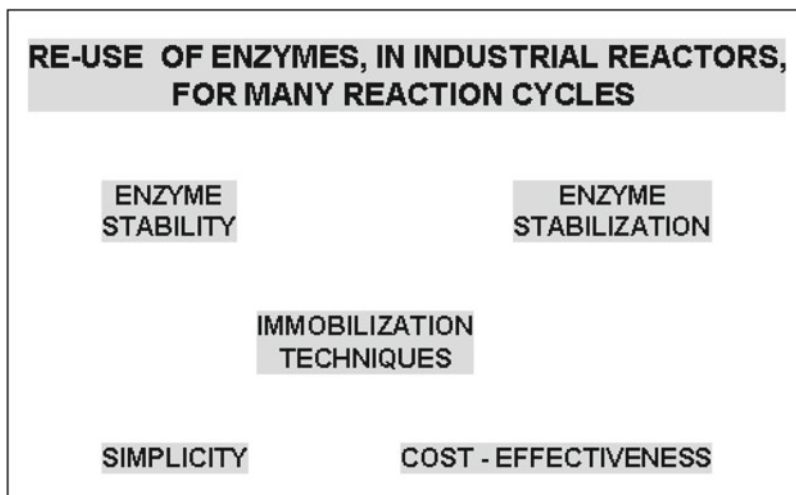


Fig. 2 Factors to be considered in the design of a biocatalyst

On the one hand, from that industrial point of view, simplicity and cost-effectiveness are key properties of immobilization techniques. On the other hand, a long-term industrial reuse of immobilized enzymes also requires the preparation of very stable derivatives also having other suitable functional properties for a given reaction (activity, selectivity, and so on). At first glance, the practical development of protocols for immobilization of enzymes is intimately related to simplicity, cost-effectiveness and stability and stabilization of enzymes (Fig. 2).

From this point of view, the thousands of protocols for enzyme immobilization, already reported in the scientific literature, should be reassess according to a number of criteria:

- (a) No need to use toxic or hazardous reagents during and after the immobilization process.
- (b) The use (in biotechnological companies) of very stable activated preexisting supports that could have been prepared by other companies (with high expertise in synthesis and activation of supports and having special security protocols).
- (c) The possibility of associating immobilization of enzymes and improvement of functional properties (activity, stability, and selectivity). In general, we can assume that the preparation of very active and very stable immobilized derivatives is a key requirement for a successful industrial application of such derivatives. Poorly active and unstable derivatives could be useful for laboratory trials but they are unlikely to be useful for industrial applications. From a practical point of view, we have to immobilize very stable enzymes or we have to be able to

greatly improve enzyme stability as a consequence of their immobilization.

- (d) The preparation of immobilized derivatives useful for use in different reactions (use of soluble or insoluble substrates, need for cofactor regeneration, presence of oxygen as enzyme substrate, etc.), in different reaction media (water, organic solvents, supercritical fluids, etc.), and in different reactors (stirred tanks, fluidized beds, etc.).
- (e) The preparation of immobilized derivatives for use in different applications: fine chemistry, biosensors, therapeutic applications, and so on.

3 The Simplicity of Immobilization of Enzymes

Enzyme can be immobilized in different places for different purposes. In general, we can assume that simplicity and cost-effectiveness of immobilization is not very important when working at the laboratory scale but it should be critical for industrial applications.

- (a) Immobilization of enzymes at the laboratory scale. This may be performed for preliminary trials of interesting biotransformations or for more basic structural and functional tests. In this case, a careful use of toxic or harmful reagents before, during and after immobilization is not necessary. In addition to that, quite unstable activated supports can be used for very rapid immobilization of a low amount of enzymes. Moreover, cost-effectiveness is hardly relevant.
- (b) Immobilization of enzymes at an industrial scale. Many companies (fine chemistry, food chemistry) are able to produce industrial enzymes but they are not able, and they do not want to be, to synthesize and to activate supports. In these cases, the development of very simple and cost-effective protocols for enzyme immobilization is critical. In addition, the use of very stable and ready-to-use activated supports is also very convenient.

4 The Improvement of Enzyme Properties Via Immobilization and Post-immobilization Techniques

Functional properties of industrial enzymes can be greatly improved by using suitable protocols for controlled and directed immobilization (Fig. 3) [12]. In this way, immobilization of enzymes, a technique necessary for the reuse of enzymes, can also become a very powerful tool for improving enzyme properties. Moreover, enzyme

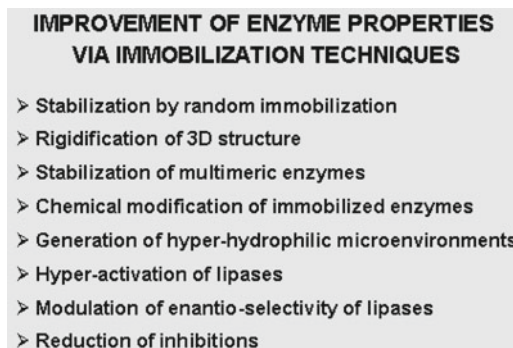


Fig. 3 Possibilities of the use of immobilization techniques to improve the enzyme properties

properties could be also improved by physical and chemical modification of immobilized derivatives. Both techniques of enzyme engineering are fairly compatible with additional engineering via preliminary biological techniques (microbiology, molecular biology, etc.) [13–15].

Next, some protocols for enzyme improvement via immobilization, already reported in literature, will be presented.

4.1 Stabilization of Enzymes by Random Immobilization

Covalent immobilization or strong physical adsorption of enzymes, fully dispersed on the internal surface of porous supports, may promote very interesting stabilizing effects [16]: (a) the immobilized enzyme is not able to undergo any Intramolecular process: autolysis, proteolysis, aggregation, and so on, (b) the immobilized enzyme (inside a porous structure) is not able to undergo undesirable interactions with large hydrophobic interfaces: air/oxygen bubbles, immiscible organic solvents, etc. In this way, under certain experimental conditions, these random immobilization protocols may promote very important stabilizations of immobilized enzymes regarding to soluble enzymes (these ones are able to undergo aggregations and interactions with hydrophobic interfaces).

4.2 Stabilization of Enzymes by Multipoint Covalent Immobilization

Multipoint covalent attachment of enzymes on highly activated preexisting supports (Fig. 4), via very short spacer arms and through a number of residues on the enzyme surface, can promote dramatic stabilization of the three-dimensional structure of the immobilized enzyme. In this case, the relative distances among all residues involved in multipoint immobilization have to be maintained unaltered during any conformational change induced by any distorting agent (heat, organic cosolvents, extremes of pH values, etc.). In this way, the intensity of conformational changes involved in enzyme inactivation may be strongly reduced and the

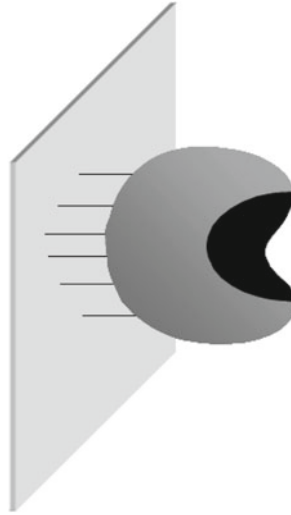


Fig. 4 Multipoint covalent attachment of proteins

immobilized enzyme may become strongly stabilized. In fact, a number of enzymes have been dramatically stabilized by multipoint covalent immobilization compared to one-point immobilized counterparts [17–20].

4.3 Stabilization of Multimeric Enzymes by Multi-subunit Immobilization

Some multimeric enzymes, under certain experimental conditions, may be inactivated by dissociation of the subunits of their quaternary structure. Some protocols for enzyme immobilization may prevent this dissociation of subunits of the immobilized enzyme and hence may promote dramatic stabilizing effects [21].

4.3.1 Multi-subunit Covalent Attachment on Preexisting Supports

By using very highly activated supports, both subunits of dimeric enzymes may be easily attached to the support. In this way, very important stabilizing effects can be obtained [22]. More difficult is the stabilization of more complex multimeric enzymes. In this case, several subunits (two or three) can firstly be covalently attached to the support and the other subunits of each enzyme molecule can then be further cross-linked to the immobilized subunits by using bifunctional or poly-functional cross-linking agents (e.g., glutaraldehyde, aldehyde-dextran, etc.) In this way, complex multimeric structures can be fully stabilized [4, 5] (Fig. 5).

4.3.2 CLEAs or CLECs of Multimeric Enzymes

The aggregation or crystallization of multimeric enzymes with further cross-linking of the aggregated or crystallized beads with bifunctional or polyfunctional reagents should fully prevent the dissociation of subunits. These protocols for immobilization of enzymes with no support may be a very powerful tool for greatly improving the stability of multimeric enzymes [23].

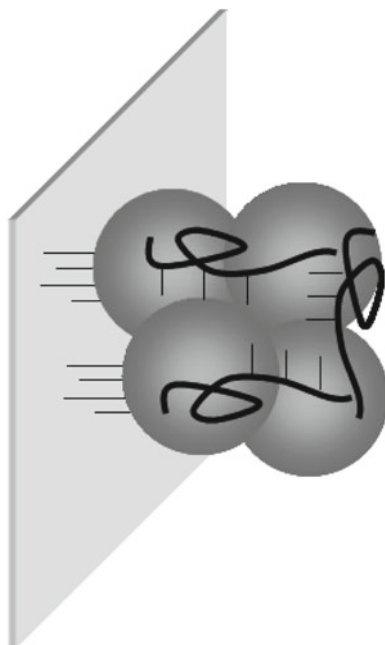


Fig. 5 Stabilization of multimeric enzymes multi-subunit covalent immobilization plus additional cross-linking

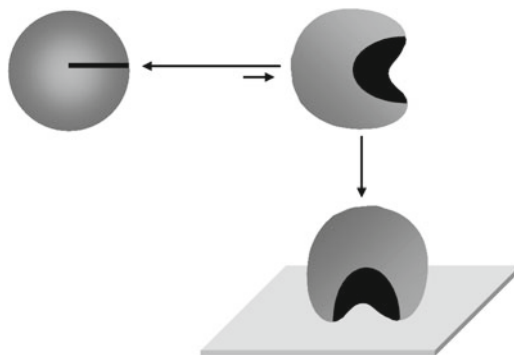


Fig. 6 Hyperactivation of lipases by interfacial activation on hydrophobic supports

4.4 Hyper-activation of Lipases by Selective Adsorption on Hydrophobic Surfaces

The adsorption of lipases, at very low ionic strength, onto hydrophobic supports can promote the immobilization and stabilization of the open structure of lipases (Fig. 6) [24–26]. In this way, these immobilized lipases may exhibit a very important hyper-activation (at least towards small and hydrophobic substrates) associated with the immobilization process.

4.5 Physicochemical Modification of Immobilized Enzymes

Immobilized enzymes can be easily modified with very different chemical reagents [27]: (a) the process of modification can be easily controlled by stopping the reaction via very fast separation of immobilized enzymes and reagents, (b) Intermolecular chemical

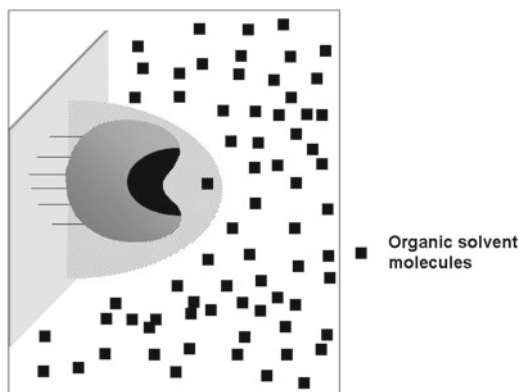


Fig. 7 Generation of hyper-hydrophilic environments surrounding immobilized enzymes

modifications are now impossible, (c) Possible aggregations promoted by the modification (via hydrophobic or electrostatic interactions) are also impossible, etc. Modifications of immobilized enzymes producing very different protein surfaces can be performed, for example hydrophobization of enzyme surfaces, physical adsorption of hyper-hydrophilic polymers, or chemical cross-linking of surface residues.

As a consequence of chemical modification, the conformational changes involved in inactivation or catalysis of immobilized enzymes can be strongly modified. In this way, some improvements in stability or selectivity may be observed.

4.6 Generation of Hyper-hydrophilic Microenvironments Surrounding Every Molecule of Immobilized Derivatives

Co-immobilization of enzymes and very high concentrations of very high MW hydrophilic polymers can promote the generation of new hyper-hydrophilic microenvironments surrounding every molecule of the immobilized derivative (Fig. 7). These microenvironments can promote partition phenomena of hydrophobic substances (cosolvents, substrates, products, etc.) between the bulk solution and the environment where every molecule of the immobilized enzyme is placed. Again, stability and catalytic behavior of these immobilized enzymes can become strongly modified and improved [28–30].

4.7 Immobilization of Enzymes Without Altering Their Properties

In some cases, e.g., highly selective and thermophilic enzymes, enzymes acting on macromolecular substrates, it may be interesting the development of immobilization protocols with minimal modification of enzyme structure and enzyme properties. One-point covalent immobilization through long hydrophilic spacer arms may be an interesting solution (Fig. 8).

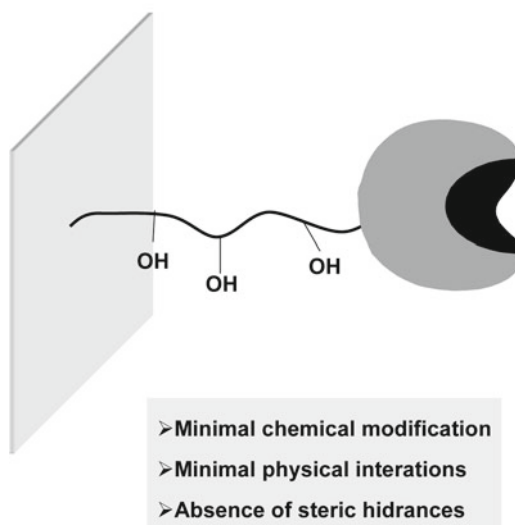
PURE IMMOBILIZATION OF ENZYMES

Fig. 8 Immobilization of enzyme without altering its properties

5 The Immobilization of the Enzymes, the Reaction Media, the Reactor, and the Application of the Immobilized Derivative

Obviously, the preparation of suitable immobilized enzyme derivatives strongly depend on the further utilization of such derivatives.

5.1 The Reaction Medium

Enzyme biotransformations can be carried out in very different reaction media: aqueous media, anhydrous organic solvents, supercritical fluid, ionic liquids, etc. The supports and the immobilization protocols are strongly dependent on the reaction medium in which the immobilized enzyme is going to be used or tested.

5.2 The Reactors

Enzyme biotransformations can be carried out in very different types of reactors: stirred tanks, packed beads, fluidized beds, basket reactors, etc. Mechanical and hydrodynamics of supports and immobilized derivatives are strongly related to the reactor to be used.

5.3 The Applications

Immobilized enzymes may be used in very different applications: chemical reactors for fine chemistry and food chemistry for many reaction cycles, different types of devices (for one or many reaction cycles) in analytical chemistry, therapeutic applications (e.g., inside human beings for long periods of time), etc. The supports, the immobilization protocols, the properties of immobilized derivatives will be very dependent on each given application.

6 Basic Applications of Immobilized Enzymes and Proteins

Immobilization of enzymes and other proteins may be also very useful, at the laboratory scale, for evaluation of some critical properties of enzymes and proteins: assembly of multimeric enzymes, studies of unfolding and refolding of proteins, studies of enzymes attached to cofactors, studies on protein–protein interactions, etc. Now, the full retention of all structural and functional properties of immobilized enzymes (even the most negative ones) has to be critical. In this way, immobilization protocols have to cover quite a range of structural and functional necessities: from unaltered immobilized enzymes to greatly modified and improved ones [10, 31].

7 Immobilization of Other Bio-macromolecules

Different protocols for enzyme immobilization can be also useful for immobilization of other interesting biomolecules: antibodies [32, 33], DNA probes [34, 35], etc. On the one hand, antibodies can be immobilized on different supports (preexisting porous supports, magnetic nanoparticles, etc.) with a correct orientation through their glycosylated chains of their Fc regions [32, 33]. This immobilization could be similar to the immobilization of other glycosylated enzymes [36]. On the other hand, DNA probes (containing amino or thiol groups inserted in one terminus) could be also covalently immobilized as reported in the previous paragraph for pure immobilization of enzymes. In both cases, the final surface of the support should be fully inert in order to prevent undesirable adsorption of antigens or DNA [35, 37]. These “tailor-made” immobilizations may be critical in very recent studies in genomics (e.g., molecular hybridization of DNA under experimental conditions promoting the “perfect match”) and proteomics (e.g., interaction of antibodies with traces of antigens, protein–protein interactions).

8 Enzyme Immobilization, Still a Fascinating Challenge

Thousands of protocols for enzyme immobilization have been reported over the last 30 years. Enzymes have, on their surfaces, very different structural moieties able to interact (adsorption/covalent attachment) with activated supports: nucleophilic residues, hydrophobic pockets, carboxylic groups, region with net positive charge, regions with net negative charge, etc. In a certain

way, and some authors maintain this point of view, we could assume that the immobilization of enzymes is an already solved problem. However, very simple and very efficient (activity, stability, selectivity, absence of inhibitions, etc.) protocols for enzyme immobilization have not been fully developed. Hence, enzyme immobilization has to be considered as a remaining fascinating challenge in modern biotechnology: much hard and interdisciplinary work is still necessary. This work for improving protocols for enzyme immobilization should encompass molecular biology, protein chemistry, material science, chemical engineering, and so on. Very simple and efficient protocols for enzyme immobilization would greatly improve the possibilities of a much more massive implementation of industrial enzymes. A much more ambitious and sustainable chemistry could be developed: e.g., the synthesis, under very mild experimental and environmental conditions, of very complex, cost-effective, and useful bioactive molecules.

9 The Immobilization of Enzymes in This Volume

As it has been indicated above, enzyme immobilization is still a fascinating challenge. This second edition of *Immobilization of Enzymes and Cells* aims to update and complement the first edition. In this Volume we show some very well developed protocols for enzyme immobilization in order to encourage the reader to develop new and more efficient methods of immobilization. Protocols to improve immobilization and use of immobilized derivatives have been presented according to the following criteria:

1. Very simple, ready for industrial application, protocols for enzyme immobilization.
2. Very efficient protocols that allow us to greatly improve the enzyme properties as a consequence of immobilization.
3. Novel protocols for enzyme immobilization that could be very useful in the future.
4. Protocols for characterization of immobilized enzymes very useful for the improvement of immobilization methods.
5. New reactors for improving the utilization of immobilized derivatives.
6. Protocols for immobilization directed to different uses and applications of industrial enzymes.

References

1. Wong C-H, Whitesides GM (1994) Enzymes in synthetic organic chemistry. In: Baldwin JE, Magnus FRS (eds) Tetrahedron organic chemistry series, vol 12. Pergamon, Oxford, pp 41–130
2. Robertson DE, Steer BA (2004) Recent progress in biocatalyst discovery and optimization. *Curr Opin Chem Biol* 8:141–149
3. van den Burg B, Eijssink VGH (2002) Selection of mutations for increased protein stability. *Curr Opin Chem Biol* 13:333–337
4. Fernández-Lafuente R, Hernández-Jústiz O, Mateo C, Fernández-Lorente G, Terreni M, Alonso J, García-López JL, Moreno MA, Guisán JM (2001) Biotransformations catalyzed by multimeric enzymes: stabilization of tetrameric ampicillin acylase permits the optimization of ampicillin synthesis under dissociation conditions. *Biomacromolecules* 2:95–104
5. Betancor L, Hidalgo A, Fernández-Lorente G, Mateo C, Fernández-Lafuente R, Guisán JM (2003) Preparation of a stable biocatalyst of bovine liver catalase. *Biotechnol Prog* 19:763–767
6. Rosell CM, Terreni M, Fernández-Lafuente R, Guisán JM (1998) A criterium for the selection of monophasic solvents for enzymatic synthesis. *Enzyme Microb Technol* 23:64–69
7. Guisán JM, Álvaro G, Rosell CM, Fernández-Lafuente R (1994) Industrial design of enzymatic processes catalyzed by very active immobilised derivatives. Utilisation of diffusional limitation (gradients of pH) as a profitable tool in enzyme engineering. *Biotech Appl Biochem* 20:357–369
8. Illanes A, Wilson L (2003) Enzyme reactor design under thermal inactivation. *Crit Rev Biotechnol* 23:61–93
9. Spiess A, Schlothauer RC, Hinrichs J, Scheidat B, Kasche V (1999) pH gradients in immobilized amidases and their influence on rates and yields of beta-lactam hydrolysis. *Biotechnol Bioeng* 62:267–277
10. Bickerstaff GF (1997) Immobilization of enzymes and cells, *Methods in biotechnology*. Humana, New York, NY
11. Katchalski-Katzir E (1993) Immobilized enzymes: learning from past successes and failures. *TIB* 11:471–478
12. Fernández-Lafuente R, Guisán JM (1998) Enzyme and protein engineering via immobilization and post-immobilization techniques. In: Pandalai SG (ed) *Recent research developments in biotechnology and bioengineering*. Research Signpost, Trivandrum, pp 299–309
13. Pessela BCC, Mateo C, Carrascosa AV, Vian A, García JL, Guisán JM, Fernández-Lafuente R (2003) One step purification, covalent immobilization and additional stabilization of a thermophilic poly-his-tagged beta-galactosidase of *Thermus* sp. strain t2, novel heterofunctional chelate-epoxy supports. *Biomacromolecules* 4:107–113
14. Abian O, Grazá V, Hermoso J, González R, García JL, Fernández-Lafuente R, Guisán JM (2004) Stabilization of penicillin G acylase from *Escherichia coli*: site directed mutagenesis of the protein surface to increase multipoint covalent attachment. *Appl Envir Microb* 70:1249–1251
15. López-Gallego F, Montes T, Fuentes M, Alonso N, Graza V, Betancor L, Guisán JM, Fernández-Lafuente R (2005) Chemical increase of the amount of reactive groups on enzyme surface to improve its stabilization via multipoint covalent attachment. *J Biotechnol* 116:1–10
16. Betancor L, Fuentes M, Dellamora-Ortiz G, López-Gallego F, Hidalgo A, Alonso-Morales N, Mateo C, Guisán JM, Fernández-Lafuente R (2005) Dextran aldehyde coating of glucose oxidase immobilized on magnetic nanoparticles prevents inactivation by gas bubbles. *J Mol Catal B Enzymatic* 32:97–101
17. Guisán JM (1988) Aldehyde gels as activated support for immobilization-stabilization of enzymes. *Enzyme Microb Technol* 10:375–382
18. Mateo C, Abian O, Bernedo M, Cuenca E, Fuentes M, Fernández-Lorente G, Palomo JM, Graza V, Pessela BCC, Giacomini C, Irazoqui G, Villarino A, Ovsejevi A, Batista-Viera F, Fernández-Lafuente R, Guisán JM (2005) Some special features of glyoxyl supports to immobilize proteins. *Enzyme Microb Technol* 37:456–462
19. Mateo C, Abian O, Fernández-Lorente G, Predoche J, Fernández-Lafuente R, Guisán JM (2002) Sepabeads: a novel epoxy-support for stabilization of industrial enzymes via very intense multipoint covalent attachment. *Biotechnol Prog* 18:629–634
20. Mateo C, Torres R, Fernández-Lorente G, Ortiz C, Fuentes M, Hidalgo A, López-Gallego F, Abian O, Palomo JM, Betancor L, Pessela BCC, Guisán JM, Fernández-Lafuente R (2003) Epoxy-amino groups: a new tool for improved immobilization of proteins by the epoxy method. *Biomacromolecules* 4:772–777
21. Poltorak OM, Chukhary ES, Torshin IY (1998) Dissociative thermal inactivation, stability and activity of oligomeric enzymes. *Biochemistry (Moscow)* 63:360–369

22. Fernández-Lafuente R, Rodríguez V, Mateo C, Penzol G, Hernández-Justiz O, Irazoqui G, Villarino A, Ovsejevi K, Batista F, Guisán JM (1999) Strategies for the stabilization of multi-meric enzymes via immobilization and post-immobilization techniques. *J Mol Catal B Enzymatic* 7:181–189
23. Wilson L, Betancor L, Fernández-Lorente G, Fuentes M, Hidalgo A, Guisán JM, Pessela BCC, Fernández-Lafuente R (2004) Crosslinked aggregates of multimeric enzymes: a simple and efficient methodology to stabilize their quaternary structure. *Biomacromolecules* 5:814–817
24. Bastida A, Sabuquillo P, Armisen P, Fernández-Lafuente R, Huguet J, Guisán JM (1998) A single step purification, immobilization and hyperactivation of lipases via interfacial adsorption on strongly hydrophobic supports. *Biotechnol Bioeng* 58:486–493
25. Fernández-Lafuente R, Armisen P, Sabuquillo P, Fernández-Lorente G, Guisán JM (1998) Immobilization of lipases by selective adsorption on hydrophobic supports. *Chem Phys Lipids* 93:185–197
26. Palomo MJ, Muñoz G, Fernández-Lorente G, Mateo C, Fernández-Lafuente R, Guisán JM (2002) Interfacial adsorption of lipases on very hydrophobic support (octadecyl Sepabeads): immobilization, hyperactivation and stabilization of the open form of lipases. *J Mol Catal B Enzymatic* 19–20:279–286
27. Fernández-Lafuente R, Rosell CM, Álvaro G, Guisán JM (1992) Additional stabilisation of penicillin G acylase by controlled chemical modification of immobilised/stabilised derivatives. *Enzyme Microb Technol* 14:489–495
28. Fernández-Lafuente R, Rosell CM, Guisán JM, Caanan-Haden L, Rodes L (1999) Facile synthesis of artificial enzyme nano-environments via solid-phase chemistry of immobilized derivatives dramatic stabilization of penicillin acylase versus organic solvents. *Enzyme Microb Technol* 24:96–103
29. Abian O, Wilson L, Mateo C, Fernández-Lorente G, Palomo JM, Fernández-Lafuente R, Guisán JM, Re D, Tam A, Daminatti M (2002) Preparation of artificial hyper-hydrophilic micro-environments (polymeric salts) surrounding immobilized enzyme molecules. New enzyme derivatives to be used in any reaction medium. *J Mol Catal B Enzymatic* 19–20:295–303
30. Wilson L, Illanes A, Abian O, Pessela BCC, Fernández-Lafuente R, Guisán JM (2004) Co-aggregation of penicillin G acylase and polyionic polymers: a simple methodology to prepare enzyme biocatalysts stable in organic media. *Biomacromolecules* 5:852–857
31. Penzol G, Armisen P, Fernández-Lafuente R, Rodes L, Guisán JM (1998) Use of dextrans as long, inert and hydrophilic spacer arms to improve the performance of immobilized proteins acting on macromolecules. *Biotechnol Bioeng* 60:518–523
32. Turkova J (1999) Oriented immobilization of biologically active proteins as a tool for revealing protein interactions and function. *J Chromatography B* 722:11–31
33. Fuentes M, Mateo C, Guisán JM, Fernández-Lafuente R (2005) Preparation of inert magnetic nano-particles for the directed immobilization of antibodies. *Biosens Bioelec* 20:1380–1387
34. Lund V, Schmid R, Rickwood D, Hornes E (1988) Assessment of methods for covalent binding of nucleic acids to magnetic beads. Dynabeads, and the characteristics of the bound nucleic acids in hybridization reactions. *Nucleic Acids Res* 16:10861–10880
35. Fuentes M, Mateo C, Garcia L, Tercero JC, Guisán JM, Fernández-Lafuente R (2004) The directed covalent immobilization of aminated DNA probes on aminated plates. *Biomacromolecules* 5:883–888
36. Pessela BCC, Torres R, Fuentes M, Mateo C, Fernández-Lafuente R, Guisán JM (2004) Immobilization of rennet from *Mucor miehei* via its sugar chain. Its use in milk coagulation. *Biomacromolecules* 5:2029–2033
37. Fuentes M, Mateo C, Rodríguez A, Casquerio M, Tercero JC, Riese H, Fernández-Lafuente R, Guisán JM (2006) Detecting minimal traces of DNA by using DNA covalently attached to superparamagnetic nanoparticles and PCR-ELISA in one step. *Biosens Bioelec* 21:1574–1580

Chapter 2

Immobilization of Enzymes: A Literature Survey

Beatriz Brena, Paula González-Pombo, and Francisco Batista-Viera

Abstract

The term immobilized enzymes refers to “enzymes physically confined or localized in a certain defined region of space with retention of their catalytic activities, and which can be used repeatedly and continuously.”

Immobilized enzymes are currently the subject of considerable interest because of their advantages over soluble enzymes. In addition to their use in industrial processes, the immobilization techniques are the basis for making a number of biotechnology products with application in diagnostics, bioaffinity chromatography, and biosensors. At the beginning, only immobilized single enzymes were used, after 1970s more complex systems including two-enzyme reactions with cofactor regeneration and living cells were developed.

The enzymes can be attached to the support by interactions ranging from reversible physical adsorption and ionic linkages to stable covalent bonds. Although the choice of the most appropriate immobilization technique depends on the nature of the enzyme and the carrier, in the last years the immobilization technology has increasingly become a matter of rational design.

As a consequence of enzyme immobilization, some properties such as catalytic activity or thermal stability become altered. These effects have been demonstrated and exploited. The concept of stabilization has been an important driving force for immobilizing enzymes. Moreover, true stabilization at the molecular level has been demonstrated, e.g., proteins immobilized through multipoint covalent binding.

Key words Immobilized enzymes, Bioaffinity chromatography, Biosensors, Enzyme stabilization, Immobilization methods

1 Background

Enzymes are biological catalysts that promote the transformation of chemical species in living systems. These molecules, consisting of thousands of atoms in precise arrangements, are able to catalyze the multitude of different chemical reactions occurring in biological cells. Their role in biological processes, in health and disease, has been extensively investigated. They have also been a key component in many ancient human activities, especially food processing, well before their nature or function was known [1].

Table 1
Technological properties of immobilized enzyme systems [3]

Advantages	Disadvantages
Catalyst reuse	Loss or reduction in activity
Easier reactor operation	Diffusional limitation
Easier product separation	Additional cost
Wider choice of reactor	

Enzymes have the ability to catalyze reactions under very mild conditions with a very high degree of substrate specificity, thus decreasing the formation of by-products. Among the reactions catalyzed are a number of very complex chemical transformations between biological macromolecules, which are not accessible to ordinary methods of organic chemistry. This makes them very interesting for biotechnological use. At the beginning of the twentieth century, enzymes were shown to be responsible for fermentation processes and their structure and chemical composition started to come under scrutiny [2]. The resulting knowledge leads to the widespread technological use of biological catalysts in a variety of other fields such as textile, pharmaceutical, and chemical industries. However, most enzymes are relatively unstable, their costs of isolation are still high, and it is technically very difficult to recover the active enzyme, when used in solution, from the reaction mixture after use.

Enzymes can catalyze reactions in different states: as individual molecules in solution, in aggregates with other entities, and as attached to surfaces. The attached or “immobilized” state has been of particular interest to those wishing to exploit them for technical purposes. The term *immobilized enzymes* refers to “enzymes physically confined or localized in a certain defined region of space with retention of their catalytic activities, and which can be used repeatedly and continuously” [3]. The introduction of immobilized catalysts has, in some cases, greatly improved both the technical performance of the industrial processes and their economy (Table 1).

The first industrial use of immobilized enzymes was reported in 1966 by Chibata and coworkers, who developed the immobilization of *Aspergillus oryzae* aminoacylase for the resolution of synthetic racemic D-L amino acids [4]. Other major applications of immobilized enzymes are the industrial production of sugars, amino acids, and pharmaceuticals (Table 2) [5]. In some industrial processes, whole microbial cells containing the desired enzyme are immobilized and used as catalysts [6].

Table 2
Major products obtained using immobilized enzymes [3, 5]

Enzyme	Product
Glucose isomerase	High-fructose corn syrup
Amino acid acylase	Amino acid production
Penicillin acylase	Semi-synthetic penicillins
Nitrile hydratase	Acrylamide
β -Galactosidase	Hydrolyzed lactose (whey)

Aside from the application in industrial processes, the immobilization techniques are the basis for making a number of biotechnology products with application in diagnostics, bioaffinity chromatography, and biosensors [7, 8]. Therapeutic applications are also foreseen, such as the use of enzymes in extra-corporeal shunts [9].

In the past four decades, immobilization technology has developed rapidly and has increasingly become a matter of rational design but there is still the need for further development [10]. Extension of the use of immobilized enzymes to other practical processes will require both new methodologies and better understanding of those used at present.

2 History of Enzyme Immobilization

It is possible to visualize four steps in the development of immobilized biocatalysts (Table 3). In the first step at the beginning of the nineteenth century, immobilized microorganisms were being employed industrially on an empirical basis. This was the case of the microbial production of vinegar by letting alcohol-containing solutions trickle over wood shavings overgrown with bacteria, and that of the trickling filter or percolating process for waste water clarification [11].

The modern history of enzyme immobilization goes back to the late 1940s, but much of the early work was largely ignored for biochemists since it was published in Journals of other disciplines [12]. Since the pioneering work on immobilized enzymes in the early 1960s, when the basis of the present technologies was developed, more than 10,000 papers and patents have been published on this subject, indicating the considerable interest of the scientific community and industry in this field [4]. In the second step, only immobilized single enzymes were used but by the 1970s more complex systems, including two-enzyme reactions with cofactor

Table 3
Steps in the development of immobilized enzymes [11, 14]

Step	Date	Use
First	1815	Empirical use in processes such as acetic acid and waste water treatment.
Second	1960s	Single enzyme immobilization: production of L-amino acids, isomerization of glucose, etc.
Third	1985–1995	Multiple enzyme immobilization including cofactor regeneration and cell immobilization. Example: production of L-amino acids from keto-acids in membrane reactors.
Fourth	1995 to present	Ever-expanding multidisciplinary developments and applications to different fields of research and industry.

regeneration and living cells were developed [13]. As an example of the latter we can mention the production L-amino acids from α -keto acids by stereoselective reductive amination with L-amino acid dehydrogenase. The process involves the consumption of NADH and regeneration of the coenzyme by coupling the amination with the enzymatic oxidation of formic acid to carbon dioxide with concomitant reduction of NAD⁺ to NADH, in the reaction catalyzed by the second enzyme, formate dehydrogenase. More recently, in the last few decades, immobilized enzyme technology has become a multidisciplinary field of research with applications to clinical, industrial and environmental samples [14].

The major components of an immobilized enzyme system are: the enzyme, the support and the mode of attachment of the enzyme to the matrix. The term solid-phase, solid support, support, carrier, and matrix are used synonymously.

3 Choice of Supports

The characteristics of the matrix are of paramount importance in determining the performance of the immobilized enzyme system. Ideal support properties include physical resistance to compression, hydrophilicity, inertness towards enzymes, ease of derivatization, bio-compatibility, resistance to microbial attack, and availability at low cost [12–15]. However, even though immobilization on solid supports is an established technology, there are still no general rules for selecting the best support for a given application.

Supports can be classified as inorganic and organic, according to their chemical composition (Table 4). The organic supports can be subdivided into natural and synthetic polymers [16].

Table 4
Classification of supports

Organic
<i>Natural polymers</i>
<ul style="list-style-type: none"> • Polysaccharides: cellulose, dextrans, agar, agarose, chitin, alginate
<ul style="list-style-type: none"> • Proteins: collagen, albumin
<ul style="list-style-type: none"> • Carbon
<i>Synthetic polymers</i>
<ul style="list-style-type: none"> • Polystyrene
<ul style="list-style-type: none"> • Other polymers: polyacrylate, polymethacrylates, polyacrylamide, polyamides, vinyl and allyl-polymers
Inorganic
<i>Natural minerals</i>
Bentonite, silica
<i>Processed materials</i>
Glass (non-porous and controlled pore), metals, controlled pore metal oxides

The physical characteristics of the matrices (such as mean particle diameter, swelling behavior, mechanical strength, compression behavior) will be of major importance for the performance of the immobilized systems and determine the type of reactor used under technical conditions (i.e., stirred tank, fluidized, fixed beds). In particular, pore parameters and particle size determine the total surface area and thus critically affect the capacity for binding of enzymes. Nonporous supports show few diffusional limitations but have a low loading capacity. Therefore, porous supports are in general preferred because the high surface area allows a higher enzyme loading and the immobilized enzyme is more protected from the environment. Porous supports should have a controlled pore distribution in order to optimize capacity and flow properties. In spite of the many advantages of inorganic carriers (e.g., high stability against physical, chemical, and microbial degradation), most of the industrial applications are performed with organic matrices. The hydrophilic character is one of the most important factors determining the level of activity of an immobilized enzyme [17].

Agarose is an excellent matrix which has been extensively used. In addition to its high porosity which leads to a high capacity for proteins, some other advantages of using agarose are hydrophilic character, ease of derivatization, absence of charged groups (which prevents nonspecific adsorption of substrate and products), and

commercial availability. However, an important limitation of agarose and other porous supports is the high cost. An approach to avoid this problem is the use of reversible methods of immobilization that allow matrix regeneration and reuse.

In turn, macroporous acrylic polymers such as Eupergit® C (Röhm, Darmstadt, Germany) and Sepabeads® EC (Resindion, Milan, Italy), are suitable carriers for covalent immobilization of enzymes for industrial applications, and are amongst the most extensively studied matrixes [18–20].

Nanomaterials can serve as excellent support materials for enzyme immobilization, offering ideal characteristics for balancing the key factors that determine the efficiency of biocatalysts: surface area, mass transfer resistance and effective enzyme loading [21, 22]. Nanotechnology has provided a wide variety of alternatives for enzyme immobilization leading to potential applications in biotechnology, immunosensing, and biomedical areas [23]. Recently, enzymes immobilized to nanosized supports such as polymer microspheres, fibers, tubes, as well as various metal and magnetic nanoparticles have been reported [23–25].

4 Methods of Immobilization

In the last decades, thousands of protocols have been reported in the literature [26–29] and various immobilization strategies can be envisioned [30]. The enzymes can be attached to the support by interactions ranging from reversible physical adsorption and ionic linkages to stable covalent bonds. One way of classifying the various approaches to immobilizing enzymes is in two broad categories: irreversible and reversible methods [31] (Fig. 1). The strength

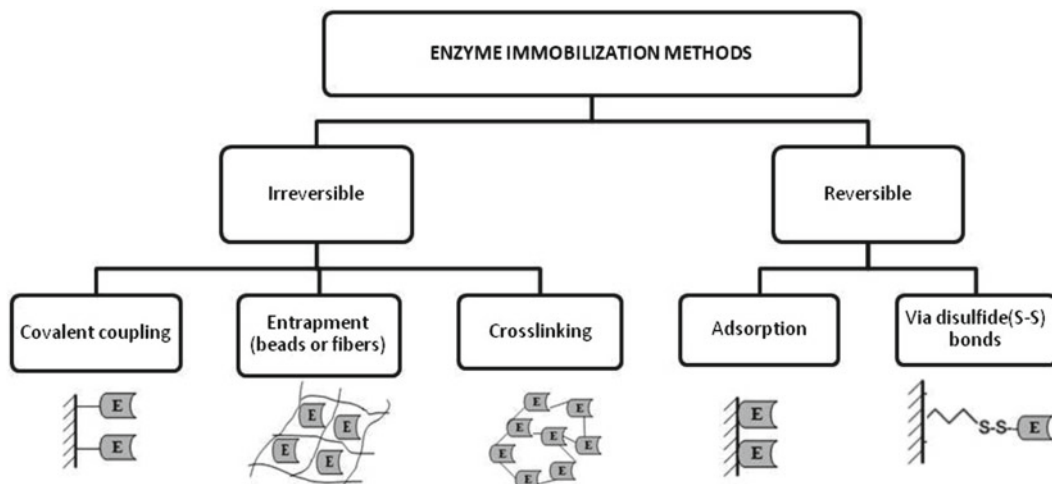


Fig. 1 Schematic representation of the main different methods of enzyme immobilization (*E* enzyme)

Table 5
Advantages and disadvantages of the main enzyme immobilization methods

Methods and binding nature	Advantages	Disadvantages
<i>Physical adsorption</i> Weak bonds: hydrophobic, Van der Waals or ionic interactions.	Simple and cheap Little conformational change of the enzyme	Desorption Nonspecific adsorption
<i>Affinity</i> Affinity bonds between two affinity partners	Simple and oriented immobilization Remarkable selectivity	High cost
<i>Covalent binding</i> Chemical binding between functional groups of the enzyme and support	No enzyme leakage Potential for enzyme stabilization	Matrix and enzyme are not regenerable Major loss of activity
<i>Entrapment</i> Occlusion of an enzyme within a polymeric network	Wide applicability	Mass transfer limitations Enzyme leakage
<i>Cross-linking</i> Enzymes molecules are cross-linked by a functional reactant	Biocatalyst stabilization	Cross-linked biocatalysts are less useful for packed beds. Mass transfer limitations Loss of activity

of the binding is usually inversely related to the ease with which it can be reversed. These two conflicting objectives, stability, and reversibility are difficult to fulfill simultaneously. The traditional approach has been to make the bond as strong as possible and sacrifice reversibility.

In addition, immobilization methods are often classified by the type of chemical reaction used for binding (Table 5). In some cases, enzyme immobilization protocols are also based on the combination of several immobilization methods. For example, an enzyme can be pre-immobilized on beads by adsorption, affinity, or covalent bonds before further entrapment in a porous polymer.

Each immobilization method presents advantages and drawbacks (Table 5). The choice of the most appropriate technique also depends on the nature of the enzyme (biochemical and kinetics properties) and the carrier (chemical characteristics, mechanical properties). So, the interaction between the enzyme and support provides an immobilized enzyme with particular biochemical and physicochemical properties that determine their applicability to specific processes.

5 Methods of Irreversible Enzyme Immobilization

The concept of irreversible immobilization means that once the biocatalyst is attached to the support, it cannot be detached without destroying either the biological activity of the enzyme or the support. The most common procedures of irreversible enzyme immobilization are covalent coupling, entrapment or micro-encapsulation, and cross-linking (Fig. 1).

5.1 Formation of Covalent Bonds

Immobilization of proteins by methods based on the formation of covalent bonds is among the most widely used. An advantage of these methods is that, because of the stable nature of the bonds formed between enzyme and matrix, the enzyme is not released into the solution upon use. However, in order to achieve high levels of bound activity, the amino acid residues essential for catalytic activity must not be involved in the covalent linkage to the support, and this may prove a difficult requirement to fulfill in some cases. A simple procedure that sometimes improves the activity yield is to carry out the coupling reaction in the presence of substrate analogues [32]. Covalent methods for immobilization are employed when there is a strict requirement for the absence of the enzyme in the product.

A wide variety of reactions have been developed depending on the functional groups available on the matrix [33]. Coupling methods in general can be divided in two main classes: (1) activation of the matrix by addition of a reactive function to a polymer; (2) modification of the polymer backbone to produce an activated group (Tables 6 and 7). The activation processes are generally designed to generate electrophilic groups on the support which in the coupling step react with the strong nucleophiles on the proteins. The basic principles controlling the course of covalent coupling to the matrices are analogous to those used for the chemical modification of proteins. The most frequently used reactions involve the following side chains of the amino acids: lysine (ϵ -amino group), cysteine (thiol group), aspartic and glutamic acids (carboxylic group).

There are many commercially available supports for immobilization; the best choice in each case requires the consideration of some relevant properties of the catalyst and the intended use. However, it is usually necessary to try more than one approach and then adapt a method to the specific circumstances [34].

The covalent reactions commonly employed give rise to enzymes linked to the support through, e.g., amide, ether, thioether, or carbamate bonds. Therefore, the enzyme is strongly bound to the matrix and in many cases it is also stabilized, which will be discussed later in Subheading 7. However, because of the covalent nature of the bond, the matrix has to be discarded together

Table 6
Covalent coupling methods of enzymes: activation of matrix hydroxyl functions

Activation method	Group that reacts (with activated matrix)	References
Tresyl chloride, sulfonyl chloride Excellent Thiols, amines 0.1–1.0 sulfonyl Chlorides	Thiol, amine	[35]
Cyanogen bromide	Amine	[36]
Bis oxiranes (epoxides)	Thiol, amine	[37]
Epichlorohydrin	Thiol, amine	[37]
Glutaraldehyde	Amine	[37]
Glycidol-Glyoxyl	Amine	[38]
N-Hydroxy-succinimidyl	Amine	[39, 40]

Table 7
Covalent coupling methods of enzymes: modification of the polymer backbone to produce an activated group

Polymer	Group that reacts	Reagent	Activated group produced	Group that reacts (with activated matrix)	References
Cellulose Agarose	Diol	Periodate	Aldehyde	Amine	[41]
Polyacrylamide	Amide	Hydrazine	Hydrazide	Amine	[42]
Polyacrylamide	Amide	Acid pH	Carboxylic acid	Amine	[42]
Polyester	Ester	Acid pH	Carboxylic acid + alcohol	Amine	[43]
Polyethylene	CH ₂	Conc. Nitric acid	Carboxylic acid	Amine	[44]
Polystyrene		Conc. Nitric acid	Nitrated aromatic ring	Histidine, Tyrosine	[45, 46]
Nylon	Amide	Hydrazine	Hydrazide	Amine	[47]

with the enzyme once the enzymatic activity decays. The benefit of obtaining a leak proof binding between enzyme and matrix resulting from these reactions could be partially offset by the cost, in terms of generally low yield of immobilized activity and by the nonreversible character of this binding. Enzymes attached covalently by disulfide bonds to solid supports, represent one way to avoid this problem, as will be described in Chapter 7.

5.2 Entrapment and Cross-linking

The entrapment method is based on the occlusion of an enzyme within a polymeric network that allows the substrate and products to pass through but retains the enzyme [48]. This method differs from the coupling methods described above, in that the enzyme is not bound to the matrix or membrane. There are different approaches to entrapping enzymes such as gel [49] or fiber entrapment [50], and micro-encapsulation [51]. The practical use of these methods is restricted by mass transfer limitations through membranes or gels.

The more recently reported technique [52, 53] for immobilization of enzymes as cross-linked enzyme aggregates (CLEAs[®]) diverges slightly from the conventional immobilization methods. CLEAs are based on multipoint attachment through intermolecular cross-linking between enzyme molecules. Successful preparation of CLEAs from a broad range of enzymes, including penicillin acylases, lipases, laccases, and horseradish peroxidase is currently being evaluated by many researchers [54].

6 Methods of Reversible Immobilization

Because of the type of the enzyme-support binding, reversibly immobilized enzymes can be detached from the support under gentle conditions. The use of reversible methods for enzyme immobilization is highly attractive, mostly for economic reasons simply because when the enzymatic activity decays the support can be regenerated and re-loaded with fresh enzyme. Indeed, the cost of the support is often a primary factor in the overall cost of immobilized catalyst. The reversible immobilization of enzymes is particularly important for immobilizing labile enzymes and for applications in bioanalytical systems [31].

6.1 Adsorption (Noncovalent Interactions)

6.1.1 Nonspecific Adsorption

The simplest immobilization method is nonspecific adsorption which is mainly based on physical adsorption or ionic binding [55, 56]. In physical adsorption the enzymes are attached to the matrix through hydrogen bonding, van der Waals forces, or hydrophobic interactions, whereas in ionic bonding the enzymes are bound through salt linkages. The nature of the forces involved in noncovalent immobilization results in a process which can be reversed by changing the conditions that influence the strength of the interaction (pH, ionic strength, temperature, or polarity of the solvent). Immobilization by adsorption is a mild, easy to perform process, and usually preserves the catalytic activity of the enzyme. Such methods are therefore economically attractive, but may suffer from problems such as enzyme leakage from matrix when the interactions are relatively weak.

6.1.2 Ionic Binding

An obvious approach to the reversible immobilization of enzymes is to base the protein-ligand interactions on principles used in chromatography. For example, one of the first applications of chromatographic principles in the reversible immobilization of enzymes was the use of ion-exchangers [4, 57, 58]. The method is simple and reversible but, in general, it is difficult to find conditions under which the enzyme remains both strongly bound and fully active. More recently, the use of immobilized polymeric ionic ligands has allowed to modulate the interactions between protein and matrix and thus to optimize the properties of the derivative. A number of patents have been filed on the use of polyethyleneimine to bind a rich variety of enzymes and whole cells [59].

However, problems may arise from the use of a highly charged support when the substrates or products are themselves charged; the kinetics are distorted due to partition or diffusion phenomena. Therefore, enzyme properties such as its optimum pH or the pH stability range may change [60, 61]. Although this could be a problem it can also be useful to shift the optimal conditions of a certain enzyme towards more alkaline or acidic conditions, depending on the application [62].

6.1.3 Hydrophobic Adsorption

Another approach is the use of hydrophobic interactions. In this method, it is not the formation of chemical bonds but rather an entropically driven interaction that takes place. Hydrophobic adsorption has been used as a chromatographic principle for more than three decades. It relies on well-known experimental variables such as pH, salt concentration, and temperature [63]. The strength of interaction relies both on the hydrophobicity of the adsorbent and that of the protein. The hydrophobicity of the adsorbent can be regulated by the degree of substitution of the support and by the size of the hydrophobic ligand molecule. The successful reversible immobilization of β -amylase and amyloglucosidase to hexyl-agarose carriers has been reported [64, 65]. Several other examples of strong reversible binding to hydrophobic adsorbents have also been reported [66–68].

6.1.4 Affinity Binding

The principle of affinity between complementary biomolecules has been applied to enzyme immobilization. The remarkable selectivity of the interaction is a major benefit of the method. However, the procedure often requires the covalent binding of a costly affinity ligand (e.g., antibody or lectin) to the matrix [69].

6.2 Chelation or Metal Binding

Transition metal salts or hydroxides deposited on the surface of organic carriers become bound by coordination with nucleophilic groups on the matrix. Mainly titanium and zirconium salts have been used and the method is known as “metal link immobilization” [16, 70, 71]. The metal salt or hydroxide is precipitated onto the support (e.g., cellulose, chitin, alginate acid, silica-based carriers) by

heating or neutralization. Because of steric factors, it is impossible for the matrix to occupy all coordination positions of the metal, and therefore some of the positions remain free to coordinate with groups from the enzymes. The method is quite simple and the immobilized specific activities obtained with enzymes in this way have been relatively high (30–80 %). However, the operational stabilities achieved are highly variable and the results are not easily reproducible. The reason for this lack of reproducibility is probably related to the existence of nonuniform adsorption sites and to a significant metal ion leakage from the support. In order to improve the control of the formation of the adsorption sites, chelator ligands can be immobilized on the solid supports by means of stable covalent bonds. The metal ions are then bound by coordination, and the stable complexes formed can be used for the retention of proteins. Elution of the bound proteins can be easily achieved by competition with soluble ligands or by decreasing pH. The support is subsequently regenerated by washing with a strong chelator such as EDTA (ethylene diamino tetraacetic acid disodium salt) when desired. These metal chelated supports were named IMA (Immobilized Metal-Ion Affinity)-adsorbents and have been used extensively in protein chromatography [72, 73]. The approach of using different IMA-gels as supports for enzyme immobilization has been studied using *E. coli* β -galactosidase as a model [74].

6.3 Formation of Disulfide Bonds

These methods are unique because, even though a stable covalent bond is formed between matrix and enzyme, this bond can be broken by reaction with a suitable agent such as dithiothreitol (DTT) under mild conditions. Additionally, since the reactivity of the thiol groups can be modulated by changing the pH, the activity yield of the methods involving disulfide bond formation is usually high, provided that an appropriate thiol-reactive adsorbent with high specificity is used [75]. Immobilization methods based on this strategy are discussed in Chapter 7.

7 Properties of Immobilized Enzymes

The properties of immobilized enzymes are determined by the characteristics of carrier material as well as by the nature and number of interactions between the enzyme and the support. As a consequence of enzyme immobilization, the stability and kinetic properties of enzymes are usually changed, mostly due to the microenvironment and modifications imposed by the supporting matrix [11, 76].

This modification in the properties may be caused either by changes in the intrinsic activity of the immobilized enzyme or by the fact that the interaction between the immobilized enzyme and the substrate takes place in a micro-environment that is different from the bulk solution. So, one of the main problems associated

with the use of immobilized enzymes is the loss of catalytic activity, especially when the enzymes are acting on macromolecular substrates. Because of the limited access of the substrate to the active site of the enzyme, the activity may be reduced to accessible surface groups of the substrate only. This steric restriction may in turn, change the characteristic pattern of products derived from the macromolecular substrate [77]. There are several strategies to avoid these steric problems such as: the selection of supports composed by networks of isolated macromolecular chains, the careful choice of the enzyme residues involved in the immobilization, and the use of hydrophilic and inert spacer arms [78].

The observed changes in the catalytic properties upon immobilization may also be due to changes in the three-dimensional conformation of the protein provoked by the binding of the enzyme to the matrix. These effects have been demonstrated and, to a lesser extent exploited for a limited number of enzyme systems. Quite often, when an enzyme is immobilized, its operational stability at higher temperature and in the presence of organic solvents is highly improved [79]. The concept of stabilization has thus been an important driving force for immobilizing enzymes. True stabilization at the molecular level has been demonstrated, such as the case of proteins immobilized through multipoint covalent binding [80]. Studies carried out by several authors using different methods have demonstrated that there is a correlation between stabilization and the number of covalent bonds to the matrix [81–83].

8 Enzyme Immobilization Mimics Biology

Although the science of enzyme immobilization has developed as a consequence of its technical utility, one should recognize that the advantages of having enzymes attached to surfaces have been exploited by living cells as long as life existed. An inquiry into the biological role of enzyme immobilization may provide some lessons for the biotechnologists and serve as a second point of departure, in addition to the purely chemical one. In fact, there is experimental evidence that the immobilized state might be the most common one for enzymes in their natural environment. In an attempt to mimic biology, co-immobilization of a number of sequential or cooperating biocatalysts on the same support has been used as a strategy to improve stability and enhance reaction kinetics [84]. The attachment of enzymes to the appropriate surface ensures that they stay at the site where their activity is required. This immobilization enhances the concentration at the proper location, and it may also protect the enzyme from being destroyed. Numerous bi-enzyme systems have been reported; a remarkable example is the co-immobilization of peroxidase and glucose oxidase onto carbon nanotubes to be used as a glucose biosensor [85, 86].

References

1. Berg JM, Tymoczko JL, Stryer L (2007) *Biochemistry*. Freeman, New York, NY
2. Creighton TE (1984) *Proteins*. Freeman, Oxford
3. Katchalski-Katzir E (1993) Immobilized enzymes: learning from past successes and failures. *Trends Biotechnol* 11:471–478
4. Tosa T, Mori T, Fuse N, Chibata I (1966) Studies on continuous enzyme reactions. I. Screening of carriers for preparation of water-insoluble aminoacylase. *Enzymologia* 31: 214–224
5. Tanaka A, Tosa T, Kobayashi T (1993) Industrial application of immobilized biocatalysts. Marcel Dekker, New York, NY
6. Swaisgood HE (1985) Immobilization of enzymes and some applications in the food industry. In: Laskin AI (ed) *Enzymes and immobilized cells in biotechnology*. Benjamin Cummings, London, pp 1–24
7. Guibault GG, Kauffmann JM, Patriarche GJ (1991) Immobilized enzyme electrodes as biosensors. In: Taylor RF (ed) *Protein immobilization. Fundamentals and applications*. Marcel Dekker, New York, NY, pp 209–262
8. Taylor RF (1991) Immobilized antibody- and receptor based biosensors. In: Taylor RF (ed) *Protein immobilization. Fundamentals and applications*. Marcel Dekker, New York, NY, pp 263–303
9. Chang MS (1991) Therapeutic applications of immobilized proteins and cells. In: Taylor RF (ed) *Protein immobilization. Fundamentals and applications*. Marcel Dekker, New York, NY, pp 305–318
10. Bickerstaff GF (1995) Impact of genetic technology on enzyme technology. *Genet Eng Biotechnol J* 15:13–30
11. Hartmeier W (1988) *Immobilized biocatalysts*. Springer, Berlin
12. Trevan M (1980) Techniques of immobilization. In *immobilized enzymes. An introduction and applications in biotechnology*. Wiley, Chichester, New York, pp 1–9
13. Brodelius P, Mosbach K (1987) Immobilization techniques for cells/organelles. In: Mosbach K (ed) *Methods in enzymology*, vol 135. Academic, London, pp 173–454
14. Khan A, Alzohairy A (2010) Recent advances and applications of immobilized enzyme technologies: a review. *Res J Biol Sci* 5(8): 565–575
15. Buchholz K, Klein J (1987) Characterization of immobilized biocatalysts. In: Mosbach K (ed) *Methods in enzymology*, vol 135. Academic, London, pp 3–30
16. Cabral JMS, Kennedy JF (1991) Covalent and coordination immobilization of proteins. In: Taylor RF (ed) *Protein immobilization. Fundamentals and applications*. Marcel Dekker, New York, NY, pp 73–138
17. Gemeiner P (1992) Materials for enzyme engineering. In: Gemeiner P (ed) *Enzyme engineering*. Ellis Horwood, New York, NY, pp 13–119
18. Katchalski-Katzir E, Kraemer DM (2000) Eupergit C. A carrier for immobilization of enzymes of industrial potential. *J Mol Catalysis B: Enzymatic* 10:157–176
19. Boller T, Meier C, Menzler S (2002) EUPERGIT oxirane acrylic beads: how to make enzymes fit for biocatalysis. *Org Process Res Dev* 6:509–519
20. Sheldon RA (2007) Enzyme immobilization: the quest for optimum performance. *Adv Synth Catal* 349:1289–1307
21. Kim J, Grate JW, Wang P (2008) Nanobiocatalysis and its potential applications. *Trends Biotechnol* 26(11):639–646
22. Feng W, Ji P (2011) Enzymes immobilized on carbon nanotubes. *Biotech Adv* 29:889–895
23. Ansari A, Husain Q (2012) Potential applications of enzymes immobilized on/in nano materials: a review. *Biotech Adv* 30:512–523
24. Kim J, Grate JW, Wang P (2006) Nanostructures for enzyme stabilization. *Chem Eng Sci* 61:1017–1026
25. Yim TJ, Kim DY, Karajanagi SS, Lu TM, Kane R, Dordick JS (2003) Silicon nanocolumns as novel nanostructured supports for enzyme immobilization. *J Nanosci Nanotechnol* 3: 479–482
26. Cao L (2005) Immobilised enzymes: science or art? *Curr Opin Chem Biol* 9:217–226
27. Guisan JM (2006) *Methods in biotechnology: immobilization of enzymes and cells*, 2nd edn. Humana Press, Totowa, NJ
28. Mateo C, Palomo JM, Fernandez-Lorente G, Guisan JM, Fernandez-Lafuente R (2007) Improvement of enzyme activity, stability and selectivity via immobilization techniques. *Enzyme Microb Technol* 40:1451–1463
29. Minteer SD (2011) *Enzyme stabilization and immobilization: methods and protocols*. Methods in molecular biology. Humana Press, Totowa, NJ
30. Sassolas A, Blum LJ, Leca-Bouvier BD (2012) Immobilization strategies to develop enzymatic biosensors. *Biotech Adv* 30:489–511
31. Gupta M, Mattiasson B (1992) Unique applications of immobilized proteins in bioanalytical systems. In: Suelter CH (ed) *Methods of*

- biochemical analysis, vol 36. Wiley, New York, NY, pp 1–34
32. Mattiasson B, Kaul R (1991) Determination of coupling yields and handling of labile proteins in immobilization technology. In: Taylor RF (ed) Protein immobilization. Fundamentals and applications. Marcel Dekker, New York, NY, pp 161–179
 33. Scouten WH (1987) A survey of enzyme coupling techniques. In: Mosbach K (ed) Methods in enzymology, vol 135. Academic, London, pp 30–65
 34. Taylor RF (1991) Commercially available supports for protein immobilization. In: Taylor RF (ed) Protein immobilization. Fundamentals and applications. Marcel Dekker, New York, NY, pp 139–160
 35. Nilsson K, Mosbach K (1987) Tresyl chloride-activated supports for enzyme immobilization. In: Mosbach K (ed) Methods in enzymology, vol 135. Academic, London, pp 65–78
 36. Axén R, Porath J, Ernback S (1967) Chemical coupling of peptides and proteins to polysaccharides by means of cyanogen halides. *Nature* 214:1302–1304
 37. Porath J, Axén R (1976) Immobilization of enzymes to agar, agarose, and sephadex supports. In: Mosbach K (ed) Methods in enzymology, vol XLIV. Academic, New York, NY, pp 19–45
 38. Guisán JM (1988) Agarose-aldehyde gels as supports for immobilization- stabilization of enzymes. *Enzyme Microb Technol* 10:375–382
 39. Wilchek M, Miron T (1982) A spectrophotometric assay for soluble and immobilized N-hydroxysuccinimide esters. *Anal Biochem* 126:433–435
 40. Drobníck J, Labský J, Kudlvasová H, Saudek V, Švec F (1982) The activation of hydroxy groups of carriers with 4-nitrophenyl and N-hydroxysuccinimidyl chloroformates. *Biotechnol Bioeng* 24:487–493
 41. Parikh I, March S, Cuatrecasas P (1974) Topics in the methodology of substitution reactions with agarose. In: Jacoby WB, Wilchek M (eds) Methods in enzymology, vol XXXIV. Academic, New York, NY, pp 77–102
 42. Inman JK, Dintzis HM (1969) The derivatization of cross-linked polyacrylamide beads. Controlled introduction of functional groups for the preparation of special-purpose, biochemical adsorbents. *Biochemistry* 8:4074–4082
 43. Rozprimova L, Franek F, Kubanek V (1978) Utilization of powder polyester in making insoluble antigens and pure antibodies. *Cesk Epidemiol Mikrobiol Immunol* 27:335–341
 44. Ngo TT, Laidler KJ, Yam CF (1979) Kinetics of acetylcholinesterase immobilized on polyethylene tubing. *Can J Biochem* 57:1200–1203
 45. Grubhofer N, Schleith L (1954) Protein coupling with diazotized polyaminostyrene. *Hoppe Seylers Z Physiol Chem* 297:108–112
 46. Beitz J, Schelleberger A, Lasch J, Fischer J (1980) Catalytic properties and electrostatic potential of charged immobilized enzyme derivatives. Pyruvate decarboxylase attached to cationic polystyrene beads of different charge densities. *Biochim Biophys Acta* 612:451–454
 47. Hornby WE, Goldstein L (1976) Immobilization of enzymes on nylon. In: Jacoby WB, Wilchek M (eds) Methods in enzymology, vol XXXIV. Academic, New York, NY, pp 118–134
 48. O'Driscoll KF (1976) Techniques of enzyme entrapment in gels. In: Mosbach K (ed) Methods in enzymology, vol XLIV. Academic, New York, NY, pp 169–183
 49. Bernfeld P, Wan J (1963) Antigens and enzymes made insoluble by entrapping them into lattices of synthetic polymers. *Science* 142:678–679
 50. Dinelli D, Marconi W, Morisi F (1976) Fiber-entrapped enzymes. In: Mosbach K (ed) Methods in enzymology, vol XLIV. Academic, New York, NY, pp 227–243
 51. Wadiack DT, Carbonell RG (1975) Kinetic behavior of microencapsulated β -galactosidase. *Biotechnol Bioeng* 17:1157–1181
 52. Tran D, Balkus K (2011) Perspective of recent progress in immobilization of enzymes. *ACS Catal* 1:956–968
 53. Cao L, van Langen L, Sheldon RA (2003) Immobilised enzymes: carrier-bound or carrier-free? *Curr Opin Biotechnol* 14:387–394
 54. Suleka F, Perez Fernandez D, Kneza Z, Habulina M, Roger A (2011) Immobilization of horseradish peroxidase as crosslinked enzyme aggregates (CLEAs). *Process Biochem* 46:765–769
 55. Messing RA (1976) Adsorption and inorganic bridge formations. In: Mosbach K (ed) Methods in enzymology, vol XLIV. Academic, New York, NY, pp 148–169
 56. Woodward J (1985) Immobilized enzymes: adsorption and covalent coupling. In: Woodward J (ed) Immobilized cells and enzymes: a practical approach. IRL, Oxford, UK, pp 3–17
 57. Tosa T, Mori T, Fuse N, Chibata I (1967) Studies on continuous enzyme reactions I. Screening of carriers for preparation of water insoluble aminoacylase. *Zyrmologia* 31:214–224

58. Sharp AK, Kay G, Lilly MD (1969) The kinetics of beta-galactosidase attached to porous cellulose sheets. *Biotechnol Bioeng* 11:363–380
59. Bahulekar R, Ayyangar NR, Ponrathnam S (1991) Polyethyleneimine in immobilization of biocatalysts. *Enzyme Microb Technol* 13:858–868
60. Goldstein L (1972) Microenvironmental effects on enzyme catalysis. A kinetic study of polyanionic and polycationic derivatives of chymotrypsin. *Biochemistry* 11:4072–4084
61. Goldman R, Kedem O, Silman I, Caplan S, Katchalski-Katzir E (1968) Papain-collodion membranes. I. Preparation and properties. *Biochemistry* 7:486–500
62. Guisan JM, Alvaro G, Rosell CM, Fernandez-Lafuente R (1994) Industrial design of enzymic processes catalysed by very active immobilized derivatives: utilization of diffusional limitations (gradients of pH) as a profitable tool in enzyme engineering. *Biotechnol Appl Biochem* 20:357–369
63. Porath J (1987) Salting-out adsorption techniques for protein purification. *Biopolymers* 26:S193–S204
64. Caldwell K, Axén R, Bergwall M, Porath J (1976) Immobilization of enzymes based on hydrophobic interaction. I. Preparation and properties of a beta-amylase adsorbate. *Biotechnol Bioeng* 18:1573–1588
65. Caldwell K, Axén R, Bergwall M, Porath J (1976) Immobilization of enzymes based on hydrophobic interaction. II. Preparation and properties of an amyloglucosidase adsorbate. *Biotechnol Bioeng* 18:1589–1604
66. Cashion P, Lentini V, Harrison D, Javed A (1982) Enzyme immobilization on trityl-agarose: reusability of both matrix and enzyme. *Biochnol Bioeng* 24:1221–1224
67. Yon R (1974) Enzyme purification by hydrophobic chromatography: an alternative approach illustrated in the purification of aspartate transcarbamoylase from wheat germ. *Biochem J* 137:127–130
68. Dixon J, Andrews P, Butler L (1979) Hydrophobic esters of cellulose: properties and applications in biochemical technology. *Biotechnol Bioeng* 21:2113–2123
69. Solomon B, Hollaander Z, Koppel R, Katchalski-Kazir E (1987) Use of monoclonal antibodies for the preparation of highly active immobilized enzymes. In: Mosbach K (ed) *Methods in enzymology*, vol 135. Academic, London, pp 160–170
70. Cabral JMS, Novais JM, Kennedy JF (1986) Immobilization studies of whole microbial cells on transition metal activated inorganic supports. *Appl Microbiol Biotechnol* 23:157–162
71. Kennedy JF, Cabral JMS (1985) Immobilization of biocatalysts by metal-link/chelation processes. In: Woodward J (ed) *Immobilized cells and enzymes*. IRL, Oxford, UK, pp 19–37
72. Porath J (1992) Immobilized metal ion affinity chromatography. *Protein Expr Purif* 3: 263–281
73. Kågedal L (2011) Immobilized metal ion affinity chromatography. In: Janson JC (ed) *Protein purification*. Wiley, New York, NY, pp 183–201
74. Brena B, Rydén L, Porath J (1994) Immobilization of β -galactosidase on metal-chelated- substituted gels. *Biotechnol Appl Biochem* 19:217–231
75. Batista-Viera F, Rydén L, Carlsson J (2011) Covalent chromatography. In: Janson JC (ed) *Protein purification: principles, high-resolution methods, and applications*. Wiley, New York, NY, pp 203–219
76. Trevan M (1980) Effect of immobilization on enzyme activity, in *Immobilized enzymes an introduction and applications in biotechnology*. Wiley, Chichester-New York, pp 11–56
77. Boundy J, Smiley KL, Swanson CL, Hofreiter BT (1976) Exoenzymic activity of alpha-amylase immobilized on a phenol-formaldehyde resin. *Carbohydr Res* 48:239–244
78. Guisán JM, Pénzol G, Armisen P, Bastida A, Blanco R, Fernández-Lafuente R, García-Junceda E (1997) Immobilization of enzymes acting on macromolecular substrates. In: Bickerstaff GF (ed) *Immobilization of enzymes and cells*. Humana, Totowa, NJ, pp 261–275
79. Mateo C, Palomo JM, Fernandez-Lorente G, Guisan JM, Fernandez-Lafuente R (2007) Improvement of enzyme activity, stability and selectivity via immobilization techniques. *Enzyme Microbial Technol* 40:1451–1463
80. Blanco RM, Calvete JJ, Guisán JM (1989) Immobilization-stabilization of enzymes. Variables that control the intensity of the trypsin (amine)-agarose-(aldehyde) -multipoint attachment. *Enzyme Microbial Technol* 11: 353–359
81. Koch-Schmidt A, Mosbach K (1977) Studies on conformation of soluble and immobilized enzymes using differential scanning calorimetry. 1. Thermal stability of nicotinamide adenine dinucleotide dependent dehydrogenases. *Biochemistry* 16:2101–2105
82. Koch-Schmidt A, Mosbach K (1977) Studies on conformation of soluble and immobilized enzymes using differential scanning calorimetry. 2. Specific activity and thermal stability of enzymes bound weakly and strongly to

- Sepharose CL 4B. *Biochemistry* 16: 2105–2109
83. Gabel D, Steinberg I, Katchalski-Kazir E (1971) Changes in conformation of insolubilized trypsin and chymotrypsin, followed by fluorescence. *Biochemistry* 10: 4661–4669
84. Betancor L, Luckarift H (2010) Co-immobilized coupled enzyme systems in biotechnology. *Biotechnol Genet Eng Rev* 27:95–114
85. Zhu L, Yang R, Zhai J, Tian C (2007) Bi enzymatic glucose biosensor based on co-immobilization of peroxidase and glucose oxidase on a carbon nanotube electrode. *Biosens Bioelectron* 23:528–536
86. Jeykumari DR, Narayanan SS (2008) Fabrication of bioenzyme nanobiocomposite electrode using functionalized carbon nanotubes for biosensing applications. *Biosens Bioelectron* 23(11):1686–1693

Chapter 3

Glutaraldehyde-Mediated Protein Immobilization

Fernando López-Gallego, Jose M. Guisán, and Lorena Betancor

Abstract

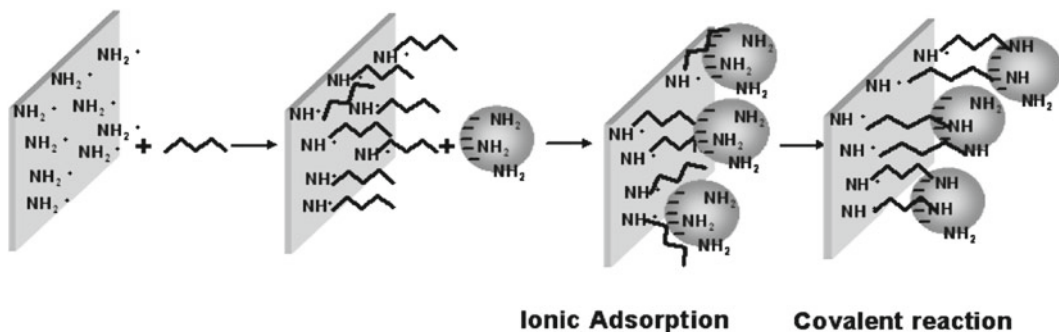
In this chapter, we describe different approaches for the utilization of glutaraldehyde in protein immobilization. First, we focus on the covalent attachment of proteins to glutaraldehyde-activated matrixes. We describe conditions for the synthesis of such supports and provide an example of the immobilization and stabilization of fructosyltransferase. We also describe how glutaraldehyde may be used for the cross-linking of protein–protein aggregates and protein adsorbed onto amino-activated matrixes. In these cases, glutaraldehyde bridges either two lysine groups from different proteic molecules or a lysine from the protein structure and an amine group from the support. Examples of cross-linking are given for the immobilization of DAAO on different amino-activated supports.

Key words Glutaraldehyde, Protein immobilization, Cross-linking, Protein stabilization

1 Introduction

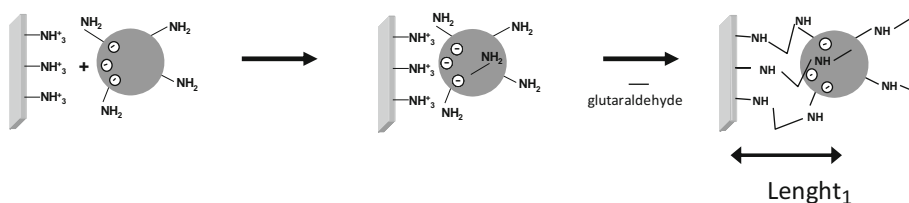
Immobilization protocols often seek simplicity and mild conditions to minimize activity loss during the process. Furthermore, the use of matrixes with facile derivatization procedures that offers multiple possibilities for covalent interaction creates a perfect scenario for an ideal immobilization protocol. Protein insolubilization procedures that involve glutaraldehyde have had great success due to the above mentioned advantages. Additional advantages are its commercial availability, low cost, and high reactivity.

Glutaraldehyde is reactive towards lysine residues of proteins and has been used for protein immobilization through covalent attachment to amino-activated matrixes or by mere cross-linking of protein–protein aggregates or protein adsorbed onto amino-activated matrixes (Scheme 1) [1–4] (or the treatment with glutaraldehyde of proteins adsorbed on supports having primary amino groups) (Scheme 2) [5–8].

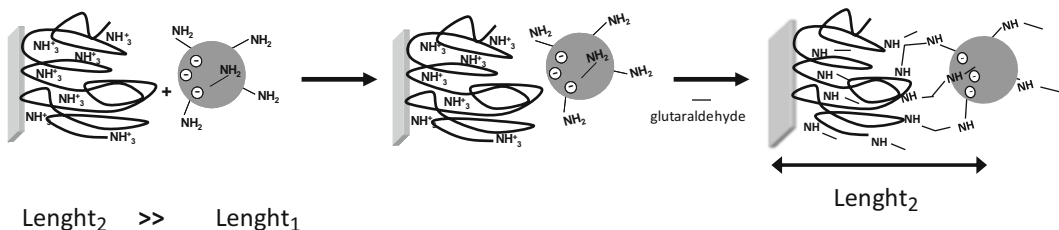


Scheme 1 Protein immobilization on aminated supports pre-activated with glutaraldehyde

Glutaraldehyde cross-linking of adsorbed proteins on MANAE



Cross-linking via glutaraldehyde of adsorbed proteins on PEI-agarose



Scheme 2 Cross-linking with glutaraldehyde of proteins ionically adsorbed onto aminated cationic supports

1.1 Glutaraldehyde-Activated Supports for Protein Immobilization

The literature on the use of this type of immobilization is vast and covers a range of supports, enzymes, and different applications. In general, surface derivatization with glutaraldehyde requires the presence of amino groups to anchor the glutaraldehyde molecule. As a consequence, some charged groups prevail after the functionalization and therefore protein interaction with the support result dual, governed first by ionic interaction and a second stage where covalent attachment is established (Scheme 1) [9].

This type of immobilization has resulted in the stabilization of a number of enzymes of biotechnological applications and we provide a few examples in this chapter [10–12].

1.2 Glutaraldehyde Cross-linking in Protein Immobilization

Another strategy to covalently immobilize proteins is using glutaraldehyde as cross-linker of ionically adsorbed biomolecules on solid surfaces. Glutaraldehyde is a bifunctional reagent able to react with two primary amine groups. It has been shown that these glutaraldehyde groups provide intense cross-linking enzyme-solid surface under a broad range of reaction conditions [13]. In most of the cases, biomolecules are ionically adsorbed onto surfaces activated with positively charged primary amine groups and later the insoluble preparation is covalently cross-linked by using a glutaraldehyde solution under mild conditions. In this scenario, one glutaraldehyde molecule bridge two primary amine groups, ideally one from the biomolecules and the other from the solid surface. However, glutaraldehyde may act as intra-molecular cross-linker by reacting with two vicinal primary amine groups within a protein. Likewise, glutaraldehyde may promote inter-molecular cross-linking between two primary amine groups of two neighbor biomolecules. Intra- or inter-molecular nature of the cross-linking may be easily controlled by controlling the protein density throughout the solid surface; a higher density, would lead to an increase in intra-molecular cross-linking. Recently, it has been reported how protein immobilization rate controls the enzyme distribution across the porous and solid surfaces and consequently the biomolecules density. Under relatively low protein concentrations, slow immobilization protocols tend to facilitate an even distribution of the biomolecules on the surface. Therefore, glutaraldehyde acts as an intra-molecular cross-linker for preparations that have been slowly immobilized, while for those rapidly immobilized, glutaraldehyde promotes an inter-molecular cross-linking.

The physic-chemical features of carrier surface may affect the cross-linking efficiency. Proteins can be absorbed onto carriers activated with monolayers of primary amine groups or the carrier surface may be coated with a polymer highly activated with primary amine groups. In the latter surface, the higher density of primary amine groups will ease glutaraldehyde cross-linking between proteins and carrier. Furthermore, coating surfaces with such highly aminated and hydrophilic polymers have been turned out in an excellent solution to apply glutaraldehyde chemistry to highly hydrophobic carriers (Duolite, Sepabeads, Lewatit, etc.) [14–16] Post-immobilization cross-linking via glutaraldehyde chemistry has been used to covalently immobilize a plethora of enzymes on preexisting carriers. This chemistry presents a high versatility since it has been successfully applied to cross-link biomolecules adsorbed onto different solid materials such as hydrogels, acrylic matrix, silica, nanoparticles. Biosensor and biocatalysis fields harness the efficiency, simplicity, and versatility of this technique that is broadly used in bioconjugation chemistry.

2 Materials

1. D-Aminoacid oxidase was kindly donated by Recordati SRL.
2. Aminated supports: Manae-agarose (Hispanagar S.A., Burgos, Spain), and EC-EA Sepabeads (Resindion S. R. L., Milan, Italy).
3. Immobilization buffer: 25 mM sodium phosphate buffer at pH 7.
4. Glutaraldehyde solution (25 % v/v), and polyethyleneimine (600 kDa) were from Fluka (Switzerland).
5. Kit glucose Trinder to measure glucose was supplied by Taper group (Alcobendas, Spain).
6. Other analytical reagents were purchased from Sigma (St Louis, MO).

3 Methods

3.1 Enzymatic Activity Assays

3.1.1 Fructosyl-transferase

Enzymatic solutions were incubated with 0.1 M Sucrose in sodium phosphate buffer 25 mM pH 6.0 at 25 °C. The reaction was stopped by boiling the reaction mixture during 5 min. The glucose formed as product was determined spectrophotometrically by indirect assay using a commercial kit (GAGO-20) and a standard curve constructed with known glucose concentrations.

3.1.2 D-Aminoacid Oxidase

It was determined following the increase in the absorbance at 420 nm produced by the coupling of oxidative deamination of Cephalosporin C and oxidation of *o*-phenyldiamine by hydrogen peroxide catalized by peroxidase. The reaction mixture was prepared with 1.5 mL of a 6.5 mM Cephalosporin C in 0.1 M potassium phosphate pH 7.5, 0.5 mL of 1.85 mM of *o*-phenyldiamine prepared in distilled water and 0.1 mL of 2 mg/mL peroxidase solution in potassium phosphate 0.1 M pH 7.5.

The enzymatic unit was defined as the amount of enzyme able to produce 1 μ mol of product per minute in the above mentioned conditions.

3.2 Preparation of Polyethyleneimine (PEI) Modified Supports

1. Prepare 100 mL of a 10 % PEI solution adjusted to pH 11.
2. Suspend 10 mL of an aldehyde containing support (i.e., Glyoxyl agarose [17]) in the solution prepared in 2.1.
3. Keep the suspension under mild stirring at 25 °C for 16 h.
4. Filter and wash exhaustively the suspension with 25 mM sodium phosphate buffer pH 7.0 (5 volumes) and then with an excess of distilled water

3.3 Glutaraldehyde Modification of Aminated Supports

1. Prepare 15 % glutaraldehyde solution in 200 mM sodium phosphate buffer and adjust the pH at 7.0 (*see Note 1*).
2. Suspend 10 mL of an aminated support in 20 mL of the glutaraldehyde solution prepared as in 3.1 (*see Note 1*).
3. Keep the suspension under mild stirring at 25 °C for 16 h (*see Note 2*).
4. Filter and wash exhaustively the suspension with 25 mM sodium phosphate buffer pH 7.0 (5 volumes) and then with an excess of distilled water.
5. Store the gel at 4 °C and use it before 24 h.

3.4 Immobilization of Enzymes on Glutaraldehyde-Activated Supports

1. Incubate 30 mL of enzymatic solution in immobilization buffer (*see Note 3*) with 10 g of the of glutaraldehyde-activated support.
2. Keep the suspension under gentle stirring at 25 °C.
3. Immobilization time will have to be assessed for each enzyme by withdrawing aliquots from the suspension and supernatant and assaying their catalytic activity until total adsorption of the enzyme.
4. Vacuum filter the derivative and wash it thoroughly with distilled water.

3.5 Adsorption of Enzymes onto Aminated Supports

1. Incubate 30 mL of enzymatic solution in immobilization buffer (*see Note 4*) with 10 g of an aminated support
2. Keep the suspension under gentle stirring at 25 °C.
3. Immobilization time will have to be assessed for each enzyme by withdrawing aliquots from the suspension and supernatant and assaying their catalytic activity until total adsorption of the enzyme.
4. Vacuum filter the derivative and wash it thoroughly with distilled water.

3.6 Cross-Linking of the Adsorbed Derivatives with Glutaraldehyde

1. Prepare a 0.5 % glutaraldehyde solution (v/v) in 25 mM sodium phosphate buffer at pH 7.0.
2. Suspend 1 wet g of the adsorbed enzyme (*see Subheading 2*) in 4 mL of the glutaraldehyde solution.
3. Keep the suspension under gentle stirring for 1 h at 25 °C.
4. Filter and wash the modified immobilized enzyme thoroughly with 25 mM sodium phosphate buffer at pH 7.0 to remove the excess of glutaraldehyde and then filter to dryness.
5. Keep the modified preparation 20 h at 25 °C and then store at 4 °C (*see Note 5*).

3.7 Desorption of Non-covalently Immobilized Proteins on the Support

1. To check if the cross-linking has been successful, resuspend 0.5 g of derivative in 2.5 mL of 1 M sodium phosphate buffer at pH 7.0. The suspension was left under mild stirring at 20 °C during 30 min.
2. Assay the activity from suspension and supernatant after of desorption process (*see* **Note 6**).

4 Notes

1. pH should be controlled as glutaraldehyde may polymerize under basic pHs, decreasing the degree of functionalization and therefore preventing enzyme immobilization by covalent interaction.
2. The suspension color is an indicator of the polymerization degree. If the suspension is brownish colored the support cannot be used since glutaraldehyde polymerization has occurred.
3. A low ionic strength during immobilization will facilitate a first ionic adsorption and a second covalent attachment between the primary amino groups of the protein and the glutaraldehyde groups of the support.
4. The low ionic strength of the immobilization buffer is necessary for the ionic adsorption between the protein and the support.
5. The additional incubation at 25 °C is necessary to achieve a higher degree of cross-linking.
6. This experiment allows for the evaluation of the covalent attachment between the protein and the support.

5 Examples

1. Immobilization-stabilization of Fructosyltransferase onto glutaraldehyde-activated MANAE agarose.
 - 1.1 Prepare 4 mL of an enzymatic solution containing 0.7 mg/mL in 25 mM sodium phosphate buffer pH 7.0.
 - 1.2 Assay the catalytic activity of the enzymatic solution as previously described.
 - 1.3 Add 1 g of MANAE agarose activated with glutaraldehyde (prepared as described in Subheading 3.3) and periodically assay the enzyme activity of both suspension and supernatant after 5 h at 25 °C.
 - 1.4 Filter and wash the derivative with an excess of distilled water.

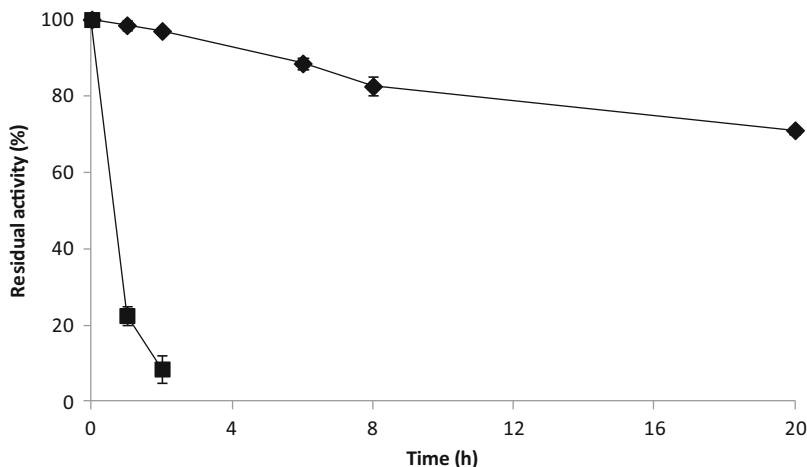


Fig. 1 Thermal stability of immobilized preparations of FST on glutaraldehyde-activated agarose. *Diamonds* control FST solution, *Squares* FST immobilized. The experiment was performed at 55°C in 10 mM sodium phosphate buffer pH 7

- 1.5 Evaluate the covalent immobilization as described above (*see* Subheading 3.7).
- 1.6 This preparation is significantly more thermostable than the soluble enzyme (Fig. 1).
2. Optimization of cross-linking glutaraldehyde concentration for enzymatic thermal stabilization: the case of DAAO immobilized.
 - 2.1 Prepare 4 mL of an enzymatic solution containing 2 mg/mL in 25 mM sodium phosphate buffer pH 7.0.
 - 2.2 Assay the catalytic activity of this solution as previously described.
 - 2.3 Proceed as in Subheading 3.3 to adsorb DAAO to MANAE or PEI modified agarose and measure the enzyme activity of both suspension and supernatant after 30 min at 25 °C.
 - 2.4 Filter the derivative.
 - 2.5 Prepare 0.2, 0.5, 0.8 and 1 % glutaraldehyde solutions in sodium phosphate buffer at pH 7.
 - 2.6 Incubate 1 g of absorbed derivative to 4 mL of the glutaraldehyde solutions prepared in 2.5. and leave the suspension 1 h at 25 °C.
 - 2.7 The suspension is filtered and washed with an excess of 25 mM sodium phosphate at pH 7, and the filtered derivative were incubated at 25 °C during 18 h.
 - 2.8 Evaluate the covalent immobilization as described above (*see* Subheading 3.7).
 - 2.9 Optimal concentration for stabilization of this enzyme was 0.5 % glutaraldehyde (Fig. 2).

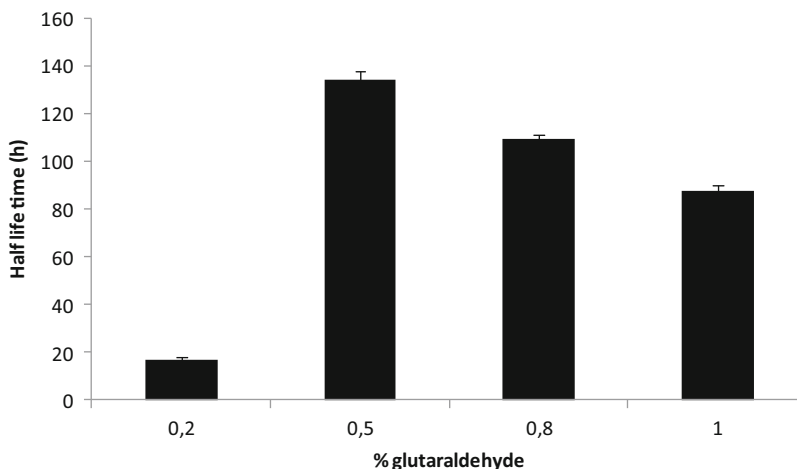


Fig. 2 Stability of DAAO absorbed on Sepabeads carriers activated with PEI and further cross-linked with different glutaraldehyde concentrations. Stability measurements are given by means of the half-life time under the following inactivation conditions: 10 mM potassium phosphate buffer at pH 7.0 at 54 °C

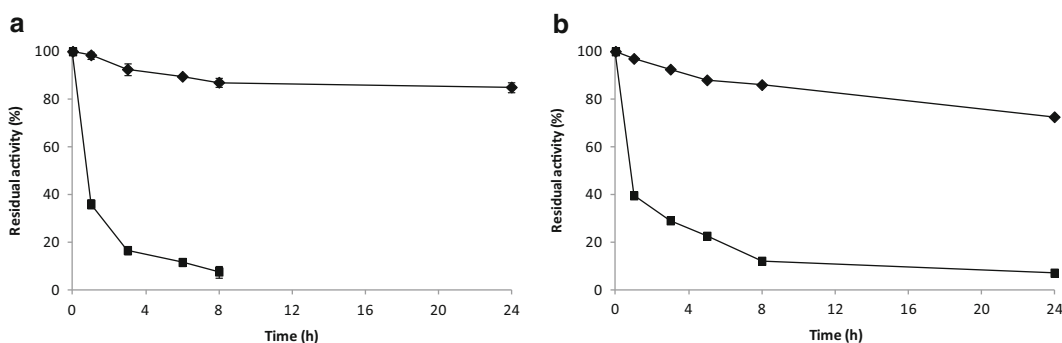


Fig. 3 Thermal stability of DAAO derivatives absorbed onto different aminated carriers and further cross-linked with glutaraldehyde. DAAO was absorbed onto MANAE-agarose (**a**) and PEI-Sepabeads (**b**) and further cross-linked with 0.5 % glutaraldehyde solution. *Squares* derivatives adsorbed onto aminated supports. *Diamonds* derivatives on aminated supports and cross-linked with 0.5 % glutaraldehyde solution. Experiments were performed by incubating 0.8 IU/mL DAAO in 10 mM potassium phosphate buffer at pH 7.0 and 50 °C

3. Stabilization of D-aminoacid oxidase (DAAO) by glutaraldehyde cross-linking of adsorbed derivatives on aminated supports.

3.1 Add 1 g of adsorbed derivative prepared as described in (2.1–2.4) to 4 mL of 0.5 % glutaraldehyde solution in sodium phosphate buffer at pH 7. This suspension is left 1 h at 25 °C under gentle stirring.

3.2 Filter and wash the suspension with an excess of 25 mM sodium phosphate at pH 7, and incubate it at 25 °C for 18 h.

3.3 These derivatives are much more thermostable than the soluble enzyme (Fig. 3a, b).

References

1. El-Aassar MR (2013) Functionalized electropun nanofibers from poly (AN-co-MMA) for enzyme immobilization. *J Mol Catal B: Enzymatic* 85–86:140–148
2. Magnan E, Catarino I, Paolucci-Jeanjean D, Preziosi-Belloy L, Belleville MP (2004) Immobilization of lipase on a ceramic membrane: activity and stability. *J Membr Sci* 241:161–166
3. Mohy Eldin MS, Elaassar MR, Elzatahry AA, Al-Sabah MMB, Hassan EA (2012) Covalent immobilization of β -galactosidase onto amino-functionalized PVC microspheres. *J Appl Polym Sci* 125:1724–1735
4. Zhou QZK, Dong CX (2001) Immobilization of β -galactosidase on graphite surface by glutaraldehyde. *J Food Eng* 48:69–74
5. Demarche P, Junghanns C, Mazy N, Agathos SN (2012) Design-of-experiment strategy for the formulation of laccase biocatalysts and their application to degrade bisphenol A. *N Biotechnol* 30:96–103
6. D'Souza SF, Kubal BS (2002) A cloth strip bioreactor with immobilized glucoamylase. *J Biochem Biophys Methods* 51:151–159
7. Hwang S, Lee KT, Park JW, Min BR, Haam S, Ahn IS, Jung JK (2004) Stability analysis of *Bacillus stearothermophilus* L1 lipase immobilized on surface-modified silica gels. *Biochem Eng J* 17:85–90
8. Zimmermann YS, Shahgaldian P, Corvini PFX, Hommes G (2011) Sorption-assisted surface conjugation: a way to stabilize laccase enzyme. *Appl Microbiol Biotechnol* 92:169–178
9. Betancor L, López-Gallego F, Hidalgo A, Alonso-Morales N, Mateo GD-OC, Fernández-Lafuente R, Guisán JM (2006) Different mechanisms of protein immobilization on glutaraldehyde activated supports: effect of support activation and immobilization conditions. *Enzyme Microb Technol* 39:877–882
10. López-Gallego F, Betancor L, Hidalgo A, Alonso N, Fernandez-Lorente G, Guisan JM, Fernandez-Lafuente R (2005) Preparation of a robust biocatalyst of D-amino acid oxidase on sephabeads supports using the glutaraldehyde crosslinking method. *Enzyme Microb Technol* 37:750–756
11. López-Gallego F, Betancor L, Mateo C, Hidalgo A, Alonso-Morales N, Dellamora-Ortiz G, Guisán JM, Fernández-Lafuente R (2005) Enzyme stabilization by glutaraldehyde crosslinking of adsorbed proteins on aminated supports. *J Biotechnol* 119:70–75
12. Betancor L, López-Gallego F, Hidalgo A, Alonso-Morales N, Dellamora-Ortiz G, Guisán JM, Fernández-Lafuente R (2006) Preparation of a very stable immobilized biocatalyst of glucose oxidase from *Aspergillus niger*. *J Biotechnol* 121:284–289
13. Fernandez-Lafuente R, Resell CM, Rodriguez V, Guisan JM (1995) Strategies for enzyme stabilization by intramolecular crosslinking with bifunctional reagents. *Enzyme Microb Technol* 17:517–523
14. Bayraktar H, Serilmez M, Karkas T, Çelem EB, Önal S (2011) Immobilization and stabilization of α -galactosidase on Sepabeads EC-EA and EC-HA. *Int J Biol Macromol* 49:855–860
15. Gouda MK, Abdel-Naby MA (2002) Catalytic properties of the immobilized *Aspergillus tamarii* xylanase. *Microbiol Res* 157:275–281
16. Chae HJ, Kim EY, In MJ (2000) Improved immobilization yields by addition of protecting agents in glutaraldehyde-induced immobilization of protease. *J Biosci Bioeng* 89:377–379
17. Guisán JM (1988) Aldehyde-agarose gels as activated supports for immobilization-stabilization of enzymes. *Enzyme Microb Technol* 10:375–382

Immobilization of Enzymes on Monofunctional and Heterofunctional Epoxy-Activated Supports

Cesar Mateo, Valeria Grazu, and Jose M. Guisan

Abstract

The immobilization of proteins on epoxy activated supports is discussed in this chapter. Immobilization on epoxy supports is carried out as a two-step mechanism: in the first step the adsorption of the protein is promoted and in the second step the intramolecular covalent linkage among epoxy groups and nucleophiles of the protein is produced. Based on this mechanism of the need of a first adsorption of the protein on the support, different epoxy supports are described. The different supports are able to immobilize proteins through different orientations being obtained catalysts with different properties of activity, stability, and selectivity.

Key words Epoxy supports, Heterofunctional epoxy supports, Immobilization, Stabilization

1 Introduction

During the last few years considerable efforts have been taken to develop effective immobilization techniques to increase the operational stability of enzymes and to facilitate their recovery and recycling, contributing to reduce the cost of the final products [1, 2]. Among the different protocols described to immobilize enzymes and proteins, many of them are only capable to resolve the problem of immobilization at laboratory scale [3–9]. Although immobilization is considered as a well-developed technique, most of the methods present different drawbacks when used to quantitative immobilize under mild conditions. The main target in this case is the necessity of immobilizing large amounts of protein per gram of support through long-term handling of the activated supports when the immobilization is carried out at industrial scale. Considering this, epoxy supports are good candidates to be almost ideal systems to develop easy protocols for enzyme immobilization. Epoxy groups are stable at neutral pH so that commercial supports can be stored for long time periods and the enzyme can be in contact with the support without significant loss of reactive groups.

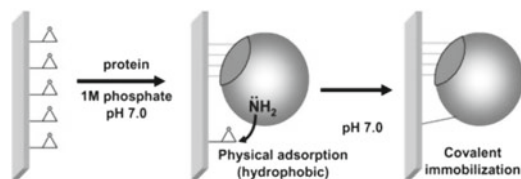


Fig. 1 Immobilization of proteins on epoxy-activated supports

Moreover, these groups can easily react with different nucleophiles highly abundant in the protein surface such as primary amine, thiol, or aromatic hydroxyl groups to form extremely strong linkages (secondary amine, thioether, or ether bonds) with a minimal modification of the protein structure. Moreover, these epoxy supports may be used to stabilize enzymes through multipoint covalent attachment controlling the enzyme–support interactions [10].

Finally, remaining epoxy groups can be easily blocked by reaction with different nucleophile molecules under very mild conditions [11].

1.1 Immobilization of Enzymes on Epoxy Supports

Epoxy groups are quite stable especially at neutral pH and consequently are not highly reactive in mild conditions. Due to this, originally epoxy supports hardly immobilize large amounts of proteins. To avoid this problem, traditionally hydrophobic epoxy supports in the presence of high ionic strengths have been used [12–15]. This is because the immobilization on these supports is performed through a two-step mechanism: first enzymes are hydrophobically adsorbed on the support and then an intramolecular covalent attachment between nucleophile groups of the enzyme (amino, thiol, or hydroxyl groups) and a high density of epoxy groups is strongly favored (Fig. 1). Thus, the immobilization of proteins on epoxy supports requires their previous adsorption on the support on a hydrophobic support in the presence of high ionic strength. In these conditions it is possible to immobilize around 70 % of the proteins contained in an *Escherichia coli* strain at neutral pH [10].

While this approach resolves the problems to immobilize proteins, this strategy presents some drawbacks such as the necessity of using a moderately highly hydrophobic support and the use of high salt concentrations. The use of hydrophobic supports can promote the wrong folding of the protein structure caused by the stabilization of anomalous structures with internal hydrophobic amino acids located in the outer layer [16]. In this sense the possibility of using supports with different nature such as hydrophilic ones is also interesting. Moreover, quite often the use of high salt concentrations can deactivate the activity of different enzymes especially of multimeric ones where the linkage among subunits is promoted by ionic forces [17]. Additionally, the immobilization on hydrophobic supports only is able to promote the orientation

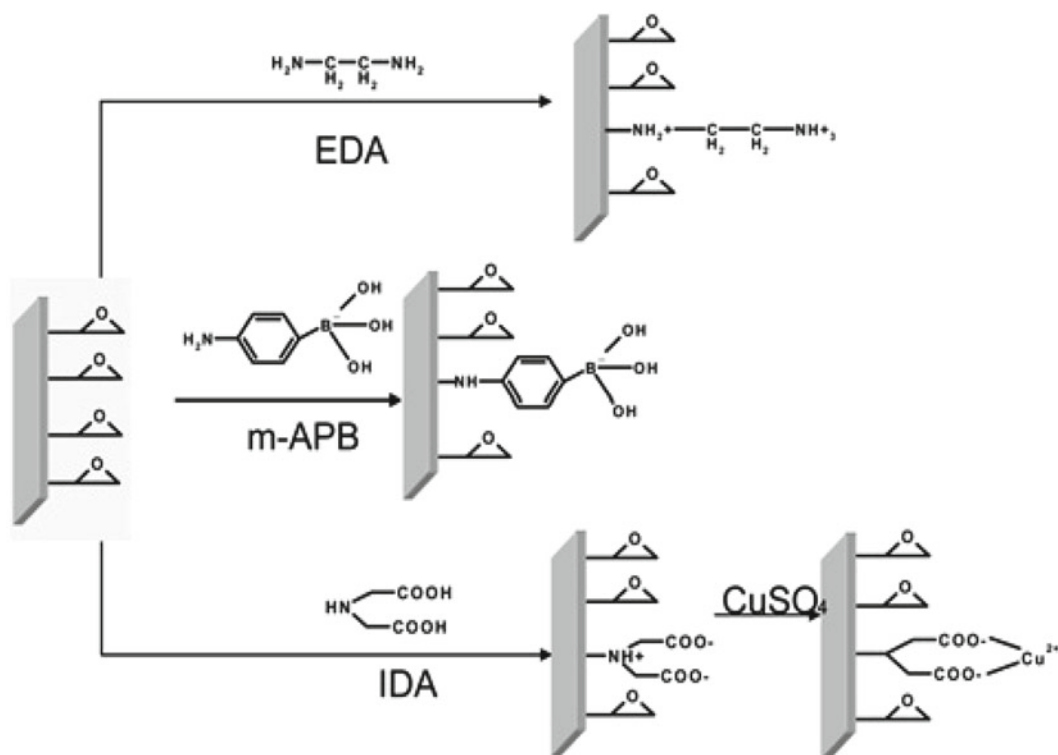


Fig. 2 Preparation of different heterofunctional epoxy supports

of the enzyme through the richest place in hydrophobic moieties. This orientation could not be the most convenient for the final properties of the catalyst (activity, stability, or selectivity).

1.2 Multifunctional Epoxy Supports for Protein Immobilization

Considering this two-step mechanism for covalent immobilization on “traditional” epoxy supports, it is possible to design new supports for the immobilization of proteins in mild conditions and using supports with different nature and not only hydrophobic ones. Thus, multifunctional supports have been proposed as a second generation of epoxy supports to immobilize different biomacromolecules [18]. These supports contain two kinds of groups: (a) groups that are able to promote the physical adsorption of the proteins (by ionic exchange, metal-chelate formation, and others) (b) epoxy groups to covalently immobilize the enzyme.

The modification of part of the epoxy groups of the support with bifunctional molecules containing an amine group to link with the epoxy and other group capable to adsorb proteins through different mechanisms can be a good alternative to achieve this goal (Fig. 2). The substitution has to be enough to promote the physical adsorption of the enzyme but keeping unaltered the maximal amount of epoxy groups to covalently immobilize the proteins (Fig. 3). The immobilization on these supports is now produced in a first step by adsorption of the proteins *via* different mechanisms

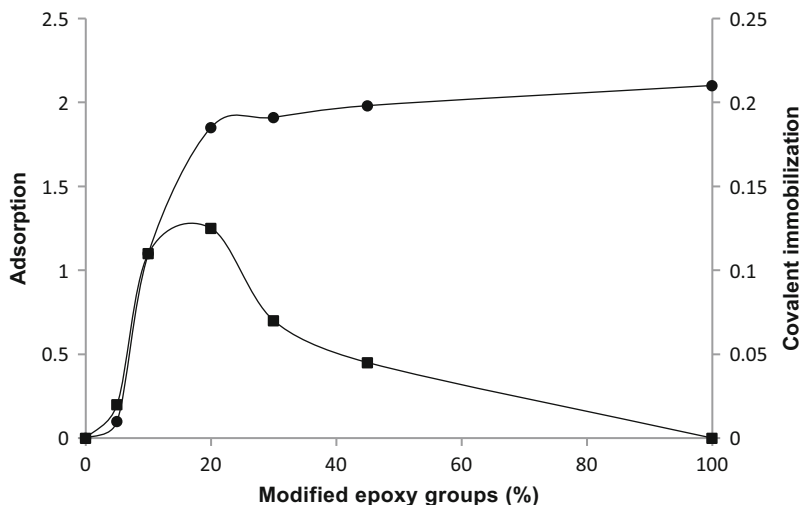


Fig. 3 Effect of the amination degree on the rates of ionic exchange and covalent attachment

(ionic exchange, metal-chelate formation, linkage to boronate compounds, and others) and then, the intramolecular covalent reaction with the epoxy groups is carried out. Different proteins from a crude *E. coli* strain were immobilized on different heterofunctional epoxy supports. Different proteins resulted immobilized on different supports (Fig. 4). Moreover, the sequential use of different heterofunctional epoxy supports has allowed the immobilization of all the proteins contained in this crude strain (Fig. 5). Most of them were immobilized on different supports implying that the enzymes were immobilized through different orientations (Table 1).

The use of these supports allows the immobilization of different enzymes on several supports through different orientations and permits the synthesis of catalysts with different properties.

1.3 Third Generation of Epoxy Supports

The synthesis of the heterofunctional supports requires the substitution of part of the epoxy groups by other capable to adsorb proteins. This promotes the decrease of the amount of epoxy groups available to covalently linking the previously adsorbed proteins. To avoid this problem, other supports have been designed, in which a group capable to adsorb proteins has been treated with epichlorohydrine to form new epoxy groups (Fig. 6) [19, 20]. The ratio between adsorbent and epoxy groups is 1:1. These supports are able to rapidly adsorb proteins promoting a strong multipoint covalent attachment.

There are numerous examples of immobilization of enzymes on these supports. Depending of the immobilized enzyme the immobilization yields are different (Table 2). The obtained stabilities are different depending of the immobilized enzyme. An interesting example is the immobilization of β -galactosidase from *Aspergillus oryzae* on different amino-epoxy supports. Different preparations of this enzyme were incubated at 50 °C and pH 4.5. The thermal

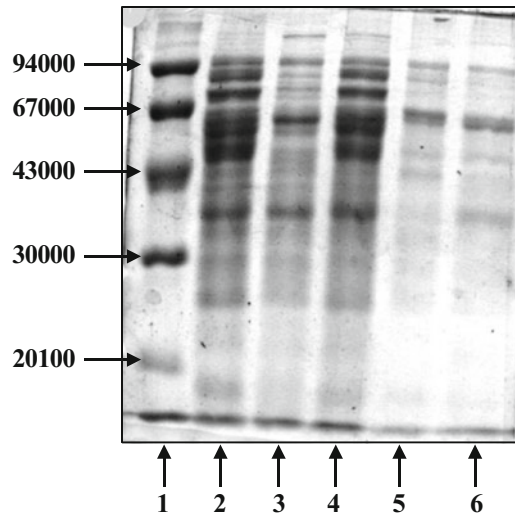


Fig. 4 Immobilization of a crude strain from *E. coli* on different heterofunctional epoxy supports. SDS-PAGE of the supernatants obtained after immobilization of the strain on the different supports. *Lane 1*: molecular weight markers; *lane 2*: *E. coli* crude strain; *lane 3*: Eupergit-EDA epoxy support; *lane 4*: Eupergit-IDA epoxy support; *lane 5*: Eupergit-IDA-Cu epoxy support; *lane 6*: Eupergit C epoxy support

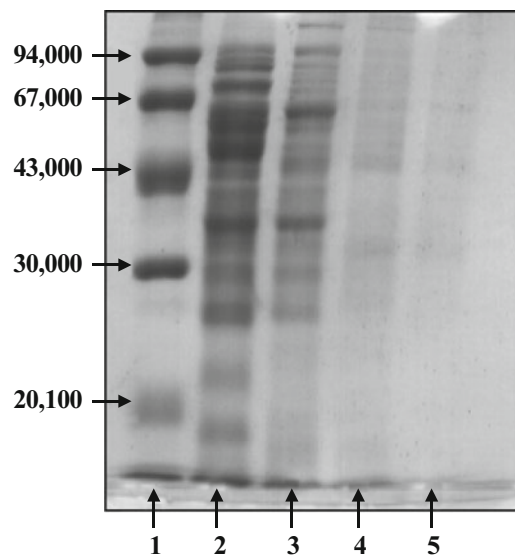


Fig. 5 SDS-PAGE analyses of the immobilization of a crude extract of *E. coli* on different epoxy supports: *Lane 1*, molecular weight markers; *lane 2*, crude protein extract from *E. coli*; *lane 3*, supernatant (I) after immobilization on aminated-Eupergit C of crude protein extract from *E. coli*; *lane 4*, supernatant (II) after immobilization on Cu-IDAEupergit C of the supernatant (I); *lane 5*, supernatant after immobilization on boronate-Eupergit C of the supernatant (II). Immobilizations were performed in 5 mM sodium phosphate at pH 7. Other conditions were as described in Subheading 3. Sequential immobilization on different supports

Table 1
Immobilization of a crude protein preparation from *E. coli* on differently modified eupergit C^a

Support	Eupergit C	Eupergit C-CU	Eupergit C-boronate	Eupergit C-IDA	Eupergit C-amino
Immobilized protein	70 %	>85 %	75 %	<10 %	65 %

^aCrude protein extract from *E. coli* was incubated in the presence of the different supports at pH 7 for 24 h. When using nonmodified Eupergit C, 1 M sodium phosphate was used. In the other cases, 5 mM of sodium phosphate was utilized as buffer. Percentage of immobilized protein was quantified by Bradford's method

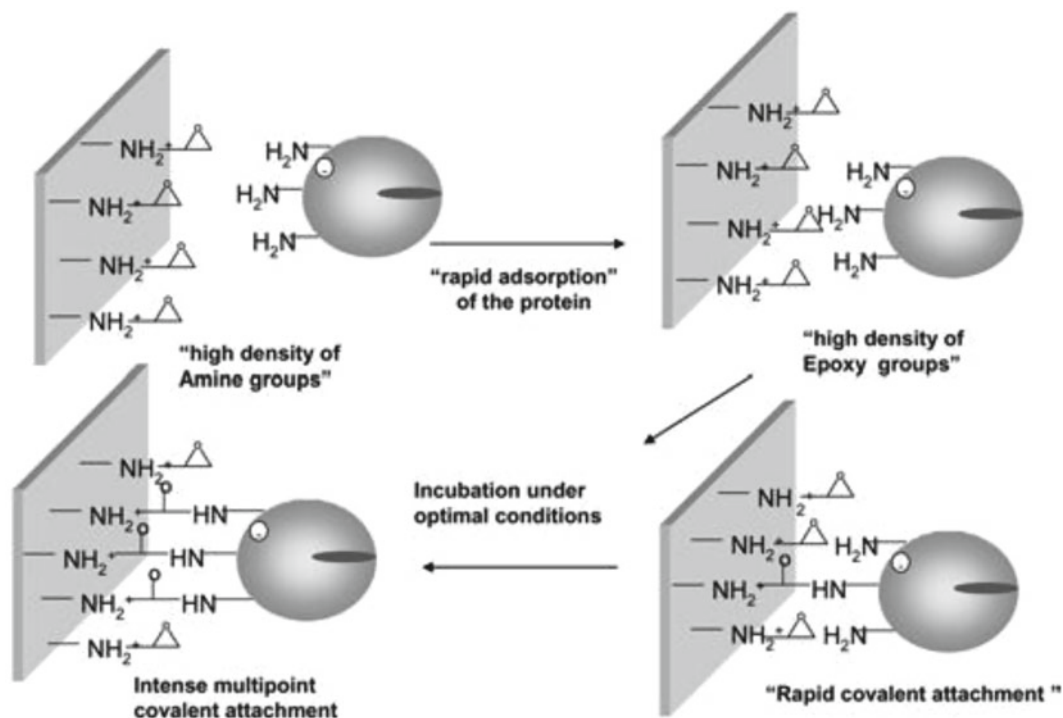


Fig. 6 Multipoint immobilization of enzymes on third generation of amino-epoxy supports

stability of the derivative immobilized on third generation amino-epoxy support was not only higher than soluble enzyme but also than that immobilized on second generation amino-epoxy support (Fig. 7). This derivative resulted around four times more stable than the immobilized on the other epoxy support [20].

1.4 Thiolated Epoxy Supports for Totally Oriented Protein Immobilization

Heterofunctional supports fulfill the requirements to immobilize different proteins through different regions of their surface. Although the use of different heterofunctional supports allows immobilizing mainly through a particular region, a 100 % pure orientation is not guaranteed because minimal populations oriented by other regions of the surface may be obtained.

Table 2
Activity recovery of the different enzymes immobilized on epoxy-sepabeads and epoxy-amino-sepabeads

Enzyme	Epoxy sepabeads recovered activity (%)	Epoxy-amino sepabeads recovered activity (%)
β -Galactosidase (<i>A. orizae</i>)	15	100
β -Galactosidase (<i>Thermus</i> sp.)	50	100
Invertase (Baker's yeast)	90	70
Glucoamilase (<i>A. niger</i>)	87	75
Lipase (<i>C. rugosa</i>)	5	65
Glutaryl acylase	100	100

Recovered activity: percentage of enzyme activity exhibited by the immobilized enzyme when compared to the soluble form. Immobilizations were performed in 5 mM and 1 M sodium phosphate pH 7 at 20 °C for 24 h with epoxy-amino and epoxy supports respectively

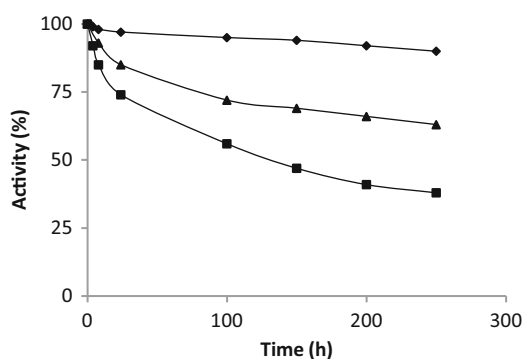


Fig. 7 Effect of the support on the stability of immobilized enzymes. (filled square) Soluble enzymes; (filled triangle) second-generation amino-epoxy immobilized enzymes; (filled diamond) third-generation amino-epoxy immobilized enzymes

Disulfide epoxy supports are able to immobilize proteins by a thiol-disulfide exchange with a surface cysteine of the protein [21, 22]. However, most of the wild proteins do not have cysteines in their surface [23] and cannot be immobilized on these supports. This fact that could be a serious drawback is an advantage because allows the introduction of a cysteine in the desired position promoting the completely oriented immobilization of the enzyme (Fig. 8). The cysteine can be introduced by site-directed mutagenesis after substitution of an amino acid of the wild protein. This methodology allows the introduction of a cysteine in different positions of the enzyme surface and after immobilization on these supports derivatives with different properties (activity, stability and selectivity) can be obtained [24]. An example of the use of this methodology is the immobilization

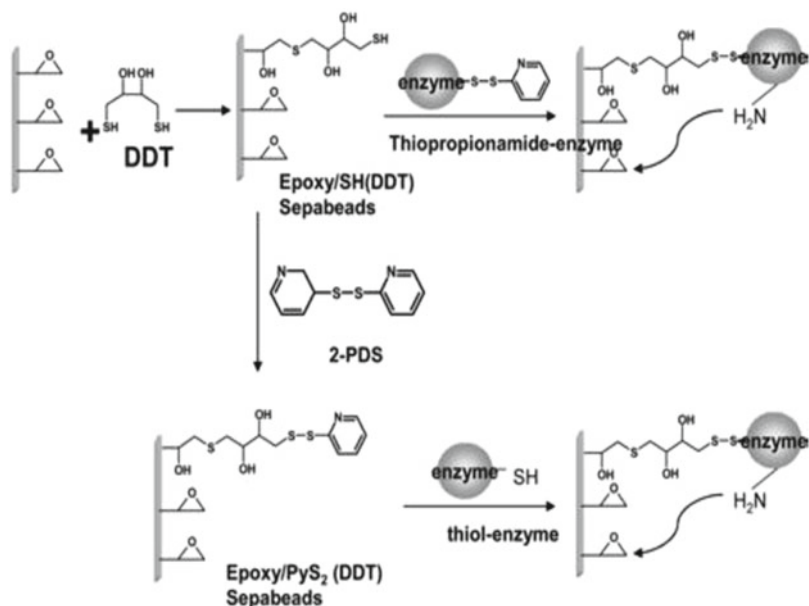


Fig. 8 Thiol epoxy support preparation and immobilization of enzymes

of different mutants of the enzyme Penicillin G Acylase from *E. coli* with a cysteine genetically introduced in different positions of the protein surface. The stability of the obtained derivatives was different depending of the orientation (dependant of the position of the introduced cysteine) of the enzyme (Fig. 9).

1.5 Optimization of the Multipoint Interaction with Epoxy Supports

The degree of enzyme-support reaction at pH 7 may be reduced because of the low reactivity of some nucleophilic residues of the enzyme at neutral pHs. Therefore, multipoint covalent attachment requires longer reaction times, higher pH values, etc. [10].

Figure 10 shows how PGA derivative stability increased when incubated at pH 9–10, with only a slight decrease in enzymatic activity (around 15 % at pH 9). Figure 11 shows how the enzyme stability reached a maximum when the reaction time increased from 1 to 4 days.

2 Materials

All the products were in general of analytical degree.

2.1 Enzymes

- β -Galactosidase grade XI (*A. orizae*) was purchased from Sigma Chem. Co.
- β -Galactosidase (*Thermus* sp.). β -galactosidase from *Thermus* sp. strain T2, (Htag-BgaA) was overproduced in *Escherichia coli* and purified as previously described [25].

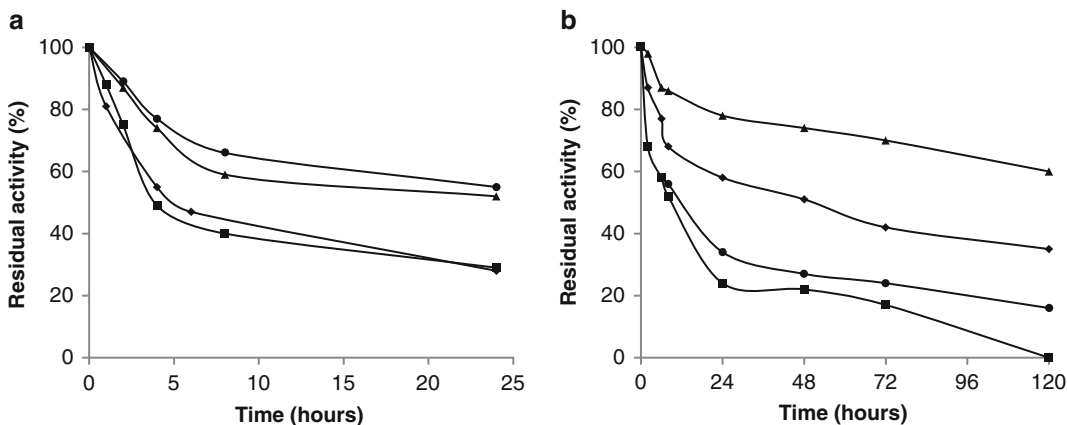


Fig. 9 Inactivation of four different mono-cysteine variants of PGA immobilized on Eupergit C under different inactivating agents. PGA mono-cysteine variants: PGA-S86C (*filled square*), PGA-Q112C (*filled diamond*), PGA-S201C (*filled circle*) and PGA-Q380C (*filled triangle*) were immobilized on Eupergit C and inactivated under 55 °C at pH 7 (**a**) and under 65 % of dioxane at pH 7 and 4 °C (**b**). Different samples were withdrawn at different times and their activity was spectrophotometrically measured using 3 mM of 6-nitro-3-phenylacetamide benzoic acid at pH 7 and 25 °C

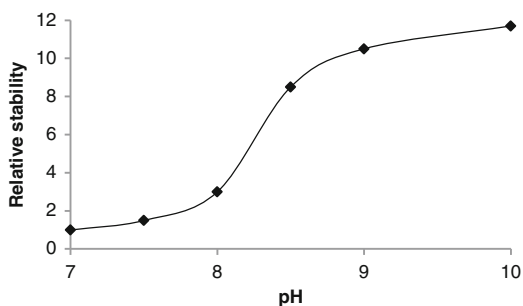


Fig. 10 Effect of pH of incubation on the stability of PGA immobilized on Sepabeads. PGA was immobilized in 1 M sodium phosphate at pH 7; after 24 h the pH was altered at the value indicated

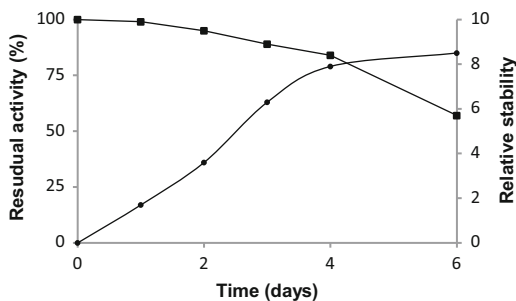


Fig. 11 Effect of incubation time on the stability of PGA immobilized on Sepabeads. PGA was immobilized at 1 M sodium phosphate at pH 7; after 24 h the pH of the immobilization suspension was increased to 9 in the presence of phenyl acetic acid and glycerin. The derivatives were blocked with 3 M of glycine at the indicated times. (*filled square*) Activity; (*filled circle*) Stabilization

- (c) Invertase (baker's yeast) was from Novo Nordisk.
- (d) Glucoamylase (*A. niger*) (Novo Nordisk AMG 300L) was from Novo Nordisk.
- (e) Lipase (*C. rugosa*) (Type VII) was from Sigma Chemical Co.
- (f) Glutaryl Acylase was kindly donated from Bioferma Murcia S.A (Murcia, Spain).
- (g) Wild type Penicillin G Acylase (*E. coli*) was donated by Antibioticos S.A. Leon (Spain). The thiolated mutants were produced as was described [24].

3 Methods

3.1 Preparation of supports [26]

3.1.1 Partial Modification of Epoxy Supports

The moieties introduced in the support may be almost any molecule able to react with the epoxy groups and permit the adsorption of the target protein. To favor multipoint covalent attachment, always introduce the minimum amount of these groups to achieve the adsorption of our target protein in a reasonable time.

1. Aminated-epoxy support:

- (a) A 10-g portion of epoxy support was incubated at 25 °C in 60 mL of 2 % v/v ethylenediamine at pH 8.5 for different times (from 15 min to 24 h) under very gently stirring.
- (b) Then, the different supports were washed with an excess of distilled water and stored at 4 °C.
- (c) Modification degree was quantified by titration of the amino groups introduced in the support.

2. Iminodiacetic acid (IDA)-epoxy supports:

- (a) A 10-g portion of epoxy support was incubated in 18 mL of 0.1 M sodium borate/2 M iminodiacetic acid pH 9 at 25 °C under very gently stirring.
- (b) At different times (from 15 min to 24 h), the different supports were washed with an excess of distilled water and stored at 4 °C.

3. Copper-IDA-epoxy supports (Cu supports)

- (a) A 10-g portion of IDA-epoxy support was incubated in 60 mL of distilled water containing 2 g of CuSO₄ under very gently stirring.
- (b) After 2 h, the support was washed with an excess of distilled water. This treatment should modify 100 % of the IDA groups in the support.
- (c) After the Cu was released from the support by treatment with EDTA, the quantification of the copper atoms by atomic absorption spectroscopy was utilized to quantify the degree of modification of the epoxy groups with the IDA groups.

4. Boronate-epoxy supports

- (a) A 10-g portion of epoxy support was incubated in 33 mL of 5 % w/v *m*-aminophenylboronic acid in 20 % dioxane at pH 8 and 25 °C.
- (b) At different times (from 30 min to 24 h) samples of the different supports were washed with 0.1 M borate pH 6 and water and stored at 4 °C.
- (c) Quantification of the modification degree was performed by elemental analysis detecting the atoms of boron.

5. Thiol-epoxy supports [21]

- (a) 10 g of epoxy supports prewashed with deionized water was incubated at room temperature with 200 mL of 0.2 M potassium bicarbonate pH 8.5 and 200 mL of 1 mM EDTA containing different DTT concentrations (5.5, 11, and 22 mM).
- (b) After 1 h, the reaction was stopped by washing the gel on a sintered glass filter with 0.1 M potassium bicarbonate pH 8.5, deionized water, and finally 0.2 M sodium acetate pH 5.0.
- (c) The partially thiolated support derivatives were stored in 50 mM sodium phosphate pH 7.0 at 4 °C until used.
- (d) Activation of Partially Thiolated Supports with 2-PDS. Partially thiolated Sepabeads with DTT (10 g) were added to a mixture of 40 mL of acetone-deionized water (60:40, v/v) and 60 mL of 0.3 M 2-PDS dissolved in acetone-0.05 M sodium bicarbonate (60:40, v/v). The solution was mixed by end-over-end rotation during the reaction, which was allowed to proceed for 1 h at room temperature. The product was washed with acetone-water (60:40, v/v) and finally with 1 mM EDTA. The activated supports were stored in 50 mM sodium phosphate pH 7.0 at 4 °C.
- (e) To determine the amount of thiol groups introduced in the support, incubate 0.5 g of the thiol containing supports with 20 mL of thiol determination buffer at 25 °C under gentle stirring for 1 h.
- (f) Take a sample of the supernatant and determine the amount of pyridine-2-thione released from the support by measuring the absorbance of the supernatant at 343 nm. The molar extinction coefficient of pyridine-2-thione is 8.020 M⁻¹ cm⁻¹ [27].

3.2 Immobilization of Proteins and Enzymes on Epoxy Supports

1. A 5-g portion of support was suspended in 45 mL of solutions of proteins or enzymes (maximum protein concentration was 1 mg/mL) in sodium phosphate pH 7, using different concentrations of buffer (from 50 mM to 1 M) at 20 °C.

2. Periodically, samples of the supernatants were withdrawn and analyzed for protein concentration (Bradford's method 24 and densitometry analyses of SDS-PAGE) or/and enzyme activity.
3. In some cases the immobilized enzyme was incubated under conditions where the physically adsorbed protein molecules were released, to check that the immobilization was actually covalent.
4. Thus, derivatives were incubated at pH 10 during different times to improve their multipoint covalent linkage degree. At different times activity was checked and was not lower than 50 % of the initial one.
5. End Point to the Support-Enzyme Reaction. To completely block the epoxy groups, 5 g of the support or enzyme-support derivative was incubated in 25 mL of 50 mM phosphate pH 7.75 containing 5 % mercaptoethanol for 16 h at 20 °C. Then, the derivatives were washed with an excess of distilled water.
6. Mercaptoethanol was found to be able to release all Cu²⁺ from the Cu supports.

3.3 Desorption of the Proteins Adsorbed but Not Covalent Attached on the Support

To test the covalent attachment of the proteins, the conditions of desorption of the proteins adsorbed on the different supports with the epoxy groups completely modified with the different reagents that promoted the physical adsorption were studied. Under these conditions the different supports were incubated to ensure that the protein molecules that remained bound to the support were really covalently attached. These conditions were as followed:

1. Eupergit C (blocked with mercaptoethanol). Most of 95 % of the proteins adsorbed in this support resulted released to the medium by incubation of 1 g of derivative in 10 mL of 25 mM phosphate, pH 7.
2. Fully modified aminated-Eupergit C released more than 95 % of the adsorbed proteins by incubation of 1 g of derivative in 10 mL of 500 mM sodium chloride, pH 7.25.
3. Fully modified IDA-Eupergit C released more than 95% of the adsorbed protein by incubation of 1 g of derivative in 10 mL sodium chloride, 500 mM, pH 7.
4. Fully modified Cu-Eupergit C released more than 95 % of the adsorbed protein by incubation of 1 g of derivative in 10 mL of 100 mM imidazole.
5. Fully modified phenylboronate supports released more than 95 % of the adsorbed protein by incubation of 1 g of derivative in 10 mL of 500 mM mannitol.
6. Fully modified thiol supports released more than 95 % of the activity after treatment of 1 g of derivative with 10 mL of mercaptoethanol 5 % pH 7.

3.4 Activity of the Enzymes

3.4.1 Penicillin G Acylase Activity Assay

Activity was determined by absorbance increasing at 405 nm resulted from hydrolysis of 6-nitro-3-(phenylacetoamide) benzoic acid. The concentration of the substrate at the assay was 0.9 mg/mL in 50 mM sodium phosphate at pH 7.5 and 25 °C. In the case of the immobilized derivatives the activity was measured under the same conditions using a spectrophotometer equipped with magnetic stirring. One enzyme activity unit is defined as the amount of enzyme needed to hydrolyze 1 μ mol of substrate per minute under the enzyme described above.

3.4.2 β -Galactosidases

1. Determination of the Activity of β -Galactosidase from *A. oryzae*.

Activity was assayed by controlling the increase in the absorbance at 405 nm caused by the hydrolysis of 10 mM *o*-nitrophenyl β -D-galactopyranoside (*o*-NPG) in 0.1 M sodium acetate pH 4.5 at 25 °C in a stirred and temperature-controlled cuvette.

2. Determination of the Activity of β -Galactosidase from *Thermus* sp. Enzyme activity was assayed at pH 6.8 and 25 °C using 10 mM *o*-NPG in 50 mM potassium phosphate, containing 0.2 M KCl and 2 mM MgCl₂. The rate of formation of free *o*-nitrophenol was determined spectrophotometrically at 405 nm using a stirred and temperature-controlled cuvette.

3.4.3 Determination of Invertase Activity from Baker's Yeast

Invertase activity was determined monitoring the hydrolysis of 5 mL of 100 mM sucrose in 0.1 M acetate buffer at pH 4.5 and 25 °C in a stirred and thermostated vessel. At different times, 100 μ L samples were withdrawn from the reaction solution. When using soluble enzymes, 20 μ L of 0.1 M NaOH was added to stop the enzymatic reaction, followed by addition of 20 μ L of 0.1 M HCl. Glucose produced by sucrose hydrolysis was measured spectrophotometrically at 505 nm using an enzymatic method (Glucose Trinder, Sigma Chemical Co).

3.4.4 Determination of Glucoamylase Activity from *A. niger*

Glucoamylase was determined monitoring the hydrolysis of 5 mL of 100 mM maltose in 0.1 M acetate buffer at pH 4.5 and 25 °C in a stirred and thermostated vessel. At different times, 100 μ L samples from the reaction solution were withdrawn. When using soluble enzymes, to stop the enzymatic reaction, 20 μ L of 0.1 M NaOH was added to inactivate the glucoamylase, followed by addition of 20 μ L of 0.1 M HCl. Glucose produced by maltose hydrolysis was measured spectrophotometrically at 505 nm using an enzymatic method (Glucose Trinder, Sigma Chemical Co).

3.4.5 Determination of Glutaryl Acylase Activity

Glutaryl acylase was measured using a pH-stat by titration of the glutaric acid released in the hydrolysis of 20 mL of 10 mM glutaryl 7-ACA in 100 mM sodium phosphate at pH 7.5 and 25 °C, using a stirred and thermostated vessel. 25 mM NaOH was used as titrating reagent.

3.4.6 *Determination of Lipase Activity from C. rugosa*

Lipase activity was determined spectrophotometrically by controlling the increase in the absorbance at 405 nm caused by the hydrolysis of 0.4 mM *p*-NPP in 25 mM sodium phosphate pH 7 at 25 °C in a stirred and temperature-controlled cuvette.

References

- Chibata I, Tosa T, Sato T (1986) Biocatalysis: immobilized cells and enzymes. *J Mol Catal* 37:1–24
- Guisan JM (ed) (2006) Immobilization of enzymes and cells, 2nd edn. Humana, Totowa, NJ
- Gupta MN (1991) Thermostatization of proteins. *Biotechnol Appl Biochem* 4:1–11
- Hartmeier W (1985) Immobilized biocatalysts—from simple to complex systems. *Trends Biotechnol* 3:149–153
- Katchalski-Katzir E (1993) Immobilized enzymes—learning from past successes and failures. *Trends Biotechnol* 11:471–478
- Kennedy JF, Melo EHM, Jumel K (1990) Immobilized enzymes and cells. *Chem Eng Prog* 45:81–89
- Klibanov AM (1983) Immobilized enzymes and cells as practical catalysts. *Science* 219:722–727
- Rosevear A (1984) Immobilized biocatalysts: a critical review. *J Chem Technol Biotechnol* 34B:127–150
- Royer GP (1980) Immobilized enzymes as catalyst. *Catal Rev* 22:29–73
- Mateo C, Abian O, Fernández-Lafuente R, Guisan JM (2000) Increase in conformational stability of enzymes immobilized on epoxy-activated supports by favoring additional multipoint covalent attachment. *Enzyme Microb Technol* 26:509–515
- Kramer DM, Lehmann K, Pennewiss H, Plainer H (1979) Oxirane acrylic beads for protein immobilization: a novel matrix for biocatalysis and biospecific adsorption. 26th international IUPAC symposium on macromolecules, Mainz, Germany
- Melander W, Corradini D, Hoorvath C (1984) Salt-mediated retention of proteins in hydrophobic-interaction chromatography. Application of solvophobic theory. *J Chromatogr* 317:67–85
- Smalla K, Turkova J, Coupek J, Herman P (1988) Influence of salt on the covalent immobilization of proteins to modified copolymers of 2-hydroxyethyl methacrylate with ethylene dimetacrylate. *Biotechnol Appl Biochem* 10:21–31
- Wheatley JB, Schmidt DE (1993) Salt induced immobilization of proteins on a high-performance liquid chromatographic epoxide affinity support. *J Chromatogr* 644:11–16
- Wheatley JB, Schmidt DE (1999) Salt induced immobilization of affinity ligands onto epoxide-activated supports. *J Chromatogr A* 849:1–12
- Fitzpatrick PA, Steinmetz ACU, Ringe D, Klibanov AM (1993) Enzyme crystal structure in a neat organic solvent. *Proc Natl Acad Sci U S A* 90:8653–8657
- Fernandez-Lafuente R (2009) Stabilization of multimeric enzymes: strategies to prevent subunit dissociation. *Enzyme Microb Technol* 45:405–418
- Mateo C, Fernández-Lorente G, Abian O, Fernández-Lafuente R, Guisán JM (2000) Multifunctional epoxy-supports: a new tool to improve the covalent immobilization of proteins. The promotion of physical adsorptions of proteins on the supports before their covalent linkage. *Biomacromolecules* 1:739–745
- Torres R, Mateo C, Fernández-Lorente G, Ortiz C, Fuentes M, Palomo JM, Guisan JM, Fernandez-Lafuente R (2003) A novel heterofunctional epoxy-amino Sepabeads for a new enzyme immobilization protocol: immobilization-stabilization of beta-galactosidase from *Aspergillus oryzae*. *Biotechnol Progr* 19:1056–1060
- Mateo C, Torres R, Fernández-Lorente G, Ortiz C, Fuentes M, Hidalgo A, López-Gallego F, Abian O, Palomo JM, Betancor L, Pessela BCC, Guisan JM, Fernández-Lafuente R (2003) Epoxy-amino groups: a new tool for improved immobilization of proteins by the epoxy method. *Biomacromolecules* 4:772–777
- Grazu V, Olga Abian O, Mateo C, Batista-Viera F, Fernandez-Lafuente R, Guisan JM (2003) Novel bifunctional epoxy/thiol-reactive support to immobilize thiol containing proteins by the epoxy chemistry. *Biomacromolecules* 4:1495–1501
- Grazu V, Abian O, Mateo C, Batista-Viera F, Fernandez-Lafuente R, Guisan JM (2005) Stabilization of enzymes by multipoint immobilization of thiolated proteins on new epoxy-thiol supports. *Biotechnol Bioeng* 90:597–605
- Hermanson GT (1996) Bioconjugate techniques. Academic, San Diego, pp 56–80
- Grazu V, López-Gallego F, Guisán JM (2012). Tailor-made design of penicillin G acylase surface enables its site-directed immobilization and

- stabilization onto commercial mono-functional epoxy supports. *Proc Biochem* 47:2538–2541. DOI: 10.1016/j.procbio.2012.07.010
25. Pessela BCC, Vian A, Mateo C, Fernandez-Lafuente R, Garcia JL, Guisan JM, Carrascosa AV (2003) Overproduction of thermus sp. strain T2 β -galactosidase in *Escherichia coli* and preparation by using tailor-made metal chelate supports. *Appl Environ Microbiol* 69:1967–1972
 26. Mateo C, Grazu V, Palomo JM, Lopez-Gallego F, Fernandez-Lafuente R, Guisan JM (2007) Immobilization of enzymes on heterofunctional epoxy supports. *Nat Protoc* 2: 1022–1033
 27. Brocklehurst K, Carlsson J, Kierstan M, Crook E (1973) Covalent chromatography. Preparation of fully active papain from dried papaya latex. *Biochem J* 133:573–584

Stabilization of Enzymes by Multipoint Covalent Immobilization on Supports Activated with Glyoxyl Groups

Fernando López-Gallego, Gloria Fernandez-Lorente,
Javier Rocha-Martin, Juan M. Bolivar, Cesar Mateo, and Jose M. Guisan

Abstract

Stabilization of enzymes via immobilization techniques is a valuable approach in order to convert a necessary protocol (immobilization) into a very interesting tool to improve key enzyme properties (stabilization). Multipoint covalent attachment of each immobilized enzyme molecule may promote a very interesting stabilizing effect. The relative distances among all enzyme residues involved in immobilization has to remain unaltered during any conformational change induced by any distorting agent. Amino groups are very interesting nucleophiles placed on protein surfaces. The immobilization of enzyme through the region having the highest amount of amino groups (Lys residues) is key for a successful stabilization. Glyoxyl groups are small aliphatic aldehydes that form very unstable Schiff's bases with amino groups and they do not seem to be useful for enzyme immobilization at neutral pH. However, under alkaline conditions, glyoxyl supports are able to immobilize enzymes via a first multipoint covalent immobilization through the region having the highest amount of Lysine groups. Activation of supports with a high surface density of glyoxyl groups and the performance of very intense enzyme–support multipoint covalent attachments are here described.

Key words Enzyme stabilization, Over-stabilization of aminated enzymes, Variables that control stabilization

1 Introduction

The low stability of most of enzymes strongly limits their implementation as industrial catalysts. The possibility of improve their stability during the development of necessary immobilization techniques is a quite interesting approach [1–3]. The most popular and most effective approach is the immobilization of enzymes by multipoint covalent attachment on highly activated supports [4, 5]. When an enzyme becomes immobilized through many surface residues on a rigid support through very short spacer arms important stabilizing effects may be achieved. Now, the relative distances among all the residues involved in multipoint immobilization

GENERAL STRATEGY FOR STABILIZATION OF ENZYMES USING MULTIPOINT COVALENT IMMOBILIZATION

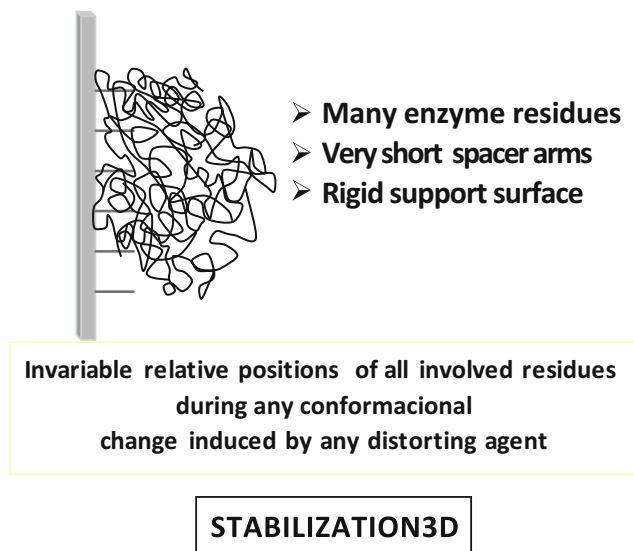


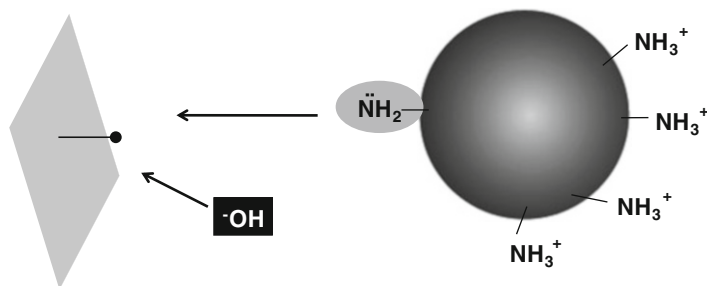
Fig. 1 A general strategy for enzyme stabilization

have to remain unaltered during any conformational change induced by any distorting agent. This idea is relatively simple, but the main problem is the achievement of such very intense enzyme-support multipoint covalent attachments (Fig. 1).

The most popular and conventional immobilization protocols are able to promote very fast enzyme immobilizations, through their amino groups, at neutral pH. Under this condition, the amino terminal residue (pK around 7.5) is thousand times more reactive than lysine residues on the enzyme surface (pK around 10.5). In this way conventional immobilization (CNBr-activated Sepharose, glutaraldehyde-activated supports, *N*-hydroxysuccinimide, etc.) occurs via the amino terminus instead, although the region with the highest amount of Lys residues would be more suitable for protein stabilization. In addition to that, conventional activation protocols utilize unstable reactive groups and they cannot be incubated under alkaline conditions in order to favor a certain additional multipoint attachment between the support and Lys residues placed in the vicinity of the amino terminal residue. In general conventional immobilization of enzymes is not very useful to get intense multipoint covalent immobilizations (Fig. 2).

The best solution for this problem would be finding a nonconventional immobilization protocol capable of direct immobilization of enzymes through the region having the highest amount of

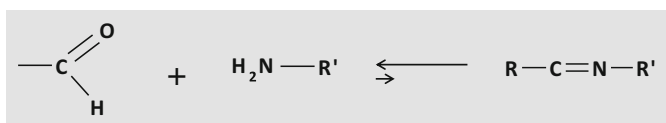
IMMOBILIZATION ENZYMES ON SUPPORTS WITH VERY REACTIVE GROUPS



- ✓ the most reactive amino group: amino terminus (pK:7,5)
<<< lysine groups (pK:10.5)
- ✓ Very unuseful to rigidify the protein surface at alkaline pH

Fig. 2 Conventional immobilization protocols

VERY POORLY REACTIVE GROUPS



Very unstable Schiff's bases

These groups are not suitable for producing covalent links between enzyme and support at neutral pH; Nevertheless, They can be converted in the best reactive groups for protein immobilization/stabilization.

Fig. 3 Poorly reactive groups may be suitable for stabilization strategies

Lys residues. For several years now our research group has reached very good stabilization protocols for industrial enzymes by using supports activated with glyoxyl groups, aldehyde groups secluded from the support surface through very short spacer arms (Support-O-CH₂-CHO) [6–22]. These supports are not useful for immobilization of enzymes at neutral pH because the formation of a unique glyoxyl-amino attachment promotes the formation of a very unstable Schiff's base and hence monomeric enzymes with a unique amino terminus are not able to become immobilized even on very highly activated glyoxyl-supports (Fig. 3).

Immobilization is also impossible under alkaline conditions (where Lys are reactive) on poorly activated supports. Again a unique enzyme-support attachment is not able to immobilize the enzyme. On the contrary the combination of alkaline conditions

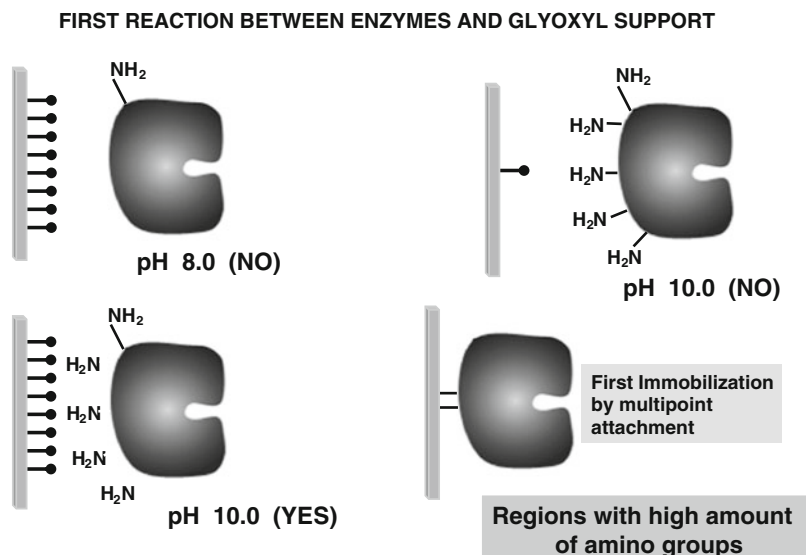


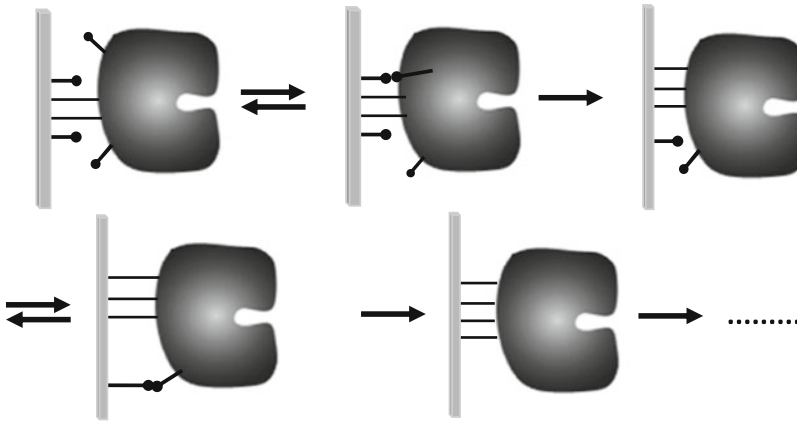
Fig. 4 Some special features of glyoxyl-supports

(e.g., pH 10) and very highly activated supports promotes a very rapid and irreversible immobilization. These results clearly demonstrated that this latter immobilization occurs via a first multipoint covalent attachment through the enzyme region having the highest amount of Lys residues. Logically, this region is the most suitable for a further intense multipoint covalent immobilization. A number of other additional results also claim for this immobilization protocol and they have been extensively reported and commented in literature [24]. At neutral pH, the amino terminus residue is 1,000-fold more reactive than Lys groups but using a nonconventional protocol, under alkaline conditions, the immobilization has been directed through the region having the highest amount of Lys residues on the enzyme surface (Fig. 4).

After this first multipoint immobilization event we may let the enzyme–support conjugate to perform an additional intramolecular reaction in which new amino groups from the enzyme surface next to the support can be aligned with new glyoxyl groups to react in order to get a more intense multipoint attachment (Fig. 5). This additional incubation has to be long (several hours after immobilization) and it occurs better at moderately high temperatures (for example, room temperature) as the vibrations of the enzyme surface is more intense and favors a more intense lysine-glyoxyl alignment and further attachment [23, 24].

The end of the enzyme–support multi-interaction is performed via a very mild borohydride reduction of the derivatives (Fig. 6). In this way, Schiff's bases between amino groups and glyoxyl ones are converted into secondary amino bond and the remaining

THE PROCESS OF MULTI-INTERACTION BETWEEN ENZYME AND SUPPORT



Time up to 24 hour safter the first immobilization.
Temperature ($25\text{ }^{\circ}\text{C} \gg 4\text{ }^{\circ}\text{C}$)

Fig. 5 The mechanism of multipoint covalent immobilization

END POINT OF ENZYME-SUPPORT MULTI-INTERACTION

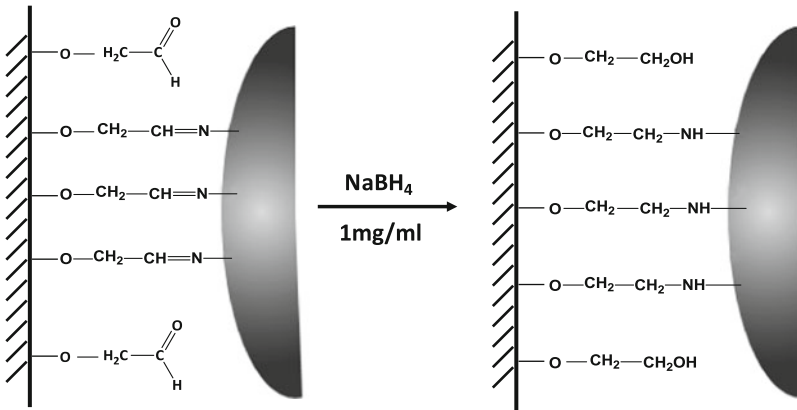


Fig. 6 End-point of multipoint covalent immobilization

glyoxyl groups are converted into inert and hydrophilic hydroxyl groups. *In this way, the chemical and physical modification of the enzyme surface will be minimal in spite of a very intense multipoint covalent attachment* [24].

Glyoxyl groups that are not useful to immobilize enzyme at pH 7.0 have a set of ideal properties for enzyme immobilization by multipoint attachment. These properties are summarized in the following Fig. 7 [24].

In addition to that, supports with highly activated large areas (for example agarose gels) seem to be optimal for the stabilization of the enzymes by multipoint covalent immobilization.

GLYOXYL GROUPS: SUPPORT -O-CH₂-CHO

- Very stable under alkaline conditions
- Very close to the support surface
- First immobilization at pH 10 is a multipoint covalent attachment
- Absence of steric hindrances for intramolecular reactions

$$\text{---O---CH}_2\text{---C} \begin{array}{l} \text{O} \\ \parallel \\ \text{H} \end{array} \leftarrow \text{:NH}_2$$

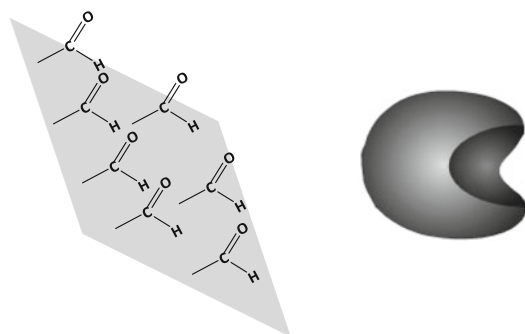
- Minimal chemical modification of the enzyme

$$\text{E---NH}_3^+ \longrightarrow \text{E---NH}_2^+ \text{---CH}_2\text{---CH}_2\text{---O} \text{---} \text{[Support]}$$

- Inert and hydrophilic final support surface

Fig. 7 Excellent properties of glyoxyl groups for multipoint covalent immobilization

GLYOXYL-AGAROSE SUPPORTS FOR ENZYME STABILIZATION



High surface density of glyoxyl groups (1.5 $\mu\text{Eq.} / \text{m}^2$)
40-80 groups per enzyme molecule

- Supports constituted by of large surfaces with a very high activation degree

Fig. 8 Special properties of glyoxyl-agarose

The enzyme support geometric congruence is very high and the density of active groups is very high. This support has also a very large density of reactive groups. For example, we can prepare agarose supports having 40–80 glyoxyl residues per immobilized enzyme molecule (Fig. 8).

Many industrial enzymes have been highly stabilized in our laboratory by multipoint covalent attachment on glyoxyl supports. In most cases the loss of catalytic activity after immobilization was very low (between 10 and 50 %) and the stabilization factors were

Table 1
Stabilization of enzymes by multipoint covalent attachment

Enzyme	Recovered activity (%)	Stabilization factor ^a
Trypsin	75	10,000 ^a
Chymotrypsin	70	10,000 ^a
Penicillin G acylase (<i>E. coli</i>)	70	8,000 ^a
Penicillin G acylase (<i>K. citrophila</i>)	70	7,000 ^a
Ferredoxin NADP reductase (<i>Anabaena</i>)	60	1,000 ^a
Esterase (<i>B. stearothermophilus</i>)	70	1,000 ^a
Glutamate racemase	70	1,000 ^a
Formate dehydrogenase (<i>Pseudomonas</i> sp. 101)	50	> 5,000 ^a
Alcohol dehydrogenase (H. liver)	90	> 3,000

^aStabilization factors are defined as the ratio between half-lives of multipoint derivatives versus one-point immobilized enzymes

very high (higher than 1,000-fold) [6–22] (Table 1). Moreover, these factors were calculated by comparing one-point with multipoint immobilizations and therefore they represent the true 3D stabilization of the enzyme against distorting agents.

As comment before, one-point immobilization could also promote interesting stabilizing effects because the elimination of different causes of enzyme inactivation: aggregation, interaction with hydrophobic interphases. Therefore 3D stabilization should be added to the stabilization by pure immobilization. The best derivatives could be millions of folds more stable than the corresponding soluble enzymes.

During the proposed immobilization process, some enzymes may be inactivated at alkaline pH. In these cases, some inhibitors may be added to the immobilization buffer to protect the enzyme. Some ways to increase the stability of soluble enzymes at pH 10.0 are summarized in the following Fig. 9.

Finally, some enzymes have a low amount of surface Lys residues and cannot be highly stabilized through this protocol. To overcome this problem, enzymes can be aminated by modification of carboxyl groups (asp and Glu residues) with ethylenediamine via previous activation with *N*-(3-Dimethylaminopropyl)-*N*-ethylcarbodiimide. Examples of amination will be given in Methods [24, 25].

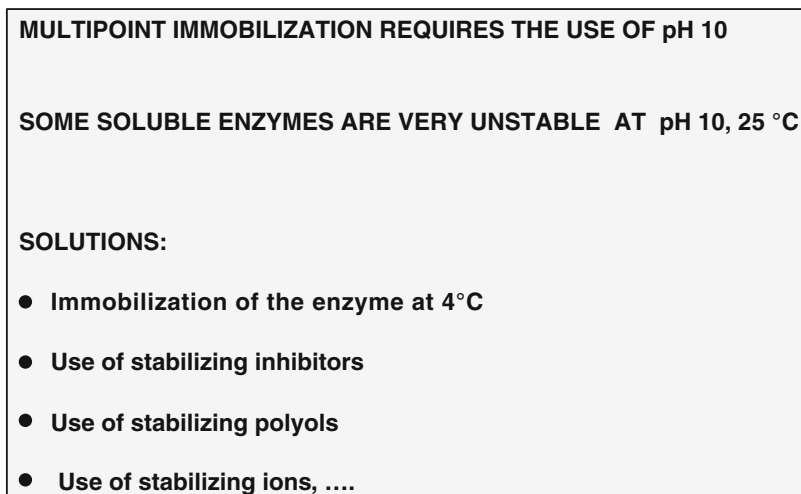


Fig. 9 Handling of enzymes at pH 10

2 Materials

1. Cross-linked 10BCL and 6BCL agarose beads were donated by Agarose Beads Technology, ABT (Madrid, Spain).
2. Glycidol (2,3-epoxy propanol) was purchased from Sigma-Aldrich S.A. (St. Louise, MO, USA) (*see Note 2*).
3. Support oxidation solution was 0.1 M sodium periodate in water (*see Note 3*).
4. Protein immobilization buffer consisted in 0.1 M bicarbonate buffer at pH 10 (*see Note 3*).

3 Methods

3.1 Preparation of Glyoxyl-Supports

3.1.1 Activation of Agarose Gel to Glyceryl-Agarose

1. Wash 105 g (150 mL) of commercial agarose 6BCL or 10BCL thoroughly with distilled water (*see Note 5*).
2. Suspend the agarose in distilled water up to a total volume of 180 mL.
3. Add to this suspension 50 mL of 1.7 N NaOH solution containing 3.4 g of sodium borohydride.
4. Take the vessel to an ice bath, keep the suspension gently stirred, and add dropwise 36 mL of glycidol (*see Note 6*).
5. Keep the suspension under mild stirring overnight (18 h) at 25 °C.
6. Filter and wash the support thoroughly with distilled water.

3.1.2 Oxidation of Glyceryl-Agarose to Glyoxyl-Agarose

1. Resuspend 105 g of glyceryl-agarose (prepared in Subheading 3.2.1) in 1,500 mL of distilled water.
2. Add the proper amount of support oxidation solution slowly to this suspension while stirring (*see Note 7*).
3. Submit the suspension for gentle stirring for 2 h.
4. Wash the support with an excess of distilled water and filter it to dryness.

3.2 Enzyme Immobilization [27]

1. Incubate 10 g glyoxyl-agarose with 100 mL of chemically aminated or non-modified enzyme solution prepared in immobilization buffer.
2. Add 1 mL of distilled water to 9 mL of enzyme solution to be used as reference solution (*see Note 8*).
3. Gently stir the mixtures by end-over-end rotation at 25 °C.
4. Aliquots of supernatant and suspension are withdrawn at regular time intervals (*see Note 9*) to assay enzyme activity.
5. Assay the activity of the reference solution using the same time intervals and aliquot volumes as in **step 5**.
6. The immobilization process finishes when activity of the supernatant is zero.
7. Then, the immobilized preparation is washed five times with three volumes of immobilization buffer.

3.3 Structural Stabilization by Multipoint Covalent Attachment

1. Resuspend the enzyme derivative (prepared in Subheading 3.3) in 100 mL of immobilization buffer.
2. Maintain the suspension for several hours (*see Note 10*). Although it is not necessary stirring because the enzyme is already immobilized on the support, stirring is necessary to measure the activity of the suspension.
3. Add 100 mg of solid sodium borohydride and stir the suspension for 30 min at 25 °C.
4. Finally, wash the enzyme derivative with 25 mM sodium phosphate pH 7.0 while vacuum filtering to eliminate the borohydride.
5. Enzyme derivatives are stored at 4 °C.

3.4 Improving the Stabilization of PGA by Multipoint Covalent Attachment on Glyoxyl Supports via Partial Amination of the Protein Surface

3.4.1 Enzyme Amination

1. 5 mL of soluble Penicillin G Acylase (PGA) from *Escherichia coli* was incubated with 45 mL of protein amination solution containing carbodiimide (EDAC) to a final concentration of 10^{-3} M. This protocol of amination allows the modification of 40–50 % of the external carboxylic groups. This means that the modified enzyme has added to the 41 amines from the Lys, 12–14 of new amino groups generated via the amination. The modification presented negligible effect in the enzyme activity, but decreased the stability of the enzyme (by a factor of eightfold).

However, as the full modification of PGA carboxylic groups caused a greater destabilization, the partial modification of the carboxylic groups with ethylenediamine (EDA) was chosen to carry out further studies.

3.4.2 Penicillin G Acylase Immobilization

1. 10 g of glyoxyl agarose 10BCL was added to 100 mL of aminated or non-modified PGA solution (0.55 mg protein/mL) in sodium bicarbonate buffer 100 mM pH 9 or 10, containing 100 mM phenylacetic acid and 20 % glycerol [4]. The suspension was then gently stirred for 3 h at pH 10 and 25 °C (*see Note 11*).

2. When immobilization was carried at pH 10, full immobilization of PGA was observed within the first moments, using both not modified and aminated PGA. Residual activity was near 100 % in both cases.

At pH 9, it was not possible to immobilize the non modified enzyme. Only the aminated enzyme could be rapidly and fully immobilized on the support. This fact could be explained because the pK value of ϵ -NH₂ of external lysines is 10.7, while the pK value of the artificially introduced primary amino groups is 9.2; therefore, they are even more reactive at pH 9 than the superficial lysines at pH 10.

3. The activity of both immobilized and soluble PGA was measured as follows: the initial reaction rates were measured using an automatic titrator (DL50 Mettler Toledo) to determine the amount of phenylacetic acid formed. The assays were carried out by adding aliquots of PGA to 10 mL of a 10 mM penicillin G in 0.1 M sodium phosphate/0.5 M NaCl at pH 8 and 25 °C. The reaction mixture was titrated with 100 mM NaOH, kept at 25 °C and mechanically stirred.

One International Unit (IU) of PGA activity was defined as the amount of enzyme that hydrolyzes 1 μ mol of Penicillin G per minute at pH 8 and 25 °C.

3.4.3 Structural Stabilization via Multipoint Covalent Attachment

1. The aminated PGA immobilized on glyoxyl agarose at pH 10, presented a half-life around two times higher than the unmodified immobilized PGA (that is 10,000-fold more stable than the one point immobilized PGA) [4] (Fig. 2).

2. The stability of the derivatives immobilized at pH 9 was lower than the ones immobilized at pH 10. However, the stability was greatly improved if after immobilization at pH 9, the pH value was increased at pH 10 to favor the reaction of the lysines of the protein surface with the aldehyde groups on the support. This derivative was found to be around a twofold factor more stable than the aminated PGA directly immobilized at pH 10 (Fig. 3). At pH 10, the enzyme is immobilized by

the region/s with the highest density of lysines plus primary amino groups introduced by the chemical modification, while at pH 9, the immobilization proceeds through the area with the highest density of primary amino groups introduced by chemical modification. This difference permits a higher number of enzyme support linkage and/or to the implication of a region in the immobilization involved in the inactivation of the enzyme.

4 Notes

1. It has been described that the use of 0.1 M EDA at pH 4.75 and 10 mM carbodiimide (EDAC) allows the full modification of the carboxylic groups of the protein surface, while using 1 mM EDAC in 1 M EDTA at pH 4.75 the modification degree is only around 40–50 % [26].
2. Store between 0 and 5 °C (toxic).
3. The choice of the amount of EDAC to be used is done by evaluating its impact on the activity and stability of the enzyme the previously immobilized enzyme. Thus, modification conditions which decrease the stability of the modified enzymes are avoided [24].
4. Avoid magnetic stirring of agarose, especially during long reaction times.
5. Glycidol addition must be very slowly to prevent the temperature rising over 25 °C.
6. Oxidation of glycols with sodium periodate is a stoichiometric reaction. Therefore, the activation degree of the support can be easily controlled through the periodate concentration used. The protocol described allows for obtaining an activation degree of 75 and 200 $\mu\text{mol}/\text{mL}$, and for this, 112.5 and 300 mL of oxidation solution have to be added to completely oxidize agarose 6BCL and 10BCL, respectively.
7. If the enzyme activity decreases during the course of immobilization due to enzyme inactivation, this effect must be distinguished from loss of the supernatant resulting from immobilization.
8. The supernatant was obtained by pipette filter or by centrifugation of the suspension.
9. Rigidification of the protein structure via the formation of multipoint covalent linkages between its nonionic amine groups and the reactive groups of the support could be obtained by keeping the suspension at pH 10 for a fairly long interaction time at 25 °C. The optimum multi-interaction

time is the shortest one that provides the maximal stability of the enzyme derivative.

10. The already immobilized enzymes were incubated under the conditions reported to yield the maximum stability for the non-modified enzyme [4].
11. Commercial preparation of GA (purchased from Roche (Basel, Switzerland) was diluted fivefold (v/v) in 25 mM potassium phosphate buffer pH 7.0 and then dialyzed threefold against 100 volumes of 25 mM potassium phosphate buffer pH 7.0. The dialyzed enzyme was then centrifuged ($6182\times g$ in a rotor JA-25.5) and the supernatant (containing 16 IU/mL and 11 mg of protein/mL) was used as the enzymatic preparation for further experiments. More than 90 % of initial activity was recovered after this process.

References

1. Haki GD, Rakshit SK (2003) Developments in industrially important thermostable enzymes: a review. *Bioresour Technol* 89:17–34
2. Wong SS, Wong LJ (1992) Chemical cross-linking and the stabilization of proteins and enzymes. *Enzyme Microb Technol* 14:866–874
3. Klibanov AM (1983) Immobilized enzymes against thermal inactivation. *Adv Appl Microbiol* 29:1–28
4. Alvaro G, Fernández-Lafuente R, Blanco RM, Guisán JM (1990) Immobilization-stabilization of penicillin acylase from *E. coli*. *Appl Biochem Biotechnol* 26:181–195
5. Guisán JM, Alvaro G, Fernández-Lafuente R, Rosell CM, Garcia-Lopez JL, Tagliatti A (1993) Stabilization of a heterodimeric enzyme by multi-point covalent immobilization: Penicillin G acylase from *Kluyvera citrophila*. *Biotechnol Bioeng* 42:455–464
6. Blanco RM, Guisán JM (1988) Protecting effect of competitive inhibitors during very intense insolubilized enzyme-activated support multipoint attachments: trypsin (amine)-agarose (aldehyde) system. *Enzyme Microb Technol* 10:227–232
7. Guisán JM, Bastida A, Cuesta AC, Fernández-Lafuente R, Rosell CM (1991) Immobilization-stabilization of chymotrypsin by covalent attachment to aldehyde agarose gels. *Biotechnol Bioeng* 39:75–84
8. Tardioli PW, Pedroche J, Giordano RL, Fernández-Lafuente R, Guisán JM (2003) Hydrolysis of proteins by immobilized-stabilized alcalase®-glyoxyl agarose. *Biotechnol Progr* 19:352–360
9. Pedroche J, Yust MM, Girón-Calle J, Vioque J, Alaiz M, Mateo C, Guisán JM, Millán F (2002) Stabilization-immobilization of carboxypeptidase to aldehyde-agarose gels. A practical example in the hydrolysis of casein. *Enzyme Microb Technol* 31:711–718
10. Tardioli PW, Fernández-Lafuente R, Guisán JM, Giordano RLC (2003) Design of new immobilized-stabilized carboxypeptidase a derivative for production of aromatic free hydrolysates of proteins. *Biotechnol Prog* 19:565–574
11. Bes T, Gomez-Moreno C, Guisán JM, Fernández-Lafuente R (1995) Selective enzymatic oxidations: stabilization by multipoint covalent attachment of ferredoxin NAD-reductase: an interesting cofactor recycling enzyme. *J Mol Catal* 98:161–169
12. Guisán JM, Polo E, Agudo J, Romero MD, Alvaro G, Guerra MJ (1997) Immobilization-stabilization of thermolysin onto activated agarose gels. *Biocatal Biotrans* 15:159–173
13. Betancor L, Hidalgo A, Fernández-Lorente G, Mateo C, Rodríguez V, Fuentes M, Fernández-Lafuente R, Guisán JM (2003) The use of physicochemical tools to solve enzyme stability problems alters the choice of the optimal enzyme: stabilization of d-aminoacid oxidase. *Biotechnol Prog* 19:784–788
14. Betancor L, Hidalgo A, Fernández-Lorente G, Mateo C, Rodríguez V, Fuentes M, Fernández-Lafuente R, Guisán JM (2003) Preparation of a stable biocatalyst of bovine liver catalase. *Biotechnol Prog* 19:763–767
15. Hidalgo A, Betancor L, Lopez-Gallego F, Moreno R, Berenguer J, Fernández-Lafuente

- R, Guisán JM (2003) Preparation of a versatile biocatalyst of immobilized and stabilized catalase from *Thermus thermophilus*. *Enzyme Microb Technol* 33:278–285
16. Otero C, Ballesteros A, Guisán JM (1991) Immobilization/stabilization of lipase from *Candida rugosa*. *Appl Biochem Biotechnol* 19:163–175
 17. Palomo JM, Muñoz G, Fernández-Lorente G, Mateo C, Fernández-Lafuente R, Guisán JM (2002) Interfacial adsorption of lipases on very hydrophobic support (octadecyl-Sepabeads): Immobilization, hyperactivation and stabilization of the open form of lipases. *J Mol Catal B Enzymatic* 19–20:279–286
 18. Suh C-W, Choi G-S, Lee E-K (2003) Enzymatic cleavage of fusion protein using immobilized urokinase covalently conjugated to glyoxyl-agarose. *Biotechnol Appl Biochem* 37:149–155
 19. Toogood HS, Taylor IN, Brown RC, Taylor SJC, McCague R, Littlechild JA (2002) Immobilisation of the thermostable L-aminoacylase from *Thermus litotalis* to generate a reusable industrial biocatalyst. *Biocatal Biotrans* 20:241–249
 20. Ichikawa S, Takano K, Kuroiwa T, Hiruta O, Sato S, Mukataka S (2002) Immobilization and stabilization of chitosanase by multipoint attachment to agar gel support. *J Biosci Bioeng* 93:201–206
 21. Kuroiwa T, Ichikawa S, Sato S, Mukataka S (2003) Improvement of the yield of physiologically active oligosaccharides in continuous hydrolysis of chitosan using immobilized chitosanases. *Biotechnol Bioeng* 84:121–127
 22. Kuroiwa T, Ichikawa S, Sosaku H, Sato S, Mukataka S (2002) Factors affecting the composition of oligosaccharides produced in chitosan hydrolysis using immobilized chitosanases. *Biotechnol Prog* 18:969–974
 23. Mateo C, Abian O, Fernandez-Lafuente R, Guisán JM (2000) Increase in conformational stability of enzymes immobilized on epoxy-activated supports by favouring additional multipoint covalent attachment. *Enzyme Microb Technol* 26:509–515
 24. Mateo C, Abian O, Bernedo M, Cuenca E, Fuentes M, Fernandez-Lorente G, Palomo JM, Grazu V, Pessela BCC, Giacomini C, Irazoqui G, Villarino A, Ovsejevi K, Batista-Viera F, Fernandez-Lafuente R, Guisán JM (2005) Some special features of glyoxyl supports to immobilize proteins. *Enzyme Microb Technol* 34(7):456–462
 25. Abian O, Grazu V, Hermoso J, González R, García JL, Fernández-Lafuente R, Guisán JM (2004) Stabilization of penicillin G acylase from *Escherichia coli*: site-directed mutagenesis of the protein surface to increase multipoint covalent attachment. *Appl Environ Microbiol* 70:1249–1251
 26. López-Gallego F, Montes T, Fuentes M, Alonso N, Grazu V, Betancor L, Guisán JM (2005) Chemical increase of the amount of reactive groups on enzyme surface to improve its stabilization via multipoint covalent attachment. *J Biotechnol* 116(1):1–10
 27. Guisán JM (1988) Agarose-aldehyde gels as supports for immobilization-stabilization of enzymes. *Enzyme Microb Technol* 10(6):375–382

Oriented Covalent Immobilization of Enzymes on Heterofunctional-Glyoxyl Supports

Cesar Mateo, Gloria Fernandez-Lorente, Javier Rocha-Martin, Juan M. Bolivar, and Jose M. Guisan

Abstract

Novel heterofunctional glyoxyl-agarose supports were prepared. These supports contained the maximal concentration of glyoxyl groups to promote maximization of covalent immobilization and groups' capability to adsorb proteins by various mechanisms (e.g., ionic exchange, metal-chelate formation). Immobilization on various supports makes it possible to orientate and rigidify an enzyme in various regions of its surface. The use of different heterofunctional supports allowed for obtaining catalysts with different activity, stability, and selectivity properties.

Key words Heterofunctional glyoxyl-agarose, Glyoxyl groups, Covalent immobilization, Enzyme

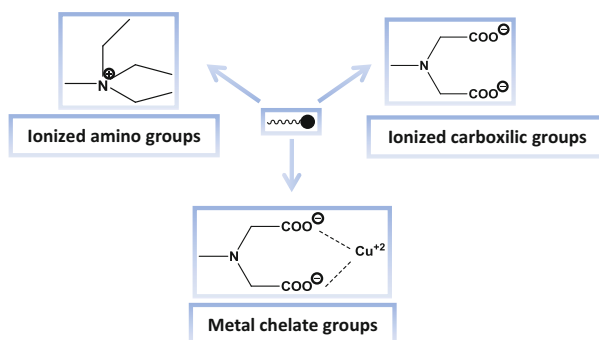
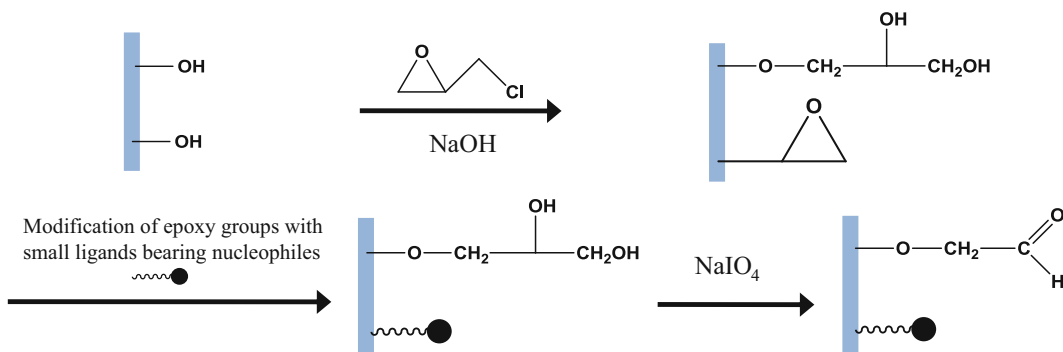
1 Introduction

The development of new immobilization methods that make it possible to obtain biocatalysts with different properties starting from one enzyme is a major aim in the industrial application of biocatalytic processes [1–6]. In many cases, immobilization allows the improvement of enzyme properties (activity, stability, and selectivity). Of these properties, the most critical is stability because in general wild enzymes can be quite unstable when they are incubated in distorting conditions such as high temperature, extreme pH, or in the presence of organic cosolvents [3, 4, 6–10]. Various methods exist for the immobilization of different enzymes, but not all of them are able to stabilize all enzymes; in fact, most of them are capable of destabilizing or inactivating some enzymes in many cases. For this reason, the development of tools that allow the immobilization of enzymes using different methodologies is of great interest. In discussions of the problem of stabilization of enzymes using immobilization methods it is accepted that when an

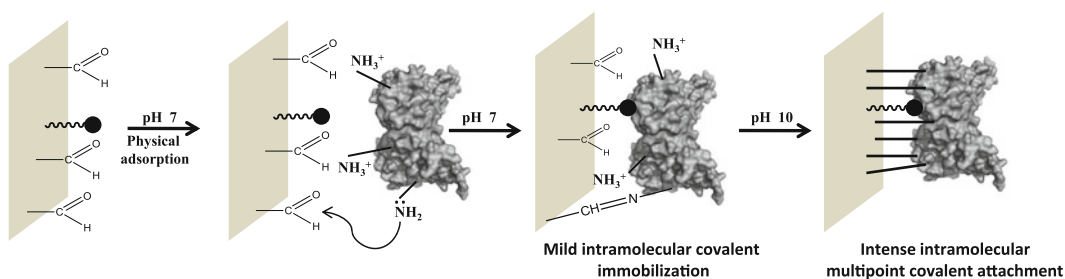
enzyme is immobilized through short spacer arms involving numerous enzyme moieties, these amino acids maintain unaltered relative positions during various distortion processes induced by various inactivating conditions [8, 11–13].

Supports activated with glyoxyl groups fulfill these requirements because they are highly reactive with primary amino groups (which are very abundant on the surface of different enzymes) and are highly activated with groups having very short spacer arms. Immobilization on these supports takes place through a multipoint mechanism; thus, immobilization occurs only if simultaneous interaction among several aldehyde groups and several primary amino groups of the enzyme surface is promoted [14–16]. Because of this, in general, enzymes are not immobilized at neutral pH because in these conditions only the most reactive amine, in general the terminal amine, is deprotonated and consequently reactive. In fact, only processes of immobilization at neutral pH have been described where the enzymes have several terminal amines in the same plane of the enzyme that can react simultaneously with different aldehyde groups at neutral pH [12]. For this reason, the immobilization of enzymes on such a support is performed at an alkaline pH, where the lysines are mainly deprotonated and, therefore, reactive. As a result, the immobilization of enzymes on these supports is performed in the region of their surface that is richest in lysine moieties. The use of these supports has allowed the immobilization and stabilization of different highly interesting enzymes with different immobilization yields as well as different stabilization factors compared with soluble enzymes. However, such enzymes are not stable at an alkaline pH and cannot be immobilized on these supports. In addition, it would be desirable to develop new methodologies that allowed for the immobilization of enzymes in other regions of their surface, allowing the rigidification of other locations that are more sensitive to inactivation such as unstable loops. This would make it possible to obtain highly stable catalysts. Therefore, the rigidification of various key regions could bring about an improvement in the selectivity or in the activity of a catalyst, for example, in the case of nonnatural substrates where often selectivity is not very high.

In this chapter, the immobilization of various enzymes on heterofunctional glyoxyl supports is proposed. These new supports have a high concentration of groups capable of promoting the physical adsorption of an enzyme at a neutral pH and the highest concentration of glyoxyl groups capable of covalently reacting with the primary amines of the enzyme (Scheme 1). The immobilization of enzymes on these supports is proposed using a two-step protocol. In the first step, the enzymes are physically adsorbed to the support in those regions of their surface that are complementary to



Scheme 1 Preparation of various heterofunctional glyoxyl supports



Scheme 2 Mechanism of immobilization-stabilization using heterofunctional glyoxyl supports

the groups of the support capable of adsorbing. In the second step, the previously adsorbed enzymes are incubated in alkaline conditions so that the lysines are reactive, with the result that the covalent interactions are as intense as possible (Scheme 2).

2 Materials

1. Chymotrypsin type II from bovine pancreas was purchased from Sigma Chemicals (St. Louis, MO).
2. *Geobacillus thermocatenulatus* lipase 2 was expressed in *E. coli*, as previously described [17].
3. The tannase strain *Lactobacillus plantarum* CECT 748T (ATCC 14917, DSMZ 20174), isolated from pickled cabbage, was purchased from the Spanish Type Culture Collection. This strain was selected on the basis of its high activity [18–21].
4. Agarose 10 BCL was purchased from Agarose Bead Technologies (Madrid, Spain).
5. Epichlorohydrin, iminodiacetic acid, *p*-aminophenylboronic acid, triethylamine, mercaptoethanol, and sodium metaperiodate were purchased from Sigma Chemicals.
6. Other reagents were of analytical grade.

3 Methods

3.1 Activation of Agarose with Epoxy Groups

1. 3.28 g NaOH was solved in 44 mL of water. The mixture was cold in ice.
2. When the solution was cold, 0.2 g NaBH₄ was added to it.
3. To this solution was added 16 mL acetone. The mixture was left in ice.
4. The solution from step 3 was added to 10 g agarose 10 BCL.
5. Finally, 11 mL epichlorohydrin was added.
6. The suspension was stirred gently for 16 h and finally washed with an excess of water.

3.2 Quantification of Activated Epoxy Groups

1. 1 g of the support was treated with 10 mL of 0.5 M H₂SO₄ for 2 h to hydrolyze the epoxy groups.
2. Then this hydrolyzed support was oxidized with NaIO₄ [14]. The number of epoxy groups was calculated by the difference in periodate consumption between the hydrolyzed support and the initial epoxy support. Periodate consumption was quantified using potassium iodide, as previously described [22]. For this, 1 mL of 10% aqueous solution potassium iodite was mixed with 1 mL of a solution of saturated NaHCO₃. To this solution was added 100 µL of the sample to be measured and recorded at 450 nm.

Table 1
Heterofunctional glyoxyl supports

Agarose	Adsorbent groups ($\mu\text{mol/mL}$)	Glyoxyl groups ($\mu\text{mol/mL}$)
10 BCL	70 ± 3	105 ± 5
6 BCL	30 ± 1.5	45 ± 2
4 BCL	16 ± 1	24 ± 1.5

3.3 Modification of Agarose Supports with Different Reactive Groups

1. Cationic supports: 1 g epoxy-agarose support was modified with 10 mL of a solution composed of 1 M triethylamine in 50 % water/acetone at pH 12 for 24 h at 25 °C.
2. Anionic supports: 1 g epoxy-agarose support was treated with 10 mL of 0.5 M iminodiacetic acid at pH 11 for 24 h at 25 °C .
3. Metal chelate supports: the anionic supports obtained in step 2 were modified with a 30 mg/mL solution of one of four different metallic salts (CuSO_4 , NiCl_2 , ZnCl_2 , and CoCl_2) at pH 7.0 for 1 h at 25 °C.
4. Boronate supports: 1 g epoxy-agarose support was modified with 10 mL of 5 % *p*-aminophenylboronic acid, dissolved in 20 % dioxane at pH 11 for 24 h at 25 °C.
5. Monofunctional supports: the epoxy-agarose supports were blocked with 5 % mercaptoethanol at pH 8.7 and 25 °C for 16 h.

Finally, the supports were oxidized with the appropriate amount (Table 1) of sodium periodate, as previously described [14], and washed with water.

3.4 Enzyme Assays

3.4.1 Chymotrypsine Assay

A chymotrypsine assay was conducted by recording the increase in absorbance at 405 nm and 25 °C promoted by the release of *p*-nitrophenol produced by the hydrolysis of *N*-benzoyl-L-tyrosine *p*-nitroanilide (BTNA) during the enzyme-catalyzed reaction.

1. Dissolve the appropriate amount of BTNA in 50 mM phosphate in the presence of 40 % ethanol at pH 7 until a final concentration of 0.3 mM is reached.
2. Mix 2 mL of substrate in a cell and add the appropriate amount of enzyme solution.
3. Record the increase in absorbance at 405 nm under stirring and thermostatisation. Spontaneous chemical hydrolysis of the substrate was <1 % related to total enzymatic hydrolysis.
4. One international unit (IU) of BTNA activity was defined as the amount of enzyme necessary to hydrolyze 1 μmol of BTNA per minute under the conditions described previously.

3.4.2 BTL2 Assay

BTL2 activity was quantified by measuring in a UV spectrum the hydrolysis of *p*-nitrophenyl butyrate (*p*NPB) (spontaneous chemical hydrolysis of the substrate was lower than 2 % related to the total enzymatic activity). The reaction was performed in 25 mM sodium phosphate at pH 7, 25 °C, and 348 nm under continuous magnetic stirring and was measured using a thermostated spectrometer.

1. A 50 mM stock solution in acetonitrile of the substrate (*p*NPB) was prepared.
2. 2.5 mL phosphate buffer and 20 μ L of substrate stock solution were added to a spectrophotometric cell, and the mixture was preincubated at 25 °C for 10 min.
3. One IU of *p*NPB activity was defined as the amount of enzyme necessary to hydrolyze 1 μ mol of *p*NPB per minute, under the conditions described previously.

3.4.3 Tannase Assay [23]

1. Aliquots of 100 μ L of soluble, suspension, or supernatant of tannase were incubated with 100 μ L of 25 mM methyl gallate in phosphate buffer (50 mM, pH 6.5) for 10 min at 37 °C.
2. After this incubation, 150 μ L of a methanolic rhodanine solution (0.667 % w/v rhodanine in 100 % methanol) was added to the mixture.
3. After 5 min of incubation at 30 °C, 100 μ L of 500 mM KOH was added and the mixture was diluted to 900 μ L with distilled water.
4. Following an additional incubation of 5–10 min, the absorbance at 520 nm was measured on a spectrophotometer. A standard curve using gallic acid concentrations ranging from 0.125 to 1 mM was prepared.
5. One unit of tannase activity was defined as the amount of enzyme required to release 1 μ mol of gallic acid per minute under standard reaction conditions.

3.5 Immobilization of Enzymes on Heterofunctional Supports

3.5.1 Immobilization of Chymotrypsin

1. 1.5 mg chymotrypsin was solubilized in 1 mL of sodium phosphate buffer (5 mM phosphate for use with ionic supports or 50 mM phosphate for use with boronate and metal-chelate supports) at pH 7 and 25 °C.
2. 1 g of support (ionic, boronate, or metal chelate) was added to 10 mL of the solution, with a maximum enzyme activity of 1 IU/mL.
3. Periodically, samples of the supernatants and suspensions must be withdrawn and the enzyme activity measured.
4. The immobilization is considered complete when there is no activity in the supernatant.

5. Wash the preparations with the phosphate buffer, dry under vacuum, and resuspend in 10 mL of sodium hydrogen carbonate (5 mM for ionic supports and 50 mM for the other supports) at pH 10 for 3 h.
6. Finally, the preparations must be reduced by the addition of 10 mg sodium borohydride. The metal-chelate supports were washed with five volumes of 50 mM EDTA at pH 7 before the reduction step. These suspensions were stirred gently for 30 min and then washed with water.
7. The yield of immobilization was considered to be the rate between the activities in the supernatant compared with the activity in the blank of soluble enzyme. (In all cases, the activity of the blank was 100 % during the immobilization process.) Activity recovery was calculated as the rate of the activity in the final suspension after the immobilization process and the initial activity of the offered enzyme.

3.5.2 Immobilization of BTL2 Lipase

Previous Purification of BTL2 Lipase

1. Dissolve 6 mg solid protein in 10 mL of 5 mM sodium phosphate solution at pH 7.0, and add 1 g of octyl-sepharose support.
2. Periodically, take samples of supernatant and suspension for assays of enzyme activity. A supernatant can be obtained using a tip filter.
3. Stir this suspension very gently for 2 h at 25 °C.
4. Evaluate the adsorption of the enzyme using the described activity assay. The immobilization process is finished when the activity of the supernatant is zero.
5. Wash and filter the suspension with distilled water.

Desorption of Purified Lipase on Support

1. Resuspend 1 g of the dried octyl-BTL2 derivative in 10 mL sodium phosphate buffer with 0.3 % triton X-100 at pH 7.0.
2. Stir this suspension for 30 min at 25 °C.
3. Check the activity or the protein concentration of the supernatant.
4. Consider that the released of pure lipase was produced when there was no activity in the suspension.

Immobilization of BTL2 Lipase on Heterofunctional Glyoxyl Supports

1. Mix 1 IU/mL purified BTL2 (Sect. 3.5.2) with 10 mL sodium phosphate solution (5 mM for use with ionic supports or 50 mM for use with boronate and metal-chelate supports) at pH 7 and 25 °C.
2. Assay the BTL2 activity of this solution. Add 1 g support (ionic, boronate, or metal-chelate) to 10 mL of the previous BTL2 and assay the activity of the suspension and supernatant after 15 min, then repeat the enzyme assays.

3. Stir this suspension very gently for 2 h at 25 °C.
4. Evaluate the adsorption immobilization.
5. The immobilization process is finished when the activity of the supernatant is zero.
6. Increase and adjust the enzyme suspension at pH 10.0; gently stir the enzyme-support reaction for 24 h at 25 °C.
7. The preparation must be reduced as described (Sect. 3.5.1).
8. Filter the suspension and wash with distilled water. Finally, filter to eliminate all interparticle water.

3.5.3 Immobilization
of Tannase from
Lactobacillus plantarum

Previous Purification
of Tannase from
Lactobacillus plantarum

1. Dilute the protein solution of tannase tenfold in 50 mM sodium phosphate buffer, 150 mM NaCl at pH 7, and 20 mM imidazole at pH 7 and a temperature of 25 °C.
2. Assay the tannase activity of this solution. Add 1 g Ni-IDA-agarose supports. Periodically, samples of supernatant and suspension were taken for assay of enzyme activity. Supernatant was achieved by using a tip filter.
3. Stir this suspension very gently for 2 h at 25 °C.
4. Evaluate the adsorption immobilization using the previously described tannase activity assay. The immobilization process is finished when the activity of the supernatant is zero.
5. Wash and filter the suspension with distilled water.

Desorption of Purified
Tannase on Support

1. Suspend 1 g of Ni-IDA-agarose supports with adsorbed proteins in 10 mL of 5 mM sodium phosphate at pH 7.0 in the presence of 100 mM of imidazole.
2. Stir this suspension for 30 min at 25 °C.
3. The percentage of desorbed enzymes was followed via the enzyme activity of the supernatant compared to the activity of the suspension (which in all cases remained constant throughout the experiment).

Immobilization of Tannase
on Heterofunctional Glyoxyl
Supports

1. Mix 1 IU/mL purified tannase (Sect. 3.2) with 10 mL sodium phosphate solution (5 mM for use with ionic supports or 50 mM for use with boronate and metal-chelate supports) at pH 7 and 25 °C.
2. Assay the enzyme activity of this solution. Add 1 g support (ionic, boronate, or metal-chelate) to 10 mL of the previous tannase dissolution and assay the activity of the suspension and supernatant after 15 min, then repeat the enzyme assays.
3. Stir this suspension very gently for 2 h at 25 °C.
4. Evaluate the adsorption immobilization.
5. The immobilization process is finished when the activity of the supernatant is zero.

6. Increase and adjust the enzyme suspension at pH 10.0, and gently stir the enzyme-support reaction for 24 h at 25 °C.
7. The preparation must be reduced as described (Sect. 3.5.1).
8. When the immobilization is finished, filter the suspension and wash with distilled water. Finally, filter to eliminate all interparticle water.

3.6 Enantioselectivity

The enantioselectivity of the various BTL2 preparations was measured using 2-O-butyryl-2-phenylacetic acid as the substrate [24].

1. 0.5 g wet immobilized preparations was added to 3 mL of 1 mM substrate in 25 mM sodium phosphate at pH 7 and 25 °C. The suspension was stirred gently.
2. During the reaction, the pH value was maintained at a constant level by automatic titration using pH-stat.
3. Blank experiments were performed using suspensions of the different matrices without enzymes.
4. The degree of hydrolysis was followed by reverse-phase high-performance liquid chromatography (HPLC) (Spectra Physics SP 100, coupled with a UV detector Spectra Physics SP 8450) on a Kromasil C18 (25 cm × 0.4 cm) column, supplied by Analisis Vinicos (Tomelloso, Spain). Each assay was performed at least in triplicate. The experimental error was <3 %. The elution was performed using a mobile phase composed of acetonitrile (35 %) and 10 mM ammonium phosphate buffer (65 %) at pH 2.95 at a flow rate of 1.5 mL/min and was monitored by recording the absorbance at 225 nm. The retention time of the butyric acid was 3.7 min, and the retention time of the 2-O-butyryl-2-phenylacetic acid was 23 min.
5. At different conversion degrees, the enantiomeric excess (ee_p) of the released acid was analyzed by chiral reverse-phase HPLC. The column was a Chiralcel OD-R, the mobile phase was an isocratic mixture of 5 % acetonitrile and 95 % 0.5 M NaClO₄/HClO₄ at pH 2.3, and the analyses were performed at a flow rate of 0.5 mL/min by recording the absorbance at 225 nm. The retention time of the *S* enantiomer was 39 min, and the retention time of the *R* enantiomer was 42 min. The asymmetry was measured as the ratio of the extent of hydrolysis of the *R* enantiomer compared with that of the *S* enantiomer.

4 Results

4.1 Activation of Mono- and Heterofunctional Glyoxyl Supports

In the first step, the supports were activated with a bifunctional reactive epichlorohydrin to obtain epoxy groups. The reaction was produced in a quite alkaline medium such that most of the primary hydroxyl groups of the support were deprotonated and then were

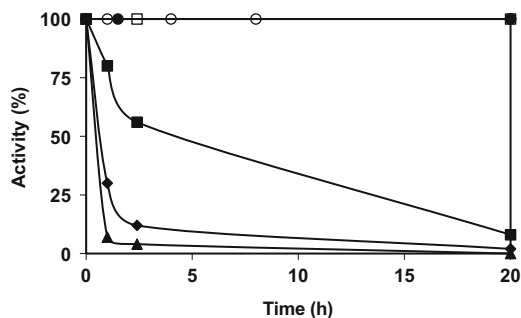


Fig. 1 Immobilization of BTL2 on heterofunctional glyoxyl supports: (*filled diamond*) glyoxyl-Cu agarose; (*filled square*) boronate-glyoxyl agarose; (*filled triangle*) amino-glyoxyl agarose; (*circle*) carboxy-glyoxyl agarose; (*filled circle*) monofunctional glyoxyl agarose; (*square*) amino-glyoxyl agarose in the presence of 1 M NaCl

able to react with the epichlorohydrin molecules. Because this reaction occurred in an alkaline environment caused some of the epoxide groups to be hydrolyzed, yielding glyceryl groups. The obtained percentage of epoxide groups compared with the total number of primary hydroxyl groups activated was around 40 % (Table 1) [25]. These epoxy groups can be easily functionalized with different bifunctional molecules capable of adsorbing proteins via various mechanisms [26, 27]. On the other hand, around 60 % of the initially activated epoxy groups that were hydrolyzed to glyceryl groups are easily oxidized with sodium periodate to glyoxyl groups that are able to establish a high density of covalent linkages with the enzyme promoting its stabilization.

4.2 Immobilization of Proteins on Various Glyoxyl Supports

The mechanism of immobilization on these supports was studied using the enzyme BTL2 as a model. To this end, the enzyme was immobilized on traditional monofunctional glyoxyl supports. These supports were only able to immobilize proteins if several linkages between some glyoxyl groups and some amine groups of the protein could be established simultaneously [14]. When the enzyme was incubated with the support at neutral pH, this monomeric enzyme was not immobilized (Fig. 1). This is because at such a pH the lysines of the enzyme are unprotonated and, consequently, not reactive. The only reactive amine group in these conditions is the terminal amine, and it cannot be simultaneously immobilized at several points. By contrast, when used glyoxyl heterofunctional supports, the enzyme could be immobilized on different supports at neutral pH. The only exception was the support activated with cationic exchange groups. This is normal that the enzyme is not adsorbed at neutral pH considering that most

of the enzymes have an isoelectric point between 4 and 5, so that at neutral pH it was negatively charged, hindering its adsorption on these groups. In fact, this enzyme could not be adsorbed on commercial supports activated with cationic exchange groups (CM-Sepharose), demonstrating that the mechanism of the immobilization strongly depends on the first step of physical adsorption. This was confirmed when the immobilization was performed on cationic-glyoxyl heterofunctional supports using high ionic strength (1 M NaCl). Under these conditions the enzyme was not immobilized. The enzyme could not be adsorbed on commercial supports activated with cationic groups (DEAE- or Q-Sepharose). Similarly, it was not possible to immobilize the enzyme on supports activated with metal chelating groups in the presence of imidazol, which is a competitor for the formation of coordination linkages with amino acids like histidine or on supports with boronate groups in the presence of mannitol. All these experiments clearly show that no immobilization can occur if the first step of adsorption is not performed. In fact, the amount of enzyme covalently immobilized with the incubation time was also studied. To this end, aliquots of suspension were taken at different times and incubated in high concentrations of NaCl (1 M). Under these conditions all the noncovalently linked protein was desorbed from the support. By increasing the protein-support incubation time it was observed as the amount of desorbed enzyme decreased. This means that the enzyme was progressively covalently immobilized. Intramolecular covalent linking occurs even at neutral pH. The first covalent bond process is very important, taking into account that in many cases the incubation conditions at an alkaline pH may disadvantage the adsorption of the enzymes on the heterofunctional groups of the support. As a final step in the immobilization process, incubation at an alkaline pH was performed to increase the reactivity of the lysines. This makes the multipoint covalent linkage processes as intense as possible.

4.3 Activity of Various Enzyme Derivatives Immobilized on Mono- and Heterofunctional Glyoxyl Supports

The activities obtained after immobilization of enzymes on different heterofunctional supports differed depending on the support used for the process. For example, the activity recovered for BTL2 when it was immobilized on monofunctional glyoxyl supports was around 60 % compared with the initial activity of the soluble enzyme. Of the initial activity, 90 % was recovered when the lipase was immobilized on amino-glyoxyl supports, and lower activity, around 20 %, was recovered after immobilization on chelate-glyoxyl supports (Table 2). These differences in the recovered activity suggest that immobilization takes place through different reaction mechanisms involving different regions of the protein surface. These regions are selected in the first physical adsorption process.

Table 2
Immobilization of BTL2 on various glyoxyl supports

Support	Immobilized BTL (%)	Activity (%)	Activity after incubation at pH 10 (%)
Cu-CHO	94	21	11
Amino-CHO	100	90	90
Monofunctional CHO	100	60	60
Boronate-CHO	95	71	67

4.4 Stability of Derivatives Immobilized on Mono- and Heterofunctional Glyoxyl Supports

The stability of the derivatives of several enzymes immobilized on different glyoxyl supports was studied. Thus, different derivatives of BTL2 were incubated at 70 °C. In the first preparation, the enzyme was adsorbed on amino-glyoxyl supports, in which glyoxyl groups were previously reduced. This derivative is only able to immobilize enzymes via ionic adsorption through the amine groups. In the second preparation, the enzyme was immobilized on bifunctional amino-glyoxyl supports at neutral pH for 12 h, and in the third preparation lipase was immobilized at neutral pH and incubated at pH 10 and 25 °C for 3 h. The most stable derivative was immobilized at neutral pH and incubated at pH 10. This may be related with the increase of the reactivity of lysine moieties by incubation at alkaline pH, allowing the formation of a higher multipoint covalent immobilization degree. The derivative immobilized at pH 8 and not incubated at alkaline pH was also more stable than a soluble enzyme, suggesting that even at this pH a certain covalent binding protein support is promoted (Fig. 2). This again confirms the validity of the proposed immobilization mechanism.

Additionally, the stability of derivatives of other enzymes immobilized on different glyoxyl supports at high temperatures or in the presence of organic cosolvents was studied. In all cases, each derivative had a different stability in the various inactivating conditions. Tannase was also immobilized on various glyoxyl supports and incubated at 55 °C. The most stable derivative was one that was immobilized on an amino-glyoxyl support (Fig. 3). Similarly, after incubation of the different derivatives of chymotrypsin at 70 °C, the most stable derivative was one immobilized on a boronate-glyoxyl support (Fig. 4). These results are curious taking into account that monofunctional glyoxyl supports direct immobilization by the richest place in lysines versus heterofunctional supports, which direct immobilization through other regions. This

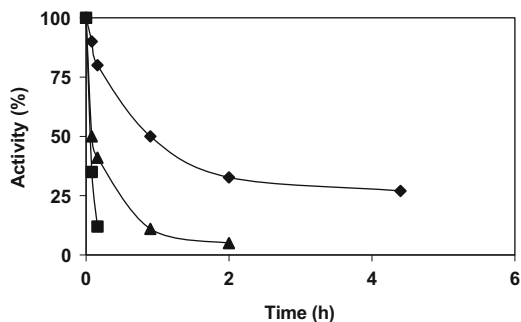


Fig. 2 Time courses of thermal inactivation of various immobilized BTL2 derivatives. Immobilized derivatives were incubated in 25 mM phosphate buffer at pH 7 and 70°C. At different times, aliquots were withdrawn from the suspension and assayed under standard conditions. (*Filled square*) BTL2 immobilized on amine supports without glyoxyl groups; (*filled triangle*) BTL2 immobilized on amino-glyoxyl at pH 8 and 12 h; (*filled diamond*) BTL2 immobilized on amino-glyoxyl supports at pH 8 and incubated at pH 10 for 3 h

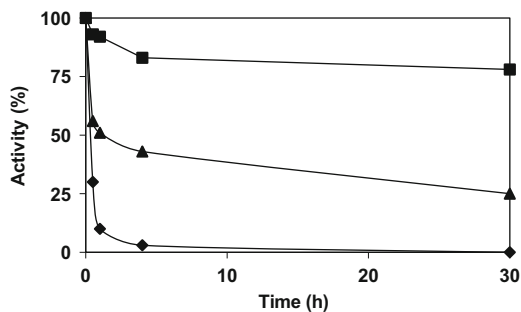


Fig. 3 Time course of inactivation of various immobilized tannase derivatives. Preparations were incubated in 25 mM phosphate at pH 7 and 55°C. (*Filled diamond*) CNBr derivatives; (*filled triangle*) monofunctional glyoxyl derivatives; (*filled square*) amino-glyoxyl derivatives

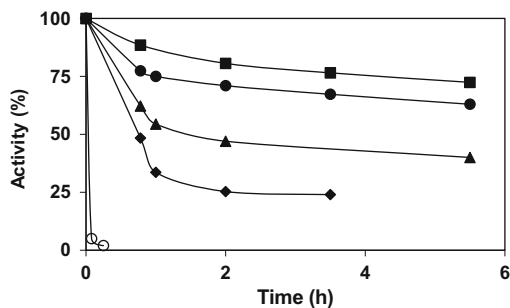


Fig. 4 Time course of thermal inactivation of various immobilized chymotrypsin derivatives. Preparations were incubated in 25 mM phosphate buffer at pH 7 and 70°C. (*Filled diamond*) glyoxyl-Cu agarose; (*filled square*) boronate-glyoxyl agarose; (*filled triangle*) amino-glyoxyl agarose; (*filled circle*) monofunctional-glyoxyl agarose; (*circle*) soluble enzyme

Table 3
Study of enantioselectivity of various BTL2 preparations

Immobilized preparation	Activity (IU/min)	Asymmetry
Amino-glyoxyl BTL2	0.0017	8
Monofunctional glyoxyl BTL2	0.00075	2

Activity is expressed as 1,000 μmol of ester hydrolyzed per minute and per milligram of immobilized lipase. Selectivity is expressed as ratio *R/S* isomers of released mandelic acid

promotes in general the highest rigidification of the structure. In these cases, the rigidification must be performed through other regions that are more sensitive to inactivation (e.g., regions containing unstable loops).

4.5 Enantioselectivity of the Different Enzyme Preparations

Different derivatives of BTL2 were used to study the selectivity of the process of resolution of 2-O-butyryl-2-phenylacetic acid. The enzyme immobilized on an amino-glyoxyl support had the best enantioselectivity, which was more than three times higher than that obtained using an enzyme immobilized on a monofunctional glyoxyl support (Table 3). This fact demonstrates again that different enzyme derivatives have different activities, stabilities, and selectivities.

5 Conclusions

A new generation of substrates was developed with various groups capable of adsorbing proteins via different mechanisms of physical adsorption and glyoxyl groups capable of covalently reacting with primary amine groups on the surface of various proteins. These supports were able to immobilize proteins according to a mechanism in two steps. In the first step, the physical adsorption of an enzyme through different regions of its surface was promoted (Table 4). In the second step, the previously adsorbed enzyme was incubated at an alkaline pH to increase the activity of lysines, resulting in a covalent immobilization process that was as intense as possible. The use of these supports allowed for the rigidification of various regions of the surface of different enzymes, which made it possible to obtain different catalysts with different activity, stability, and selectivity properties.

Table 4
Various orientations of enzymes immobilized on different glyoxyl supports

Support	Immobilization pH	Probable orientation of enzyme
Monofunctional glyoxyl	10.0	Richest region on lysine
Monofunctional glyoxyl + thiols	7.0–8.0	Region with most reactive amine group
Amine glyoxyl	7.0	Region with richest net negative charge
Chelate glyoxyl	7.0	Region richest in histidine
Carboxylic glyoxyl	7.0	Region with richest net positive charge
Boronate glyoxyl	7.0	Region with highest affinity for boronate

References

- Klibanov AM (1983) Immobilized enzymes and cells as practical catalysts. *Science* 219:722–727
- Katchalski-Katzir E, Kraemer D (2000) Eupergit C, a carrier for immobilization of enzymes of industrial potential. *J Mol Catal B Enzym* 10:157–176
- Hartmeier W (1985) Immobilized biocatalysts—from simple to complex systems. *Trends Biotechnol* 3:149–153
- Chibata I, Tosa T, Sato T (1986) Biocatalysis: immobilized cells and enzymes. *J Mol Catal B: Enzym* 37:1–24
- Cao L, van Langen L, Sheldon RA (2003) Immobilised enzymes: carrier-bound or carrier-free? *Curr Opin Biotechnol* 14:387–394
- Katchalski-Katzir E (1993) Immobilized enzymes—learning from past successes and failures. *Trends Biotechnol* 11:471–478
- Khare SK, Vaidya S, Gupta MN (1991) Entrapment of proteins by aggregation within sephadex beads. *Appl Biochem Biotechnol* 27:205–216
- Klibanov AM (1983) Stabilization of enzymes against thermal inactivation. *Adv Appl Microbiol* 29:1–28
- Mateo C, Palomo JM, Fernandez-Lorente G, Guisan JM, Fernandez-Lafuente R (2007) Improvement of enzyme activity, stability and selectivity via immobilization techniques. *Enzyme Microb Technol* 40:1451–1463
- Cao L (2005) Immobilised enzymes: science or art? *Curr Opin Chem Biol* 9:217–226
- Pedroche J, Yust MM, Mateo C, Fernandez-Lafuente R, Giron-Calle J, Alaiz M, Vioque J, Guisan JM, Millan F (2007) Effect of the support and experimental conditions in the intensity of the multipoint covalent attachment of proteins on glyoxyl-agarose supports: correlation between enzyme-support linkages and thermal stability. *Enzyme Microb Technol* 40:1160–1166
- Bolivar JM, Rocha-Martin J, Mateo C, Cava F, Berenguer J, Vega D, Fernandez-Lafuente R, Guisan JM (2009) Purification and stabilization of a glutamate dehydrogenase from *Thermus thermophilus* via oriented multisubunit plus multipoint covalent immobilization. *J Mol Catal B: Enzym* 58:158–163
- Rosevear A (1984) Immobilised biocatalysts—a critical review. *J Chem Technol Biotechnol* 34B:127–150
- Guisan JM (1988) Aldehyde-agarose gels as activated supports for immobilization-stabilization of enzymes. *Enzyme Microb Technol* 10:375–382
- Mateo C, Abian O, Bernedo M, Cuenca E, Fuentes M, Fernandez-Lorente G, Palomo JM, Grazu V, Pessela BCC, Giacomini C, Irazoqui G, Villarino A, Ovsejevi K, Batista-Viera F, Fernandez-Lafuente R, Guisan JM (2005) Some special features of glyoxyl supports to immobilize proteins. *Enzyme Microb Technol* 37:456–462
- Blanco RM, Calvete JJ, Guisan JM (1989) Immobilization-stabilization of enzymes;

- variables that control the intensity of the trypsin (amine)-agarose (aldehyde) multipoint attachment. *Enzyme Microb Technol* 11:353–359
17. Palomo JM, Fernandez-Lorente G, Rúa ML, Guisan JM, Fernandez-Lafuente R (2003) Evaluation of the lipase from *Bacillus thermocatenulatus* as an enantioselective biocatalyst. *Tetrahedron Asymmetry* 14:3679–3687
 18. Nishitani Y, Osawa R (2003) A novel colorimetric method to quantify tannase activity of viable bacteria. *J Microbiol Methods* 54:281–284
 19. Nishitani Y, Sasaki E, Fujisawa T, Osawa R (2004) Genotypic analyses of lactobacilli with a range of tannase activities Isolated from human feces and fermented foods. *Syst Appl Microbiol* 27:109–117
 20. Vaquero I, Marcobal A, Muñoz R (2004) Tannase activity by lactic acid bacteria isolated from grape must and wine. *Int J Food Microbiol* 96:199–204
 21. Rodriguez H, de las Rivas B, Gomez-Cordoves C, Muñoz R (2008) Characterization of tannase activity in cell-free extracts of *Lactobacillus plantarum* CECT 748T. *Int J Food Microbiol* 121:92–98
 22. Nevell TP (1963) In: Whistler B (ed) *Methods in carbohydrate chemistry*, vol 3, NaIO₄ oxidation of cellulose. Academic, New York, p 164–168
 23. Inoue KH, Hagerman AE (1988) Determination of gallotannin with rhodanine. *Anal Biochem* 169:363–369
 24. Palomo JM, Muñoz G, Fernandez-Lorente G, Mateo C, Fuentes M, Guisan JM, Fernandez-Lafuente R (2003) Modulation of *Mucor miehei* lipase properties via directed immobilization on different hetero-functional epoxy resins: Hydrolytic resolution of (R, S)-2-butyroyl-2-phenylacetic acid. *J Mol Catal B: Enzym* 21:201–210
 25. Mateo C, Bolivar JM, Godoy CA, Rocha-Martin J, Pessela BCC, Curiel JA, Muñoz R, Guisan JM, Fernandez-Lorente G (2010) Improvement of enzyme properties with a two-step immobilization process on novel hetero-functional supports. *Biomacromolecules* 11:3112–3117
 26. Mateo C, Fernandez-Lorente G, Abian O, Fernandez-Lafuente R, Guisan JM (2000) Multifunctional epoxy supports: A new tool to improve the covalent immobilization of proteins. The promotion of physical adsorptions of proteins on the supports before their covalent linkage. *Biomacromolecules* 1:739–745
 27. Wheatley JB, Schmidt DE (1993) Salt-induced immobilization of proteins on a high-performance liquid chromatographic epoxide affinity support. *J Chromatogr* 644:11–16

Reversible Covalent Immobilization of Enzymes via Disulfide Bonds

Karen Ovsejevi, Carmen Manta, and Francisco Batista-Viera

Abstract

This enzyme immobilization approach involves the formation of disulfide ($-S-S-$) bonds with the support. Thus, enzymes bearing exposed nonessential thiol (SH) groups can be immobilized onto thiol-reactive supports provided with reactive disulfides or disulfide oxides under mild conditions. The great potential advantage of this approach is the reversibility of the bonds formed between the activated solid phase and the thiol-enzyme, because the bound protein can be released with an excess of a low-molecular-weight thiol (e.g., dithiothreitol [DTT]). This is of particular interest when the enzyme degrades much faster than the adsorbent, which can be reloaded afterwards. The possibility of reusing the polymeric support after inactivation of the enzyme may be of interest for the practical use of immobilized enzymes in large-scale processes in industry, where their use has often been hampered by the high cost of the support material. Disulfide oxides (thiolsulfinate or thiolsulfonate groups) can be introduced onto a wide variety of support materials with different degrees of porosity and with different mechanical resistances. Procedures are given for the preparation of thiol-activated solid phases and the covalent attachment of thiol-enzymes to the support material via disulfide bonds. The possibility of reusing the polymeric support is also shown.

Key words Thiol-enzymes, Enzyme thiolation, Reversible enzyme immobilization, Thiol-activated supports, Pyridyldisulfide-agarose, Solid phase disulfide oxides, Thiolsulfinate-agarose, Thiolsulfonate-agarose, β -Galactosidase

1 Introduction

Enzyme immobilization methods based on thiol-disulfide exchange reactions are unique since they allow the formation of a stable and reversible covalent bond, of disulfide ($-S-S-$) type [1]. Thus, enzymes bearing exposed nonessential thiol (SH) groups can be immobilized onto thiol-reactive supports under mild conditions (e.g., low-ionic-strength buffer with pH 7.0–8.0 at room temperature). However, the applicability of these methods is not restricted to those thiol enzymes. Enzymes containing masked or unreactive thiol groups, or not containing thiol groups at all, can be modified chemically or by genetic engineering techniques, in order to provide them with reactive SH groups.

The great potential advantage of this approach is the reversibility of the bonds formed between the activated solid phase and the thiol-enzyme, because the bound protein can be released by the reduction of the disulfide bonds with an excess of a low-molecular-weight (MW) thiol (e.g., β -mercaptoethanol or dithiothreitol). This is of particular interest when the enzyme degrades much faster than the adsorbent, which can be reloaded afterwards.

This chapter focuses exclusively on enzyme immobilization onto thiol-activated solid phases provided with reactive disulfides (2-Pyridyldisulfide-agarose) or disulfide oxides (Thiolsulfinate and Thiolsulfonate-gels).

1.1 2-Pyridyldisulfide-agarose (PyS₂-gel)

In the most traditional method, 2-pyridyldisulfide-agarose (so called PyS₂-gel) reacts with thiol groups in proteins, forming a gel-bound mixed disulfide with the protein, with concomitant liberation of 2-thiopyridone (*see* Fig. 1). The coupling reaction is driven essentially to completion because of the formation of the thione, a compound stabilized by thiol–thione tautomerism. The release of 2-thiopyridone (the leaving group) can be monitored, in order to follow the advance of the reaction of the activated solid phase with thiols. However, its release contaminates the non-immobilized material, which sometimes can be of interest. The use of 2-pyridyldisulfide as a ligand is very advantageous because it is reactive in a wide pH range.

2-Pyridyldisulfide-agarose has been used both for enzyme immobilization and for purification of thiol-proteins by covalent chromatography [1]. Thus, crude Jack bean meal urease (a thiol-rich multimeric protein containing several nonessential thiol groups) has been reversibly immobilized onto PyS₂-gel by thiol-disulfide exchange with concomitant purification [2]. A column packed with this immobilized urease derivative could hydrolyze urea very efficiently when a solution of the substrate was passed through it. Because the gel-bound active enzyme could be eluted

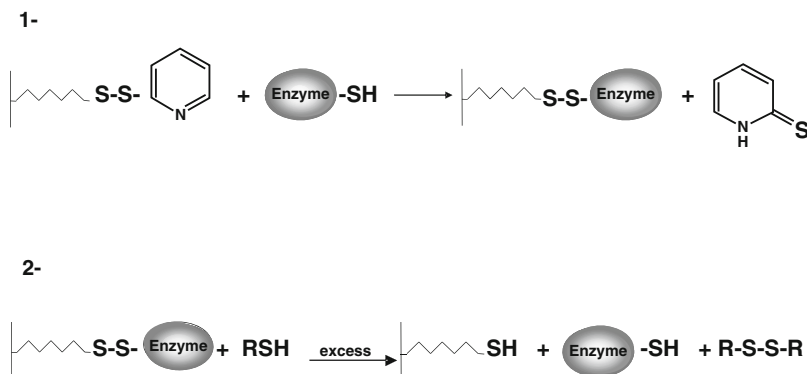


Fig. 1 Reversible covalent immobilization of thiol-enzymes onto 2-pyridyldisulfide-agarose. (1) Enzyme coupling with liberation of 2-thiopyridone. (2) Elution of gel-bound enzyme with an excess of a low MW thiol (e.g., dithiothreitol or β -mercaptoethanol)

quantitatively after incubation with low MW thiols (*see* Fig. 1), the method was also useful for the purification of urease (e.g., 167-fold) by covalent chromatography. Moreover, the resulting thiol-support could be used for regenerating the PyS₂-gel and re-loading with fresh enzyme.

A disadvantage of these gels is that at high ionic strength (e.g., 0.5 M sodium or potassium sulfate) 2-pyridyldisulfide-gels bind some proteins lacking thiol groups, especially immunoglobulins, through a noncovalent interaction, a property that has been utilized in the so-called thiophilic adsorption chromatography [3].

Thiol-reactive adsorbents based on pyridyldisulfide groups are commercially available. Thus, General Electric Healthcare (Uppsala, Sweden) provides two types of such agarose derivatives which differ both in the length of the spacer arm and the degree of substitution. Activated Thiol Sepharose 4B contains about 1 μmol pyridyldisulfide groups per mL packed gel, and a glutathione (ten atoms) spacer arm. Thiopropyl Sepharose 6B contains about 20 μmol pyridyldisulfide groups per mL packed gel, and a 2-hydroxypropyl (four atoms) spacer arm. It should be borne in mind that in spite of its trade name, Thiopropyl Sepharose 6B is not a thiol-gel but a mixed reactive disulfide gel.

1.2 Thiolsulfinate- and Thiolsulfonate-Gels (TSI- and TS-Gels)

A new approach based on agarose-bound disulfide oxides groups (thiolsulfonates and thiolsulfonates) has been developed for the reversible immobilization of thiol-containing substances [4]. These agarose-derivatives display high reactivity and selectivity towards both low- and high-MW thiols and can be used for the reversible immobilization of thiol-peptides and thiol-proteins [4–7]. Enzymes containing exposed SH groups are covalently immobilized onto solid phase disulfide oxides under mild conditions. The immobilization process involves the formation of disulfide bonds between thiol groups on the enzyme and disulfide oxide structures on the supports. Because of displacement of the electrons around the two sulfur atoms, disulfide oxides show high *S* reactivity. Thiol-containing molecules react with the more electrophilic of the two sulfur atoms (the unoxidized one) and become, as a result, immobilized to the solid phase by disulfide bonds (*see* Fig. 2). Contrary to the case with 2-pyridyldisulfide-based gels, the leaving groups (sulfenic or sulfinic acid) remain attached to the support.

All the techniques for introducing either reactive disulfides of 2-pyridyldisulfide type or disulfide oxides (thiolsulfonates or thiolsulfonates) into beaded agarose gels start with the same support derivative: thiol-agarose, which is prepared by means of a three step thiolation process. Thus, to obtain a thiol-substituted agarose, the support is first reacted with epichlorohydrin in a strong alkaline medium to introduce oxirane moieties into the gel; the oxirane groups are then converted with sodium thiosulfate to gel-bound thiosulfate-ester groups (Bunte salt derivative), which finally are reduced with DTT to thiol groups (*see* Fig. 3).

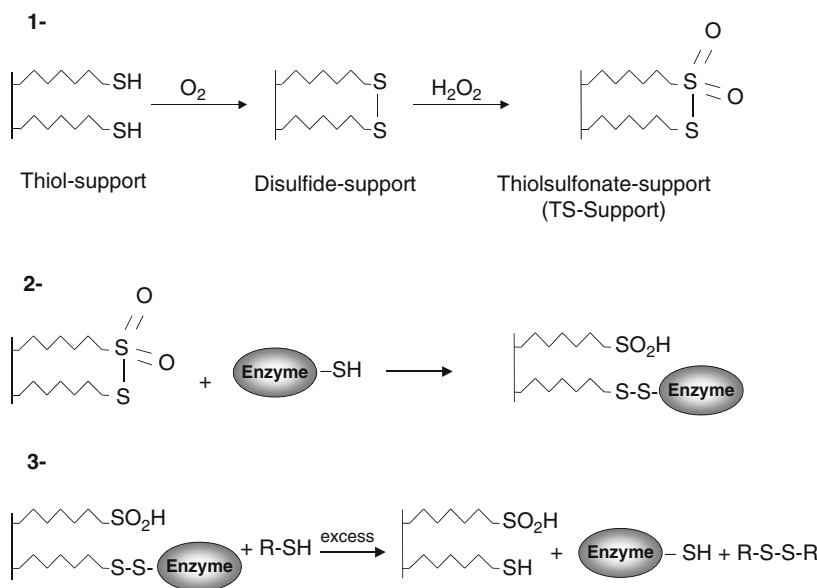


Fig. 2 Reversible covalent immobilization of thiol-enzymes onto a thiol-sulfonate-support. (1) Preparation of a thiol-sulfonate-support through oxidation of thiol-support. (2) Immobilization of a thiol-enzyme onto a thiol-sulfonate-support; the leaving group (sulfenic acid group) remains attached to the support. (3) Release of gel-bound enzyme with an excess of a low MW thiol

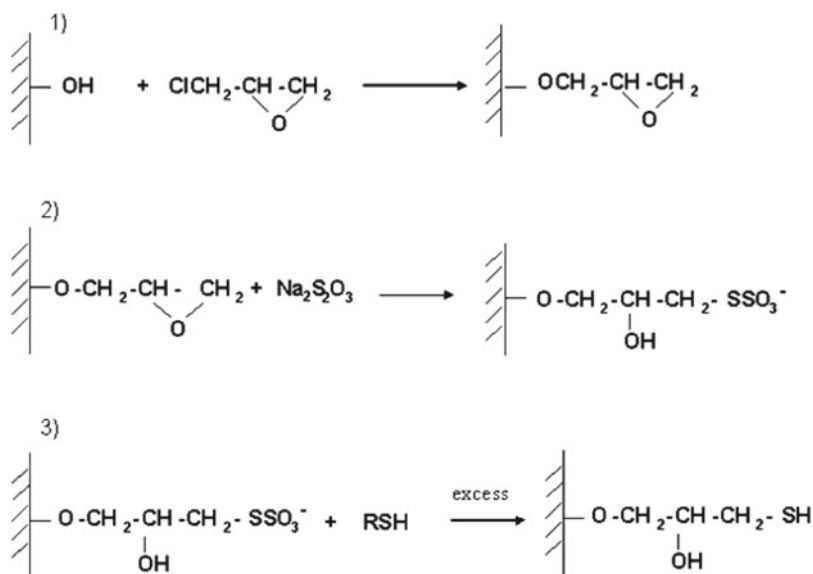


Fig. 3 Synthesis of a thiol-support through a three step procedure. (1) Epoxy-activation of the solid phase. (2) Formation of thiosulfate-ester structures (Bunte salt derivative). (3) Reduction of the Bunte salt by an excess of a low MW thiol

The degree of substitution in the thiol-agarose can be regulated by the amount of epichlorohydrin added as well as by the incubation conditions (e.g., incubation period, temperature) [8].

Thiol-agarose can be subsequently converted to TS-gel or TSI-gel through different oxidation procedures. Thus, oxidation of thiol-agarose with hydrogen peroxide at moderately acidic pH and room temperature for extended periods (20–30 h) converts thiol groups on the support (via disulfide and thiolsulfinate) into thiolsulfonate (disulfide dioxide) moieties (*see* Fig. 2) [5]. The thiolsulfinate (disulfide monoxide) groups are introduced by oxidation of thiol-agarose. The method comprises two steps: first, mild oxidation of agarose-bound thiol groups to disulfide structures with potassium ferricyanide; second, controlled oxidation with magnesium monoperoxyphthalate (MPP) of the agarose disulfide groups so formed to thiolsulfinate groups (*see* Fig. 2) [6, 7]. This reagent makes possible the introduction of only one oxygen atom per immobilized aliphatic disulfide group, to form a thiolsulfinate moiety. The number of thiolsulfinate groups introduced can be regulated at will by choosing a certain molar ratio between the oxidizing agent and the gel-bound disulfide structures. When the stoichiometric quantity of monoperoxyphthalate is used, maximum thiol-binding capacity is achieved; if half of this amount is used, 50 % of the maximum thiol-binding capacity is obtained, and so on.

Therefore, it is possible to prepare thiolsulfinate-agarose gels with different thiol-binding capacities from the same thiol-agarose batch.

The gel-bound thiolsulfinate/thiolsulfonate groups are very stable in the pH range of 3.0–8.0; therefore, solid phases containing these groups can be stored as suspensions at pH 5.0 at 4 °C for extended periods, without a decrease in their thiol-binding capacity. Furthermore, disulfide oxide gels do not need any preservative agent since no bacterial or fungal growth was observed after storing at 4 °C and pH 5.0 for 2 year.

After extensive reuse of an enzyme derivative until its inactivation, the disulfide bonds can be split under reducing conditions at alkaline pH to remove the bound protein (*see* Fig. 2). Then, the gel can be regenerated following the activation techniques described above and reloaded with fresh enzyme. This is achieved more efficiently with a TSI-gel, resulting from the fact that the sulfenic acid groups (–SOH) formed during thiol coupling can easily be converted back to SH moieties by using an excess of a mild reducing agent (*see* Fig. 2). Thus thiolsulfinate-agarose can at least in theory (as is also the case with 2-pyridyldisulfide-agarose), be regenerated an unlimited number of times. In contrast, TS-gels can be regenerated only a few times, due to the formation of gel-bound nonreducible sulfinate groups (–SO₂H) (*see* Fig. 2), with a concomitant decrease of about 50 % of its thiol-binding capacity after each cycle [6].

Besides beaded agarose, thiol-sulfonate and thiol-sulfinate groups can be introduced onto a wide variety of support materials with different degrees of porosity and with different mechanical resistances (e.g., soft particles such as Sephadex[®] and cellulose; semi-rigid ones such as Toyopearl[®] resins, Sephacryl[™], Eupergit[®], Superdex[™] and Superose[®]; and rigid particles such as controlled porous glass). Thiolation of the different supports is carried out using the same procedure as reported for agarose, except for porous glass which is directly thiolated by silanization in organic solvent with 3-mercaptopropyltriethoxysilane, and for oxirane-carrying acrylic beads (Eupergit[®] C, Sepabeads[®] EP), for which the first step in the thiolation procedure is omitted [7]. Table 1 shows thiol-binding capacities of different thiol-sulfinate-supports prepared according to the methods described. These figures represent the total number of thiol-reactive structures because they are determined by measuring the maximum binding of a thiol-peptide (reduced glutathione). In spite of the disparate types of support assayed, it is possible to provide all of them with thiol-reactive groups. In some cases the degrees of activation achieved were lower than expected, as a consequence of the rigidity of some matrices that makes impossible the formation of disulfide bonds between SH groups located far from each other.

Table 1
Thiol-binding capacities for different thiol-sulfinate-supports determined by glutathione binding [7]

Support: nature and identification	SH group content of thiol-support ($\mu\text{mol/g}$ dried deriv.)	TSI-group content ($\mu\text{mol/g}$ dried deriv.)	TSI-group content ($\mu\text{mol/g}$ wet deriv.) ^a
<i>Polysaccharides</i>			
Sepharose 4B	1009	500	27
Cellulose	194	82	34
Sephadex G-75	397	386	38
Superose 12	414	183	22
<i>Composite support</i>			
Superdex 75	272	212	26
Sephacryl S-200 SF	244	217	31
TSK-gel HW-65F	355	105	20
Eupergit	313	61	15
Sepabeads	124	52	32
<i>Inorganic supports</i>			
Porous glass (CPG)	474	125	74

^aBecause supports have quite different swelling factors in water, it is sometimes more useful to know the binding capacity in μmoles of GSH per gram of swollen and suction-dried (wet) derivative

The application of TS- and TSI-gels to the immobilization of high molecular weight thiols was assessed using different enzymes: with exposed nonessential SH groups, with buried thiol groups, with *de novo* thiol groups, and with reducible disulfides. Thus, immobilization of β -galactosidase (*Escherichia coli*) on TS- and TSI-agarose has been performed without any previous modification of the enzyme obtaining yields higher than 80 % and a high percentage of expressed activity [6, 9]. Moreover, tobacco-etch-virus NIa protease (TEV-protease) has been immobilized through its two exposed cysteine thiol groups onto TSI-gel with high yields (75–97 %) while keeping only 30 % of expressed activity [10]. This TEV protease immobilized onto TSI-agarose has proved to be a potentially useful tool for the cleavage of His tags of recombinant proteins.

The maximum capacity of these thiol-reactive adsorbents is on the order of 10 mg protein/mL packed gel. In the case of commercial β -galactosidases such as those from *Kluyveromyces lactis* and *Aspergillus oryzae*, a previous reduction process was shown to be essential in order to unblock their more exposed thiol groups [11]. This can be done either with soluble reducing agents such as dithiothreitol (DTT) or more conveniently with solid phase reducing agents [12].

A continuous solid phase process for reduction and thiol-dependent covalent immobilization of *Kluyveromyces lactis* β -galactosidase onto thiolsulfinate-agarose has been developed [13]. When enzyme solution was recirculated through two fixed-bed mini-reactors connected in series, one packed with thiopropyl-agarose (a solid phase reducing agent) and the other with thiolsulfinate-agarose (a thiol-reactive support), immobilization yield reached 42 % and the expressed activity 56 %.

When enzymes lack reactive SH groups, one alternative can be the introduction of *de novo* thiol groups by a thiolation process using suitable heterobifunctional reagents such as *N*-succinimidyl 3-(2-pyridyldithiopropionate) (SPDP) (*see* Fig. 4). The modification of proteins with this reagent involves mainly the ϵ -amino

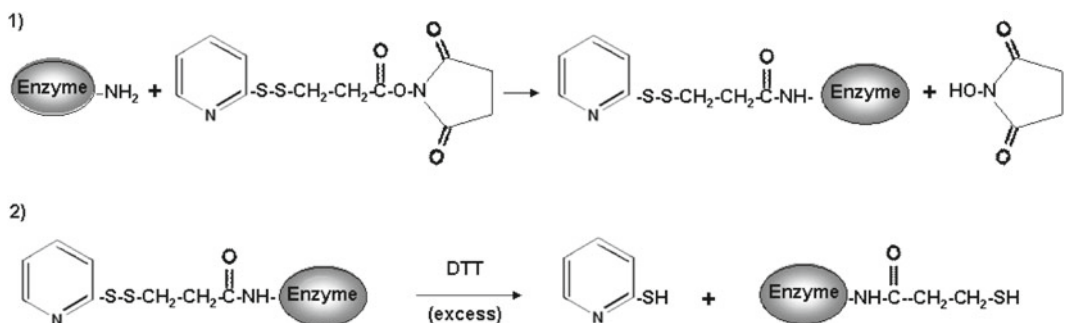


Fig. 4 Enzyme thiolation. (1) Reaction of protein amino groups with *N*-succinimidyl-3-(2-pyridyldithio) propionate (SPDP). (2) Reduction of the pyridyldisulphide-substituted protein with DTT

groups from lysine residues and the amino-terminal group which is more reactive than the ϵ -amino groups because of its lower pK_a [14, 15]. Pancreatic hog α -amylase [16], sweet potato β -amylase, pullulanase, and cyclodextrin glucantransferase (CGTase from *Thermoanaerobacter* sp.) have been chemically modified to allow their covalent immobilization onto thiol-reactive supports while preserving the enzymatic activity [17–19]. A critical parameter for the thiolation process while preserving the enzymatic activity is the SPDP/protein molar ratio, which determines the degree of chemical modification in the enzyme. The achieved degree of modification represents an average for the whole population of enzyme molecules, and it can be monitored by measuring the amount of released 2-TP after reduction with DTT (see Fig. 4). The number of thiol groups incorporated per protein molecule can then be calculated from the absorbance at 343 nm, using the $\epsilon_{2-TP} = 8.02 \times 10^3 \text{ M}^{-1} \text{ cm}^{-1}$.

Furthermore, site-directed mutagenesis techniques can be used to introduce a free cysteine at a suitable position on the protein, which can be used subsequently for immobilization. Thus, genetically engineered glucose dehydrogenase has been immobilized on a Thiopropyl-Sepharose column [20]. More recently, six different variants of penicillin G acylase (PGA) from *E. coli* (which lacks Cys) were designed, introducing a unique Cys residue via site-directed mutagenesis in six different enzyme regions which were rich in Lys residues, as a way to perform the immobilization of these PGA variants by site-directed thiol-disulfide intermolecular exchange onto a bifunctional thiol-reactive/epoxy support [21]. Derivatives were then incubated for long periods at alkaline pH to promote the reaction of Lys residues with epoxy groups to favor multipoint attachment.

When enzyme immobilization onto TS/TSI-gels is achieved it is important to take into account that the remaining reactive groups in the matrix could react with hidden thiol groups in the protein leading to an activity loss, specifically during thermal treatments. In order to avoid this effect, excess reactive structures can be blocked by coupling polar low-MW thiols. Thus, a β -galactosidase derivative blocked with glutathione retained 100 % of initial activity after 1 h at 50 °C, whereas the unblocked derivative only retained 16 % of the activity [9]. On the other hand, different nano-environments can be generated by reacting the excess of gel-bound disulfide oxides moieties with apolar, polar, anionic, or cationic thiols. In that way, it might be possible to tailor the matrix surface so as to maximize enzyme stability in particular applications [9, 22].

In conclusion, reversible covalent immobilization of enzymes through thiol-disulfide exchange reactions has the following advantages:

- It involves thiol groups, which are generally the most reactive groups found in proteins, because of the high nucleophilicity of the corresponding thiolate ions.

- Because thiolate ions exist at reasonable concentrations at neutral to weakly alkaline pH values, it is possible to perform enzyme immobilization under mild conditions and at relative high rates.
- These immobilization methods are absolutely specific for thiols.
- Resulting from the fact that thiol groups are scarce in proteins and located in specific regions, the enzyme can be immobilized in an oriented way, exposing the active site.
- Immobilization methods based on thiol-disulfide exchange reactions are unique, because they combine a very stable covalent attachment with the possibility of releasing the bound material. Thus, after enzyme inactivation, the immobilized material can be easily released by reduction.
- Disulfide oxides can be introduced onto a wide variety of support materials with different degrees of porosity and with different mechanical resistances that make them suitable for many analytical and preparative applications.
- The activated supports show high storage stability because thiol-reactive groups remain unchanged after 2 years at 4 °C.
- Sulfur content makes these gels highly resistant to microbial growth, so it is not necessary to use sodium azide as a preservative.
- The activated gel structures are completely regenerable for TSI- and PyS₂-gels, and 50 % regenerable for TS-gels.
- The possibility of reusing the polymeric support after inactivation of the enzyme may be of interest for the practical use of immobilized enzymes in large-scale processes in industry, where their use has often been hampered by the high cost of the support material.

In Subheading 3, procedures are given for the preparation of thiol-activated solid phases and the covalent attachment of thiol-enzymes to the support material via disulfide bonds. The possibility of reusing the polymeric support is also shown after reductive detachment, chemical reactivation, and reattachment of fresh thiol protein.

2 Materials

2.1 Preparation of Activated Solid Phases

2.1.1 Preparation of Thiol-Agarose and Titration of Thiol Groups

1. Sepharose 4B (Pharmacia BTG, Uppsala, Sweden).
2. Epichlorohydrin (1-chloro-2,3-epoxypropane) (Sigma, St. Louis, MO, USA).
3. Sodium thiosulfate (Fluka AG, Buchs, Switzerland).
4. Dithiothreitol (DTT) (Sigma, St. Louis, MO, USA).
5. 2,2'-Dipyridyldisulfide (2-PDS) (Sigma, St. Louis, MO, USA).

2.1.2 *Preparation of 2-Pyridyldisulfide Agarose and Titration of Pyridyl Disulfide Groups*

1. 2-Mercapto pyridine (2-TP) (Fluka AG, Buchs, Switzerland).
2. 2-PDS (Sigma, St. Louis, MO, USA).
3. DTT (Sigma, St. Louis, MO, USA).

2.1.3 *Preparation of Thiolsulfonate-Agarose (TS-gel)*

1. Perhydrol® (30 % Hydrogen peroxide) (Merck AG, Darmstadt, Germany).

2.1.4 *Preparation of Thiolsulfinate-Agarose (TSI-gel)*

1. Magnesium monoperoxyphthalate (MMPP) (Merck AG, Darmstadt, Germany).
2. Potassium ferricyanide (Baker, Phillipsburg, NJ, USA).

2.1.5 *Titration of Thiol-Reactive Structures in the Agarose Derivatives*

1. Reduced glutathione (Sigma, St. Louis, MO, USA).
2. 2-PDS (Sigma, St. Louis, MO, USA).

2.2 Immobilization of *E. coli* β -galactosidase onto Thiol-Reactive Agarose

For each of the following techniques it is necessary to have:

1. Empty PD-10 columns.
2. End-over-end mixer.
3. Vacuum pump.

2.2.1 *Activity Determination*

1. β -Galactosidase (β -D-galactoside galactohydrolase; EC 3.2.1.23) grade VIII from *E.coli*. (Sigma, St. Louis, MO, USA).
2. Activity buffer: 0.1 M potassium phosphate buffer, pH 7.5, 3 mM MgCl₂.
3. *o*-Nitrophenyl- β -D-galactopyranoside (ONPG) (Sigma, St. Louis, MO, USA).

2.2.2 *Enzyme Immobilization*

1. Thiolsulfonate-agarose, prepared as described in Subheading 3.1.5.
2. Immobilization buffer: 0.1 M potassium phosphate buffer, pH 7.0.
3. 0.1 M potassium phosphate buffer, pH 7.0, 0.5M sodium chloride.
4. β -Galactosidase grade VIII from *E.coli*. (Sigma, St. Louis, MO, USA).

2.2.3 *Blocking Excess of Active Groups*

1. Glutathione (GSH) (Sigma, St. Louis, MO, USA).

2.2.4 *Enzyme Elution*

1. DTT (Sigma, St. Louis, MO, USA).

2.3 Immobilization of *Kluyveromyces lactis* β -galactosidase onto Thiol-Reactive Supports (Fig. 5)

2.3.1 Activity Determination

1. β -Galactosidase (β -D-galactoside galactohydrolase; EC 3.2.1.23) from *K. lactis*, Gist-Brocades (Cedex, France).
2. Activity buffer: 20 mM potassium phosphate buffer, pH 7.0, 2 mM MgCl₂, 0.1 M KCl.
3. ONPG (Sigma, St. Louis, MO, USA).

2.3.2 Protein Determination

1. Coomassie Plus protein assay reagent (Pierce, Rockford, IL, USA).

2.3.3 Enzyme Reduction

1. DTT (Sigma, St. Louis, MO, USA).

2.3.4 Enzyme Immobilization

1. Thiolsulfonate-agarose (TS-gel) and thiolsulfinate-agarose (TSI-gel) prepared as described in Subheadings 3.1.5 and 3.1.6, respectively.
2. Immobilization buffer: 0.1 M potassium phosphate buffer, pH 7.0.
3. 0.1 M potassium phosphate buffer, pH 7.0, 0.5 M NaCl.
4. β -Galactosidase (β -D-galactoside galactohydrolase; EC 3.2.1.23) from *K. lactis*, Gist-Brocades (Cedex, France).
5. DTT (Sigma, St. Louis, MO, USA).

2.3.5 Blocking Excess of Active Groups

1. GSH (Sigma, St. Louis, MO, USA).

2.3.6 Enzyme Elution

1. DTT (Sigma, St. Louis, MO, USA).

2.4 Immobilization of *Thermoanaerobacter* sp. Cyclodextrin glucantransferase onto Thiolsulfinate Agarose

2.4.1 Activity Determination

1. Toruzyme® (CGTase; EC 2.4.1.19) from *Thermoanaerobacter* sp. (Novozymes, Bagsvaerd, Denmark).
2. Soluble starch (Panreac, Montplet and Esteban SA, Madrid, Spain).
3. Activity buffer: 10 mM sodium acetate buffer, pH 5.4, 0.15 mM CaCl₂.

2.4.2 Protein Determination

Bicinchoninic acid (BCA) Protein Assay Kit, Pierce (Rockford, IL, USA)

2.4.3 Enzyme Reduction

1. DTT (Sigma, St. Louis, MO, USA).
2. 5, 5'-Dithiobis (2-nitrobenzoic acid) (DTNB) (Sigma, St. Louis, MO, USA).

- 2.4.4 *Enzyme Thiolation*
1. *N*-Succinimidyl-3-(2-pyridyldithio) propionate (SPDP) (Sigma, St. Louis, MO, USA)
 2. DTT (Sigma, St. Louis, MO, USA).
- 2.4.5 *Enzyme Immobilization*
1. Thiolsulfinate-agarose prepared as described in Subheading 3.1.6.
 2. Immobilization buffer: 50 mM Phosphate buffer, pH 6.8–7.0, 0.15 M sodium chloride.
 3. Toruzyme® CGTase from *Thermoanaerobacter* sp. (Novozymes, Bagsvaerd, Denmark).
- 2.4.6 *Enzyme Elution*
1. DTT (Sigma, St. Louis, MO, USA).

3 Methods

3.1 Preparation of Activated Solid Phases

3.1.1 Preparation of Thiol-Agarose

The preparation of mercaptohydroxypropyl ether agarose gel (thiol agarose) is carried out essentially as described by Axén et al. [8]. In this method the agarose beads (Sephacrose 4B) are first reacted with epichlorohydrin in an alkaline medium. The oxirane groups thus formed are then converted with sodium thiosulfate to gel-bound thiosulfate groups (Bunte-salt), which are finally reduced with DTT to thiol groups (*see* Fig. 3).

1. Suspend 15 g suction-dried Sepharose 4B in 15 mL of 1 M NaOH.
2. Add slowly with agitation 2.5 mL epichlorohydrin (*see* Note 1).
3. Incubate overnight at 22 °C under shaking (*see* Note 2).
4. Transfer the epoxy-activated gel to a sintered-glass filter and wash it with distilled water. Use it immediately.
5. Equilibrate the gel with 0.5 M sodium phosphate buffer, pH 6.3 and suspend it in 15 mL of the same buffer.
6. Add 15 mL 2 M sodium thiosulfate and incubate overnight under shaking at 22 °C (minimum 6 h).
7. Transfer the Bunte-salt gel to a sintered-glass filter and wash it with water. Store it in distilled water at 4 °C until use (very stable) (*see* Note 3).
8. Suspend 15 g suction-dried Bunte-salt gel with 15 mL 0.2 M sodium bicarbonate buffer, pH 8.5.
9. Dissolve 3 g DTT in 15 mL 1mM ethylene diamine tetraacetic acid (EDTA) and add it to the Bunte-salt gel suspension (*see* Note 4).
10. Incubate the mixture during 1 h under shaking at 22 °C.

11. Transfer to a sintered-glass filter and wash with:
 - (a) 0.2 M sodium bicarbonate buffer, pH 8.5.
 - (b) Distilled water.
 - (c) 0.1 M acetic acid, until absence of DTT.

These conditions will give a thiol-agarose derivative containing between 400 and 600 μmol of thiol groups per gram of dried gel (*see Note 5*).

3.1.2 Thiol Group Analysis

1. The thiol content of both soluble and insoluble material is determined spectrophotometrically at 343 nm by titration with 2-PDS (saturated solution, 1.5 mM, prepared by 30 min agitation followed by filtration) dissolved in 0.1 M sodium phosphate, pH 8.0 according to Brocklehurst et al. [23].

3.1.3 Preparation of 2-Pyridyldisulfide-Agarose

Preparation of 2-pyridyldisulfide-agarose is carried out as reported by Oscarsson et al. [3].

1. Suspend 10 g of suction-dried thiol-agarose gel in 40 mL of 50 mM sodium phosphate buffer, pH 8.5.
2. Dissolve 1.8 g of 2-TP and 3.5 g of 2-PDS in 40 mL of 98 % ethanol.
3. Add this solution to the gel suspension and stir for 15 h at room temperature.
4. Wash with ethanol and water on a glass filter.

3.1.4 Titration of Pyridyldisulfide Groups

The determination is based on the release of 2-TP after reduction of 2-pyridyldisulfide-gel. The extinction coefficient at 343 nm for 2-TP is $8.02 \times 10^3 \text{ M}^{-1} \text{ cm}^{-1}$.

1. A filter-dried gel aliquot is weighted and suspended in 25 mM DTT in 0.1 M phosphate buffer pH 8.0.
2. After incubation under shaking at room temperature for 30 min, the supernatant is filtered and the absorbance at 343 nm is measured.

3.1.5 Preparation of Thiolsulfonate-Agarose (TS-Gel) [4, 5]

1. Suction-dried thiol-agarose (15 g containing 500–800 μmol SH groups/g dried gel) is suspended in 45 mL of 0.2 M sodium acetate, pH 5.0.
2. Add aliquots of 30 % hydrogen peroxide under continuous shaking, 1.8 mL initially and then 2.2 mL after 30, 90, and 150 min. The incubation is then continued to give a total reaction time of 30 h (*see Note 6*).
3. Transfer the oxidized gel to a sintered-glass filter and wash with 0.1 M acetic acid until free of hydrogen peroxide.
4. Store the activated gel in 0.2 M sodium acetate, pH 5.0 at 4°C until use.

5. The thiol-sulfonate group content of the gel thus obtained is between 250 and 400 μmol TS groups per gram of dried gel.

3.1.6 Preparation of Thiolsulfinate-Agarose (TSI-Gel) [6, 7]

Disulfide-Agarose (S_2 -Gel)

1. Suspend 15 g of suction-dried thiol-agarose gel in 30 mL of 0.1 M sodium phosphate buffer pH 7.0 and 0.1 M potassium ferricyanide is added (by 0.5 mL aliquots under shaking until the yellow color persists for at least 30 min).
2. Then, wash thoroughly the gel on a sintered-glass filter with 1 M NaCl solution, and 0.2 M sodium acetate buffer, pH 5.0. It can be assumed that the disulfide (S-S) group content of obtained S_2 -gel is 50 % of the thiol content in starting thiol-agarose.

Thiolsulfinate-Agarose (TSI-Gel)

1. Suspend 15 g of suction-dried S_2 -gel in 100 mL 0.2 M sodium acetate, pH 5.0 in which the required amount of MMPP has been dissolved (0.5 mol per mol of S-S groups) (*see Note 7*).
2. Incubate the suspension while shaking for 2 h at room temperature (22 °C).
3. Then, wash thoroughly the gel derivative on a sintered-glass filter with 50 mM sodium acetate buffer, pH 5.0 and 0.1 M acetic acid solution.
4. Store the gel at 4 °C as a suspension in 0.2 M sodium acetate buffer, pH 5.0 (*see Notes 8 and 9*).

3.1.7 Titration of Thiol-Reactive Structures in the Agarose Derivatives

This is performed by back titration of remaining GSH free in solution, after its incubation with thiol-reactive gels. A blank is performed for spontaneous oxidation of GSH.

1. Equilibrate 2.0 g suction-dried gel aliquots (TS- or TSI-gel) with 0.1 M sodium phosphate buffer, pH 7.0 in centrifuge tubes.
2. Adjust the amount in each tube to 3.0 g with the same phosphate buffer.
3. Add 3-mL aliquots of 15 mM GSH dissolved in the same buffer to each tube while mixing (Vortex).
4. Incubate the suspensions for 30 min at 22 °C, mix every 5 min, and then centrifuge.
5. Mix 50- μl aliquots of supernatants with 3.0 mL of 1.5 mM 2-PDS dissolved in 0.1 M sodium phosphate buffer, pH 8.0.
6. Measure absorbances at 343 nm.

3.2 Immobilization of *E. coli* β -galactosidase onto Thiol-Reactive Agarose [9]

3.2.1 Activity Determination

1. Free β -galactosidase activity is determined using 14 mM ONPG as a substrate in 0.1 M potassium phosphate buffer, pH 7.5, containing 3 mM magnesium chloride (activity buffer) (*see Note 10*). The released o-nitrophenol (ONP) is determined spectrophotometrically at 405 nm [24]. One *unit of enzyme activity (EU)* is defined as the amount of enzyme able to catalyze the hydrolysis of 1 μ mol of ONPG per minute under the specified conditions.
2. Immobilized enzyme activity is assayed by incubating 100 μ L aliquots of gel suspensions (containing 10 mg of suction-dried gel derivatives) with ONPG in activity buffer, using a 1 cm path length cuvette provided with magnetic stirring.

3.2.2 Protein Determination

1. Protein concentration is estimated from the absorbance values at 280 nm and using an extinction coefficient of 2.09 for a 1.0 mg/mL solution of *E. coli* β -galactosidase [24].
2. Protein content of the gel derivatives is determined by total amino acid analysis, after extensive drying in a dessicator over phosphorus pentoxide and hydrolysis in 6 M HCl for 24 h at 110 $^{\circ}$ C.

3.2.3 Preparation of Immobilized Enzyme Derivatives

1. Wash thiolsulfonate-agarose (TS-gel) in a sintered-glass filter connected to a vacuum pump, with 0.1 M potassium phosphate buffer, pH 7.0 (immobilization buffer) (*see Note 11*).
2. Transfer 2.0 g aliquots of suction-dried TS-gel (equilibrated in immobilization buffer) to empty PD-10 columns (*see Note 12*).
3. Add 7.5 mL of β -galactosidase solutions (containing between 1.0 and 50.0 mg of protein, respectively) in 0.1 M potassium phosphate buffer, pH 7.0 (*see Note 13*).
4. Mix the suspensions gently in an end-over-end mixer for 16 h at 4 $^{\circ}$ C.
5. Wash the resulting insoluble derivatives sequentially with 25 mL portions of 0.1 M potassium phosphate buffer, pH 7.0 with and without 0.5 M NaCl (*see Note 14*).
6. Equilibrate and dilute the conjugates to 22 mL with 0.1 M potassium phosphate buffer, pH 7.5, containing 3 mM MgCl_2 (activity buffer).
7. Store at 4 $^{\circ}$ C (*see Note 15*).

3.2.4 Blocking the Excess of Active Groups

1. Incubate for 30 min under mixing, 2.0 g of suction-dried gel derivatives with 20.0 mL of 8 mM of GSH solution. After incubation, filtrate, wash and dilute to 20.0 mL with activity buffer.

2. Assay β -galactosidase activity in both the filtrates and blocked-gel suspensions (*see* **Note 16**).

3.2.5 Enzyme Elution

1. Incubate aliquots of suction-dried derivatives (100 mg) with 4.0 mL of fresh 50 mM DTT in 0.1 M sodium phosphate, pH 8.5 under agitation for 1 h under end-over-end rotation.
2. After filtration, determine activity in the filtrates (*see* **Note 17**).

3.3 Immobilization of *K. lactis* β -Galactosidase onto Thiol-Reactive Supports [11]

The activity determination is performed as in Subheading 3.3.1.

3.3.1 Activity Determination

3.3.2 Protein Determination

1. The protein content of the enzyme solutions is determined with Coomassie Plus reagent.
2. Immobilized protein is estimated as the difference between the amount of protein added to the gel and that recovered in the pooled supernatant and washing fractions. It is also determined by total amino acid analysis after extensive drying over phosphorus pentoxide in a desiccator and hydrolysis in 6 M HCl for 24 h at 110 °C.

3.3.3 Enzyme Reduction with a Soluble Reducing Agent

1. Incubate 1.0 mL-aliquots of enzyme (60 mg/mL, 1,400 EU/mL) at 22 °C with 1.0 mL DTT 200 mM dissolved in 20 mM potassium phosphate, pH 8.0, under magnetic agitation (*see* **Note 18**).
2. After 30 min, remove the excess of DTT by gel-filtration.
3. Determine protein SH content [25].

3.3.4 Enzyme Reduction with a Solid Phase Reducing Agent

Thiol-agarose containing 1,000 μ mol SH groups per gram of dried gel is used, prepared as described in Subheading 3.1.1.

1. Incubate aliquots of enzyme (8 mg/mL, 240 EU/mL) at 22 °C with 1.0 g suction-dried thiopropyl-agarose (*see* **Notes 19–20**).
2. After 2 h, remove the excess of reducing agent by filtration on a sintered glass filter.
3. Titrate the thiol content of the reduced enzyme as described by Ellman [25] (*see* **Notes 21–22**).

3.3.5 Preparation of Immobilized Enzyme Following a Batch Procedure

1. Follow the protocol described in Subheading 3.2.3 using reduced enzyme (*see* **Notes 23–25**).

3.3.6 Preparation of Immobilized Enzyme Following Column Procedure

1. Equilibrate TS-agarose or TSI-agarose as in Subheading 3.2.3.
2. Pack 5 mL of this gel into a plexiglass column.
3. Recirculate for 16 h at 22 °C, reduced and gel filtered enzyme in 0.1 M phosphate buffer, pH 7.0 at a flow rate of 10 mL/h.
4. Wash the column sequentially with 0.1 M phosphate buffer (pH 7.0) with and without 0.5 M NaCl.
5. Measure β -galactosidase activity in the recirculated and washing fractions, and in the gel-derivative obtained (*see Note 26*).

3.3.7 Blocking the Excess of Active Groups

1. Incubate for 30 min, 300 mg of suction-dried gel derivatives with 3.0 mL of fresh 8 mM glutathione solution.
2. After incubation, filter, wash, and dilute to 3.0 mL with activity buffer (*see Note 27*).

3.3.8 Enzyme Elution

1. Follow the protocol described in Subheading 3.2.5.
2. After filtration, determine protein content and activity in the filtrates (*see Note 28*).

3.3.9 Lactose Hydrolysis in Batch

1. Incubate at 22 and 37 °C, aliquots of free and immobilized enzyme suspensions with 5 % lactose saline solution, whey, whey permeates and skimmed milk (ratio 1/10 [v/v]).
2. Glucose formation is followed by an enzymatic method (*see Note 29*).

3.3.10 Lactose Hydrolysis in Column

1. A column with 5 mL of packed gel is fed with the same lactose solutions specified above, using a flow rate between 6.0 and 10.0 mL/h.
2. Determine the glucose formed (*see Note 30*).

3.3.11 Reuse of the Immobilized Enzyme

1. Incubate with whey at 22 °C for 2.5 h an aliquot of the TSI-agarose- β -galactosidase derivative.
2. Determine the amount of formed glucose.
3. Wash the derivative with activity buffer.
4. Use the washed derivative for a second time in the same way as in the first time.
5. This protocol is carried out four times (*see Note 31*).

3.3.12 Regeneration of Thiol-Reactive Gels

After release of bound material from the gel derivative by reductive cleavage and thorough washing, reactivation is performed according to the two-step procedure described for TSI-gel synthesis or the one-step procedure described for TS-gel (*see Notes 32 and 33*).

3.4 Immobilization of *Thermoanaerobacter sp.* Cyclodextrin glucantransferase onto Thioisulfinate Agarose [19]

The production of β -cyclodextrin (β -CD) is detected spectrophotometrically at 550 nm on the basis of its ability to form a stable, colorless inclusion complex with phenolphthalein [26] (*see Note 34*). One *unit of enzyme activity (EU)* is defined as the amount of enzyme able to produce 1 μ mol of β -CD per minute under the specified conditions.

3.4.1 Assay of β -CD Cyclization Activity

Cyclodextrin
Glucantransferase
(CGTase) Activity in
Solution

1. Incubate the enzyme (0.29 EU/mL) at 85 °C in the presence of 5 % (w/v) starch in 10 mM sodium acetate buffer, pH 5.4, 0.15 mM CaCl₂ (activity buffer) (*see Note 35*).
2. Withdraw aliquots at time intervals and perform the following assay:
 - Mix 0.5 mL of each aliquot (containing β -CD) with 2.5 mL of a 60 μ M phenolphthalein solution, in 0.12 M carbonate-bicarbonate buffer, pH 10.5.
 - Measure absorbance at 550 nm after 15 min reaction.
 - Calculate β -CD concentration with calibration curve.

Immobilized Enzyme
Activity

1. Incubate 50 mg of suction-dried gel derivative with 5.0 mL of 5 % (w/v) starch in activity buffer at 85 °C under magnetic stirring.
2. Take samples of the reaction mixture at 1-min intervals and filter by suction to interrupt the immobilized enzyme reaction.
3. Determine β -CD content as described above.

3.4.2 Protein Determination

Protein content is determined using the bicinchoninic acid (BCA) assay [27] (*see Note 36*). Bovine serum albumin is used as standard. Immobilized protein is estimated as the difference between the amount of protein added to the gel and that recovered in the pooled supernatant and washing fractions.

3.4.3 Enzyme Reduction with DTT

1. Incubate CGTase (Toruzyme®, 10 mg/mL, 330 EU/mL) with 100 mM DTT in 100 mM potassium phosphate, pH 8.0 for 30 min.
2. Remove excess of reducing agent and other low molecular weight molecules by gel filtration.
3. Determine spectrophotometrically thiol content of the enzyme, before and after the reduction process, by titration with DTNB dissolved in 100 mM sodium phosphate buffer, pH 8.0 [25] (*see Notes 37–39*).

3.4.4 Enzyme Thiolation

1. Dilute ten times aliquots of Toruzyme® (10 mg/mL, 330 EU/mL) with 50 mM sodium phosphate pH 6.8, 0.15 M NaCl

and perform a gel filtration on PD-10 columns equilibrated in the same buffer solution (*see Note 40*).

2. Incubate for 30 min aliquots of gel filtered CGTase (0.7 mg/mL, 21 EU/mL) with SPDP, at SPDP/protein molar ratio of 100 in 50 mM sodium phosphate pH 6.8, 0.15 M NaCl (*see Notes 41 and 42*).
3. After treatment with SPDP, a 1.5 M excess of DTT over the starting amount of SPDP is added and incubated for 1 h under stirring.
4. The resulting modified enzyme is gel filtered on a PD-10 column to remove DTT excess.
5. The SH content and residual activity are determined as described above.

3.4.5 Enzyme Immobilization onto TSI-Agarose

Perform the following protocol using thiolated enzyme (*see Notes 43 and 44*):

1. Incubate thiolated enzyme (30 EU/mg) with 0.5 g of suction-dried TSI-gel under the following conditions: pH (6.8–7.0), concentration of phosphate buffer 50 mM, 0.15 M NaCl, and enzyme load (0.3 mg protein/g suction-dried gel).
2. Gently agitate the mixtures for 24 h at 22 °C.
3. Sequentially washed the insoluble derivatives obtained with: immobilization buffer, with and without 0.5 M NaCl.
4. Store CGTase derivatives at 4 °C until used (*see Notes 45–47*).

3.4.6 Reusability/Stability Experiments

1. Measure β -CD cyclization activity of the resulting derivative after the immobilization process.
2. Then, wash the insoluble biocatalyst with activity buffer.
3. Add to the suction-dried derivative fresh substrate in order to restart the reaction.
4. Perform five consecutive reuses along 12 days, washing the derivative between each run and keeping it at 4 °C until the next use (*see Note 48*).

3.4.7 Immobilized Protein Elution

1. Incubate suction-dried aliquots of CGTase derivative (100 mg) with 4 mL of 100 mM DTT in 0.1 M sodium phosphate, pH 8.0.
2. Agitate for 30 min at room temperature,
3. Filter and wash with the same buffer the reduced gel.
4. Measure the released activity (*see Note 49*).

4 Notes

1. According to Axén et al. [8] it is possible to regulate the degree of thiol agarose substitution (thiol content) by varying the amount of epichlorohydrin used in the epoxy activation step.
2. This reaction is highly dependent on temperature and on incubation time. It is possible to decrease incubation time by working at 60 °C.
3. It is possible to confirm the highly charged properties of the Bunte-salt gel by observing the increase in the swelling and in the volume of the gel.
4. Reduction of the Bunte-salt gel is carried out by using a small excess of DTT (e.g., 10 %) with respect to the stoichiometric amount. This is important because of the high cost of this reagent.
5. A higher content of thiol groups (e.g., 1,000 µmol per gram of dried gel) would be desirable if the thiol-agarose is intended for use as a solid phase reducing agent.
6. Longer incubation periods lead to a loss of activated groups [5].
7. Magnesium monoperoxyphthalate hexahydrate (MMPP) is a cheap and safe oxidant which can be purchased from Merck Schuchardt (Darmstadt, Germany)(Merck Schuchardt MS Info 88–1, Cat. No.818372). It is a crystalline solid that is soluble in water and low MW alcohols, and it was originally recommended for the selective oxidation of organic sulfides to sulfoxides and sulfones [28, 29].
8. TS- and TSI-gels show high stability in 0.2 M sodium acetate (pH 5.0) at 4 °C, because no decrease in reactivity can be detected after long storage periods under these conditions [5, 7].
9. The antibacterial properties of alkyl thiol-sulfonates are well known and we have never observed microbial growth in these gel suspensions.
10. This potassium phosphate buffer is the most suitable for this β-galactosidase because sodium ions inactivate the enzyme, and also because of the presence of magnesium (stabilizing ion).
11. Use gentle suction to remove liquid until the moment when the gel forms a firm cake and then stop suction; the gel is then called suction-dried gel.
12. Plastic reservoir with a bottom membrane and top and bottom caps.
13. This *E. coli* β-galactosidase is selected because of its high cysteine content; it should therefore be possible to use its nonessential thiol groups for its immobilization.

14. Sodium chloride is included in the washing buffer to elute nonspecifically bound proteins.
15. The percentage of gel-bound activity depends on the amount of protein added, ranging from 70 to 80 % for the low- and intermediate-load derivatives, to 41 % for the high-load derivative. A control gel (with its thiol-reactive groups previously blocked with glutathione) does not retain the enzyme.
16. In 3.0 mL of 8 mM glutathione solution there is a tenfold excess of glutathione with respect to the number of active groups present on the activated gel. Other thiol compounds, like mercaptopropionic acid and mercaptoethanol (in activity buffer) can be used for blocking the excess of active groups. Because of its low pKa value, cysteamine (pKa = 8.3) is the only thiol-compound assessed which has an eluting effect (after the blocking treatment with cysteamine under the conditions described, nearly 30 % of the bound enzyme is released).
17. More than 90 % of the total immobilized activity is eluted, proving that the matrix-enzyme bonds formed are of disulfide type.
18. Under these conditions, the ratio $\mu\text{moles SH groups of reductant/mg of protein}$ is 3.4.
19. Prior to its use, this commercial lactase preparation (Maxilact LX-5,000) is diluted 20-fold with 20 mM phosphate buffer (pH 7.0) and gel filtered through Sephadex G-25.
20. Achieving a ratio of $\mu\text{moles SH groups of reducing agent/mg of protein}$ of 0.5.
21. The reduction of this lactase with both reductants allowed a threefold increase of its initial content of SH groups. Nearly sevenfold less $\mu\text{moles of SH groups/mg of protein}$ were needed to perform the reduction of *K. lactis* β -galactosidase with thiopropyl-agarose than the SH amount required for the reduction with DTT.
22. After the reduction process, the remaining content of SH groups of the solid phase reducing agent was quantified; nearly 60 % of the initial SH groups remained.
23. The reduction process dramatically improved the immobilization yield onto thiol-reactive supports, from 0 % for the native enzyme up to 90 % for the reduced enzyme.
24. Using an acrylic resin as support, like Toyopearl HW-65F, the expressed β -galactosidase activity is strongly dependent on the salt concentration present during the immobilization process, increasing from 32 % in absence of salt to 60 % in the presence of 0.3 M K_2SO_4 (Table 2).

Table 2
Immobilization yields of reduced β -galactosidase onto thiol-reactive supports

Thiol-reactive support	Immobilization yield (%) ^a	Expressed activity (%) ^b
TS-agarose	91	82
TSI-agarose	90	86
TSI-Toyopearl	74	60

^aEstimated on the basis of the difference between the amount of protein applied and that remaining in supernatants and washings

^bPercentage of expressed activity (gel-bound activity/applied activity)

25. The immobilization process requires incubation periods of at least 8 h for quantitative binding of the reduced enzyme to TS- and TSI-supports (*see* Fig. 5).
26. After overnight recirculation, the immobilization yield for the reduced enzyme is 69 %.
27. The blocking treatment markedly improves the thermal stability at 37 °C (optimum temperature for the hydrolysis of lactose) of β -galactosidase derivatives (Table 3).
28. Nearly 70 % of the total immobilized activity and 90 % of the bound protein are eluted, showing the reversibility of the immobilization process.
29. The percentages of lactolysis (lactose hydrolysis) at 22 °C are similar, regardless of the lactose solution (nearly 75 % after 90 min of reaction).
30. When this mini-reactor is fed with whey permeate at 22 °C, steady state lactose conversion reaches 90 % and remains constant for 12. When it is fed for another 5 day with skimmed milk, the percentage of lactolysis is maintained.
31. After five cycles of 2.5 h each, the degree of lactolysis remains greater than 75 %.
32. It is important to emphasize the differences found between TS- and TSI-gels from the point of view of regeneration. TSI-gels can be regenerated to 100 % of their initial reactivity, whereas TS-gels can only be regenerated to 50 % (Table 4).
33. In order to demonstrate the feasibility of reusing the support, several cycles of immobilization, elution of bound protein, regeneration of thiol-reactive adsorbent (TSI-gel), and reuse is performed. As high amounts of a model thiol-protein are required, bovine serum albumin (BSA) provided with 4.0 mol

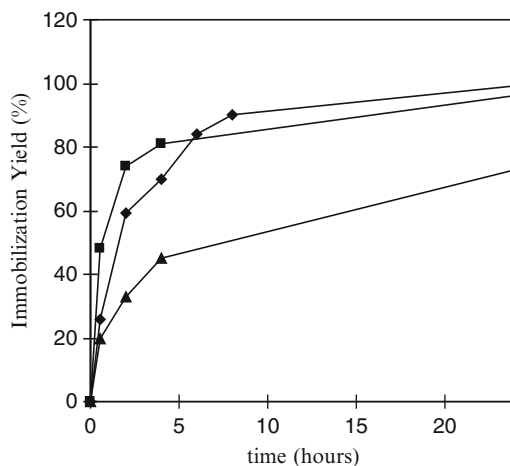


Fig. 5 Kinetics for the immobilization of reduced *K. lactis* β -galactosidase onto thiol-reactive supports. (Filled diamonds) TS-agarose; (filled squares) TSI-agarose; (filled triangles) TSI-Toyopearl

Table 3

Stability of immobilized β -galactosidase derivatives (before and after blocking with GSH) as a function of the incubation period at 37 °C

Enzyme derivative	Remaining activity (%) after incubation (h)		
	0.5	1	2
TS-agarose- β -gal	80	60	52
Blocked TS-agarose- β -gal	100	100	92
TSI-agarose- β -gal	94	84	50
Blocked TSI-agarose- β -gal	100	100	81
TSI-Toyopearl- β -gal	76	69	55
Blocked TSI-Toyopearl- β -gal	100	100	100

of de novo thiol groups per mole of protein through chemical modification with SPDP) is selected for this purpose (Table 5).

34. It is necessary to make a calibration curve ($A_{550\text{nm}}$ vs. β -cyclodextrin concentration) for determining the amount of synthesized β -cyclodextrin. For this purpose, solutions of standard β -cyclodextrin (in the range 50–300 μM) are incubated with phenolphthalein in activity buffer.

The absorbances at 550 nm measured during the activity assay (five time intervals between 0 and 60 s), are then interpolated in the curve $A_{550\text{nm}}$ vs. β -cyclodextrin concentration in

Table 4
Regenerability of thiosulfonate agarose (TS-gel) and thiosulfinate-agarose (TSI-gel)

Gel type	Gel-bound SH		μ moles thiol reactive groups/g dried gel
	(μ moles SH/g dried gel)	%	
SH-gel (starting point)	712	100	0
TSI-gel	<10	–	388
Regenerated SH-gel (after TSI gel) ^a	683	96	0
TS-gel	<10	–	382
Regenerated SH-gel (after TS-gel) ^a	370	52	0

^aThe regeneration was carried out after glutathione immobilization

Table 5
Reuse of TSI-Gel

Step	Gel bound SH groups (μ mol SH/g dried gel)	Thiol-reactive groups (μ mol/g dried gel)	Bound BSA (mg/g dried gel)
SH-gel	1,027	–	–
TSI-gel (first use)	0	415	133
TSI-BSA derivative, after DTT	1,083	0	5
TSI-gel (third use) ^a	0	545	132
TSI-BSA derivative after DTT	–	0	19

^aAfter each use, elution was carried out and then the gel was regenerated

order to determine the synthesized β -cyclodextrin concentration at each interval. The slope of the curve synthesized β -cyclodextrin concentration vs time gives the rate of the reaction allowing the determination of the EU/mL.

35. Stability and half life of CGTase is able to be increased by addition of CaCl_2 in the activity buffer.
36. The BCA Protein Assay combines the Biuret assay with the highly sensitive and selective colorimetric detection of the cuprous cation (Cu^{1+}) by bicinchoninic acid. The first step involves the chelation of copper with protein in an alkaline environment to form a light blue complex. In the second step

bicinchoninic acid (BCA) reacts with the reduced (cuprous) cation that was formed in **step 1**. The BCA/copper complex exhibits a strong linear absorbance at 562 nm with increasing protein concentrations.

37. Since *Bacillus* CGTases have one disulfide bridge [30] in order to increase the SH content, the enzyme is reduced with DTT.
38. The optimal conditions for the reduction of the enzyme are 30 min incubation with 100 mM DTT in 100 mM potassium phosphate buffer pH 8.0. These conditions allow a twofold increase in enzyme SH group content with a slight decrease in the specific activity (data not shown).
39. DTNB is known as the Ellman's reagent, it readily undergoes the thiol-disulfide interchange reaction in the presence of a free thiol, giving a TNB dianion with a relatively intense absorbance at 412 nm (Molar absorption coefficient $13.6 \times 10^3 \text{ M}^{-1}\text{cm}^{-1}$). Since the stoichiometry of protein thiol to TNB formed is 1:1, TNB formation can be used to assess the number of thiols present.
40. Prepacked and disposable desalting columns containing Sephadex® G-25 Medium for group separation of high ($M_r > 5,000$) from low molecular weight substances.
41. Since CGTase from *Thermoanaerobacter* contains 23 Lys residues [31], its chemical modification by thiolation with a heterobifunctional reagent (SPDP) is attempted in order to increase reactivity towards thiol-reactive adsorbents.
42. The number of thiol groups introduced grows remarkably with increasing SPDP/protein molar ratio (*see* Table 6). The optimal conditions for the thiolation process of the enzyme, which allow an eightfold increase in SH group content without affecting the specific activity, are 30 min incubation with a SPDP/protein molar ratio of 100 in 50 mM sodium phosphate pH 6.8, 0.15 M NaCl (Table 6).

Table 6
Thiolation of CGTase From *Thermoanaerobacter* sp.

Molar ratio (SPDP/prot)	Incubation time (min)	$\frac{\text{SH}_{\text{thiolated enzyme}}}{\text{SH}_{\text{native enzyme}}}$	Specific activity (EU/mg)
0	30	1.0	29
3	30	1.2	29
100	30	8.0	29
0	60	1.0	29
44	60	4.5	29
100	60	8.0	26

Table 7
Dependence on the conditions for the batchwise immobilization of CGTase onto TSI-agarose

Enzyme	Enzyme load (mg prot/g suction dried gel)	pH	Phosphate buffer conc (mM)	NaCl (M)	Immobilized protein (%) ^a	Expressed activity (%) ^b	Coupling efficiency (%) ^c
Native	0.3	7.0	50	0	0	0	
Thiolated ^d	0.3	6.8	50	0	52	40	80
	0.3	6.8	50	0.15	89	80	100
	0.3	6.8	200	0.15	87	60	74
	0.3	6.8	1000	0.15	90	25	40
	0.3	7.0	50	0	38	40	100
	0.3	7.0	50	0.15	88	80	100
	1.2	6.8	50	0.15	78	40	52
	2.4	6.8	50	0.15	84	27	40
	6.0	6.8	50	0.15	Nd ^e	7	25
	2.4	7.5	50	0.15	80	23	40

^aEstimated on the basis of the difference between the amount of protein applied and that remaining in supernatants and washings

^bDefined as: $(EU_{\text{expressed on the gel}}) \times 100 / (EU_{\text{applied}})$

^cDefined as: $(EU_{\text{expressed on the gel}}) \times 100 / (EU_{\text{applied}} - EU_{\text{recovered in supernatants and washings}})$

^dCGTase thiolated under optimal conditions, e.g.: $(SH_{\text{thiolated enzyme}} / SH_{\text{native enzyme}}) = 8.0$

^eNd = not determined

43. In CGTase from *Thermoanaerobacter* sp. it was possible to detect the presence of a low level of free SH groups, but they were not reactive towards thiol reactive supports (*see* Table 7).
44. The reduced enzyme showed no reactivity towards thiol-sulfinate-agarose since no covalent immobilization was achieved (data not shown).
45. Thiolation process dramatically improves the immobilization yield, from 0 % for the native enzyme up to nearly 90 % for the thiolated enzyme under the optimized conditions. Higher immobilization yields are achieved in the pH range 6.8–7.0. Ionic strength is a critical parameter since nearly a 3.5-fold decrease in the expressed activity is achieved when phosphate concentration changes from 50 to 1,000 mM. An almost two-fold increase in the percentage of immobilized protein in the presence of 0.15 M NaCl is also observed (*see* Table 7).
46. The percentage of gel-bound protein remained almost unchanged (between 78 and 90 %) for all the enzyme loads assessed (*see* Table 7); however, expressed activity varied, ranging from 80 to 7 % (for the lowest and highest loads, respectively).

47. The optimized conditions for the covalent reversible immobilization of CGTase from *Thermoanaerobacter* sp. onto thiol-sulfinate-agarose were: incubation of 0.3 mg of thiolated enzyme per gram of suction dried gel in 50 mM phosphate, pH 6.8–7.0, 0.15 M NaCl, at 22 °C for 24 h.
48. The CGTase derivative shows good stability under the assayed conditions, keeping almost 90 % of its initial activity after five reuses performed along 12 days.
49. More than 80 % of the total immobilized activity is eluted by 100 mM DTT in sodium phosphate, pH 8.0.

References

1. Batista-Viera F, Carlsson J, Rydén L (2011) Covalent chromatography. In: Janson JC (ed) Protein purification: principles: high-resolution methods, and applications, 3rd edn. Wiley-VCH, New York, NY, pp 203–219
2. Carlsson J, Axén R, Brocklehurst K, Crook E (1974) Immobilization of urease by thiol-disulphide interchange with concomitant purification. *Eur J Biochem* 44:189–194
3. Oscarsson S, Porath J (1989) Covalent chromatography and salt-promoted thiophilic adsorption. *Anal Biochem* 176:330–337
4. Carlsson J, Batista-Viera F (1991) Solid phase disulfide oxides: a new approach to reversible immobilization and covalent chromatography of thiol compounds. *Biotechnol Appl Biochem* 14:114–120
5. Batista-Viera F, Barbieri M, Ovsejevi K, Manta C, Carlsson J (1991) A new method for reversible immobilization of thiol biomolecules based on solid phase bound thiol-sulfonate groups. *Appl Biochem Biotechnol* 31:175–195
6. Batista-Viera F, Manta C, Carlsson J (1994) Solid-phase thiol-sulfonates for the reversible immobilization of thiols. *Appl Biochem Biotechnol* 44:1–14
7. Batista-Viera F, Manta C, Carlsson J (1996) Covalent binding of thiols to thiol-sulfinate-containing supports. *Biotechnol Appl Biochem* 24:231–239
8. Axén R, Drevin H, Carlsson J (1975) Preparation of modified agarose gels containing thiol groups. *Acta Chem Scand B29*:471–474
9. Ovsejevi K, Brena B, Batista-Viera F, Carlsson J (1995) Immobilization of *E. coli* β -galactosidase on thiol-sulfonate agarose. *Enzyme Microb Technol* 17:151–156
10. Puhl AC, Giacomini C, Irazoqui G, Batista-Viera F, Villarino A, Terenzi H (2009) Covalent immobilization of tobacco-etch-virus NIa protease: a useful tool for cleavage of the histidine tag of recombinant proteins. *Biotechnol Appl Biochem* 53:165–174
11. Ovsejevi K, Grazú V, Batista-Viera F (1998) β -galactosidase from *Kluyveromyces lactis* immobilized on to thiol-sulfinate/thiol-sulfonate supports for lactose hydrolysis in milk and dairy by-products. *Biotechnol Tech* 12:143–148
12. Grazú V, Ovsejevi K, Cuadra K, Betancor L, Manta C, Batista-Viera F (2003) Solid phase reducing agents as alternative for reducing disulfide bonds in proteins. *Appl Biochem Biotechnol* 110:23–32
13. Ovsejevi K, Cuadra K, Batista-Viera F (2009) Development of a continuous solid phase process for reduction and thiol-dependent immobilization of yeast β -galactosidase. *J Mol Catal B Enzymatic* 57:188–193
14. Brena B, Lidholm J, Batista-Viera F, Carlsson J (1998) Selective removal of enzymes from substrate and products. An alternative to immobilization for enzymes acting on macromolecular or solid substrates. *Appl Biochem Biotechnol* 75:323–341
15. Giacomini C, Irazoqui G, Batista-Viera F, Brena B (2007) Chemical thiolation strategy: a determining factor in the properties of thiol-bound biocatalysts. *Biocatal Biotransform* 25:373–381
16. Carlsson J, Axén R, Unge T (1975) Reversible, covalent immobilization of enzymes by thiol-disulphide interchange. *Eur J Biochem* 59:567–572
17. Brena B, Ovsejevi K, Luna B, Batista-Viera F (1993) Thiolation and reversible immobilization of sweet potato beta-amylase on thiol-sulfonate-agarose. *J Mol Catal* 84:381–390
18. Díaz T, Stahl U, Batista-Viera F, Carlsson J (1995) Reversible immobilization of chemically modified pullulanase. *Biotechnol Tech* 9:533–538
19. Viera SE, Batista-Viera F, Ovsejevi K (2012) Development and characterization of a solid

- phase biocatalyst based on cyclodextrin glucantransferase reversibly immobilized onto thiolsulfinate-agarose. *Appl Biochem Biotechnol* 167:164–176
20. Persson M, Bülow L, Mosbach K (1990) Purification and site-specific immobilization of genetically engineered glucose dehydrogenase on thiopropyl-sepharose. *FEBS Lett* 270: 41–44
 21. Grazú V, López-Gallego F, Montes T, Abian O, González R, Hermoso JA, García JL, Mateo C, Guisán JM (2010) Promotion of multipoint covalent immobilization through different regions of genetically modified penicillin G acylase from *E. coli*. *Process Biochem* 45:390–398
 22. Irazoqui G, Villarino A, Batista-Viera F, Brena B (2002) Generating favorable nano-environments for thermal and solvent stabilization of immobilized β -galactosidase. *Biotechnol Bioeng* 77:430–434
 23. Brocklehurst K, Carlsson J, Kierstan M, Crook E (1973) Covalent chromatography. Preparation of fully active papain from dried papaya latex. *Biochem J* 133:573–584
 24. Worthington V (1993) β -galactosidase. In *Worthington enzyme manual*, Freehold, NJ, p 179
 25. Ellman GL (1958) A colorimetric method for determining low concentrations of mercaptans. *Arch Biochem Biophys* 74:443–450
 26. Vikmon M (1982) Rapid and simple spectrophotometric method for determination of microamounts of cyclodextrins. In: Szejtli J (ed) *First symp on cyclodextrins*. Reidel Publishing, Budapest, Hungary, pp 69–74
 27. Smith PK, Khron RI, Hermanson GT, Mallia AK, Gartner FH, Provenzano MD, Fujimoto EK, Goeke NM, Olson B:J, Klenk DC (1985) Measurement of protein using bicinchoninic acid. *Anal Biochem* 150:76–85
 28. MERCK Schuchardt technical information (1988) *A versatile new peroxyacid*. Magnesium monoperoxyphthalate MS Info 88–1
 29. Ali M, Stevens W (1997) A facile and selective procedure for oxidation of sulfides and sulfoxides on silica gel supported magnesium monoperoxyphthalate (MMPP) in dichloromethane. *Synthesis* 7:764–768
 30. Costa H, Del Canto S, Ferrarotti S, Biscoglio M (2009) Structure-function relationship in cyclodextrin glycosyltransferase from *Bacillus circulans* DF 9R. *Carbohydr Res* 344:74–79
 31. Alcalde M, Plou FJ, Andersen C, Martin MT, Pedersen S, Ballesteros A (1999) Chemical modification of lysine side chains of cyclodextrin glycosyltransferase from *Thermoanaerobacter* causes a shift from cyclodextrin glycosyltransferase to α -amylases specificity. *FEBS Lett* 445: 333–337

Immobilization of *Candida rugosa* Lipase on Superparamagnetic Fe₃O₄ Nanoparticles for Biocatalysis in Low-Water Media

Joyeeta Mukherjee, Kusum Solanki, and Munishwar Nath Gupta

Abstract

A simple immobilization method for *Candida rugosa* lipase on superparamagnetic Fe₃O₄ nanoparticles is described. The Fe₃O₄ nanoparticles were coated with PEI and *Candida rugosa* lipase was adsorbed on these particles via electrostatic interactions. The immobilization resulted in marginal simultaneous purification. However, the immobilized preparation showed 110× higher transesterification activity in low-water media. It was also efficient in kinetic resolution of (±)-1-phenylethanol with ee_p of 99 % and *E*=412 within 24 h.

Key words Iron oxide nanoparticles, Lipase, Enzyme immobilization, Lipase adsorption, Nonaqueous enzymology, Kinetic resolution, Transesterification reaction, Nanoparticles as immobilization support, Superparamagnetic particles

1 Introduction

Preparation of bioconjugates of proteins with nanomaterials has generated considerable interest in recent years [1, 2]. Magnetic nanoparticles of Fe₃O₄ (especially with <30 nm diameter) in particular seem to offer many advantages as support materials for proteins. These include the following: (1) large surface to volume ratio (as is the case with any nanomaterial); (2) biocompatibility [3]; (3) superparamagnetic nature (when size is <30 nm diameter) [4, 5]. This property means that these particles show Brownian motion but cluster together in the presence of an external magnetic field; (4) Just like micron sized Fe₃O₄ particles, the possibility of separation by magnetism makes such materials an excellent support for designing biocatalysts for use in viscous medium [6, 7]. Like on any other matrix, both covalent and non covalent methods have been employed for immobilization on Fe₃O₄ nanoparticles [8, 9]. With covalent methods, there is a risk of modifying those

Table 1
Adsorption and purification of *Candida rugosa* lipase on iron oxide nanoparticles

Nanoparticle on which lipase is adsorbed	Total protein bound (μg)	Total activity bound (U)	Specific activity (U/mg protein)
Iron oxide	23.1	12	519
Tween 80 modified iron oxide	29.4	13	442
Oleic acid modified iron oxide	28.0	11	393
Stearic acid modified iron oxide	39.9	12	300
PEI modified iron oxide	19.6	13	663

The total activity added was 16.3 U and specific activity of this preparation was 233 U/mg protein. The experiments were done in duplicates and average of the two is reported. The difference between each set of readings was within 4 %. [Reproduced by permission from The Royal Society of Chemistry (RSC) on behalf of the Centre National de la Recherche Scientifique (CNRS) and the RSC]

side chains on the protein which are essential for biological activity. Such predicaments have been expectedly observed [10, 11]. Efforts to use non covalent methods have also been described [12, 13]. Recently, we have reported that Fe_3O_4 particles coated by PEI can bind to *Candida rugosa* lipase [14]. Given the zeta potential on the particles (+22.1 mV) and the enzyme (−11.9 mV) at the adsorption pH, electrostatic interactions undoubtedly played an important role in excellent binding capacity of the particles (see Table 1). This binding was somewhat specific and hence was accompanied by increase in specific activity of lipase (see Table 1).

Enzymes in low-water media are known to display several advantages which have been frequently discussed [15–17]. Immobilization of the enzymes for use in such media offers the additional benefit of spreading the enzyme over a larger surface in view of the fact that this is a case of heterogeneous catalysis [18, 19]. In that respect, nanoparticles (with their large surface to volume ratio) are especially attractive.

Candida rugosa lipase has a molecular lid covering its active site [20, 21]. It is very likely that binding to the PEI coated surface also results in opening of the lid and is partly responsible for considerable enhancement of biological activity of the immobilized lipase in nonaqueous media (see Table 2).

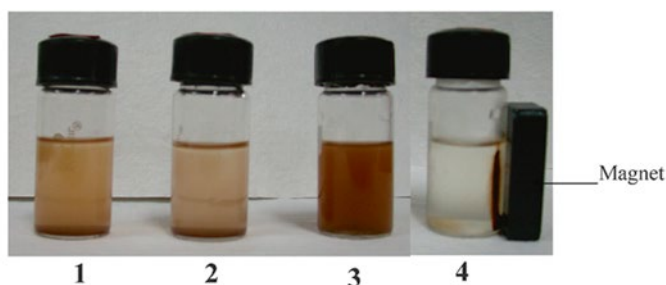
The coating of the particles followed by binding of the enzymes did not abolish the superparamagnetic nature of the nanoparticles (see Fig. 1). Recently, a CD accessory has been described which allows recording of CD of suspensions by spinning the cuvette holding the sample [22, 23]. This is a valuable tool to look at structural changes in protein upon immobilization [24]. CD spectra of the free lipase solution and suspension of the lipase

Table 2

Initial rates of transesterification of ethyl butyrate by butanol catalyzed by *Candida rugosa* lipase immobilized on modified iron oxide nanoparticles

Nanoparticle on which lipase is adsorbed	Initial rates (nmol/mg/min)	Fold increase
Straight out of the bottle	0.1	1
Unmodified Iron oxide	4.5	45
Tween 80 modified iron oxide	6.8	68
Oleic acid modified iron oxide	6.7	67
Stearic acid modified iron oxide	2.0	20
PEI modified iron oxide	11.0	110

Initial rates were calculated from the aliquots taken within 30–120 min. The percentage conversions during these time periods were in the range of 1–25 % and were in the linear range. All the experiments were carried out in duplicates and average of the two is reported. The difference between each set of readings was within 5 %. [Reproduced by permission from The Royal Society of Chemistry (RSC) on behalf of the Centre National de la Recherche Scientifique (CNRS) and the RSC]



- 1) Lipase immobilized on iron oxide nanoparticles
- 2) Lipase immobilized on oleic acid coated iron oxide nanoparticles
- 3) Lipase immobilized on PEI coated iron oxide nanoparticles
- 4) Lipase immobilized on PEI coated iron oxide nanoparticles attracted by a magnet.

Fig. 1 Dispersion of lipase immobilized on different modified iron oxide nanoparticles in aqueous media: *Candida rugosa* lipase (10 mg) was immobilized on different nanoparticles (5 mg) and suspended in 50 mM phosphate buffer (pH 7.0). [Reproduced by permission from The Royal Society of Chemistry (RSC) on behalf of the Centre National de la Recherche Scientifique (CNRS) and the RSC]

immobilized on PEI coated Fe_3O_4 particle is shown in Fig. 2. CD spectra show that no significant changes in the secondary structure content of lipases took place as a result of this immobilization. This is in agreement with the high activity displayed by the lipase preparation in low-water media [14].

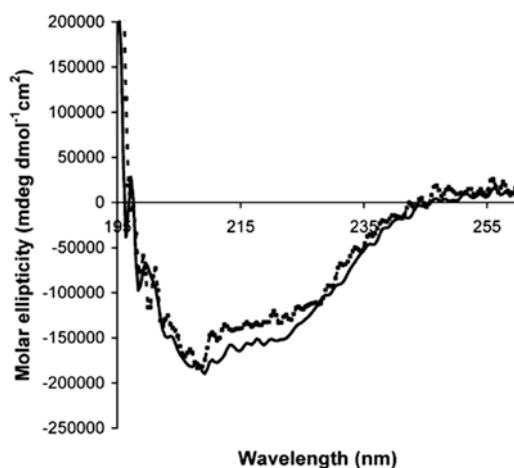


Fig. 2 Far UV CD spectra of *Candida rugosa* lipase straight out of the bottle (*solid line*) and immobilized on PEI coated iron oxide nanoparticles (*dotted line*). [Reproduced by permission from The Royal Society of Chemistry (RSC) on behalf of the Centre National de la Recherche Scientifique (CNRS) and the RSC]

The enzymes in low-water media have also been extensively used for kinetic resolution of the racemic preparation of organic compounds [25–27]. Kinetic resolution of 1-phenylethanol has often been used as a model system to evaluate the process efficiency [28, 29]. The use of immobilized lipase resulted in resolution of (\pm)-1-phenylethanol with $ee_p = 99\%$ with $E = 412$ in a reasonable time of 24 h. It is noteworthy that the free commercial preparation did not show any significant conversion during this period.

The protocol for the immobilization on Fe_3O_4 particles described here is one of the simplest available in the literature [14] and yet it results in an extremely efficient biocatalyst design both for the synthesis and kinetic resolution in low-water media.

2 Materials

2.1 Assay of *Candida rugosa* Lipase Activity

1. *Candida rugosa* lipase (Amano Enzyme Inc., Nagoya, Japan).
2. *p*-Nitrophenylpalmitate (*p*-NPP) (Sigma Chemical Co., St. Louis, USA) (*see Note 1*).
3. Buffer 1: 0.1 M sodium phosphate buffer, pH 7.0.
4. Buffer 2: 0.1 M sodium phosphate buffer, pH 7.0 containing 0.15 M NaCl and 0.5 % (v/v) Triton X-100.
5. Acetonitrile (anhydrous grade, Sigma Aldrich, St. Louis, USA).
6. Milli-Q water.

2.2 Synthesis of Iron Oxide Nanoparticles and Lipase Immobilization

1. Ferrous chloride ($\text{FeCl}_2 \cdot 4\text{H}_2\text{O}$) and Ferric chloride ($\text{FeCl}_3 \cdot 6\text{H}_2\text{O}$) (Merck, Mumbai, India) (*see Note 2*).
2. Deoxygenated Milli-Q water (*see Note 3*).
3. Polyethyleneimine (PEI) (Sigma Chemical Co., St. Louis, USA).
4. Fatty acids: oleic acid, lauric acid, stearic acid.
5. Tween 80.

2.3 Transesterification Reaction

1. Ethyl butyrate (Sigma Chemical Co., St. Louis, USA) (*see Note 4*).
2. *n*-Butanol (Sigma Chemical Co., St. Louis, USA) (*see Note 4*).
3. *n*-Hexane (Anhydrous grade with water content less than 0.001, Sigma Chemical Co., St. Louis, USA) (*see Note 4*).

2.4 Kinetic Resolution of (\pm)-1-Phenylethanol (See Note 4)

1. (\pm)-1-phenylethanol (Merck, Hohenbrunn, Germany).
2. Vinyl acetate (Merck, Hohenbrunn, Germany).

3 Methods

3.1 Assay of *Candida rugosa* Lipase Activity [30]

1. Weigh 10 mg of lipase and dissolve it in 10 ml of buffer 1. Incubate the enzyme sample (solution containing 1–10 μg of enzyme) in a reaction mixture containing 1.8 ml of buffer 2 and 20 μl of 0.05 M *p*-NPP in acetonitrile at 37 °C for 30 min (*see Note 1*).
2. Quench the reaction after 30 min of incubation by irradiating it with microwaves for 30 s (*see Note 5*).
3. Read the absorbance of liberated *p*-nitrophenol at 410 nm. One unit enzyme liberates one micromole of *p*-nitrophenol in 1 min at 37 °C, pH 7.0.
4. For estimating the amount of lipase adsorbed onto the nanoparticles, apply external magnetic fields to the vial containing nanoparticle and lipase suspension (Fig. 1 [4]). Collect supernatant after all the nanoparticles separate from the solution. Wash the nanoparticles thrice with buffer 1. Then determine unadsorbed lipase in supernatant and washes (*see Table 1*).

3.2 Synthesis of Iron Oxide Nanoparticles [31]

1. Prepare 90 ml of solution containing 1.28 M $\text{FeCl}_3 \cdot 6\text{H}_2\text{O}$ and 0.64 M $\text{FeCl}_2 \cdot 4\text{H}_2\text{O}$ in deoxygenated Milli-Q water at room temperature. Add 10 ml of 10 M NaOH to it under vigorous shaking conditions so that the final concentration of NaOH becomes 1 M (*see Note 3*). Wash the nanoparticles thus formed with Milli-Q water, ethanol and acetone to remove unreacted reagents.

2. For coating the nanoparticles with fatty acid/Tween 80, incubate the nanoparticles with 1 M fatty acid (oleic acid, stearic acid, lauric acid) in deoxygenated Milli-Q water at 80 °C, 250 rpm for 4 h. Wash the coated nanoparticles with Milli-Q water (*see Note 6*).
3. Incubate the lauric acid coated magnetic nanoparticles with 25 ml of 8 % (v/v) solution of PEI in 50 % (v/v) in methanol. Keep it at 80 °C under vigorous shaking overnight. Wash with water, ethanol and acetone (*see Note 7*).

3.3 Lipase Immobilization on Nanoparticles

1. Suspend 5 mg (dry weight) of nanoparticles in 5 ml of Buffer 1 containing 10 mg of *Candida rugosa* lipase. Disperse the nanoparticles by sonicating for 1 min at 40 kHz and at 70 W power rating. Incubate the mixture at 4 °C with shaking at 200 rpm for 10 h (*see Note 8*).
2. With the help of a magnet, separate lipase bound nanoparticles from the supernatant. Determine amount of protein and enzyme activity present in the supernatant and calculate amount of lipase bound to the nanoparticles (*see Table 1*).

3.4 Transesterification Reaction Catalyzed by Immobilized Lipase [32]

1. In a 10 ml vial, take 1 ml of anhydrous *n*-hexane as a solvent and add substrates ethyl butyrate (60 mM) and *n*-butanol (120 mM) (*see Note 4*). Add 1 mg of free lipase/1 mg of lipase adsorbed on nanoparticles. Sonicate for 10 min (water in the ultrasonicator bath was replaced with cold water in between the sonication so as to avoid heating due to sonication) to disperse the nanoparticles at 40 kHz and at 70 W power rating.
2. Incubate the reaction mixture at 37 °C at 200 rpm.
3. Take aliquots at different time points and analyze for the product formation by GC (*see Note 9*, Table 2).

3.5 Kinetic Resolution of (±)-1-Phenylethanol [28]

1. In a 10 ml vial, take 1 ml of anhydrous *n*-hexane as a solvent and add substrates (±)-1-phenylethanol (1 mmol) and vinyl acetate (1 mmol) (*see Note 4*). Add 1 mg of free lipase/1 mg of lipase adsorbed on nanoparticles. Sonicate for 10 min to disperse the nanoparticles at 40 kHz and at 70 W power rating.
2. Incubate the reaction mixture at 37 °C at 200 rpm.
3. Take aliquots at different time points and analyze for the product formation (*see Table 3*) by HPLC using chiralcel OD-RH column (Diacel, Japan) (*see Notes 10 and 11*).

Table 3
Kinetic resolution of 1-phenylethanol by transacetylation with vinyl acetate using *Candida rugosa* lipase immobilized on nanoparticles

Nanoparticle on which lipase is adsorbed	Total conversion after 24 h (%)	ee _p (%)	E
Straight out of the bottle	2	–	–
Unmodified Iron oxide	19	71	7
Oleic acid modified iron oxide	19	75	8
Stearic acid modified iron oxide	28	40	3
PEI modified iron oxide	41	99	412

All experiments were carried out in duplicates and the results within each pair differed by <5 %. [Reproduced by permission from The Royal Society of Chemistry (RSC) on behalf of the Centre National de la Recherche Scientifique (CNRS) and the RSC]

4 Notes

1. *p*-NPP hydrolyzes in presence of light. It should be weighed in a light protected vial. The *p*-NPP does not dissolve in acetonitrile at room temperature so suspension needs to be warmed in order to get a clear solution. The incubation of samples after adding enzyme should also be done in dark.
2. Gloves and goggles must be worn at all times. The Fe²⁺ chloride salt is toxic, corrosive, and a mutagen. The Fe³⁺ chloride salt (iron (III) chloride, ferric chloride, or FeCl₃) is corrosive.
3. Milli-Q water is deoxygenated by bubbling nitrogen for 1 h prior to use. Nitrogen gas not only protects oxidation of nanoparticles but also reduces the particle size. The chemical reaction of Fe₃O₄ precipitation is as follows:



A complete precipitation of Fe₃O₄ should be expected between pH 7.5–14 while maintaining a molar ratio of Fe²⁺:Fe³⁺ = 1:2 under nonoxidizing environment.

4. The organic solvents are further dried by shaking them overnight with 3 Å molecular sieves in a closed vial and then storing under these conditions only.
5. The samples should be kept in a domestic oven along with a beaker containing a volume of water sufficient to make the total volume of the liquid in the cavity as 100 ml. As additional water absorbs a significant amount of microwave energy, overheating of the samples is avoided.

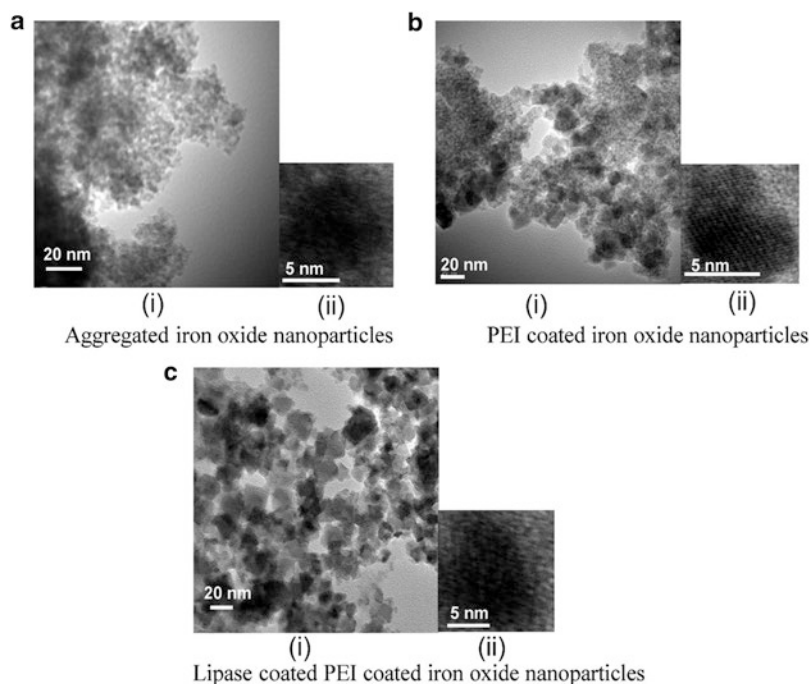


Fig. 3 HRTEM micrographs of (a*i*) Fe_3O_4 nanoparticles, (b*i*) PEI coated Fe_3O_4 nanoparticles, (c*i*) Lipase adsorbed on PEI coated Fe_3O_4 nanoparticles. (a*ii*), (b*ii*), and (c*ii*) are the atomic lattice fringes corresponding to the nanoparticles. [Reproduced by permission from The Royal Society of Chemistry (RSC) on behalf of the Centre National de la Recherche Scientifique (CNRS) and the RSC]

6. 1 M solution of oleic acid is prepared by adding oleic acid in small amount, letting each installment dissolve and maintaining its pH at 10 by adding 1 M NaOH solution and then adding the next lot.
7. The coating of iron oxide nanoparticles with PEI and immobilization of lipase on it leads to change in its properties like dispersion in aqueous media (*see* Fig. 1), aggregation behavior (*see* Fig. 3) and zeta potential (*see* Table 4). The nanoparticles synthesized were about 5 nm in diameter as measured by HRTEM and they were in the aggregated form (*see* Fig. 3a). Coating them with PEI did not result in substantial increase in their size and it still remained aggregated due to bridging aggregation [14]. However, on coating the PEI- Fe_3O_4 nanoparticles with lipase, aggregation was not observed as seen in the TEM micrograph (*see* Fig. 3c) and the size of the particles was about 10 nm. Figure 3a(ii), b(ii), c(ii) show the atomic lattice fringes corresponding to the nanoparticles and they clearly indicate that the nanoparticles are crystalline.
8. Physical adsorption of proteins on matrices by ionic, hydrophobic or affinity interactions often results in retention of secondary structure in proteins (*see* Fig. 2).

Table 4
Zeta potential values of different iron oxide nanoparticles at pH 7.0

	Zeta potential (mV)
Iron oxide nanoparticles	-16.4
PEI coated iron oxide nanoparticles	+22.1
<i>Candida rugosa</i> lipase solution	-11.9
<i>Candida rugosa</i> lipase coated iron oxide nanoparticles	-20.9
<i>Candida rugosa</i> lipase coated PEI modified iron oxide nanoparticles	-5.0

Reproduced by permission from The Royal Society of Chemistry (RSC) on behalf of the Centre National de la Recherche Scientifique (CNRS) and the RSC

9. The alkyl esters are analyzed on Agilent Technologies 6890 network GC systems, USA with flame ionization detector. The capillary column used for separation of ethyl butyrate (substrate) from butyl butyrate (product) was EQUITY™-5 (30 m × 0.32 mm × 0.25 μm film thickness, Supelco, Bellefonte, USA). The column oven temperature is programmed in the range of 150–250 °C at 10 °C/min with injector and detector temperatures at 240 °C and 250 °C, respectively.
10. The eluent for HPLC consists for 96.5 % (v/v) *n*-hexane, 3 % (v/v) propane-2-ol and 0.5 % (v/v) ethanol with flow rate of 1 ml/min and detection is carried out with a UV detector at 254 nm [28].
11. The enantiomeric excess values the enantioselectivity are calculated using Chen's equation [33].

$$E = \ln[1 - c(1 + ee_p)] / \ln[1 - c(1 - ee_p)]$$

“*c*” is the degree of conversion which is calculated using the following expression:

$$C = \text{product concentration} / (\text{unreacted substrate concentration} + \text{product concentration})$$

Acknowledgments

Financial support from the Department of Science and Technology (DST-SERB) [Grant No.: SR/SO/BB-68/2010], the Department of Biotechnology (DBT) [Grant Number: BT/PR14158/NNT/28/484/2010], and Council for Scientific and Industrial Research (CSIR), all Government of India organizations, is gratefully acknowledged.

References

1. Reukov V, Maximov V, Vertegel A (2010) Proteins conjugated to poly(butyl cyanoacrylate) nanoparticles as potential neuroprotective agents. *Biotechnol Bioeng* 108:243–252
2. Ren Y, Rivera JG, He L, Kulkarni H, Lee DK, Messersmith PB (2011) Facile, high efficiency immobilization of lipase enzyme on magnetic iron oxide nanoparticles via a biomimetic coating. *BMC Biotechnol* 11:63–70
3. Safarik I, Pospiskova K, Horska K, Safarikova M (2012) Potential of magnetically responsive (nano)biocomposites. *Soft Matter* 8: 5407–5413
4. Mikhaylova M, Kim DK, Bobrysheva N, Osmolowsky M, Semenov V, Tsakalakos T, Muhammed M (2004) Superparamagnetism of magnetite nanoparticles: dependence on surface modification. *Langmuir* 20: 2472–2477
5. Kim J, Grate JW, Wang P (2008) Nanobiocatalysis and its potential applications. *Trends Biotechnol* 26:639–646
6. Safarik I, Safarikaova M (2004) Magnetic techniques for the isolation and purification of proteins and peptides. *Biomagn Res Technol* 2:7–24
7. Safarik I, Safarikova M (2009) Magnetic nano- and microparticles in biotechnology. *Chem Papers* 63:497–505
8. Wu W, He Q, Chiang C (2008) Magnetic iron oxide nanoparticles: synthesis and surface functionalization strategies. *Nanoscale Res Lett* 3:397–415
9. Gupta MN, Kaloti M, Kapoor M, Solanki K (2011) Nanomaterials as matrices for enzyme immobilization. *Artif Cells Blood Substit Immobil Biotechnol* 39:98–108
10. Dyal A, Loos K, Noto M, Chang SW, Spagnoli C, Shafi KVPM, Ulman M, Cowman M, Gross RA (2003) Activity of *Candida rugosa* lipase immobilized on γ -Fe₂O₃ magnetic nanoparticles. *J Am Chem Soc* 125:1684–1685
11. Gardimalla HMR, Mandal D, Stevens PD, Yen M, Gao Y (2005) Superparamagnetic nanoparticle-supported enzymatic resolution of racemic carboxylates. *Chem Commun* 35: 4432–4434
12. Huang S-H, Liao M-H, Chen D-H (2003) Direct binding and characterization of lipase onto magnetic nanoparticles. *Biotechnol Prog* 19:1095–1100
13. Bai S, Guo Z, Liu W, Sun Y (2006) Resolution of (\pm)-menthol by immobilized *Candida rugosa* lipase on superparamagnetic nanoparticles. *Food Chem* 96:1–7
14. Solanki K, Gupta MN (2011) Simultaneous purification and immobilization of *Candida rugosa* lipase on superparamagnetic Fe₃O₄ nanoparticles for catalyzing transesterification reactions. *New J Chem* 35:2551–2556
15. Mattiasson B, Adlercreutz P (1991) Tailoring the microenvironment of enzymes in water-poor systems. *Trends Biotechnol* 9:394–398
16. Gupta MN (1992) Enzyme function in organic solvents. *Eur J Biochem* 203:25–32
17. Halling PJ (2000) Biocatalysis in low-water media: understanding effects of reaction conditions. *Curr Opin Chem Biol* 4:74–80
18. Adlercreutz P (2006) Immobilization of enzymes for use in organic media. In: Guisan JM (ed) *Immobilization of enzymes and cells. Methods in Biotechnology*, vol 2. Humana Press, Towota, NJ, pp 251–256
19. Mateo C, Palomo JM, Fernandez-Lorente G, Guisan JM, Fernandez-Lafuente R (2007) Improvement of enzyme activity, stability and selectivity via immobilization techniques. *Enzyme Microb Tech* 40:1451–1463
20. Palomo JM, Munoz G, Fernandez-Lorente G, Mateo C, Fernandez-Lafuente R, Guisan JM (2002) Interfacial adsorption of lipases on very hydrophobic support (Octadecyl-Sephabeads): immobilization, hyperactivation and stabilization of the open form of lipases. *J Mol Catal B: Enzym* 19–20:279–286
21. De Maria PD, Sanchez-Montero JM, Sinisterra JV, Alcantara AR (2006) Understanding *Candida rugosa* lipases: an overview. *Biotechnol Adv* 24:180–196
22. Ganesan A, Price NC, Kelly SM, Petry I, Moore BD, Halling PJ (2006) Circular dichroism studies of subtilisin Carlsberg immobilized on micron sized silica particles. *Biochim Biophys Acta* 1764:1119–1125
23. Ganesan A, Moore BD, Kelly SM, Price NC, Rolinski OJ, Birch DJS, Dunkin IR, Halling PJ (2009) Optical spectroscopic methods for probing the conformational stability of immobilised enzymes. *Chemphyschem* 10:1492–1499
24. Solanki K, Gupta MN, Halling PJ (2012) Examining structure–activity correlations of some high activity enzyme preparations for low water media. *Bioresour Technol* 115:147–151
25. Hudson EP, Eppler RK, Clark DS (2005) Biocatalysis in semi-aqueous and nearly anhydrous conditions. *Curr Opin Biotechnol* 16: 637–643
26. Majumder AB, Shah S, Gupta MN (2007) Enantioselective transacetylation of (R, S)- β -citronellol by propanol rinsed immobilized

- Rhizomucor miehei lipase. Chem Cent J 1:10–14
27. Shah S, Gupta MN (2007) Kinetic resolution of (\pm)-1-Phenylethanol in [Bmim][PF₆] using high activity preparations of lipases. Bioorg Med Chem Lett 17:921–924
 28. Schöfer SH, Kaftzik N, Wasserscheid P, Kragl U (2001) Enzyme catalysis in ionic liquids: lipase catalysed kinetic resolution of 1-phenylethanol with improved enantioselectivity. Chem Commun 425–426
 29. Lozano P, Diego TD, Larnicol M, Vaultier M, Iborra JL (2006) Chemoenzymatic dynamic kinetic resolution of *rac*-1-phenylethanol in ionic liquids and ionic liquids/supercritical carbon dioxide systems. Biotechnol Lett 28:1559–1565
 30. Jain P, Jain S, Gupta MN (2005) A microwave assisted microassay for lipase. Anal Bioanal Chem 381:1480–1482
 31. Chiang C-L, Sung C-S, Wu T-F, Chen C-Y, Hsu C-Y (2005) Application of superparamagnetic nanoparticles in purification of plasmid DNA from bacterial cells. J Chromatogr B 822:54–60
 32. Shah S, Gupta MN (2008) The effect of ultrasonic pre-treatment on the catalytic activity of lipases in aqueous and non-aqueous media. Chem Cent J 2:1–5
 33. Chen C-S, Fujimoto Y, Girdalukas G, Sih CJ (1982) Quantitative analysis of biochemical kinetic resolution of enantiomers. J Am Chem Soc 104:7294–7299

Immobilization of Enzymes by Bioaffinity Layering

Veena Singh, Meryam Sardar, and Munishwar Nath Gupta

Abstract

Bioaffinity immobilization exploits the affinity of the enzyme to a macro-(affinity ligand). Such a macro-(affinity ligand) could be a lectin, a water-soluble polymer, or a bioconjugate of a water-soluble polymer and the appropriate affinity ligand. Successive layering of the enzyme and the macro-(affinity ligand) on a matrix allows deposition of a large amount of enzyme activity on a small surface. Illustrative protocols show affinity layering of a pectinase and horseradish peroxidase on Concanavalin A-agarose and Concanavalin A-Sephadex matrices, respectively.

Key words Bioaffinity layering, Concanavalin A, Pectinase, Immobilized enzymes, Bioaffinity immobilization

1 Introduction

Bioaffinity immobilization is a gentle method of protein/enzyme immobilization. An excellent account of this approach has been provided by Mattiasson [1]. It essentially consists of binding a protein to an immobilized affinity ligand. The association constant between the protein and the affinity ligand should be high enough so that the protein does not come off the matrix during the use of the biocatalyst [1]. An illustrative protocol for this is also available in the earlier edition of this book [2]. A challenge in the area of enzyme immobilization is to be able to deposit large amount of catalytic activity on a small surface. Layering technique, i.e., depositing layers of the protein with an appropriate macroaffinity ligand sandwiched in between allows one to do that. The macroaffinity ligand chosen for this purpose could be a water soluble polymer having an inherent affinity for the enzyme [3, 4] or could be a lectin [5]. The technique has been successfully demonstrated in a number of cases (*see* Table 1). The first protocol illustrates the affinity layering of a plant pectinase. This tomato pectinase is a Concanavalin A (Con A) binding glycoprotein [6].

Table 1
Enzymes immobilized by affinity layering

Matrix	Layer of affinity ligand	Layer of enzyme	References
Sepharose 4B	Con A	Invertase	[14]
Sepharose 4B	Con A	Glucose oxidase	[14]
Sepharose 4B	Con A	Amyloglucosidase	[14]
Sepharose 4B	Con A	Beta galactosidase	[14]
Sepharose	IgG	Glucose oxidase/HRP	[15]
Cellulose Beads	Con A	Invertase	[16]
Triazine bead cellulose	Con A	Invertase/glucoamylase	[17]
Sephadex	Con A	HRP	[8]
Seralose 4B	Con A	Pectinase	[6]
Cross-linked alginate beads	Alginate	Pectinase	[18]
Iminodiacetate-sepharose 4B	Anti-enzyme antibodies	Glucose oxidase	[19]
Sepharose	Polyclonal antibodies	Glucose oxidase	[20]

Con A covalently bound to an agarose column was used as the immobilization matrix. Successive layers of pectinase and Con A could be created on these beads by bioaffinity immobilization (*see* Fig. 1). Interesting enough, the effectiveness factor of immobilization improves with successive layering (*see* Table 2). Initially, most of the Con A is bound to the interior of the agarose bead. Hence, first layer of the enzyme also binds to the interior of the bead. Mass transfer limitations give poor activity. The successive layers of the enzyme are outside the bead and more accessible.

The second protocol exploits the affinity of the lectin Con A to the sephadex beads. Hence, initial Con A layer is also bound to the matrix by bioaffinity immobilization. Horseradish peroxidase (HRP) is also a well known glycoenzyme having affinity for Con A [7]. Hence, it could be bound to Con A-sephadex bead by bioaffinity immobilization. The successive layers of Con A and HRP could be created just like in protocol I. This affinity layered preparation of HRP was found to be useful in treatment of phenolic waste water [8].

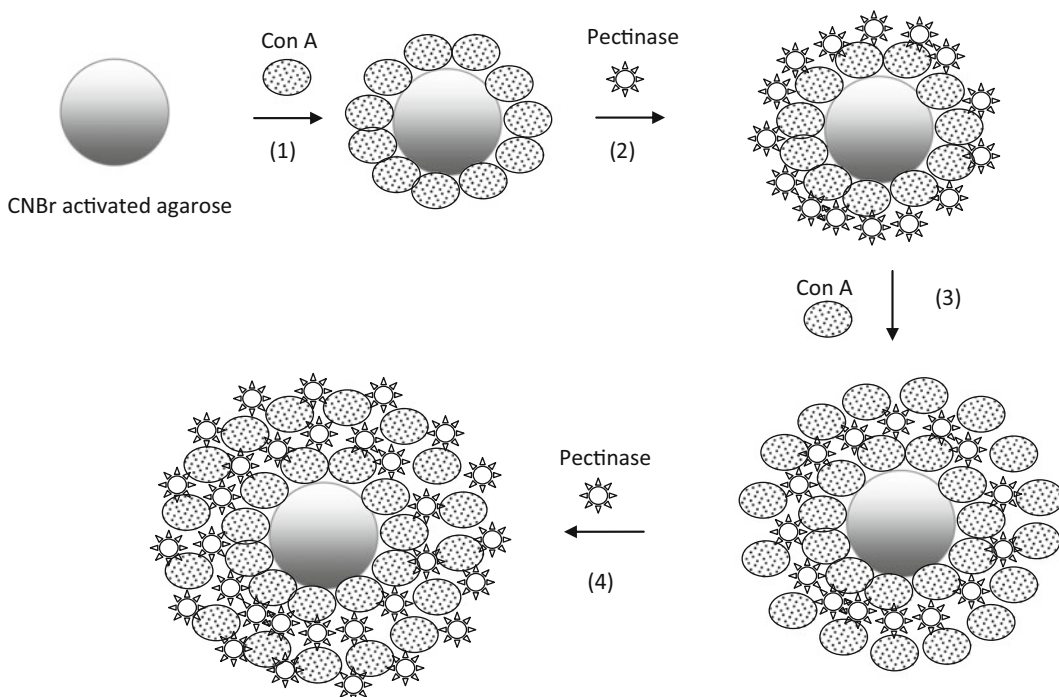


Fig. 1 Diagrammatic sketch showing bioaffinity layering of Con A and pectinase on agarose matrix. The pectinase and Con A were added alternately to Con A immobilized on agarose particles. Each layer is formed by bioaffinity immobilization. Here Con A is the affinity ligand for the glucoenzyme pectinase

Table 2

Immobilization of tomato pectinase on Con A–Seralose 4B by affinity layering

No. of layers	Enzyme bound (U) theoretical (A)	Expressed activity (U) actual (B)	Effectiveness factor, $\eta = (BA^{-1})$
1	12.75	4.08	0.32
2	27.2	13	0.48
3	42.5	23.8	0.56
4	55.2	40.15	0.73
5	60.0	43.8	0.73

Reprinted from *Enzyme and Microbial Technology*, 37, M. Sardar and M.N. Gupta, Immobilization of tomato pectinase on Con A–Seralose 4B by bioaffinity layering, 355–359, Copyright (2012) with permission from Elsevier

2 Materials

2.1 Immobilization of Tomato Pectinase on Con A–Agarose by Bioaffinity Layering

2.1.1 Extraction of Pectinase

1. Tomatoes from local market.
2. Dinitrosalicylic acid Reagent (Merck, Mumbai, India) (Dissolve 1 g of 3,5-dinitrosalicylic acid in 50 mL of water). Add 30 g of sodium potassium tartrate (Merck, Mumbai, India) and 20 mL of 2 N NaOH (Fisher Scientific, Mumbai, India). Dilute it by making up the volume to 100 mL with distilled water.
3. Buffer 1: 50 mM Sodium citrate, pH 4.5 containing 15 mM EDTA (Merck, Mumbai, India) and 1.7 M NaCl (Fisher Scientific, Mumbai, India).
4. Buffer 2: 50 mM Sodium acetate buffer, pH 5.0.

2.1.2 Assay of Pectinase Activity

1. Polygalactouronic acid (Sigma chemical Co., St. Louis, MO).
2. Buffer 2: same as in Subheading 2.1.1 (item 4).
3. Dinitrosalicylic acid Reagent: same as in Subheading 2.1.1 (item 2).

2.1.3 Preparation of Bioaffinity Layered Pectinase

1. Seralose 4B (an agarose preparation) (Sisco Research Laboratories, Mumbai, India) (*see Note 1*).
2. Buffer 2: same as in Subheading 2.1.1 (item 4).
3. Buffer 3: 50 mM sodium acetate buffer, pH 5.0 (containing the metal ions Mn^{2+} and Ca^{2+} added as their chloride salt in 1 mM concentration).
4. Cyanogen Bromide (Sigma chemical Co., St. Louis, MO).

2.2 Horseradish Peroxidase (HRP) Immobilized by Bioaffinity Layering on Con A Sephadex Beads

2.2.1 Assay of Horseradish Peroxidase

1. Horseradish Peroxidase (Sisco Research Lab, Mumbai, India).
2. 3,3',5,5'-Tetramethylbenzidine (TMB) (Sigma chemical Co., St. Louis, MO).
3. Buffer 4: 30 mM Citrate—Phosphate, pH 5.5.

2.2.2 Preparation of Bioaffinity Layered Horseradish Peroxidase

1. Sephadex G 100 (Pharmacia, Uppsala, Sweden). The gel is swollen and deaerated per the vendor's instructions [9].
2. Buffer 5: 20 mM Tris–HCl, pH 7.4.
3. Buffer 6: 20 mM Tris–HCl buffer, pH 7.4 (containing the metal ions Mn^{2+} and Ca^{2+} added in the form of their chloride salt in 1 mM concentration).

3 Methods

3.1 Immobilization of Tomato Pectinase on Con A–Agarose by Bioaffinity Layering

3.1.1 Extraction of Pectinase [10]

1. Homogenize 200 g ripe tomatoes with 200 g of ice and adjust the pH of the homogenate to 3.0 with 1 M HCl.
2. Separate the insoluble material by centrifugation at $9,000 \times g$ for 10 min at 4 °C.
3. Wash the pellet with cold dilute HCl, pH 3.0 till no reducing sugars are detected in the supernatant by dinitrosalicylic acid method [11].
4. Resuspend the pellet in the buffer 1 and homogenize for 15 min at 4 °C.
5. Centrifuge the mixture obtained in **step 4** above at $9,000 \times g$ for 10 min at 4 °C.
6. Dialyze the supernatant obtained after centrifugation against buffer 2. Dialysis is carried out against 2 L of buffer 2 with 5 changes at 4 °C for 48 h.
7. Lyophilize the dialyzed supernatant. The solid powder obtained is used as crude pectinase.

3.1.2 Assay of Pectinase Activity [6]

1. Substrate solution: 0.5 % (w/v) Polygalacturonic acid in buffer 2.
2. Weigh 10 mg of pectinase and dissolve it in 10 mL of buffer 2. Incubate the enzyme sample (solution containing 10–100 μ g of enzyme) in a reaction mixture containing 0.4 mL buffer 2 and 0.5 mL of substrate solution at 37 °C for 10 min with shaking at 150 rpm.
3. Stop the reaction by adding 1 mL of DNSA reagent. Keep in boiling water bath for 10 min, cool the samples, and add 10 mL distilled water.
4. Read the absorbance at 540 nm. One enzyme unit (U) liberates 1 μ mol of d-galacturonic acid from polygalacturonic acid per min at 37 °C, pH 5.0.
5. For estimating the enzyme activity of the immobilized enzyme preparation, the enzyme suspension is pipetted with a precision air displacement pipette. The end of the tip is cut so that the particles in suspension do not block the tip. The enzyme suspension is continuously shaken at 150 rpm and an aliquot of 50 μ L of enzyme suspension is taken out and added to 450 μ L of buffer 2, incubated with the substrate and assayed as above. The immobilized enzyme preparation is continuously shaken at 150 rpm at 25 °C for the entire duration of the assay.

3.1.3 Preparation of the Bioaffinity Layered Tomato Pectinase [6]

1. Wash agarose (50 mL settled gel) with 500 mL distilled water in a sintered glass funnel, suction dry to a wet cake, and transfer to a 250 mL beaker.

2. Suspend the gel in 50 mL deionized water and stir with a glass rod (*see Note 2*).
3. Add CNBr (10 g) to the gel suspension (*see Notes 3 and 4*). Maintain the pH of the reaction mixture at 11.0 by dropwise addition of 20 % (w/v) NaOH. Occasionally add ice to the reaction mixture to maintain the temperature at around 25 °C [12].
4. When all the CNBr dissolves (10–15 min), the rate of consumption of NaOH will decrease. At this time, pour the reaction mixture into a sintered glass funnel containing ice. Quickly wash the gel with 500 mL ice-cold water and 250 mL ice-cold coupling buffer (0.1 M sodium bicarbonate, pH 8.5).
5. Transfer the gel to 150 mL beaker and incubate with 200 mg of Con A dissolved in 10 mL of buffer 4 for 30 min at 25 °C with shaking at 150 rpm (*see Note 5*).
6. Remove the unbound Con A by extensive washing with the buffer 2.
7. Activate the resulting Con A–agarose matrix with metal ions (*see Note 6*). For this incubate 10 mL of settled matrix with 10 mL of buffer 3 (which contains the metal ions Mn^{2+} and Ca^{2+}) for 1 h at 25 °C. To remove the unbound metal ions, wash the matrix extensively with buffer 2.
8. Incubate Con A–agarose matrix (settled volume, 3 mL) with 2 mL of tomato pectinase (30 mg in buffer 2) for 6 h at 25 °C.
9. Separate the matrix bound enzyme from the unbound enzyme by centrifugation at $3,000 \times g$ for 5 min at 25 °C. Wash the matrix extensively with buffer 2 for removing the nonspecifically bound enzyme.
10. The immobilized enzyme preparation was finally suspended in 3 mL of buffer 2. The preparation thus obtained was considered to contain one affinity layer.
11. Determine the pectinase activity in the supernatant, washings, and immobilized preparation as described in Subheading 3.1.2.
12. For the formation of successive affinity layers incubate the preparation with 3 mL of Con A (20 mg/mL in the buffer 2) for 6 h at 25 °C. Wash the preparation with the buffer 2, till no Con A activity is determined in the washings, then incubate for 6 h with 45 mg of tomato pectinase (in 2 mL buffer 3). To get the desired number of affinity layers incubate the preparation alternatively with Con A and pectinase (i.e., repeat steps 8–11).

3.2 Horseradish Peroxidase (HRP) Immobilized by Bioaffinity Layering

3.2.1 Estimation of HRP Activity [13]

1. Substrate solution: 2 μL of 30 % v/v H_2O_2 and 1 mL of dimethyl sulfoxide solution containing 1.5 mg TMB (*see Note 5*) is added to 15 mL of buffer 4.
2. Weigh 10 mg of HRP and dissolve it in 10 mL of buffer 4. Incubate the enzyme sample (solution containing 1–10 μg of enzyme) in a reaction mixture containing 0.4 mL buffer 4 and 1.5 mL of substrate solution at 25 °C for 10 min.
3. Stop the reaction with 0.5 mL of 2 M H_2SO_4 .
4. Read the absorbance at 450 nm. One unit of enzyme activity (U) is defined as the amount of enzyme that catalyzes the oxidation of 1 μmol of TMB per min at 25 °C to the colored product (*see Notes 7 and 8*).
5. For estimating the enzyme activity of the bioaffinity layered enzyme, the enzyme sample is pipetted with a precision air displacement pipette. The aliquot is withdrawn from the enzyme suspension for measurement of enzyme activity as explained in **step 5** of Subheading 3.1.2. An aliquot of 100 μL enzyme suspension is pipetted and added to 400 μL of buffer 4, incubated with the substrate and assayed as above. The immobilized enzyme preparation is continuously shaken at 150 rpm for the entire duration of the assay.

3.2.2 Preparation of Bioaffinity Layered HRP [8]

1. Dissolve 25 mg Con A in 1 mL of buffer 5.
2. Swell Sephadex G 100 (0.070 g) in boiling water bath for 5 h.
3. Incubate the Con A with 1 mL settled gel suspension for 12 h at 25 °C.
4. Remove the unbound Con A by extensive washing with the buffer 5.
5. Activate the resulting Con A–Sephadex G 100 matrix with metal ions (*see Note 6*) by incubating the settled matrix with buffer 6 (which contains the metal ions Mn^{2+} and Ca^{2+} at 25 °C for 1 h).
6. Wash the matrix extensively with buffer 5, to remove the unbound metal ions. The settled activated gel (1 mL) was used for further experiments.
7. For enzyme immobilization, incubate 1 mL (settled volume) of the activated gel with 260 U of HRP dissolved in 2 mL of buffer 5, for 6 h at 25 °C.
8. Separate the unbound enzyme from the matrix bound enzyme by centrifugation at $3,000\times g$ for 5 min at 25 °C. Remove the nonspecifically associated enzyme by repeated washing with buffer 5.
9. Determine the HRP activity in the supernatant, washings, and the immobilized preparation as described in Subheading 3.2.1.
10. The matrix bound enzyme preparation obtained is considered to contain one affinity layer.

11. For the formation of successive affinity layers incubate the enzyme preparation obtained above with 1 mL of Con A for 12 h at 25 °C. Activate the Con A with metal ions as described above and incubate with 260 U of HRP dissolved in 2 mL of buffer 5.

4 Notes

1. While we had sourced this locally, others may like to use any agarose preparation, e.g., Sepharose 4B from Pharmacia.
2. Do not use magnetic stirring, since this can deform the beads of agarose.
3. CNBr activation procedure should be carried out in a well ventilated hood since CNBr is highly toxic.
4. Cyanogen bromide activation is the most common method for preparing affinity gels because it reacts with the hydroxyl groups on agarose to form cyanate esters and imidocarbonates. These groups are reacted with primary amines in order to couple the protein onto the agarose matrix.
5. Due to the limited shelf life of the CNBr activated matrix, it is advisable to prepare the gel just before use. Alternatively, one can buy CNBr activated matrices commercially and go by the vendors instructions about the stability.
6. Con A is a metalloprotein each subunit of which contains one Ca^{2+} and one Mn^{2+} ion. These ions are necessary for full activity of the lectin. Hence, it is advisable to carry out this step to replenish these ions which may have been lost during purification or at any other step.
7. TMB is a relatively less noncarcinogenic substrate as compared to 3,3'-diaminobenzidine and o-dianisidine for HRP.
8. In the presence of HRP and hydrogen peroxide (H_2O_2), TMB is oxidized first to a blue cation free radical having an absorption maximum at 653 nm ($\epsilon = 3.9 \times 10^4 \text{ M}^{-1} \text{ cm}^{-1}$). Upon further reaction with HRP/ H_2O_2 , or addition of acid, the radical is converted to a terminal oxidation product, a yellow diimine that absorbs light at 450 nm ($\epsilon = 5.9 \times 10^4 \text{ M}^{-1} \text{ cm}^{-1}$).

Acknowledgments

The authors thank Dr. Sohel Dalal for some of his work described in this chapter. Financial support from the Department of Science and Technology (DST-SERB) [Grant No.: SR/SO/BB-68/2010] and the Department of Biotechnology (DBT) [Grant No: BT/PR14103/BRB/10/808/2010], all Government of India organizations, is gratefully acknowledged.

References

1. Mattiasson B (1988) Affinity immobilization. In: Mosbach K (ed) *Methods in Immobilization*, vol 137. Academic Press, New York, pp 647–656
2. Roy I, Gupta MN (2006) Bioaffinity immobilization. In: Guisan JM (ed) *Immobilization of enzymes & cells*. Humana Press Inc, USA, pp 107–116
3. Roy I, Gupta MN (2003) Smart polymeric materials: emerging biochemical applications. *Chem Biol* 10(12):1161–1171
4. Gautam S, Dubey P, Singh P, Kesavardana S, Varadarajan R, Gupta MN (2012) Smart polymer mediated purification and recovery of active proteins from inclusion bodies. *J Chromatogr A* 1235:10–25
5. Liener IE, Sharon N, Goldstein IJ (1986) *The lectins: properties, functions and applications in biology and medicine*. Academic Press, Inc., Orlando, Florida
6. Sardar M, Gupta MN (2005) Immobilization of tomato pectinase on Con A-Seralose 4B by bioaffinity layering. *Enzyme Microb Tech* 37: 355–359
7. Ryan BJ, Carolan N, Ó'Fágáin C (2006) Horseradish and soybean peroxidases: comparable tools for alternative niches? *Trends Biotechnol* 24(8):355–363
8. Dalal S, Gupta MN (2007) Treatment of phenolic wastewater by horseradish peroxidase immobilized by bioaffinity layering. *Chemosphere* 67:741–747
9. Gel Filtration. Principles and Methods. Handbooks from Amersham Biosciences. [Can be downloaded from the following website: http://kirschner.med.harvard.edu/files/protocols/GE_gelfiltration.pdf]
10. Benhura MAN, Mavhudzi I (1996) Use of crosslinked mucilage prepared from ruredzo (*Dicerocaryum zanguibarium*) in the purification of polygalacturonase extracted from tomato. *Food Chem* 56:433–437
11. Miller GL (1959) Use of dinitrosalicylic acid reagent for determination of reducing sugar. *Anal Chem* 31:426–428
12. Hermanson GT, Mallia AK, Smith PK (1992) *Immobilized affinity ligand technique*. Academic Press, San Diego, CA
13. Bos ES, Doelen AA, Rooy N, Schuurs AHWM (1981) 3,3',5,5'-Tetramethylbenzidine as an ames test negative chromogen for horseradish peroxidase in enzyme immunoassay. *J Immunoassay* 2:187–204
14. Farooqui M, Saleemuddin M, Ulber R, Sosnitza P, Scheper T (1997) Bio-affinity layering: a novel strategy for the immobilization of large quantities of glycoenzymes. *J Biotechnol* 55:171–179
15. Farooqui M, Sosnitza P, Saleemuddin M, Ulber R, Scheper T (1999) Immunoaffinity layering of enzymes. *Appl Microbiol Biotechnol* 52: 373–379
16. Gemeiner P, Docolomansky P, Vikartovska A, Stefuca V (1998) Amplification of flow-microcalorimetry signal by means of multiple bioaffinity layering of lectin and glycoenzyme. *Biotechnol Appl Biochem* 28: 155–161
17. Danica Mislovicova D, Gemeiner P, Sandula J, Masarova J, Vikartovska A, Docolomansky P (2000) Examination of bioaffinity immobilization by precipitation of mannan and mannan-containing enzymes with legume lectins. *Biotechnol Appl Biochem* 31: 153–159
18. Sardar M, Varandani D, Mehta B, Gupta MN (2008) Affinity directed assembly of multilayers of pectinase. *BioCAT Biotrans* 26(4): 313–320
19. Jan U, Hussain Q, Saleemuddin M (2001) Preparation of stable highly active and immobilized glucose oxidase using the anti enzyme antibodies and F(ab)₂. *Biotechnol Appl Biochem* 34:13–17
20. Jan U, Hussain Q (2004) Preparation of a highly stable, very active and high yield multi-layered assembly of glucose oxidase using carbohydrate-specific polyclonal antibodies. *Biotechnol Appl Biochem* 39:233–239

Chapter 10

Immobilization of Enzymes on Magnetic Beads Through Affinity Interactions

Audrey Sassolas, Akhtar Hayat, and Jean-Louis Marty

Abstract

The development of enzyme immobilization techniques that will not affect catalytic activity and conformation is an important research task. Affinity tags that are present or added at a specific position far from the active site in the structure of the native enzyme could be used to create strong affinity bonds between the protein structure and a surface functionalized with the complementary affinity ligand. These immobilization techniques are based on affinity interactions between biotin and (strept)avidin molecules, lectins and sugars, or metal chelate and histidine tag.

Recent developments involve immobilization of tagged enzymes onto magnetic nanoparticles. These supports can improve the performance of immobilized biomolecules in analytical assay because magnetic beads provide a relative large numbers of binding sites for biochemical reactions resulting in faster assay kinetics.

This chapter describes immobilization procedures of tagged enzymes onto various magnetic beads.

Key words Affinity interactions, Magnetic beads, Tagged enzyme, Faster assay kinetics, Enzyme immobilization

1 Introduction

In recent years, advances in immobilization techniques have remarkably influenced the design and performance of a variety of enzymatic systems ranging from bioreactors to biosensor devices. Various immobilization methods such as adsorption, covalent binding, or physical entrapment in a polymer matrix have been used to immobilize enzymes onto different surfaces. Numerous immobilization techniques involve random distribution or poor orientation of enzyme molecules inducing a partial or a total loss of activity due to enzyme denaturation or blocking of the active site from substrate accessibility. A strategy is to create (bio)affinity bonds between an activated support (e.g., with lectin, avidin, metal chelates) and a specific group (a tag) of the protein sequence (e.g., carbohydrate residue, biotin, histidine). This method allows to

control the biomolecule orientation in order to avoid enzyme deactivation and/or active site blocking. Several affinity methods have been described to immobilize enzymes through (strept)-avidin–biotin, lectin–carbohydrate, and metal cation–chelator interactions. An enzyme can contain affinity tags in its sequence (e.g., a sugar moiety) but, in some cases, the affinity tag (e.g., biotin, histidine tag) needs to be attached to the protein sequence. The His tag is attached by genetic engineering methods such as site-directed mutagenesis, protein fusion technology, and post-transcriptional modification, whereas the biotin incorporation is based on a covalent coupling reaction to a specific lysine residue.

Recent developments involve immobilization of enzymes onto magnetic beads. Magnetic beads are known to be powerful and versatile tools in a variety of analytical and biotechnology applications [1–3]. The use of magnetic beads presents many advantages.

1. An increase in the surface area.
2. The magnetic beads can be easily magnetically manipulated by using permanent magnets or electromagnets. Magnetic separation can be used for an easy removal of unbound binding molecules.
3. Numerous commercial magnetic particles are available. The particles are functionalized with different groups (e.g., Ni modified magnetic beads).

This chapter describes the principles and experimental strategies for affinity immobilization of enzymes onto magnetic beads.

1.1 Biotin–Streptavidin

1.1.1 Principle

A strategy to immobilize enzymes is to use the strong affinity existing between biotin and (strept)avidin (dissociation constant of 10^{-15} M). Biotinylation of proteins can be achieved through a covalent coupling of biotin to the protein by the use of biotin-ester reagents that preferentially modify lysine residues [4]. Enzymes can also be genetically biotinylated using a biotin acceptor peptide sequences fused to the C-terminus of enzyme [5].

Biotinylated enzymes have been used to develop chemiluminescent biosensors for choline and acetylcholine (ACh) detection [6]. Streptavidin was first entrapped in a polyacrylamide gel by using a very small quantity of glutaraldehyde. Then, this membrane was incubated in the presence of biotinylated ChOD and AChE. In the same way, an electrochemical biosensor for H_2O_2 detection was developed [7]. HRP conjugated with streptavidin was immobilized on a mixed self-assembled monolayer formed by 1,2-dipalmitoyl-*sn*-glycero-3-phosphoethanolamine-*N*-(biotinyl) and 16-mercaptopentadecanoic acid previously grafted on a gold

electrode. An electropolymerizable pyrrole-modified biotin [8] has also been used to develop several glucose and catechol biosensors [9–11]. This strategy involved the electropolymerization of a biotin derivative. Then, the attachment of biomolecules to the electrode surface could be achieved by the functionalization of the resulting conducting polypyrrole by (strept)avidin and subsequent coupling using biotinylated molecules. This strategy was also used to develop a clinical biosensor for urea detection [12].

This affinity method was also used for the immobilization of biotinylated nucleases on streptavidin-coated magnetic beads [13].

2 Materials

1. Streptavidin-coated magnetic beads (*see Note 1*).
2. Biotinylated enzymes (*see Note 2*).
3. AdemMag SV magnetic support (Ademtech SA, Pessac, France).
4. Eppendorf tubes.
5. Automatic pipettes.

2.1 **Materials for Magnetic Lectin Purification**

1. Streptavidin-coated superparamagnetic Fe₃O₄ microparticles (magnetic beads) (*see Note 1*).
2. Glycoenzyme.
3. Biotinylated lectins from *T. vulgaris* (wheat germ) or *A. hypogaea* (peanut) (Sigma Aldrich, USA).
4. AdemMag SV magnetic support (Ademtech SA, Pessac, France).
5. Eppendorf tubes.
6. Automatic pipettes.

2.2 **Materials for IMAC Magnetic IMAC Purification**

1. Pre-activated magnetic beads carrying Ni-IDA complexes (diameter 300 nm) obtained from “Histidine Adem-kit for His-tagged protein purification” (Ademtech SA, Pessac, France).
2. Binding buffer: 20 mM Tris-HCl, pH 7.5, containing 500 mM NaCl and 0.09 % sodium azide (Ademtech SA, Pessac, France).
3. AdemMag SV magnetic support (Ademtech SA, Pessac, France).
4. His-tagged enzyme.
5. Eppendorf tubes.
6. Automatic pipettes.

3 Methods

1. 100 μL of the magnetic bead solution is mixed with 100 μL of biotinylated enzyme diluted buffer solution (*see Note 3*).
2. The mixture is shaken for 1 h to allow the binding of the biotinylated enzyme with the streptavidin-coated beads.
3. The tube is placed on a magnetic support.
4. The beads are washed three times with 200 μL of PBS. These three repetitive washing steps ensured the suppression of nonspecifically adsorbed species on the magnetic beads (*see Note 4*).
5. The beads are stored at 4 $^{\circ}\text{C}$ until use.

3.1 Lectin–Carbohydrate

Affinity immobilization was also described between a sugar moiety naturally present in some enzymes such as AChE and concanavalin A (Con A) deposited onto a surface. Con A is a lectin which has multiple sites with high affinity for carbohydrates. First, the lectin is immobilized on a support and then glycosidic enzyme is bound to specific lectins. The enzyme and Con A have to operate under the same experimental conditions (e.g., temperature, pH buffer), and measurement solution does not contain carbohydrates that could have a higher affinity for the lectin than the enzyme carbohydrate chain [23]. This method is based on a tag that is naturally present in the enzyme. Thus, no enzyme modification is necessary. The affinity of lectins for carbohydrate chains provides reversible immobilization, good steric substrate accessibility, and protection of the enzyme against proteolytic digestion.

Strong affinity links between Con A and the mannose residues of AChE allowed to develop amperometric biosensors for acetylthiocholine and insecticide detection [14–16].

The layer-by-layer self-assembly technique allows to obtain organized molecular assemblies with alternate layers of concanavalin A and glycoenzyme. Enzymes, such as HRP [17, 18], GOD [19], or LOD [19], have been incorporated into multilayers without any chemical modification. The response of the electrode modified by the Con A/enzyme multilayers was related to the number of assembled bilayers of Con A/enzyme [18]. The increase of the number of bilayers induced an increase of the enzyme quantity immobilized on the electrode surface and thus exhibited a better sensitivity of the biosensor to the enzymatic substrate. On the other hand, thicker layers of assembled film could obstruct the diffusion of the substrate.

Recently, yeast invertase has been immobilized on lectin-modified magnetic beads [20]. Yeast invertase exists in at least two forms which are related to its location in the cell [21]. The external

enzyme which is localized in the cell wall is a glycoprotein containing about 50 % carbohydrate. First, biotinylated lectins were bound to streptavidin-coated superparamagnetic iron oxide beads. Then, invertase was introduced to the lectin-modified magnetic beads to allow the interaction between the lectin and the sugar moieties. In this work, these modified beads were used to develop a sandwich-type bioassay to detect lectin–glycoprotein interactions using fluorescein isothiocyanate (FITC). For this purpose, a biotinylated secondary lectin was bound to the glycoenzyme, forming a sandwich-type complex. The biotinylated ends of the secondary lectins allowed the binding of avidin-conjugated FITC onto the complex.

This protocol was used for the immobilization of yeast invertase [20]. However, this technique can be applied to any glycoenzyme.

3.2 Preparation of Lectin-Modified Magnetic Beads

1. 100 μL of the magnetic bead solution is mixed with 100 μL of biotinylated lectin diluted in PBS (*see Note 5*).
2. The mixture is shaken at 300 rpm for 1 h to allow the binding of the biotinylated lectins with the streptavidin-coated beads.
3. The tube is placed on a magnetic support.
4. The beads are washed three times with 200 μL of PBS. These three repetitive washing steps ensured the suppression of nonspecifically adsorbed species on the magnetic beads (*see Note 4*).

3.3 Immobilization of Enzyme on the Lectin-Modified Magnetic Beads

5. 100 μL of enzyme solution is mixed with 100 μL of the lectin-modified magnetic beads (*see Note 3*).
6. The solution is shaken at 300 rpm for 1 h.
7. The beads are washed three times with PBS to suppress the amount of nonspecifically adsorbed biomolecules (*see Note 4*).
8. The modified beads are stored at 4 °C until use (*see Note 6*).

3.4 Metal Ion-Chelator

3.4.1 Principle

The strong affinity link between a metal cation and a chelator such as nitrilotriacetic acid (NTA), iminodiacetic acid (IDA) or tag poly(histidine) can be used for the enzyme immobilization on a surface. This method is based on the principle of Immobilized Metal Affinity Chromatography (IMAC), currently used for protein purification and separation. Immobilization of the metal ion on a chromatographic resin by chelation allows the separation of histidine-tagged proteins from untagged proteins. The bound molecule can be eluted from the resin by reducing the pH and increasing the ionic strength of the buffer or using EDTA or imidazole. Based on this principle, enzymes with His residues in their structure can be easily attached to a support containing a metal chelate. However, few His residues are present on enzyme

surface and are accessible for binding to a chelate-modified surface. To solve this problem, genetic engineering methods allow the production of tagged enzyme by attaching His at a specific position of the protein without affecting the activity or the folding of the enzyme. These tags are usually placed in poly(histidine) tail attached to the N- or C- terminus of recombinant proteins.

In this case, the enzyme is immobilized in a diffusion-free barrier design, which ensures low response time, low detection limit and high sensitivity of the system. The His tag affinity method is generic and can be easily applied to any enzyme containing a His tag.

This approach was used for the development of enzyme biosensors. The immobilization of enzymes through specific His tag affinity interactions involves two main requirements: the use of a surface that contains a metal chelate onto its surface and the availability of a His-tagged enzyme. A biosensor for lactate detection based on this immobilization method has been described [22]. First, polyaniline–polyacrylate films were formed on an electrode. This copolymer could be loaded with Ni^{2+} ions, which acted as coordination sites for histidine residues present on his-tagged lactate dehydrogenase.

NTA was also commonly used as a chelator for selective enzyme attachment. In this case, four of six coordinations of Ni^{2+} ions were occupied by the four ligands of the NTA chelate, while the other two positions were occupied by water or buffer molecules which could be selectively replaced by the His tag that were incorporated in the enzyme sequence [23, 24]. This strategy also allowed to immobilize His-tagged AChE on functionalized graphite used for SPE fabrication [25]. The graphite was modified in order to incorporate a NTA group that could interact with nickel ions. Then, immobilization of the enzyme was possible via a histidine tail. This immobilization also allowed to develop an electrochemical biosensor for glucose detection using an histidine-tagged GOD [26]. In this study, the pyrrole monomer functionalized with an NTA group was electropolymerized on a platinum electrode. Then, copper ions interacted with NTA groups. In the presence of the enzyme, a complex between GOD-His, Cu^{2+} ions and NTA was formed (Fig. 1).

Recently, colorimetric assays for OA detection have been developed by immobilizing genetically engineered protein phosphatase with hexa-His tail on Ni-modified magnetic beads. The oriented and site-specific immobilization of a highly sensitive genetically engineered acetylcholinesterase (B394) with a hexa(histidine) tail by affinity interactions on metal chelate-functionalized magnetic microbeads carrying Ni-IDA complexes was also reported [27]. The ability to easily control the charging/discharging of the electrode surface by application of a magnetic field provided reusability of the same electrode for several analyses

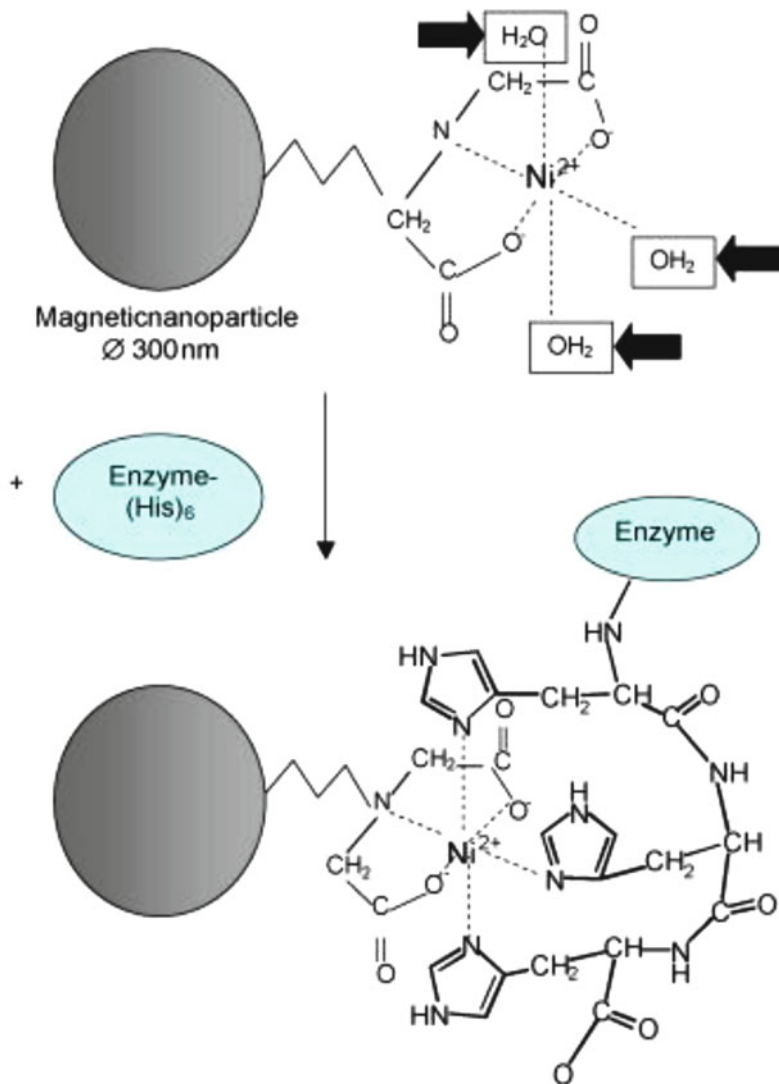


Fig. 1 Schematic representation of enzyme immobilization on magnetic microbeads via Ni-His affinity. *Black arrows* show histidine-exchangeable water molecules [27]

by simply removing the magnet and recharging the surface with fresh enzyme functionalized beads.

This protocol was used to immobilize genetically engineered AChE by affinity on metal chelate-functionalized magnetic beads [27]. The His tag affinity method is generic and can be easily applied to any enzyme containing a His tag.

3.5

1. 30 μ L of colloidal suspension of Ni-IDA beads were placed in an Eppendorf tube containing 300 μ L binding buffer (*see* **Notes 7** and **8**).

2. The tube is placed on a magnetic support to facilitate the washing steps.
3. The beads are washed twice using 300 μL binding buffer.
4. The beads are mixed with 1 mL enzymatic solution (*see* **Notes 3** and **9**).
5. The mixture is stirred for 15 min.
6. The solution is removed by placing the tube in the magnetic support.
7. The activated beads are washed twice with 200 μL of binding buffer (*see* **Note 4**).
8. The activated beads are stored in pH 7 PBS buffer (*see* **Note 10**).

4 Notes

1. Numerous streptavidin-coated magnetic beads are commercially available (e.g., Pierce, Invitrogen, Roche, Merck) and can be used in this protocol.
2. Biotinylated peroxidase, alkaline phosphatase, glucose oxidase, and β -galactosidase are commercially available. For the immobilization of most enzymes, a preliminary step that consists in the binding of the biotin tag to the protein sequence is required. The most commonly used method to incorporate biotin is based on the covalent coupling reaction to a specific lysine residue using biotin-ester reagents, typically an *N*-hydroxysuccinimide (NHS) ester [23].
3. The concentration of enzyme has to be optimized.
4. The washing procedure consists of separating the magnetic beads from the solution by putting the tube against the magnet. The beads aggregate against the wall of the tube. A micropipette is used to remove the supernatant solution without disturbing the aggregated magnetic beads. Then, 200 μL of buffer are added in the tube. The beads are dispersed for 10 s. This process constituted one wash step and is repeated for each washing procedure.
5. The concentration of biotinylated lectin has to be optimized.
6. The beads are ready to use. The modified beads were used to develop a sandwich-type bioassay to detect lectin–glycoprotein interactions using FITC. For this purpose, the immobilization of the yeast invertase was followed by the attachment of a biotinylated secondary lectin onto the enzyme, creating a sandwich-type complex. The detection was achieved using a FITC-conjugated avidin. However, these beads can also be used for other applications.

7. Other types of metal chelate-functionalized magnetic beads with different sizes can be used.
8. According the type of pre-activated magnetic beads, the composition of the binding buffer can be modified.
9. This protocol was used for the immobilization of His-tagged AChE. However, this protocol is also applicable to other His-tagged enzymes.
10. The activated beads are ready to use. These beads were employed for the development of an electrochemical biosensor. In this case, 1 μL of bead suspension was deposited on a working electrode, beforehand fitted with magnet on the back of the electrode. These activated beads can also be used for other applications.

References

1. Solé S, Merkoçi A, Alegret S (2001) New materials for electrochemical sensing III. *Trends Anal Chem* 20:102–110
2. Plata MR, Contento AM, Rios A (2010) State-of-the-art of (bio)chemical sensor developments in analytical spanish groups. *Sensors (Basel)* 10:2511–2576
3. Richardson J, Hawkins P, Luxton R (2001) The use of coated paramagnetic particles as a physical label in a magneto-immunoassay. *Biosens Bioelectron* 16:989–993
4. Nilsson J, Stahl S, Lundeberg J, Uhlen M, Nygren P-A (1997) Affinity fusion strategies for detection, purification and immobilization of recombinant proteins. *Protein Expr Purif* 11:1–16
5. Zhang J, Cass AEG (2000) Electrochemical analysis of immobilised chemical and genetic biotinylated alkaline phosphatase. *Anal Chim Acta* 408:241–247
6. Yao D, Vlessidis AG, Evmiridis NP (2002) Development of an interference-free chemiluminescence method for monitoring acetylcholine and choline based on immobilized enzymes. *Anal Chim Acta* 462:199–208
7. Esseghaier C, Bergaoui Y, Tlili A, Abdelghani A (2008) Impedance spectroscopy on immobilized streptavidin horseradish peroxidase layer for biosensing. *Sensors Actuat B* 134:112–116
8. Cosnier S, Lepellec A (1999) Poly(pyrrole-biotin): a new polymer for biomolecule grafting on electrode surfaces. *Electrochim Acta* 44:1833–1836
9. Cosnier S, Stoytcheva M, Senillou A, Perrot H, Furiel RPM, Leone FA (1999) A biotinylated conducting polypyrrole for the spatially controlled construction of an amperometric biosensor. *Anal Chem* 71:3692–3697
10. Cosnier S, Gondran C, Lepellec A, Senillou A (2001) Controlled fabrication of glucose and catechol microbiosensors via electropolymerized biotinylated polypyrrole films. *Anal Lett* 34:61–70
11. Mousty C, Lepellec A, Cosnier S, Novoa A, Marks RS (2001) Fabrication of organic phase biosensors based on multilayered polyphenol oxidase protected by an alginate coating. *Electrochem Commun* 3:727–732
12. Barhoumi H, Maaref A, Martelet C, Jaffrezic-Renault N (2008) Urease immobilization on biotinylated polypyrrole coated ChemFEC devices for urea biosensor development. *IRBM* 29:192–201
13. Gast F-U, Franke I, Meiss G, Pingoud A (2001) Immobilization of sugar-non-specific nucleases by utilizing the streptavidin-biotin interactions. *J Biotechnol* 87:131–141
14. Bucur B, Andreescu S, Marty J (2004) Affinity methods to immobilize acetylcholinesterases for manufacturing biosensors. *Anal Lett* 37:1571–1588
15. Bucur B, Danet AF, Marty JL (2005) Cholinesterase immobilisation on the surface of screen-printed electrodes based on concanavalin A affinity. *Anal Chim Acta* 530:1–6
16. Bucur B, Danet AF, Marty JL (2004) Versatile method of cholinesterase immobilisation via affinity bonds using concanavalin A applied to the construction of a screen-printed biosensor. *Biosens Bioelectron* 20:217–225
17. Liu L, Chen Z, Yang S, Jin X, Lin X (2008) A novel inhibition biosensor constructed by layer-by-layer technique based on biospecific affinity for the determination of sulfide. *Sensors Actuat B* 129:218–224

18. Yang S, Chen Z, Jin X, Lin X (2006) HRP biosensor based on sugar-lectin biospecific interactions for the determination of phenolic compounds. *Electrochim Acta* 52:200–205
19. Anzai J-I, Kobayashi Y, Nakamura N, Hoshi T (2000) Use of Con A and mannose-labeled enzymes for the preparation of enzyme films for biosensors. *Sensors Actuat B* 65:94–96
20. Rambihar C, Kernan K (2010) Magnetic bead-based fluorometric detection of lection-glycoprotein interactions. *Talanta* 81:1676–1680
21. Neumann NP, Lampen JO (1969) Glycoprotein structure of yeast invertase. *Biochemistry* 8:3552–3556
22. Halliwell CM, Simon E, Toh CS, Bartlett PN, Cass AEG (2002) Immobilisation of lactate dehydrogenase on poly(aniline)-poly(acrylate) and poly(aniline)-poly-(vinyl sulphonate) films for use in a lactate biosensor. *Anal Chim Acta* 453:191–200
23. Campas M, Bucur B, Andreescu S, Marty JL (2004) Application of oriented immobilisation methods to enzyme sensors. *Curr Top Biotechnol* 1:95–107
24. Andreescu S, Magearu V, Lougarre A, Fournier D, Marty JL (2001) Immobilization of enzymes on screen-printed sensors via an histidine tail. Application to the detection of pesticides using modified cholinesterase. *Anal Lett* 34:529–540
25. Andreescu S, Fournier D, Marty JL (2003) Development of highly sensitive sensor based on bioengineered acetylcholinesterase immobilized by affinity method. *Anal Lett* 36:1865–1885
26. Haddour N, Cosnier S, Gondran C (2005) Electrogeneration of a poly(pyrrole)-NTA chelator film for a reversible oriented immobilization of histidine-tagged proteins. *J ACS* 127:5752–5753
27. Istamboulie G, Andreescu S, Marty JL, Noguier T (2007) Highly sensitive detection of organophosphorus insecticides using magnetic microbeads and genetically engineered acetylcholinesterase. *Biosens Bioelectron* 23:506–512

Chapter 11

Tips for the Functionalization of Nanoparticles with Antibodies

Ester Polo, Sara Puertas, María Moros, Pilar Batalla, José M. Guisán, Jesús M. de la Fuente, and Valeria Grazú

Abstract

Multiple antibody immobilization methodologies have been developed for several applications including affinity chromatography, immunosensing, and drug delivery. Most of them have been carried out without considering the orientation of the antigen binding site of the antibody, or after the chemical modification of the antibody. An efficient immobilization to improve the biological activity of the antibody is one of the key fundamental issues to pursue. A simple and effective methodology for well-oriented covalently immobilization of antibodies on nanoparticles is reported in this chapter.

Key words Oriented antibody, Immobilization methods, Covalent immobilization, Ionic adsorption, Nanoparticles

1 Introduction

Immunoglobulins (Igs) or Antibodies (Abs) are glycoproteins produced by the immune system that are implied in specific defense mechanisms in animals. Igs are divided in five classes or isotypes (IgG, IgA, IgM, IgD, and IgE) and are characterized by their high specificity and selectivity to recognize antigens. The basic functional unit of each of them is an immunoglobulin (Ig) monomer. Each Ig monomer or basic unit has a Y-shaped basic structure formed by two identical light chains of 25 kDa and two identical heavy chains of 50–70 kDa, held together by disulfide bonds (Fig. 1) [1]. The light chains (L) contain a variable domain (VL) in the amino terminal end and one constant domain (CL) in the carboxyl terminal end, whereas the heavy chains (H) contain one variable domain (VH) and three constant domains (CH1, CH2, CH3). Abs are bifunctional, with the polypeptide chains arranged to form two antigen-recognition regions (Fab fragments) that are linked to an Fc region with effector functions [2]. The variable

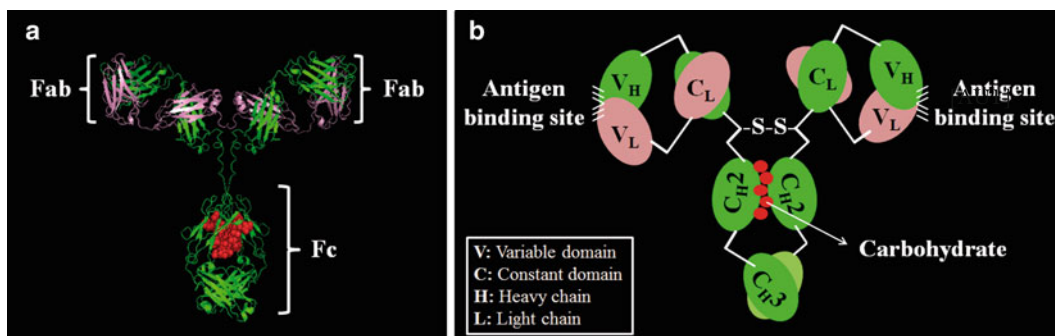


Fig. 1 Three-dimensional model of Ab from studies by X-ray crystallography. The Protein Data Bank (PDB) entry 1IGY was selected for this 3D representation and visualized using PyMol v0.99. **(a)** The three-dimensional structure of Ab can be depicted as a Y-shaped molecule; **(b)** Schematic cartoon showing the constant and variable regions of light and heavy chains of an Ab. Reprinted with permission from reference. [3](#) Copyright 2011, American Chemical Society

regions of the amino terminal ends are those which form the antigen-binding sites, which are highly specific. IgG, IgD, and IgE are secreted by B cells as monomers. But secreted antibodies could also be dimeric as in the case of IgA or even pentameric like mammalian IgM. However, from the aforementioned IgG is the most widely used when attaching Abs to nanoparticles (NPs).

1.1 Usual Coupling Strategies for Immobilizing Abs onto Nanoparticles

Antibodies have been conjugated to nanoparticles for many biotechnological and biomedical applications like cell sorting, bioseparation, protein purification, development of nanomaterial based biosensors, in vivo diagnosis, and human therapy [4, 5]. For the binding of Abs onto NPs, it is preferred that the Fab regions are not involved in the immobilization process, so that the Ab does not lose its antigen recognition sites. As Abs are asymmetric molecules, they can adopt different spatial orientations when conjugated onto the surface of the NPs [6]. Some of the protocols that are used for NP functionalization are based on the antibody attachment onto the nanoparticle surface in a random orientation [7, 8], which involves hampering the Ab capability of antigen recognition [9]. Therefore, the development of strategies that allow attaching the Abs in an oriented manner is a key issue to overcome the reduction of randomly immobilized Abs. For that reason, over the last years, several strategies that propose an oriented Ab immobilization have been reported in literature. These methodologies are based on the antibody conjugation through the Fc fragment of the IgG antibody, maintaining the antigen binding sites still available for the recognition event. Due to the Fc region being similar in all IgG antibodies of the same isotope and species, and well-conserved between different species, these oriented conjugations strategies have the advantage of their generality. The main oriented binding methodologies consists of (a) binding

through biotin binding proteins, (b) binding through thiol groups of the antibody, (c) binding through sugar chains of the antibody, (d) binding through Fc-binding proteins.

It is true that it is possible to take advantage of the existing experience in the functionalization of microbeads and surfaces for the development of Ab coupling strategies of NPs. However, the adaptation of these protocols optimized for the functionalization of microstructured materials is not trivial as it is essential that NPs remain stable during their functionalization. This is a problematic task as the colloidal stability of NPs is governed by a delicate balance among attractive (van der Waals and/or magnetic) and repulsion forces (electrostatic and/or steric). Therefore, depending on the nanoparticle characteristics (the colloidal stability, the density of functional groups, the surface area, size, etc.) some coupling strategies will work better than the others. Currently, coupling Abs to NPs is achieved (a) by physical adsorption, (b) by direct covalent immobilization, (c) using adapter molecules, or (d) by taking advantage of ionic interactions prior to Ab covalent binding.

1.1.1 Physical Adsorption

Physical adsorption of Abs onto NPs is a widely used methodology for the reversible binding of Abs to the surface of the NPs [10]. This physical adsorption is generally based on hydrophobic, electrostatic, hydrogen bonding and van der Waals attractive forces between the Ab and the surface of the NP. This binding strategy is the easiest to achieve as it does not imply the chemical modification of the NP or the Ab. However, this methodology has different drawbacks. For instance, hydrophobic interactions can lead to denaturation and loss of activity of the immobilized Abs, as a consequence of conformational changes induced in the adsorption process [11, 12]. On the other hand, electrostatic interactions between oppositely charged NPs and Abs can give rise to weak attachments, where the Ab can be detached by pH or ionic strength changes [13].

1.1.2 Covalent Binding

Covalent binding of Abs is not as easy to carry out as physical adsorption. In fact, it requires the introduction of functional groups on the NP surface, or the chemical modification of the Ab. The major advantages of covalent attachment compared with physical Ab adsorption are the higher reproducibility and that the Ab molecules remain strongly attached to the NPs surface so that they cannot be desorbed with pH or ionic strength changes.

Random Covalent Immobilization

One of the most popular ways of covalently attaching Abs to NPs entails the binding through their primary amines. The amine groups of Abs are abundant throughout their surface and they are very reactive without any chemical modification with a variety of reactive groups of the NP. In the case of NPs bearing carboxylic groups on their surface, these groups have to be activated prior to

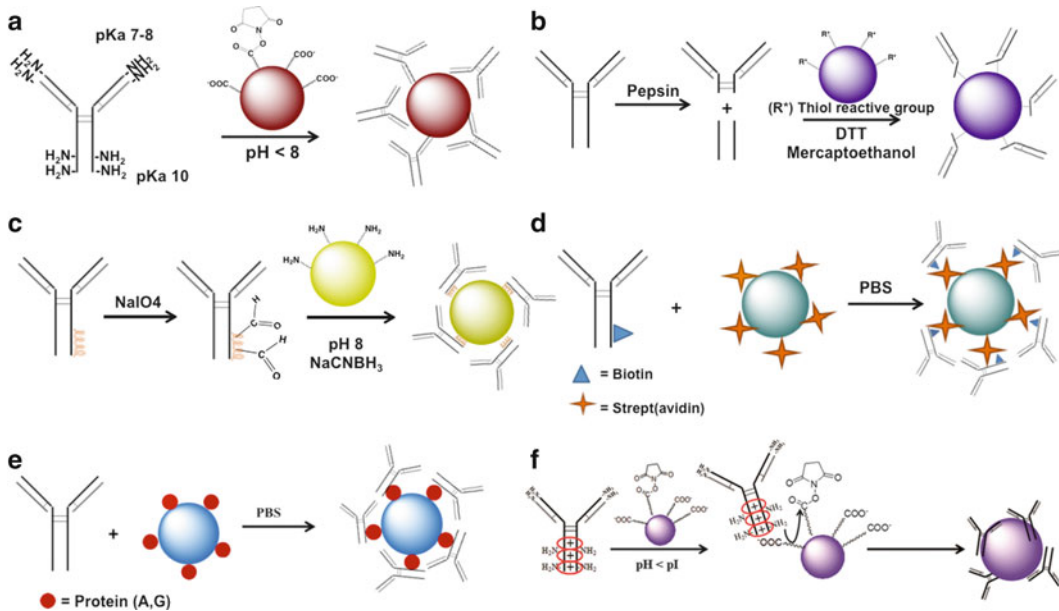


Fig. 2 Scheme of Ab immobilization by using: **(a)** binding through Ab primary amine groups, **(b)** binding through thiol groups of the Ab, **(c)** binding through sugar chains of the Ab, **(d)** binding through biotin binding proteins, **(e)** binding through Fc-binding proteins, **(f)** ionic adsorption plus covalent binding

Ab binding, using carbodiimide (EDC) and *N*-hydroxysuccinimide (NHS) [8, 14]. This binding chemistry, however, can lead to a random immobilization of the Abs on the NP surface (Fig. 2a). This is because at the usual working pH (generally around 7), the most reactive amine groups are placed in the Fab region, that is, the antigen binding site [15]. Therefore, this methodology can lead to the loss of biological activity [16, 17]. For this reason, other techniques that result in an oriented immobilization are preferred.

Oriented Covalent Immobilization

To avoid Ab random covalent immobilization, different alternative strategies have been developed over the last years. However, these oriented covalent binding strategies require several steps, including the Ab chemical modification that includes the oxidation of its sugar moieties or the reduction of disulfide bonds.

One of the strategies that ensure the Ab covalent oriented immobilization is based on reducing the disulfide bonds present in the hinge region of the Ab structure, by reducing agents (mercaptoethanol, dithiotreitol) [18]. Due to disulfides in the hinge region are the most susceptible to reduction, it is possible to selectively cleave only these disulfides and thus to split the antibody into monovalent halves without altering their 3D structure and

antigen-binding efficiency. This chemical modification could also be combined with fragmentation of the IgG within the hinge region by the use of proteolytic enzymes (pepsin, papain, etc.) [19]. In this way, it is possible to selectively bind an Ab fragment ($F(ab')_2$ or Fab'), through thiol groups, without altering the 3D structure of the Ab, and maintaining a high binding affinity. The main disadvantages of this methodology are the need of a previous Ab chemical modification, and that it is necessary to introduce thiol reactive groups on the nanoparticles surface such as maleimide, iodoacetyl or 2-pyridyl disulfide among others. In the case of gold nanoparticles, for instance, it is possible to directly conjugate the Ab through Au-S bond.

Binding through the sugar chains of the Ab is also another way to ensure the oriented covalent binding of Abs. However, this methodology involves the oxidation of sugar moieties present in the Fc region of the Ab structure [20] in order to create aldehyde groups in the Ab that could react through reductive amination with aminated nanoparticles [21] (Fig. 2c). Thus, to carry out this coupling strategy a mild oxidation by sodium periodate is necessary to maintain the integrity of Ab structure. The major drawback of this strategy, apart from the chemical Ab modification, is the necessity of having glycosylated Abs. However, some monoclonal Abs or some recombinant Abs do not have carbohydrates in their structure.

1.1.3 Binding by Adapter Molecules

This strategy also ensures that the antibody Fab region will be available for antigen recognition due to the oriented Ab immobilization through the Fc region. The main problem is that most of these methodologies require complex processes such as the Ab modification, or the nanoparticle functionalization with expensive binding proteins. Moreover, although the binding is much stronger than the one achieved by physical adsorption still remains to be reversible.

One way to achieve oriented Ab immobilization is using biotin binding proteins (Fig. 2d). The strept(avidin)–biotin interaction is one of the most rapid and strongest non-covalent interaction known. The bond between biotinylated Ab and streptavidin occurs in a natural way with a high affinity constant, and it is very resistant to different conditions (pH, ionic strength, temperature, etc.) [22–24]. In this case it is necessary to functionalize the nanoparticle surface with streptavidin, and label the Fc region of the antibody with biotin to ensure an oriented Ab immobilization (there are many biotinylated Abs commercially available). Another procedure for the oriented immobilization of Abs using adapter molecules describes the use of Fc binding proteins such as protein G or protein A (Fig. 2e). These proteins specifically bind to the Fc region of the immunoglobulin IgG [25, 26]. The advantage of this strategy is that it is not necessary the Ab modification, nevertheless the nanoparticles need to be functionalized with these Fc binding proteins.

1.1.4 Ionic Adsorption Plus Covalent Binding

As it has been previously reported, there are several strategies described for the functionalization of NPs with Abs. Nevertheless, none of them allows binding the protein in an oriented and irreversible way without involving the chemical modification of the antibody or the use of expensive adapter proteins. Considering this and the fact that the biosensing field requires higher sensitivities, fast and reliable results at a low cost of production, it is necessary to develop new, simple and universal conjugation methodologies. Among the aforementioned methodologies, the covalent coupling of the superficial amine groups of the Ab with carboxylic moieties present on the NPs via carbodiimide chemistry is by far the simplest covalent coupling methodology. However, despite the advantage that this approach does not require the chemical modification of the Ab, the oriented attachment of this molecule is usually compromised. However, we recently demonstrated that a rational design of Ab incubation conditions favors its ionic pre-adsorption followed by its site-specifically covalent attachment rather than its direct covalent binding through its more reactive amine groups [3] (Fig. 2f).

Knowing that ionic interactions occur faster than covalent ones, it is possible to favor a fast ionic adsorption of the Ab through the region with the greatest number of positive charges. Therefore, covalent binding only occurs through the region of the Ab surface where ionic adsorption took place. As ionic adsorption rate depends mainly on the number and position of charged groups present on the protein surface it can be used to orient Abs. When the charge distribution of the Ab is analyzed it is observed that both positive and negative charges are located all around the biomolecule. However, as the Ab is not a symmetric molecule, there is an interaction plane with the largest area, i.e., the region with the greatest number of positive charges. This plane is the one involving the four Ab subunits. Therefore, if the Ab is adsorbed through its richest positive zone, the antigen recognition sites will stay close to the NP but will not be involved during the conjugation process (Fig. 3). Thus, the biological activity of the Ab is preserved and the antigen binding capacity of the Ab-MNPs will be preserved.

This strategy requires two simple requirements: (a) to determine the isoelectric point (pI) of the Ab in order to find the pH of the media that favor its ionic adsorption, and (b) to design a bifunctional NP. This second factor is due to the fact that ionizable groups are needed to absorb the Ab onto the NP surface and, on the other hand, reactive groups are needed to allow its covalent attachment.

Thus, to ensure an oriented covalent immobilization of Abs onto negatively charged NPs, it is necessary a partial activation of the carboxylic groups of NPs, with EDC and NHS. It is important to note that a negative charge is lost per each carboxylic group that results activated with EDC assisted by NHS. Therefore, it is important to optimize the molar ratio between EDC/NHS and carboxylic

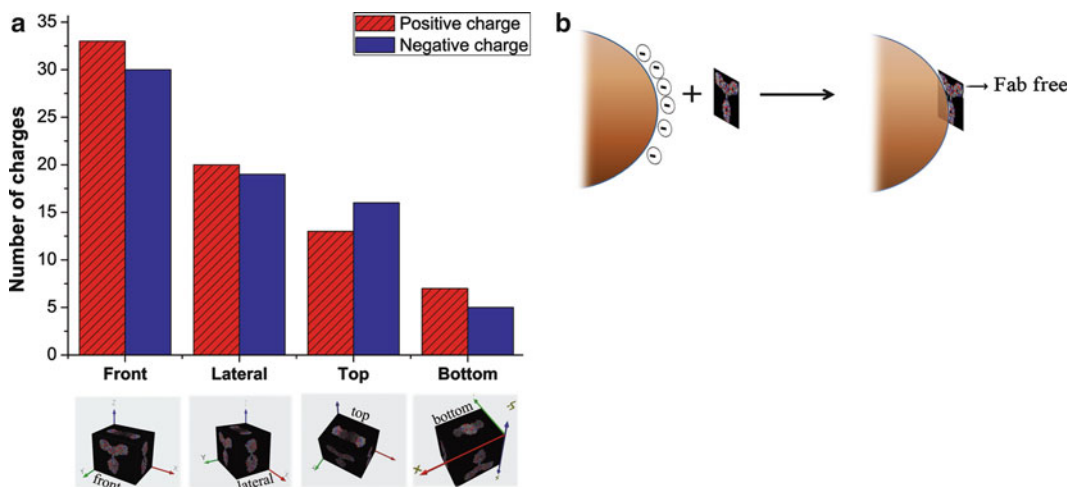


Fig. 3 (a) Number of antibody charged residues per possible plane of interaction with nanoparticles; (b) Ab interaction plane with largest area. Reprinted with permission from reference. 3 Copyright 2011, American Chemical Society

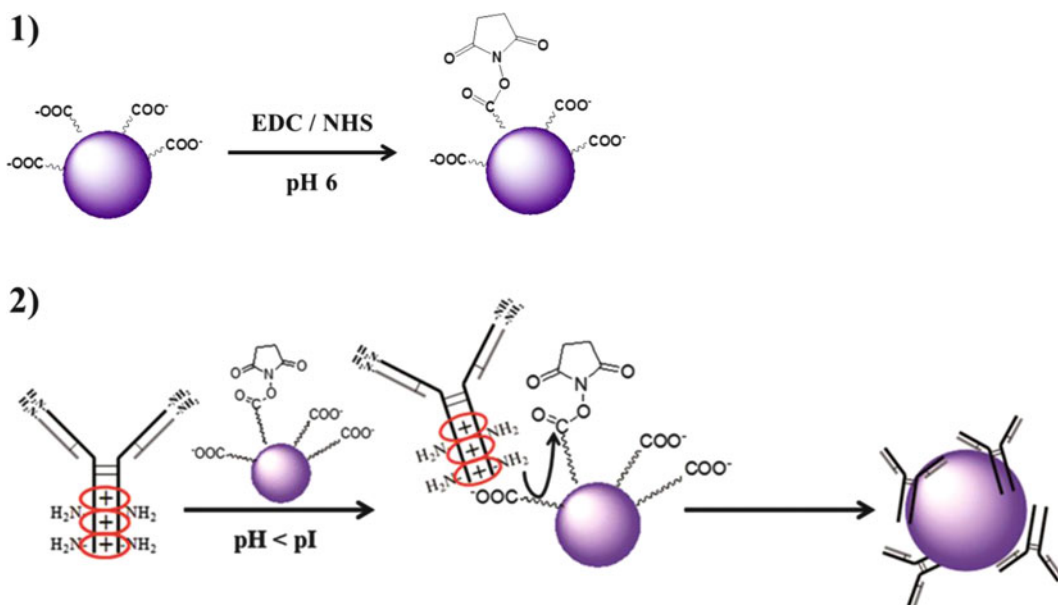


Fig. 4 (1) partial activation with EDC/NHS to obtain a bifunctional NP; (2) Scheme of the oriented Ab immobilization using carbodiimide chemistry when a ionic adsorption plus a covalent two-step coupling strategy is favored

groups, to assure there are enough unmodified carboxylic groups for the previous ionic Ab adsorption (Fig. 4).

The ionic adsorption between Abs and carboxylated NPs only takes place when working at a pH lower than the Ab pI, as at this pH the net Ab charge is positive. After the two binding steps, validation of the covalent immobilization can be confirmed due to the

reversible character of ionic interactions. Increasing the ionic strength or changing the pH of the media give rise to desorption from the NP surface of ionically adsorbed Abs. On the other hand, Abs that are covalently immobilized cannot be eluted. Therefore, all Abs attached on the nanoparticle surface will be well-oriented and covalently immobilized.

In summary, it is possible the Ab attachment onto carboxylated NPs in a well-oriented way without modifying the biomolecule using the simple and well-known carbodiimide chemistry. Thus, avoiding possible damages on the Ab structure, that could produce a decrease on its biological activity, and also complex protocols with several time-consuming steps or that imply the use of expensive reagents.

Next, we will explain the steps that are needed to carry out in order to achieve the oriented covalently binding of antibodies on carboxylated NPs using this two-step coupling methodology.

2 Materials

1. Commercial magnetic nanoparticles (fluidMAG-PAA 4108 Chemicell).
2. Homemade magnetic nanoparticles with a diameter of 8 nm determined by transmission electron microscopy (TEM) and 50 nm by dynamic light scattering (DLS) prepared as reported elsewhere [21].
3. Rabbit Anti-Horseradish Peroxidase fractionated antiserum (P7899 Sigma-Aldrich) named as Ab IgG anti HRP.
4. Mouse Anti-carcinoembryonic antigen clon 3C1 (Hytest Ltd) named as Ab IgG anti CEA1.
5. Mouse Anti-carcinoembryonic antigen clon 3C6 (Hytest Ltd) named as Ab IgG anti CEA2.
6. Rabbit Anti-human chorionic gonadotropin hormone clon 5014 (Medix Biochemica) named as Ab IgG anti hCG1.
7. Rabbit Anti-human chorionic gonadotropin hormone clon 5016 (Medix Biochemica) named as Ab IgG anti hCG2.
8. Peroxidase from Horseradish Type VI (P8375 Sigma-Aldrich).
9. EDC, 1-ethyl-3(3-dimethyl aminopropyl)carbodiimide hydrochloride (E1769 Sigma-Aldrich).
10. NHS, *N*-hydroxysuccinimide (130672 Sigma-Aldrich).
11. ABTS, 2,2'-Azino-bis(3-ethylbenzothiazoline-6-sulfonic acid) diammonium salt (A1888 Sigma-Aldrich).
12. H₂O₂, Hydrogen peroxide solution (141077.1211 Pancreac).

13. Bovine serum albumin (A2153 Sigma-Aldrich).
14. Adsorption buffer: 10 mM MES buffer pH 5.
15. Desorption buffer: 10 mM sodium phosphate buffer pH 7.5, 0.3 M sodium chloride.
16. Activation buffer: 10 mM MES buffer pH 6.1.
17. HRP activity buffer: 50 mM sodium phosphate pH 6.0.
18. Coomassie Plus (Bradford) Assay Reagent (23238 Thermo Scientific).
19. PhastGel™ IEF 3-9 (17-0543-01 GE Healthcare).
20. PAGER® Gold Precast 4–20 % Trys-Glycine gels (59511 Lonza).

3 Methods

3.1 Determination Ab Isoelectric Point

In order to determine the pI of the antibody, the isoelectric focusing can be carried out using Pharmacia Phast System. Phast Gel® IEF gels between pH 3–9 can be used. 2 µl of Ab solution 100 µg/ml is applied to the gel and separated according to Phast System Technique File No. 100. The gel is silver stained according to the instructions of Pharmacia's Phast System. As it could be observed in Fig. 5 different antibodies can have large differences in their pI values. Therefore, it is critical to check the pI of the antibody in order to select the incubation conditions that ensure the two-step coupling methodology proposed.

TECHNICAL SPECIFICATIONS (Kit pI 3,5-9,3)

Protein	pI (Native)
Amylglucosidase	3.50
Methyl red (dye)	3.75
Trypsin inhibitor	4.55
b-Lactoglobulin A	5.20
Carbonic anhydrase B (bovine)	5.85
Carbonic anhydrase B (human)	6.55
Myoglobin, acidic band	6.85
Myoglobin, basic band	7.35
Lentil lectin, acidic	8.15
Lentil lectin, middle	8.45
Lentil lectin, basic	8.65
Trypsinogen	9.30



Samples:
 1.- Ladder
 2.- Ab IgG anti HRP
 3.- Ab IgG anti hCG1
 4.- Ab IgG anti hCG2
 5.- Ab IgG anti Fc
 6.- Ab IgG anti CEA1
 7.- Ab IgG anti CEA 2
 8.- ---

Fig. 5 IEF gel of Abs with different pI values

3.2 Nanoparticle Colloidal Stability

Not all nanoparticles present the same colloidal stability, as it depends on the size, the type of reactive groups on their surface and the density of these groups per nm^2 [2]. It is very important to avoid MNPs aggregation during the different Ab immobilization process steps. For that reason it is necessary to study the colloidal stability of the nanoparticles at different pH solutions and ionic strength media before Ab immobilization is carried out.

Resuspend 0.1 mg of COOH-MNPs in 0.25 ml of different buffer solutions, with pH ranging from 1 to 9. Incubate for 2 h at room temperature and check the MNPs stability (Fig. 6). When aggregation is not observed by eye view, you have to check the colloidal stability by dynamic light scattering (DLS) measurements. Figure 7 confirms that no aggregation occurs between pH 3 and 9

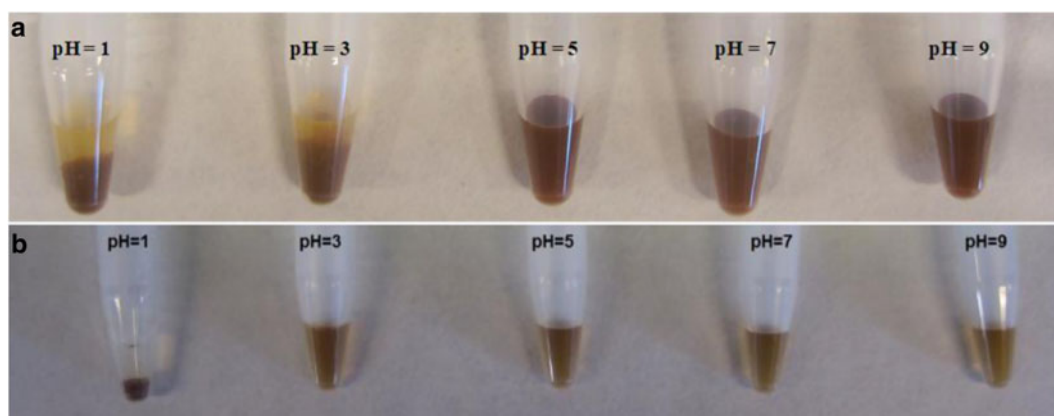


Fig. 6 Effect of the pH on the stability of different MNPs: (a) Magnetic nanoparticle 200 nm diameter from Chemicell® by DLS, (b) homemade magnetic nanoparticle 50 nm diameter by DLS [27]

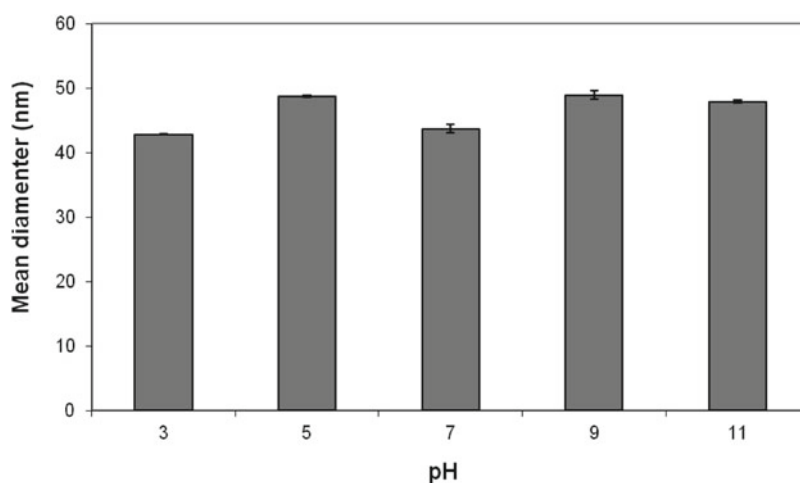


Fig. 7 DLS measurements of homemade magnetic nanoparticles at pH values where aggregation by eye view was not observed

in the case of the home made magnetic MNPs. Any significant change in the hydrodynamic diameter of Chemicell NPs was also not observed between pH 5 and 9. Therefore, in order to favor the ionic adsorption of the Ab it would not be possible to work at pH values lower than 3 or 5 in the case of homemade or Chemicell MNPs respectively.

3.3 Optimization of Ab-Nanoparticle Ionic Interactions

Prior to the covalent attachment of the Ab, it is necessary to check if the Ab can be ionically adsorbed on and desorbed of the MNP surface, in order to remove any non covalent bound Ab molecule after the two-step covalent conjugation. Once the Ab pI has been determined and the stability of MNPs has been studied, the proper conditions for Ab adsorption/desorption have to be optimized. Below, all the steps that are needed to be carried out in order to validate the adsorption/desorption process are described using Chemicell MNPs and anti-HRP as model antibody.

1. Incubate 100 µg of Ab IgG anti HRP with 10 mg of COOH-MNPs (fluidMAG-PAA 4108) in 1 ml of 10 mM MES pH 5 (adsorption buffer) during 30 min (*see Note 1*).
2. Separate MNPs with a magnet and remove the supernatant to determinate the amount of Ab that has not been adsorbed on the nanoparticle.
3. Resuspend MNPs in 1 ml of 10 mM NaP buffer pH 7.5, 0.3 M NaCl (desorption buffer) and incubate during 30 min (*see Note 2*).
4. Separate MNPs with a magnet and remove the supernatant to determinate the amount of Ab that has been desorbed from the nanoparticle.
5. The amount of Ab present in the supernatants after the adsorption and desorption can be quantified using a very fast colorimetric protein determination kit (*Bradford assay*) and/or Native PAGE electrophoresis (*see Note 2*).

3.4 Two-Step Oriented Covalent Immobilization Protocol

1. Wash MNPs as follows: Add 1 mL of 10 mM MES pH 6.1 to 10 mg of carboxylated magnetic nanoparticles (COOH-MNPs, fluidMAG-PAA 4108). Then, centrifuge the nanoparticles at $12,100 \times g$ during 10 min. Repeat the process three times.
2. *Activation Step.* Incubate 10 mg of COOH-MNPs with 1 mL of 10 mM MES pH 6.1 containing 5 µmol of EDC and 7.5 µmol of NHS during 30 min at 37 °C (*see Note 3*).
3. Wash three times the COOH-MNPs with 1 mL of 10 mM MES pH 6.1 (*see step 1*).
4. *Immobilization Step.* Incubate the MNPs with 1 mL of 100 µg/mL of Ab IgG anti HRP prepared in 10 mM MES pH 5 during 2 h at 37 °C (*see Note 4*).

5. Centrifuge at $12,100 \times g$ during 5 min and discard the supernatant (*see Note 5*).
6. Remove the Ab that has not been covalently attached to the MNP by washing with 1 ml of 10 mM NaP pH 7.5, NaCl 0.3 M 30 min at 37 °C (*see Note 6*).
7. Centrifuge at $12,100 \times g$ during 5 min and discard the supernatant (*see Note 5*).
8. *Blocking Step*. Resuspend the MNPs with 1 mL of BSA 1 % in 10 mM MES pH 6.1. Incubate during 16 h at 4 °C (*see Note 7*).
9. Wash three times the MNPs with 1 mL of 10 mM MES pH 6.1.
10. Store at 4 °C.

3.5 Determination of the Biological Activity of the Immobilized Ab IgG Anti HRP

1. Incubate 10 mg of Ab-MNPs with 1 mL of 1 mg/mL of peroxidase in 10 mM sodium phosphate pH 7.5 300 mM NaCl during 30 min.
2. Wash three times the Abs-MNPs with 10 mM sodium phosphate pH 7.5 300 mM NaCl and resuspend in 1 mL of 10 mM sodium phosphate pH 7.5.
3. Add 10 μ l of Ab-MNPs suspension on 1 mL of a solution ABTS-H₂O₂ (100:1, v/v) prepared in 50 mM sodium phosphate pH 6.0.
4. Measure the increase in the absorbance at 414 nm during 15 min (Fig. 8) (*see Notes 8 and 9*).

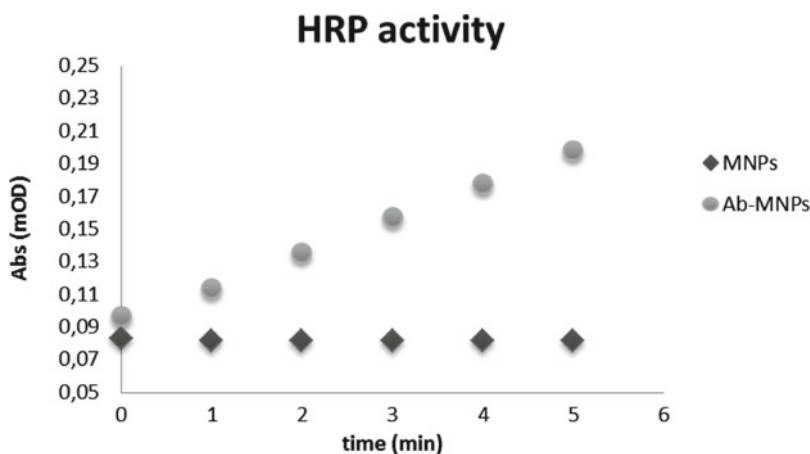


Fig. 8 Biological activity of the immobilized Ab: HRP activity of Ab-MNPs

4 Notes

1. In this case negatively charged nanoparticle and Ab with a pI around 6.1 are being used; therefore, a solution of pH 5 is needed in order to have a net positive charge of the Ab. It is necessary to work at least 0.5 U of pH below the Ab pI to guarantee its ionic adsorption onto the nanoparticle surface.
2. Due to the reversible character of ionic interactions it is possible to desorb the Ab changing the pH and the ionic strength of the media. It is necessary to increase the pH of the media over the Ab pI and add a high concentration of NaCl, in order to change the global net charge of the Ab and increase the ionic strength. A fully Ab desorption has to be carried out to be sure that after the covalent attachment of the Ab takes place, it would be possible the desorption of the non-covalent (ionic) attached Ab molecules. As it could be observed in Fig. 9, in the case of Chemicell MNPs the binding of the anti-HRP Ab by physical adsorption only occurred when a buffer with low ionic strength and a pH lower than the pI of the antibody was used. Besides, absorption only took place through electrostatic binding since quantitative desorption of the bound antibody occurred when the pH and ionic strength of the buffer was increased.
3. Depending on the selected nanoparticle (on the amount of reactive groups present on the nanoparticle surface), it could be necessary to use sulfo-NHS instead of NHS. This is due to the fact that sulfo-NHS preserves the negative net charge of the nanoparticles, while NHS generates a neutral molecule. This negative intermediate can avoid nanoparticle aggregation.

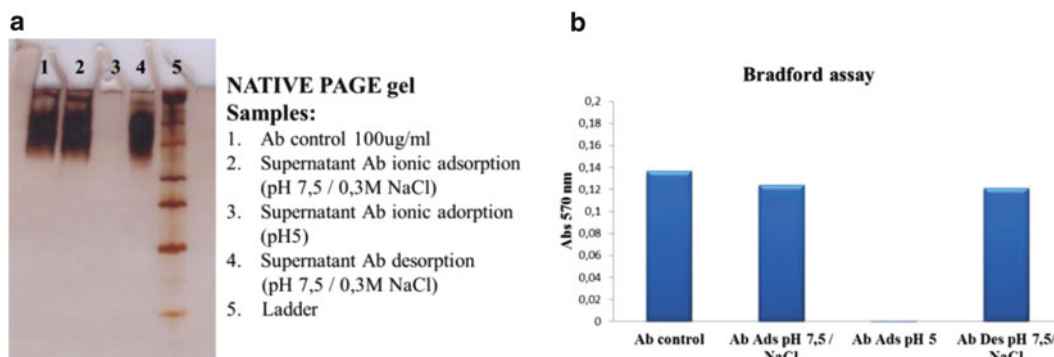


Fig. 9 Ab adsorption/desorption processes: (a) native polyacrylamide electrophoresis gel (4–20 %), (b) colorimetric Bradford assay

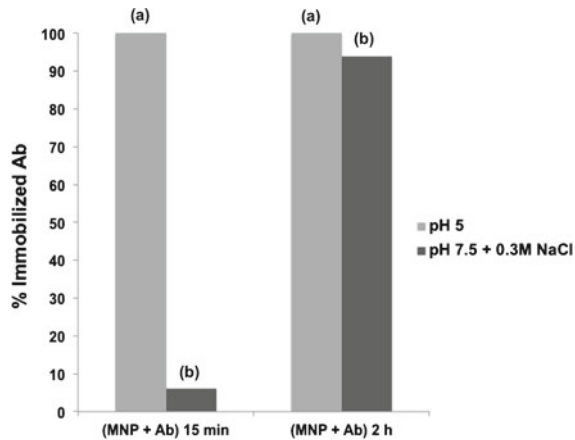


Fig. 10 Results that confirm the two-step immobilization process proposed after quantifying by Bradford assay the amount of protein present in the supernatant after: **(a)** incubating the partially activated MNPs with the Ab solution prepared in the absorption buffer (pH 5) for 15 min and 2 h respectively (to quantify the ionic adsorption ratio); and **(b)** incubating both Ab-MNPs with desorption buffer (pH 7.5 + 0.3 M NaCl) for 30 min (to quantify the covalent binding ratio)

4. The pH of incubation depends on the Ab pI. To use this methodology, the pH of the incubation buffer must be lower than the Ab pI.
5. The supernatant could be used to determine the amount of attached Ab by Bradford assay, polyacrylamide gels, etc. (*see* Subheading 3.3). This would allow confirming that immobilization proceeds through the two-step immobilization process proposed. Figure 10 shows that most of the attached anti-HRP Ab could be desorbed from EDC/NHS activated COOH-MNPs after 15 min of incubation when increasing the pH and ionic strength of the incubation buffer (desorption buffer). This demonstrates that ionic adsorption is very rapid and faster than the irreversible covalent binding of the Ab molecules. The incubation for a longer period of time reduces the percentage of Ab that could be released from the MNPs activated with EDC/NHS as most Ab molecules were irreversible covalently attached after 2 h [3].
6. The pH and ionic strength of the media should be adjusted so that the ionically adsorbed Ab can be desorbed from the nanoparticle surface (this pH has to be previously determined as shown in Subheading 3.3).
7. Depending on the Np size, it could be necessary to use other small blocking agents (i.e.: TRIS, ethanolamine, glycine, polyethylene glycol).

8. One unit of enzyme (IU) was defined as the amount of enzyme catalyzing the hydrolysis of 1 μmol of substrate per minute under the specified conditions.
9. The biological activity of the MNPs functionalized using the proposed methodology is similar to the MNPs functionalized through the carbohydrates moieties placed on the Fc region of the Ab (one of the most frequently used methodologies that ensures an oriented Ab binding) [3].

References

1. Edelman GM, Cunningh BA, Gall WE, Gottlieb PD, Rutishau U, Rutishau U, Waxdal M (1969) *Proc Nat Acad Sci USA* 63:78
2. Woof JM, Burton DR (2004) *Nat Rev Immunol* 4:89
3. Puertas S, Batalla P, Moros M, Polo E, del Pino P, Guisan JM, Grazu V, de la Fuente JM (2011) *ACS Nano* 5:4521
4. Jung Y, Jeong JY, Chung BH (2008) *Analyst* 133:697
5. Kausaite-Minkstimiene A, Ramanaviciene A, Kirlyte J, Ramanavicius A (2010) *Anal Chem* 82:6401
6. Wiseman ME, Frank CW (2012) *Langmuir* 28:1765
7. Chou S-W, Shau Y-H, Wu P-C, Yang Y-S, Shieh D-B, Chen C-C (2010) *J Am Chem Soc* 132:13270
8. Pham TT-H, Sim SJ (2010) *J Nanopart Res* 12:227
9. Puertas S, Moros M, Fernández-Pacheco R, Ibarra MR, Grazu V, de la Fuente, JM (2010) *J Physics D-Appl Phys* 43:474012
10. Roque ACA, Bispo S, Pinheiro ARN, Antunes JMA, Goncalves D, Ferreira HA (2009) *J Mol Recognit* 22:77
11. Butler JE, Ni L, Nessler R, Joshi KS, Suter M, Rosenberg B, Chang J, Brown WR, Cantarero LA (1992) *J Immunol Methods* 150:77
12. Torcello-Gomez A, Santander-Ortega MJ, Manuel Peula-Garcia J, Maldonado-Valderrama J, Jose Galvez-Ruiz M, Luis Ortega-Vinuesa J, Martin-Rodriguez A (2011) *Soft Matter* 7:8450
13. Pei Z, Anderson H, Myrskog A, Duner G, Ingemarsson B, Aastrup T (2010) *Anal Biochem* 398:161
14. Mu B, Huang X, Bu P, Zhuang J, Cheng Z, Feng J, Yang D, Dong C, Zhang J, Yan X (2010) *J Virol Methods* 169:282
15. Sesay MA (2003) *Biopharm Int Applied Tech Biopharm Dev* 16:32
16. Fuentes M, Mateo C, Guisan JM, Fernandez-Lafuente R (2005) *Biosens Bioelectron* 20:1380
17. Rao SV, Anderson KW, Bachas LG (1998) *Mikrochim Acta* 128:127
18. Tiefenauer LX, Kuhne G, Andres RY (1993) *Bioconjug Chem* 4:347
19. Brogan KL, Wolfe KN, Jones PA, Schoenfish MH (2003) *Anal Chim Acta* 496:73
20. Batalla P, Fuentes M, Grazu V, Mateo C, Fernandez-Lafuente R, Guisan JM (2008) *Biomacromolecules* 9:719
21. Lin P-C, Chen S-H, Wang K-Y, Chen M-L, Adak AK, Hwu J-RR, Chen Y-J, Lin C-C (2009) *Anal Chem* 81:8774
22. Dinauer N, Balthasar S, Weber C, Kreuter J, Langer K, von Briesen H (2005) *Biomaterials* 26:5898
23. Koh I, Hong R, Weissleder R, Josephson L (2009) *Anal Chem* 81:3618
24. Wang J, Cao Y, Xu Y, Li G (2009) *Biosens Bioelectron* 25:532
25. Jung Y, Lee JM, Jung H, Chung BH (2007) *Anal Chem* 79:6534
26. Wang H, Liu Y, Yang Y, Deng T, Shen G, Yu R (2004) *Anal Biochem* 324:219
27. Moros M, Pelaz B, Lopez-Larrubia P, Garcia-Martin ML, Grazu V, de la Fuente JM (2010) *Nanoscale* 2:1746

Design and Characterization of Functional Nanoparticles for Enhanced Bio-performance

Pablo del Pino, Scott G. Mitchell, and Beatriz Pelaz

Abstract

Recent years have witnessed the rapid development of inorganic nanomaterials for medical applications. At present, nanomedicines—nanoparticles (NPs) destined for therapy or diagnosis purposes—can be found in a number of medical applications including therapeutics (either self-therapeutics or drug carriers) and diagnosis agents (e.g., contrast agents for imaging or transducers in biosensors). Pushing the limits of nanotechnology towards enhanced nanomedicines will surely help to reduce side effects of traditional treatments and to achieve earlier diagnosis. As for all medical approaches, the ultimate aim of nanomedicine is improving the well-being of patients. However, mixing nanomaterials with biological components such as fluids, living cells, and tissues does not always result as expected. The interplay between engineered nanomaterials and biological components is influenced by complex interactions which make predicting their biological fate and performance a nontrivial issue. Indeed, the structural integrity and the a priori function of nanomaterials can change dramatically due to unwanted nano–bio interactions. For medical applications in particular, any new nanomaterial has to be exhaustively studied when it comes in close contact with biological fluids and living cells or organisms. The motivation is clear: first, many unwanted effects can be turned on unexpectedly (e.g., leakage of toxic ions, ROS production, and sequestration by the phagocytic system) and second, their purpose as therapeutic or diagnostic agent can be lost as they are transferred to the desired working environment. This chapter aims to highlight key factors that should be taken into account when choosing and characterizing such functional materials for a given application, with a view to minimizing unwanted nano–bio interactions, rather than providing an exhaustive compilation of recent work. We hope that both early-stage and experienced researchers will find it valuable for designing nanoparticles for enhanced bio-performance.

Key words Nanomedicines, Nanoparticles, Nanomedicine, Nanomaterials, Medical applications, Nano–bio interactions

1 Introduction

Within the broad field of nanotechnology, which has developed rapidly over the last two decades, colloidal nanoparticles containing primarily inorganic components (herein inorganic NPs) have emerged as rich and versatile systems whose specific properties aid in medicine, be it as novel therapeutics or diagnostic tools [3, 4].

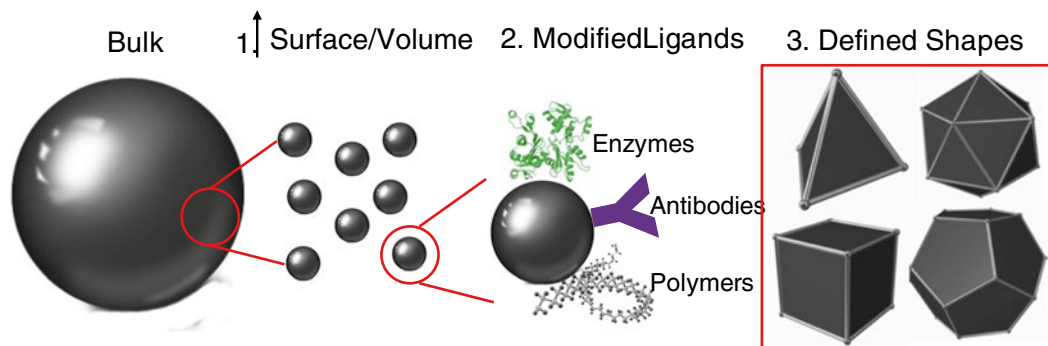


Fig. 1 Representation of the most important characteristics of inorganic nanoparticles: their high surface-to-volume ratio, ability to be modified by various types of ligand, and the wealth of well-defined geometric shapes that can be accessed

Inorganic particles themselves are a diverse range of materials—and will be described in turn—however, several key properties are commensurate across each discrete particle type, namely, that each provides a modifiable molecular “scaffold” to build upon, high surface to volume ratio, immense variety of shape and size, as well as unique physicochemical properties such as bright fluorescence, plasmonic effects, or superparamagnetism, to name a few [5]. Furthermore, these properties can be fine-tuned by minor alteration of the synthetic conditions and modification of anchor points on their surface for the further attachment of molecules, aiming medical purposes [6]. As an example, Fig. 1 illustrates inorganic nanoparticles which possess a high surface-to-volume ratio, modifiable ligands, and defined shapes. In order to discuss functionalization, we must first provide a short description of the each “scaffold,” how these are synthesized, and perhaps more significantly, how the distinctive properties of each type may enhance their potential for biomedical applications. As mentioned previously, inorganic NPs encompass a wide variety of materials, displaying unique and diverse properties. Importantly, the term “inorganic” refers to the core component of the material, the “scaffold” upon which a diverse range of functionality can be built. It should be noted, however, that in the context of biological applications, the term *inorganic* nanomaterials, typically refers to *inorganic-organic hybrids* [1]. These are composed of (1) an inorganic core, (2) a purposely constructed primary coating made of organic or inorganic material and last, (3) an organic layer typically formed by proteins, resulting from the interaction with the biological environment. Typically, layer (2) confers colloidal stability to the system and it can also accommodate molecules of biological relevance, with a view towards specific bioapplications, e.g.,

targeting, drug, peptide-like properties. Layer (3) is in general the result of unspecific adsorption of proteins which form the so-called protein corona.

In the following section we introduce different types of inorganic core and in Subheading 3 move on to discuss the chemically designed primary coating in detail (*see* Fig. 12.1). Due to space limitations, the central focus of this chapter concerns the most common inorganic materials used in nanomedicine, i.e., noble metals such Au, and Ag (some of the less common transition metal NPs will also be introduced), semiconductor NPs called quantum dots (QDs), upconverting NPs (UC NPs), and Fe-containing superparamagnetic NPs. We have left out prolific systems such as silica (SiO₂) NPs and carbon nanotubes, the former one because they serve principally for hosting drugs, fluorescence markers, or other NPs [7, 8]. Silica coatings are also used for encapsulating other inorganic materials [9]. Carbon nanotubes are omitted here because of toxicity concerns [10, 11]. It should, however, be mentioned that important developments are being made in the use of graphene (the “other” carbon NP) and nano-diamond in biomedical applications [12, 13]. Please forgive us for any omissions in citing articles from the literature.

2 Inorganic NPs

2.1 *Choosing the Right Inorganic Material*

The composition of the core material itself determines the most relevant physicochemical properties of the system which in turn confers “unique” attributes such as useful optical, magnetic or catalytic properties, to name a few. The advance in nanoparticle science over the last two decades is such that a tremendous variety of NPs can be accessed by varying precursors and kinetic and/or thermodynamic variables in the syntheses [14, 15]. Parameters such as the composition, crystallinity, size, charge, shape, and structure (core@shell or hollow shell) are of the utmost importance [16]. In addition to the physicochemical properties of the core, these properties influence greatly in the suitability of the system for a given bioapplication. However, how these nanomaterials perform in physiological media is far from a trivial issue which in general cannot be broken down to just a few parameters [1].

Next we discuss some sound examples concerning the composition of inorganic NPs, aimed for biological applications. But first, let us give some hints and tips on the direction to take when designing a NP to be in contact with living “things.” The first choice depends on the application, be it as a carrier, imaging agent, signal transducer, etc. Applications are typically connected to the properties of one class of NPs, i.e., plasmonic, photoluminescence, superparamagnetic, etc. For instance, plasmonic NPs such as Au, Ag, or Cu NPs display strong optical properties due to surface

plasmons, i.e., collective oscillations of conduction electrons which can couple to light in the visible and NIR range. These properties have been widely exploited for a variety of applications in sensing (e.g., localized surface plasmon resonance (LSPR) spectroscopy and surface enhanced Raman spectroscopy (SERS)), imaging (e.g., photoacoustic and photothermal) and photothermal therapy. In other example, semiconductor NPs, also called QDs, can be used as photoluminescence probes for labeling or sensing. They exhibit strong (high quantum yield) and stable (low photobleaching) photoluminescence, greatly improving the performance of traditional fluorophores. Also very prolific in literature are iron oxide NPs (mostly maghemite, $\gamma\text{-Fe}_2\text{O}_3$, or magnetite, Fe_3O_4 , single domains of about 5–20 nm in diameter) which have received a great deal of interest in the fields of biotechnology and nanomedicine [17, 18]. This interest has been motivated by the fascinating superparamagnetic behavior that iron oxide NPs exhibit and which make them very suitable candidates for bioapplications such as targeted drug delivery [17, 19, 20], magnetofection [21–23], magnetic hyperthermia [17–19, 24–29], magnetic resonance imaging (MRI) [20, 30–32], biosensing [33, 34], or magnetic separation [25, 35].

Following the critical selection of a material for a given application, the second important point rests on its toxicity. Ideally, the system should not corrode to produce toxic ions (Ag^+ , Au^{3+} , Cd^{2+} , etc.), produce ROS species, trigger protein denaturation, intercalate with nuclear DNA, accumulate in organs, or cause an allergic response. Please note that these can be interconnected and of course, toxicity is a matter of dose [1].

The composition of the inorganic material can have a determining influence in the toxicity of the system and thereby, in its range of applicability. For example, for surface enhanced Raman spectroscopy (SERS), a widely used high-sensitivity spectroscopic technique, Ag NPs perform much better than Au NPs, producing larger signal enhancements due to the particular optical properties of these types of NPs. However, since Au NPs are less prone (more noble) to corrosion than their Ag counterparts, the former are preferred for applications with living cells or in vivo. Similarly, other applications such photothermal heating and photoacoustic imaging employ Au NPs over other plasmonic NPs. Many parameters must therefore be taken into account when choosing the “right” core for a given application. As previously stated, Au NPs are widely used for many bioapplications; some authors have recently acknowledged the numerous and important applications of Au NPs in a paper entitled “the golden age: biomedical applications of Au NPs” [36]. Although Au NPs are very versatile, and have proven biocompatibility, there are applications where other plasmonic materials such Ag or Cu might be more suitable, even though they have thus far been largely unused. One remarkable example is the area of photothermal heating mediated by

plasmonic NPs for destroying tumors. At this point it is worth making some brief remarks about photothermal heating: plasmonic nanoparticles can produce heat upon illumination with light of energy matching their plasmon band [37]. Typically, NIR sources can penetrate deeply into tissue without causing damage (biological window). However, when light reaches plasmonic NPs, it can be absorbed and transformed into heat which ultimately can be used to destroy tumors [38]. The mechanism is equivalent to magnetic hyperthermia where nanoheaters are made of superparamagnetic NPs and the source is RF radiation. In general, most of the plasmonic nanoheaters are based on anisotropic Au NPs (nanorods [39], nanoshells [40], nanoprisms [41], etc.), even clinical studies and commercially available solutions are mostly based on Au (AuroLase® Therapy from Nanospectra Biosciences). The size (or at least one of the dimensions) of these Au nanoheaters does not allow for renal clearance. Therefore, if delivered in vivo, these will typically accumulate in organs such liver and spleen which is not always the ideal scenario. Very recently, some works involving CuS and CuSe NPs as nanoheaters in photothermal therapy have been proven very efficient in killing tumoral cells [42, 43]. Importantly, the size of these Cu NPs (~10 nm) allows for renal clearance. Although much is still to be done to test the impact of the release of Cu ions in vivo (Cu is less noble than Au or Ag), these recent results illustrate how relatively solid trends can be challenged by new results. These, and others to come, might allow for a change in the direction concerning some relevant applications such photothermal heating (e.g., Cu-containing NPs) [10, 11], photoacoustic imaging (e.g., CuSe [44] or Ag NPs [45]), or antibacterial applications (e.g., Ag NPs) [46, 47], among many others.

Although we have mainly discussed noble metal NPs, one can find similar trends in other classes of inorganic NPs, which are also widely used in bionanotechnology. For instance, although the bright and stable photoluminescence of QDs has attracted much attention in their use as tags for bioapplications, their uses have been traditionally limited to in vitro because they can trigger cytotoxicity effects. The best probes are high quantum yield QDs that typically contain cadmium (CdS, CdSe, CdTe, CdS@ZnS, etc.) although they are easily oxidized to produce toxic Cd ions, well-known carcinogens. Despite the wide use of Cd-based QDs as fluorescence labels in vitro, other less hazardous alternatives have been explored over the past decade. For instance, indium phosphide (InP) QDs promise a safer alternative although less toxic, they can also produce reactive oxygen species under illumination [48]. It is unlikely that current formulations of QDs will be approved for in vivo experimentation, but novel approaches such Ag₂S QDs hold promise for new opportunities in the medical field [49]. On the route to safer approaches, a relatively new alternative type

of imaging agent, upconverting NPs (UC NPs), have generated excitement and expectation in relation to bioimaging [50, 51]. The upconversion process refers to the sequential absorption of two or more photons leading to the emission of light of higher energy than that of the energy absorbed, by anti-Stokes emission. UC NPs are generally formed by an inorganic host and lanthanide dopant ions such as Er^{3+} , Tm^{3+} , and Ho^{3+} embedded in the lattice host; adding Yb^{3+} as dopant enhances the emission efficiency. Host NPs include Y_2O_3 , $\text{Y}_2\text{O}_2\text{S}$, LaF_3 , NaYF_4 and NaGdF_4 among the most frequent host NPs used in biological studies [52]. Wang et al. have made important contributions by producing core@shell UC NPs with tunable emission which open a lot of possibilities in the bioimaging area [53]. Quoting N. Kotov “the broad tunability of these nanoparticles seems to be matched only by the broad range of possible applications” [51].

In other applications, the superparamagnetic behavior of Fe-containing NPs confers two crucial properties of remarkable potential in the context of bioapplications: (1) iron oxide NP-based nanosystems (also assemblies based on superparamagnetic NPs) can be remotely manipulated by an external magnetic field (EMF) [21, 54] and (2) they can resonantly couple to an alternating magnetic field (AMF) [26, 27, 29, 55, 56]. Importantly, the concept of superparamagnetism is intrinsically linked to the nanometer range. In contrast to ferromagnetic particles, larger in size, superparamagnetic NPs are very suitable candidates for *in vivo* bioapplications since the absence of coercivity, among other reasons, prevents potential NP aggregation. In the context of *in vivo* experimentation, NP aggregation represents a potential danger that can lead to embolisms [57]. Concerning the composition of superparamagnetic NPs, iron oxide is the most used in bioapplications as a result of its “good” biocompatibility. However, biocompatibility has to be accompanied by optimal performance for achieving success. For instance, iron oxide NPs are typically used for magnetic hyperthermia *in vivo*. Indeed, magnetic hyperthermia has been recently approved to treat humans (Magforce AG). So far this treatment is only available in Germany at the Charité-Universitätsmedizin Berlin; there, they use ca. 15 nm iron oxide NPs with an aminosilane coating (NanoTherm[®]) and “bio-suitable” AC fields with a frequency of 100 kHz and variable field strength ($0\text{--}18\text{ kA}\times\text{m}^{-1}$). It should be noticed that heating by “more magnetic” particles (ferromagnetic or ferrimagnetic) would require non biocompatible AC fields. These treatments required a high dose of iron oxide NPs for achieving hyperthermia temperatures within the tumor. It would be therefore of great value to find superparamagnetic nanoheaters of superior performance, meaning heating more efficiently so that doses can be decreased. As recently described by Lee et al., the specific loss power (SLP) of NPs (their approximately ability to heat) can be

largely improved by making nanocomposites (core@shell NPs) where a magnetically hard core (e.g., CoFe_2O_4) and magnetically soft shell (e.g., MnFe_2O_4) exhibit exchange coupling. This new type of superparamagnetic NP can dramatically enhanced the SPL values compared to common nanoheaters (more than 34 times higher) [58]. However, all the systems that they discuss contain Co in the core which obviously brings a lot of toxicity concerns for in vivo experimentation. In the same work, Lee et al. performed animal experimentation and reported that apparently, this system does not cause toxicity. There is one obvious open question left within this discussion; since the nanocomposite can achieve the same SLP values than common iron oxide agents, but with 34 times less dose, what is best for treatment, considerably less dose but more toxic Co content or high dose of bare iron oxide? Future studies will surely add more data in this direction, allowing us to safely answer this question.

In summary, in the last two decades, a vast collection of research has established a number of trends concerning the most appropriate choice of inorganic core for a given application. However, as the currently “accepted” materials are imperfect to some extent (such as size, poor magnetic saturation, corrosion), these trends can be challenged as new materials are developed. Table 1 provides a summary of selected current inorganic nanomaterials, their corresponding bioapplications, pros and cons, and relevant and recent work for their synthesis.

In the following, we briefly discuss how inorganic NPs, including the systems highlighted in Table 1, can be formed from molecular precursors.

2.2 Formation of Inorganic NPs

Practitioners of synthetic nanoparticle science have no shortage of synthetic tools and methods at their disposal. There are two main approaches to synthesize nanocrystals, i.e., the “top-down” using physical methods such as laser ablation [87], and the “bottom-up” which employs solution-phase colloidal chemistry. Typically, by using colloidal chemical synthetic methods, a variety of NPs sizes and shapes can be accessed synthetically enabling tailoring for specific purposes. Herein, we focus on wet-chemical approaches, which are prolific in the literature. There are a variety of methods for producing inorganic NPs, for example the use of coprecipitation methods, sol-gel processing, microemulsions, hydrothermal/solthermal methods, or templated syntheses [88]. Due to this diversity, researchers must often choose the most appropriate method to match the desired NP type whilst taking into account the necessary subsequent functionalization steps.

In general, chemical synthetic methods to obtain nanocrystals from a precursor are based on its decomposition (to basic ionic units) or its reduction to zero-valent atoms (metallic NPs); in this context, the crystallization of these atoms to form a nanocrystal

Table 1
Summary of the most important nanomaterials, their applications, and pros and cons

Type	Application	Choices	Pros	Cons	Synthesis
Plasmonic NPs	Therapy	Au, Ag, Cu	High light-to-heat conversion Clinical trials	Few centimeters of laser light into the tissues NPs coating The safety of nanomaterials is still under study	Au [40, 59–64] Ag [45, 65–67]
	Imaging		Provide structural, functional, and molecular information in preclinical studies [71] Real-time imaging	Acceptable resolution The safety of nanomaterials is still under study	
	Sensing		Information at molecular level Sensitive to small changes Reduce biological background interactions	Spatial imaging limitations [72] The safety of nanomaterials is still under study	Cu [43, 68–70]
Semiconductor QDs	Imaging	CdSe, ZnS; CdTe, CdSe, CuInS ₂ , InAs, etc.	Size tunable absorption/emission High fluorescence quantum yields [73] Single-molecule analyses are possible.	Lifetime discrimination between QDs not yet shown Toxicity	CdSe, ZnS; CdTe, CdSe [74, 75], CuInS ₂ , InAs, etc. [76]
	Sensing		Fluorescence energy transfer energy (FRET) and electrochemical sensors [77]	Cytotoxicity due to cation release	

UC NPs	Imaging	In vitro and in vivo labeling [50]	La F ₃ , NaYF ₄ (Yr ³⁺ -Er ³⁺), Y ₂ O ₃ , etc.	High sensitivity Less toxicity than QDs High penetration depths High photostability Optical tunability Single molecule and ions analysis	Improvements of the synthetic methodologies New ions of interest are still to be discovered Quality in the resolution is still not the best Fluorescence issues must be solved	La F ₃ , NaYF ₄ (_{Yr³⁺-Er³⁺}), Y ₂ O ₃ , etc. [50, 52]
	Sensing	Molecular-based fluorescence energy transfer energy (FRET) [79]				
Fe-containing NPs	Therapy	Magnetic hyperthermia	F ₃ O ₄ , MFe ₂ O ₄	Enhance the typical anticancer treatments Clinical trials underway Treatments of imaging and therapy can be applied	NP stabilization, to avoid unspecific interaction and side damage Enhance the efficiency of heat generation of the actual hyperthermia agents The safety of nanomaterials is still under study	F ₃ O ₄ , MFe ₂ O ₄ [80–85]
	Imaging	MRI		Less toxicity than classical contrast agents Clinical uses Excellent spatial resolution generation of 3D images Detection of a broad range of biological species (e.g. DNA, proteins, pathogens, enzymatic)	NP modification Limitation to cross the blood–brain barrier The safety of nanomaterials is still under study The safety of nanomaterials is still under study	
	Sensing	Magnetic relaxation switches (T ₂ -based) [86]		Good sensitivity and accuracy [80]		

can be typically described by the model proposed by LaMer and coworkers [89]. In this model, the concentration of atoms steadily increases as the precursor is decomposed or reduced; then, once the concentration of atoms reaches a supersaturation state, the atoms start to crystallize to form small clusters or so-called nuclei (nucleation process). Following nucleation, clusters grow up to a critical size, where structural fluctuations become so energetically costly that the cluster becomes locked into a well-defined structure, the so-called seed. Importantly, the crystal structure of the seed (single-crystal, singly twinned, or multiply twinned structure) determines ultimately the shape and monodispersity of the final product(s). For instance, in the case that different seeds coexist, different nanocrystal (in shape and/or size) will result. Then, seeds will grow into nanocrystals of increasingly larger size until an equilibrium state is reached between the atoms on the surface of the nanocrystal and the atoms in the solution [90].

Contrary to the atom-by-atom addition, the final nanocrystals can be formed via agglomeration of the nuclei and preformed nanocrystals [91, 92]. Importantly, the shape of the final NPs is determined by a combinations of thermodynamic (e.g., temperature, reduction potential) and kinetic factors (e.g., reactant concentration, diffusion, solubility concentration rate), as well as the presence of capping agents. In principle, by finely tuning the reaction conditions (i.e., seeds structure), it is possible to access different shapes such as octahedral [93], tetrahedral [94], hexagonal plates [95], nanorods [96], triangular plates [97], and dendrites [98]. For more details on the shape of metallic NPs see the excellent review by Xia and coworkers [90]. In addition, the reader is referred to the review of Cushing and coworkers for details on liquid-phase synthesis of inorganic NPs [88]. For information on the synthetic methods for the synthesis of some biomedical-relevant NPs, we urge the interested reader to seek out the references in Table 1.

What follows aims to assist researchers consider the *in vivo* interactions of NPs by considering their organic coatings and NP-protein interactions in greater detail.

2.3 Organics Coatings Towards Stabilization and Functionalization

Although the importance of the inorganic core of any NP is crucial for assessing their bio-performance, the hybrid nature of any “inorganic” NP should be also put into perspective. There are no truly “bare” inorganic NPs—at least colloiddally stable ones—since inorganic NPs require a coating to prevent irreversible agglomeration due to inter-NP van der Waals attractions. This is an important remark which must be taken into account; especially when designing nanomaterials for bioapplications. The coating of choice represents a crucial part of the design of colloidal inorganic NPs as this determines the degree of colloidal stability (to high ionic strengths, shielding against corrosion, unspecific absorption of biomolecules, etc.) and the possibility to further derivatize the

nanomaterials with molecules of biological relevance. Typically, the availability of “free” chemical groups allows for multifunctional derivatization using standard coupling chemistry strategies [99]. Nanomaterials designed for use in biological environments (containing cells, macromolecules, organic and inorganic molecules present in physiological media, etc.) therefore possess an organic layer [100] which ultimately determines their interaction with macromolecules such as nucleic acids, proteins, carbohydrates, and lipids [101]. These interactions at the nano–bio interface normally represent a complex scenario which greatly influences the success of a particular engineered nanomaterial for a certain application (as a sensor, diagnostic tool, drug carrier or more complex multitask systems) [16, 102]. Therefore, especially in a bio-context, materials scientists must critically analyze how both a particular complex nanomaterial and their constituents (surfactants, precursors, macromolecules or organic polymers, etc.) perform in physiological environments that normally are far from the environment where the original synthesis of the nanomaterials took place, i.e., polar or nonpolar solvents with very particular attributes such as ionic strength, pH or presence of multivalent ions, salts or polymers, to name a few. For instance, synthesis of highly monodisperse inorganic nanocrystals made of metals (e.g., Au, FePt), metal oxides (e.g., ferrites, Fe oxides, ZnO), and semiconductor (e.g., CdSe, CdSe/ZnS, CdS, CdTe) are typically done in organic solvents in the presence of capping agents containing aliphatic chains including alkyl phosphine oxides, alkyl phosphonic acids, alkyl phosphines, or fatty acids [100]. In order to use nanocrystals made in organic solvents for bioapplications, these have to be transformed into water soluble materials, as physiological media contains mainly water, among other constituents such as proteins, lipids, salts, or multivalent ions.

Over the past decade different approaches have been used for water-transfer of nanocrystals by for example ligand-exchange (exchanging aliphatic chains by hydrophilic molecules) [103], silanization (growing a glass shell around the NPs) [104], and polymer coating methods (intercalating amphiphilic polymers in the aliphatic shell of the NPs) [105]. All these methods provide material scientists with tools for designing, at the molecular level, the outermost shell of the material. To ensure optimal performances, NPs must be physically and chemically stable in aqueous conditions, namely, they should not aggregate, dissociate, or suffer any irreversible chemical reaction with the surrounding media. Generally, the stabilization and functionalization routes to surface-modified materials are determined by the chemical composition of the NP core as it determines the subsequent suitable stabilization and functionalization processes. For bioapplications, avoiding aggregation and provide NPs with a load of molecules with biological relevance is of the most importance. Many synthetic

routes towards NPs use surfactants or molecules that can act as ligands. The nature of the coating can be very diverse, ranging from small molecules (e.g., forming highly charged monolayers that prevent inter-NP interactions via charge repulsion) [106] to large polymers (that prevent inter-NPs interactions via steric hindrance) [107]. Typically, ligand molecules must be bound onto the NPs surface by some attractive interaction such as chemisorption, electrostatic attraction, or hydrophobicity, or coordination bonds [108, 109]. Different groups (thiol, phosphine, amine, carboxy, etc.) present in a molecule of interest can be used to promote the derivatization of NPs [110]. Also due to the nature of NPs (typically, via electrostatic attraction or hydrophobicity) NPs suspended in biological fluids will normally adsorb organic molecules, typically proteins, to form the so-called protein corona (*see* Subheading 3) [111, 112].

Once stabilization in physiological environments has been achieved by one of the aforementioned methods, NPs can be engineered into complex functional materials for a particular bioapplication. Nowadays, there is a wide variety of chemical methods to anchor molecules of biological relevance onto NPs, i.e., fluorescence tags, polyethylene glycol (PEG) chains, proteins, carbohydrates, DNA, peptides, siRNA, enzymes, antibodies, cyclodextrins, biotin, etc. [41, 113–118]. There are different approaches depending on the chemical groups present on the NPs and the ligand of interest. For instance, conjugation of NPs bearing carboxylates with amine-containing molecules/proteins can be achieved by classical carbodiimide cross coupling approaches; linkage to sulfhydryl groups can be similarly achieved by way of maleimide-terminal ligands, widely commercially available. Click chemistry has been similarly employed in a number of gold nanoparticle conjugation strategies [119]. Different derivatization approaches allow for an extraordinary control over the arrangement of ligands onto NPs which can be used to “tailor” and predict how a nanomaterial of interest is for instance internalized by cells, among other biointeractions [120]. The pioneering work of Stellacci and coworkers showed that by patterning the coating of Au NPs (making “stripes” or defined hydrophobic/hydrophilic domains on monolayer protected NPs), the internalization process can be controlled [121]. In this fascinating work, the authors show how “stripped” NPs penetrate the plasma membrane without bilayer disruption, whereas the equivalent NPs but “non-stripped” are mostly trapped in endosomes.

For most bioapplications, preventing unspecific interactions that otherwise determine the organic coating of NPs (and consequently, their bio-performance) is critical. Understanding how the coating interacts with the biological entities, i.e., cell membranes, serum proteins, polyelectrolytes, and so forth represents a challenge that is often poorly explored. However, relevant and sometimes unexpected results can be derived from accurate control

over unspecific protein adsorption, size distribution, grafting density, and an extensive physicochemical characterization. For instance, although PEG-protected NPs are generally preferred for avoiding unspecific protein absorption, carbohydrate-protected NPs (with a well-defined density of the grafted molecules) can also avoid absorption of proteins and promote specific internalization pathways [113, 115]. Also in this line, enhanced immunosensors can be achieved by controlling the orientation and density of antibodies onto NPs [114].

Sometimes it appears “vague” whether adverse effects are consequence of the inorganic core and/or the organic coating; this is motivated by the great degree of interconnection between physicochemical properties of NPs. For instance, in former studies on the interaction of gold nanorods (a widely used nanomaterial in photothermal therapy) [122] and cells, one can find statements referring to gold nanorods as being toxic whereas it is now clear now that the toxic agent here is the coating, most frequently cetyltrimethylammonium bromide (CTAB). CTAB is the most widely used and convenient surfactant for high-yielding syntheses of Au nanorods even though it is a well-known highly toxic component. CTAB can be released from the surface of nanorods upon exposure to physiological environments [123].

To conclude this section, we wish to stress the importance of suitable NP surface derivatives (organic coating and functional ligands) and the corresponding complete physicochemical characterization. It is of the utmost importance to specify and characterize the coating of NPs (intended or result of unspecific bio-interactions) as these can determine the bio-performance even to a greater extent than the inorganic core. Rigorous characterization helps to avoid misleading (or irreproducible) results and “catastrophic” messages. In the following section, we discuss how the properties of NPs intended for use in physiological environments will typically change due to the absorption of proteins, which ultimately become part of the “hybrid” nanomaterial.

3 Influence of the Organic Coating in Toxicity: Charge, Hydrophobicity and Protein Corona

The possibility of custom-made organic-coated nanomaterials with a wide variety of chemical groups (neutral, positively or negatively charged as well as different hydrophobicity patterns) allows for tailoring the net charge of the nanomaterials as well as a well-defined surface/charge and hydrophilic/hydrophobic patterns [121]. Independent of the synthetic route (in polar or non-polar solvent, inorganic or organic core material), the shape, size, surface area, roughness, porosity or crystallinity, charge and distribution of charges arising from different functional groups play a

critical role in the fate of nanomaterials for bioapplications. This is principally because Coulomb interactions (as well as hydrophobic/hydrophilic interactions) lead a nanomaterial to interact with macromolecules in the physiological milieu (such as proteins or carbohydrates) both in the media or in the cell (membrane receptors, chaperones, genetic material, and so on) [124]. It is noteworthy that when a NP encounters a cell, what the cell “sees” is a patchwork made of the organic molecules (and their corresponding functional groups) covering the NP. Furthermore, these can be as originally designed or result from unspecific protein absorption. The surface charge of NPs, as directly resulting from any synthetic method, comes determined from the nature of the ligands, i.e., the outermost layer of the nanomaterials (such as a wide variety of polymers, highly charged inorganic or organic molecules, macromolecules, and the like) as used in each particular case. However, the charge of nanomaterials can also be greatly modified in physiological media due to the absorption of biomolecules present in the physiological milieu; absorption of proteins and following physiochemical surface changes on nanomaterials are the focus of several studies [111, 113, 125–128]. Thus the adsorption of serum proteins on the surface of nanomaterials can hide the synthetic organic layer, change the net charge, and lead to unspecific uptake of nanomaterials into cells by receptor-mediated endocytosis [129–131].

In general, in the context of *in vitro* studies, cationic NPs of the most diverse nature varying in both the core material and cationic coating are generally believed to be more toxic to cells than their neutral or anionic counterparts [39, 121, 129, 132–136]. Compared to neutral and negatively charged NPs, cationic NPs present the highest degree of cell interaction and/or internalization [132, 137–141]; although this fact can be speculatively related to the proven higher cytotoxicity of cationic NPs, the “big picture” seems to be more complex [142]. Distinct mechanisms have been proposed to explain the cytotoxicity of cationic NPs such as strong interaction of cationic NPs with the cell membrane leading to hole formation, membrane thinning and/or erosion [133, 142, 143] damage to the acidifying endosomal compartment by the proton sponge effect [39, 144–146] followed by mitochondrial injury [38, 39], increase of intracellular Ca^{2+} concentration following membrane depolarization [132, 147], or release of cytotoxic surfactants like the widely used cetyltrimethylammonium bromide (CTAB), as CTAB-coated NPs are added to cell cultures [123, 131].

NPs coated with a variety of cationic molecules such as polyamidoamine (PMAM) and polypropylenimine (PPI) dendrimers of different generations, cell penetrating peptides, amine molecules, polyethyleneimine (PEI), diethylaminoethyl-dextran, to name a few, have been proven to induce defects in lipid membranes [142, 143, 148–150].

In other work, previously mentioned, Verma et al. studied the role of different arrangements of capping ligands onto NP on their penetration in cells; [121] NPs with ordered ribbon-like anionic domains are able to penetrate the cell membrane; whereas equivalent NPs differing only in the coating arrangement (random) were inefficient in breaching cell membrane barriers, and were instead trapped in vesicular bodies. These anionic NPs did not impair cellular viability whereas equivalent cationic NPs caused membrane disruption and consequently, cellular leakage which was linked to the observed cytotoxicity as expected from previous work [142, 143].

Arvizo et al. studied the effect of surface charge of NPs in modulating membrane potential of different malignant and non-malignant cell types [132]. Based on their findings, uptake of cationic NPs caused an increase of cellular Ca^{2+} influx following membrane depolarization (it is not clear here whether there is membrane disruption). High Ca^{2+} intracellular concentration is shown here to inhibit the proliferation of normal cells, whereas malignant cells remained unaffected; however, both normal and malignant cell lines showed apoptotic features.

In vivo nanotoxicity, i.e., blood, spleen, kidney, respiratory system, liver or immune system (immunotoxicity) [151–153], is generally triggered by the induction of oxidative stress by free radical formation following administration of nanomaterials [154]. Sequestration of NPs by phagocytic cells in the organs of the reticuloendothelial system (RES) makes organs such as the liver and spleen main targets of oxidative stress. Other organs exposed to high blood flow such as the kidneys and lungs are also subject of oxidative stress. Here, it is important to note the important opsonization process that occurs on nanomaterials in physiological media, which ultimately leads to phagocytosis of the opsonized body [155]. Non-passivated nanomaterials in physiological media will absorb proteins forming the so known protein corona. By this process the mononuclear phagocyte system (MPS) can recognize easily estranges bodies that irrputed in the body. Therefore, if a NP is not well-passivated by a surface that prevents unspecific protein absorption, opsonization occurs and most probably the complement system will be activated producing an immunological response against them [152]. Typically, this immunological response leads to accumulation of nanomaterials in the liver and spleen [151]. As previously mentioned, the surface charges of NPs exert significant influence on the interaction with the proteins of the physiological medium; neutral NPs such as polyethylene glycol (PEG) coated NPs remain “invisible” to the phagocytic system [113, 156].

Recently, Deng et al. have proposed an alternative mechanism to the more commonly described role of oxidative stress in the inflammatory response to nanomaterials; they showed that negatively charged NPs (Polyacrylic acid-coated gold NPs) can

strongly bind to (forming a “hard” protein corona) and consecutively induce unfolding of fibrinogen, a plasma protein. Following, a chain of activation (receptor Mac-1) and corresponding signaling pathway (NF- $\alpha\beta$) result in the release of inflammatory cytokines.

In general, once introduced in the circulatory system, cationic nanomaterials have been shown to strongly interact with red blood cells, destabilize cell membranes, and cause cell lysis [151]. Malik et al. showed that cationic dendrimers, in contrast to neutral or anionic ones, show concentration and generation dependent hemolysis and are able to induce morphology changes in red blood cells [157]. Also, cationic dendrimers (PAMAM, G5) as well as other cationic nanomaterials, have been shown to induce strong complement activation [158].

To sum up this point, it is important to stress the diversity of levels that must be considered (inorganic core, first intended organic core and last, unspecific interaction with proteins) when determining and describing the toxicity and performance of any nanomaterial aimed for bioapplications. Yet, these are interconnected and always, a deep physicochemical characterization is key to ensure optimal performance. Many current ongoing investigations are attempting to understand the interplay between engineered NPs and physiological environments. What follows is a modest list of characterization techniques which, as stated several times in this chapter, are required for becoming “better acquainted” with NPs that are intended for bioapplications.

4 Analytical Techniques for Characterizing Nanoparticles, Their Toxicity, and Their Interactions with Proteins

As research and development into inorganic nanoparticles (NPs) continues to move at an alarming rate from fundamental laboratory-based work to “real world” application in areas associated to medicine, sensing and environmental products there is an ever-growing need to for more comprehensive understanding of their properties and behaviors. The need to understand both their physicochemical and applied properties—those that relate ultimately to their function—stems from several factors: from the fundamental interest of researchers across broad disciplines such as physics, chemistry, biology and medicine; to those seeking rigorous consumer quality; as well those studying the health, safety, and environmental impact of these unique materials. And the principal means of understanding is of course obtaining data from a rigorous combination of routine analytical techniques as well as more specialist instrumentation. For an overview of the principal techniques involved in assessing nanoparticles, their toxicity and interaction with proteins, please refer to Table 2.

Table 2
A list of common techniques used for characterizing nanoparticles which mentions their principal advantages and characteristics as well as some additional details on the information that can be extracted using these analytical tools

Technique	Advantages	Information available
<i>Basic spectroscopies</i>		
Fourier transform infrared (FTIR)	Rapid and inexpensive	Appearance or disappearance of an IR band originating from a chromophore Easily observe NP-bound ligands, amide and carboxylic groups of proteins
Ultraviolet-visible (UV-Vis)	Fast and flexible method	The NP LSPR band provides information on the following: (a) Types of NPs present, (b) concentration of NPs, (c) extent of any NP aggregation
Fluorescence	Quantitative, sensitive	Detecting the presence of surface-bound ligands and their quantification using appropriate calibration curves
Dynamic light scattering (DLS)	Assesses NP size and size distribution range	Measurements of the hydrodynamic radius of the NPs, and provides information about the size distribution of the sample Ideal for spherical NPs but less useful for non-spherical ones
ζ-Potential	Unique technique to evaluate the surface charge of the NPs	Surface charge distribution of the NPs. Data from it can be used as relative parameter to confirm chemical surface modifications on the NPs
Nuclear magnetic resonance (NMR)	Identification of NP-bound groups and binding site mapping	A powerful tool in solution phase organic synthesis for structural characterization of small organic molecules. However, line broadening in spectrum occurs when organic molecules and proteins bind to NPs Multinuclear element probes provide complimentary data to traditional ^1H and ^{13}C NMR

(continued)

Table 2
(continued)

Technique	Advantages	Information available
<p><i>Elemental analysis</i></p> <p>Inductively coupled plasma (ICP)</p>	<p>Several techniques available ICP-OES, ICP-MS and ICP-AES Quantitative and rapid sample processing Sensitive down to the ppb and ppt ranges</p>	<p>Analyte concentrations in the sub-parts-per-trillion level can be determined by ICP-MS ICP discharges are relatively free of contamination because the detection electrodes are located outside the reaction chamber Unlike flame atomic absorption spectroscopy (FAAS), which can only measure a single element at a time, ICP techniques have the capability to scan for all elements simultaneously</p>
Chromatography	Quantitative	<p>HPLC is a chromatographic technique that can separate a mixture of compounds for identifying, quantifying and purifying the individual components of the mixture Limited application range Exclusion size chromatography is also available in precast columns ready to use, without expensive equipment</p>
Electrophoresis	Quantitative, easy, and fast	<p>Separation of NPs by charge and size, and allows for differentiation between surface-modified NPs and their unmodified counterparts There are different electrophoretic techniques which can be selected as function as the system, e.g., to increase the spatial resolution</p>
Centrifugation	Gravimetric separation, easy, and relatively cheap and rapid	<p>Separation of particles as function of their weight If the NP stability is high enough different sizes or even NP compositions can be resolved. The speed and time needed depends on each NP type Provide an idea of the colloidal stability of the NPs</p>

Quartz crystal microbalance	Real-time analysis, label-free, sensitive, and quantitative	Measures a mass-per-unit area by measuring the change in frequency of a quartz crystal resonator Can be used under vacuum, in gas, and in liquid environments
<i>Microscopies</i>		
Scanning electron microscopy (SEM)	Quantitative, rapid and cheap 2-D surface profile	Ideal for quantifying the size and shape of NPs in the 10–100 nm-range EDX provides qualitative elemental composition
Transition electron microscopy (TEM)	Quantitative and extremely detailed 3-D data can be obtained	Appropriate for obtaining size and shape information on NPs in the 1–100 nm-range Detailed information regarding in vitro NP uptake and localization from visualization of NP location within a cell or tissue Composition of the internalized NP is possible
<i>Scanning probe microscopies</i>		
Atomic force microscopy (AFM)	Qualitative and/or quantitative A powerful tool, AFM provides a three-dimensional surface profile	3D imaging/visualization of NPs distributed on a flat surface Information about physical properties of NPs including size, morphology, surface texture, and roughness When structure is known can provide information about crystallographic orientation
Scanning tunneling microscopy (STM)	Individual atoms within materials routinely imaged and manipulated	Electrical characteristics of individual particles NP formation and/or size distribution of particles deposited or grown on a surface Although, STM can be a challenging technique, requiring extremely clean and stable surfaces, sharp tips, excellent vibration control, and sophisticated electronics

(continued)

Table 2
(continued)

Technique	Advantages	Information available
<i>Electron spectroscopies</i>		
Auger Electron Spectroscopy (AES)	High resolution, spatially resolved chemical images	Surface composition of individual large NPs or distribution of smaller NPs (depending on special resolution of specific instrument) Presence and/or thickness of coatings and/or contaminants
X-ray photoelectron spectroscopy (XPS)	Elemental composition, empirical formula, chemical state and electronic state of elements present	Surface composition and chemical state Presence and nature of functional groups Enrichment or depletion of elements on the surface Presence and/or thickness of coatings or contaminants Electrical properties of NPs
<i>Others</i>		
Mass spectrometry (MS)	Efficient, requires a low quantity of sample; yet less quantitative than other methods	Although compounds have to be cleaved first, mass spectrometry (MS) is a very sensitive and convenient method for analysis of surface molecules
Circular dichroism (CD)	Useful for studying the secondary structures of proteins in the absence or presence of NPs	Qualitative analysis of NP-protein corona but no residue-specific information
Isothermal titration calorimetry (ITC)	Quantitative technique. Directly measures the binding affinity (K_b), enthalpy changes (ΔH), and binding stoichiometry (n) of the interaction between two or more molecules in solution	Study the binding of small molecules to larger molecules or NPs Thermodynamic parameters of interactions in solution
Thermogravimetric analysis (TGA)	Monitors changes in weight in relation to a temperature program in a controlled atmosphere	Can determine degradation temperatures, absorbed moisture content of materials, the level of inorganic and organic components in materials, decomposition points, and solvent residues

SEERS Surface enhanced Raman spectroscopy, LSPR localized surface plasmon resonance, MRI magnetic resonance imaging

Composition and stability are the fundamental properties contributing to the application of NPs in materials science and medicine; yet, all too often, their characterization is poor or incomplete. Thus, for a “complete” characterization of novel inorganic NPs, a comprehensive analysis of their elemental composition and colloidal stability is required in the first instance because this platform serves as the primary scaffold upon which functionality is built. Across many disciplines, characterization of any new material is frequently based on a limited number of analytical techniques and can therefore suffer from misinterpretation. Furthermore, conclusions drawn from limited data and subject to conflicting interpretations could of course affect their ability in subsequent application. Consequently, there are some key complimentary techniques that should be used routinely to obtain vital data on nanoparticles. These data can be obtained using readily available tools; although very often certain information must be obtained using more specialized analytical equipment.

More often than not, to achieve colloidal stability, nanoparticles themselves are coated with surfactants and/or contaminants (typically from the unspecific adsorption of for example proteins, charged molecules) and, time and again, these are often not subject to rigorous analysis and, unfortunately, often remain as unidentified. As previously mentioned, nanoparticle surface composition and structure play vital roles in their subsequent functionalization, properties, and performance and their surface composition and properties can also be radically altered with time and as they evolve, either through effects from application or from environmental exposure. As a result, detailed reports on NP structure, stability and composition should be routine steps at many stages whilst assessing functionality.

Most recently, the marked increase in biomedical applications of nanomaterials and their potential toxicity as antiviral and antitumoral agents has resulted in the requirement for versatile analytical techniques to determine protein–nanoparticle interactions to characterize both *in vitro* and *in vivo* studies. For example, in many cases NP binding affinity, binding ratio, and binding mechanisms must all be adequately assessed.

In this section we examine the most important analytical techniques required for comprehensive characterization of NPs, their surfaces, toxicity and interactions with proteins. In addition, we briefly address some of the main issues and challenges faced when performing such analyses in the hope that it will serve as a starting point for both early and experienced researchers.

4.1 Characterizing Their Composition and Colloidal Stability

Detailed analysis of the composition of nanoparticles is the first and single most important step towards their application to other areas of science. However, their colloidal stability is the other principal physicochemical parameter exerting great influence on their

behavior and its effect must also be assessed. The tendency of NPs to agglomerate due to van der Waals attraction means that their surfaces require modification with organic coatings: either charged molecules or with sterically bulky polymer brushes to which provide colloidal stability by electrostatic or steric repulsion between discrete particles, respectively, to prevent aggregation.

Importantly, agglomeration due to limited colloidal stability can smear out effects of different NP sizes and colloidal stability is also paramount for purification of NP solutions from residual reactants or leached constituents. Ultrafiltration, size exclusion chromatography, electrophoresis, and flow field fractionation are some of the common methods for NP purification. In case of limited colloidal stability NPs may irreversibly precipitate upon purification by some of the aforementioned methods due to partly stripping off the organic surface layer or by screening of surface charge in the required buffer solutions. Great care must therefore be taken to assess purity and stability over a period of months and of course throughout the purification process in order to assess the stability of these suspensions to unwanted changes, such as flocculation and aggregation. The standard analytical tools found in most laboratories for the characterization of NPs are ultraviolet–visible (UV–Vis) absorption spectroscopy (optical properties), zeta potential (ZP) measurements and dynamic light scattering (DLS) based particle size analysis (PSA) measurements, and Fourier transform infrared (FTIR). Complementary techniques include multinuclear nuclear magnetic resonance spectroscopy (NMR) as well as electron microscopies such as scanning electron microscopy (SEM) and transmission electron microscopy (TEM). Figure 2 provides a practical example of how both TEM and UV–Vis can be used to monitor the colloidal stability of NPs. In this figure small gold nanoparticles (Au NPs) of ca. 3 nm aggregate after a sterilizing treatment with plasma gas. Aggregation is visible by TEM (Fig. 2b), and in UV–Vis spectroscopy (Fig. 2c) [159].

For elemental analysis of colloidal inorganic nanoparticles, ICP sources, especially when combined with mass spectrometric detection, provide high sensitivity and are excellent analytical tools [160]. Analyte concentrations in the sub-parts-per-trillion level can be determined by ICP-MS and for mixed-element samples such as alloys and core-shell nanoparticles, the signal intensities obtained are highly selective for the element observed and nearly independent of the sample matrix. This latter observation is vital for bioapplications, where elemental markers are embedded in complex organic matrices. Both ICP-MS and ICP optical emission spectrometry (ICP-OES) are ideal tools to determine the concentration of nanoparticles and nanoparticle-based elemental markers; although ICP-MS is about three orders of magnitude more sensitive than ICP-OES. In addition, combustion elemental analysis, titrimetric analysis (Isothermal titration calorimetry (ITC) and

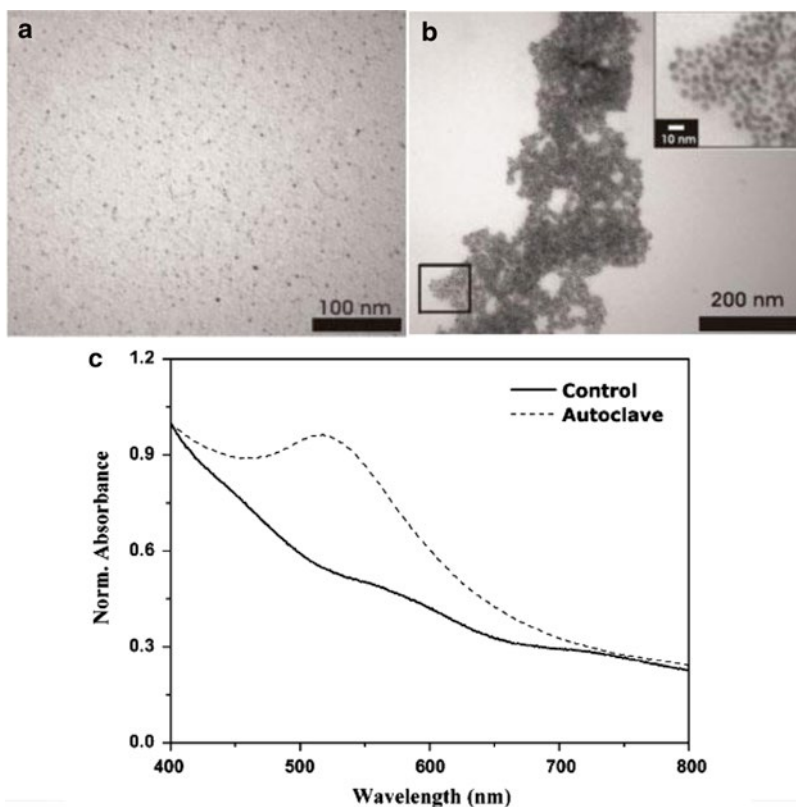


Fig. 2 TEM micrographs (a) 3 nm Au NPs control and (b) 3 nm Au NPs after autoclave treatment, (c) UV-Vis absorption spectra. Adapted from França et al. [159]

differential scanning calorimetry (DSC)), or thermogravimetric analyses (TGA) are methods which are also applicable in characterization of “bare” NPs and their surface-bound molecules.

It is important to note that the stability of nanoparticles is primarily dictated by their surface chemistry. The interface between the particles and their surrounding medium determines how the particles interact with each other, as well as with any molecules or ions in the solution. Damage to the surface coatings could result from chemical attack, or destabilization of the interactions between the capping molecules and the surfaces of the nanoparticles.

5 Materials

5.1 Practical Example: Evaluating the Stability of Bare Gold Nanoparticles by UV-Vis Spectroscopy

Synthesis of 9 nm gold nanoparticles

1. Sodium citrate (71497 Sigma Aldrich).
2. Hydrogen tetrachloroaurate (III) hydrate (12325 Alfa Aesar).
3. Distilled water.

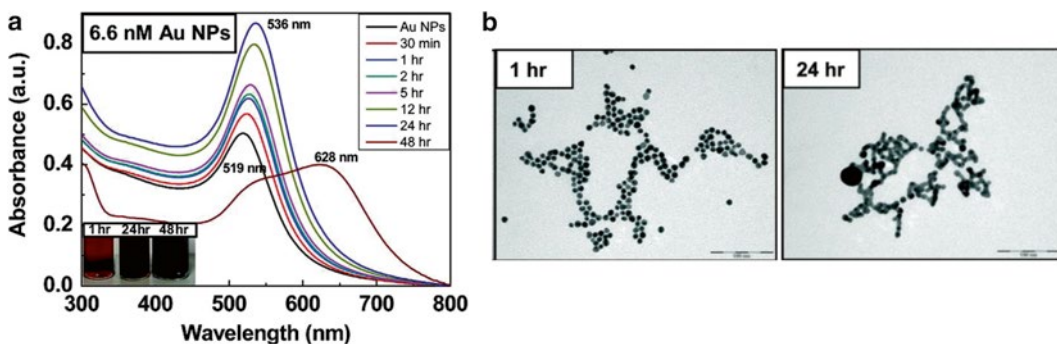


Fig. 3 (a) Plasmon band shifting of 9 nm Au NPs due the presence of the Hg^{2+} cations. (b) TEM images of the Au NPs at different times showing different aggregation rates. Adapted from Ojea-Jiménez et al. [161]

4. Procedure.

- (a) Prior to use, all the glassware must be washed with aqua regia and rinsed thoroughly with distilled water.
- (b) 150 mL of 2.2 mM (aq) sodium citrate solution was heated to 100 °C in a round bottomed flask.
- (c) When the sodium citrate solution started to boil 1 mL of 25 mM of HAuCl_4 was added. At this point, the speed of stirring is quite important to obtain a narrow size distribution of NPs.
- (d) The solution quickly turns red and after 5 min of heating the solution is allowed to cool down to room temperature.

Evaluation of the Au NPs stability against Hg^{2+} cations [161].

The aggregation of gold nanoparticles has been widely applied to develop new sensors. In this example the aggregation of Au NPs is used to detect the presence of mercury (II) ions in water. It is used here as an illustration of how the plasmon band variations are correlated with the aggregation of the particles. This aggregation can be followed using UV-Vis spectroscopy.

5. 8 mL of Au NPs as synthesized were mixed with 2 mL of a 1.6 mM (aq) HgCl_2 solution.
6. The mixture was stirred at room temperature and the aggregation of Au NPs was tracked over time by recording taking several UV-Vis spectra (Fig. 3).
7. A blue-shifting of the maximum peak due the aggregation of the Au NPs was observed with respect to time. This maximum peak displacement can be correlated with the extent of aggregation subsequently observed by TEM. Note that in order to observe this effect the absorption of the solution of Au NPs must be in the linear range of the spectrophotometer.

5.2 Surface Chemistry Characterization

We have already mentioned the importance of surface analysis of NPs but data can be obtained from various different techniques, each providing key information. Fourier transform infrared (FTIR), UV–Vis absorption, and nuclear magnetic resonance (NMR) spectroscopies, have all been used as effective and convenient methods to monitor organic reactions directly on NPs and enable a rapid optimization of reaction conditions. These tools, along with mass spectrometry (MS), are readily available in most laboratories, companies or university departments; but more essential information can be obtained from electron spectroscopies. These include Auger electron spectroscopy (AES) and X-ray photoelectron spectroscopy (XPS); ion-based methods such as secondary ion mass spectrometry (TOF-SIMS) and low energy ion scattering (LEIS); as well as scanning probe microscopy (SPM), including atomic force microscopy (AFM) and scanning tunneling microscopy (STM). It is important to recognize that these different surface analysis techniques provide comprehensive and complementary information relating to topography, elemental composition, molecular and chemical state, and structure. For detailed look at electron spectroscopies, Ion-Based Surface Analysis Methods, and Scanning Probe Microscopies along with specific considerations for NP surface analysis please refer to recent reviews [162, 163].

Infrared spectroscopy (FTIR) has long been the favored, most convenient, and highly sensitive technique for characterizing supported organic compounds. Monitoring either the appearance or disappearance of an IR band originating from a chromophore in a molecule can provide a direct means of monitoring the kinetics of solid-phase reactions; meanwhile peak intensities can be used as qualitative means of identification of multiple ligands since they may be proportional to the relative amount of each ligand on the particle. While Nuclear magnetic resonance (NMR) spectroscopy is undoubtedly still the most powerful tool in solution phase organic synthesis where inorganic nanoparticles are concerned, the line widths of grafted organic components in NMR spectra are greatly broadened by both the restricted mobility of atoms in a solid sample and the inhomogeneity of the sample matrix. However, these issues can be complimented by NMR of heteroatom-containing compounds (containing elements such as N, P, and F) due to the large chemical shift dispersion. Matrix-assisted laser desorption/ionization time-of-flight mass spectrometry (MALDI-TOF MS) is also a sensitive and convenient method for analysis of surface molecules in anchored on NPs. UV–Vis absorption and Fluorescence spectroscopy excel in the quantification of ligands and, in addition, UV–Vis provides a convenient mechanism to monitor NP stability over time. When metal NPs aggregate, and become electronically coupled they exhibit a different SPR than the individual particles. For the case of a multi-nanoparticle aggregate, the plasmon resonance will be red-shifted to a longer

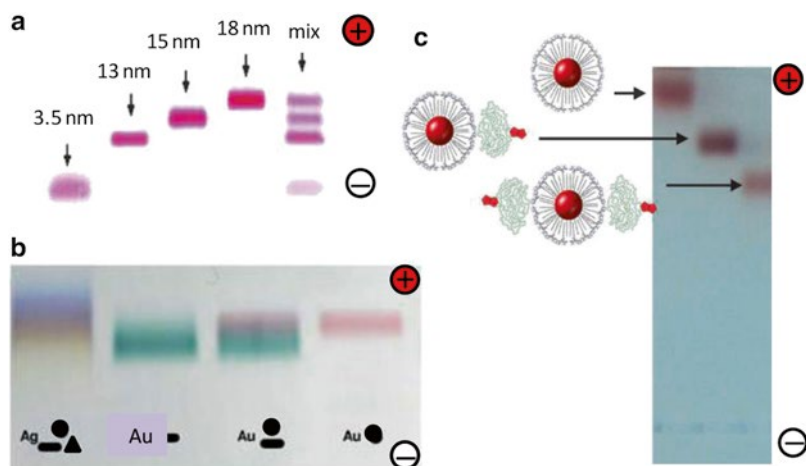


Fig. 4 Electrophoresis gel-separations of (a) different sizes of Au NPs (adapted from Xu et al.) [164] (b) silver and Au NPs with different shapes (adapted from Hanauer et al.) [166]; and (c) different modified NPs with different number of biotin-polyethylene glycol (PEG) chains (adapted from Lin et al.) [167]

wavelength than the resonance of an individual nanoparticle, and aggregation is observable as an intensity increase in the red/infrared region of the spectrum.

Electrophoretic techniques are powerful tools to both characterize and purify surface-modified nanoparticles. These techniques can be used to separate water-soluble particles by their charge-to-size ratio and also those samples containing mixtures of shapes and sizes [164] (*see* Fig. 4a, b) [165, 166]. Typically, citrate capped NPs are not suitable for this technique. Regarding the surface modification of NPs, as soon as this modification alters the charge and size of the NPs, the electrophoretic mobility of the functionalized particle will change. Thus, this technique is commonly employed to assess, qualitatively, the success of a chemical modification on the NP's surface. However, it is even possible to quantify the number of introduced chains (Fig. 4c) [167].

By the use of centrifugal force, it is possible to sediment and separate NPs in monodisperse populations. This technique is often used for the purification of NPs after their chemical surface modification [113]. The exact conditions for centrifugation are highly dependent on the composition, size, shape and charge of the NPs; not to mention the nature of the surface modified components. Density Gradient centrifugation can be used to separate NPs by size or separate nanoclusters in discrete populations using bands with different density which finally determine where the particles sediment (Fig. 5) [168, 169]. Mirkin and coworkers have developed a methodology using DNA strands to separate Au NPs based on size-selective aggregation [170]. Whitesides et al. have also recently demonstrated the use of aqueous multiphase systems (MuPSs) as media for rate-zonal centrifugation to separate different

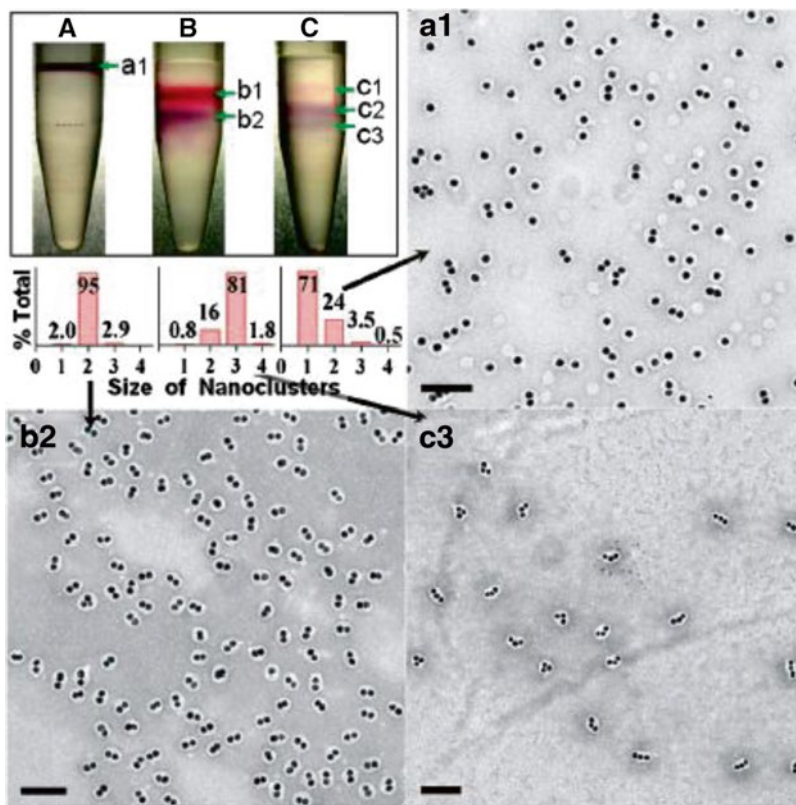


Fig. 5 Separation using a density gradient centrifugation of CsCl of monomers, dimers, or trimers. TEM micrographs have a scale bar of 100 nm (adapted from Chen et al.) [169]

shapes and sizes of NPs in a three-phase system which isolates reaction products of nanorods, nanospheres, and large particles into well-separated and isolatable zones [170]. This technique could also be applied to surface-modified particles, which also often require longer periods of ultracentrifugation than their unfunctionalized counterparts.

Dynamic light scattering (DLS) is now used as an indispensable technique to characterize NPs and accurately evaluate their size distribution. This technique is a fast and very convenient tool to evaluate changes in the hydrodynamic radius of the NPs due to chemical surface modification. Electrophoretical light scattering (ζ -potential) can also provide complimentary information and give a relative parameter of NPs stability as function of their surface charge. Recently, Doane and coworkers have published a very useful review concerning this topic [171].

Although electron spectroscopies may not be as used in every situation where they might be appropriate, they are increasingly employed for nanoparticle characterization in a variety of ways. It is, however, valuable to identify specific analysis objectives based

on the type of research involved since these assist both the data collection and the nature of the data processing, both of which can significantly improve the quality and value of the resulting information. The presence, composition, and thickness of coatings on nanoparticles, as well as surface enrichment and depletion at particle surfaces can be determined by both AES and XPS spectroscopies, and the latter can also be used to determine particle sizes when conditions are not appropriate for analysis by other methods.

Like the electron spectroscopies one of the primary uses of time-of-flight secondary ion mass spectrometry (TOF-SIMS) is to extract molecular information about the functional groups and, possibly, molecular orientation of molecular coatings on particles surfaces. The main difference between the electron spectroscopies and SIMS is the higher detection sensitivity of TOF-SIMS making it a useful for examining the basic composition of NPs as well as their surfaces. LEIS, also known as Ion Scattering Spectrometry (ISS), is a well-established, but uncommon method reserved for specialists. Recent developments have made it more useful predominantly because of the increased sensitivity for measuring the outermost atomic layers of a sample.

The scanning probe microscopies STM and AFM have enabled major advances in nanotechnology in recent years and are particularly useful and powerful tools for analyzing NPs. AFM readily provides 3D imaging/visualization of nanoparticles distributed on a flat surface. It can provide qualitative and/or quantitative information about physical properties of NPs including size, morphology, surface texture, and roughness. By collecting many images vital information about particle size distributions and volumes can be extracted and, importantly, AFM can be conducted in vacuum, ambient conditions, liquids, or other environments.

Generally, data required for quantifying the size and shape of inorganic NPs is best obtained from electron microscopies such as transition electron microscopy (TEM) and scanning electron microscopy (SEM). In addition, TEM can provide extremely detailed information regarding in vitro NP uptake and localization by allowing both visualization of particle location within a cell or tissue and, in conjunction with spectroscopic methods, characterization of the composition of the internalized species. In the following section NP uptake and toxicity are dealt with in more detail.

5.3 Practical Example: Characterization of Gold NPs Stabilized with Different Lengths of Poly (Ethylene Glycol) [172]

Stabilization of Citrate-Capped Au NPs with Poly (Ethylene Glycol) (PEG) [41]

1. Au NPs.
2. Thiol modified PEG. These kinds of molecule are commercially available from Rapp Polymer, Sigma Aldrich, and Iris Biotech with different lengths.
3. 2 M (aq) Sodium hydroxide solution.

5.4 Characterization of Au NPs Stabilized with PEG of Different Polymer Chain Lengths by Gel Electrophoresis, Dynamic Light Scattering (DLS) and ζ -Potential [172]

1. Various samples of Au NPs stabilized using PEG of different polymer chain lengths, e.g., 500 Da, 1,000 kDa, 2,000 kDa, 5,000 kDa, and 10,000 kDa.
2. Agarose powder (Invitrogen).
3. 1× Tris Acetate EDTA (TAE) buffer pH 8.06.
4. Glycerol (G 5516 Sigma Aldrich).

5.5 Practical Example: Evaluation of NP Toxicity by MTT Colorimetric Assays

1. NPs to be studied.
2. MTT salt: 3-(4,5-dimethylthiazol-2-yl)-2,5-diphenyltetrazolium (M 2128 Sigma Aldrich).
3. Cells (immortal cells such as HeLa, Vero, 3T3).
4. Cell culture media, note that this can vary with the cell type (e.g., Dulbecco's modified Eagle's media, DMEM, Sigma Aldrich).
5. Sterile PBS buffer or Dulbecco's phosphate-buffered saline (PBS) (D1408 Sigma Aldrich).
6. Dimethylsulfoxide (DMSO, Sigma Aldrich).

5.6 Practical Example: Evaluation of Protein Absorption in Negatively Charged Iron Oxide NPs as Function of the pH [113]

1. NPs to be studied. In this example we discuss the use of iron oxide NPs stabilized with poly (maleic anhydride-alt-1-octadecene) (PMAO). These particles were also modified with PEG, or with glucose (4-aminophenyl β -D- glucopyranoside) and the protein absorption prevention was studied compared with the particles coated only with PMAO.
2. PBS buffer pH 7.4.
3. 10 mM sodium acetate/acetic acid buffer pH 4.7.
4. Bovine Serum Albumin (67 kDa, Isoelectric point 4.7, BSA, Sigma Aldrich).
5. 15 % polyacrilamide (w/v) gels (Lonza).
6. Sodium dodecyl sulfate (SDS, Sigma Aldrich).
7. Mercaptoethanol (Sigma Aldrich).
8. Molecular weight standards (Sigma Aldrich).

6 Methods

6.1 Characterization of gold NPs stabilized with different lengths of poly (ethyleneglycol) [172]

1. 10 mL of Au NPs ($\sim 3 \times 10^{12}$ NPs/mL) solution was mixed with 0.2 μ mol of thiolated-PEG with the desired polymer chain length.
2. The pH was raised to exactly pH 12 with the NaOH solution. This adjustment is crucial in order to increase the amount of

PEG attached to the NP surface, because the thiol groups are more reactive at this pH.

3. The sample was allowed to react overnight to complete the ligand exchange.
4. Samples were washed by centrifugation for 30 min at $52,000 \times g$. Three washes were performed using milli Q water to remove the ligands excess. The final sample must be characterized by UV-Vis spectroscopy to ensure that the plasmon band of the modified particles is comparable with the initial spectra and has not shifted (indicating aggregation of the particles).

6.2 Characterization of Au NPs stabilized with PEG of different polymer chain lengths by gel electrophoresis, dynamic light scattering (DLS) and ζ -potential [172]

1. Agarose was mixed with the buffer. The percentage of the gel can be varied by controlling the ration w/w of agarose. The normal agarose percentages range is from 0.7 to 2 %.
2. The solution was heated until the agarose was completely dissolved.
3. Solution was placed in a gel-cassette with the comb to create the wells. The solution was cooled down for 45–60 min.
4. The gel was placed into the electrophoresis cuvette.
5. Samples were mixed with a solution of glycerol 25 % in TEA.
6. Samples were loaded into the gel. The sample volume will depend with the well size.
7. Current source was switched on and the gel was run. A typical gel run may be 100 V for 1 h.
8. The electrophoretical mobility is a function of both the charge and size of the particles. This is why we can observe differences between the NPs (Fig. 6a). Smaller particles will run faster than larger ones and similarly, particles of higher charge will run more than more neutral particles.

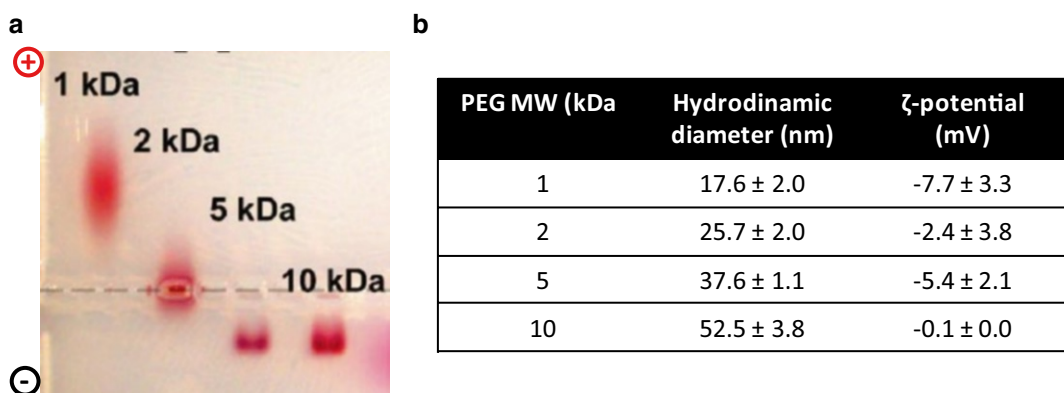


Fig. 6 (a) 1 % Agarose electrophoresis gel of PEG-modified Au NPs. (b) summary of results from DLS and ζ -potential for these particles (adapted from Donae et al.) [172]

9. To measure the hydrodynamic radius of the particles by DLS, samples must be filtered using a 0.2 μm filter before being introduced into the cuvette (Fig. 6b).
10. To measure the ζ -potential values the use of 1 mM of KCl in the final Au NPs solution is recommended (Fig. 6b).

6.3 Characterization of NP Toxicity

The emerging field of nanotoxicology has formed in response to the lack of information on potential impact of nanoparticles on environmental health and safety. Nanotoxicology relies on a broad spectrum of analytical methods for the characterization of nanomaterials as well as their impacts on *in vitro* and *in vivo* function. As a rapidly developing research area, the analytical chemistry involved poses many interesting challenges which draw from nanomaterial characterization and bioanalytical chemistry. The most common analytical methods can be organized into the characterization of cellular uptake of NPs, *in vitro* toxicity characterization, and *in vivo* toxicity studies.

Characterizing *in vitro* NP uptake and localization is inherently associated to cytotoxicological studies since uptake provides evidence of nanoparticle-cell interaction. In such cases, delicate intracellular machinery is exposed to NPs and so quantifying the uptake of nanomaterial by cells and locating these materials presents a variety of analytical challenges that must be addressed with not one, but a range of complimentary techniques. Frequently, quantification of NP uptake is often obtained at the cost of spatial resolution, and intracellular localization information is predominantly qualitative. As a result of these limitations, combinations of techniques provide a more complete understanding of uptake [173].

Undoubtedly the most detailed information regarding *in vitro* NP uptake and localization is obtained using TEM as it allows allowing both visualization of their location within a cell or tissue and, in conjunction with spectroscopic methods, characterization of their composition. However, TEM struggles to provide high resolution images of diffuse electron materials, therefore dynamic light scattering (DLS) measurements can be performed in conjunction with TEM to validate data. Qualitative elemental analysis techniques may also be used in conjunction with TEM to provide more information on biological samples exposed to NPs, for example, electron-dispersive X-ray analysis (EDX) and electron energy loss spectroscopy (EELS).

Elemental analysis is of course a useful means of determining NP uptake. Inductively coupled plasma-atomic emission spectroscopy (ICP-AES), -optical emission spectrometry (ICP-OES), and -mass spectrometry (ICP-MS) are once again regarded as the most powerful and convenient techniques for the quantification of internalized NP elemental composition and are often used to quantify their uptake both *in vitro* and *in vivo*.

In a similar fashion, fluorescence spectroscopy lends itself well to the quantitative assessment of NP uptake and also provides a qualitative assessment of their localization. Quantitative data can be attained through use of bulk fluorescence or on a cell-to-cell basis using confocal fluorescence.

The most commonly used *in vitro* assessment techniques for measuring NP toxicity are, generally, either viability (live/dead ratio) or toxicity mechanisms. The major viability based assays can be organized into the categories of proliferation, necrosis or apoptosis, and the major toxicity mechanism analyses into those operating via either oxidative stress or DNA damage detection techniques. A review concerning the *in vitro* techniques currently applied to nanotoxicology provides an overview of the principal *in vitro* viability assays and discusses some novel toxicological techniques [173].

6.3.1 Methods

1. Seed 5×10^3 cell per well in a 96 well plate at 37 °C and 5 % CO₂ in cell culture media with a final volume of 100 µL.
2. After 24 h, the particles were filtered using a 0.2 µm syringe filter to sterilize the particles. Then, dilutions in fresh media of the particles in a range of concentration were prepared. The old media replaces the NPs dilutions. At least three replicates per concentration of NPs and per NPs type are required in order to carry out a comprehensive study to obtain appropriate statistics.
3. After 24 h in the incubator, the media was removed, and cells were washed with PBS three times to remove the particles that can be attached on the membrane of the cells.
4. Then, 100 µL of a sterile solution of 1 mg/mL MTT in DMEM was added to the cells. Cells were incubated for a time period from 1 to 4 h in the incubator. This time period will be dependent on the rate of metabolism of the cells but typically 3 or 4 h are adequate. During this time, mitochondria will produce formazan crystals inside the cells.
5. After this incubation time, cells were centrifuged at $15,000 \times g$ for 10 min, and the media was removed.
6. Formazan crystals were dissolved in 100 µL of DMSO, which produce a violet color.
7. The absorbance of each well was read on a microplate reader at 570 nm. The zero of the absorbance was calibrated using cell culture medium without cells.
8. To calculate the cell viability (%) according to the control was applied the next equation:

$$\% \text{ Cell viability} = ([A]_{\text{test}} / [A]_{\text{control}}) \times 100$$

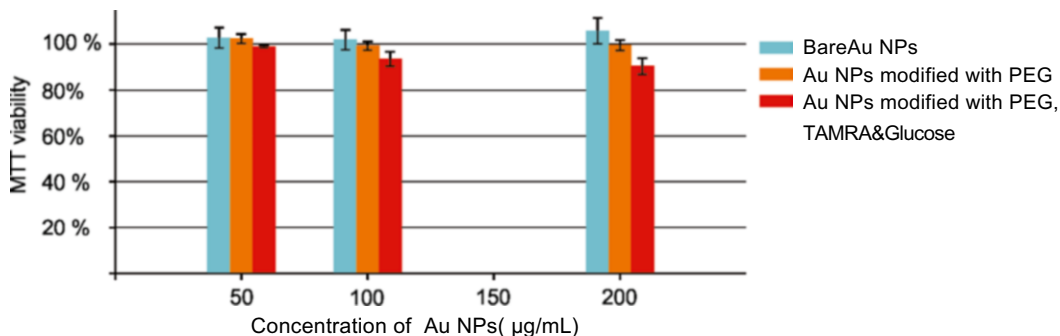


Fig. 7 Cell viability results of differently modified Au NPs obtained by MTT colorimetric assay (adapted from the supporting information of Pelaz et al.) [41]

- Results are represented containing the value for the standard deviation obtained by the use of the replicates. Figure 7 provides an exemplary representation of the data obtained using this methodology [41].

6.4 Analytical Tools for Identifying Nanoparticle-Protein Interactions

We have already discussed that when nanoparticles enter human blood or cells, they strongly interact with proteins (see Section 3). The NP-protein interface can give rise to perturbed signaling transduction in cells which may then have adverse effects on cellular function, causing toxicity *in vitro* and *in vivo*. Investigations into the strong interactions between NPs and biomacromolecules, such as proteins play a key role in both the determination of the biocompatibility of any given NP for various biomedical applications and also for appropriate safety evaluations. There are currently several analytical methods and strategies used to investigate NP-protein interactions effectively, helping researchers to understand the mechanistic basis for their biological activity and making safe use of nanotechnology.

A recent comprehensive review discussed the most appropriate analytical methods for NP-protein interactions and we encourage interested readers to seek further information there [174]. Importantly, the NP-protein interactions can be classified into two categories: either interaction with single proteins or with a proteome. For the former, we assume that the bound protein has been identified and studies mainly focus on the determination of binding affinity, the binding ratio, binding-induced protein conformational changes, and mechanism of interactions. For the latter, the proteome contains hundreds of proteins, therefore studies focus on separating and identifying NP-bound proteins. Separately, NP-protein binding kinetics involves other special approaches [174].

For NP-single-protein interactions, particularly in relation to binding affinity and binding ratio, UV-Vis and fluorescence spectroscopy are valuable techniques. The former can be used to

evaluate binding and makes use of changes in the absorption spectra of the NPs resulting from protein binding to NPs. Conveniently, UV-Vis is fast, flexible and uncomplicated, but absorption spectra vary from one NP type to another. Thus, it is necessary to complement UV-Vis data with another analytic method to collect conclusive results. Fluorescence spectroscopy, on the other hand, is sensitive to protein dynamics and is an extremely powerful method for assessing NP-protein interactions. As proteins are polymeric complexes of amino acids they may contain fluorophores, such as tyrosine, tryptophan and phenylalanine so can be monitored easily. NPs can also be intrinsically luminescent or labeled with fluorescence probes meaning that fluorescence emission can also be detected from NPs. Consequently, NP-protein binding can be monitored by several easily accessible spectroscopic methods. Furthermore, dynamic light scattering (DLS) can be used to determine discrete changes in the hydrodynamic size of NPs. As proteins bind to the NP surface, the size of NP increases resulting eventually in binding saturated, so this technique can be used to monitor the NP-protein binding ratio.

Protein interactions with NPs may induce protein conformational changes that can expose unknown epitopes and subsequently activate undesired signaling pathways. If information on conformational change of NP-bound proteins is desired there are several approaches that can be used to shed light on the protein conformation. Circular dichroism (CD), Fourier transform infrared (FTIR) spectroscopy, Raman spectroscopy and fluorescence anisotropy (FA) are all of use in this instance.

The binding of NPs with plasma proteins (Proteomes—which contain hundreds of proteins) or cellular proteins may influence the biological activities of many proteins. When analyzing NP-proteome interactions the most challenging issue is to accurately quantify and identify proteins attached to NPs, therefore the separation of proteins is a prerequisite to examining their identity. As a result, such protein separation requires chromatography and electrophoresis. High performance liquid chromatography (HPLC) is the most frequently used and effective chromatographic method, including size exclusion chromatography (SEC), reverse phase chromatography (RPC) and ion exchange chromatography (IEC). Among the different electrophoresis techniques, capillary electrophoresis and gel electrophoreses are the two methods most commonly used for analyzing NP-protein complexes. Following separation of proteins from proteomic complexes, MALDI-TOF-MS can be used for identifying proteins bound to NPs. Protein spots are excised and digested with a specific protease and the fragments analyzed by MALDI-TOF-MS and the peptide mass fingerprints can be searched for on databases to identify proteins.

Assessing NP-protein binding events is no easy task; yet the combination of readily available analytical methods makes the

analyses more approachable than they may seem at the outset. As research in this area progresses, new techniques will be added to the current inventory allowing more detail to be obtained.

6.4.1 Methods

1. 0.5 mg of each type of NPs was mixed with 25 μg of protein solution (125 $\mu\text{g}/\text{mL}$ in PBS pH 7.4) to a final volume of 200 μL . Other samples using the same conditions were incubated with BSA dissolved in acetate/acetic buffer (pH 4.7) in order to evaluate the influence of pH.
2. Samples were gently shaken at 37 $^{\circ}\text{C}$ for 90 min in an orbital shaker.
3. After which time the NPs were centrifuge in a centrifugal filter with 100,000 Da MW cutoff (Millipore).
4. The proteins contained in the supernatant were denatured by the use of a buffer containing 20 % of SDS and 10 % of mercaptoethanol. This buffer was added in a 10 % of the final volume of the sample.
5. Samples were boiled for 10 min before their loading into a precast gel of polyacrylamide 15 % (w/v).
6. Electrophoresis was performed using a constant voltage of 150 V for 1.5 h in a vertical electrophoresis slab apparatus. As molecular weight markers were used 190, 127, 77, 49, 38, 25, 18, and 12 kDa.
7. Finally, the gel was silver stained using the standard procedure.
8. Figure 8 illustrates the results at both pHs. The presence of PEG or glucose avoids the unspecific absorption of BSA (Lanes 2 and 6 for glucose NPs, and Lanes 3 and 7 for PEG NPs). In the case of PMAO NPs, which present a major negative charge in their surface, the BSA absorption depends with the pH. As BSA exhibits an isoelectric point (pI) of 4.7, at pH 7.4 both

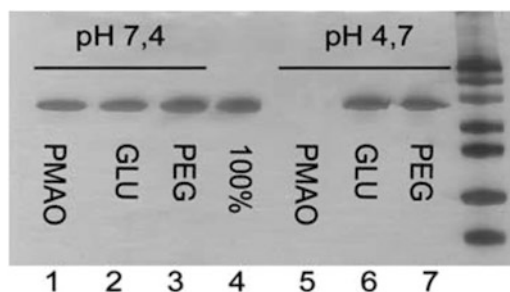


Fig. 8 SDS PAGE analysis performed to study the protein adsorption on the iron oxide NPs with different surface modifications: supernatants of the BSA adsorption for PMAO NPs (lanes 1 and 5), glucose NPs (lanes 2 and 6) and PEG NPs (lanes 3 and 7) at pH 7.4 and 4.7, respectively (adapted from Moros et al.) [113]

PMAO NPs and BSA possess negative charge which prevents their interaction (Lane 1). However, at pH 4.7 which is the pI of the BSA, the charge of the protein is zero but the PMAO NPs still have negative charge. Consequently, the interaction is possible and is clear due the disappearance of the BSA band into the gel (Lane 5). In the Lane 4 the 100 % of BSA used as control is presented.

References

- Rivera-Gil P, Jimenez De Aberasturi D, Wulf V, Pelaz B, Del Pino P, Zhao Y, De La Fuente JM, Ruiz De Larramendi I, Rojo T, Liang X-J, Parak WJ (2013) The challenge to relate the physico-chemical properties of colloidal nanoparticles to their cytotoxicity. *Acc Chem Res* 6:743–749
- Duncan R, Gaspar R (2011) Nanomedicine(S) under the Microscope. *Mol Pharm* 8: 2101–2141
- Doane TL, Burda C (2012) The unique role of nanoparticles in nanomedicine: imaging, drug delivery and therapy. *Chem Soc Rev* 41: 2885–2911
- Arvizo RR, Bhattacharyya S, Kudgus RA, Giri K, Bhattacharya R, Mukherjee P (2012) Intrinsic therapeutic applications of noble metal nanoparticles: past present and future. *Chem Soc Rev* 41:2943–2970
- Parak WJ, Gerion D, Pellegrino T, Zanchet D, Micheel C, Williams SC, Boudreau R, Le Gros MA, Larabell CA, Alivisatos AP (2003) Biological applications of colloidal nanocrystals. *Nanotechnology* 14:R15–R27
- Mout R, Moyano DF, Rana S, Rotello VM (2012) Surface functionalization of nanoparticles for nanomedicine. *Chem Soc Rev* 41: 2539–2544
- Ow H, Larson DR, Srivastava M, Baird BA, Webb WW, Wiesner U (2004) Bright and stable core–shell fluorescent silica nanoparticles. *Nano Lett* 5:113–117
- Yang HH, Zhang SQ, Chen XL, Zhuang ZX, Xu JG, Wang XR (2004) Magnetite-containing spherical silica nanoparticles for biocatalysis and bioseparations. *Anal Chem* 76:1316–1321
- De M, Ghosh PS, Rotello VM (2008) Applications of nanoparticles in biology. *Adv Mater* 20:4225–4241
- Kostarelos K, Bianco A, Prato M (2009) Promises, facts and challenges for carbon nanotubes in imaging and therapeutics. *Nat Nanotechnol* 4:627–633
- Boczkowski J, Lanone S (2007) Potential uses of carbon nanotubes in the medical field: how worried should patients be? *Nanomedicine* 2:407–410
- Yang K, Zhang S, Zhang G, Sun X, Lee S-T, Liu Z (2010) Graphene in mice: ultrahigh in vivo tumor uptake and efficient photothermal therapy. *Nano Lett* 10:3318–3323
- Mohan N, Chen CS, Hsieh HH, Wu YC, Chang HC (2010) In vivo imaging and toxicity assessments of fluorescent nanodiamonds in caenorhabditis elegans. *Nano Lett* 10:3692–3699
- Parak WJ (2011) Complex colloidal assembly. *Science* 334:1359–1360
- Manna L, Scher EC, Alivisatos AP (2002) Shape control of colloidal semiconductor nanocrystals. *J Cluster Sci* 13:521–532
- Nel AE, Madler L, Velegol D, Xia T, Hoek EMV, Somasundaran P, Klaessig F, Castranova V, Thompson M (2009) Understanding biophysicochemical interactions at the nano-bio interface. *Nat Mater* 8:543–557
- Gupta AK, Gupta M (2005) Synthesis and surface engineering of iron oxide nanoparticles for biomedical applications. *Biomaterials* 26:3995–4021
- Pankhurst QA, Connolly J, Jones SK, Dobson J (2003) Applications of magnetic nanoparticles in biomedicine. *J Phys D: Appl Phys* 36:R167–R181
- Neuberger T, Schopf B, Hofmann H, Hofmann M, von Rechenberg B (2005) Superparamagnetic nanoparticles for biomedical applications: possibilities and limitations of a new drug delivery system. *J Magn Magn Mater* 293:483–496
- Nasongkla N, Bey E, Ren JM, Ai H, Khemtong C, Guthi JS, Chin SF, Sherry AD, Boothman DA, Gao JM (2006) Multifunctional polymeric micelles as cancer-targeted, mri-ultrasensitive drug delivery systems. *Nano Lett* 6:2427–2430
- del Pino P, Munoz-Javier A, Vlaskou D, Rivera Gil P, Plank C, Parak WJ (2010) Gene silencing mediated by magnetic lipospheres tagged with small interfering RNA. *Nano Lett* 10:3914–3921

22. Mykhaylyk O, Antequera YS, Vlaskou D, Plank C (2007) Generation of magnetic non-viral gene transfer agents and magnetofection in vitro. *Nat Protoc* 2:2391–2411
23. Schillinger U, Brill T, Rudolph C, Huth S, Gersting S, Krotz F, Hirschberger J, Bergemann C, Plank C (2005) Advances in magnetofection—magnetically guided nucleic acid delivery. *J Magn Magn Mater* 293: 501–508
24. Fortin JP, Wilhelm C, Servais J, Menager C, Bacri JC, Gazeau F (2007) Size-sorted anionic iron oxide nanomagnets as colloidal mediators for magnetic hyperthermia. *J Am Chem Soc* 129:2628–2635
25. Goya GF, Grazu V, Ibarra MR (2008) Magnetic nanoparticles for cancer therapy. *Curr Nanosci* 4:1–16
26. Hergt R, Dutz S (2007) Magnetic particle hyperthermia-biophysical limitations of a visionary tumour therapy. *J Magn Magn Mater* 311:187–192
27. Hergt R, Dutz S, Muller R, Zeisberger M (2006) Magnetic particle hyperthermia: nanoparticle magnetism and materials development for cancer therapy. *J Phys Condens Matter* 18:S2919–S2934
28. Johannsen M, Gneveckow U, Eckelt L, Feussner A, Waldoefner N, Scholz R, Deger S, Wust P, Loening SA, Jordan A (2005) Clinical hyperthermia of prostate cancer using magnetic nanoparticles: presentation of a new interstitial technique. *Int J Hyperthermia* 21: 637–647
29. Jordan A, Scholz R, Maier-Hauff K, van Landeghem FKH, Waldoefner N, Teichgraber U, Pinkernelle J, Bruhn H, Neumann F, Thiesen B, von Deimling A, Felix R (2006) The effect of thermotherapy using magnetic nanoparticles on rat malignant glioma. *J Neurooncol* 78:7–14
30. Huh YM, Jun YW, Song HT, Kim S, Choi JS, Lee JH, Yoon S, Kim KS, Shin JS, Suh JS, Cheon J (2005) In vivo magnetic resonance detection of cancer by using multifunctional magnetic nanocrystals. *J Am Chem Soc* 127:12387–12391
31. Lee JH, Huh YM, Jun Y, Seo J, Jang J, Song HT, Kim S, Cho EJ, Yoon HG, Suh JS, Cheon J (2007) Artificially engineered magnetic nanoparticles for ultra-sensitive molecular imaging. *Nat Med* 13:95–99
32. Martina MS, Fortin JP, Menager C, Clement O, Barratt G, Grabielle-Madelmont C, Gazeau F, Cabuil V, Lesieur S (2005) Generation of superparamagnetic liposomes revealed as highly efficient MRI contrast agents for in vivo imaging. *J Am Chem Soc* 127:10676–10685
33. Mannix RJ, Kumar S, Cassiola F, Montoya-Zavala M, Feinstein E, Prentiss M, Ingber DE (2008) Nanomagnetic actuation of receptor-mediated signal transduction. *Nat Nanotechnol* 3:36–40
34. Wang SX, Li G (2008) Advances in giant magnetoresistance biosensors with magnetic nanoparticle tags: review and outlook. *IEEE Trans Magn* 44:1687–1702
35. Ramadan Q, Samper V, Poenar D, Yu C (2006) Magnetic-based microfluidic platform for biomolecular separation. *Biomed Microdevices* 8:151–158
36. Dreaden EC, Alkilany AM, Huang X, Murphy CJ, El-Sayed MA (2012) The golden age: gold nanoparticles for biomedicine. *Chem Soc Rev* 41:2740–2779
37. Govorov AO, Richardson HH (2007) Generating heat with metal nanoparticles. *Nano Today* 2:30–38
38. Dreaden EC, Mackey MA, Huang XH, Kang B, El-Sayed MA (2011) Beating cancer in multiple ways using nanogold. *Chem Soc Rev* 40:3391–3404
39. Dickerson EB, Dreaden EC, Huang X, El-Sayed IH, Chu H, Pushpanketh S, McDonald JF, El-Sayed MA (2008) Gold nanorod assisted near-infrared plasmonic photothermal therapy (PpTT) of squamous cell carcinoma in mice. *Cancer Lett* 269:57–66
40. Lal S, Clare SE, Halas NJ (2008) Nanoshell-enabled photothermal cancer therapy: impending clinical impact. *Acc Chem Res* 41:1842–1851
41. Pelaz B, Grazu V, Ibarra A, Magen C, del Pino P, de la Fuente JM (2012) Tailoring the synthesis and heating ability of gold nanoprisms for bioapplications. *Langmuir*, 28:8965–8970
42. Tian Q, Jiang F, Zou R, Liu Q, Chen Z, Zhu M, Yang S, Wang J, Wang J, Hu J (2011) Hydrophilic Cu₉S₅ nanocrystals: a photothermal agent with a 25.7% heat conversion efficiency for photothermal ablation of cancer cells in vivo. *ACS Nano* 5:9761–9771
43. Hessel CM, Pattani PV, Rasch M, Panthani MG, Koo B, Tunnell JW, Korgel BA (2011) Copper selenide nanocrystals for photothermal therapy. *Nano Lett* 11:2560–2566
44. Ku G, Zhou M, Song S, Huang Q, Hazle J, Li C (2012) Copper sulfide nanoparticles as a new class of photoacoustic contrast agent for deep tissue imaging at 1064 Nm. *ACS Nano*, 6:7489–7496
45. Homan KA, Souza M, Truby R, Luke GP, Green C, Vreeland E, Emelianov S (2011) Silver nanoplate contrast agents for in vivo molecular photoacoustic imaging. *ACS Nano* 6:641–650

46. Mahmoudi M, Serpooshan V (2012) Silver-coated engineered magnetic nanoparticles are promising for the success in the fight against antibacterial resistance threat. *ACS Nano* 6:2656–2664
47. Xiu Z-M, Zhang Q-B, Puppala HL, Colvin VL, Alvarez PJJ (2012) Negligible particle-specific antibacterial activity of silver nanoparticles. *Nano Lett* 12:4271–4275
48. Chibli H, Carlini L, Park S, Dimitrijevic NM, Nadeau JL (2011) Cytotoxicity of Inp/Zns quantum dots related to reactive oxygen species generation. *Nanoscale* 3:2552–2559
49. Zhang Y, Hong G, Zhang Y, Chen G, Li F, Dai H, Wang Q (2012) Ag₂s quantum dot: a bright and biocompatible fluorescent nanoprobe in the second near-infrared window. *ACS Nano* 6:3695–3702
50. Haase M, Schäfer H (2011) Upconverting nanoparticles. *Angew Chem Int Ed* 50:5808–5829
51. Kotov N (2011) Bioimaging: the only way is up. *Nat Mater* 10:903–904
52. Wang F, Banerjee D, Liu Y, Chen X, Liu X (2010) Upconversion nanoparticles in biological labeling, imaging, and therapy. *Analyst* 135:1839–1854
53. Wang F, Deng R, Wang J, Wang Q, Han Y, Zhu H, Chen X, Liu X (2011) Tuning upconversion through energy migration in core-shell nanoparticles. *Nat Mater* 10:968–973
54. Erb RM, Son HS, Samanta B, Rotello VM, Yellen BB (2009) Magnetic assembly of colloidal superstructures with multipole symmetry. *Nature* 457:999–1002
55. Gazeau F, Levy M, Wilhelm C (2008) Optimizing magnetic nanoparticle design for nanothermotherapy. *Nanomedicine* 3:831–844
56. Thiesen B, Jordan A (2008) Clinical applications of magnetic nanoparticles for hyperthermia. *Int J Hyperthermia* 24:467–474
57. Figuerola A, Di Corato R, Manna L, Pellegrino T (2010) From iron oxide nanoparticles towards advanced iron-based inorganic materials designed for biomedical applications. *Pharmacol Res* 62:126–143
58. Lee J-H, Jang J-T, Choi J-S, Moon SH, Noh S-H, Kim J-W, Kim J-G, Kim I-S, Park KI, Cheon J (2011) Exchange-coupled magnetic nanoparticles for efficient heat induction. *Nat Nanotechnol* 6:418–422
59. Jana NR, Gearheart L, Murphy CJ (2001) Wet chemical synthesis of high aspect ratio cylindrical gold nanorods. *J Phys Chem B* 105:4065–4067
60. Skrabalak SE, Chen J, Sun Y, Lu X, Au L, Copley CM, Xia Y (2008) Gold nanocages: synthesis, properties, and applications. *Acc Chem Res* 41:1587–1595
61. Millstone JE, Park S, Shuford KL, Qin L, Schatz GC, Mirkin CA (2005) Observation of a quadrupole plasmon mode for a colloidal solution of gold nanoprisms. *J Am Chem Soc* 127:5312–5313
62. Oldenburg SJ, Jackson JB, Westcott SL, Halas NJ (1999) Infrared extinction properties of gold nanoshells. *Appl Phys Lett* 75:2897–2899
63. Chen J, Saeki F, Wiley BJ, Cang H, Cobb MJ, Li Z-Y, Au L, Zhang H, Kimmey MB, Li X, Xia Y (2005) Gold nanocages: bioconjugation and their potential use as optical imaging contrast agents. *Nano Lett* 5:473–477
64. Hu M, Chen J, Li Z-Y, Au L, Hartland GV, Li X, Marquez M, Xia Y (2006) Gold nanostructures: engineering their plasmonic properties for biomedical applications. *Chem Soc Rev* 35:1084
65. Zhang Q, Li N, Goebel J, Lu Z, Yin Y (2011) A systematic study of the synthesis of silver nanoplates: is citrate a “magic” reagent? *J Am Chem Soc* 133:18931–18939
66. Pastoriza-Santos I, Liz-Marzan LM (2008) Colloidal silver nanoplates. State of the art and future challenges. *J Mater Chem* 18:1724–1737
67. Jana NR, Gearheart L, Murphy CJ (2001) Wet chemical synthesis of silver nanorods and nanowires of controllable aspect ratio. *Chem Comm* 617–618
68. Gou L, Murphy CJ (2002) Solution-phase synthesis of Cu₂O nanocubes. *Nano Lett* 3:231–234
69. Garitaonandia JS, Insausti M, Goikolea E, Suzuki M, Cashion JD, Kawamura N, Ohsawa H, Gil de Muro I, Suzuki K, Plazaola F, Rojo T (2008) Chemically induced permanent magnetism in Au, Ag, and Cu nanoparticles: localization of the magnetism by element selective techniques. *Nano Lett* 8:661–667
70. Scotognella F, Della Valle G, Srimath Kandada AR, Dorfs D, Zavelani-Rossi M, Conforti M, Miszta K, Comin A, Korobchevskaya K, Lanzani G, Manna L, Tassone F (2011) Plasmon dynamics in colloidal Cu₂-Xse nanocrystals. *Nano Lett* 11:4711–4717
71. Mallidi S, Luke GP, Emelianov S (2011) Photoacoustic imaging in cancer detection, diagnosis, and treatment guidance. *Trends Biotechnol* 29:213–221

72. Zheng YB, Kiraly B, Weiss PS, Huang TJ (2012) Molecular plasmonics for biology and nanomedicine. *Nanomedicine* 7:751–770
73. Resch-Genger U, Grabolle M, Cavaliere-Jaricot S, Nitschke R, Nann T (2008) Quantum dots versus organic dyes as fluorescent labels. *Nat Methods* 5:763–775
74. Murray CB, Norris DJ, Bawendi MG (1993) Synthesis and characterization of nearly monodisperse Cde (E=sulfur, selenium, tellurium) semiconductor nanocrystallites. *J Am Chem Soc* 115:8706–8715
75. Somers RC, Bawendi MG, Nocera DG (2007) Cdse nanocrystal based chem-/biosensors. *Chem Soc Rev* 36:579–591
76. Mattoussi H, Palui G, Na HB (2012) Luminescent quantum dots as platforms for probing in vitro and in vivo biological processes. *Adv Drug Deliv Rev* 64:138–166
77. Freeman R, Willner I (2012) Optical molecular sensing with semiconductor quantum dots (Qds). *Chem Soc Rev* 41:4067–4085
78. Jimenez de Aberasturi D, Montenegro J-M, Ruiz de Larramendi I, Rojo T, Klar TA, Alvarez-Puebla R, Liz-Marzán LM, Parak WJ (2011) Optical sensing of small ions with colloidal nanoparticles. *Chem Mater* 24:738–745
79. Chen J, Zhao JX (2012) Upconversion nanomaterials: synthesis, mechanism, and applications in sensing. *Sensors (Basel)* 12:2414–2435
80. Colombo M, Carregal-Romero S, Casula MF, Gutierrez L, Morales MP, Bohm IB, Heverhagen JT, Prospero D, Parak WJ (2012) Biological applications of magnetic nanoparticles. *Chem Soc Rev* 41:4306–4334
81. Sun SH, Zeng H, Robinson DB, Raoux S, Rice PM, Wang SX, Li GX (2004) Monodisperse Mfe₂o₄ (M=Fe, Co, Mn) nanoparticles. *J Am Chem Soc* 126:273–279
82. Park J, An K, Hwang Y, Park J-G, Noh H-J, Kim J-Y, Park J-H, Hwang N-M, Hyeon T (2004) Ultra-large-scale syntheses of monodisperse nanocrystals. *Nat Mater* 3:891–895
83. Laurent S, Forge D, Port M, Roch A, Robic C, Elst LV, Muller RN (2008) Magnetic iron oxide nanoparticles: synthesis, stabilization, vectorization, physicochemical characterizations, and biological applications. *Chem Rev* 108:2064–2110
84. Lu A-H, Salabas EL, Schüth F (2007) Magnetic nanoparticles: synthesis, protection, functionalization, and application. *Angew Chem Int Ed* 46:1222–1244
85. Jana NR, Chen Y, Peng X (2004) Size- and shape-controlled magnetic (Cr, Mn, Fe, Co, Ni) oxide nanocrystals via a simple and general approach. *Chem Mater* 16:3931–3935
86. Perez JM, Josephson L, O’Loughlin T, Hogemann D, Weissleder R (2002) Magnetic relaxation switches capable of sensing molecular interactions. *Nat Biotechnol* 20:816–820
87. Barcikowski S, Mafune F (2011) Trends and current topics in the field of laser ablation and nanoparticle generation in liquids. *J Phys Chem C* 115:4985
88. Cushing BL, Kolesnichenko VL, O’Connor CJ (2004) Recent advances in the liquid-phase syntheses of inorganic nanoparticles. *Chem Rev* 104:3893–3946
89. LaMer VK, Dinegar RH (1950) Theory, production and mechanism of formation of monodispersed hydrosols. *J Am Chem Soc* 72:4847–4854
90. Xia YN, Xiong YJ, Lim B, Skrabalak SE (2009) Shape-controlled synthesis of metal nanocrystals: simple chemistry meets complex physics? *Angew Chem Int Ed* 48:60–103
91. Watzky MA, Finke RG (1997) Transition metal nanocluster formation kinetic and mechanistic studies. a new mechanism when hydrogen is the reductant: slow, continuous nucleation and fast autocatalytic surface growth. *J Am Chem Soc* 119:10382–10400
92. Jana NR, Gearheart L, Murphy CJ (2001) Seed-mediated growth approach for shape-controlled synthesis of spheroidal and rod-like gold nanoparticles using a surfactant template. *Adv Mater* 13:1389–1393
93. Lim B, Xiong YJ, Xia YN (2007) A water-based synthesis of octahedral, decahedral, and icosahedral Pd nanocrystals. *Angew Chem Int Ed* 46:9279–9282
94. Zhang JG, Gao Y, Alvarez-Puebla RA, Buriak JM, Fenniri H (2006) Synthesis and sers properties of nanocrystalline gold octahedra generated from thermal decomposition of H₂ucl₄ in block copolymers. *Adv Mater* 18:3233
95. Ah CS, Yun YJ, Park HJ, Kim W-J, Ha DH, Yun WS (2005) Size-controlled synthesis of machinable single crystalline gold nanoplates. *Chem Mater* 17:5558–5561
96. Murphy CJ, Thompson LB, Chernak DJ, Yang JA, Sivapalan ST, Boulos SP, Huang J, Alkilany AM, Sisco PN (2011) Gold nanorod crystal growth: from seed-mediated synthesis to nanoscale sculpting. *Curr Opin Colloid Interface Sci* 16:128–134
97. Millstone JE, Hurst SJ, Métraux GS, Cutler JJ, Mirkin CA (2009) Colloidal gold and silver triangular nanoprisms. *Small* 5:646–664

98. Guerrero-Martínez A, Barbosa S, Pastoriza-Santos I, Liz-Marzán LM (2011) Nanostars shine bright for you. *Curr Opin Colloid Interface Sci* 16:118–127
99. Hermanson GT (2008) Bioconjugate techniques. Academic, San Diego CA
100. Yin Y, Alivisatos AP (2005) Colloidal nanocrystal synthesis and the organic-inorganic interface. *Nature* 437:664–670
101. Niemeyer CM (2001) Nanoparticles, proteins, and nucleic acids: biotechnology meets materials science. *Angew Chem Int Ed* 40:4128–4158
102. Nel A, Xia T, Mädler L, Li N (2006) Toxic potential of materials at the nanolevel. *Science* 311:622–627
103. Ackerson CJ, Jadzinsky PD, Kornberg RD (2005) Thiolate ligands for synthesis of water-soluble gold clusters. *J Am Chem Soc* 127:6550–6551
104. Liz-Marzán LM, Giersig M, Mulvaney P (1996) Synthesis of nanosized gold-silica core-shell particles. *Langmuir* 12:4329–4335
105. Pellegrino T, Kudera S, Liedl T, Javier AM, Manna L, Parak WJ (2005) On the development of colloidal nanoparticles towards multifunctional structures and their possible use for biological applications. *Small* 1:48–63
106. Bastus NG, Comenge J, Puntès V (2011) Kinetically controlled seeded growth synthesis of citrate-stabilized gold nanoparticles of up to 200 Nm: size focusing versus ostwald ripening. *Langmuir* 27:11098–11105
107. He QJ, Zhang JM, Shi JL, Zhu ZY, Zhang LX, Bu WB, Guo LM, Chen Y (2010) The effect of pegylation of mesoporous silica nanoparticles on nonspecific binding of serum proteins and cellular responses. *Biomaterials* 31:1085–1092
108. Schmid G, Corain B (2003) Nanoparticulated gold: syntheses, structures, electronics, and reactivities. *Eur J Inorg Chem* 2003:3081–3098
109. Sperling RA, Parak WJ (2010) Surface modification, functionalization and bioconjugation of colloidal inorganic nanoparticles. *Philos Transact R Soc Math Phys Eng Sci* 368:1333–1383
110. Khlebtsov NG, Dykman LA (2010) Optical properties and biomedical applications of plasmonic nanoparticles. *J Quant Spectrosc Radiat Transf* 111:1–35
111. Cedervall T, Lynch I, Lindman S, Berggård T, Thulin E, Nilsson H, Dawson KA, Linse S (2007) Understanding the nanoparticle-protein corona using methods to quantify exchange rates and affinities of proteins for nanoparticles. *Proc Natl Acad Sci USA* 104:2050–2055
112. Lynch I, Dawson KA (2008) Protein-nanoparticle interactions. *Nano Today* 3:40–47
113. Moros M, Pelaz B, Lopez-Larrubia P, Garcia-Martin ML, Grazu V, de la Fuente JM (2010) Engineering biofunctional magnetic nanoparticles for biotechnological applications. *Nanoscale* 2:1746–1755
114. Puertas S, Batalla P, Moros MA, Polo E, del Pino P, Guisán JM, Grazu V, de la Fuente JSM (2011) Taking advantage of unspecific interactions to produce highly active magnetic nanoparticle-antibody conjugates. *ACS Nano* 5:4521–4528
115. Moros M, Hernández B, Garet E, Dias JT, Sáez B, Grazu V, González-Fernández Á, Alonso C, de la Fuente JM (2012) Monosaccharides versus peg-functionalized Nps: influence in the cellular uptake. *ACS Nano* 6(2):1565–1577
116. Child HW, Del Pino PA, De La Fuente JM, Hursthouse AS, Stirling D, Mullen M, McPhee GM, Nixon C, Jayawarna V, Berry CC (2011) Working together: the combined application of a magnetic field and penetratin for the delivery of magnetic nanoparticles to cells in 3d. *ACS Nano* 5:7910–7919
117. Mirkin CA, Letsinger RL, Mucic RC, Storhoff JJ (1996) A dna-based method for rationally assembling nanoparticles into macroscopic materials. *Nature* 382:607–609
118. Algar WR, Prasuhn DE, Stewart MH, Jennings TL, Blanco-Canosa JB, Dawson PE, Medintz IL (2011) The controlled display of biomolecules on nanoparticles: a challenge suited to bioorthogonal chemistry. *Bioconjug Chem* 22:825–858
119. Gole A, Murphy CJ (2007) Azide-derivatized gold nanorods: functional materials for “click” chemistry. *Langmuir* 24:266–272
120. Verma A, Stellacci F (2010) Effect of surface properties on nanoparticle-cell interactions. *Small* 6:12–21
121. Verma A, Uzun O, Hu Y, Han H-S, Watson N, Chen S, Irvine DJ, Stellacci F (2008) Surface-structure-regulated cell-membrane penetration by monolayer-protected nanoparticles. *Nat Mater* 7:588–595
122. Park J-H, von Maltzahn G, Xu MJ, Fogal V, Kotamraju VR, Ruoslahti E, Bhatia SN, Sailor MJ (2009) Cooperative nanomaterial system to sensitize, target, and treat tumors. *Proc Natl Acad Sci* 107:981–986
123. Alkilany A, Murphy C (2010) Toxicity and cellular uptake of gold nanoparticles: what we have learned so far? *J Nanopart Res* 12:2313–2333

124. Rosi NL, Giljohann DA, Thaxton CS, Lytton-Jean AKR, Han MS, Mirkin CA (2006) Oligonucleotide-modified gold nanoparticles for intracellular gene regulation. *Science* 312:1027–1030
125. Monopoli MP, Walczyk D, Campbell A, Elia G, Lynch I, Baldelli Bombelli F, Dawson KA (2011) Physical–chemical aspects of protein corona: relevance to in vitro and in vivo biological impacts of nanoparticles. *J Am Chem Soc* 133:2525–2534
126. Walczyk D, Bombelli FB, Monopoli MP, Lynch I, Dawson KA (2010) What the cell “sees” in bionanoscience. *J Am Chem Soc* 132:5761–5768
127. Gref R, Lück M, Quellec P, Marchand M, Dellacherie E, Harnisch S, Blunk T, Müller RH (2000) ‘stealth’ corona-core nanoparticles surface modified by polyethylene glycol (peg): influences of the corona (peg chain length and surface density) and of the core composition on phagocytic uptake and plasma protein adsorption. *Colloids Surf B Biointerfaces* 18:301–313
128. Rocker C, Potzl M, Zhang F, Parak WJ, Nienhaus GU (2009) A quantitative fluorescence study of protein monolayer formation on colloidal nanoparticles. *Nat Nanotechnol* 4:577–580
129. George S, Pokhrel S, Xia T, Gilbert B, Ji Z, Schowalter M, Rosenauer A, Damoiseaux R, Bradley KA, Mädler L, Nel AE (2009) Use of a rapid cytotoxicity screening approach to engineer a safer zinc oxide nanoparticle through iron doping. *ACS Nano* 4:15–29
130. Chithrani BD, Ghazani AA, Chan WCW (2006) Determining the size and shape dependence of gold nanoparticle uptake into mammalian cells. *Nano Lett* 6:662–668
131. Alkilany AM, Nalaria PK, Hexel CR, Shaw TJ, Murphy CJ, Wyatt MD (2009) Cellular uptake and cytotoxicity of gold nanorods: molecular origin of cytotoxicity and surface effects. *Small* 5:701–708
132. Arvizo RR, Miranda OR, Thompson MA, Pabelick CM, Bhattacharya R, Robertson JD, Rotello VM, Prakash YS, Mukherjee P (2010) Effect of nanoparticle surface charge at the plasma membrane and beyond. *Nano Lett* 10:2543–2548
133. Chen J, Glaus C, Laforest R, Zhang Q, Yang M, Gidding M, Welch MJ, Xia Y (2010) Gold nanocages as photothermal transducers for cancer treatment. *Small* 6:811–817
134. El Badawy AM, Silva RG, Morris B, Scheckel KG, Suidan MT, Tolaymat TM (2010) Surface charge-dependent toxicity of silver nanoparticles. *Environ Sci Technol* 45:283–287
135. Lundqvist M, Stigler J, Elia G, Lynch I, Cedervall T, Dawson KA (2008) Nanoparticle size and surface properties determine the protein corona with possible implications for biological impacts. *Proc Natl Acad Sci USA* 105:14265–14270
136. Goodman CM, McCusker CD, Yilmaz T, Rotello VM (2004) Toxicity of gold nanoparticles functionalized with cationic and anionic side chains. *Bioconjug Chem* 15:897–900
137. Chung T-H, Wu S-H, Yao M, Lu C-W, Lin Y-S, Hung Y, Mou C-Y, Chen Y-C, Huang D-M (2007) The effect of surface charge on the uptake and biological function of mesoporous silica nanoparticles in 3T3-L1 cells and human mesenchymal stem cells. *Biomaterials* 28:2959–2966
138. Gratton SEA, Ropp PA, Pohlhaus PD, Luft JC, Madden VJ, Napier ME, DeSimone JM (2008) The effect of particle design on cellular internalization pathways. *Proc Natl Acad Sci* 105:11613–11618
139. Hauck TS, Ghazani AA, Chan WCW (2008) Assessing the effect of surface chemistry on gold nanorod uptake, toxicity, and gene expression in mammalian cells. *Small* 4: 153–159
140. Martin AL, Bernas LM, Rutt BK, Foster PJ, Gillies ER (2008) Enhanced cell uptake of superparamagnetic iron oxide nanoparticles functionalized with dendritic guanidines. *Bioconjug Chem* 19:2375–2384
141. Cho EC, Xie J, Wurm PA, Xia Y (2009) Understanding the role of surface charges in cellular adsorption versus internalization by selectively removing gold nanoparticles on the cell surface with a I2/Ki etchant. *Nano Lett* 9:1080–1084
142. Leroueil PR, Hong S, Mecke A, Baker JR, Orr BG, Banaszak Holl MM (2007) Nanoparticle interaction with biological membranes: does nanotechnology present a janus face? *Acc Chem Res* 40:335–342
143. Leroueil PR, Berry SA, Duthie K, Han G, Rotello VM, McNerny DQ, Baker JR, Orr BG, Banaszak Holl MM (2008) Wide varieties of cationic nanoparticles induce defects in supported lipid bilayers. *Nano Lett* 8: 420–424
144. Yezhelyev MV, Qi L, O’Regan RM, Nie S, Gao X (2008) Proton-sponge coated quantum dots for siRNA delivery and intracellular imaging. *J Am Chem Soc* 130:9006–9012
145. El-Sayed IH, Huang X, El-Sayed MA (2006) Selective laser photo-thermal therapy of epithelial carcinoma using anti-EGFR antibody conjugated gold nanoparticles. *Cancer Lett* 239:129–135

146. Lin J, Zhang H, Chen Z, Zheng Y (2010) Penetration of lipid membranes by gold nanoparticles: insights into cellular uptake, cytotoxicity, and their relationship. *ACS Nano* 4:5421–5429
147. Albanese A, Sykes EA, Chan WCW (2010) Rough around the edges: the inflammatory response of microglial cells to spiky nanoparticles. *ACS Nano* 4:2490–2493
148. Harper SL, Carriere JL, Miller JM, Hutchison JE, Maddux BLS, Tanguay RL (2011) Systematic evaluation of nanomaterial toxicity: utility of standardized materials and rapid assays. *ACS Nano* 5:4688–4697
149. Duncan R, Izzo L (2005) Dendrimer biocompatibility and toxicity. *Adv Drug Deliv Rev* 57:2215–2237
150. Stasko NA, Johnson CB, Schoenfish MH, Johnson TA, Holmuhamedov EL (2007) Cytotoxicity of polypropylenimine dendrimer conjugates on cultured endothelial cells. *Biomacromolecules* 8:3853–3859
151. Aillon KL, Xie Y, El-Gendy N, Berkland CJ, Forrest ML (2009) Effects of nanomaterial physicochemical properties on in vivo toxicity. *Adv Drug Deliv Rev* 61:457–466
152. Dobrovolskaia MA, McNeil SE (2007) Immunological properties of engineered nanomaterials. *Nat Nanotechnol* 2:469–478
153. Zolnik BS, González-Fernández Á, Sadrieh N, Dobrovolskaia MA (2010) Minireview: nanoparticles and the immune system. *Endocrinology* 151:458–465
154. Chomposor A, Saha K, Ghosh PS, Macarthy DJ, Miranda OR, Zhu Z-J, Arcaro KF, Rotello VM (2010) The role of surface functionality on acute cytotoxicity, ROS generation and DNA damage by cationic gold nanoparticles. *Small* 6:2246–2249
155. Owens III DE, Peppas NA (2006) Opsonization, biodistribution, and pharmacokinetics of polymeric nanoparticles. *Int J Pharm* 307:93–102
156. Lin S, Zhao Y, Xia T, Meng H, Ji Z, Liu R, George S, Xiong S, Wang X, Zhang H, Pokhrel S, Mädler L, Damoiseaux R, Lin S, Nel AE (2011) High content screening in zebrafish speeds up hazard ranking of transition metal oxide nanoparticles. *ACS Nano* 5:7284–7295
157. Malik N, Wiwattanapatapee R, Klopsch R, Lorenz K, Frey H, Weener JW, Meijer EW, Paulus W, Duncan R (2000) Dendrimers: relationship between structure and biocompatibility in vitro, and preliminary studies on the biodistribution of 125I-labelled polyamidoamine dendrimers in vivo. *J Control Release* 65:133–148
158. Plank C, Mechtler K, Szoka FC, Wagner E (1996) Activation of the complement system by synthetic DNA complexes: a potential barrier for intravenous gene delivery. *Hum Gene Ther* 7:1437–1446
159. França Á, Pelaz B, Moros M, Sánchez-Espinel C, Hernández A, Fernández-López C, Graú V, de la Fuente JM, Pastoriza-Santos I, Liz-Marzán LM, González-Fernández Á (2010) Sterilization matters: consequences of different sterilization techniques on gold nanoparticles. *Small* 6:89–95
160. Scheffer A, Engelhard C, Sperling M, Buscher W (2008) ICP-MS as a new tool for the determination of gold nanoparticles in bioanalytical applications. *Anal Bioanal Chem* 390:249–252
161. Ojea-Jiménez I, López X, Arbiol J, Puentes V (2012) Citrate-coated gold nanoparticles as smart scavengers for mercury(II) removal from polluted waters. *ACS Nano* 6:2253–2260
162. Baer D, Gaspar D, Nachimuthu P, Techane S, Castner D (2010) Application of surface chemical analysis tools for characterization of nanoparticles. *Anal Bioanal Chem* 396:983–1002
163. Liu Y, Yan B (2011) Characterizing the surface chemistry of nanoparticles: an analogy to solid-phase synthesis samples. *Comb Chem High Throughput Screen* 14:191–197
164. Romo-Herrera JM, Alvarez-Puebla RA, Liz-Marzán LM (2011) Controlled assembly of plasmonic colloidal nanoparticle clusters. *Nanoscale* 3:1304–1315
165. Xu X, Caswell KK, Tucker E, Kabisatpathy S, Brodhacker KL, Scrivens WA (2007) Size and shape separation of gold nanoparticles with preparative gel electrophoresis. *J Chromatogr A* 1167:35–41
166. Hanauer M, Pierrat S, Zins I, Lotz A, Sönnichsen C (2007) Separation of nanoparticles by gel electrophoresis according to size and shape. *Nano Lett* 7:2881–2885
167. Lin C-AJ, Sperling RA, Li JK, Yang T-Y, Li P-Y, Zanella M, Chang WH, Parak WJ (2008) Design of an amphiphilic polymer for nanoparticle coating and functionalization. *Small* 4:334–341
168. Kowalczyk B, Lagzi I, Grzybowski BA (2011) Nanoseparations: strategies for size and/or shape-selective purification of nanoparticles. *Curr Opin Colloid Interface Sci* 16:135–148

169. Chen G, Wang Y, Tan LH, Yang M, Tan LS, Chen Y, Chen H (2009) High-purity separation of gold nanoparticle dimers and trimers. *J Am Chem Soc* 131:4218–4219
170. Lee J-S, Stoeva SI, Mirkin CA (2006) DNA-induced size-selective separation of mixtures of gold nanoparticles. *J Am Chem Soc* 128:8899–8903
171. Doane TL, Chuang CH, Hill RJ, Burda C (2012) Nanoparticle zeta-potentials. *Acc Chem Res* 45:317–326
172. Doane TL, Cheng Y, Babar A, Hill RJ, Burda C (2010) Electrophoretic mobilities of pegylated gold nps. *J Am Chem Soc* 132:15624–15631
173. Marquis BJ, Love SA, Braun KL, Haynes CL (2009) Analytical methods to assess nanoparticle toxicity. *Analyst* 134:425–439
174. Li L, Mu Q, Zhang B, Yan B (2010) Analytical strategies for detecting nanoparticle-protein interactions. *Analyst* 135: 1519–1530

Immobilization of Enzymes on Ethynyl-Modified Electrodes via Click Chemistry

Akhtar Hayat, Audrey Sassolas, Amina Rhouati, and Jean-Louis Marty

Abstract

This paper describes a novel, simple, and versatile protocol for covalent immobilization of enzyme on electrode. The immobilization method is based on the combination of diazonium salt electrografting and click chemistry. The ethynyl-terminated monolayers are obtained by diazonium salt electrografting, then, in the presence of copper (I) catalyst, the ethynyl modified surfaces reacts efficiently and rapidly with enzyme bearing an azide function (azido-enzyme), thus forming a covalent 1,2,3-triazole linkage by means of click chemistry. The ethynyl-terminated film preserves the activity of the immobilized enzyme. The click chemistry along with binary film of diazonium salts offers a variety of good characteristics including high sensitivity, good repeatability and reusability, rapid response and long term stability of the system. Thus, because of the chemoselective reactivity and quantitative yield of the click reaction, an ethynyl-terminated monolayer can be treated as a general platform for obtaining reliable coverage of a wide range of azido-terminated species of interest for various sensing applications.

Key words Click chemistry, Diazonium salt, Direct electrochemistry, Enzyme immobilization, Azido-enzyme

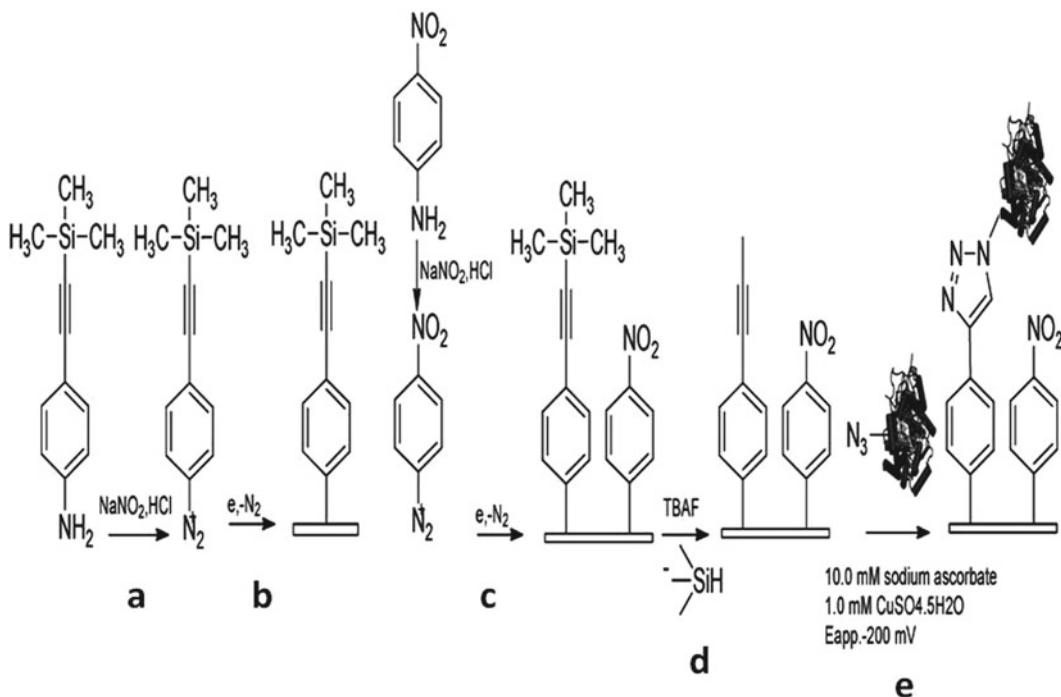
1 Introduction

Robust immobilization technique remains a critical variable for the optimal performance of the enzyme electrode. Many potential and interesting applications can be achieved only if enzymes are properly immobilized on solid surface with their activity preserved [1, 2]. The approaches used for enzyme immobilization used include sol-gel encapsulation [3], polymer entrapment [4], physical adsorption (electrostatic and hydrophobic adhesion) [5], and bio-specific recognition [6]. Although appropriate, these schemes can, at times, be limited by the reduction of enzyme activity due to protein denaturation, unintended reactions at the solid-liquid interface that reduces access to molecular recognition sites.

Recently, the direct immobilization and covalent immobilization of enzymes have been used to functionalize solid interface, such as carbon, silicon, metals, and diamonds [7-9].

However, covalent immobilization is difficult to control and yields randomly bound enzymes with poor orientation or inappropriate alignment, which results in inefficient electron transfer to electrode surface. The key issue in the proper immobilization of enzyme is to design a biocompatible interface, which is able to immobilize enzyme with reproducible binding, conformation preserving, distance controlling, and proper molecular-level orientation in addition to stability of the method. Among the few enzyme immobilization techniques able to meet these multiple criteria, the click chemistry could be an attractive approach to enhance the direct electron transfer between the enzyme and electrode surface [10–12].

Click chemistry is attracting lot of interest and importance in recent years. As an azide/alkyne 1, 3-dipolar cycloaddition, it was first introduced by Huisgen in 1984 as a reaction at high temperature in organic solvent [13]. In 2001, Sharpless et al. performed this reaction in aqueous phase with Cu (I) as catalyst under very mild conditions [14]. From then on, click chemistry received vital importance not only because it is irreversible, quantitative and mildly processed, but also because the 1, 2, 3-triazole ring formed in the reaction is similar to peptide bond in atom placement and electronic properties. The ring-like peptide could help to maintain biological activity of the immobilized enzyme [15, 16]. Moreover, this heterogeneous coupling reaction is fast, resistant to side reactions, selective, compatible to various solvents (including water), reproducible, highly tolerant to reaction conditions and has high yield. Additionally, the formed 1, 4-disubstituted 1, 2, 3-triazole is very stable under physiological conditions, and the azides are highly energetic and inert to biomolecules, which is useful for site-specific immobilization of enzymes on solid surface [17, 18]. These advantages make click chemistry suitable for electrochemical grafting of enzymes onto electrode surface. Although covalent attachment based on other chemistries is widely studied, the concept of using click chemistry in enzyme immobilization is very new and recent. In 2011, Ran et al. used an alkynylation/click chemistry based on diazonium salts to immobilize horseradish peroxidase (HRP) on gold electrode surface. The developed electrochemical biosensors showed good electrocatalytic performance toward hydrogen peroxide with high sensitivity [10, 11]. The possible drawback in the immobilization methods of Ran et al. could be the difficulty of controlling the vertical extension of the produced layer because aryl radicals may react on the grafted layer leading to multilayer coatings with irregular morphology [19]. An alternative strategy was proposed by Leroux et al., who successfully used a binary layer containing two reagents to obtain the uniform, compact and controlled modified electrode surface [20]. On the basis of this concept, recently, our group has reported a novel, simple, and versatile protocol based on click chemistry for the



Scheme 1 The steps involved in electrode modification and immobilization of the azido-enzyme: (a) In situ generation of TMSi-Eth-Ar diazonium salt; (b) electrochemical reduction of in situ generated TMSi-Eth-Ar diazonium salt on SPCE surface; (c) electrochemical reduction of in situ generated p - NO_2 -Ar diazonium salt on modified SPCE surface; (d) treatment of protected TMSi-Eth-Ar- $p\text{NO}_2$ -Ar with TBAF to remove the TMSi group; (e) immobilization of azido-enzyme via click chemistry on ethynyl-modified SPCE

immobilization of horseradish peroxidase [12]. The immobilization strategy was based on the electroreduction of aryldiazonium salt derivatives bearing a silyl protection group. After chemical deprotection, a dense and active phenylethynylene monolayer was obtained on the electrode surface that was used to specifically immobilize HRP through the click chemistry (Scheme 1).

The developed biosensor was used to detect hydrogen peroxide with high sensitivity, good repeatability and reusability, rapid response, and long-term stability. The controlled electrochemical grafting of two diazonium salt on the same transducer surface resulted in the formation of uniform layer on the transducer surface and improved the reproducibility of the system. Additionally, compact uniform layer also prevented the nonspecific adsorption. The obtained results demonstrated the advantages displayed by combining click chemistry and uniform and compact modified electrode surface to immobilize the enzyme. The high quantitative yield of the click reaction opens the door to design simple and efficient immobilization protocol for enzyme. Although, the use of click chemistry is reported only for HRP to date, but this immobilization strategy could be easily extended to immobilize other enzyme molecules due its simple and efficient characteristics.

It is not just different enzymes that can be immobilized using the click chemistry technique but other molecules as well. This immobilization method could be applied to all the azide-terminated species of interest for various sensing applications. However, biomolecules such as enzymes, aptamers, antibodies, regulatory protein are required for modification with azide functional group prior to surface immobilization on ethynyl-modified electrode.

This chapter presents the steps involved in the immobilization of enzyme onto electrode surface via click chemistry. The immobilization procedure is divided into three parts

- Electrochemical grafting of binary functional layers to have a uniform and compact modified electrode surface with ethynyl terminal group.
- Modification of enzyme with azide functional group.
- Immobilization of azido-enzyme onto ethynyl modified electrode surface via click chemistry.

2 Materials

2.1 Electrochemical Grafting of Binary Functional Layer onto Electrode

1. 4-((Trimethylsilyl) ethynyl) aniline (TMSi-Eth-Ar-NH₂) to have ethynyl functional group on modified electrode (Sigma).
2. 4-Nitroaniline to cover the pinholes of the first layer for the design of uniform and compact modified electrode surface (Sigma).
3. Sodium nitrite (NaNO₂) for the formation of diazonium radical (Sigma).
4. Tetrabutylammonium fluoride (TBAF) to deprotect the ethynyl group on the modified electrode (Sigma).
5. Ethanol to release the loosely attached oligophenylene layers (Sigma).
6. 0.5 M HCl and 0.5 M H₂SO₄ (sigma).
7. Screen printed carbon electrodes (SPCEs) from IMAGES Université de Perpignan, France.

2.2 Modification of Enzyme with Azide Functional Group

1. Enzyme to be immobilized.
2. Potassium carbonate (K₂CO₃) (sigma).
3. Copper (II) sulfate pentahydrate (CuSO₄·5H₂O) (sigma).
4. Imidazole-1 sulfonyl azide hydrochloride.
5. Dialysis bag (molecular weight 8,000–14,000).
6. Phosphate buffer saline solution (PBS) (1×, pH 7.0).

2.3 Immobilization of Azido-Enzyme onto Ethynyl Modified Electrode Surface via Click Chemistry

1. Azido-enzyme.
2. Sodium ascorbate (Sigma).
3. Copper (II) sulfate pentahydrate ($\text{CuSO}_4 \cdot 5\text{H}_2\text{O}$) (Sigma).
4. Disodium ethylenediaminetetraacetate dehydrate (EDTA) to wash any physically adsorbed azide moieties and excess copper.
5. Phosphate buffer saline solution (PBS) (1×, pH 7.2).
6. Modified electrodes having ethynyl functional groups.

3 Methods

3.1 Electrochemical Grafting of Binary Functional Layer onto SPCE Electrode

1. The screen printed carbon electrodes were modified by slightly modifying the strategy undertaken early by Leroux et al. [20] (*see Note 1*).
2. Clean the electrode surface electrochemically in 0.5 M H_2SO_4 between 1.0 and 1.6 V versus pseudo reference silver electrode until a reproducible cyclic voltammogram is obtained (*see Note 2*).
3. Rinse the clean electrode with de-ionized water.
4. Prepare the starting surface modified with protected 4-((trimethylsilyl)ethynyl) benzene (TMSi-Eth-Ar) by electroreduction upon one potential cycling between 0.4 and -0.5 V versus pseudo reference silver electrode in a solution of 4-((trimethylsilyl)ethynyl) aniline TMSi-Eth-Ar- NH_2 (2.0 mM) and sodium nitrite (2.0 mM) in 0.5 M HCl (*see Note 3*).
5. Immerse the protected TMSi-Eth-Ar electrode for 1 min in ethanol to release the loosely attached oligophenylene layers (*see Note 4*).
6. Consequently, perform the electroreduction of *p*- NO_2 -Ar N_2^+ ion on the TMSi-Eth-Ar electrode (*see Note 5*).
7. Then, treat the protected surface TMSi-Eth-Ar-*p*- NO_2 -Ar with tetrabutylammonium fluoride (TBAF) (0.05 M) to remove the TMSi group, leading to a carbon surface modified by a covalently bound ethynyl benzene monolayer (HEth-Ar-*p*- NO_2 -Ar-SPCE) (*see Note 6*).

3.2 Modification of Enzyme with Azide Functional Group

1. The azido-enzyme conjugate was synthesized by following the protocol described by Van Dongen et al. [21] (*see Note 7*).
2. Briefly, add K_2CO_3 (100 μL , 2 mg/mL) and $\text{CuSO}_4 \cdot 5\text{H}_2\text{O}$ (25 μL , 1 mg/mL) to enzyme aqueous solution (200 μL , 2.5 mg/mL) (*see Note 8*).
3. After mixing, add a solution of imidazole-1 sulfonyl azide hydrochloride (15 μL , 2 mg/mL, 1.75 equiv. relative to amines in enzyme) (*see Note 9*).

4. Agitate the solution overnight.
5. Then, transfer the mixture to a dialysis bag (molecular weight 8,000–14,000), and dialyze three times with 500 mL phosphate buffered solution (PBS, pH 7.0) for 36 h.

3.3 Immobilization of Azido-Enzyme onto Ethynyl Modified Electrode Surface via Click Chemistry

1. Perform the cycloaddition reaction by contacting the ethynyl-coated carbon electrode with a solution of the enzyme-N₃ with sodium ascorbate (10.0 mM) and copper (II) sulfate pentahydrate (1.0 mM).
2. Poise the electrode at –200 mV versus pseudo reference silver electrode over a period of few minutes.
3. This potential is roughly 300 mV negative of the Cu(II/I) standard potential of the catalyst, ensuring that Cu(I) is formed at the electrode surface.
4. Then, rinse the electrode carefully with distilled water, and an EDTA solution to ensure washing off any physically absorbed azide moieties and excess copper.
5. After rinsing in distilled water, the enzyme modified electrodes are ready to be used for electrochemical experiments.

4 Notes

1. Our experiments were based on the modification of screen printed carbon electrodes (SPCEs); however, other immobilization supports can also be modified with this procedure.
2. The reported cleaning protocol is for SPCEs; however, other immobilization supports can be clean by varying the range of applied potential or by following the other reported method specific for each support.
3. 4-((trimethylsilyl)ethynyl) aniline benzene (TMSi-Eth-Ar-NH₂) was used in our experiments; however, this can be replaced by other compounds having protected ethynyl functional group.
4. The reported incubation time in ethanol is for SPCEs; however, this can be varied according to immobilization support. Long incubation time can damage the surface of screen printed electrodes.
5. The sequence of immobilizing two diazonium compounds on the immobilization support is very important. The click reaction does not work in case of immobilizing 4-nitroaniline before or simultaneously with diazonium compound having protected ethynyl group.
6. The concentration of TBAF should be optimized according to immobilization support. Long TBAF treatment can destroy the modified electrode.

7. Our experiments were based on the modification of HRP; however, this modification method is also applicable to other enzymes.
8. Use the optimal concentration of the enzyme to be modified.
9. Each enzyme has different number of amine groups in its chemical structure. Use the concentration of imidazole-1 sulfonyl azide hydrochloride according to number of amine groups in the enzyme to be modified. The reported concentration is for HRP enzyme.

References

1. Burnham MR, Turner JN, Szarowski D, Martin DL (2006) Biological functionalization and surface micropatterning of polyacrylamide hydrogels. *Biomaterials* 27:5883–5891
2. Shi Q, Chen X, Lu T, Jing X (2008) The immobilization of proteins on biodegradable polymer fibers via click chemistry. *Biomaterials* 29:1118–1126
3. Hayat A, Barthelmebs L, Marty J-L (2012) A simple colorimetric enzymatic-assay for okadaic acid detection based on the immobilization of protein phosphatase 2A in sol-gel. *Appl Biochem Biotechnol* 166:47–56
4. Sassolas A, Catanante G, Hayat A, Marty J-L (2011) Development of an efficient protein phosphatase-based colorimetric test for okadaic acid detection. *Anal Chim Acta* 702:262–268
5. Wang J, Wang L, Di J, Tu Y (2009) Electrodeposition of gold nanoparticles on indium/tin oxide electrode for fabrication of a disposable hydrogen peroxide biosensor. *Talanta* 77:1454–1459
6. Sassolas A, Blum LJ, Leca-Bouvier BD (2012) Immobilization strategies to develop enzymatic biosensors. *Biotechnol Adv* 30:489–511
7. Rahman MA, Park DS, Shim YB (2004) A performance comparison of choline biosensors: anodic or cathodic detections of H₂O₂ generated by enzyme immobilized on a conducting polymer. *Biosens Bioelectron* 19:1565–1571
8. Nan C, Zhang Y, Zhang G, Dong C, Shuang S, Choi MMF (2009) Activation of nylon net and its application to a biosensor for determination of glucose in human serum. *Enzyme Microb Technol* 44:249–253
9. Arya SK, Prusty AK, Singh SP, Solanki PR, Pandey MK, Datta M, Malhotra BD (2007) Cholesterol biosensor based on N-(2-aminoethyl)-3-aminopropyl-trimethoxysilane self-assembled monolayer. *Anal Biochem* 363: 210–218
10. Ran Q, Peng R, Liang C, Ye S, Xian Y, Zhang W, Jin L (2011) Covalent immobilization of horseradish peroxidase via click chemistry and its direct electrochemistry. *Talanta* 83:1381–1385
11. Ran Q, Peng R, Liang C, Ye S, Xian Y, Zhang W, Jin L (2011) Direct electrochemistry of horseradish peroxidase immobilized on electrografted 4-ethynylphenyl film via click chemistry. *Anal Chim Acta* 697:27–31
12. Hayat A, Marty J-L, Radi A-E (2012) Novel amperometric hydrogen peroxide biosensor based on horseradish peroxidase azide covalently immobilized on ethynyl-modified screen-printed carbon electrode via click chemistry. *Electroanalysis* 24:1446–1452
13. Huisgen R (1984) 1,3-dipolar cycloadditions – introduction, survey, mechanism, In: Padwa A (ed) 1,3 Dipolar cycloaddition chemistry, vol 1. Wiley, New York, pp 1–176
14. Kolb HC, Finn MG, Sharpless KB (2001) Click chemistry: diverse chemical function from a few good reactions. *Angew Chem Int Ed* 40:2004–2021
15. Qi H, Ling C, Huang R, Qiu X, Shangguan L, Gao Q, Zhang C (2012) Functionalization of single-walled carbon nanotubes with protein by click chemistry as sensing platform for sensitized electrochemical immunoassay. *Electrochim Acta* 63:76–82
16. Devaraj NK, Collman JP (2007) Copper catalyzed azide-alkyne cycloadditions on solid surfaces: applications and future directions. *QSAR Comb Sci* 26:1253–1260
17. Devaraj NK, Decreau RA, Ebina W, Collman JP, Chidsey CED (2006) Rate of interfacial electron transfer through the 1,2,3-triazole linkage. *J Phys Chem B* 110:15955–15962
18. Daugaard AE, Hansen TS, Larsen NB, Hvilsted S (2011) Microwave assisted click chemistry on a conductive polymer film. *Synth Met* 161:812–816

19. Leroux YR, Fei H, Noël J-M, Roux C, Hapiot P (2010) Efficient covalent modification of a carbon surface: use of a silyl protecting group to form an active monolayer. *J Am Chem Soc* 132:14039–14041
20. Leroux YR, Hui F, Noël J-M, Roux C, Downard AJ, Hapiot P (2011) Design of robust binary film onto carbon surface using diazonium electrochemistry. *Langmuir* 27: 11222–11228
21. van Dongen SFM, Teeuwen RLM, Nallani M, van Berkel SS, Cornelissen JJLM, Nolte RJM, van Hest JCM (2008) Single-step azide introduction in proteins via an aqueous diazo transfer. *Bioconjugate Chem* 20: 20–23

Modification of Carbon Nanotube Electrodes with 1-Pyrenebutanoic Acid, Succinimidyl Ester for Enhanced Bioelectrocatalysis

Guinevere Strack, Robert Nichols, Plamen Atanassov, Heather R. Luckarift, and Glenn R. Johnson

Abstract

Conductive materials functionalized with redox enzymes provide bioelectronic architectures with application to biological fuel cells and biosensors. Effective electron transfer between the enzyme (biocatalyst) and the conductive materials is imperative for function. Various nanostructured carbon materials are common electrode choices for these applications as both the materials' inherent conductivity and physical integrity aids optimal performance. The following chapter presents a method for the use of carbon nanotube buckypaper as a conductive architecture suitable for biocatalyst functionalization. In order to securely attach the biocatalyst to the carbon nanotube surface, the conductive buckypaper is modified with the heterobifunctional cross-linker, 1-pyrenebutanoic acid, succinimidyl ester. The technique effectively tethers the enzyme to the carbon nanotube which enhances bioelectrocatalysis, preserves the conductive nature of the carbon surface, and facilitates direct electron transfer between the catalyst and material interface. The approach is demonstrated using phenol oxidase (laccase) and pyrroloquinoline quinone-dependent glucose dehydrogenase PQQ-GDH, as representative biocatalysts.

Key words Direct electron transfer (DET), 1-Pyrenebutanoic acid, succinimidyl ester (PBSE), Buckypaper (BP), Carbon nanotube (CNT), Laccase, Pyrroloquinoline quinone-dependent glucose dehydrogenase (PQQ-GDH), Biological fuel cell, Glucose, Cathode, Anode, Cyclic voltammetry, Polarization curve, Contact angle, Enzyme, Bioelectrochemistry, Multi-copper oxidase, Oxygen reduction reaction (ORR)

1 Introduction

The incorporation of carbon nanotubes (CNTs) into bioelectronic interfaces has been explored with respect to various applications, in particular, biological fuel cells [1]. One promising approach is to link biocatalysts that catalyze the oxidization or reduction of a dissolved chemical species to CNTs in such a manner that allows the direct transfer of electrons between the conductive material and the redox biocatalyst. In order to achieve the electron tunneling or

direct electron transfer (DET), the biomaterial interface should be designed to establish a robust electronic connection between the biomolecule and the conductive material. The two part challenge is to secure the biocatalyst to the surface and retain catalytic activity within the constructed architecture.

CNTs are excellent nanostructure candidates for bioelectronics due to their high conductivity and an aspect ratio that allows close association between the enzyme and material surface. Many methodologies have been described for coupling enzymes and CNTs. One common approach to covalently attach enzymes to CNTs is carbodiimide chemistry in which the CNT surface is first oxidized to produce carboxyl groups that react with lysine residues on the surface of the enzyme to form a covalent attachment between the enzyme and CNT [2]. A disadvantage to this approach, however, is that the oxidation process generates surface defects, which decrease materials conductivity due to loss of sp^2 hybridization on the CNT. One way to overcome this disadvantage is to use a cross-linker that first allows direct physical interaction with a pristine (i.e., defect-free) CNT surface through π - π stacking via a pyrene moiety. Second, the cross-linker contains a functional region that reacts with amines groups available on the surface of the protein to form a covalent bond [3]. In this chapter, 1-pyrenebutanoic acid, succinimidyl ester (PBSE) is demonstrated to tether enzymes to CNT electrodes in the described manner; however, other analogous bifunctional reagents can act as tethering molecules [4].

To simplify bio-electrode fabrication, CNTs can be organized as pressed “buckypaper” (BP) that is easy to handle and readily scalable [5–8]. The product used herein—referred to as BuckyShield®—is an optimized blend of 100 % multi-wall carbon nanotubes (MWCNTs) with high conductivity (354 S/cm). Electrode dimensions were chosen to reduce capacitance and enhance conductivity in order to characterize the DET process. BP can also be tailored to accommodate various applications or biocatalyst combinations by selecting CNTs with other aspect ratio and functionalities.

Selection of an enzyme suitable for DET between the biocatalyst and the CNT surface depends on the desired application [2, 3, 9]. For demonstrative purposes, we selected a biocatalyzed reduction reaction and an oxidation reaction. For example, the oxygen reduction reaction (ORR) can be catalyzed by enzymes such as the laccase from *Trametes versicolor* for cathodic reactions [3, 5, 10]. We also demonstrate the production of anodic current (via glucose oxidation) by immobilizing pyrroloquinoline quinone-dependent glucose dehydrogenase (PQQ-GDH) using the same PBSE tethering method [2, 11–13].

The application of the PBSE tether enhances catalytic efficiency and increases current density from both oxidative and reductive

catalytic reactions and facilitates the DET processes. The described immobilization method can be modified to most any biocatalyst of choice, although there must be amine groups on the protein that will react with the ester group of the tethering reagent. For bioelectrochemical applications, cyclic voltammetry (CV) and potentiostatic polarization can be used to evaluate the efficiency of immobilization. CV is a qualitative assessment of bioelectrocatalysis, while potentiostatic polarization is a preliminary characterization of the steady-state current density obtained at several applied potentials. In addition, a method to determine the surface energy change of BP after modification with PBSE is included to confirm that the tether has been successfully deposited on the CNTs as evidenced by a change in surface hydrophobicity.

2 Materials

All chemicals were obtained from Sigma–Aldrich, St. Louis, MO, unless otherwise stated. PBSE was purchased from AnaSpec, Fremont, CA. PQQ-GDH (E.C. 1.1.5.2) was purchased from Toyobo Co., Ltd., Osaka, Japan, and used as supplied. Follow standard laboratory safety protocols; be sure to use protective eye-wear and gloves as directed. BP (BuckyShield®) was purchased from Buckeye Composites; NanoTechLabs, Kettering, OH (average thickness ~20 μm).

Prepare all solutions using deionized water (DI) unless otherwise stated. All presented methods are performed at room temperature unless otherwise indicated.

2.1 Protein Preparation

Two model systems are described herein for laccase and PQQ-GDH. The crude laccase powder is ~10 % protein and was purified via dialysis in order to improve the quality of subsequent experiments. The requirement for pre-purification of the biocatalyst of choice must be determined on an individual basis, depending upon the final application and the purity of the manufacturer's preparation.

2.1.1 Laccase Dialysis

1. Prepare 20 mM phosphate buffer, pH 7.3 in 3×4 L batches. Weigh 13.92 g K_2HPO_4 and 10.88 g KH_2PO_4 and dissolve in 3.5 L of DI H_2O . After adjusting the pH to 7.3 with NaOH, adjust the total volume to 4 L. Prepare an extra 0.5 L of the same buffer by modifying the quantities accordingly and set aside.
2. Dissolve 0.638 g CuSO_4 in 4 L of the phosphate buffer to give a final concentration of 1 mM.
3. Dissolve 1.489 g of ethylenediaminetetraacetic acid (EDTA) in 4 L of phosphate buffer to give a final concentration of 1 mM.
4. Prepare a stock solution of the commercial laccase (20 mg/mL) in potassium phosphate buffer (20 mM, pH 7.3).

2.1.2 Preparation of PQQ-GDH

1. Prepare a stock solution of PQQ-GDH by dissolving directly in 10 mM potassium phosphate (pH 7.0) to a concentration of 20 mg/mL.

2.2 Modification of BP with PBSE and Enzyme Immobilization

2.2.1 Enzyme Buffer

1. Prepare a stock solution of 1 M K_2HPO_4 by dissolving 87.09 g in 0.5 L of DI water.
2. Prepare a stock solution of 1 M KH_2PO_4 by dissolving 68.045 g in 0.5 L of DI water.
3. Prepare 10 mM phosphate buffer, pH 7.0, by mixing 6.15 mL of 1 M K_2HPO_4 with 3.85 mL of 1 M KH_2PO_4 and make up to 1 L with DI water. Check that the pH is 7.0.
4. Dilute protein stock solution (20 mg/mL) or dialyzed protein preparation to a working concentration of 1 mg/mL (*see Note 1*). Store on ice until needed.

2.2.2 Preparation of PBSE Solution

1. Remove PBSE from freezer 15 min before opening the container. Weigh 3.8 mg of PBSE and add to 1 mL dimethylsulfoxide (DMSO) DMSO (*see Note 1*) to give a final concentration of 10 mM.

2.2.3 Preparation of the BP Electrodes

1. BP can be stored and handled at room temperature. Protect BP from dust and carefully handle using forceps.
2. Cut circular BP electrodes (geometric area, $A=0.13\text{ cm}^2$) using a cork borer. Set aside for later use.

2.2.4 Preparation of BP for Lyophilization and Contact Angle Measurements

1. Cut circular BP electrodes (geometric area, $A=2\text{ cm}^2$) using a cork borer. Set aside for later use.

2.3 Electrochemical Measurements

2.3.1 Preparation of Electrochemical Electrolyte for CV (Laccase)

1. Prepare 0.1 M phosphate buffer, pH 6.0. Using buffer stock solutions (Subheading 2.2.1) mix 13.2 mL of 1 M KH_2PO_4 and 86.8 mL K_2HPO_4 and make up to a final volume of 1 L in DI water. Ensure that the pH is 6.0.

2.3.2 Preparation of Electrochemical Electrolyte for Potentiostatic Polarization (PQQ-GDH)

1. Prepare 20 mM 3-(N-morpholino)propanesulfonic acid (MOPS) MOPS solution, pH 6.0, containing 6 mM $CaCl_2$ and 10 mM KCl to serve as the electrochemical electrolyte. Dissolve 4.18 g of MOPS in 0.9 L of distilled H_2O . Adjust the solution pH to 6.0 with NaOH and HCl as required. Add 0.880 g $CaCl_2$ and 0.740 g KCl to the solution and adjust the final volume to 1 L.

2.3.3 Fabrication of a Teflon® Electrode Cap

In order to secure the BP electrode against the glassy carbon (GC) current collector (Metrohm), an electrode retainer cap was fabricated from Teflon®. Teflon® was chosen due to its inert properties

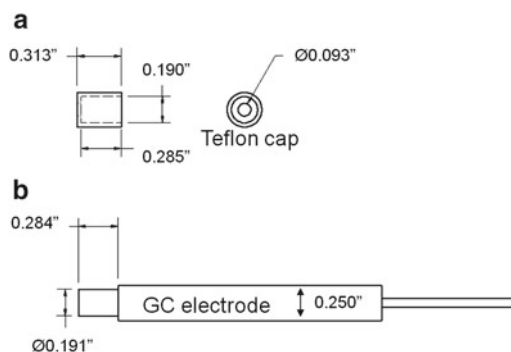


Fig. 1 Depiction of (a) Teflon[®] cap dimensions and (b) GC electrode dimensions. *Note:* Dimensions correspond to a GC electrode (Metrohm)

and ease of cleaning. The fit of the retainer cap is snug enough to hold the BP electrode in place while allowing for easy removal. The dimensions of the retainer cap were selected to maintain the original electrode geometry (Fig. 1a).

Adhere to safety protocols for lathe operation.

1. Position a 0.5" Teflon[®] rod in a self-centering three jaw chuck. Machine the end of the Teflon[®] stock to a good finish perpendicular to the axis of the material (*see Notes 2 and 3*).
2. Using a center drill, make a slight indentation in the machined face of the Teflon[®] stock. The indentation provides a concentric starting point for subsequent holes.
3. Remove the center drill from the drill chuck and replace it with a 0.093" diameter drill bit. Drill to a depth of 0.4" in the Teflon[®] stock. This will provide a circular opening matching the GC working electrode diameter.
4. Remove the 0.093" diameter drill bit and replace the drill bit with a 0.187" endmill. With the endmill touching the machined end of the Teflon[®] stock, set the depth reference (lathe tailstock spindle) to zero. Machine a hole in the stock using the endmill to a depth of 0.285". This produces a flat-bottom hole that secures the BP against the GC surface for good electrical contact.
5. Using an outside turning tool, remove the material from the outside diameter of the Teflon[®] stock in order to arrive at the outside diameter (0.250") of the electrode body.
6. Remove any sharp edges from the outer diameter of the cap.
7. Using a lathe parting tool, cut off the machined cap to a length of 0.313".
8. Remove the excess material (resulting from the parting of the cap) using a utility knife (*see Note 4*).

**Modification
of the GC Electrode**

This modification allows the Teflon® cap (fabricated in Subheading 2.3.3) to fit flush with the GC shaft. GC electrode dimensions are depicted in Fig. 1b.

1. Precisely measure the inside diameter of the Teflon® cap using an inside micrometer (*see Note 5*). Record this dimension.
2. Securely clamp the GC electrode, with the GC surface facing out, in the self-centering three jaw chuck (or collet). Machine the outside diameter 0.001–0.002" larger than the inside dimension of the cap in order to provide interference fit with the cap. Machine to a length of 0.284" along the length of the GC shaft.
3. Confirm the fit of the cap by sliding the cap onto the machined surface (*see Note 6*).

3 Methods

The molecular tether method presented herein is demonstrated with two model systems, laccase and PQQ-GDH, immobilized to CNT by using PBSE as the tethering reagent. Techniques required to determine effective DET are included, but final activity measurements may vary depending upon the application and the choice of biocatalyst.

3.1 Protein Preparation

It is recommended that contaminating materials be removed from protein preparations before attempting to immobilize enzymes to an electrode; the purification lessens non-catalytically active components that may lead to misinterpretation of data. For the examples described herein, laccase was purified from the commercial preparation via dialysis. Note that copper is included in dialysis of laccase in order to retain activity of the catalytic copper centers. The method described can be modified to suit the biocatalyst of choice. Dialysis was not required for PQQ-GDH as the commercial preparation is deemed to be of adequate purity.

3.1.1 Laccase Dialysis

1. Using a syringe, inject the laccase stock solution into a dialysis membrane (5 mL Slide-A-Lyzer dialysis cassette (10 kDa molecular weight cutoff; Thermo Fisher Scientific, Inc.)) prepared according to the manufacturer's instructions and suspend in 4 L of precooled 20 mM potassium phosphate, pH 7.3 containing 1 mM CuSO₄ for 12 h at 4 °C. Be sure to gently agitate the buffer solution with a magnetic stir bar during each dialysis step.
2. Transfer the dialysis cassette to 10 mM potassium phosphate, pH 7.0 containing 1 mM EDTA (4 L) for 12 h at 4 °C.
3. Finally, transfer to buffer only (4 L) for a final 12 h step.

4. Remove the dialyzed enzyme from the dialysis cassette and centrifuge at $208 \times g$ for 15 min to clarify enzyme suspension. Discard the pellet and divide the supernatant into aliquots and immediately store at $-20\text{ }^{\circ}\text{C}$.
5. Determine the protein concentration of the preparation before and after dialysis using a bicinchoninic acid protein assay kit (Thermo Fisher Scientific, Inc.) according to the manufacturer's instructions.

3.2 Modification of BP with PBSE and Enzyme Immobilization

Herein, the described method is applied to BP, but this method can also be applied to other conductive carbon surfaces, for example, CNT. In our experience, the methodology works well with BP, but substrate choice will depend upon the biocatalyst, and the final application, and may require further optimization.

1. Incubate BP electrodes in PBSE solution (in DMSO) for 1 h.
2. Remove BP electrodes from the PBSE solution and place on filter paper (Whatman[®], qualitative circles; 150 mm) for 1 min to remove excess liquid.
3. Immediately remove BP electrodes from filter paper and submerge in 10 mM potassium phosphate, pH 7.0, total volume 50 mL. Gently agitate the buffer for 2 min or until excess DMSO is removed from the porous body of the electrode.
4. Immediately transfer the BP electrodes into enzyme solution for 2 h.
5. Remove BP electrodes from the enzyme solution and rinse three times with electrochemical electrolyte (20 mM MOPS solution, pH 6.0, containing 6 mM CaCl_2 and 10 mM KCl for PQQ-GDH; 100 mM potassium phosphate, pH 6.0 for laccase).
6. Store enzyme modified BP electrodes in buffered electrolyte at $4\text{ }^{\circ}\text{C}$ until used in characterization tests.

Contact angle measurements can be used to qualitatively determine the presence of PBSE on the BP surface. PBSE modification of BP changes the interfacial energy and enhances surface wetting, which is indicated by a decreased contact angle. A Kruss 100 Drop Shape Analyzer (goniometer) with associated software package was used to obtain the contact angle of water on BP samples shown here (Fig. 2).

3.2.1 Contact Angle Measurements on PBSE-Functionalized BP

1. Dry the BP samples before contact angle measurements. The steps described below are for a VirTis Sentry Freeze Dryer/Lyophilizer and may need to be modified according to the manufacturer's instructions.
2. Prepare a minimum of three PBSE-modified BP electrodes using the previously described method.
3. Prepare three control electrodes without PBSE by incubating in DMSO only.

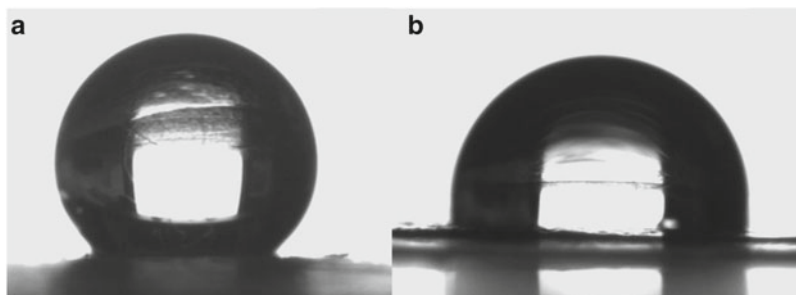


Fig. 2 Contact angle image of BP (a) without PBSE- and (b) with PBSE-modification

4. Rinse the electrodes in phosphate buffer and place in 50 mL Falcon tubes or other suitable container.
5. Cover tubes with folded laboratory tissues, e.g. kimwipes held in place with rubber bands.
6. Place Falcon tubes vertically in 600 mL Vir-Tis jar with the Kimwipe covers facing the opening of the jar.
7. Turn on freeze dryer refrigeration and allow the temperature to reach $-25\text{ }^{\circ}\text{C}$. Turn on the vacuum when the temperature reaches $-25\text{ }^{\circ}\text{C}$ and connect the jar when the vacuum reaches 100 mtorr.
8. Slowly turn the valve to the open position. Lyophilize to dryness (typically 5 hours to overnight).
9. Turn off vacuum and refrigeration when freeze drying is complete. Release the pressure and remove the sample jar.
10. Secure lyophilized BP to the goniometer sample platform with double-sided sticky tape.
11. Apply $5 \times 5\ \mu\text{L}$ water drops (flow rate = $195\ \mu\text{L}/\text{min}$) to the paper and allow 2 min to equilibrate.
12. Obtain the contact angle for each drop using the tangent 1 method according to the manufacturer's instructions.
13. Repeat contact angle measurements on at least three replicate BP samples with and without PBSE to establish statistical variation (Fig. 2).

3.3 Electrochemical Measurements

BP modified with PBSE and functionalized with enzyme is contacted with the GC current collector in order to perform electrochemical characterization of the bioelectronic interface. In this method, the BP is secured against a planar GC electrode using a modified Teflon[®] cap (described in Subheading 2.3.3) (Fig. 3).

1. Enzyme functionalized electrodes were placed in the modified cap and placed into an electrochemical cell (50-mL European five-neck flask with three 14/20 fittings and two #7 threads; Ace Glass, Vineland, NJ) filled with electrolyte.

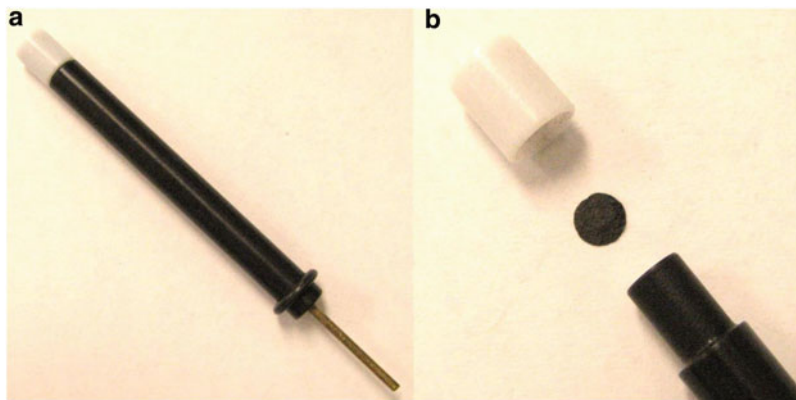


Fig. 3 (a) GC disk electrode with fabricated Teflon[®] cap. (b) The cap fits securely, holding the BP in contact with the surface of the GC surface. The cap is removed for easily exchanging BP electrodes and cleaning

2. CV and potentiostatic polarization are measured using a potentiostat (Versastat 3, Princeton Applied Research; Oak Ridge, TN) and the associated software.
3. The GC disk electrode is the working electrode (Metrohm). All data and methods described are presented in respect to a Ag|AgCl|KCl (3 M KCl; Metrohm) reference electrode and a platinum wire counter electrode (Metrohm).

3.3.1 Cyclic Voltammetry

Electrochemical characterization by CV allows a rapid and qualitative evaluation of enzyme immobilization by visualizing the redox chemistry associated with a specific electro-active biocatalyst. The example shown here allows for the assessment of the ORR as catalyzed by laccase. CV may not provide qualitative result for all biocatalysts used for electrode preparation and other techniques may be required.

1. Polish the GC surface with Gamma Micropolish II, Deagglomerated Alumina, 0.05 μm (Buehler[®]) and polishing cloth (TexMet[®] PSA-backed). Place the alumina on the polishing cloth and use to burnish the electrode in a gentle figure 8 motion.
2. Rinse the GC electrode with water and sonicate in denatured ethanol for 2 min to remove adsorbed alumina particles.
3. Rinse with ethanol and then with 0.1 M potassium phosphate buffer, pH 6.0.
4. Place enzyme-functionalized BP electrodes onto the GC surface (*see Note 7*) and position the Teflon[®] cap to hold the electrode securely in place (Fig. 3).
5. Fill the electrochemical chamber with 50 mL of 0.1 M potassium phosphate, pH 6.0.

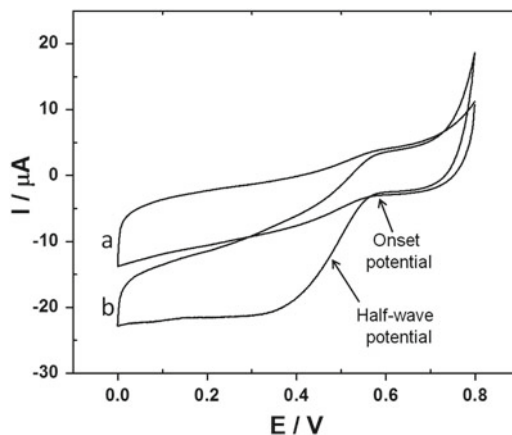


Fig. 4 Cyclic voltammogram of laccase immobilized to PBSE-functionalized BP in O_2 saturated phosphate buffer, 0.1 M, pH=6.0 (a) without PBSE and (b) with PBSE; scan rate = 5 mV/s. Onset potential and half-wave potential are marked by arrows

6. Bubble O_2 in the electrolyte to saturate the solution with the electron acceptor (*see Note 8*).
7. Place electrodes in the electrochemical chamber and connect each electrode to the appropriate potentiostat connection (*see Note 9*).
8. Use CV to assess the biocatalytic performance of electrodes fabricated with and without the PBSE tether. The scan window is +0.8 to 0 V at a suggested scan rate of 5 mV/s. Use the second scan to estimate the onset potential and half wave potential (Fig. 4) and compare to known or reported values.

3.3.2 Polarization Curves

As an alternative method for determining electrocatalytic activity of an enzyme-modified BP electrode, potentiostatic polarization curves can be determined. This method is described as an example for assessment of the activity of immobilized PQQ-GDH.

1. Remove oxygen from the MOPS solution by bubbling with N_2 and add 10 mM glucose as the electron donor (*see Note 8*).
2. Monitor the open circuit potential (OCP) with respect to time until a constant value is reached.
3. Potentiostatic polarization curves: Apply a series of potentials to the working electrode (*see Note 10*). In the case of PQQ-GDH apply potential values beginning at the OCP and adjust stepwise to approach +0.5 V. Select a minimum of 15 potentials concentrating several values close to the OCP (Fig. 5).
4. Determine steady-state current values normalized to the geometric area of the BP electrode and fit lines to the data using graphing software (Fig. 5).

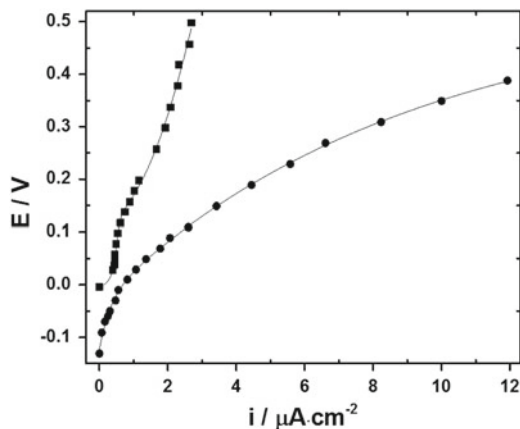


Fig. 5 Potentiostatic polarization curves of PQQ-GDH physisorbed on BP (*filled square*), and PBSE-modified BP with immobilized PQQ-GDH (*filled circle*). All polarization curves were performed with N_2 -purged electrolyte (10 mM glucose in 20 mM MOPS solution, pH 6.0 with 6 mM CaCl_2 and 10 mM KCl)

4 Notes

1. Prepare fresh solution on the same day as the immobilization procedure.
2. Using a right hand turning tool, set the turning tool perpendicular to the travel of the cross feed.
3. The diameter of the Teflon[®] rod can be larger. Be sure to choose a diameter large enough to ensure rigidity during machining.
4. Remove flash or burr left inside of the Teflon[®] cap by gently rotating a 0.148" drill bit against the bore of the 0.093" diameter hole.
5. If an inside micrometer is not available, an adjustable ball gauge and an outside micrometer can be used.
6. The cap should be held in place by the interference of the electrode outside diameter, which is slightly larger than the inside diameter of the cap. The cap should not be so tight as to prevent removal by hand.
7. When placing the BP electrode onto the GC surface, check for air trapped between the two electrodes.
8. Remove accumulated air bubbles from the surface of the working electrode by gently shaking or tapping.
9. Do not allow buffer to splash onto the conductive surface used to connect electrodes.
10. Monitor current with respect to time. Obtain data points from potential regimes that result in steady-state current. For example, >15 min for laccase and >30 min for PQQ-GDH are typically required at each potential to obtain steady-state readings.

References

1. Rincon RA, Lau C, Luckarift HR, Garcia KE, Adkins E, Johnson GR, Atanassov P (2011) Enzymatic fuel cells: integrating flow-through anode and air-breathing cathode into a membrane-less biofuel cell design. *Biosens Bioelectron* 27:132–136
2. Ivnitski D, Atanassov P, Apblett C (2007) Direct bioelectrocatalysis of PQQ-dependent glucose dehydrogenase. *Electroanalysis* 19:1562–1568
3. Ramasamy RP, Luckarift HR, Ivnitski DM, Atanassov PB, Johnson GR (2010) High electrocatalytic activity of tethered multicopper oxidase-carbon nanotube conjugates. *Chem Commun* 46:6045–6047
4. Lau C, Adkins ER, Ramasamy RP, Luckarift HR, Johnson GR, Atanassov P (2011) Design of carbon nanotube-based gas-diffusion cathode for O₂ reduction by multicopper oxidases. *Adv Energy Mater* 2:162–168
5. Strack G, Luckarift HR, Nichols R, Cozart K, Katz E, Johnson GR (2011) Bioelectrocatalytic generation of directly readable code: harnessing cathodic current for long-term information relay. *Chem Commun* 47:7662–7664
6. Narvaez Villarrubia CW, Rincon RA, Radhakrishnan VK, Davis V, Atanassov P (2011) Methylene green electrodeposited on SWNTs-based “bucky” papers for NADH and L-malate oxidation. *ACS Appl Mater Interfaces* 3:2402–2409
7. Hussein L, Rubenwolf S, Von Stetten F, Urban G, Zengerle R, Krueger M, Kerzenmacher S (2011) A highly efficient buckypaper-based electrode material for mediatorless laccase-catalyzed dioxygen reduction. *Biosens Bioelectron* 26:4133–4138
8. Hussein L, Urban G, Krueger M (2011) Fabrication and characterization of buckypaper-based nanostructured electrodes as a novel material for biofuel cell applications. *Phys Chem Chem Phys* 13:5831–5839
9. Ivnitski D, Artyushkova K, Rincon RA, Atanassov P, Luckarift HR, Johnson GR (2008) Entrapment of enzymes and carbon nanotubes in biologically synthesized silica: glucose oxidase-catalyzed direct electron transfer. *Small* 4:357–364
10. Vaz-Dominguez C, Campuzano S, Rudiger O, Pita M, Gorbacheva M, Shleev S, Fernandez VM, De Lacey AL (2008) Laccase electrode for direct electrocatalytic reduction of O₂ to H₂O with high operational stability and resistance to chloride inhibition. *Biosens Bioelectron* 24:531–537
11. Tanne C, Gobel G, Lisdat F (2010) Development of a (PQQ)-GDH-anode based on MWCNT-modified gold and its application in a glucose/O₂ biofuel cell. *Biosens Bioelectron* 26:530–535
12. Flexer V, Durand F, Tsujimura S, Mano N (2011) Efficient direct electron transfer of PQQ-glucose dehydrogenase on carbon cryogel electrodes at neutral pH. *Anal Chem* 83:5721–5727
13. Razumiene J, Vilkanauskyte A, Gureviciene V, Barkauskas J, Meskys R, Laurinavicius V (2006) Direct electron transfer between PQQ dependent glucose dehydrogenases and carbon electrodes: an approach for electrochemical biosensors. *Electrochim Acta* 51:5150–5156

Enzyme Immobilization by Entrapment Within a Gel Network

Audrey Sassolas, Akhtar Hayat, and Jean-Louis Marty

Abstract

This chapter provides a detailed description of the three immobilization methods based on the biomolecules entrapment into polymer matrices. The poly (vinyl alcohol) bearing styrylpyridinium groups (PVA-SbQ), a soluble pre-polymer bearing photo-cross-linkable groups, has widely been used to entrap enzymes, and several bioassays based on this immobilization matrix have been reported. Similarly, immobilization of enzymes via sol-gel has been described in this chapter. Sol-gel process is based on the ability to form solid metal or semi-metal oxides via the aqueous process of hydrolytically labile precursors. Enzymes can also be entrapped in an agarose gel. Contrary to synthetic polymers such as polyacrylamide, this matrix is biocompatible, non-toxic, provides natural microenvironment to the enzyme and also gives sufficient accessibility to electrons to shuttle between the enzyme and the electrode. The entrapment strategies are easy-to-perform, and permit to deposit enzyme, mediators, and additives in the same sensing layer. Moreover, the activity of the enzyme is preserved during the immobilization process, as biological element is not modified. Biosensors based on physically entrapped enzymes are often characterized by increased operational and storage stability

Key words Gel network, Photopolymerization, Sol-gel, agarose gel, Enzyme entrapment

1 Introduction

Enzymes can be immobilized in different three-dimensional matrices [1]. This chapter describes three immobilization methods based on the biomolecule entrapment into polymer matrices: the photopolymerization, the sol-gel process and the entrapment within an agarose gel. The sol-gel technology is based on the ability to form metal-oxide, silica, and organosiloxane matrices of defined porosity by the reaction of organic precursors at room temperature. The photopolymerization involves the use of a pre-polymer bearing photo-cross-linkable groups. In this case, the polymerization is initiated by light exposition. Agarose gels can also be used for enzyme immobilization. This biological polymer is formed upon temperature-induced gelation.

The entrapment strategies are easy-to-perform. Enzyme, mediators and additives can be simultaneously deposited in the same sensing layer. There is no modification of the biological element so that the activity of the enzyme is preserved during the immobilization process. Biosensors based on physically entrapped enzymes are often characterized by increased operational and storage stability. However, possible diffusion barriers can restrict the performances of the systems.

1.1 Entrapment Within a Photopolymer

1.1.1 Photo- polymerization Principle

The poly(vinyl alcohol) bearing styrylpyridinium groups (PVA-SbQ), a soluble pre-polymer bearing photo-cross-linkable groups, has widely been used to entrap enzymes. It was synthesized for the first time by Ichimura and Watanabe [2–4]. An insoluble matrix was obtained upon light-induced polymerization (Fig. 1). The PVA-SbQ matrix allowed the entrapment of different enzymes.

Several PVA-SbQ-based biosensors were developed for the detection of pesticides [5]. For this purpose, acetylcholinesterase (AChE) can be entrapped within a photopolymer formed on a screen-printed electrode [6–10]. For instance, a PVA-SbQ-based biosensor was developed for the detection of paraoxon and chlorpyrifos ethyl oxon in water miscible organic solvents [10]. In this work, *p*-aminophenyl acetate was used as the AChE substrate instead of acetylthiocholine. Detection limits as low as 1.9×10^{-8} M paraoxon and 1.24×10^{-4} M chlorpyrifos ethyl oxon were obtained when experiments were carried out in a phosphate buffer containing 5 % acetonitrile. NAD⁺-dependent dehydrogenases were also entrapped within a PVA-SbQ photopolymer formed on SPE surface to detect pesticides [5], lactate [11], or acetaldehyde [11]. A PVA-SbQ-based biosensor was also developed for the detection of microcystin, an aquatic toxin produced by cyanobacteria [12]. For this purpose, protein phosphatase was immobilized on a SPE surface by entrapment in PVA-SbQ polymer. The PVA-SbQ photopolymer was also used to immobilize oxidases at the surface of electrodes of a screen-printed array [13]. The study was performed with a single microarray of nine independent 1 mm × 1 mm electrodes. The different sensing layers were obtained through the entrapment of glucose oxidase and lactate oxidase in PVA-SbQ photopolymer deposited at the surface of two from the nine electrode array. An automated nano-spotter was employed to precisely drop spots of entrapped enzyme at an electrode surface. Electrochemiluminescent measurements allowed the simultaneous detection of L-lactate and G-glucose with detection limits of 3 and 10 μM, respectively. In some cases, enzyme was successfully pre-immobilized by ionic interactions with charged beads before entrapment in the photopolymer in order to limit enzyme leaching [14–17].

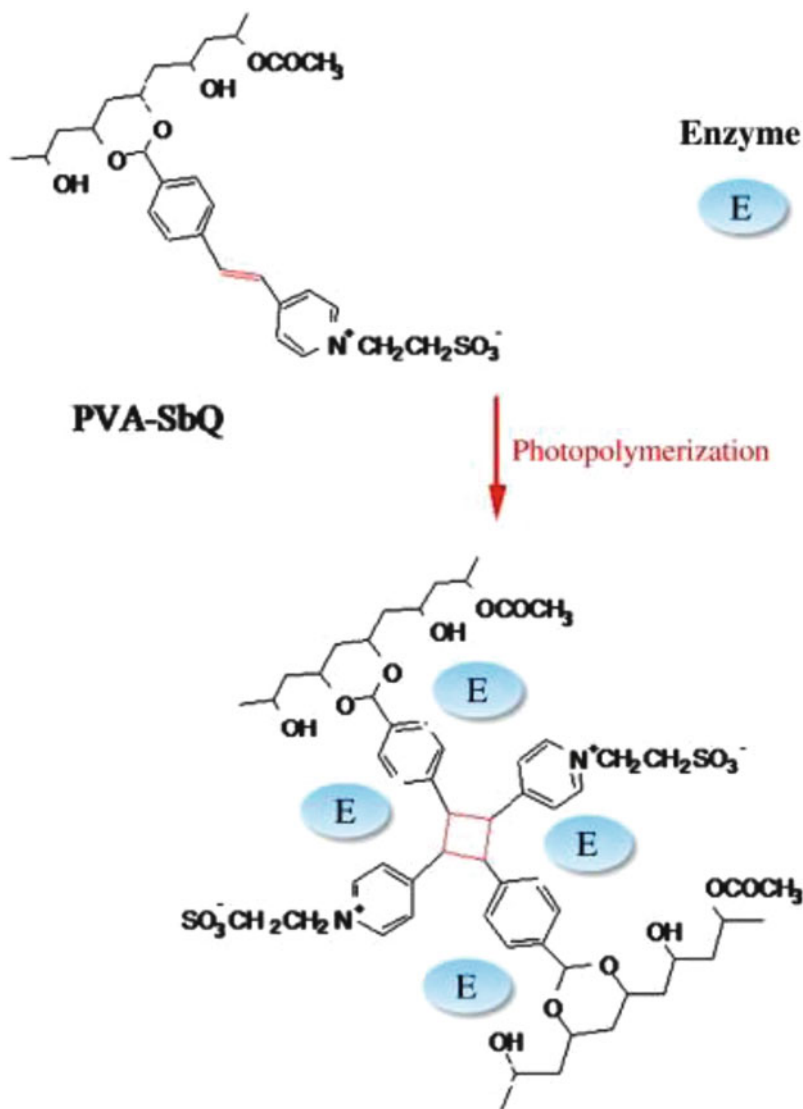


Fig. 1 PVA-SbQ entrapment of enzymes [1]

PVA-SbQ is not the only photopolymer that can be used to develop enzymatic biosensors. Recently, azide-unit pendant water-soluble photopolymer (PVA-AWP) has been used to entrap protein phosphatases [18], laccase [19], or AChE [20–24]. An amperometric acetylcholinesterase biosensor was developed for quantification of pesticides in a phosphate buffer containing 5 % acetonitrile using three different acetylcholinesterases [24]. Enzymes were immobilized on cobalt(II) phthalocyanine-modified electrodes by entrapment in PVA-AWP. The biosensor based on genetically engineered AChE (B394) showed a detection limit of 9.6×10^{-11} M of dichlorvos. The developed biosensor was used for

the determination of pesticides in spiked apple samples. Recently, the new PVA-super porous hydrogel (PVA-SPH) bearing methylpyridinium groups has been used for the entrapment of enzymes [25]. This immobilization matrix was employed to develop colorimetric protein phosphatase inhibition assays for the detection of microcystin and okadaic acid, a toxin responsible of gastrointestinal troubles. In optimal conditions, the PVA-SPH-based tests allowed the detection of okadaic acid and microcystin-LR with detection limits of 0.18 and 0.36 $\mu\text{g/L}$, respectively.

2 Materials

1. PVA-super porous hydrogel (PVA-SPH) bearing methylpyridinium groups (Toyo Gosey Kogyo Co., Chiba, Japan).
2. Milli-Q water.
3. Enzyme.
4. Automatic pipettes (and automatic pipettes special for viscous solutions).
5. Eppendorf tubes.
6. Vortex mixer.
7. Maxisorp microtiter plates (Nunc, Roskilde, Denmark).
8. Refrigerator or cold chamber.
9. Tetramethoxysilane (TMOS , Aldrich).
10. Milli-Q water.
11. 1 mM HCl.
12. Polyethylene glycol (PEG) with average mol wt: 600 (PEG₆₀₀) (Sigma).
13. Enzyme.
14. Hydroxyethyl cellulose (HEC, Fluka).
15. Automatic pipettes (and automatic pipettes special for viscous solutions).
16. Eppendorf tubes.
17. Vortex mixer.
18. Sonicator.
19. Maxisorp microtiter plates (Nunc, Roskilde, Denmark).
20. Refrigerator or cold chamber.
21. Agarose (type IX, Sigma).
22. Milli-Q water.
23. Enzyme.

24. Automatic pipettes (and automatic pipettes special for viscous solutions).
25. Eppendorf tubes.
26. Vortex mixer.
27. Maxisorp microtiter plates (Nunc, Roskilde, Denmark).
28. Refrigerator or cold chamber.

3 Methods

1. Dissolve the enzyme in the convenient buffer using Milli-Q water.
2. Mix the enzymatic solution with PVA-SPH in a 1:1 ratio (v:v) in a 1.5 mL Eppendorf tube (use an automatic pipette special for viscous solutions for PVA-SPH) (*see* **Notes 1** and **2**).
3. Cap the Eppendorf tube and homogenize the mixture using a vortex mixer (*see* **Note 3**).
4. Spread the mixture on the support surface using an automated pipette (*see* **Notes 4** and **5**).
5. Expose the support surface to neon light for 3 h at 4 °C to allow entrapment of enzymes by photopolymerization (*see* **Note 6**).
6. Dry the support surface for 24 h at room temperature (*see* **Note 7**).
7. Rinse the support with water prior utilization. While rinsing, carefully look to see if any desorption of the gel from the surface has occurred (*see* **Note 8**).

3.1 Entrapment Within a Silica gel

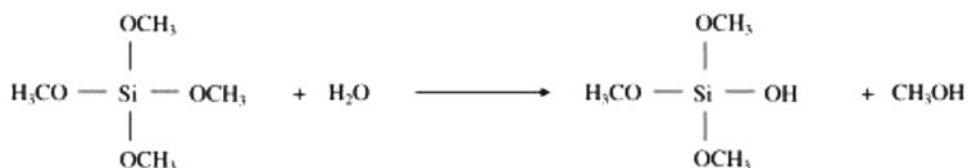
3.1.1 Sol-Gel Process

Sol-gel process is based on the ability to form solid metal or semi-metal oxides via the aqueous process of hydrolytically labile precursors (e.g., ester of silicic, polysilicic acid, alkoxide, halide of aluminum).

Sol-gel process involves hydrolysis of alkoxide precursors under acidic (or alkaline) conditions followed by condensation of the hydroxylated units, which leads to the formation of a porous gel (Fig. 2). First, a low-molecular weight metal alkoxide precursor molecule such as tetramethoxysilane (TMOS) or tetraethoxysilane (TEOS) is hydrolyzed in the presence of water at acid (or alkaline) pH, resulting in the formation of (Si-OH) groups. In the second step, the condensation reaction between silanol moieties at alkaline (or acidic) pH results in the formation of siloxane (Si-O-Si) polymers, creating a matrix in which an enzyme can be successfully entrapped [26–28].

Silica gels are highly porous, showing physical rigidity, chemical and biological inertness and thermal stability. However, these matrices suffer from considerable shrinkage during the drying

1. Hydrolysis of precursor



2. Condensation

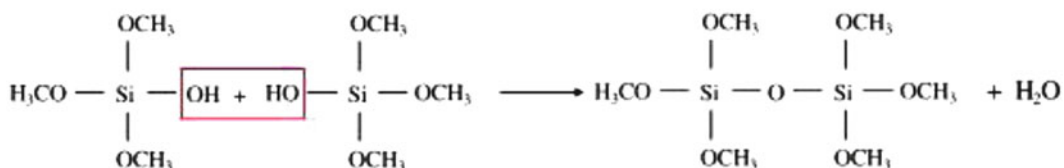
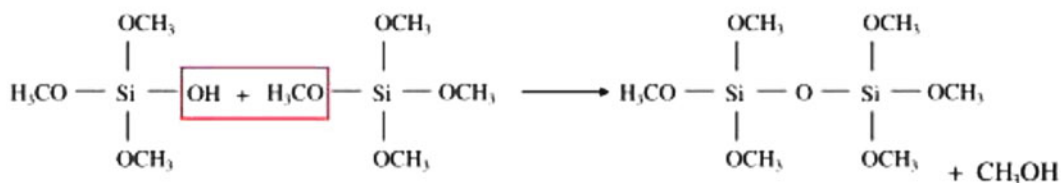


Fig. 2 Sol-gel process, which is composed of two steps: hydrolysis of TMOS (1) and condensation of silanol groups (2) [1]

process, which leads to fracture of the material and pore collapse. Recent reports suggest that the use of additives might help to overcome these problems by decreasing internal stress and shrinkage of the materials. For example, the use of trehalose or glycerol as a drying control chemical additive is considered as an interesting possibility in the sol-gel process [29]. In the same way, some polymers such as the natural polymer chitosan, poly(ethyleneglycol) or Nafion can also be used to prevent cracking [30].

Sol-gel process is used classically to immobilize enzymes in order to develop biosensors. For example, an electrochemiluminescent (ECL) biosensor for glucose detection was developed with a GOD-immobilizing silica matrix formed on a glassy carbon electrode surface [31]. Glucose was detected in a concentration range comprised between 5×10^{-5} M and 1×10^{-2} M (detection limit of 2.6×10^{-5} M). A fluorescent biosensor for xanthine detection based on the immobilization of xanthine oxidase, superoxide dismutase and peroxidase, in a silica matrix coupled to the Amplex Red probe was also described [32]. This system allowed to detect xanthine up to 3.5×10^{-6} M (detection limit of 2×10^{-8} M). This biosensor remained stable for 2 weeks under appropriate storage conditions. Numerous electrochemical sol-gel-based biosensors were also

described [6, 12, 33–36]. A system based on GOD-immobilizing silica gel formed onto a glassy carbon electrode allowed to detect glucose from 6×10^{-5} M to 4.4×10^{-3} M [36]. A biosensor for ATP detection was also developed by co-immobilization of GOD and hexokinase (HK) in a silica gel. ATP detection was based on competitive enzymatic reactions for glucose. This biosensor allowed to detect ATP between 5×10^{-7} M and 2×10^{-5} M. The electrode-to-electrode reproducibility was satisfactory (relative standard deviation of 5.6 %). The stability of the biosensor was estimated over a period of 3 weeks. The response to ATP decreased by about 35 % during 4 days and then remained remarkably stable.

3.2 Sol-Gel Entrapment

1. Mix TMOS (15 %), Milli-Q water (41.3 %), 1 mM HCl (40 %) and PEG₆₀₀ (3.7 %) in a 1.5 mL Eppendorf tube (*see Note 9*).
2. Cap the Eppendorf tube and sonicate 15 min to homogenize the mixture.
3. Store the Eppendorf tube at 4 °C overnight to allow hydrolysis of the precursors (*see Note 10*).
4. Dissolve the enzyme in a basic buffer using Milli-Q water precursors (*see Note 11*).
5. Mix the enzymatic solution with HEC in a 1:1 ratio in a 1.5 mL Eppendorf tube (*see Note 12*).
6. Mix the sol solution with the enzymatic solution in a 1:2 ratio in a 1.5 mL Eppendorf tube to start the condensation (*see Note 13*).
7. Cap the Eppendorf tube and homogenize the mixture using a vortex mixer.
8. Spread the mixture on the support surface using an automated pipette (*see Note 14*).
9. Dry the support surface for 1 h at room temperature.
10. Rinse the support with water prior utilization. While rinsing, carefully look to see if any desorption of the gel from the surface occurred (*see Note 8*).

3.3 Entrapment Within an Agarose gel

3.3.1 Entrapment Principle

Enzymes can also be entrapped in an agarose gel (Fig. 3). Contrary to synthetic polymers such as polyacrylamide, this matrix is biocompatible, non-toxic, provides natural microenvironment to the enzyme and also gives sufficient accessibility to electrons to shuttle between the enzyme and the electrode.

Agarose powder is dissolved in a buffer by heating. This mixture gellifies when temperature decreases. An enzyme incorporated in the mixture during gelling can be entrapped [37–39]. For instance, an electrochemical biosensor based on tyrosinase immobilized in a composite biopolymeric film of agarose and guar gum was developed [38]. This composite enzyme-entrapping matrix was formed

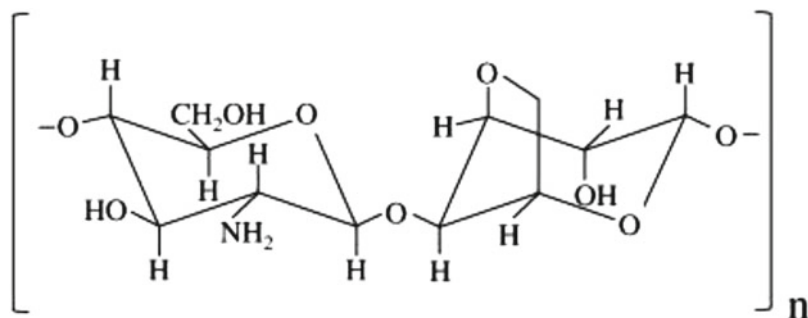


Fig. 3 Chemical structure of agarose [1]

on a glassy carbon electrode. For example, dopamine was detected by the direct reduction of the biocatalytically liberated quinone species at -0.18 V vs. Ag/AgCl. This biosensor could be reused up to 15 assays and had a shelf life of more than 2 months. Recently, Marty's group has described the first agarose-based colorimetric assays for the detection of okadaic acid [25] and microcystin [40]. For this purpose, different protein phosphatases were entrapped within an agarose gel formed at the bottom of a microwell. In optimal conditions, the agarose gel-based colorimetric tests allowed the detection of okadaic acid and microcystin-LR with detection limits of 0.18 $\mu\text{g/L}$ and 0.0039 $\mu\text{g/L}$, respectively.

3.3.2 Protocol

1. Prepare a 2 % (w:v) agarose solution by heating the agarose powder in a convenient buffer at 60 $^{\circ}\text{C}$ for 5 min.
2. Let the agarose solution cooled to 27 $^{\circ}\text{C}$.
3. Mix the agarose solution with the enzymatic solution in a 1:1 volume ratio in a 1.5 mL Eppendorf tube (*see Note 2*).
4. Cap the Eppendorf tube and homogenize the mixture using a vortex mixer.
5. Spread the mixture on the support surface (microwell) using an automated pipette (*see Notes 4 and 5*).
6. Dry the support surface for 4 h at 4 $^{\circ}\text{C}$.
7. Rinse the support with water prior utilization. While rinsing, carefully look to see if any desorption of the gel from the surface occurred (*see Note 8*).

4 Notes

1. PVA-SPH is suggested but other pre-polymers such as PVA-SbQ and PVA-AWP can be used
2. The 1:1 volume ratio is suggested but other ratios can be tested.

3. If foam or bubbles are observed after vortex mixing, briefly centrifuge using a benchtop centrifuge.
4. The volume of mixture deposited on the support surface depends on the particular interest, but it has never to spread out from the surface of interest.
5. Our experience is based on the immobilization at the bottom of Maxisorp microtiter wells. However, the immobilization on other supports is also possible.
6. Exposure to ultraviolet light for 2 min at 4 °C is also possible. However, exposure to neon light for 3 h at 4 °C is more convenient, as it provides slower polymerization and higher reproducibility.
7. This step can be performed at room temperature. However, 4 °C are preferred to maintain the enzyme activity.
8. Buffer can also be used to rinse the modified support.
9. Other ratios and other precursors can be used. It should be taken into account that the higher the TMOS proportion, the faster the subsequent polymerization process.
10. Hydrolysis time depends on each case and should be optimized.
11. At basic pH, the condensation is favored. The appropriate basic pH will depend on the enzyme performance (not too high to inactivate it). The buffer composition is not particularly important. However, $(\text{NH}_4)_2\text{SO}_4$ should not be used to avoid precipitation.
12. HEC allows to prevent cracking. Other ratios can be used.
13. The 1:2 ratio is suggested. However, other ratios can be used.
14. Sometimes the condensation occurs at faster rates. As a result the sol-gel starts to form before its deposition on the surface. It is then convenient to carry out this step at 4 °C (cold chamber).

References

1. Sassolas A, Blum LJ, Leca-Bouvier BD (2012) Immobilization strategies to develop biosensors. *Biotechnol Adv* 30:189–511
2. Ichimura K, Watanabe S (1980) Immobilization of enzymes with use of photosensitive polymers having the stilbazolium group. *J Polym Sci Polym Chem Ed* 18:891–902
3. Ichimura K, Watanabe S (1982) Preparation and characteristics of photocross-linkable poly(vinyl alcohol). *J Polym Sci Polym Chem Ed* 20:1419–1432
4. Ichimura K, Watanabe S (1982) Preparation of water-soluble photoresist derived from poly(vinyl alcohol). *J Polym Sci Polym Chem Ed* 20:1411–1417
5. Noguer T, Balasoiu A-M, Avramescu A, Marty J-L (2001) Development of a disposable biosensor for the detection of metam-sodium and its metabolite MITC. *Anal Lett* 344:513–528
6. Andreescu S, Barthelmebs L, Marty J-L (2002) Immobilization of acetylcholinesterase on screen-printed electrodes: comparative study between three immobilization methods and applications to the detection of organophosphorus insecticides. *Anal Chim Acta* 464:171–180

7. De Oliveira Marques PRB, Nunes GS, Dos Santos TCR, Andreescu S, Marty JL (2004) Comparative investigation between acetylcholinesterase obtained from commercial sources and genetically modified *Drosophila melanogaster*. Application in amperometric biosensors for methamidophos pesticide detection. *Biosens Bioelectron* 20:825–832
8. Sikora T, Istamboulie G, Jubete E, Ochoteco E, Marty JL, Noguer T (2011) Highly sensitive detection of organophosphate insecticides using biosensors based on genetically engineered acetylcholinesterase and poly(3,4-ethylenedioxythiophene). *J Sens* 2011:1–7
9. Nunes GS, Jeanty G, Marty JL (2004) Enzyme immobilization procedures on screen-printed electrodes used for the detection of anticholinesterase pesticides. *Anal Chim Acta* 523:107–115
10. Andreescu S, Noguer T, Magearu V, Marty JL (2002) Screen-printed electrode based on AChE for the detection of pesticides in presence of organic solvents. *Talanta* 57:169–176
11. Avramescu A, Noguer T, Avramescu M, Marty JL (2002) Screen-printed biosensors for the control of wine quality based on lactate and acetaldehyde determination. *Anal Chim Acta* 458:203–213
12. Campas M, Szydłowska D, Trojanowicz M, Marty JL (2002) Towards the protein phosphatase-based biosensor for microcystin detection. *Biosens Bioelectron* 20:1520–1530
13. Corgier BP, Marquette CA, Blum LJ (2005) Screen-printed electrode microarray for electrochemiluminescent measurements. *Anal Chim Acta* 538:1–7
14. Leca B, Blum LJ (2000) Luminol electrochemiluminescence with screen-printed electrodes for low-cost disposable oxidase-based optical sensors. *Analyst* 125:789–791
15. Leca BD, Verdier A, Blum LJ (2001) Screen-printed electrodes as disposable or reusable optical devices for luminol electrochemiluminescence. *Sens Actuators B Chem* 74:190–193
16. Marquette CA, Degiuli A, Blum LJ (2003) Electrochemiluminescent biosensors array for the concomitant detection of choline, glucose, glutamate, lactate, lysine and urate. *Biosens Bioelectron* 19:433–439
17. Sassolas A, Blum LJ, Leca-Bouvier BD (2009) New electrochemiluminescent biosensors combining poly(luminol) and an enzymatic matrix. *Anal Bioanal Chem* 394:971–980
18. Campas M, Marty JL (2007) Enzyme sensor for the electrochemical detection of the marine toxin okadaic acid. *Anal Chim Acta* 605:87–93
19. Ibarra-Escutia P, Gomez JJ, Calas-Blanchard C, Marty JL, Ramirez-Silva M (2012) Amperometric biosensor based on a high resolution photopolymer deposited onto a screen-printed electrode for phenolic compounds monitoring in tea infusions. *Talanta* 81:1636–1642
20. Mishra RK, Dominguez RB, Bhand S, Munoz R, Marty JL (2012) A novel automated flow-based biosensor for the determination of organophosphate pesticides in milk. *Biosens Bioelectron* 32:56–61
21. Istamboulie G, Sikora T, Jubete E, Ochoteco E, Marty JL, Noguer T (2010) Screen-printed poly(3,4-ethylenedioxythiophene) (PEDOT): a new electrochemical mediator for acetylcholinesterase-based biosensors. *Talanta* 82:957–961
22. Istamboulie G, Fournier D, Marty JL, Noguer T (2009) Phosphotriesterase: a complementary tool for the selective detection of two organophosphate insecticides: chlorpyrifos and chlorfenvinfos. *Talanta* 77:1627–1631
23. Galezowska A, Sikora T, Istamboulie G, Trojanowicz M, Polec I, Nunes GS, Noguer T, Marty JL (2008) Application of genetically engineered acetylcholinesterase in screen-printed amperometric biosensor for detection of organophosphorus insecticides. *Sens Mater* 20:29–308
24. Valdes-Ramirez G, Cortina M, Ramirez-Silva M, Marty JL (2008) Acetylcholinesterase-based biosensors for quantification of carbofuran, carbaryl, methylparaoxon, and dichlorvos in 5% acetonitrile. *Anal Bioanal Chem* 392:699–707
25. Sassolas A, Catanante G, Hayat A, Marty JL (2011) Development of an efficient protein phosphatase-based colorimetric test for okadaic acid detection. *Anal Chim Acta* 702
26. Gupta R, Chaudhury NK (2007) Entrapment of biomolecules in sol-gel matrix for applications in biosensors: problems and future prospects. *Biosens Bioelectron* 22:2387–2399
27. Jeronimo PCA, Araujo AN, Montenegro MC (2007) Optical sensors and biosensors based on sol-gel films. *Talanta* 72:13–27
28. Kandimalla VB, Tripathi VS, Ju H (2006) Immobilization of biomolecules in sol-gels: biological and analytical applications. *Crit Rev Anal Chem* 36:73–106
29. Desimone MF, Matiacevich SB, Del Pilar Buera M, Diaz LE (2008) Effects of relative humidity on enzyme activity immobilized in sol-gel-derived silica nanocomposites. *Enzyme Microb Technol* 42:583–588
30. Choi HN, Kim MA, Lee W-Y (2005) Amperometric glucose biosensor based on sol-gel-derived metal oxide/nafion composite films. *Anal Chim Acta* 537:179–187

31. Zhu L, Li Y, Zhu G (2002) A novel flow through optical fiber biosensor for glucose based on luminol electrochemiluminescence. *Sens Actuators B Chem* 86:209–214
32. Salinas-Castillo A, Pastor I, Mallavia R, Mateo R (2008) Immobilization of a trienzymatic system in a sol-gel matrix: a new fluorescent biosensor for xanthine. *Biosens Bioelectron* 24: 1053–1056
33. Gurban AM, Nogue T, Bala C, Rotariu L (2008) Improvement of NADH detection using prussian blue modified screen-print electrodes and different strategies of immobilisation. *Sens Actuators B Chem* 128:536–544
34. Nogue T, Tencaliec A, Calas-Blanchard C, Avramescu A, Marty JL (2002) Interference-free biosensor based on screen-printing technology and sol-gel immobilization for the determination of acetaldehyde in wine. *J AOAC Int* 85:1382–1389
35. Jena BK, Raj CR (2006) Electrochemical biosensor based on integrated assembly of dehydrogenase. *Anal Chem* 78:6332–6339
36. Liu S, Sun Y (2007) Co-immobilization of glucose oxidase and hexokinase on silicate hybrid sol-gel membrane for glucose and ATP detections. *Biosens Bioelectron* 22:905–911
37. Tembe S, Inamdar S, Haram S, Karve M, D'Souza SF (2007) Electrochemical biosensor for catechol using agarose-guar gum entrapped tyrosinase. *J Biotechnol* 128:80–85
38. Tembe S, Karve M, Inamdar S, Haram S, Melo J, D'Souza SF (2006) Development of electrochemical biosensor based on tyrosinase immobilized in composite biopolymeric film. *Anal Biochem* 349:72–77
39. Shumyantseva V, Deluca G, Bulko T, Carrara S, Nicolini C, Usanov SA, Archakov A (2004) Cholesterol amperometric biosensor based on cytochrome P450sc. *Biosens Bioelectron* 19:971–976
40. Sassolas A, Catanante G, Fournier D, Marty JL (2011) Development of a colorimetric inhibition assay or microcystin-LR detection: comparison of the sensitivity of different protein phosphatases. *Talanta* 85:2498–2503

Practical Protocols for Lipase Immobilization via Sol–Gel Techniques

Manfred T. Reetz

Abstract

Lipases can be efficiently entrapped in the pores of hydrophobic silicates by a simple and cheap sol–gel process in which a mixture of a hydrophobic alkylsilane $\text{RSi}(\text{OCH}_3)_3$ and $\text{Si}(\text{OCH}_3)_4$ is hydrolyzed under basic conditions in the presence of the enzyme. Additives such as isopropanol, polyvinyl alcohol, cyclodextrins, ionic liquids or surfactants enhance the efficiency of this type of lipase-immobilization. The main area of application of these heterogeneous biocatalysts concerns esterification or transesterification in organic solvents, ionic liquids, or supercritical carbon dioxide. Rate enhancements (relative to the traditional use of lipase powders) of several orders of magnitude have been observed, in addition to higher thermal stability. The lipase-immobilizates are particularly useful in the kinetic resolution of chiral esters, enantioselectivity often being higher than what is observed when using the commercial forms of these lipases (powder or classical immobilizates). Thus, due to the low price of sol–gel entrapment, the excellent performance of the lipase-immobilizates, and the ready recyclability, the method is industrially viable.

Key words Lipases, Sol–gel immobilization, Esterification, Transesterification, Thermal stability, Kinetic resolution, Enantioselectivity, Recyclability

1 Introduction

Lipases (EC 3.1.1.3) are the most often used enzymes in synthetic organic chemistry and biotechnology [1–5], new applications being reported almost daily. A milestone in the application of lipases and of certain other enzymes as catalysts for synthetic organic chemistry was the discovery that they can be used in nonaqueous media, allowing transformations of interest to organic chemists to be performed that are not possible in the natural aqueous environment [3]. Lipases catalyze the hydrolysis of carboxylic acid esters in aqueous medium or the reverse reaction (esterification) as well as transesterification in organic solvents [1–5]. When working in organic media, nucleophiles other than alcohols can be used, e.g., amines or H_2O_2 affording amides or carboxylic acid peroxides, respectively. Numerous examples involving enantioselectivity in the production of chiral

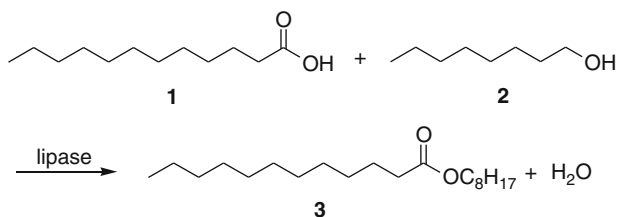


Fig. 1 Model esterification of lauric acid (1) by *n*-octanol (2) catalyzed by a lipase [18]

alcohols, amines and carboxylic acids have been reported. Lipases are structurally characterized by a so-called lid. When hydrophobic substrates interact with certain hydrophobic regions of a lipase, the lid opens and thus exposes the active site (serine) in a process called interfacial activation [4–7].

When the reactions are performed in organic solvents (which corresponds to the majority of cases), commercially available lipase powders are often employed. In spite of the obvious advantages in such simple protocols, several drawbacks need to be considered, primarily the considerably reduced lipase activities relative to those observed in aqueous medium, and the extreme difficulty in recycling the enzyme. Thus, for real (industrial) applications of lipases some form of immobilization is necessary which not only allows for efficient separation and reuse of the enzyme, but which also leads to a significant enhancement of catalyst activity and stability, sometimes enhanced stereoselectivity also being observed. Several approaches have been described (*see* Chapters 3, 7 and 17). The present chapter focuses on the entrapment of lipases in hydrophobic sol–gel silicates.

The general process of sol–gel encapsulation is a particularly easy and effective way to immobilize many different types of enzymes [8]. Following isolated reports describing special examples [9, 10], it was the seminal work of Avnir and coworkers which led to the generalization of this technique [8, 11–15]. Sol–gel techniques involve the acid- or base-catalyzed hydrolysis of tetraalkoxysilanes Si(OR)₄ [16, 17]. Mechanistically, the silane-precursor undergoes hydrolysis and cross-linking condensation with formation of a SiO₂ matrix in which the enzyme is trapped. This type of encapsulation, not to be confused with adsorption on silica, works well for a number of enzymes [8, 11–15]. However, in the case of lipases, materials were obtained which showed disappointingly low enzyme activities, as measured by the rate of the model reaction involving the esterification of lauric acid (1) by *n*-octanol (2) in isooctane as solvent (Fig. 1) [18]. Only 5–10 % activity relative to the traditional use of the respective lipase powder was observed, equivalent to relative rates of 0.05–0.1.

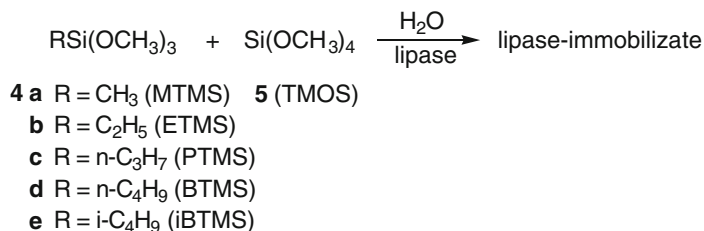


Fig. 2 Encapsulation of lipases in typical hydrophobic sol–gel materials [18, 19]

Following this disappointing observation, it was speculated that the microenvironment in the SiO₂ matrix may be too polar, and therefore mixtures of Si(OCH₃)₄ (**5**) and alkylsilanes of the type RSi(OCH₃)₃ (**4**) or polydimethylsiloxane (PDMS) having non-hydrolyzable lipophilic alkyl groups (R) were tested for the first time (Fig. 2) [18]. This strategy was developed because the silicon oxide matrix is now hydrophobic, which can facilitate or simulate a type of interfacial activation of the entrapped lipase. Basic catalysts such as NaF were used for the sol–gel process, because such conditions lead to large pores in the silicate matrix, in contrast to most acidic catalysts. Indeed, dramatically improved relative lipase activities typically amounting to 200–800 % were observed in the model reaction, which corresponds to an enhancement of relative enzyme activity by a factor ranging from 2 to 8 with respect to the traditional use of the corresponding lipase powder (lyophilizate) [18, 19]. Relative activity is defined as $[\nu(\text{immobilized lipase})/\nu(\text{commercial lipase})]$, where ν is the initial rate of the reaction in each case. A pronounced increase in thermal stability was also observed. In most cases the optimal ratio of RSi(OCH₃)₃ to Si(OCH₃)₄ turned out to be about 5:1, although it was not possible to present an experimental protocol which is completely general for all lipases and substrates of interest. In the early work CH₃Si(OCH₃)₃ was generally used as the precursor and polyvinyl alcohol (PVA) as an additive, the latter possibly acting as a stabilizer of the lipase [18, 19]. However, other RSi(OCH₃)₃ precursors with for example R = *n*-butyl proved to be superior in many cases, suggesting that optimization in new situations is advisable.

Although these heterogeneous biocatalysts proved to work quite well for a variety of applications, further improvements followed. An important extension of this method pertains to the use of additional porous solid supports during the sol–gel process [20]. This type of “double immobilization” involves binding of the lipase-containing gels in the large hollow spaces of the solid support (e.g., silicates of the type SIRAN[®] or Celite[®]) as gelation occurs (Fig. 3). Such a process results in higher mechanical stability and enhanced enzyme activity (up to a factor of 88). It is now routinely used.

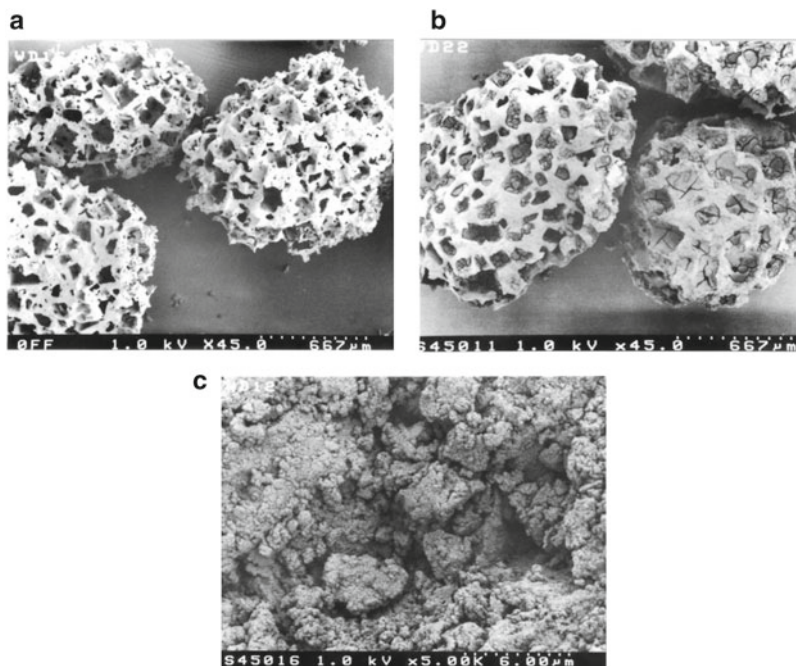


Fig. 3 (a) Scanning electron microscopic (SEM) image of untreated SIRAN[®] showing hollow pores in which the lipase-containing sol–gel material can be bound. (b) SEM image of a lipase SP 523 containing TMOS/PDMS (4:1) gel in the pores of SIRAN[®]. (c) ca. 100-fold magnification of the SEM image of (b) [20]

Sol–gel *encapsulation* is crucial in both variants since conventional *adsorption* on hydrophobic silicates or on SIRAN[®] alone affords poor catalysts. The structural and morphological properties of the first-generation lipase immobilizates were characterized by scanning electron microscopy (SEM), solid state ²⁹Si and ¹³C NMR spectroscopy and studies concerning specific surface area and pore volume [21]. Moreover, kinetic studies clearly point to an “alkyl effect,” i.e., enhancement of lipase-activity upon using RSi(OCH₃)₃ in the series methyl < ethyl < *n*-propyl < *n*-butyl [21]. Enhanced hydrophobicity in the silicon oxide matrix correlates with increased enzyme activity. Higher thermal stability and activity appears to result from multipoint interactions through hydrogen bonding as well as ionic and hydrophobic interactions (van der Waals), which can be schematized as shown in Fig. 4. Hydrophobic interactions can result in a type of interfacial activation. The lipase may be conformationally arrested in the matrix in a “lid-opened” and therefore active form [22].

A crucial issue of any type of enzyme immobilization concerns the question of recyclability. Successful recycling of sol–gel lipase immobilizates derived from eight different lipases was originally demonstrated [19, 22]. For example, the entrapped lipase from *Pseudomonas cepacia* in MTMS or MTMS/PDMS gels was repeatedly used in batch esterification involving the model reaction of

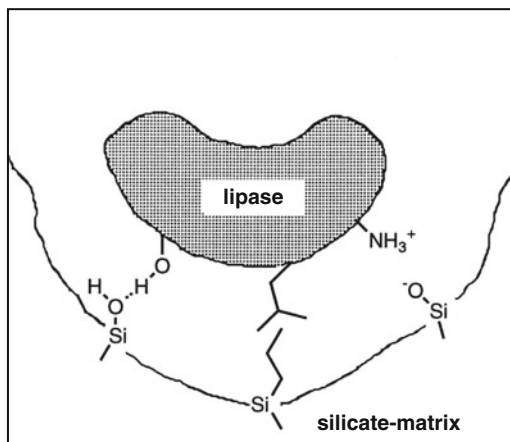


Fig. 4 Schematic view of non-covalent interactions between the gel matrix and the lipase [22]

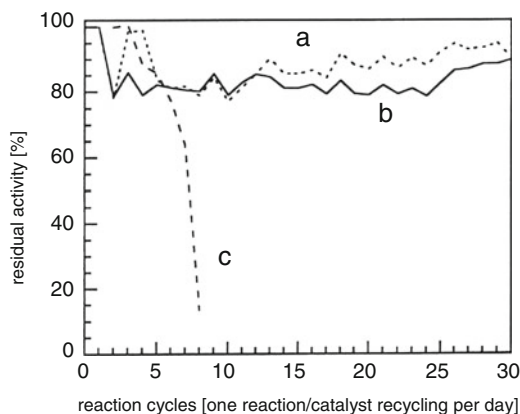


Fig. 5 Activity of immobilized lipase PS (Amano) after repeated use in esterification reactions involving $1 + 2 \rightarrow 3$. (a) MTMS/PDMS (6:1) gel with entrapped lipase PS. (b) MTMS gel with entrapped lipase PS. (c) MTMS gel with adsorbed lipase PS [19, 22]

1 and **2**. After shaking the reaction mixture at 30 °C for 23 h, the lipase-containing gels were recovered by filtration or centrifugation, washed with isooctane and pentane, and reused. In addition, the gels were washed with acetone after every fifth reaction. After a slight loss of enhanced activity, probably due to loss of surface adsorbed lipase, enzyme activity remained constant for at least 30 reactions at about 85 % of the original high value. Under the same conditions a control experiment in which the lipase was physically *adsorbed* to the hydrophobic gel showed that the material loses its activity completely after only a few reactions (Fig. 5) [19, 22]. These experiments illustrate an important point, namely that immobilization by adsorption is certainly viable in this system (and

in other types of immobilizates), but only for a very limited number of cycles involving reaction/recyclization (which is not always reported in the literature). Thus, the advantages of this type of lipase immobilization include the following: (1) higher stability, (2) enhanced rate, (3) often improved stereoselectivity, and (4) recyclability. Some of the first-generation sol-gel lipase immobilizates are commercially available, although they appear to have considerably lower activity than home-made samples [23].

Whereas the sol-gel lipase-encapsulation was designed for application in nonaqueous media, the immobilizates can also be used as heterogeneous catalysts for ester hydrolysis in aqueous medium [24]. Another development concerns the possibility of magnetic separation as a means to recycle the lipase catalysts, specifically by incorporating magnetite (iron oxide) during the sol-gel process [25]. Moreover, the concept of lipase entrapment in hydrophobic silicates has been extended to aerogels [26, 27].

The development of second-generation sol-gel lipase-immobilizates in 2003 [28] opened the way to heterogeneous catalysts which are even more active, while retaining enhanced thermal and mechanical stability and the possibility to recycle efficiently. It involves the optimal choice of the hydrophobic alkyl group in the sol-gel precursor $\text{RSi}(\text{OCH}_3)_3$ (**4**) as well as the use of additives such as 18-crown-6, Tween-80[®], other surfactants, cyclodextrins, isopropanol and/or KCl. Sometimes combinations of these additives work particularly well. Such additives had been used previously to activate lipases in the absence of sol-gels (29–39). The most active lipase-gels are based on *n*-butyl- or isobutylsilane-precursors (**4d**, **e**) and contain either 18-crown-6 or Tween-80[®] as additives [28]. Nine different lipases (Pfl, BcL, MmL, AnL, CrL (type VII), CrL(L-3), TIL, PpL, and PrL as described in Subheading 3) were subjected to sol-gel immobilization of the second-generation, and all of them displayed improved catalytic performance [28]. In some cases “double” immobilization, i.e., performing the sol-gel lipase-entrapment not only in the presence of an appropriate additive, but also in the presence of a solid support such as SIRAN[®] (Fig. 3) or Celite[®] leads to additional enhancement of activity as well as thermal and mechanical stability. Although this actually increases the amount of solid support (Celite[®] plus attached sol-gel silicate) relative to the amount of lipase, weight-wise less total heterogeneous catalyst needs to be employed. This is due to the fact that enzyme activity in the model reaction is dramatically higher relative to the use of lipase powders. For example, in the case of the lipase TIL the factor is 1,391 (relative activity), corresponding to an activity of 1,237 $\mu\text{mol}/\text{min g gel}$ and a specific activity of 8,899 $\mu\text{mol}/\text{min g protein}$. Sol-gel encapsulation of lipases also enhances stability, activity, and enantioselectivity in most reactions tested, as in the kinetic resolution of *rac*-**6** (Table 1) [28] and in other early cases as well (Fig. 6) (40–44).

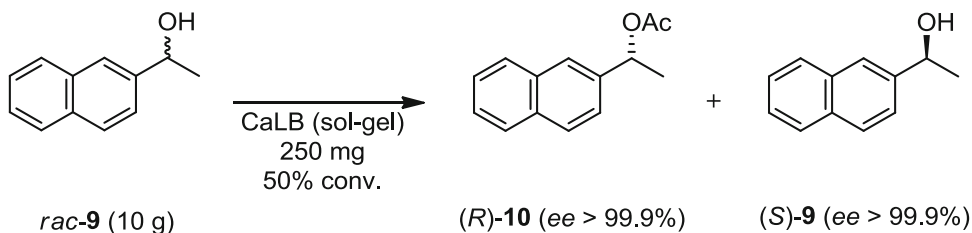


Fig. 7 Kinetic resolution of *rac-9* by lipases [28]

precursor and/or additive have led to further improvements. A selection of examples is presented here, although a universal protocol suitable for all lipases and substrates is not possible. For example, further fine tuning of second-generation lipase-immobilizates can be achieved by the use of ternary alkoxy silane precursors, medium-chain *n*-octylSi(OC₂H₅)₃ and the perfluoro-analog [46], or disubstituted dialkoxy silanes [47] being prime candidates. In another important contribution, the superiority of the sol-gel lipase catalysts relative to several other types of lipase-immobilizates including cross-linked enzyme crystals (CLECs) and cross-linked enzyme aggregates (CLEAs) was demonstrated [48]. This study included the use of sucrose as an additive and the in situ double immobilization technique using Celite® (see above), practical applications referring to the lipase from *Pseudomonas fluorescens* (AK Amano 20) as a catalyst in the kinetic resolution of structurally different chiral alcohols. Even after ten cycles of reusing the heterogeneous catalysts, the selectivity factors remained high ($E=100$ to -200) [48]. Yet another contribution pertains to the use of ionic liquids bearing hydrophobic alkyl groups in the cationic component as additives in the sol-gel process, this leading to enormous rate and stereoselectivity enhancements [49]. In another study focusing on the kinetic resolution of secondary alcohols, the double-immobilization technique was also applied [50].

Notable advances in sol-gel encapsulation of lipases were also made by introducing novel concepts. For example, the catalytic properties of *Candida rugosa* lipase were dramatically improved by sol-gel encapsulation in the presence of Fe₃O₄ magnetic particles attached to calix[4]arene [51]. In the enantioselective hydrolysis of Naproxen methyl ester, a selectivity factor of $E=460$ was observed, relative to $E=166$ of the free enzyme. The same group also reported enhancement of rate and enantioselectivity by performing the sol-gel encapsulation onto a β -cyclodextrin-based polymer [52]. Another way to tune sol-gel lipase immobilizates for even higher activity or selectivity is to include chiral template substrates or substrate analogs, efficient bioimprinting sometimes being involved [53, 54]. Sol-gel lipase immobilizates have also been used in continuous-flow or column reactors [55, 56].

In conclusion, sol–gel encapsulation of lipases based on the use of hydrophobic precursors of the type $\text{RSi}(\text{OCH}_3)_3$ in combination with tetraethoxysilane constitutes a viable and practical way to immobilize this important class of enzymes. A variety of additives can be used to fine-tune these heterogeneous catalysts. In situ double-immobilization by performing the sol–gel encapsulation in the presence of porous solid supports provides mechanically stable catalysts that can be used in column or continuous-flow reactors. Generally, intellectual property (IP) aspects do not pose any problems. For these reasons the use of these lipase-immobilizates is rapidly increasing. Controlling the pore size of the silicate matrix is a task for future studies. Finally, application of the sol–gel technique has continued to be applied to other types of enzymes as well [11, 14, 58].

2 Materials

2.1 Substrates, Solvents, and Reagents for Lipase-Catalyzed Reactions

1. Lauric acid (Fluka, Switzerland).
2. *n*-Octanol (Fluka).
3. *rac*-2-Octanol (Aldrich, Germany).
4. Vinyl acetate (Acros, U.K.).
5. *rac*-2-Naphthyl-2-ethanol (Aldrich).
6. Isooctane (Fluka).
7. Toluene (Overlack, Germany).

2.2 Sol–Gel Process

1. *n*-Butyltrimethoxysilane (ABCR, Germany).
2. Isobutyltrimethoxysilane (Lancaster, U.K.).
3. Tween-80® [poly-oxyethylene (20) sorbitan monooleate] (Fluka).
4. Sodium fluoride (Fluka).
5. Celite® 577 (Fluka).
6. Methyl- β -cyclodextrin (Aldrich).
7. Tetramethoxysilane (Fluka).
8. Polyvinyl alcohol (PVA; MW = 15,000) (Merck, Germany).

2.3 Lipases

The lipases from *Candida antarctica* (CaLB; Chirazyme L-2®), *C. rugosa* (CrL; Chirazyme L-3®), and *Mucor miebei* (MmL; ChirazymeL-9®) are accessible from Roche; *Aspergillus niger* (AnL; Amano AS), *Burkholderia cepacia* (BcL; Amano PS), and *P. fluorescens* (PfL; Amano AK “20”) from Amano Pharmaceutical Co.; *C. rugosa* type VII (CrL type VII) from Sigma; *Penicillium roqueforti* (PrL) from Fluka; *Thermomyces lanuginosa* (TIL; Novozym SP) from Novo Nordisk.

3 Methods

3.1 Sol–Gel

Entrapment of Lipases

General Procedure

1. A commercial lipase powder (lyophilizate) such as AnL (150 mg), BcL (150 mg), CaLB (125 mg), CrL (150 mg), CrL type VII (60 mg), MmL (150 mg), Pfl (150 mg), PpL (150 mg), PrL (150 mg), or TIL (70 mg) is placed in a 50 mL Falcon-tube (Corning) together with TRIS/HCl-buffer (390 μ L; 0.1 M; pH 7.5) and the mixture is vigorously shaken with a Vortex-Mixer. In the case of an additive or an additional porous solid support, these materials are included as needed [28]. In a typical procedure, 0.5 mmol of 18-crown-6 as an additive is added. In the case of “double immobilization,” the additive is used as above in addition to 50 mg of Celite®.
2. Then 100 μ L of aqueous PVA (4 % W/V), 50 μ L of a 1 M aqueous sodium fluoride, and 100 μ L isopropanol are added, and the mixture is homogenized using a vortex mixer.
3. Then the alkylsilane (Fig. 2, 4d or 4e) (2.5 mmol) and TMOS 5 (Figs. 2, 5) (0.5 mmol; 74 μ L; 76 mg) are added. The mixture is agitated once more for 10–15 s. Gelation is usually observed within seconds or minutes while the reaction vessel is gently shaken.
4. Following drying over night in the opened Falcon-tube, 10 or 15 mL isopropanol is added in the order to facilitate removal of the white solid material (filtration).
5. The gel is washed with 10 mL distilled water, 10 mL isopropanol, and 10 mL *n*-pentane. During this process a spatula is used to crush the gel.
6. The lipase immobilizate is placed in an open 2-mL plastic vessel and dried at room temperature [28].

3.2 Determination of Protein Content

In order to determine the protein content of the commercial lipases as well as the degree of loading, the *BCA Protein Assay Kit* (Sigma) can be used. Accordingly, solutions of the commercial lipase or the wash-solutions following the sol–gel process are incubated for 30 min and measured at 37 °C using a UV–Vis-spectrometer at 562 nm according to the *Technical Bulletin* (Sigma). Distilled water is used as a reference and bovine serum albumin (BSA) as standards. The degree of immobilization ranges between 0.3 and 0.9 [28].

3.3 Determination of Lipase Activity

1. Depending on the activity, between 1 and 50 mg of the sol–gel lipase-immobilizate is placed in a Falcon-tube together with a solution of lauric acid (100 mg; 0.5 mmol) solution and *n*-octanol (158 μ L; 130 mg; 1.0 mmol) in nondried (H₂O-saturated) iso-octane.

2. The mixture is then shaken at 180 rounds per minute (rpm) at 30 °C. At defined intervals (usually after 15, 30, 45 and 60 min) 300 μ L samples are taken and centrifuged ($39,000\times g$) before the gas chromatographic determination of lauric acid and lauric acid *n*-octyl ester is carried out using 150 μ L of the supernatant.
3. By applying a linear regression of the measured values the initial reaction rate in μ mol/min and therefore the activity relative to 1 g of immobilizate can be determined. By considering the degree of loading, the specific activity is calculated.
4. The relative activity is determined by dividing the specific activity of the immobilizate by the specific activity of the commercial lipase powder [28].

3.4 Typical Kinetic Resolution on a Preparative Scale

1. Similar to the above protocol a mixture of *rac*-1-(2-naphthyl)-ethanol (10 g; 58 mmol), vinyl acetate (8.1 mL; 7.5 g; 87 mmol), and 250 mg of a sol-gel CaLB-immobilizate (prepared in the presence of 18-crown-6 as additive) in 300 mL toluene is shaken at 35 °C for 48 h.
2. Following filtration gas chromatography analysis shows a conversion of 50.0 %, the enantiomeric excess of non-reacted (*S*)-1-(2-naphthyl)ethanol and product ((*R*)-acetate) each being >99.9 %.
3. The immobilizate is removed by filtration, washed with toluene and pentane, and can be reused, showing no significant loss in activity or enantioselectivity [28].

3.5 Sol-gel Immobilization of Lipases Using Ionic Liquids as Additives

A microbial lipase suspension (120 mg/mL) in TRIS/HCl 0.1 M, pH 8.0 buffer, was stirred at 700 rpm for 30 min, centrifuged, and the supernatant used for immobilization. In a 4 mL glass vial, 1 mL of this lipase solution was mixed (magnetic stirrer) with 200 μ L ionic liquid or PEG 20,000, followed by addition of 100 μ L 1 M NaF solution, and 200 μ L isopropyl alcohol. This mixture was kept for 30 min under continuous stirring for homogenization, and subsequently a binary or tertiary mixture of silane precursors (total 6 mmol) was added. The mixture was stirred at room temperature until start of gelation. The obtained gel was kept for 24 h at room temperature to complete polymerization. The bulk gel was washed with isopropyl alcohol (7 mL), distilled water (5 mL), isopropyl alcohol again (5 mL) and finally hexane (5 mL), filtered, dried at room temperature for 24 h, and in a vacuum oven at room temperature for another 24 h. Finally, it was crushed in a mortar and kept in refrigerator [49, 57].

References

- Faber K (2011) *Biotransformations in organic chemistry*, 6th edn. Springer, Berlin
- Drauz K, Gröger H, May O (2012) *Enzyme catalysis in organic synthesis: a comprehensive handbook*, 3rd edition, vol I–III, 3rd edn. VCH, Weinheim
- Klibanov AM (2001) Improving enzymes by using them in organic solvents. *Nature* 409: 241–246
- Schmid RD, Verger R (1998) Lipases: interfacial enzymes with attractive applications. *Angew Chem Int Ed* 37:1608–1633
- Reetz MT (2002) Lipases as practical biocatalysts. *Curr Opin Chem Biol* 6:145–150
- Brzozowski AM, Derewenda U, Derewenda ZS, Dodson GG, Lawson DM, Turkenburg JP, Bjorkling F, Huge-Jensen B, Patkar SA, Thim L (1991) A model for interfacial activation in lipases from the structure of a fungal lipase-inhibitor complex. *Nature* 351:491–494
- Van Tilbeurgh H, Egloff M-P, Martinez C, Rugani N, Verger R, Cambillau C (1993) Interfacial activation of the lipase-procolipase complex by mixed micelles revealed by X-ray crystallography. *Nature* 362:814–820
- Avnir D, Braun S, Lev O, Ottolenghi M (1994) Enzymes and other proteins entrapped in sol-gel materials. *Chem Mater* 6:1605–1614
- Johnson P, Whateley TL (1971) Use of polymerizing silica gel systems for immobilization of trypsin. *J Colloid Interface Sci* 37:557–563
- Glad M, Norrlöw O, Sellergren B, Siegbahn N, Mosbach K (1985) Use of silane monomers for molecular imprinting and enzyme entrapment in polysiloxane-coated porous silica. *J Chromatogr* 347:11–23
- Avnir D (1995) Organic chemistry within ceramic matrices: doped sol-gel materials. *Acc Chem Res* 28:328–334
- Livage J (1996) Bioactivity in sol-gel glasses. *C R Acad Sci Ser Iib Mec Phys Chim Astron* 322:417–427
- Gill I (2001) Bio-doped nanocomposite polymers: sol-gel bioencapsulates. *Chem Mater* 13: 3404–3421
- Avnir D, Coradin T, Lev O, Livage J (2006) Recent bio-applications of sol-gel materials. *J Mater Chem* 16:1013–1030
- Nassif N, Livage J (2011) From diatoms to silica-based biohybrids. *Chem Soc Rev* 40:849–859
- Hench LL, West JK (1990) The sol-gel process. *Chem Rev* 90:33–72
- Brinker CJ, Scherer GW (1990) *Sol-gel science: the physics and chemistry of sol-gel processing*. Academic, Boston
- Reetz MT, Zonta A, Simpelkamp J (1995) Efficient heterogeneous biocatalysts by entrapment of lipases in hydrophobic sol-gel materials. *Angew Chem Int Ed Engl* 34:301–303
- Reetz MT, Zonta A, Simpelkamp J (1996) Efficient immobilization of lipases by entrapment in hydrophobic sol-gel materials. *Biotechnol Bioeng* 49:527–534
- Reetz MT, Zonta A, Simpelkamp J, Könen W (1996) In situ fixation of lipase-containing hydrophobic sol-gel materials on sintered glass—highly efficient heterogeneous biocatalysts. *Chem Commun*:1397–1398
- Reetz MT, Zonta A, Simpelkamp J, Ruffńska A, Tesche B (1996) Characterization of hydrophobic sol-gel materials containing entrapped lipases. *J Sol Gel Sci Technol* 7:35–43
- Reetz MT (1997) Entrapment of biocatalysts in hydrophobic sol-gel materials for use in organic chemistry. *Adv Mater* 9:943–954
- When the author compared the first generation lipase-immobilizates as prepared in his own laboratory with analogous commercial samples (Fluka), large differences in activity were observed, a finding that was corroborated by another group: Galarneau A, Mureseanu M, Atger S, Renard G, Fajula F (2006) Immobilizates of lipase on silicas. Relevance of textural and interfacial properties on activity and selectivity. *New J Chem* 30:562–571
- Reetz MT, Wenkel R, Avnir D (2000) Entrapment of lipases in hydrophobic sol-gel materials: efficient heterogeneous biocatalysts in aqueous medium. *Synthesis* 781–783
- Reetz MT, Zonta A, Vijayakrishnan V, Schimossek K (1998) Entrapment of lipases in hydrophobic magnetite-containing sol-gel materials: magnetic separation of heterogeneous biocatalysts. *J Mol Catal A Chem* 134:251–258
- Pierre M, Buisson P, Fache F, Pierre A (2000) Influence of the drying technique of silica gels on the enzymatic activity of encapsulated lipase. *Biocatal Biotransform* 18:237–251
- Buisson P, Hernandez C, Pierre M, Pierre AC (2001) Encapsulation of lipases in aerogels. *J Non-Cryst Solids* 285:295–302
- Reetz MT, Tielmann P, Wiesenhöfer W, Könen W, Zonta A (2003) Second generation sol-gel encapsulated lipases: robust heterogeneous biocatalysts. *Adv Synth Catal* 345: 717–728
- Reinhoudt DN, Eendebak AM, Nijenhuis WF, Verboom W, Kloosterman M, Schoemaker HE (1989) The effect of crown ethers on enzyme-catalyzed reactions in organic solvents. *J Chem Soc Chem Commun*:399–400

30. Engbersen JFJ, Broos J, Verboom W, Reinhoudt DN (1996) Effects of crown ethers and small amounts of cosolvent on the activity and enantioselectivity of alpha-chymotrypsin in organic solvents. *Pure Appl Chem* 68: 2171–2178
31. van Unen D-J, Engbersen JFJ, Reinhoudt DN (2002) Why do crown ethers activate enzymes in organic solvents? *Biotechnol Bioeng* 77: 248–255
32. Griebenow K, Laureano YD, Santos AM, Clemente IM, Rodríguez L, Vidal MW, Barletta G (1999) Improved enzyme activity and enantioselectivity in organic solvents by methyl- β -cyclodextrin. *J Am Chem Soc* 121: 8157–8163
33. Santos AM, Clemente IM, Barletta G, Griebenow K (1999) Activation of serine protease subtilisin Carlsberg in organic solvents: combined effect of methyl- β -cyclodextrin and water. *Biotechnol Lett* 21:1113–1118
34. Khmelnitsky YL, Welch SH, Clark DS, Dordick JS (1994) Salts dramatically enhance activity of enzymes suspended in organic solvents. *J Am Chem Soc* 116:2647–2648
35. Altreuter DH, Dordick JS, Clark DS (2002) Nonaqueous biocatalytic synthesis of new cyclotoxic doxorubicin derivatives: exploiting unexpected differences in the regioselectivity of salt-activated and solubilized subtilisin. *J Am Chem Soc* 124:1871–1876
36. Liu Y-Y, Xu J-H, Hu Y (2000) Enhancing effect of Tween-80 on lipase performance in enantioselective hydrolysis of ketoprofen ester. *J Mol Catal B: Enzym* 10:523–529
37. Colton IJ, Ahmed SN, Kazlauskas RJ (1995) A 2-propanol treatment increases the enantioselectivity of *Candida rugosa* lipase toward esters of chiral carboxylic acids. *J Org Chem* 60: 212–217
38. Zhu K, Jutila A, Tuominen EKJ, Kinnunen PKJ (2001) Effects of i-propanol on the structural dynamics of *Thermomyces lanuginosa* lipase revealed by tryptophan fluorescence. *Protein Sci* 10:339–351
39. Cipiciani A, Bellezza F (2002) Primary allenic alcohols of high optical purity via lipase catalyzed resolution. *J Mol Catal B: Enzym* 17: 261–266
40. Badjic JD, Kadnikova EN, Kostic NM (2001) Enantioselective aminolysis of an α -chloroester catalyzed by *Candida cylindracea* lipase encapsulated in sol-gel silica glass. *Org Lett* 3: 2025–2028
41. Furukawa S-Y, Kawakami K (1998) Characterization of *Candida rugosa* lipase entrapped into organically modified silicates in esterification of menthol with butyric acid. *J Ferment Bioeng* 85:240–242
42. Pfau R, Kunz H (1999) Selectively deprotectable carbohydrates based on regioselective enzymatic reactions. *Synlett* 1817–1819
43. Gill I, Pastor E, Ballesteros A (1999) Lipase-silicone biocomposites: efficient and versatile immobilized biocatalysts. *J Am Chem Soc* 121: 9487–9496
44. Ragheb A, Brook MA, Hrynyk M (2003) Highly activated, silicone entrapped, lipase. *Chem Commun*:2314–2315
45. Margolin has stated that “it is not unusual to see processes employing more enzyme than substrate by weight”: Khalaf N, Govardhan CP, Lalonde JJ, Persichetti RA, Wang Y-F, Margolin AL (1996) Cross-linked enzyme crystals as high active catalysts in organic solvents. *J Am Chem Soc* 118:5494–5495
46. Tomin A, Weiser D, Hellner G, Bata Z, Corici L, Péter F, Koczka B, Poppe L (2011) Fine-tuning the second generation sol-gel lipase immobilization with ternary alkoxysilane precursor systems. *Process Biochem* 46:52–58
47. Weiser D, Boros Z, Hornyánszky G, Tóth A, Poppe L (2012) Disubstituted dialkoxysilane precursors in binary and ternary sol-gel systems for lipase immobilization. *Process Biochem* 47:428–434
48. Brem J, Turcu MC, Paizs C, Lundell K, Toşa M-I, Irimie F-D, Kanerva LT (2012) Immobilization to improve the properties of *Pseudomonas fluorescens* lipase for the kinetic resolution of 3-aryl-3-hydroxy esters. *Process Biochem* 47:119–126
49. Zarcu C, Croitoru R, Corici L, Csunderlik C, Peter F (2009) Improvement of lipase catalytic properties by immobilization in hybrid matrices. *World Acad Sci Eng Technol* 52: 179–184
50. Ursoiu A, Paul C, Marcu C, Peter F (2011) Double immobilized lipase for the kinetic resolution of secondary alcohols. *World Acad Sci Eng Technol* 76:70–74
51. Sayin S, Yilmaz E, Yilmaz M (2011) Improvement of catalytic properties of *Candida rugosa* lipase by sol-gel encapsulation in the presence of magnetic calix[4]arene nanoparticles. *Org Biomol Chem* 9: 4021–4024
52. Yilmaz E, Sezgin M (2012) Enhancement of the activity and enantioselectivity of lipase by sol-gel encapsulation immobilization onto β -cyclodextrin-based polymer. *Appl Biochem Biotechnol* 166:1927–1940

53. Furukawa SY, Ono T, Ijima H, Kawakami K (2002) Effect of imprinting sol-gel immobilized lipase with chiral template substrates in esterification of (R)-(+)- and (S)-(-)-glycidol. *J Mol Catal B Enzym* 17:23–28
54. Cao X, Yang J, Shu L, Yu B, Yan Y (2009) Improving esterification activity of *Burkholderia cepacia* lipase encapsulated in silica by bioimprinting with substrate analogues. *Process Biochem* 44:177–182
55. Kuncova G, Szilva J, Hettflejs J, Sabata S (2003) Catalysis in organic solvents with lipase immobilized by sol-gel technique. *J Sol Gel Sci Technol* 26:1183–1187
56. Tomin A, Hornyánszky G, Kupai K, Dorkó Z, Úrge L, Darvas F, Poppe L (2010) Lipase-catalyzed kinetic resolution of 2-methylene-substituted cycloalkanols in batch and continuous-flow modes. *Process Biochem* 45: 859–865
57. Peter F, Paul C, Ursoiu A (2011) Applications of ionic liquids to increase the efficiency of lipase biocatalysis. In: Kokorin A (ed) *Ionic liquids: applications and perspectives*. InTech, Rijeka, Croatia, pp 481–498
58. Buthe A (2011) Entrapment of enzymes in nanoporous sol-gels. *Methods Mol Biol* 743: 223–237

Improving Lipase Activity by Immobilization and Post-immobilization Strategies

Jose M. Palomo, Marco Filice, Oscar Romero, and Jose M. Guisan

Abstract

One important parameter for the application of lipase catalysts in chemical industries is the specific activity displayed towards natural or unnatural substrates. Different strategies to enhance the lipase activity have been described. The immobilization of lipases on hydrophobic supports by interfacial adsorption at low ionic strength permitted the hyper-activation of these enzymes by fixing the open conformation of the lipase on the hydrophobic support. Improvements of activity from 1.2- up to 20-fold with respect to the initial one have been observed for lipases from different sources.

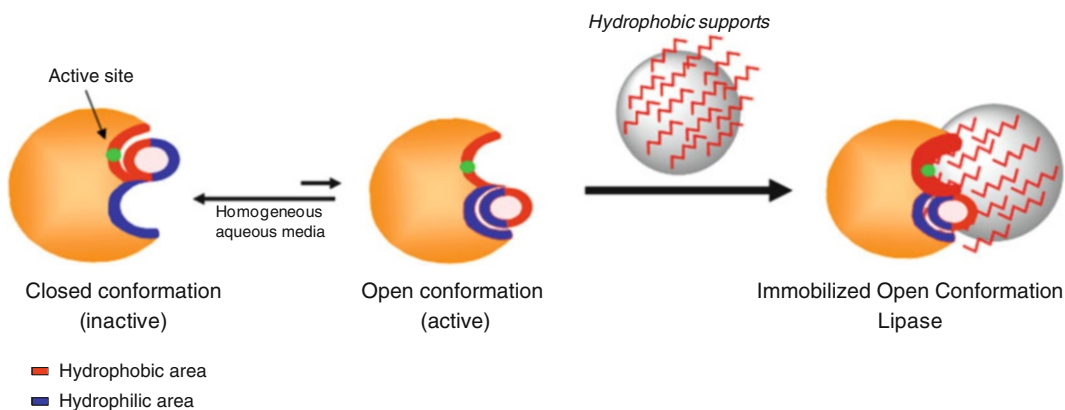
A second strategy was based on the presence of additives, in particular surfactants or ionic liquids, with hydrophobic character to enhance the activity of lipases immobilized on macroporous supports up to eightfold and even more than 100-fold in some cases for soluble lipases.

Finally, a third strategy to improve the activity in immobilized lipases was based on a site-directed chemical modification of the protein by glycosylation on the enzyme N-terminal group or on a unique reactive cysteine of the enzyme by disulfide exchange using different tailor-made disulfide activated polymers.

Key words Lipase, Activation, Immobilization, Site-directed modification, Additives, Polymers

1 Introduction

The improvement of the catalytic activity of enzymes is important for their different industrial applications, in particular, processes, where the enzyme is quite selective but exhibits very low activity towards non-natural substrates [1, 2]. One of the most interesting examples is lipases. These are acyl-glycerol hydrolases with a high activity towards substrate–water interfaces but very low towards soluble oils or non-natural substrates [3]. This behavior is based on a complex catalytic mechanism. Lipases exist in certain equilibrium between a closed conformation (inactive), where the active site is isolated from the reaction medium by a polypeptide chain called lid, and an open conformation (active), where this lid is displaced and the active center is fully exposed to the reaction medium



Scheme 1 Immobilization of lipases on hydrophobic surfaces

[4–7]. In homogeneous aqueous media this equilibrium is mainly shifted to the closed form (Scheme 1).

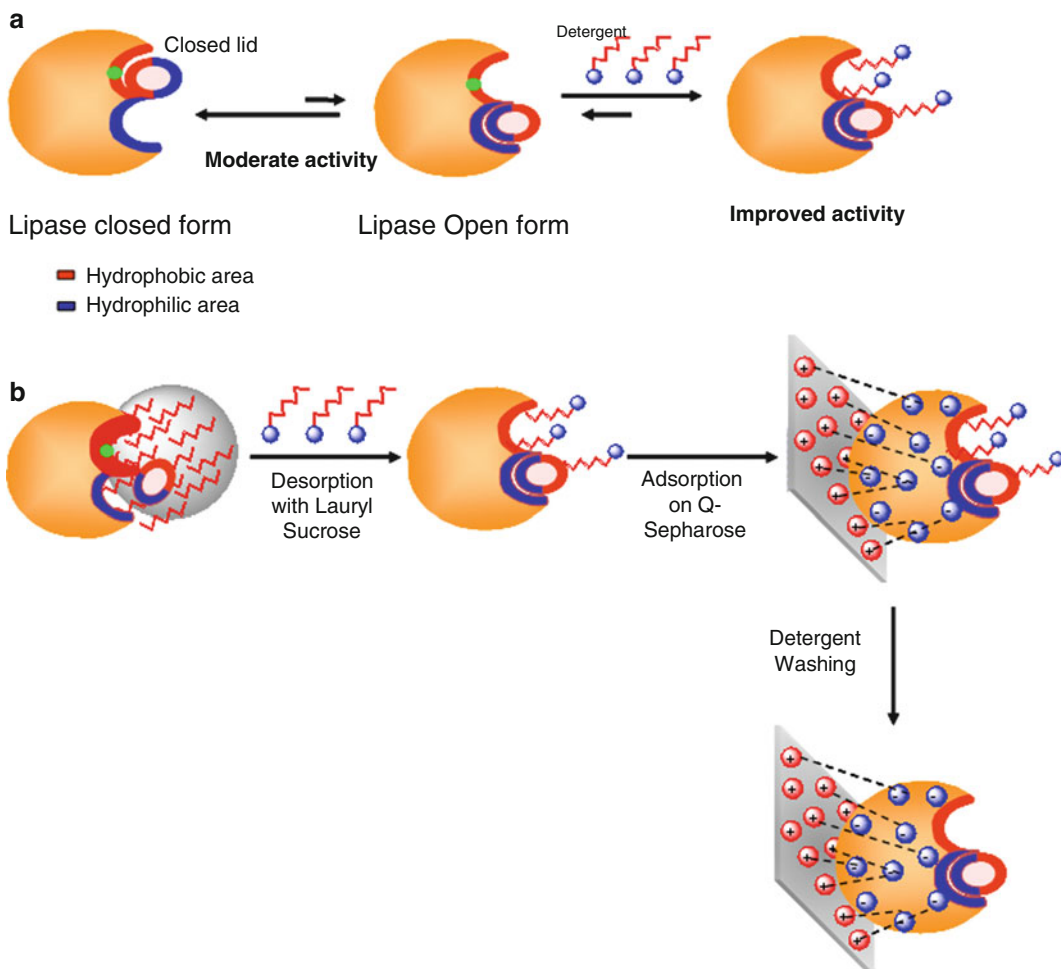
Therefore, the development of strategies to shift this equilibrium to the open and active form could achieve an enhancement on the activity of lipases.

The immobilization of lipases on hydrophobic supports by interfacial adsorption (e.g., octyl-Sepharose, octadecyl-Sepabeads, etc.) [8, 9] permits to fix the open conformation on a solid phase (Scheme 1) representing a simple and elegant methodology to get very high active lipase catalysts. The hydrophobic nature of the support affected to the hyperactivation [10]. This depended on the hydrophobic nature of the lid (e.g. number of amino acids) or the surrounding area of the active site of a particular lipase.

The presence of additives, in particularly those with certain hydrophobicity, has been found to be another methodology to enhance lipase activity [11].

Detergents usually may prevent the negative interaction between the water and the hydrophobic pocket and the hydrophobic face of the lid (*see Note 1*), in this way shifting the close–open equilibrium between the forms of lipases towards the open form (Scheme 2a). For example, the lyophilization and the preparation of Cross-Linked Enzyme Aggregates (CLEAs) of lipases in the presence of detergents have been optimal strategies to get higher active lipases [12, 13].

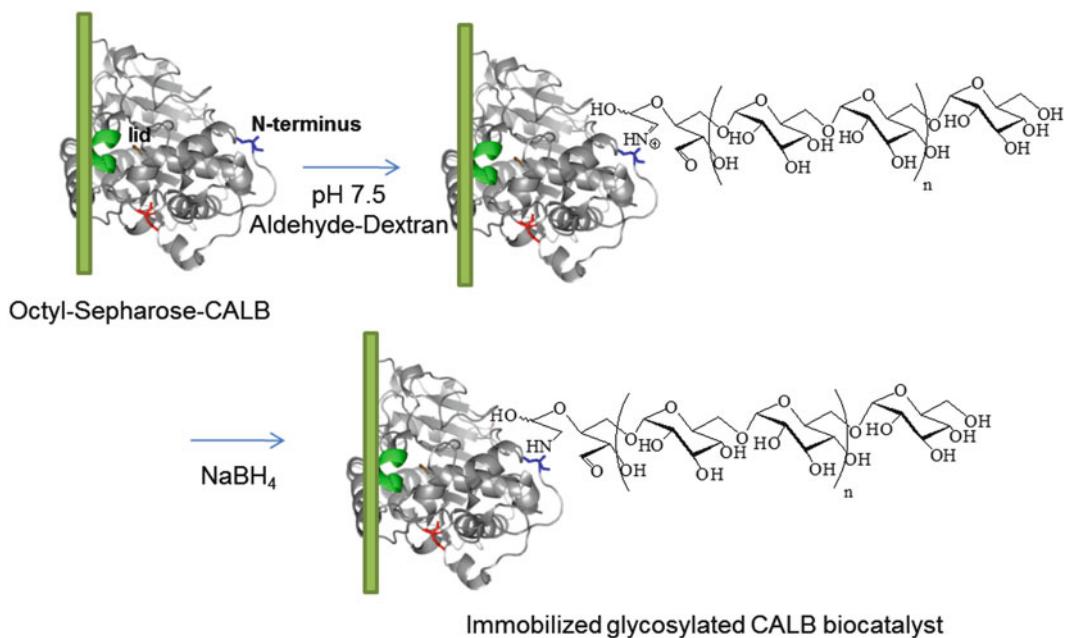
Another application of the use of detergents it has been recently reported by our group. *Rhizomucor miehei* lipase (RML) has been greatly hyperactivated (around 20- to 25-fold towards pNPB) in the presence of lauryl sucrose as detergent (Scheme 2b). This hyperactivated form of the enzyme was fixed (in the presence of detergent) and maintained on Q-Sepharose (strong cationic exchange resin) even after detergent removing [14]. By this strategy, a lipase derivative more active than those adsorbed onto hydrophobic surfaces it has been easily prepared.



Scheme 2 (a) Enhanced activities of lipases by detergent treatment. (b) Immobilization of RML on strong cationic exchanger in presence of detergent

Also the cross-linking of immobilized lipases with glutaraldehyde exhibited better activity than the native immobilized enzymes [15, 16].

In the case of soluble lipases, the addition of detergents caused two effects, breaking the lipase–lipase bimolecular aggregates [17] and the stabilization of the open form of individual lipase molecules (Scheme 2). In this sense, the use of lipases immobilized under dissociation conditions (e.g., in the presence of detergents) may permit to have fully dispersed immobilized enzyme molecules, studying the effect of the interaction between the individual lipase molecules and the detergent. Using enzymes immobilized on porous supports, the small size of the micelles (e.g., 18 kDa for SDS) [18] could permit the entry of the micelles and its interaction with the immobilized enzyme.



Scheme 3 Solid-phase chemical glycosylation of CalB

Following the research-line of the presence of the additives during the biocatalytic process, the presence of very small amounts (5 equiv. compared to the substrate) of ionic liquids in the reaction medium has permitted greatly alter the activity of differently immobilized *R. miehei* lipase preparations in the hydrolysis of peracetylated lactal [19].

Chemical modification of amino acid side chains has been also broadly used to introduce a high variety of groups to improve the enzyme properties [20]. Most strategies for chemical protein modification rely on the nucleophilic side chains of amino acids (such as aspartic and glutamic acids or lysines) [20]. However, this approach is often nonspecific because proteins contain several of these groups throughout the whole structure. Therefore, site-specific modification of the protein is a better approach to prepare such biomolecules. A good example is the surface chemical glycosylation of immobilized lipase in the *N*-terminal amino acid enzyme residue by using dextran polymers, on the basis of the reactivity of amino terminal of proteins at neutral pH (Scheme 3). The formed immobilized glycosylated lipase biocatalysts were more stable, active, and selective toward different substrates than unmodified one [21].

Cysteine represents another convenient target for selective modification owing to the strong nucleophilic side chain sulfhydryl that enables thiol-disulfide exchange [22]. This amino acid can be naturally presented on the protein or can be introduced by directed mutagenesis [20].

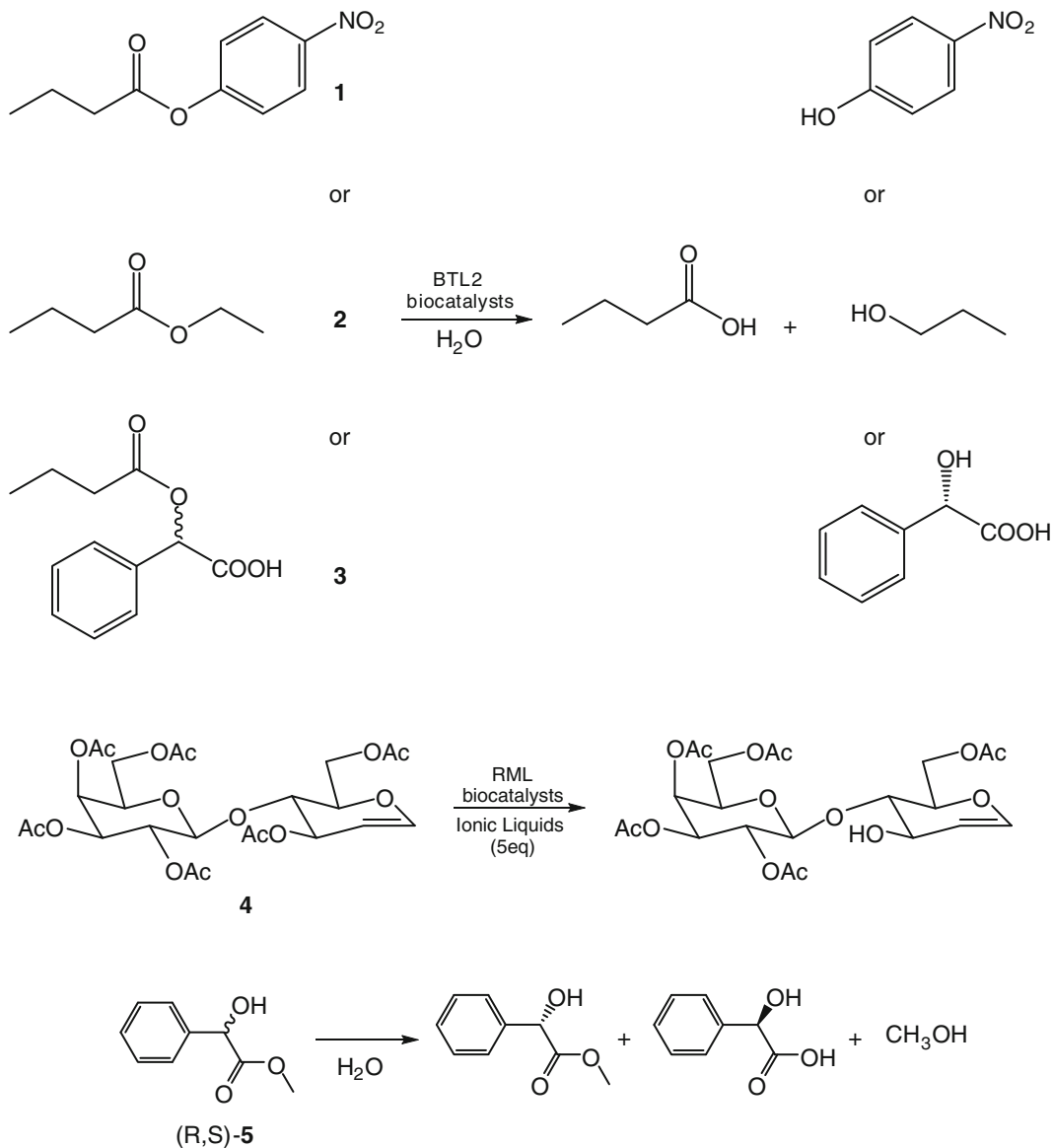


Fig. 1 Substrates used for lipase activity assay: **1**: *p*-nitrophenyl butyrate (pNPB), **2**: ethyl butyrate, **3**: 2-*O*-butryl-2-phenylacetic acid, **4**: hexaacetyl lactal, **5**: methyl mandelate

- Substrate **2**: 50 mM ethyl butyrate (Fig. 1, compound **2**) in assay buffer.
- Substrate **3**: 0.5 mM 2-*O*-butryl-2-phenylacetic acid (Fig. 1, compound **3**) in assay buffer [21].
- Substrate **4**: 5 mM Hexaacetyl lactal (Fig. 1, compound **4**) in 25 mM acetate buffer with 3 % (v/v) acetonitrile, pH 5.
- Substrate **5**: 5 mM methyl mandelate (Fig. 1, compound **5**) in assay buffer.

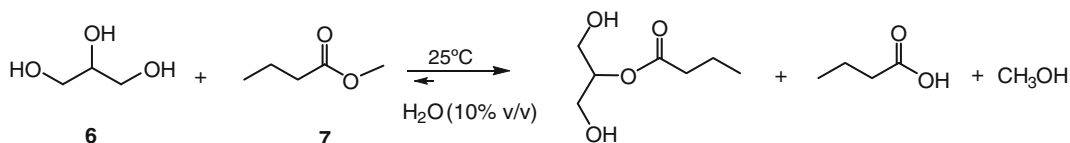


Fig. 2 Transesterification of glycerol (6) with methyl butyrate (7) catalyzed by chemical glycosylated CALB derivatives

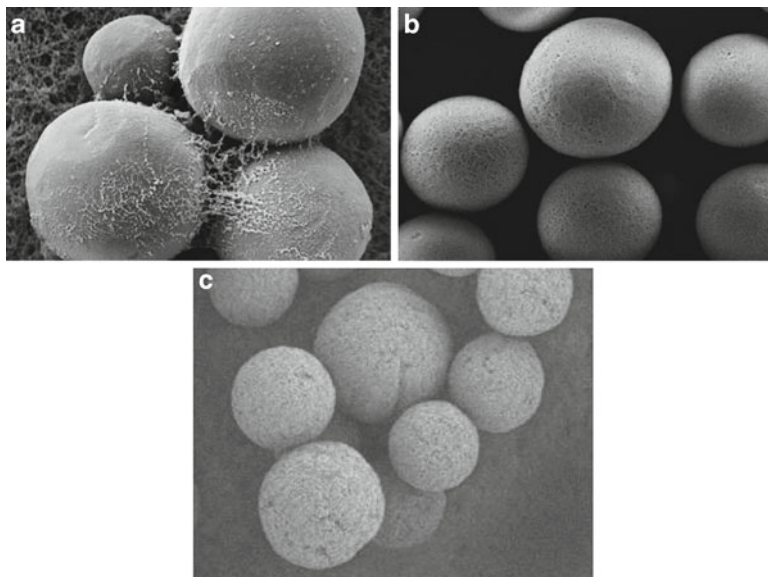


Fig. 3 SEM pictures of different supports for lipase immobilization. Sepharose beads (a), Sepabeads (b), Toyopearl (c)

7. Transesterification reaction buffer: 100 mM sodium phosphate, pH 7.
8. Substrate 6: Glycerol 99 % (Fig. 2, compound 6).
9. Substrate 7: Methyl butyrate (Fig. 2, compound 7) [21].

2.3 Detergents

Triton X-100, Triton X-45, hexadecyltrimethylammonium (CTAB), sodium dodecyl sulfate (SDS), lauryl sucrose.

2.4 Immobilization on Hydrophobic Supports (See Fig. 3)

1. Butyl-, Octyl-, and Q-Sepharose (GE healthcare, Sweden).
2. Butyl- and hexyl-Toyopearl (Tosoh Corporation, Tokyo, Japan).
3. Octadecyl-Sepabeads (Resindion SRL, Italy).
4. Immobilization buffer: 10 mM sodium phosphate, pH 7.

2.5 Chemical Modification

2.5.1 Glycosylation Polymers

1. Dext-CHO solution: 33 mg/mL 10 % oxidated (aldehyde) dextran (Mr 1,500, 6,000, 20,000 Da) in 10 mM sodium phosphate, pH 7.5 [21].
2. Dext-Gly solution: 33 mg/mL glycine-dextran (Mr 1,500) in 10 mM sodium phosphate, pH 6.0 [21].
3. PEG-COOH solution: 33 mg/mL monocarboxylated-polyethyleneglycol (Mr 1,500, 35,000 Da) in 10 mM sodium phosphate, pH 7.5.

2.5.2 Tailor-Made Disulfide Activated Polymers: PDP-Dext-NH₂ Polymer

1. Dext-NH₂ solution: 14 mg/mL aminated-aspartic-dextran (Mr 1,500, 6,000 Da) [20].
2. Polymer buffer: 250 mM phosphate, pH 7.
3. SPDP-Dext solution: 0.10 equiv./mL 3-(2-pyridyldithio) propionic acid *N*-hydroxysuccinimide ester (SPDP) in acetonitrile.

2.5.3 Tailor-Made Disulfide Activated Polymers: PDP-PEG-COOH Polymer

1. PEG-COOH solution: 166.67 mg/mL monocarboxylated-polyethyleneglycol (Mr 1,500, 35,000 Da) in chloroform.
2. SPDP-PEG solution: 3 equiv./mL 3-(2-pyridyldithio) propionic acid *N*-hydroxysuccinimide ester (SPDP) in chloroform.
3. Dimethylaminopyridine (DMAP).

2.5.4 Chemical Glycosylation

1. Octyl-Sepharose (GE healthcare, Sweden).
2. Sodium borohydride.
3. 4-Dimethylaminopyridine (DMAP).
4. 1-Ethyl-3-(3-dimethylaminopropyl) carbodiimide (EDC).

2.5.5 Tailor-Made Polymers

1. Dialysis membrane (200–500 Da cut-off).
2. DTT solution: 50 mM dithiothreitol in 25 mM sodium phosphate, pH 8.
3. Triton solution: 0.5 % (w/v) [Triton X-100].
4. CNBr-Sepharose (GE healthcare, Sweden).
5. Octyl-Sepharose (GE healthcare, Sweden).
6. Modification buffer: 500 mM sodium phosphate, pH 8.3.
7. NaCl solution: 500 mM NaCl.

2.6 Analysis

1. UV spectrophotometer (e.g. Shimadzu UV UVmini1240).
2. HPLC system coupled with an UV detector (e.g. Spectra Physic SP 100 coupled with an UV detector Spectra Physic SP 8450).
3. Kromasil C18 (25 cm × 0.46 cm, 5 μm Ø) HPLC column.
4. Kromasil C8 (25 cm × 0.46 cm, 5 μm Ø) HPLC column (for substrate 7).

5. Mobile phase: 10 mM ammonium phosphate, in acetonitrile, 35:65 v/v pH 3.0 for substrate **2** and **3**.
6. Mobile phase: 10 mM ammonium phosphate, in acetonitrile, 40:60 v/v pH 3.8 for substrate **4**.
7. Mobile phase: 10 mM ammonium phosphate, pH 3.0 (for substrate **5**) or pH 3.8 (for substrate **6** and **7**) in acetonitrile, 30:70 v/v.

3 Methods

3.1 Activity Assay of Lipases

3.1.1 Hydrolysis of *p*-Nitrophenol Esters

1. Add 2.5 mL of assay buffer and 20 μ L of substrate stock solution to a spectrophotometric cell and pre-incubate the mixture at 25 °C for 2 min.
2. Measure esterase lipase activity using an ultraviolet spectrophotometer by following the increase in absorbance at 348 nm (*see Note 5*) produced by the release of *p*-nitrophenol in the hydrolysis of pNPP or **1** prepared as described in Subheading 2.2.
3. To start the reaction add 0.05–0.1 mL of lipase solution or suspension (*see Note 6*) to 2.5 mL of the pre-incubate mixture of pNPP or **1** stock solution and assay buffer.

3.1.2 Hydrolysis of Substrates **2**, **3** and **5**

1. In a syringe reactor (*see Note 7*) add the substrate and biocatalyst (5 mL of substrate **2** solution and 0.1 g of immobilized enzyme; 1.5 mL of substrate **3** solution and 0.5 g of immobilized enzyme; 2 mL of substrate **5** solution and 0.3 g of immobilized enzyme).
2. Extract 100 μ L of reaction solution periodically (each 5 min up to 30 min for substrate **2** and **5**; each 3 h up to 17 h for substrate **3**).
3. Analyze the degree of hydrolysis by reverse-phase HPLC using a flow rate of 1.5 mL/min (*see Subheading 2.6* for mobile phase and column). Follow the elution at 225 nm for substrate **2** and **5** and at 254 nm for substrate **3**.

3.1.3 Hydrolysis of Substrate **4**

1. In a syringe reactor (*see Note 7*) add 2 mL of substrate **4** solution with 5 eq. of the selected ionic liquid and 0.4 g of immobilized enzyme.
2. Withdraw 50 μ L of reaction solution periodically (each 2 h up to 24 h).
3. Analyze the degree of hydrolysis by reverse-phase HPLC using a flow rate of 1 mL/min (*see Subheading 2.6* for mobile phase and column). Follow the elution at 210 nm.

3.1.4 Transesterification of **6**

1. In a glass bottle add 1 mL of reaction buffer and 23 μ L of substrate **7**. Then add 9 mL of **6** and set the pH at 7.0. To this solution add 62 mg of immobilized enzyme to start the reaction (*see* Fig. 2) and maintain under vigorous magnetic stirring (*see* **Note 8**).
2. Take 100 μ L of reaction solution periodically (each 2.5 min up to 30 min) and centrifuge at 30,000 $\times g$ for 10 min.
3. Take the supernatant and dilute five times and analyze the degree of synthesis by reverse-phase HPLC using a flow rate of 0.7 mL/min (*see* Subheading 2.6 for mobile phase and column). Follow the elution at 210 nm.

3.2 Hyperactivation of Lipases by Immobilization on Hydrophobic Supports

3.2.1 Immobilization of Lipase on Different Hydrophobic Supports

1. Wash different commercial supports (butyl, octyl-Sepharose; octadecyl-Sepabeads; butyl, hexyl-Toyopearl) (*see* Fig. 3) with three volumes of distilled water and drain (*see* **Note 8**).
2. Mix 10 mL of enzyme solution in 90 mL of immobilization buffer and 1 g of swollen support at 25 °C
3. Stir for 3 h at 25 °C (*see* **Note 9**).
4. Filter by vacuum and wash the solid five times with 100 mL distilled water.
5. Dry and store at 4 °C.

3.2.2 Hyperactivation of Lipases Resulting from the Interfacial Activation on Hydrophobic Supports

The immobilization of lipases on different supports (Sepharose, Sepabeads, or Toyopearl) with different degrees of hydrophobicity (butyl, hexyl, octyl, octadecyl groups) or adsorbed on an ionic support (Q-Sepharose) in the presence of detergent caused a significant increase in the lipase activity (hyper-activation) towards completely soluble substrates. Table 1 shows the hyperactivation on lipases from different sources by this technique in the hydrolysis of pNPP as model substrate. Table 2 shows the improvement in enzyme activity after immobilization of different lipases in the hydrolysis of **2**.

3.2.3 Lipase Immobilization on Cationic Q-Sepharose Support in the Presence of Detergent

1. Perform the **steps 1–4** described in Subheading 3.2.1.
2. Mix 1 g of immobilized enzyme in 10 mL of 0.5 % sucrose laurate solution in 25 mM sodium phosphate pH 7 at 25 °C for 1 h.
3. Measure the esterase lipase activity using the method described in Subheading 3.1.
4. Once the activity values of supernatant and suspension result equals filter the suspension by vacuum.
5. Wash Q-Sepharose commercial support with three volumes of distilled water and finally with one volume of 25 mM sodium phosphate pH 7 and drain (*see* **Note 8**).
6. Mix 10 mL of desorbed enzyme solution with 1 g of support at 25 °C.

Table 1
Hyperactivation of different lipases by immobilization on different supports measured in the hydrolysis of pNPP

Lipase	Support	Support modification	Activity ^a (%)
BTL2	Sepharose	Octyl	300
	Sepharose	Butyl	200
	Sepabeads	Octadecyl	120
	Toyopearl	Hexyl	200
	Toyopearl	Butyl	150
CAL-B	Sepharose	Octyl	200
	Sepabeads	Octadecyl	110
	Toyopearl	Hexyl	40
TLL	Sepharose	Octyl	2000
	Toyopearl	Butyl	60
CRL	Sepharose	Octyl	250
	Sepabeads	Octadecyl	110
RML	Sepharose	Octyl	750
	Sepabeads	Octadecyl	500
ANL	Sepharose	Octyl	180
	Sepabeads	Octadecyl	150
QL	Sepharose	Octyl	130
	Sepabeads	Octadecyl	130
LecitaseUltra	Sepharose	Octyl	220
TTL	Sepabeads	Octadecyl	400
CAL-A	Sepharose	Octyl	200
MJL	Sepharose	Octyl	300
PFL	Sepharose	Octyl	150
RNL	Sepharose	Octyl	600
RML ^b	Sepharose	Q	1,800

^a100 % was referred to the activity of the soluble lipase b measured in the hydrolysis of 1

^bIn presence of 0.5 % of lauryl sucrose

Table 2
Hyperactivation of different lipases by immobilization on different hydrophobic supports measured in the hydrolysis of substrate 2

Lipase	Support	Hydrophobic modification	Activity ^a (%)
BTL2	Sepabeads	Octadecyl	340
CAL-B	Sepharose	Octyl	400
	Sepabeads	Octadecyl	200
CRL	Sepharose	Octyl	600
	Sepabeads	Octadecyl	400
RML	Sepabeads	Octadecyl	2,000

^a100 % was referred to the activity of the soluble lipase

7. Stir for 1 h at 25 °C (*see Note 9*).
8. Filter by vacuum and wash the solid five times with 20 mL distilled water.
9. Dry and store at 4 °C.

3.3 Hyperactivation of Immobilized Lipases by Detergents

3.3.1 Determination of Enzymatic Activity in the Presence of Detergents

1. Add 2.5 mL assay buffer and 20 µL of substrate stock solution to a spectrophotometric cell and different concentrations (0.001–1 %, v/v) of Triton X-100, Triton X-45, SDS, sucrose laurate, or CTAB. Pre-incubate the mixture was at 25 °C for 2 min.
2. Measure the esterase lipase activity using the method described in Subheading 3.1.
3. 0.1 mL lipase suspension (1 g biocatalyst dissolved in 4 mL 25 mM sodium phosphate pH 7) was added to 2.5 mL of pNPP or **1** solution (*see Note 6*).

3.3.2 Hyperactivation of Immobilized Lipases by the Addition of Detergents

The presence of a particular concentration of detergents (Triton X-100, Triton X-45, CTAB, SDS, sucrose laurate) in the immobilized lipase suspension greatly enhanced the enzyme specific activity towards the hydrolysis of different substrates. Table 3 shows the hyperactivation by detergents at the best concentration to get the highest activity value for different covalent immobilized lipases in the hydrolysis of pNPP at pH 7 and 25 °C.

3.3.3 Hyperactivation of Immobilized Lipases by the Addition of Ionic Liquids

The presence of small amount of ionic liquids (i.e. [emim][BF₄], [bdmim][PF₆], and [emim][MeOSO₃]) in the immobilized lipase suspension can greatly enhance the enzyme specific activity. Table 4 shows the hyperactivation by addition of 5 eq. of ionic liquids for different RML derivatives in the hydrolysis of **4** at pH 7 and 25 °C.

Table 3
Increase of the lipase activity by the addition of different detergents

Biocatalyst	Detergent	Concentration ^a (w/v) (%)	Activity ^b (%)
Glyoxyl-PFL	Triton X-100	0.1	372
	Triton X-45	1	330
	CTAB	0.01	817
	SDS	0.1	117
CNBr-PFL	Triton X-100	0.01	293
	CTAB	0.01	613
	CTAB	0.01	800
CNBr-TLL	SDS	0.001	700
CNBr-BTL2	Triton X-100	0.01	275
Glyoxyl-BTL2	Triton X-100	0.1	290
CNBr-RML	Sucrose Laurate	0.5	1,000
CNBr-CAL-B	Triton X-100	0.1	239
	Triton X-45	0.1	196
	SDS	0.001	97

^aThe best concentration to get highest activity value

^b100 % was referred to the activity of the soluble lipase in the hydrolysis of pNPP

Table 4
Activity of different immobilized preparations of RML in the hydrolysis of substrate 4 in the presence of small amount of different ionic liquids (ILs)

Support	ILs ^a	Time (h)	Activity (%)
CNBr	–	144	100
	[emim][BF ₄]	144	136
	[bdmim][PF ₆]	144	168
Octyl	–	24	100
	[emim][BF ₄]	8	413
	[bdmim][PF ₆]	7	568
Q-Sepharose	–	48	100
	[emim][NO ₃]	72	27
	[emim][MeOSO ₃]	26	213

^a5 equivalents

3.4 Hyperactivation by Site-Directed Chemical Modification

3.4.1 Site-Specific Glycosylation of Immobilized Lipase with Polymers: Dextran-CHO

1. 20 mL of dext-CHO solution (Mr 1,500, 6,000, 20,000 Da) was added to 1 g of octyl-CalB (Subheading 3.2.1 for lipase immobilization) (0.5 mg of lipase/mL). Then the pH was set to 7.5 and maintain under gently stirring for 36 h.
2. Then add 20 mg of sodium borohydride. After 15 min, another 20 mg of sodium borohydride was added for 15 min.
3. Filter by vacuum and wash the solid five times with 100 mL of distilled water
4. Analyze the incorporation of the polymer to the immobilized enzyme by SDS-PAGE.
5. Dry and store at 4 °C.

3.4.2 Site-Specific Glycosylation of Immobilized Lipase with Polymers: Dextran-Gly

1. 20 mL of dext-Gly solution (Mr 1,500, 6,000, 20,000 Da) was added to 1 g of octyl-CalB (Subheading 3.2.1 for lipase immobilization) (0.5 mg of lipase/mL).
2. Then add 192 mg of EDC and maintain under gently stirrer for 1.5 h.
3. Filter by vacuum and wash the solid five times with 100 mL of distilled water.
4. Analyze the incorporation of the polymer to the immobilized enzyme by SDS-PAGE.
5. Dry and store at 4 °C.

3.4.3 Site-Specific Glycosylation of Immobilized Lipase with Polymers: PEG-COOH

1. 20 mL of PEG-COOH solution (Mr 1,500, 6,000, 20,000 Da) was added to 192 mg of EDC and 1 mg of DMAP, the pH was adjusted to 7.5.
2. Then 1 g of octyl-CalB (Subheading 3.2.1 for lipase immobilization) or 1 mL of CalB solution (0.5 mg of lipase/mL) was added to the polymer solution and maintain under gently stirrer for 48 h.
3. Filter by vacuum and wash the solid five times with 100 mL of distilled water.
4. Analyze the incorporation of the polymer to the soluble or immobilized enzyme by SDS-PAGE.
5. Dry and store at 4 °C.

3.4.4 Hyperactivation of Immobilized Lipases by Site-Directed Chemical Glycosylation

The chemical glycosylation of the *N*-terminal in immobilized CalB by different polymers (Dext-CHO, Dext-Gly and PEG-COOH) allowed improving the biocatalysts properties. Therefore, the formed immobilized glycosylated lipase biocatalysts showed enhanced activity towards different substrates [21]. Table 5 shows the hyperactivation values of different chemical glycosylated biocatalysts in the hydrolysis of substrates **1** y **5** and the synthesis of butyryl ester of **6** at pH 7 and 25 °C.

Table 5
Improvement of the activity of Octyl-CalB preparations by solid-phase glycosylation

Biocatalyst	Activity (%) ^a		
	1	5	6 + 7
Cal-B	100 (12.1) ^b	100 (2.8) ^b	100 (3.0) ^{b, c}
Cal-B-Dext-1500	134	244	228
Cal-B-Dext-gly-1500	183	278	–
Cal-B-Dext-6000	196	331	238
Cal-B-Dext-20000	171	306	–
Cal-B-PEG-1500	192	91	–
Cal-B-PEG-35000	188	263	–
Cal-B-NH ₂	125	93	214
Cal-B-NH ₂ -Dext-1500	252	92	214

^a100 % was referred to the activity of the non-modified catalyst

^bSpecific activity of non-modified Cal-B defined as $\mu\text{mol}/\text{min}/\text{mg}_{\text{lip}}$

^cSpecific activity of synthesis of glyceryl ester

3.4.5 Site-Directed Modification of Immobilized Lipases with Tailor-Made Polymers. Preparation of PDP-Activated Dext-NH₂ Polymers

1. Mix 30 mL of Dext-NH₂ solution (14 mg/mL) with 9 mL of polymer buffer and 1 mL of SPDP-Dext solution.
2. Maintain under magnetic stirring for 2 h at 25 °C.
3. Dialyze the solution three times against distilled water.
4. Store the solution at 4 °C.

3.4.6 Site-Directed Modification of Immobilized Lipases with Tailor-Made Polymers. Preparation of PDP-Activated PEG-COOH Polymers

1. Add drop wise 0.5 mL of SPDP-PEG solution to 0.6 mL of PEG-COOH solution. 100 mg of COOH-PEG-OH were dissolved in 0.6 mL of chloroform.
2. Add a catalytic amount of DMAP (*see Note 10*).
3. Maintain under magnetic stirring for 24 h at 25 °C and afterwards take the reaction mixture to dryness (*see Note 11*).
4. Treat the solid residue with 15 mL of assay buffer and dialyze using 200–500 Da cut-off membrane (3 volumes of 1 L water) at 25 °C. Store at 4 °C.

3.4.7 Site-Directed Modification of Immobilized Lipases

1. Treat CNBr-BTL2 derivative (*see Note 12*) with DTT solution for 30 min (*see Note 13*).
2. Dissolve 0.345 mL of polymer solution (Subheading 3.4.1 or 3.4.2) in 2.7 mL of modification buffer. Adjust the final pH at 8.0. Then add 0.2 g of reduced BTL2 immobilized preparation.

Table 6
Improvement of the hydrolytic activity of CNBr-BTL2 preparations by site-specific modification

Modification	Activity (%) ^a		
	1	2	3
–	100 (10.0) ^b	100 (2.1) ^b	100 (0.8) ^c
Dext1500-NH ₂	193	249	61
Dext6000-NH ₂	174	226	107
PEG1500-COOH	186	280	208
PEG35000-COOH	162	143	113

^a100 % was referred to the activity of the non-modified catalyst

^bSpecific activity of non-modified octyl-Cal-B defined as $\mu\text{mol}/\text{min}/\text{mg}_{\text{lip}}$

^cSpecific activity of non-modified octyl-Cal-B defined as $\text{nmol}/\text{h}/\text{mg}_{\text{lip}}$

- Analyze the supernatant at 343 nm (*see Note 14*) after 1 h incubation.
- Analyze the incorporation of the polymer to the enzyme by S-S interaction (thiol-disulfide exchange) by SDS-PAGE using the lipase in solution by the following procedure: reduce with DTT solution for 30 min the lipase on octyl-agarose, desorb with Triton solution for 45 min and afterwards immobilize on Q-Sepharose at pH 10.2 for 20 min. After that, the modification procedure is performed and the modified enzyme must be immediately desorbed using NaCl solution.
- Filter by vacuum and wash the solid five times with 100 mL distilled water.
- Dry and store at 4 °C.

3.4.8 Hyperactivation of Immobilized Lipases by Site-Directed Chemical Modification with Tailor-Made Polymers

The site-directed modification of Cys64 in immobilized BTL2 by tailor-made disulfide activated polymers (Dext-NH₂, PEG-COOH) permitted to enhance the specific activity of the native enzyme towards different soluble substrates [20]. Table 6 shows the hyperactivation values after modification with different polymers with different molecular mass in the hydrolysis of three different substrates 1–3 at pH 7 and 25 °C.

4 Notes

- However, detergents at concentrations higher than 1 % normally inhibit the lipase activity.
- These lipases are sold in liquid form.
- These lipases are sold as a powder.

4. This is a recombinant lipase produced in *E. coli* in collaboration with ICTAN-CSIC and it is in liquid form.
5. 348 nm corresponds to the maximum absorbance (isoblastic point of *p*-nitrophenol), but in the case that this wavelength is not available, it is possible to measure the *p*-nitrophenol at wavelengths between 348 and 415 nm.
6. To take suspension the micropipette tips have to be cut.
7. The reaction was performed in a special syringe reactor and samples were simply obtained by pushing the piston and dropping 100 μ L of sample. Other systems such as glass vessels or plastic bottles with screw top can be used.
8. Cause of the high viscosity of reaction media is mandatory a vigorous stirring agitation ($3,000 \times g$).
9. These supports are commercial available dissolved in ethanol solution. Then the suspension is filtrated on a funnel with fritted disk under vacuum to eliminate ethanol. Then 200 mL of distilled water is added to the funnel and the suspension is stirred using a spatula. After 30 s, the liquid is filtrated and procedure is repeated at least five times. Then, the liquid is removed under vacuum and the solid is recovered.
10. Maintain in a roller stirrer to avoid the breaking of the resin. Avoid use magnetic stirring or other kind of aggressive stirring methods.
11. A spatula tip of DMAP was used.
12. Solvent was removed by using an evaporator.
13. The enzyme was purified from *E. coli* crude extract by interfacial adsorption on butyl-Sepharose (*see* Subheading 3.2.1). The lipase was desorbed from the support adding 20 mL of 25 mM phosphate buffer pH 7 with 0.5 % triton X-100 (v/v) per gram of support. After that, 10 mL of lipase solution was added to 1 g of CNBr-activated support (previously swollen in acidic solution aqueous HCl solution at pH 3 for 1 h and just filtered to draining using a vacuum pump) for 15 min at 4 °C to obtain a one-point covalent attachment of the lipase on the support. Periodically, activity of suspensions and supernatants was measured (*see* Subheading 3.1.1). The enzyme-support immobilization was ended by incubating the support with 1 M ethanolamine at pH 8 for 2 h. Finally, the immobilized preparation was washed with abundant water (5×200 mL) to eliminate the detergent. The immobilization yield was >95 % obtaining a biocatalyst of $4 \text{ mg}_{\text{lipase}}/\text{g}_{\text{support}}$.
14. To maintain the Cys64 thiol in a reduced form.
15. The reaction was followed spectrophotometrically by the release of 2-mercaptopyridine, which quickly tautomerizes into 2-thiopyridone which has an absorption maximum at 343 nm (molar extinction coefficient at 343 nm: $8,080 \text{ M}^{-1} \text{ cm}^{-1}$).

Acknowledgments

This work has been sponsored by the Spanish Ministry of Science and Innovation (AGL-2009-07526) and the CSIC by Intramural project (200980I133). The authors are grateful to CSIC for the JAE-DOC contract of M.F. and to CONICYT and Programa Bicentenario Becas-Chile for financial support of O.R.

References

- Patel RN (2006) Biocatalysis: synthesis of chiral intermediates for pharmaceuticals. *Curr Org Chem* 10:1289–1321
- Fukuda H, Hama S, Tamalampudi S, Noda H (2008) Whole-cell biocatalysts for biodiesel fuel production. *Trends Biotechnol* 26:668–673
- Verger R (1997) Interfacial activation of lipases: facts and artifacts. *Trends Biotechnol* 15:32–38
- Brzozowski AM, Derewenda U, Derewenda ZS, Dodson GG, Lawson DM, Turkenburg JP, Bjorkling F, Høge-Jensen B, Patkar SA, Thim L (1991) A model for interfacial activation in lipases from the structure of a fungal lipase-inhibitor complex. *Nature* 351:491–494
- Derewenda U, Brzozowski AM, Lawson DM, Derewenda ZS (1992) Catalysis at the interface: the anatomy of a conformational change in a triglyceride lipase. *Biochemistry* 31:1532–1541
- Lowrier A, Drtina GJJ, Klivanov AM (1996) On the issue of interfacial activation of lipase in non-aqueous media. *Biotechnol Bioeng* 50:1–5
- Sarda L, Desnuelle P (1958) Actions of pancreatic lipase on esters in emulsions. *Biochim Biophys Acta* 30:513–521
- Bastida A, Sabuquillo P, Armisen P, Fernández-Lafuente R, Hugué J, Guisán JM (1998) A single step purification, immobilization and hyperactivation of lipases via interfacial adsorption on strongly hydrophobic supports. *Biotechnol Bioeng* 58:486–493
- Palomo JM, Muñoz G, Fernández-Lorente G, Mateo C, Fernández-Lafuente R, Guisán JM (2002) Interfacial adsorption of lipases on very hydrophobic support (octadecyl-Sepabeads): immobilization, hyperactivation and stabilization of the open form of lipases. *J Mol Catal B Enzym* 19–20:279–286
- Fernández-Lorente G, Cabrera Z, Godoy C, Fernández-Lafuente R, Palomo JM, Guisán JM (2008) Interfacially activated lipases against hydrophobic supports: effect of the support nature on the biocatalytic properties. *Process Biochem* 43:1061–1067
- Mogensen JE, Sehgal P, Otzen DE (2005) Activation, inhibition, and destabilization of *Thermomyces lanuginosus* lipase by detergents. *Biochemistry* 44:1719–1730
- Fishman A, Cogan U (2003) Bio-imprinting of lipases with fatty acids. *J Mol Catal B Enzym* 22:193–202
- Lopez-Serrano P, Cao L, Van Rantwijk F, Sheldon RA (2002) Cross-linked enzyme aggregates with enhanced activity: application to lipases. *Biotechnol Lett* 24:1379–1383
- Filice M, Marciello M, Betancor L, Carrascosa AV, Guisán JM, Fernández-Lorente G (2011) Hydrolysis of fish oil by hyperactivated rhizomucor miehei lipase immobilized by multipoint anion exchange. *Biotechnol Prog* 27(4):961–968
- Fernández-Lorente G, Palomo JM, Mateo C, Munilla R, Ortiz C, Cabrera Z et al (2006) Glutaraldehyde crosslinking in the presence of detergents of lipases adsorbed on aminated supports: improving lipases performance. *Biomacromolecules* 7:2610–2615
- Palomo JM, Segura RL, Fernández-Lorente G, Guisán JM, Fernández-Lafuente R (2007) Glutaraldehyde modification of lipases adsorbed on aminated supports: a simple way to improve their behaviour as enantioselective biocatalyst. *Enzyme Microb Technol* 40:704–707
- Palomo JM, Fuentes M, Fernández-Lorente G, Mateo C, Guisán JM, Fernández-Lafuente R (2003) General trend of lipase to self-assemble giving bimolecular aggregates greatly modifies the enzyme functionality. *Biomacromolecules* 4:1–6
- Helenius A, Simons K (1975) Solubilization of membranes by detergents. *Biochem Biophys Acta* 415:29–79
- Filice M, Guisán JM, Palomo JM (2010) Effect of ionic liquids as additives in the catalytic properties of different immobilized preparations of *Rhizomucor miehei* lipase in the hydrolysis of peracetylated lactal. *Green Chem* 12:1365–1369

20. Hackenberger CPR, Schwarzer D (2008) Chemoselective ligation and modification strategies for peptides and proteins. *Angew Chem Int Ed* 47:10030–10074
21. Gutarra MLE, Romero O, Abian O, Torres FAG, Freire DMG, Castro AM, Guisan JM, Palomo JM (2011) Enzyme surface glycosylation in the solid phase: improved activity and selectivity of *Candida antarctica*. *ChemCatChem* 3:1902–1910
22. Chalker JM, Bernardes GJL, Lin YA, Davis BG (2009) Chemical modification of proteins at cysteine: opportunities in chemistry and biology. *Chem Asian J* 4:630–640
23. Godoy C, de las Rivas B, Filice M, Fernández-Lorente G, Guisan JM, Palomo JM (2010) Enhanced activity of an immobilized lipase promoted by site-directed chemical modification with polymers. *Process Biochem* 45:534–541

Chapter 18

High Activity Preparations of Lipases and Proteases for Catalysis in Low Water Containing Organic Solvents and Ionic Liquids

Ipsita Roy, Joyeeta Mukherjee, and Munishwar Nath Gupta

Abstract

Simple precipitation of enzymes has shown impressive catalytic efficiencies in organic solvents. Inasmuch as these can be recovered after the reaction, these can be viewed as immobilized preparations just like more extensively used cross-linked enzyme aggregates (CLEAs). This chapter describes three protocols which use these enzyme precipitated and rinsed with propanol/some other appropriate organic solvent. The first two protocols show their applications in ionic liquids for a transesterification reaction and a kinetic resolution. The third protocol presumably incorporates an “imprinting” effect so that the precipitates are now able to efficiently catalyze transesterification of tributyrin with tertiary alcohols.

Key words Enzymes in organic solvent, Enzymes in ionic liquids, Kinetic resolution by enzymes, Transesterification reactions, Enzyme precipitation, Lipases, Proteases, Biotransformation with tertiary alcohols, Enzyme imprinting

1 Introduction

Use of hydrolases for synthesis in non aqueous media containing very low amount of water is now well established [1–5]. This is a relatively new area of enzymology and our understanding of various reaction parameters (and their interrelationship) is slowly emerging. Most of the early work in this area was carried out with lyophilized powders. About a decade back, it became clear that very low catalytic activity observed in non aqueous enzymology was largely due to this practice [6, 7]. Currently, it is common to use commercially available immobilized enzymes [Novozyme 435, an immobilized form of CaL B is a good example of this practice], which are relatively expensive. At the same time, some other enzyme formulations have been described as high activity preparations or high performance enzyme preparations for use in low water media. These are exemplified by Cross-Linked Enzyme

Crystals (CLEC) [8], Cross-Linked Enzyme Aggregates (CLEA) [9], Propanol Rinsed Enzyme Preparations (PREP) [10], Three Phase Partitioned (TPP) enzymes [11, 12], Protein Coated Micro Crystals (PCMC) [13], and Cross-Linked Protein Coated Micro Crystals (CLPCMC) [14, 15]. A common feature of all these preparations is that the buffer (the media in which enzymes are normally present after purification) is not removed by freeze drying/spray drying. This circumvents the problems associated with structural changes in proteins due to lyophilization [6, 16]. Instead, crystallization (in the case of CLEC) or precipitation (CLEA, TPP treated enzymes, PCMC, CLPCMC) by (mostly) organic solvents is used for “drying” of the enzyme. A similar formulation, using propanol as the solvent, is called Enzyme Precipitated and Rinsed with Propanol (EPRP) [17]. In some cases, other solvents were found to be more appropriate [18] and a more general name, Enzyme Precipitated and Rinsed with Organic Solvent (EPROS) was used to describe such preparations. The present chapter describes some successful applications of this simplest formulation. This formulation can only be included in the list of immobilized preparations by interpreting the term in its broadest sense; these precipitates remain insoluble in the reaction media, and can be recovered for reuse. This is in agreement with the current thinking that CLEAs, the enzyme aggregates (without any support), are considered immobilized enzymes [19].

While nearly anhydrous organic solvents have dominated the reaction media in non aqueous enzymology; ionic liquids have been fast emerging as attractive options [12, 20, 21]. A protocol described in this chapter (*see* Subheading 3.1) illustrates how these simple formulations (of protease subtilisin Carlsberg protein) worked very well in ionic liquids. The improvement in initial rates as compared to when lyophilized powders are used was significant (*see* Table 1, Fig. 1). The second protocol (*see* Subheading 3.2) describes an application for a widely used lipase (from *Candida rugosa*) for kinetic resolution of (\pm)-1-phenylethanol in an ionic liquid (*see* Fig. 2). Enzymatic methods for obtaining chirally pure compounds are emerging as a powerful approach in organic synthesis for application in the area of drug intermediates, agrochemicals and material sciences [22, 23]. Again, the comparison with lyophilized powders shows the advantage of using EPRPs (*see* Table 2, Scheme 1). The third protocol (*see* Subheading 3.3) describes a somewhat different application and one which needs wider exploration. Transformation of *t*-alcohols and their esters by most of the lipases is extremely slow or not possible [24, 25]. Only few lipases, with space available in their active sites to accommodate the *t*-alkyl groups, can carry it out. Protocol described in Subheading 3.3 shows that a simple precipitation with a *t*-alcohol

Table 1
Transesterification catalyzed by different preparations of subtilisin
in ionic liquid [Bmim][PF₆]

Enzyme preparation	Initial rates (mmol/h/mg)	Times increase
pH tuned subtilisin	0.01	1
Subtilisin ^a	0.10	10
Subtilisin ^b	0.03	3
Subtilisin ^c	0.32	24
EPRP of subtilisin	41.60	4,160

All experiments were done in duplicate and the results within each pair differed by <3 %. (Reprinted from Obtaining high transesterification activity for subtilisin in ionic liquids, with permission from Elsevier)

^aLyophilized with 1 % (w/w) PEG 6000

^bLyophilized with 2 % (w/w) trehalose

^cLyophilized with 1 % (w/w) PEG 6000 and 2 % (w/w) trehalose

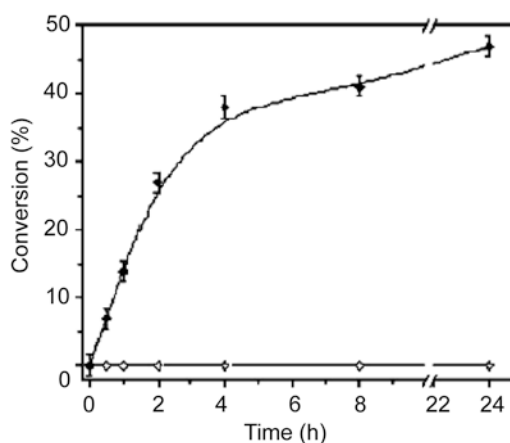


Fig. 1 Time course of transesterification reaction catalyzed by different preparations of subtilisin in [Bmim][BF₄]: lyophilized subtilisin (*diamond*) and EPRP of subtilisin (*open circle*). (Reprinted from Obtaining high transesterification activity for subtilisin in ionic liquids, with permission from Elsevier)

helps (*see* Fig. 3). It also probably involves some “imprinting” effects [26]. The protocol involves employing one of the substrates, tributyrin (taken in excess), as the reaction medium. Such media are sometimes called solvent free media and certain advantages are associated with this approach [27].

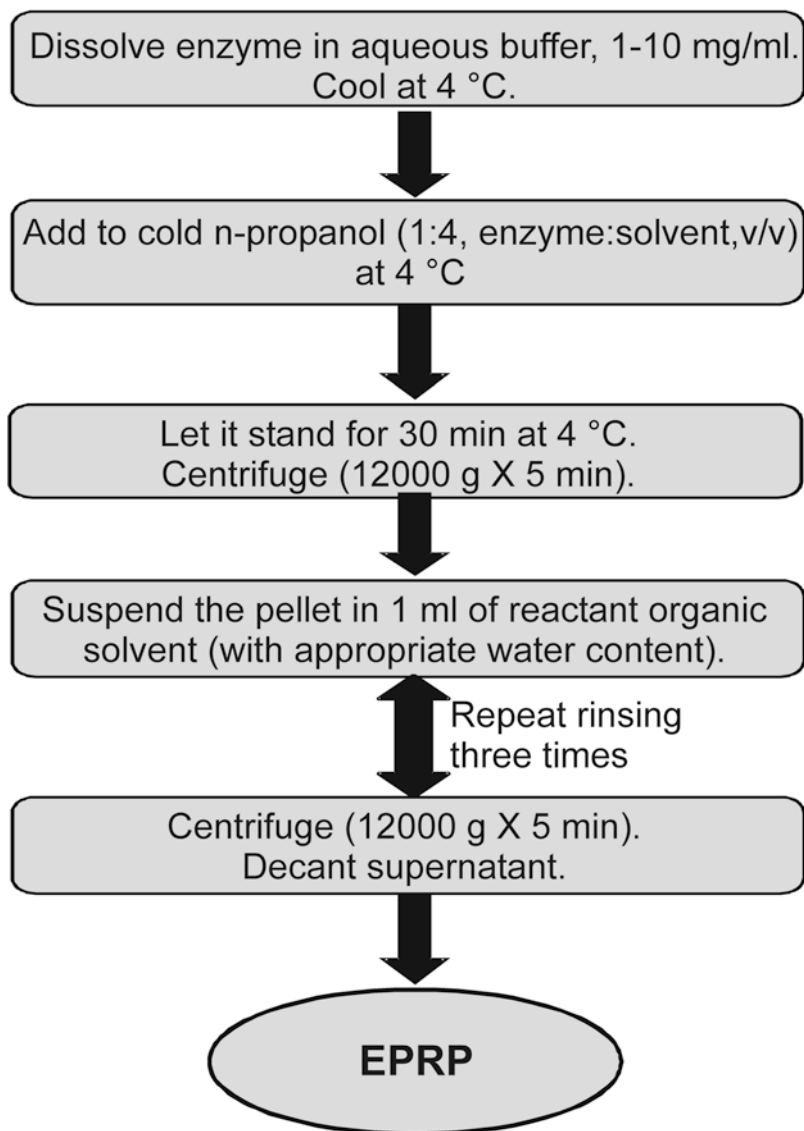


Fig. 2 Protocol for preparation of EPRP. In the present case, the precipitated enzyme was rinsed with *n*-propanol since the organic solvent was the substrate as well as the solvent. (Reprinted from Obtaining high transesterification activity for subtilisin in ionic liquids, with permission from Elsevier)

A few papers (unfortunately literature comparing catalytic efficiency of various formulations is scarce) show that other formulations may be better for catalyzing some biotransformation [15, 28]. However, EPRP/EPROS are extremely simple to obtain. It should be pointed out that precipitation with organic solvents may lead to simultaneous purification of the enzyme activity present in starting commercial preparations [19].

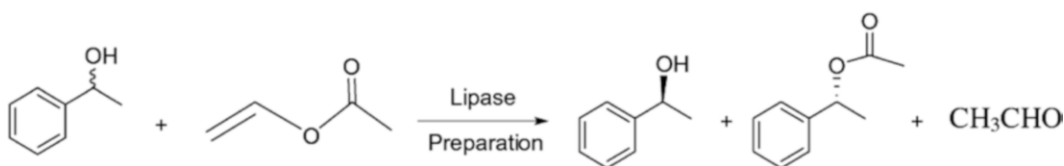
Table 2

Kinetic resolution of (\pm)-1-phenylethanol in [Bmim][PF₆] catalyzed by *Candida rugosa* lipase and its EPRP preparation, measured by HPLC

Enzyme preparation	Time (h)	Conversion (%)	ee _p (%)	ee _s (%)	E ^a
pH tuned	12	5	80	5	11
pH tuned	24	7	83	6	12
EPRP	12	22	97	28	123
EPRP	24	26	98	34	153

(Reprinted from Kinetic resolution of (\pm)-1-phenylethanol in [Bmim][PF₆] using high activity preparations of lipases, with permission from Elsevier)

^a $E = \ln[1 - c(1 + ee_p)] / \ln[1 - ce_p]$, where $c = ee_s / (ee_s + ee_p)$



Scheme 1 Kinetic resolution of (\pm)-1-phenylethanol with vinylacetate in ionic liquid. (Reprinted from Kinetic resolution of (\pm)-1-phenylethanol in [Bmim][PF₆] using high activity preparations of lipases, with permission from Elsevier)

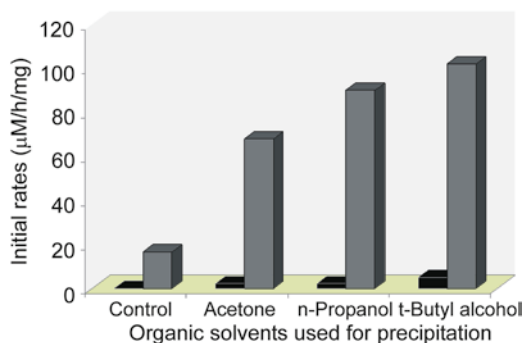


Fig. 3 Transesterification of *t*-butyl alcohol with tributyrin under solvent free conditions. In the control freeze dried preparation of the enzyme was used. 1 mL reaction medium containing tertiary alcohol (1 M) in excess tributyrin [29] was incubated with 10 mg lipase formulations at 20 °C under constant shaking at 250 rpm for 72 h. Initial rates were based upon conversions obtained by gas chromatography analysis. The reactions were carried out with 0 % water added (w/w enzyme) (black bars) and 3 % water added (w/w enzyme) (grey bars) [18]

2 Materials

2.1 Formation of EPRP of Subtilisin Carlsberg and *Candida rugosa* Lipase

1. Subtilisin Carlsberg (Type VII, Sigma Aldrich, St. Louis, USA).
2. Lipase from *Candida rugosa* (lipase AYS, Amano Enzymes Inc., Nagoya, Japan).
3. *n*-Propanol (>99 %, Sigma Aldrich, St. Louis, USA).

2.2 Transesterification Reaction of *N*-Acetyl-L-phenylalanine ethyl ester and *n*-Propanol by Subtilisin Carlsberg in Ionic Liquids

1. [Bmim][PF₆] (Acros Organics, New Jersey, USA) (99.6 % pure by HPLC, water content of 0.05 %, v/v, by Karl Fischer titration, as specified by the manufacturer) (*see Note 1*).
2. [Bmim][BF₄] (Acros Organics, New Jersey, USA) (97.5 % pure by NMR, water content of <0.1 %, v/v, by Karl Fischer titration, as specified by the manufacturer) (*see Note 1*).
3. *N*-acetyl-L-phenylalanine ethyl ester (Sigma Aldrich, St. Louis, USA).
4. Acetonitrile (anhydrous grade (containing <0.2 % water), J. T. Baker, Griesheim, Germany).
5. Acetic Acid (Merck, Hohenbrunn, Germany).
6. C18 column (we used Zorbax SB-C18 column, Agilent Technologies, USA).

2.3 Kinetic Resolution of (±)-1-Phenylethanol with Vinyl Acetate

1. (±)-1-Phenylethanol (Merck, Hohenbrunn, Germany).
2. Vinyl acetate (Merck, Hohenbrunn, Germany).
3. *n*-Hexane (anhydrous grade, J. T. Baker, Griesheim, Germany).
4. *i*-propanol (anhydrous grade, J. T. Baker, Griesheim, Germany).
5. Ethanol (anhydrous grade, J. T. Baker, Griesheim, Germany).
6. Chiracel OD-RH column, Diacel, Japan.

2.4 Solvent Free Transesterification Reaction Between Tributyrin and *t*-Alkyl Alcohols

1. Tributyrin (>99 %, Himedia Laboratories Pvt. Ltd., Mumbai, India).
2. *t*-Butyl alcohol (>98 %, Merck, Mumbai, India) (*see Note 2*).
3. *t*-Amyl alcohol (>99 %, Merck, Hohenbrunn, Germany) (*see Note 2*).
4. EQUITY™-5 30 m × 0.32 mm × 0.25 μm film thickness, Supelco, Bellefonte, USA.

3 Methods

3.1 EPRP (Enzyme Precipitated and Rinsed with *n*-Propanol) as a High Performance Biocatalyst Design for the Enhancement of Transesterification Rates in Ionic Liquids

1. Dissolve subtilisin Carlsberg (1 mg) in 1 mL of 0.02 M sodium phosphate buffer, pH 7.8.
2. Add the above solution dropwise to dry chilled *n*-propanol (4 mL) at 4 °C and let it stand for 30 min at 4 °C (*see Note 3*).
3. Centrifuge the suspension at 12,000 × *g* for 5 min.
4. Decant supernatant. Rinse with ice-cold *n*-propanol containing 0.5 % (v/v) water followed by **step 3**.
5. Repeat this rinsing three times.

3.1.1 Formation of EPRP of Subtilisin Carlsberg (See Fig. 1)

3.1.2 Transesterification
**Reaction of *N*-Acetyl-L-
PHENYLALANINE ethyl ester
and *n*-Propanol by
Subtilisin Carlsberg
in Ionic Liquids**

1. Dissolve *N*-acetyl-L-phenylalanine ethyl ester (20 mM) and *n*-propanol (0.85 mM) in 1 mL of [Bmim][PF₆].
2. Add the enzyme formulation as prepared in Subheading 3.1.1.
3. Incubate at 40 °C in an orbital shaker with constant shaking (200 rpm).
4. Withdraw 20 µL samples each after different time intervals and analyze by HPLC.
5. Dilute samples four times with acetonitrile.
6. Inject into a C18 column.
7. Elute the substrates and products with 60 % aqueous acetic acid (1 %, v/v), 40 % acetonitrile, at a flow rate of 1 mL/min.
8. Detect the product formed at 258 nm using a UV detector (*see* **Note 4**).
9. Calculate the rate of formation of product.

**3.2 Kinetic
Resolution of
(±)-1-Phenylethanol
by EPRP of *Candida
rugosa* Lipase in Ionic
Liquids**

**3.2.1 Formation of EPRP
of *Candida rugosa* Lipase**

1. Dissolve *Candida rugosa* lipase (10 mg) in 1 mL of 0.05 M sodium phosphate buffer, pH 7.0.
2. Add the above solution dropwise to dry chilled *n*-propanol (4 mL) at 4 °C and let it stand for 30 min at 4 °C.
3. Centrifuge the suspension at 12,000 × *g* for 5 min.
4. Decant supernatant. Rinse with dry chilled *n*-propanol and repeat **step 3**.
5. The rinsing was repeated twice (*see* **Note 5**).

**3.2.2 Kinetic Resolution
of (±)-1-Phenylethanol
with Vinyl Acetate by
Candida rugosa Lipase**

1. Take the enzyme formulation (prepared from 10 mg solid enzyme powder) as prepared in Subheading 3.2.1 in a screw-capped vial.
2. Add 1 mmol of (±)-1-phenylethanol and 1 mmol of vinyl acetate in a total volume of 1 mL of [Bmim][PF₆].
3. Incubate at 35 °C in an orbital shaker with continuous shaking at 250 rpm.
4. Withdraw aliquots (50 µL each) after different time intervals.
5. Extract with 500 µL of *n*-hexane-*i*-propanol (97.5:2.5, v/v).
6. Inject into a chiral column and elute with *n*-hexane-*i*-propanol-ethanol (96.5:3.0:0.5, v/v/v) as the mobile phase at 1 mL/min.
7. The product is detected at 254 nm using a UV detector (*see* **Note 6**).

3.3 EPROS (Enzyme Precipitated and Rinsed with Organic Solvents) as a Lipase Preparation for Biotransformation in Transesterification of *t*-Alkyl Alcohols

3.3.1 Formation of EPROS of *Candida rugosa* Lipase

1. Dissolve *Candida rugosa* lipase (10 mg) in 0.05 M sodium phosphate buffer, pH 7.0 (100 μ L).
2. Add the enzyme solution dropwise in ice-cold anhydrous organic solvent and allow to stand for 1 h at 4 °C.
3. Centrifuge at 9,000 $\times g$ for 5 min at 4 °C.
4. Discard the supernatant. Rinse the precipitate with 1.5 mL of ice-cold precipitating solvent (either anhydrous or containing a defined amount of water).
5. Centrifuge at 9,000 $\times g$ for 5 min at 4 °C.
6. Repeat **steps 4** and **5** three times.

3.3.2 Solvent Free Transesterification Reaction Between Tributyrin and *t*-Alkyl Alcohols by *Candida rugosa* Lipase

1. Take the enzyme formulation (as prepared in Subheading **3.3.1**, from 10 mg of solid enzyme powder) in a screw-capped vial.
2. Add *t*-butyl alcohol or *t*-amyl alcohol (*see* **Note 7**) containing water in tributyrin such that the final concentration of the alcohol is 1 M and the concentration of water is 3 % (w/enzyme w) in a total volume of 1 mL.
3. Incubate at 20 °C in an orbital shaker with constant shaking (250 rpm).
4. Withdraw aliquots at different time intervals and analyze by gas chromatography.
5. Inject aliquots into a capillary column fitted into a gas chromatograph (we used Agilent 6890 N) with a flame ionization detector.
6. Program the initial oven temperature at 100 °C; increase the temperature at 10 °C/min up to 150 °C followed by a ramp rate of 15 °C/min till 250 °C.
7. Assign retention times of products by running authentic samples (*see* [18] for the protocol for purification of authentic samples).

4 Notes

1. Ionic liquids are highly unstable species and proper storage facilities need to be used for them. We use vacuum desiccators with anhydrous CaCl₂. All experiments need to be carried out in air-tight vessels. Special care also needs to be taken to ensure that HF fumes are not generated. For these reasons, it is recommended that old bottles of ionic liquids should not be used.
2. All alcohols were distilled and dried overnight on 3 Å molecular sieves before use.

3. The aqueous enzyme solution should be added to the organic solvent and not vice versa as it sometimes causes greater denaturation of the enzyme [28].
4. The substrate peak appears at a retention time of ~2.1 min and the product (*N*-acetyl-L-phenylalanine propyl ester) appears at ~2.5 min. The ionic liquid [Bmim][PF₆] appears as a small peak at ~1.7 min.
5. Rinse the precipitate twice with 1 mL of chilled vinyl acetate before use for kinetic resolution.
6. The peak corresponding to vinyl acetate appears at ~2.4 min and the enantiomers of 1-phenylethanol appear at 5.7 and 7.1 min. The product 1-phenylethyl acetate also appears as enantiomers at ~2.8 and 3.1 min.
7. Precipitation in *t*-alkyl alcohol leads to greater transesterification rates when the same alcohol is used as one of the substrates. This may be due to some marginal “imprinting effect” of the kind observed by Stähl et al. [26] while precipitating an enzyme in the presence of a substrate [18].

Acknowledgments

The authors thank Dr. Shweta Shah and Dr. Abir B. Majumder for the work described in this chapter. Financial support from the Department of Science and Technology (DST-SERB) [Grant No.: SR/SO/BB-68/2010], the Department of Biotechnology (DBT) [Grant No: BT/PR14103/BRB/10/808/2010], and Council for Scientific and Industrial Research (CSIR), all Government of India organizations, is gratefully acknowledged.

References

1. Mattiasson B, Adlercreutz P (1991) Tailoring the microenvironment of enzymes in water poor systems. *Trends Biotechnol* 9:394–398
2. Gupta MN (1992) Enzyme function in organic solvents. *Eur J Biochem* 203:25–32
3. Halling PJ (2000) Biocatalysis in low-water media: understanding effects of reaction conditions. *Curr Opin Chem Biol* 4:74–80
4. Carrea G, Riva S (2000) Properties and synthetic applications of enzymes in organic solvent. *Angew Chem Int Ed Engl* 36:2226–2254
5. Grunwald P (2009) *Biocatalysis: biochemical fundamentals and applications*. Imperial College Press, London
6. Lee M-Y, Dordick JS (2002) Enzyme activation for nonaqueous media. *Curr Opin Biotechnol* 13:376–384
7. Gupta MN, Roy I (2004) Enzymes in organic media: forms, functions and applications. *Eur J Biochem* 271:1–9
8. Govardhan CP (1999) Crosslinking of enzymes for improved stability and performance. *Curr Opin Biotechnol* 10:331–335
9. Sheldon RA (2007) Enzyme immobilization: the quest for optimum performance. *Adv Synth Catal* 349:1289–1307
10. Partridge J, Halling PJ, Moore BD (1998) Practical route to high activity enzyme preparations for synthesis in organic media. *Chem Commun* 841–842
11. Roy I, Sharma A, Gupta MN (2004) Obtaining high transesterification rates with Subtilisin Carlsberg in non-aqueous media. *Bioorg Med Chem Lett* 14:887–889

12. Shah S, Gupta MN (2007) Obtaining high transesterification activity for subtilisin in ionic liquids. *Biochim Biophys Acta* 1770:94–98
13. Kreiner M, Moore BD, Parker MC (2001) Enzyme-coated microcrystals: a 1-step method for high activity biocatalyst preparation. *Chem Commun* 1096–1097
14. Shah S, Sharma A, Gupta MN (2008) Cross-linked protein-coated micro-crystals as biocatalysts in non aqueous solvents. *Biocatal Biotransfor* 26:266–271
15. Kapoor M, Gupta MN (2012) Obtaining monoglycerides by esterification of glycerol with palmitic acid using some high activity preparations of *Candida antarctica* lipase B. *Process Biochem* 47:503–508
16. Roy I, Gupta MN (2004) Freeze-drying of proteins: some emerging concerns. *Biotechnol Appl Biochem* 39:165–177
17. Roy I, Gupta MN (2004) Preparation of highly active alpha chymotrypsin for catalysis in organic media. *Bioorg Med Chem Lett* 14:2191–2193
18. Majumder AB, Gupta MN (2011) Increasing catalytic efficiency of *Candida rugosa* lipase for the synthesis of tert-alkyl butyrates in low-water. *Biocatal Biotransfor* 29:238–245
19. Schoevaart R, Wolbers MW, Golubovic M, Ottens M, Kieboom APG, van Rantwijk F, van der Wielen LAM, Sheldon RA (2004) Preparation, optimization and structures of cross-linked enzyme aggregates (CLEAs). *Biotechnol Bioeng* 87:754–762
20. Irimescu R, Kato K (2004) Investigation of ionic liquids as reaction media for enzymatic enantioselective acylation of amines. *J Mol Catal B Enzym* 30:189–194
21. Moniruzzaman M, Nakashima K, Kamiya N, Goto M (2010) Recent advances of enzymatic reactions in ionic liquids. *Biochem Eng J* 15: 295–314
22. Patel RN (ed) (2000) *Stereoselective biocatalysis*. Marcel Dekker, New York
23. Gotor V, Alfonso I, Garcia-Urdiales E (2008) *Asymmetric organic synthesis with enzymes*. Wiley-VCH Verlag GmbH & Co. KGaA, Weinheim, Germany
24. O'Hagan D, Zaidi NA (1994) The resolution of tertiary α -acetylene-acetate esters by the lipase from *Candida cylindracea*. *Tetrahedron Asymmetry* 5:1111–1118
25. Bosley JA, Casey J, Macrae AR, Mycock G (1997) Process for the esterification of carboxylic acids with tertiary alcohols using a lipase from *Candida antarctica*. US patent 5658769, 5, 658–769
26. Stähl M, Månsson M-O, Mosbach K (1990) The synthesis of a D-amino acid ester in an organic media with alpha-chymotrypsin modified by a bio-imprinting procedure. *Biotechnol Lett* 13:161–166
27. Shah S, Gupta MN (2007) Lipase catalysed preparation of biodiesel from Jatropha oil in a solvent free system. *Process Biochem* 42: 409–414
28. Solanki K, Gupta MN, Halling PJ (2012) Examining structure–activity correlations of some high activity enzyme preparations for low water media. *Bioresour Technol* 115: 147–151
29. Zaks A, Klibanov AM (1994) Enzyme catalysis in organic media at 100 °C. *Science* 224: 1249–1251

Biomedical Applications of Immobilized Enzymes: An Update

Marta Pastor, Amaia Esquisabel, and José Luis Pedraz

Abstract

Immobilized enzymes have been widely studied during the last few decades. Biocatalyst systems may work as biosensors or may be used for the treatment of different diseases. This chapter presents different attempts to immobilize enzymes in the biomedical field, particularly the use of prolidase and superoxide dismutase as two examples of this approach. Although this chapter focuses on liposomes and nanoparticles for the entrapment of these enzymes, the methods detailed here could be adapted for the immobilization of other enzymes with therapeutic purposes.

Key words Superoxide dismutase, Prolidase, Liposomes, Nanoparticles

1 Introduction

Immobilized enzymes were first applied in the biomedical field aiming to detect bioactive substances. Enzymes are able to promote chemical reactions in a highly regio- and stereo-selective manner. Moreover, enzymes are highly active under mild physiological environment. Therefore, enzymes can provide an extremely selective and biocompatible therapeutic toll [1, 2]. However, the utility of isolated enzymes in medicine is limited due to the labile nature of these molecules, the possibility of immunogenic reaction and their difficulty to accumulate at the target site [3].

To overcome these disadvantages, several enzyme modification approaches have been reported lately, such as encapsulation or cross-linking [4]. An immobilized enzyme is constituted by two main components, the non-catalytic part (carrier or support), and catalytic functional part (enzyme). Both elements, when forming a composite, should be able to provide a stable and functional entity [5].

Modified enzymes can act as a biosensor for diagnosis of an illness by detecting, measuring and recording levels of a biomarker [6]. Alternatively, immobilized enzymes can also be useful in the

Table 1
Enzymes that have been immobilized for therapeutic purposes

Enzyme	Disease treated	Ref
Adenosine deaminase	SCID	[7]
Alcohol dehydrogenase and acetaldehyde dehydrogenase	Alcohol intoxication	[8, 9]
Arginine deiminase	Human melanoma and hepatocarcinoma	[10, 11]
Cytochrome P450 (cells producing the enzyme)	Cancer therapy, to convert ifosfamide to its cytotoxic metabolite	[12]
Deoxyribonuclease I	Cystic fibrosis	[13]
Fibrinolytic enzyme	Cardiovascular therapy	[14]
Glucose oxidase-peroxidase	Oral infections	[15]
L-asparaginase	Leukemia	[16, 17]
Organophosphorous hydrolase	Organophosphate intoxication	[18]
Pepsin, chymotrypsin, trypsin	Replacement therapy in gastrointestinal diseases, treatment of fat malabsorption	[19, 20]
Phenylalanine ammonia lyase	Phenylketonuria	[21]
Prolidase	Prolidase deficiency	[22]
Streptokinase	Thrombolytic therapy	[23]
Thymidine phosphorylase	Mitochondrial Neurogastrointestinal Encephalomyopathy (MNGIE)	[24]
Tissue plasminogen activator	Thrombolytic therapy	[25]
Trypsin and urokinase	Thrombolytic therapy	[26]
Urease (<i>E. coli</i> cells engineered to produce urease)	Removal of urea in kidney failure	[27]
β -Glucosidase	Gaucher's disease	[28, 29]
β -Glucuronidase	Cancer therapy, for activation of anticancer prodrugs	[30]

treatment of certain illnesses, for instance, in inborn metabolic defects, cardiovascular diseases, cancer, intestinal diseases or for the treatment of intoxication. Enzymes can work by scavenging an accumulation of a metabolic pathway product or by eliminating toxic xenobiotics. Moreover, enzymes can ameliorate some pathological states, namely, oxidative stress and inflammation (Table 1).

Many approaches have been developed in order to achieve enzyme immobilization. Among them, two main strategies have arisen, the first one is based on binding the enzyme, either covalently or by adsorption to a support (*immobilization by binding*) and the second one consists of entrapping the enzyme into a matrix (*immobilization by entrapment*) [4].

Regarding *immobilization by binding*, two main methods can be distinguished, cross-linking and support-based immobilization. In the early 1960s, researchers discovered that by mixing enzymes and a cross linker active aggregates were formed. CLE (Cross-Linked Enzyme), CLEC (Cross-Linked Enzyme Crystals), and CLEA (Cross-Linked Enzyme Aggregate) are the best known enzyme cross-linked product. The difference between them lies in the state that enzyme presents prior to cross linking process, i.e., it is dissolved, in crystals or aggregated. CLECs show improved thermal and mechanical stability, broader pH stability and withstanding of organic solvents and the possibility of controlling size from 1 to 100 μm , compared to CLE. However, the crystallization of enzyme is quite a laborious step. In order to avoid the purifying and crystallization steps, CLEAs were developed and therefore the elaboration technique was greatly simplified [5].

Support based immobilization can be performed by bonding an enzyme and support through an ionic or covalent manner. Still, the binding should be strong enough not to release the enzyme, but mild enough to ensure the preservation of enzymatic activity. Several supports are currently marketed, such as Eupergit[®] and Sepabeads[®] and their derivatives [2, 4].

When *enzyme entrapment* is employed, no chemical reaction involving the enzyme itself is undergone. Moreover, protection level and enzyme loading is substantially enhanced in these systems [2]. The enzyme is enclosed in a wide range of polymers. The entrapment can be achieved by holding into synthetic polymer, biodegradable polymers (polymers and copolymers derived from lactic and glycolic acid, alginate, chitosan, etc.) or by the use of other biocompatible materials like liposomes or even red blood cells [4, 31, 32].

Liposomes are vesicles formed by phospholipid bilayer in the nanometric range (Fig. 1). This drug delivery system has been extensively studied over the last few decades. As a consequence, different liposome formulations are currently commercially available, such as AmBisome[®] or DOXIL[®] [33]. Liposomes enclose hydrophilic drugs in its inner aqueous spaces and thus prolong in vivo circulation time and what is more, they may enhance targeting to specific body sites by ligand coupling. In addition, as the enzyme is encapsulated inside the vesicle its antigen determinants are masked from the immune system [34–36].

Another drug delivery system approach spans the use of polymeric nano/microparticles. For this encapsulation attempt

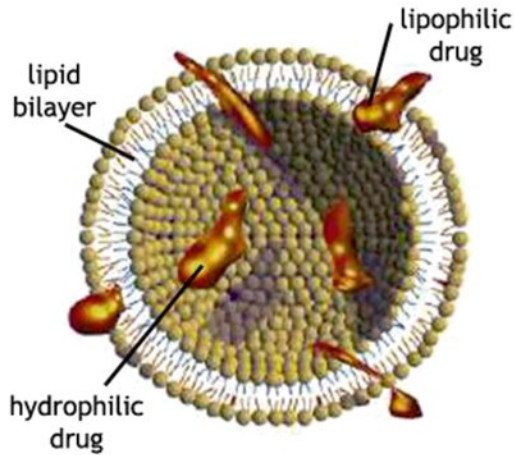


Fig. 1 Structure of a liposome. Hydrophilic drugs are encapsulated in the inner aqueous space, whereas lipophilic drugs are entrapped in the phospholipid membrane

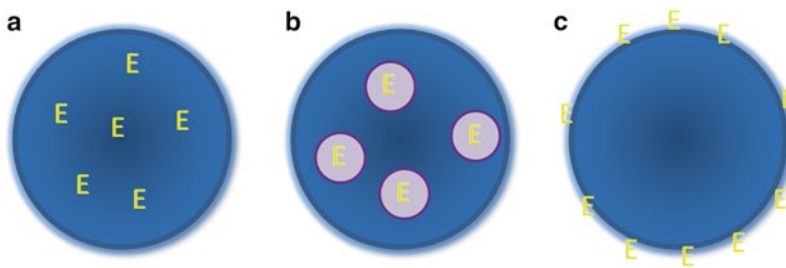


Fig. 2 Drug delivery system for enzyme (E: enzyme), microparticles and nanoparticles. Immobilized enzyme may be dispersed (a), dissolved (b), or adsorbed (c) into the polymers forming the particle

biodegradable polymers can be used in order to obtain particles above 10 nm [37]. In these colloidal systems the drug can be dissolved, entrapped or adsorbed (Fig. 2). Nanoparticles display some advantages for enzyme delivery due to their controlled release capability, formulation versatility, sub cellular size and biocompatibility [38, 39].

Among the different therapeutic areas in which enzyme immobilization could be of interest, enzyme replacement therapy is one of the most frequently used approaches. Rare disorders are defined in the European Union as a disease affecting six patients per 10,000 inhabitants. Although as a single illness presents low prevalence, all the rare disorders taken together sum up to 5,000–8,000 disorders. In many of these cases, a missing or dysfunctional enzyme is the responsible of the clinical manifestations [40]. Among these rare diseases prolidase deficiency can be found. Prolidase deficiency

appears as a consequence of a defect in the prolidase gene (PEPD, 19cen-q13.11) leading to a rare autosomal recessive disorder distinguished by chronic skin ulceration, mental retardation and respiratory infections. Prolidase (E.C. 3.4.13.9) hydrolyzes dipeptides containing residues of proline or hydroxyproline at a C terminal end. The lack of this enzyme leads to altered matrix remodelling and cell growth and it is postulated that it may be necessary for healing, inflammation, angiogenesis, proliferation, and protein synthesis [41]. In this regard, exogenous supply of the immobilized enzyme in order to modify the pathology of this disease has been examined.

Another application field of immobilized enzymes lies on the use of enzymes with antioxidant properties. Increased reactive oxygen species (ROS) involve cell and tissue damage, being this accumulation produced due to oxidative stress occurring in many different situations and illnesses. ROS could be neutralized by antioxidant enzymes, mainly by superoxide dismutase (SOD). ROS are associated to a wide range of illnesses where an inflammatory pathology underlies, for instance atherosclerosis, Parkinson's disease, autoimmune disorders, or cancer [42]. As superoxide dismutase presents a short half-life of around 6 min and poor cellular penetration, its immobilization in drug delivery systems is a feasible strategy towards an improved therapeutic effect of this enzyme in a wide range of illness, such as myocardial infarctions or age-related macular degeneration [43].

The aim of this chapter is to describe different methods to entrap prolidase and superoxide dismutase in drug delivery systems, namely, nanoparticles made of chitosan or PLGA or liposomes. These techniques could also be applied for other enzymes for clinical purposes.

2 Materials

2.1 Immobilization of Prolidase Into Chitosan Nanoparticles

2.1.1 Materials for the Preparation of Prolidase-Loaded Nanospheres

1. Prolidase from porcine kidney, lyophilized powder, ≥ 100 U/mg protein (Sigma-Aldrich, St. Louis, MO, USA).
2. Chitosan glutamate, Protosan G213, MW 150,000–600,000 g/mol, 25–10 % of acetylation (FMC Biopolymer, Norway).
3. Tripolyphosphate pentasodium salt hexahydrate, TPP (MW 475.9 g/mol, Sigma-Aldrich, St. Louis, MO, USA).

2.2 Materials for the Characterization of Prolidase-Loaded Nanospheres

1. Tris (hydroxymethyl) aminomethane, TRIS (Sigma, St. Louis, MO, USA).
2. Hydrochloric acid, HCl (Panreac Quimica, Barcelona, Spain).
3. MnCl_2 (Panreac Quimica, Barcelona, Spain).

4. Glycine-proline (Sigma-Aldrich, St. Louis, MO, USA).
5. Glutathione reduced form (Sigma-Aldrich Co., St. Louis, MO, USA).
6. Trichloroacetic acid (Sigma-Aldrich Co., St. Louis, MO, USA).
7. Sodium tetraborate (Panreac Quimica, Barcelona, Spain).
8. Cyclodextrin (Sigma-Aldrich Co., St. Louis, MO, USA).

2.3 Materials for the Preparation of Prolidase-Loaded Liposomes

1. Prolidase from porcine kidney, lyophilized powder, ≥ 100 U/mg protein (Sigma-Aldrich, St. Louis, MO, USA).
2. Bovine serum albumin, fraction V (Sigma-Aldrich Co., St. Louis, MO, USA).
3. Egg L, α -phosphatidylcholine type XI-E, EPC (Sigma-Aldrich Co., St. Louis MO, USA).
4. Cholesterol (Sigma-Aldrich Co., St. Louis, MO, USA).
5. Distearoylphosphatidylcholine-polyethylene glycol 2000, DSPE-PEG 2000 (Corden Pharma, Switzerland)
6. Chloroform-*d* containing 0.03 % of tetramethylsilane (Sigma, St. Louis, MO, USA).
7. $MnCl_2$ (Panreac Quimica, Barcelona, Spain).
8. Tris (hydroxymethyl) aminomethane, TRIS (Sigma, St. Louis, MO, USA).
9. Glutathione reduced form, GSH (Sigma-Aldrich Co., St. Louis, MO, USA).

2.4 Materials for the Characterization of Prolidase-Loaded Liposomes

1. Triton X-100 (Sigma, St. Louis, MO, USA).
2. Bicinchoninic acid microassay, BCA protein assay reagent kit (Thermo Scientific-Pierce Protein Research Products, Rockford, IL, USA).
3. Glutathione reduced form, GSH (Sigma-Aldrich Co., St. Louis, MO, USA).
4. Tris (hydroxymethyl) aminomethan, TRIS (Sigma, St. Louis, MO, USA).
5. Gly-Pro peptide (Sigma-Aldrich Co., St. Louis, MO, USA).
6. Trichloroacetic acid, TCA (Sigma, St. Louis, MO, USA).
7. Potassium dihydrogen phosphate, KH_2PO_4 (Panreac Quimica, Barcelona, Spain).
8. Sodium hexanesulfonate (Sigma, St. Louis, MO, USA).

2.5 Materials for the Preparation of Super Oxide Dismutase-Loaded Nanoparticles

1. Super Oxide Dismutase, SOD, lyophilized powder form bovine erythrocytes (Sigma-Aldrich, St. Louis, MO, USA).
2. Poly (D,L-Lactic-co-glycolic) acid, lactide:glycolide 50:50 ratio, PLGA (LACTEL Absorbable Polymers, Birmingham, AL, USA).

3. Dimethyl tartaric acid, DMT (Sigma-Aldrich, St. Louis, MO, USA).
4. Rat Serum Albumin, RSA (Sigma-Aldrich, St. Louis, MO, USA).
5. Polyvinyl alcohol, PVA, average MW 30,000–70,000 (Sigma-Aldrich, St. Louis, MO, USA).
6. Chloroform (Panreac Quimica, Barcelona, Spain).

2.5.1 Materials for the Characterization of SOD Loaded Nanospheres

1. BCA Protein Assay Kit (Thermo Fisher Scientific, Rockford, IL, USA).
2. SOD assay kit (Dojindo Molecular Technologies, Gaithersburg, MD, USA).

2.6 Materials for the Preparation of SOD-Loaded Liposomes

1. Super Oxide Dismutase, SOD, lyophilized powder form bovine erythrocytes (Sigma-Aldrich, St. Louis, MO, USA).
2. 1,2-Dioleoyl-*sn*-glycero-3-phosphatidylethanolamine, DOPE (Avanti Polar Lipids, Alabaster, AL, USA).
3. Phosphatidic Acid, PA (Sigma-Aldrich Co., St. Louis MO, USA).
4. Chloroform (Panreac Quimica, Barcelona, Spain).
5. 10 mM HEPES(4-(2-hydroxyethyl)-1-piperazineethane-sulfonic acid), pH 7.4 (Gibco, Life Technologies, Paisley, UK).

2.6.1 Materials for the Characterization of SOD-Loaded Liposomes

1. SOD assay kit (Dojindo Molecular Technologies, Gaithersburg, MD, USA).
2. BCA Protein Assay Kit (Thermo Fisher Scientific, Rockford, IL, USA).

3 Methods

3.1 Preparation of Prolidase-Loaded Chitosan Nanospheres

Prolidase loaded nanospheres can be prepared by ionotropic gelation followed by an ultrasonication step [44].

1. Add 250 μ L of 200 IU/mL of prolidase to 1 mg/mL chitosan glutamate solution.
2. Add 1 mL TPP solution at a constant rate of 0.5 mL/min to 2.5 mL of 1 mg/mL solution of chitosan glutamate containing the enzyme under magnetic stirring of 300 rpm.
3. Emulsify the mixture by sonication for 4 min at discontinuous mode at 20 kHz (GM 2070 Bandelin Sonopuls, Germany, 70W High Intensity, Germany) (*see Note 1*).
4. Separate the nanoparticles with ultracentrifugation at 12,000 $\times g$ for 15 min at 4 °C (repeat the procedure three times in order to wash the nanoparticles).
5. Resuspend the nanoparticles in 500 μ L of distilled water.

3.2 Determination of Encapsulation Efficiency

The encapsulation efficiency (EE) indicates the percentage of the enzyme encapsulated with respect to the total amount used for the preparation of the nanoparticles.

1. Take the supernatants recovered at the centrifugation step.
2. Determine the amount of enzyme in the clear supernatants by UV spectrophotometry (Beckmann DU7500) at 280 nm.
3. Calculate the amount of encapsulated protein by subtracting the non-encapsulated protein amount to the added protein proportion.

$$\text{Protein encapsulation(\%)} = \frac{\text{added protein amount} - \text{protein in supernatants}}{\text{total protein amount}} \times 100$$

3.3 Determination of Prolidase Activity

1. The biological activity of the enzyme is determined by the capillary electrophoresis method described by Viglio [45]. The enzymatic activity of one unit prolidase corresponds to the hydrolysis of 1 μmol of Gly-Pro per min at 37 °C.
2. Weigh a suitable amount of prolidase loaded chitosan nanoparticles and disperse in 2 mL of 50 mM Tris-HCl, pH 7.8.
3. Take 1 mL of the nanoparticle suspension and incubate it overnight at 37 °C in an activation buffer consisting of 50 mM Tris-HCl, 1 mM MnCl_2 , 0.75 mM glutathione reduced form, freshly prepared at pH 7.8.
4. Start the reaction by adding 0.4 mM glycyl-L-proline for a 1 h at 37 °C.
5. Stop the reaction with 70 μL of 2.7 M trichloroacetic acid.
6. Centrifuge the samples using Microcon concentrator (Millipore) at 6,000 rpm for 5 min.
7. Inject the samples under pressure (10s, 0.07 MPa) onto an uncoated fused silica capillary of 50 cm effective length \times 50 μm I.D. operating at 25 °C and applying voltage of 25 kV by a Beckmann P/ACE 2100 system.
8. Use 50 mM sodium tetraborate, pH 9.3 containing 30 mM α -cyclodextrin as background electrolyte to separate.
9. Determine the analytes at 214 nm.
10. Calculate the μmol of Gly-Pro hydrolyzed at 37 °C per min (IU)
11. Results can be express as Residual Enzyme Activity percentage.

3.4 Preparation of Prolidase-Loaded Liposomes

Prolidase loaded liposomes can be prepared by a thin film hydration method followed by a 100 nm pore size extrusion process [46].

1. Prepare a chloroformic lipidic solution by mixing at 1:1 molar ratio cholesterol and EPC.

2. Add 10 mol% of DSPE-PEG.
3. Dry the lipid mixture in a rotary evaporator for 1 h at 40 °C in order to reduce to a thin film.
4. Formed film undergoes a N₂ stream at 0.01 atm for 1 h to ensure organic solvent evaporation.
5. Perform film hydration for 1 h at 27 °C with an aqueous of prolidase solution (0.266–1.064 mg/mL) in 0.5 % BSA (at prolidase BSA 1:5 w/w ratio) in 1.2 mM MnCl₂, 0.1 mM in 50 mM Tris-HCl (TMG solution).
6. Centrifuge at 16,400 rpm as a washing step in an Eppendorf 5417R centrifuge.
7. Suspend the pellet in TMG solution.
8. Extrude the resuspended formulation through 100 nm pore size membrane using Liposofast-100 extruder device.
9. Filter sterile the liposomes with a 0.22 μm filter.

3.5 Determination of Encapsulation Efficiency in Liposomes

Allow liposomes to solubilize in Triton X-100 (10 % w/v aqueous solution).

Define total amount of protein in liposomes by means of Bicinchoninic acid (BBCA) microassay, compared to standard curve between 20 and 2,000 μg/mL.

1. Prepare reagent by mixing 1 part of reagent B to 50 parts of reagent A.
2. Place 25 μL of samples and standard curve in the microplate, bearing in mind that working range in is 20–2,000 μg/mL.
3. Add 200 μL of reagent to each well and mix thoroughly.
4. Let it incubate for 30 min at 37 °C.
5. Cool the plate to room temperature and read at 562 nm wavelength.
6. Subtract blank value to standard curve and to samples.
7. Plot standard curve from blank corrected standard value versus concentration μg/mL.
8. Use the standard curve to determine protein amount in samples.
9. Take into account that apart from enzyme nanoparticles contains BSA. Calculate protein amount in the formulation following this equation

Protein encapsulation(%)

$$= \frac{\text{added protein amount} - \text{protein in supernatants}}{\text{total protein amount}} \times 100$$

3.6 Determination of Prolidase Activity

Prolidase activity can be determined by a HPLC method [47].

1. Prepare the following solutions.
 - (a) Solution A: 1.2 mM of MnCl_2 containing 0.1 mM Glutathione reduced form, in 50 mM of Tris-HCl.
 - (b) Solution B: 30 mM Gly-Pro peptide in 50 mM of Tris-HCl.
 - (c) Solution C: 0.45 M of trichloroacetic acid.
2. Incubate the enzyme containing samples with 100 μL of Solution A for 45 min at 37 °C.
3. Add 100 μL of Solution B (Gly-Pro solution) to the previous mixture.
4. Stop the reaction at different time intervals by adding Solution C.
5. Centrifuge the samples at 21,900 g for 5 min.
6. Inject the supernatant in HPLC system:
 - (d) C18 reversed phase column, 5 μm pore size, 250 \times 4.6 mm.
 - (e) Mobile phase: 10 mM KH_2PO_4 buffer containing 0.5 mM hexanesulfonic acid and sodium salt pH 2.7.
 - (f) Flow rate: 1.9 mL/min.
 - (g) 210 nm detection wavelength.
7. Calculate the amount of remaining Gly-Pro. Peptide decrease is linearly related to the incubation time. Use a reference calibration curve of Gly-Pro.
8. Express enzyme activity as Unit, bearing in mind that 1 IU of prolidase corresponds to the hydrolysis of 1 μmol of Gly-Pro per min at 37 °C.

3.7 Immobilization of Superoxide Dismutase into PLGA Nanoparticles. Preparation of SOD-Loaded PLGA Nanospheres

SOD loaded nanospheres can be prepared by a double emulsion solvent evaporation technique [48].

1. Weigh 81 mg of PLGA and 9 mg of DMT and dissolve them in 3 mL of chloroform (*see Note 2*).
2. Weigh the needed amount for 50,000 IU of SOD and 18 mg of RSA (*see Note 3*).
3. Emulsify the mixture by sonication for 2 min at 55W (Sonicator[®] XL, Misonix, Farmingdale, NY) (*see Note 1*).
4. Pour the first emulsion onto a 2 % PVA solution. Vortex it and then sonicate it as in **step 3**.
5. Leave the double emulsion under magnetic stirring overnight at room temperature.
6. Stir it for 1 h under vacuum, so that the organic solvent is removed.

7. Separate the nanoparticles by ultracentrifugation at 30,000 rpm for 20 min at 4 °C (repeat the procedure three times in order to wash the nanoparticles).
8. Resuspend the nanoparticles in 10 mL of distilled water and lyophilize for 48 h.

3.8 Determination of Protein Encapsulation in PLGA Nanoparticles

Define total amount of protein in nanoparticles by means of Bicinchoninic acid microassay, compared to standard curve between 20 and 2,000 µg/mL.

1. Collect supernatants from washing step and determine the protein content using Pierce BCA Protein Assay Kit.
2. Prepare reagent by mixing 1 part of reagent B to 50 parts of reagent A.
3. Place 25 µL of samples and standard curve in the microplate, bearing in mind that working range in is 20–2,000 µg/mL.
4. Add 200 µL of reagent to each well and mix thoroughly.
5. Let it incubate for 30 min at 37 °C.
6. Cool the plate to room temperature and read at 562 nm wavelength.
7. Subtract blank value to standard curve and to samples.
8. Plot standard curve from blank corrected standard value versus concentration µg/mL.
9. Use the standard curve to determine protein amount in samples.
10. Take into account that apart from enzyme, nanoparticles contains RSA. Calculate protein amount in the formulation following this equation

Protein encapsulation (%)

$$= \frac{\text{added protein amount} - \text{protein in supernatants}}{\text{total protein amount}} \times 100$$

3.9 Determination of SOD Activity

1. Take the supernatants recovered at the centrifugation step.
2. Place 20 µL of the sample in replicates wells. Apart from various sample dilutions three different controls or blanks are required. Sample should be added in blank 2 and bi-distilled water in blanks 1 and 3.
3. Add 200 µL of WST Working Solution to all wells and mix.
4. Add dilution buffer to blanks 2 and 3.
5. Add 20 µL of Enzyme Working solution to sample wells and blank 1.

	Sample (μL)	Blank 1 (μL)	Blank 2 (μL)	Blank 3 (μL)
Sample solution	20	–	20	–
ddH ₂ O	–	20	–	20
WST Working solution	200	200	200	200
Dilution Buffer	–	–	20	20
Enzyme Working solution	20	20	–	–

6. Incubate at 37 °C for 20 min.
7. Read the absorbance 450 nm.
8. Calculate SOD activity. Bear in mind that 1 U of SOD is defined as the amount of SOD that inhibits the reduction reaction of WST with superoxide anion by 50 %. So, for instance, if the activity of SOD is 50 % at the 1/120 dilution. SOD activity prior to dilution would be 120 IU/20 μL , so 1 mL 120/0.02 = 10,800 IU/mL.

$$\text{SOD activity} = \frac{[(A_{\text{blank1}} - A_{\text{blank3}}) - (A_{\text{sample}} - A_{\text{blank2}})]}{(A_{\text{blank1}} - A_{\text{blank3}})} \times 100$$

3.10 Immobilization of SOD into Liposomes. Preparation of SOD-Loaded Liposomes

SOD loaded liposomes can be prepared by a film hydration method [49].

1. Prepare the chloroformic lipidic solution at 550 nmol concentration (DOPE/PA molar ratio 7:2) and 1.8 nmol of SOD.
2. Let the chloroform evaporate.
3. Add 250 μL of 10 mM HEPES and incubate for 15 min at room temperature to moisture the lipids (final lipid concentration, 2.2 mM).
4. Sonicate the mixture in a bath type sonicator for 1 min.

3.11 Determination of SOD Encapsulation

1. Solubilize liposomes in Triton X-100 (10 % w/v aqueous solution).
2. Prepare reagent by mixing 1 part of reagent B to 50 parts of reagent A.
3. Place 25 μL of samples and standard curve in the microplate, bearing in mind that working range is in 20–2,000 $\mu\text{g}/\text{mL}$.
4. Add 200 μL of reagent to each well and mix thoroughly.
5. Let it incubate for 30 min at 37 °C.
6. Cool the plate to room temperature and read at 562 nm wavelength.
7. Subtract blank value to standard curve and to samples.

8. Plot standard curve from blank corrected standard value versus concentration $\mu\text{g}/\text{mL}$.
9. Use the standard curve to determine protein amount in samples.
10. Calculate the amount of protein in the formulation following the equation mentioned in Subheading 3.2, step 2.

3.12 Determination of SOD Activity

1. Disrupt liposome by mixing them with Triton X-100 (10 % w/v aqueous solution).
2. Place 20 μL of the sample in replicants wells. Apart from various sample dilutions three different controls or blanks are required. Sample should be added in blank 2, and bi-distilled water in blanks 1 and 3.
3. Add 200 μL of WST Working Solution to all wells and mix.
4. Add dilution buffer to blanks 2 and 3.
5. Add 20 μL of Enzyme Working solution to sample wells and blank 1.

	Sample (μL)	Blank 1 (μL)	Blank 2 (μL)	Blank 3 (μL)
Sample solution	20	–	20	–
ddH ₂ O	–	20	–	20
WST Working solution	200	200	200	200
Dilution Buffer	–	–	20	20
Enzyme Working solution	20	20	–	–

6. Incubate at 37 °C for 20 min.
7. Read the absorbance 450 nm.
8. Calculate SOD activity as in Subheading 3.9. One unit of SOD is defined as the amount of SOD that inhibits the reduction reaction of WST with superoxide anion by 50 %.

$$\text{SOD activity} = \frac{[(A_{\text{blank1}} - A_{\text{blank3}}) - (A_{\text{sample}} - A_{\text{blank2}})]}{(A_{\text{blank1}} - A_{\text{blank3}})} \times 100$$

4 Notes

1. The sonication energy used in this step is gentle enough to preserve enzyme activity.
2. DMT is added to ease enzyme release from NP.
3. RSA is used in order to stabilize the enzyme from interfacial activation.

References

1. Laurent N, Haddoub R, Flitsch SL (2008) Enzyme catalysis on solid surfaces. *Trends Biotechnol* 26:328–337
2. Betancor L, Luckarift HR (2008) Bioinspired enzyme encapsulation for biocatalysis. *Trends Biotechnol* 26:566–572
3. Park Y, Liang J, Song H, Li YT, Naik S, Yang VC (2003) ATTEMPTS: a heparin/protamine-based triggered release system for the delivery of enzyme drugs without associated side-effects. *Adv Drug Deliv Rev* 55:251–265
4. Brady D, Jordaan J (2009) Advances in enzyme immobilisation. *Biotechnol Lett* 31:1639–1650
5. Cao L, Langen LV, Sheldon RA (2003) Immobilised enzymes: carrier-bound or carrier-free? *Curr Opin Biotechnol* 14:387–394
6. Kotanen CN, Moussy FG, Carrara S, Guiseppi-Elie A (2012) Implantable enzyme amperometric biosensors. *Biosens Bioelectron* 35:14–26
7. Liu P, Santisteban I, Burroughs LM, Ochs HD, Torgerson TR, Hershfield MS et al (2009) Immunologic reconstitution during PEG-ADA therapy in an unusual mosaic ada deficient patient. *Clin Immunol* 130:162–174
8. Lizano C, Pérez MT, Pinilla M (2001) Mouse erythrocytes as carriers for coencapsulated alcohol and aldehyde dehydrogenase obtained by electroporation: in vivo survival rate in circulation, organ distribution and ethanol degradation. *Life Sci* 68:2001–2016
9. Lizano C, Sanz S, Luque J, Pinilla M (1998) In vitro study of alcohol dehydrogenase and acetaldehyde dehydrogenase encapsulated into human erythrocytes by an electroporation procedure. *Biochim Biophys Acta* 1425:328–336
10. Holtsberg FW, Ensor CM, Steiner MR, Bomalaski JS, Clark MA (2002) Poly(ethylene glycol) (PEG) conjugated arginine deiminase: effects of peg formulations on its pharmacological properties. *J Control Release* 80:259–271
11. Glazer ES, Piccirillo M, Albino V, Di Giacomo R, Palaia R, Mastro AA et al (2010) Phase II study of pegylated arginine deiminase for non-resectable and metastatic hepatocellular carcinoma. *J Clin Oncol* 28:2220–2226
12. Löhr M, Hummel F, Faulmann G, Ringel J, Saller R, Hain J et al (2002) Microencapsulated, CYP2B1-transfected cells activating ifosfamide at the site of the tumor: the magic bullets of the 21st century. *Cancer Chemother Pharmacol* 49:21–24
13. Osman R, Kan PL, Awad G, Mortada N, El-Shamy A, Alpar O (2011) Enhanced properties of discrete pulmonary deoxyribonuclease I (DNaseI) loaded PLGA nanoparticles during encapsulation and activity determination. *Int J Pharm* 408:257–265
14. Cheng M, Wang J, Li Y, Liu X, Zhang X, Chen D et al (2008) Characterization of water-in-oil microemulsion for oral delivery of earthworm fibrinolytic enzyme. *J Control Release* 129:41–48
15. Hill KJ, Kaszuba M, Creeth JE, Jones MN (1997) Reactive liposomes encapsulating a glucose oxidase-peroxidase system with antibacterial activity. *Biochim Biophys Acta* 1326:37–46
16. Ghosh S, Chaganti SR, Prakasham RS (2012) Polyaniline nanofiber as a novel immobilization matrix for the anti-leukemia enzyme l-asparaginase. *J Mol Catal B: Enzym* 74:132–137
17. Kwon YM, Chung HS, Moon C, Yockman J, Park YJ, Gitlin SD et al (2009) L-asparaginase encapsulated intact erythrocytes for treatment of acute lymphoblastic leukemia (ALL). *J Control Release* 139:182–189
18. Kapoor M, Rajagopal R (2011) Enzymatic bioremediation of organophosphorus insecticides by recombinant organophosphorous hydrolase. *Int Biodeterior Biodegradation* 65:896–901
19. Patchell CJ, Desai M, Weller PH, MacDonald A, Smyth RL, Bush A et al (2002) Creon® 10,000 Minimicrospheres™ vs. Creon® 8000 microspheres—an open randomised crossover preference study. *J Cyst Fibros* 1:287–291
20. Santini B, Antonelli M, Battistini A, Bertasi S, Collura M, Esposito I et al (2000) Comparison of two enteric coated microsphere preparations in the treatment of pancreatic exocrine insufficiency caused by cystic fibrosis. *Dig Liver Dis* 32:406–411
21. Shah RM, D'mello AP (2008) Strategies to maximize the encapsulation efficiency of phenylalanine ammonia lyase in microcapsules. *Int J Pharm* 356:61–68
22. Genta I, Perugini P, Pavanetto F, Maculotti K, Modena T, Casado B et al (2001) Enzyme loaded biodegradable microspheres in vitro: ex vivo evaluation. *J Control Release* 77:287–295
23. Liang JF, Li YT, Yang VC (2000) A novel approach for delivery of enzyme drugs: preliminary demonstration of feasibility and utility in vitro. *Int J Pharm* 202:11–20
24. De Vocht C, Ranquin A, Willaert R, Van Ginderachter JA, Vanhaecke T, Rogiers V et al (2009) Assessment of stability, toxicity and immunogenicity of new polymeric nanoreactors for use in enzyme replacement therapy of MNGIE. *J Control Release* 137:246–254

25. Kaminski MD, Xie Y, Mertz CJ, Finck MR, Chen H, Rosengart AJ (2008) Encapsulation and release of plasminogen activator from biodegradable magnetic microcarriers. *Eur J Pharm Sci* 35:96–103
26. Piras AM, Chiellini F, Fiumi C, Bartoli C, Chiellini E, Fiorentino B et al (2008) A new biocompatible nanoparticle delivery system for the release of fibrinolytic drugs. *Int J Pharm* 357:260–271
27. Prakash S, Chang TMS (1996) Microencapsulated genetically engineered live *E. coli* DH5 cells administered orally to maintain normal plasma urea level in uremic rats. *Nat Med* 2:883–887
28. Korablyov VF, Zimran AF, Barenholz Y (1999) Cerebroside- β -glucosidase encapsulation in liposomes for gaucher's disease treatment revisited. *Pharm Res* 16:466–469
29. Belchetz P, Crawley JCW, Braidman I, Gregoriadis G (1977) Treatment of gaucher's disease with liposome-entrapped glucocerebrosidase: β -glucosidase. *Lancet* 310:116–117
30. Storm G, Vingerhoeds MH, Crommelin DJA, Haisma HJ (1997) Immunoliposomes bearing enzymes (immuno-enzymosomes) for site-specific activation of anticancer prodrugs. *Adv Drug Deliv Rev* 24:225–231
31. Bilati U, Allémann E, Doelker E (2005) Strategic approaches for overcoming peptide and protein instability within biodegradable nano- and microparticles. *Eur J Pharm* 59:375–388
32. Ansari SA, Husain Q (2012) Potential applications of enzymes immobilized on/in nano materials: a review. *Biotechnol Adv* 30:512–523
33. Szebeni J, Bedőcs P, Rozsnyay Z, Weiszhar Z, Urbanics R, Rosivall L et al (2012) Liposome-induced complement activation and related cardiopulmonary distress in pigs: factors promoting reactivity of doxil and ambisome. *Nanomedicine* 8:176–184
34. Bakás L (2000) Influence of encapsulated enzyme on the surface properties of freeze-dried liposomes in trehalose. *Colloids Surf B Biointerfaces* 17:103–109
35. Landesman-Milo D, Peer D (2012) Altering the immune response with lipid-based nanoparticles. *J Control Release* 161:600–608
36. Gutiérrez Millán C, Sayalero Marinero ML, Zaruelo Castañeda A, Lanao JM (2004) Drug, enzyme and peptide delivery using erythrocytes as carriers. *J Control Release* 95:27–49
37. Mundargi RC, Babu VR, Rangaswamy V, Patel P, Aminabhavi TM (2008) Nano/micro technologies for delivering macromolecular therapeutics using poly(D, L-lactide-co-glycolide) and its derivatives. *J Control Release* 125:193–209
38. Couvreur P, Vauthier C (2006) Nanotechnology: intelligent design to treat complex disease. *Pharm Res* 23:1417–1450
39. Ye M, Kim S, Park K (2010) Issues in long-term protein delivery using biodegradable microparticles. *J Control Release* 146:241–260
40. Heemstra HE, van Weely S, Büller HA, Leufkens HGM, de Vruhe RLA (2009) Translation of rare disease research into orphan drug development: disease matters. *Drug Discov Today* 14:1166–1173
41. Besio R, Monzani E, Gioia R, Nicolis S, Rossi A, Casella L et al (2011) Improved prolidase activity assay allowed enzyme kinetic characterization and faster prolidase deficiency diagnosis. *Clin Chim Acta* 412:1814–1820
42. Ratnam DV, Ankola DD, Bhardwaj V, Sahana DK, Kumar MNVR (2006) Role of antioxidants in prophylaxis and therapy: a pharmaceutical perspective. *J Control Release* 113:189–207
43. Celik O, Akbuga J (2007) Preparation of superoxide dismutase loaded chitosan microspheres: characterization and release studies. *Eur J Pharm Biopharm* 66:42–47
44. Colonna C, Conti B, Perugini P, Pavanetto F, Modena T, Dorati R et al (2007) Chitosan glutamate nanoparticles for protein delivery: development and effect on prolidase stability. *J Microencapsul* 24:553–564
45. Viglio S, Annovazzi L, Conti B, Genta I, Perugini P, Zanone C et al (2006) The role of emerging techniques in the investigation of prolidase deficiency: from diagnosis to the development of a possible therapeutical approach. *J Chromatogr B* 832:1–8
46. Perugini P, Hassan K, Genta I, Modena T, Pavanetto F, Cetta G et al (2005) Intracellular delivery of liposome-encapsulated prolidase in cultured fibroblasts from prolidase-deficient patients. *J Control Release* 102:181–190
47. Colonna C, Conti B, Perugini P, Pavanetto F, Modena T, Dorati R et al (2008) Site-directed pegylation as successful approach to improve the enzyme replacement in the case of prolidase. *Int J Pharm* 358:230–237
48. Reddy MK, Labhasetwar V (2009) Nanoparticle-mediated delivery of superoxide dismutase to the brain: an effective strategy to reduce ischemia-reperfusion injury. *FASEB J* 23:1384–1395
49. Furukawa R, Yamada Y, Takenaga M, Igarashi R, Harashima H (2011) Octaarginine-modified liposomes enhance the anti-oxidant effect of lecithinized superoxide dismutase by increasing its cellular uptake. *Biochem Biophys Res Commun* 404:796–801

Immobilization of Whole Cells by Chemical Vapor Deposition of Silica

Susan R. Sizemore, Robert Nichols, Randi Tatum, Plamen Atanasov, Glenn R. Johnson, and Heather R. Luckarift

Abstract

Effective entrapment of whole bacterial cells onto solid-phase materials can significantly improve bioprocessing and other biotechnology applications. Cell immobilization allows integration of biocatalysts in a manner that maintains long-term cell viability and typically enhances process output. A wide variety of functionalized materials have been explored for microbial cell immobilization, and specific advantages and limitations were identified. The method described here is a simple, versatile, and scalable one-step process for the chemical vapor deposition of silica to encapsulate and stabilize viable, whole bacterial cells. The immobilized bacterial population is prepared and captured at a predefined physiological state so as to affix bacteria with a selected metabolic or catalytic capability to compatible materials and surfaces. Immobilization of *Shewanella oneidensis* to carbon electrodes and immobilization of *Acinetobacter venetianus* to adsorbent mats are described as model systems.

Key words Chemical vapor deposition, Silica, *Shewanella oneidensis*, *Acinetobacter venetianus*, Whole cell immobilization

1 Introduction

There are many well-established methods for immobilizing whole bacterial cells, primarily by entrapment in various organic or inorganic matrices or by attachment to a surface [1–3]. Immobilization of living cells is intended to provide a biocompatible environment that allows retention of biocatalytic activity, but without hindering the flow of essential nutrients. In many cases, encapsulated cells remain viable but do not grow, thereby maintaining catalytic activity for extended periods of time without loss of viability.

Sol–gel formulations in particular provide a versatile material for whole cell encapsulation [1]. The one-step vapor deposition of silica described herein provides an alternative to aqueous sol–gel

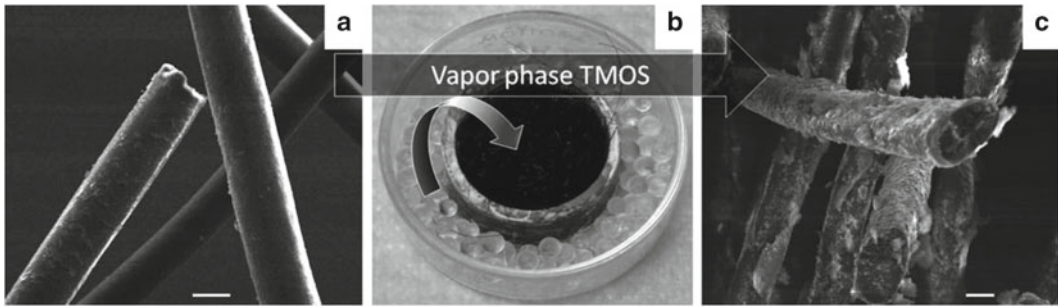


Fig. 1 Immobilization of *Acinetobacter venetianus* 2AW by silica CVD to hair fibers within an adsorbent mat as visualized by scanning electron microscopy

formations by eliminating the use of co-solvents (alcohols) or catalysts (acid or base) commonly used in sol-gel synthesis, better preserving the integrity of whole cells [4–7].

In the vapor phase, silicon alkoxides such as tetramethyl orthosilicate (TMOS) undergo hydrolysis and condensation upon contact with aqueous solvents of high salt concentration. Further cross-linking of the hydrolyzed silica monomers then occurs and leads to particulate silica formation [8]. As a result, chemical vapor deposition (CVD) is a simple method to create of an inorganic matrix, in this case silica. The silica polymerization process occurs at room temperature without the production of toxic by-products that may compromise biomolecular function and can thus be used to affix bacteria with a selected metabolic or catalytic capability to compatible materials and surfaces (Fig. 1).

By preparing the bacterial culture of interest *ex situ*, rather than relying on natural biofilm formation, this method of cell immobilization provides a homogenous population of bacterial cells that is captured at a high and predefined cell density. In addition, the speed and ease of the reaction (1 h or less) confers a significant advantage compared to the time required for natural microbial colonization of surfaces [5].

2 Materials

All laboratory reagents noted here are available from Sigma-Aldrich (St Louis, MO) or Fisher Scientific (Pittsburgh, PA) unless otherwise stated. Solutions are prepared using deionized (DI) water and analytical-grade solvents unless otherwise stated.

2.1 Growth and Preparation of Bacterial Cells for Immobilization

2.1.1 Example 1: *Shewanella oneidensis* DSP-10

1. Phosphate buffered saline (PBS): add 8 g NaCl, 0.2 g KCl, 1.44 g Na₂PO₄, 0.24 g KH₂PO₄ to 0.8 L of distilled H₂O. Adjust the pH to 7.4 with HCl and make up to 1 L with DI water (*see Note 1*). Sterilize by autoclaving at 121 °C for 15 min.
2. Growth medium: Prepare Difco Luria Broth (LB) (Becton Dickinson, Sparks, MD) according to the manufacturer's instructions. 50 mL of LB in a 250-mL Erlenmeyer flask is typically used for bacterial growth. Sterilize the medium by autoclaving at 121 °C for 15 min and then allow to cool.
3. Rifampicin stock: Prepare a stock solution of rifampicin by mixing 20 mg of rifampicin in 1 mL methanol in a suitable container (*see Note 2*).
4. Culture medium: To LB, aseptically add rifampicin from the stock solution to give a final concentration of 5 µg/mL (i.e., add 12.5 µL of stock solution to 50 mL LB). For agar plates, (2 % Bacto Agar, Becton Dickinson) dilute the stock to a final concentration of 10 µg/mL in tempered medium.
5. Determine optical density (OD₆₀₀) of cell culture by spectrophotometric measurement ($\lambda = 600$ nm) against a buffer (i.e., PBS) blank using a Cary 3E spectrophotometer (Varian, Inc., Palo Alto, CA) or similar equipment (*see Note 3*).

2.1.2 Example 2: *Acinetobacter venetianus* 2AW

1. Growth medium: Prepare Bushnell–Haas (BH) broth (Becton Dickinson) according to the manufacturer's instructions. 50 mL of BH in a 250-mL Erlenmeyer flask is typically used for bacterial growth. Sterilize the medium by autoclaving at 121 °C for 15 min and then allow to cool.

2.2 Immobilization of Bacterial Cells to a Solid Substrate

2.2.1 Example 1: Preparation of Carbon Felt Electrodes

1. Graphite felt (GF) circles were cut from 3.2 mm graphite felt (Morgan AM&T, Inc., Greenville, SC) with a punch (5-cm diameter), which gives an electrode weighing ~0.5 g.
2. Titanium wire (~20 cm length, 0.25 mm diameter; Goodfellow, Oakdale, PA) was woven by hand (2× around the perimeter using fairly large stitches) through the GF circle, allowing trailing ends of wire ~10 cm for connections.
3. The wired GF was sterilized in PBS by autoclaving at 121 °C for 15 min before use (*see Note 4*).

2.2.2 Example 2: Preparation of Adsorbent Material

1. Adsorbent mats made from human hair were obtained from Ottimat™ (World Response Group Inc. Huntsville, AL) and cut using a punch (2.2-cm diameter) which gives a sample of ~1 g dry weight. The sample was sterilized by autoclaving in PBS.

2.2.3 Silica Chemical Vapor Deposition

1. Tetramethyl orthosilicate, 98 % (TMOS). *TMOS is toxic and should be handled with care in a fume hood. Appropriate gloves and eye protection must be worn and exposure to fumes should be limited.*

CVD Reaction Vessel

The silica deposition procedure must occur in a vessel that allows TMOS vapors to coat bacterial cells without allowing the liquid TMOS to come in direct contact with the sample. Glass is recommended (*see Note 5*). Two vials (one containing sample and a second containing TMOS) located in close proximity can be used for CVD of silica [4]. In our experience, however, a petri dish fabricated with an inner well that holds the solid substrate/material provides much more uniform vapor deposition. Glass reaction dishes for this purpose are not commercially available, but can be readily fabricated in-house using the procedure defined below. Reaction dishes can be built for any sample size. Herein, dishes were built in two sizes, specifically for the size of the material used for cell immobilization and based on design considerations.

1. Modify glass reaction vessels by attaching a circular section of borosilicate glass tube (*see Note 6*) (Wale Apparatus Co., Hellertown, PA) in the center of the bottom of a petri dish with waterproof, transparent epoxy (Hardman, Royal Adhesives & Sealants, LLC, Belleville, NJ) or an equivalent adhesive.
2. Clean the inside bottom of the glass reaction dish and the center well with acetone to remove any residue that may prevent the epoxy from adhering to the glass.
3. Mix the epoxy according to the manufacturer's instruction and apply it to the contact side of the glass ring.
4. Center the glass ring in the bottom of the petri dish and press in place.
5. Allow the epoxy to dry at room temperature overnight under weighted pressure.
6. Test for leaks the next day by filling the center well with water (*see Note 7*).
7. Make some allowance in the center well to accommodate sol-gel formation and expansion of support materials (~5-mm diameter in the following examples). For graphite felt electrodes, a 15- \times 100-mm glass petri dish was prepared with a pre-cut 13 \times 55-mm glass ring glued to the bottom. For the OttimatTM adsorbent material, the reaction dish was built as described above, except using a 15 \times 60-mm glass petri dish and a pre-cut 13- \times 28-mm glass ring (Fig. 2).

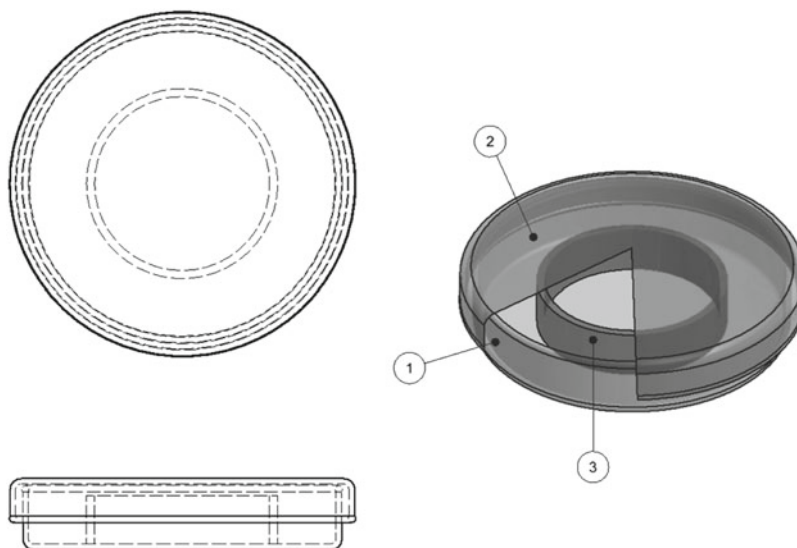


Fig. 2 Schematic for fabrication of a glass reaction vessel for chemical vapor deposition of silica. Key: Glass petri dish (1) and lid (2) modified with an inner glass central well (3)

2.3 Calculating Immobilization Efficiency

2.3.1 Measuring Bacterial Viability by ATP Production

2.3.2 Colony Counting

1. Prepare BacTiter-Glo™ reagent according to the manufacturer's instructions (Promega, Madison, WI).
1. Luria Agar Plates with Rifampicin
Prepare Luria Agar Base, Miller (Becton Dickinson, Sparks, MN) according to manufacturer's instruction. After autoclaving, cool with gentle stirring to ~55 °C. Add 0.5 mL of 20 mg/mL rifampicin stock (*see* Subheading 2.1.1, **item 3**) to give a final antibiotic concentration of 10 µg/mL. Pour plates using aseptic technique. Yield should be 40–50 plates per liter.
2. Serial dilution: Suspend *S. oneidensis* DSP-10 overnight culture to an OD₆₀₀ of ~5 in PBS buffer. Prepare serial dilutions of the culture in the range 10⁻¹–10⁻¹⁰ by combining 0.9 mL PBS buffer with 0.1 mL of culture in a suitable vial and mix thoroughly. Take 0.1 mL from the first vial (10⁻¹) and repeat the procedure stepwise to a 10⁻¹⁰ dilution. Plate 0.1 mL of each dilution by standard spread plating. Invert the plates and incubate at 30 °C until visible colonies can be seen and counted. Multiply the number of colonies by the dilution of that plate to determine the colony forming units (CFU)/mL; for example = 29 colonies on a plate of 10⁻⁷ dilution = 2.9 × 10⁸ CFU/mL (*see* **Note 8**).

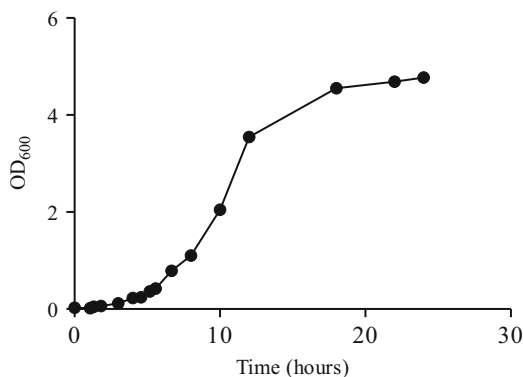


Fig. 3 Representative growth curve for *Shewanella oneidensis* in LB

3 Methods

The methodology defined herein will help outline the ease, speed and effectiveness of the CVD silica encapsulation procedure for immobilization of whole cells. In the examples provided, two different bacterial species are described to demonstrate the versatility of the technique for various support materials and applications. In practice, individual researchers will substitute their biocatalyst of interest. Recent work demonstrates the applicability of the method to various classes of biomolecules and encourages investigation with a variety of catalysts [4] (*see Note 9*).

3.1 Growth and Preparation of Bacterial Cells for Immobilization

3.1.1 Example 1: *Shewanella oneidensis* DSP-10

The first example demonstrated herein is the immobilization of *S. oneidensis* DSP-10 for fabrication of microbial fuel cell anodes. *S. oneidensis* is a dissimilatory, metal-reducing bacterium that is able to couple metal reduction with metabolism [9, 10]. These organisms can respire by passing electrons directly to insoluble metals and metal oxides, a process that can be harnessed at the anode of a microbial fuel cell to provide electrical current [9, 11–14].

1. Inoculate *S. oneidensis* from a starter culture to LB broth containing rifampicin and incubate at 30 °C, with gentle agitation (100 rpm) (*see Note 10*).
2. Monitor the bacterial population at regular intervals by aseptically removing 0.1 mL of cell culture, mixing with 0.9 mL of PBS and measuring the absorbance spectrophotometrically at 600 nm against a buffer blank. Record the increase in optical density (OD₆₀₀) with time as a growth curve (Fig. 3) (*see Note 11*).

3. Harvest cells at late stationary phase ($OD_{600} \sim 4-5$) by centrifugation ($7650 \times g$ for 4 min at $10^\circ C$) in suitable centrifuge tubes.
4. Suspend the cell pellet (from **step 3**) by mixing in 30–40 mL PBS buffer and repeat the centrifugation step three times in total. This step is intended to wash the cells of any residual growth medium.
5. Suspend the washed cell pellet in a small volume of PBS (~ 10 mL) and measure the OD_{600} . The cell pellet will need to be diluted to the readable range of the spectrophotometer (*see Note 3*).
6. Adjust the cell suspension by dilution with PBS to give a final OD_{600} of 5.
7. Determine CFU/mL of the cell suspension by serial dilution of the cell preparation and plate counts (*see Note 8*).

3.1.2 Example 2:
Acinetobacter
venetianus 2AW

1. Inoculate *A. venetianus* 2AW from a starter culture to BH broth supplemented with tetradecane and hexadecane (1:1) at 1 % v/v of each alkane. Incubate the culture at $30^\circ C$ with agitation (200 rpm).
2. Monitor the bacterial culture at regular intervals by aseptically removing 0.1 mL of cell culture, mix with 0.9 mL of PBS and measure the absorbance spectrophotometrically at 600 nm against a buffer blank. Record the increase in optical density with time as a growth curve as before (*see Note 11*).
3. Harvest cells at late stationary phase ($OD_{600} 2-2.5$) by centrifugation ($17,600 \times g$ for 4 min at $10^\circ C$) in suitable centrifuge tubes.
4. Proceed through **steps 4–7** (Subheading **3.1.1**) as described above.

**3.2 Immobilization
of Bacterial Cells to a
Solid Substrate**

3.2.1 Silica
Encapsulation of
S. oneidensis to Carbon
Felt

For fabrication of microbial fuel cell anodes, the substrate for cell immobilization is a conductive carbon felt, but any solid, semi-porous material architecture can be substituted depending upon application.

1. Place the sterilized GF in the center well of the reaction vessel (modified glass petri dish).
2. Add 5 mL of the harvested and washed culture (from Subheading **3.1.1**) to the GF to completely saturate the sample.
3. Distribute a single layer of sterilized glass beads (3-mm diameter solid borosilicate, Kimble Chase, Inc., Vineland, NJ) to the outer well to increase the surface area for evaporation.
4. Add TMOS (1 mL) evenly dropwise onto the glass beads in the outer ring of the petri dish. Cover the petri dish and seal with Parafilm (American National Can, Greenwich, CT).

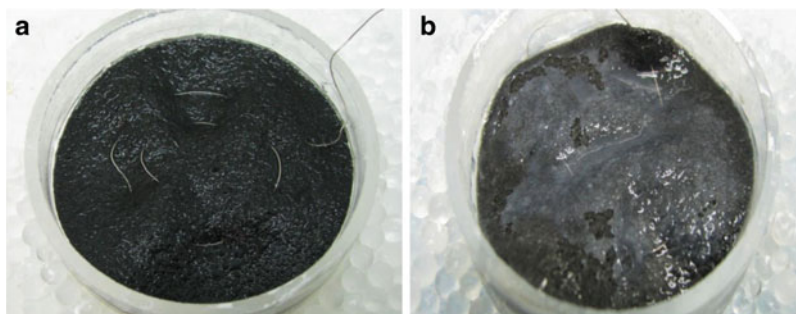


Fig. 4 Silica formation on the substrate surface (**a**; before) is visible as a translucent sheen (**b**; after)

5. Incubate the reaction sealed vessel in an airtight container for 30 min at 37 °C. After 30 min, check for a translucent iridescent film on the surface (Fig. 4). If no film is present, continue incubation until a visible film forms, up to 1 h (*see Note 12*).
6. The *S. oneidensis*-coated GF is removed and used in microbial fuel cell assemblies.
7. Reaction dishes can be reused, but one must allow the TMOS to evaporate completely in a fume hood before washing (*Remember—TMOS is toxic!*) Some dried silica residue may adhere to the glass, but this does not affect subsequent performance.

3.2.2 Silica Encapsulation of *Acinetobacter venetianus* 2AW to Adsorbent Mats

A number of adsorbent materials, including natural and synthetic polymeric materials, have been investigated for whole-cell immobilization for use in chemical synthesis and for bioremediation [6, 15, 16]. Immobilization of cells to an adsorbent matrix typically enhances cell viability and operational longevity, particularly under continuous flow.

1. Place the sterilized adsorbent mat in the center well of the reaction vessel (modified glass petri dish). Add 5 mL of the harvested and washed culture (from Subheading 3.1.2) to completely saturate the sample.
2. Distribute a single layer of sterilized glass beads (3-mm diameter solid borosilicate, Kimble Chase, Inc., Vineland, NJ) to the outer well to increase the surface area for evaporation.
3. Add TMOS (1 mL) evenly dropwise onto the glass beads in the outer ring of the petri dish. Cover the petri dish and seal with Parafilm (American National Can, Greenwich, CT).
4. Incubate the reaction sealed vessel in an airtight container for 60 min at 37 °C. After 30 min, open the reaction vessel (*see Note 13*) and turn the material over, reseal and return to the incubator for an additional 30 min. After 60 min of incubation check for a translucent, iridescent film on the surface (Fig. 4).

If no film is present, continue incubation until a visible film forms, up to 1.5 h (*see Note 12*).

5. Remove the *A. venetiannus*-coated mat from the chamber. It is ready to be used for biodegradation testing.

3.3 Calculating Immobilization Efficiency

3.3.1 Protocol for Measuring Bacterial Viability by ATP Production

Measuring ATP Production in Cell Suspensions

The efficiency for immobilizing bacterial cells using the method described can be determined by enumerating population density. The assay for bacterial viability is based on quantification of ATP by luminescence as an indicator of metabolically active cells.

1. Aliquot 100 μL of cells into a black polystyrene 96-well assay plate (Costar VR, Corning, NY) and add an equal volume of BacTiter-Glo™ reagent.
2. Aliquot 100 μL of medium without cells to obtain a value for background luminescence.
3. Mix contents briefly and incubate at 25 °C and record the relative luminescence (RLU) at 5-min intervals using a Synergy 4 hybrid plate reader (Biotek, Winooski, VT) or similar equipment (*see Note 14*).

Measuring ATP Production in Cell-Immobilized Solid Samples

1. Remove a sample of the cell-immobilized substrate of a known size and incubate with 100 μL of BacTiter-Glo™ reagent (*see Note 15*) for 5 min.
2. Remove the supernatant into a black polystyrene 96-well assay plate and measure immediately for relative luminescence using a Synergy 4 hybrid plate reader (Biotek, Winooski, VT) or similar equipment (*see Note 14*).
3. Transfer a 100- μL aliquot of medium alone to obtain a value for background (without cells) luminescence.

3.3.2 Colony Counting

1. Prepare serial dilutions of the broth culture. For a tenfold logarithmic serial dilution on a 1-mL scale, vials are filled with 0.9 mL of buffer or growth medium and 0.1 mL of the cell suspension is transferred, with thorough mixing after every dilution step. Repeat the dilution step as needed.
2. Spread 0.1 mL of each cell dilution evenly over the surface of an LB agar plate (or equivalent solid growth medium)
3. Invert the plates and incubate at 30 °C (or suitable growth temperature depending upon species) until visible colonies can be observed.
4. Count the colonies and calculate the number of CFU/mL for each dilution step (*see Note 8*).
5. Plot RLU against CFU/mL to create a standard curve for viable cell counts (Fig. 5).

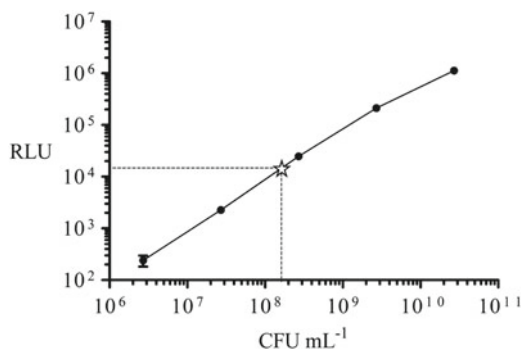


Fig. 5 Calibration plot of relative luminescence units (RLU) vs. colony-forming units/mL (CFU/mL) for *S. oneidensis* DSP-10. The RLU of the silica-immobilized cells is measured (unknown; designated by *star*) and extrapolated from the calibration curve to determine the CFU/mL, from which immobilization efficiency can be calculated

4 Notes

1. Any 0.1 M potassium (or sodium) phosphate buffer at pH 7 can be substituted.
2. Rifampicin (and many other antibiotic solutions) is light and heat sensitive and should be stored in a suitable amber-colored container or wrapped in aluminum foil and stored in the freezer.
3. The readable range of most spectrophotometers is $OD_{600} < 3$, but OD_{600} within the range 0.1–1 is considered most accurate.
4. Wiring of the sample is required in this instance only for preparing electrode materials.
5. Glass is recommended as it is non-reactive, inexpensive, and readily available and, in our experience, TMOS is not compatible with other materials.
6. The circular glass sections were sliced from the tubing using either a diamond abrasive saw or a hot-wire glass tubing cutter. This service should be available at most good glass shops. The center ring must always be shorter than the bottom of the petri dish to allow the silica vapors to readily diffuse onto the anode material.
7. Most epoxy does not withstand autoclaving temperatures, so the modified dishes are sterilized with alcohol before use.
8. Thirty to 300 colonies on a plate are typically considered statistically valid for cell counting. Note that only 0.1 mL of cell suspension is spread to the agar plate, so all cell counts must be multiplied by 10 to allow for the dilution.
9. For work with alternative biocatalysts, media formulations and growth conditions should be modified to suit the researcher's requirements.

10. Most bacterial strains are maintained on agar plates or slants but can be subcultured from small starter cultures (for example, 10 mL of LB in a 50-mL test tube incubated until growth is visible and then subcultured by dilution; 1:100). The bacterial species can be substituted as required, in which case, media formulations, antibiotic addition and growth conditions should be modified according to documented procedures.
11. The spectrophotometer reading should be multiplied by 10 to allow for the initial dilution with PBS.
12. Heavy deposits of sol-gel will form if the reaction is left too long and typically proves detrimental to activity.
13. Always open the reaction vessel in the fume hood; TMOS is toxic. Note here that the incubation time for the adsorbent mat is extended compared to the GF electrode. This is due to the substantially increased density and surface area of the adsorbent mat, which requires longer for a silica film to form. Some optimization may be necessary for alternative materials.
14. Instrument settings depend on the manufacturer. An integration time of 0.25–1 s per well should serve as a guideline.
15. The sample size and volume of reagent may require optimization beyond the procedure described.

References

1. Desimone MF, Alvarez GS, Foglia ML, Diaz LE (2009) Development of sol-gel hybrid materials for whole cell immobilization. *Recent Pat Biotechnol* 3:55–60
2. Michelini E, Roda A (2012) Staying alive: new perspectives on cell immobilization for biosensing purposes. *Anal Bioanal Chem* 402:1785–1797
3. Zhou M, Dong S (2011) Bioelectrochemical interface engineering: toward the fabrication of electrochemical biosensors, biofuel cells, and self-powered logic biosensors. *Acc Chem Res* 44:1232–1243
4. Gupta G, Staggs KW, Ista LK, Oucherif KA, Atanassov PB, Tartis MS, Montano GA, Lopez GP (2009) CVD for the facile synthesis of hybrid nanobiomaterials integrating functional supramolecular assemblies. *Langmuir* 25:13322–13327
5. Luckarift HR, Sizemore SR, Roy J, Lau C, Gupta G, Atanassov P, Johnson GR (2010) Standardized microbial fuel cell anodes of silica-immobilized *Shewanella oneidensis*. *Chem Commun (Camb)* 46:6048–6050
6. Luckarift HR, Sizemore SR, Farrington KE, Fulmer PA, Biffinger JC, Nadeau LJ, Johnson GR (2011) Biodegradation of medium chain hydrocarbons by *Acinetobacter venetianus* 2AW immobilized to hair-based adsorbent mats. *Biotechnol Prog* 27:1580–1587
7. Luckarift HR, Sizemore SR, Farrington KE, Roy J, Lau C, Atanassov PB, Johnson GR (2012) Facile fabrication of scalable, hierarchically structured polymer/carbon architectures for bioelectrodes. *ACS Appl Mater Interfaces* 4:2082–2087
8. Coiffier A, Coradin T, Roux C, Bouvet OMM, Livage J (2001) Sol-gel encapsulation of bacteria: a comparison between alkoxide and aqueous routes. *J Mater Chem* 11:2039–2044
9. Bretschger O, Obraztsova A, Sturm CA, Chang IS, Gorby YA, Reed SB, Culley DE, Reardon CL, Barua S, Romine MF, Zhou J, Beliaev AS, Bouhenni R, Saffarini D, Mansfeld F, Kim BH, Fredrickson JK, Nealon KH (2007) Current production and metal oxide reduction by *Shewanella oneidensis* MR-1 wild type and mutants. *Appl Environ Microbiol* 73:7003–7012

10. Lies DP, Hernandez ME, Kappler A, Mielke RE, Gralnick JA, Newman DK (2005) *Shewanella oneidensis* MR-1 uses overlapping pathways for iron reduction at a distance and by direct contact under conditions relevant for biofilms. *Appl Environ Microbiol* 71:4414–4426
11. Bretschger O, Cheung ACM, Mansfeld F, Nealsen KH (2010) Comparative microbial fuel cell evaluations of *Shewanella* spp. *Electroanalysis* 22:883–894
12. Biffinger JC, Ray R, Little BJ, Fitzgerald LA, Ribbens M, Finkel SE, Ringeisen BR (2009) Simultaneous analysis of physiological and electrical output changes in an operating microbial fuel cell with *Shewanella oneidensis*. *Biotechnol Bioeng* 103:524–531
13. Fredrickson JK, Romine MF, Beliaev AS, Auchtung JM, Driscoll ME, Gardner TS, Nealsen KH, Osterman AL, Pinchuk G, Reed JL, Rodionov DA, Rodrigues JL, Saffarini DA, Serres MH, Spormann AM, Zhulin IB, Tiedje JM (2008) Towards environmental systems biology of *Shewanella*. *Nat Rev Microbiol* 6:592–603
14. Ringeisen BR, Henderson E, Wu PK, Pietron J, Ray R, Little B, Biffinger JC, Jones-Meehan JM (2006) High power density from a miniature microbial fuel cell using *Shewanella oneidensis* DSP-10. *Environ Sci Technol* 40:2629–2634
15. Jia L, Deng R, Song H (2011) Reversible removal of SO₂ at low temperatures by *Bacillus licheniformis* immobilized on γ -Al₂O₃. *Bioresour Technol* 102:524–528
16. Wu J, Yu HQ (2007) Biosorption of 2,4-dichlorophenol by immobilized white-rot fungus *Phanerochaete chrysosporium* from aqueous solutions. *Bioresour Technol* 98:253–259

Chapter 21

Encapsulation of Cells in Alginate Gels

Pello Sánchez, Rosa María Hernández, José Luis Pedraz,
and Gorka Orive

Abstract

Cell microencapsulation is based on the immobilization of cells for continuous release of therapeutics. This approach has been tested in the treatment of many diseases and several clinical trials have been performed. Factors such as the choice of cells to be encapsulated, the biomaterial used, and the procedure for carrying out the capsules are important issues when implementing this technology.

This book chapter makes a comprehensive description of alginate, the most frequently employed biomaterial, passing by its structure, the extraction and treatment, and finishing with the process of gelation. It also describes the various modifications that can be carried out to allow the interaction between the alginate and the integrin receptors of encapsulated cells. The main microencapsulation technologies are presented as well as how 100 μm alginate–Poly-L-Lysine–alginate microcapsules can be fabricated with Flow-focusing technology.

Key words Cell encapsulation, Microencapsulation, Hydrogel, Alginate, Flow focusing

1 Introduction

Cell microencapsulation consists on the immobilization of biologically active materials in a polymer matrix surrounded by a semipermeable membrane designed to protect them. Since Chang made the first encapsulation in 1964 [1] and the first mammalian cell was enclosed in polymers [2], the field has evolved progressively and many different encapsulation technologies have been developed.

Cell encapsulation allows provides a constant and prolonged release of therapeutic products of better quality because they are synthesized “de novo,” thus preventing its degradation and facilitating their administration directly into the damaged area. In theory, using this technology it would be possible to treat chronic diseases as it allows reducing the number of shots and therefore improving patients’ life quality [3].

The selection of biopolymers is one of the most important requirements to make the cell encapsulation technique feasible.

This selection would generate the best conditions for cell surveillance so that cells could synthesize the therapeutic product in the desired manner. There is a wide range of polymers and biomaterials that have been used in cell encapsulation but there is no doubt that alginate is by far the most frequently employed material due to its high biocompatibility, biodegradability, and easy manipulation.

1.1 Alginate as Biomaterial

Alginate is a natural polysaccharide found in brown algae species and in some bacterial species such as *Pseudomonas* and *Azotobacter*. Although it was discovered and recorded in 1880, it was not until 1936 when it was first commercially exploited. The bacteria are able to produce alginate by four stages biosynthesis pathway: (1) synthesis of precursor substrate, (2) polymerization and cytoplasmic membrane transfer, (3) periplasmic transfer and modification, and (4) export through the outer membrane [4]. Nowadays commercially available most common alginates are extracted from brown seaweed such as *Laminaria digitata*, *Laminaria hyperborea*, *Laminaria japonica*, *Macrocystis pyrifera*, and *Ascophyllum nodosum* [5]. The extraction and treatment of these polysaccharides for commercial use is made using aqueous alkali solutions, usually with NaOH. Subsequently, the extract is filtered and in order to obtain the alginate from the extract by precipitation, it is added or sodium chloride or calcium chloride. If that salt of alginate is treated with HCl diluted, it can be transformed in alginic acid. Finally, after purification and conversion, water-soluble sodium alginate powder is produced [6].

As cells are very sensitive to the environment around them, the presence of traces of chemicals and microstructure within the gel may affect their behavior. Therefore, the purity of alginates is a very important requirement for the improvement of the viability of the encapsulated cells and for the reduction of the foreign body reaction that may happen every time a device is injected in patients. If the alginate is purified by a multistep extraction procedure to obtain ultrapure product the foreign body immune response is significantly reduced [7]. The purification process would also permit to eliminate other types of alginate contaminants including polyphenols, endotoxins, and proteins [8].

Not only the purity of the alginate is important but also the viscosity of the gel, which is directly proportional to the molecular weight. To improve the physical properties of alginate gels, the molecular weight of the polymer should be high. However, the solution becomes largely viscous, which is often difficult and undesirable in processing [9]. Using a combination of high and low molecular weight alginate polymers, the elastic modulus of gels can be increased without changing the viscosity of the solution [10]. The molecular weights of commercially available sodium alginate range between 32,000 and 400,000 g/mol.

Table 1
Percentages of the main blocks (MM, GG, MG/GM) of alginates extracted from some species of brown seaweed

Seaweed specie	M/G ratio	MM (%)	GG (%)	MG/GM (%)
<i>Ascophyllum nodosum</i>	1.5	38.4	20.7	41.0
<i>Laminaria digitata</i>	1.43	49.0	25.0	26.0
<i>Laminaria japonica</i>	2.26	36.0	14.0	50.0
<i>Macrocystis pyrifera</i>	1.56	40.6	17.7	41.7

Depending on the species the M/G ratio varies

Table 2
According to the technology used the size range of the obtained microcapsules is different, as well as the alginate solution viscosity that can be used

Technology	Capsules size	Alginate solution viscosity
Simple extrusion	0.5–2 mm	Low
Vibrating nozzle	0.3–0.6 mm	Low
JetCutter	0.2 to several mm	High
Electrostatic	0.3–0.6 mm	Low
Flow focusing	0.1–0.4 mm	Low

1.2 Structure and Gelling of Alginate

Chemically alginates are linear copolymers formed by units of D-mannuronic acid (M) and L-guluronic acid (G) arranged in a chain of alternating sequences of blocks. This G-M ratio of the block structures depends on the algal source [11] (Tables 1 and 2) and it is important to define the ideal relationship of G-M blocks (usually 70 % minimal G). G blocks make ionic exchange and calcium entrapment and the particular spatial configuration that the alginate acquires during its polymerization is known as the “egg box” model [12] (Fig. 1). Thus G-blocks enriched alginates form more rigid gels have greater mechanical strength while M-blocks enriched alginates create more elastic and flexible gels. Although this is the most accepted theory, there are some authors that suggest MGM sequences could have a direct involvement in alginate gel network [13] and other studies have reported that Ba²⁺ can bind to M blocks [14].

The gelation of the alginate can be given with numerous divalent cations thus varying the stiffness of the gel, which generally

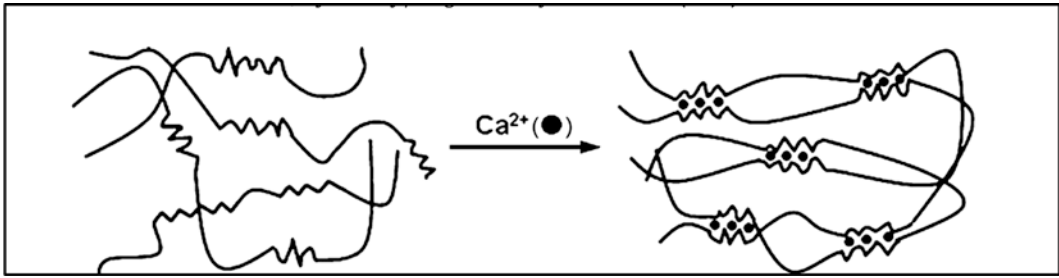


Fig. 1 “Egg-box model.” G blocks make ionic exchange and calcium entrapment

increases with the affinity of the alginate by the cation $Mn > Co > Zn > Cd > Ni > Cu > Pb > Ca > Sr > Ba$. However, most of these ions cannot be used for immobilization of therapeutic active cells. In general, the Ca^{2+} is the most frequently employed ion for such purposes because of its low toxicity. Depending on the calcium agent, the gelation and the resultant gels will have different properties. For example, whereas $CaCl_2$, which is the most used agent, has high solubility in aqueous solutions and leads to rapid and poorly controlled gelation, $CaSO_4$, which has low solubility, leads to slow gelation. Moreover it has reported that at low temperatures the exchanges of divalent cations are slower, forming better structure of the hydrogel and improving its mechanical properties [15]. In an atmosphere of physiological conditions, alginate gels are not very stable over a long period of time, since the divalent cations, which form the bridges between G blocks, are exchanged with monovalent cations. Thus, alginate chains are separated and the gel is dissolved.

Alginate hydrogels are three-dimensional matrices that have similar structure to extracellular matrix and they are typically used for wound healing and release of bioactive agents such as chemical drugs or proteins. As a consequence these type of alginate hydrogels have also been used for cell transplantation in tissue engineering delivering them to the desired site and providing a space for new tissue formation [16]. The alginate despite being a biocompatible material that can hold inside cells is unable to interact with them. There are different techniques and methods to modify the biomaterial providing it the capacity to interact directly with cells [17]. Thus alginate will behave more like an extracellular matrix allowing the interaction with the integrin receptors of encapsulated cells and enhancing cellular viability [18, 19]. One of the most frequent modifications to tailor alginate or create biomimetic alginates is the inclusion of peptides sequences found in the ECM like arginine–glycine–aspartic acid (RGD), which is derived from fibronectin [15] through carbodiimide chemistry [20]. These types of peptides act as adhesion sequences that favor cell attachment to the gel by means of integrins [21] (Fig. 2). Another fragments

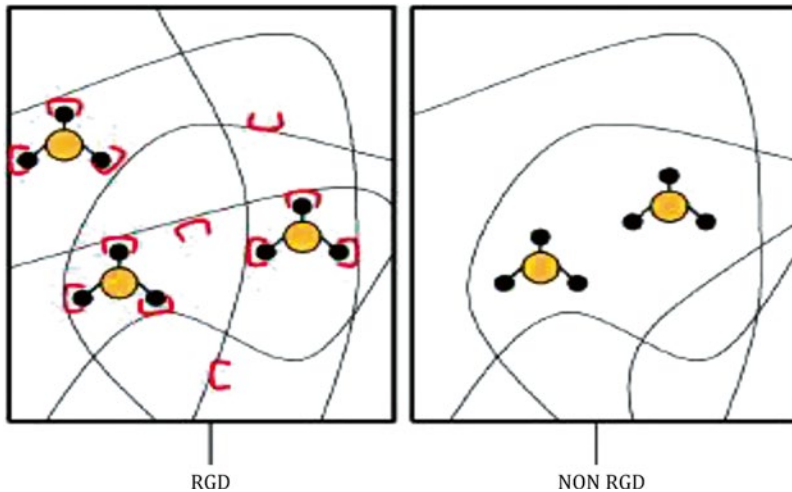


Fig. 2 Schematic description of interaction between cells and alginate hydrogel with or without RGD sequences. RGD modification provides a specific mechanism for cell adhesion [17]

of extracellular matrix proteins like Asp–Gly–Glu–Ala (DGEA) and tyrosine–isoleucine–glycine–serine–arginine (YIGSR) which is derived from laminin can also be used to functionalize alginate gels enhancing adhesive interactions between gel and cells [22, 23]. Another important consideration is the disposition and organization of those peptides within the alginate gel, as the latter may affect cell behavior including differentiation, proliferation, and migration [24, 25].

1.3 Cell Encapsulation Technology with Alginate Hydrogels

In the last few decades many different technologies for cell encapsulation have been reported. In general, the final aim of these techniques is to create an alginate bead in which the therapeutic cells can be enclosed. Once these beads are formed and gelled, they can be coated with different types of agents leading to the formation of microcapsules. These spherical structures provide to the gels more resistance and have increased contact surface thereby improving conditions for cell survival [26, 27]. To maintain viable cells save from the host immune system, the pore size must be large enough to allow the cycling of nutrients, and small enough to prevent the passage of cells and antibodies.

There are different materials, such as polycations that can be used to coat the capsules with the aim of forming a net that provides a suitable pore size range for the enclosed cells.

Some of the most important encapsulation methods include emulsion techniques and extrusion methods. The former is based on mixing aqueous solution with an immiscible organic phase (i.e., oil). When the dispersion is in equilibrium, gel formation is

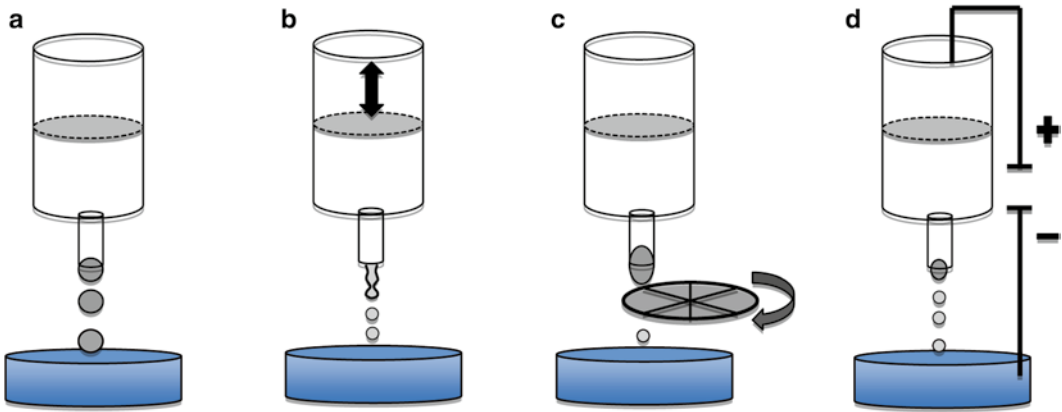


Fig. 3 Main extrusion technologies for cell encapsulation in alginates. **(a)** Simple extrusion. **(b)** Vibrating nozzle. **(c)** Jet Cutter. **(d)** Electrostatic potential

made adding the gelation agent. Finally, the beads are washed. This method is unsuitable when using alginate because CaCl_2 is insoluble in the oil phase. On the other hand, in the extrusion methods the alginate solution mixed with cells is extruded through a needle or a cannula into a gelification bath where they are cross-linked.

Different extrusion methods have been reported and even commercialized so far (Fig. 3). Some critical differences among the different technologies include the simplicity, predictability, repeatability, and the size of the final bead. With the simple extrusion method, it is possible to fabricate capsules in the range of 0.5–3 mm. The capsule size is important, as all necessary nutrients for cell survival diffuse through the entire capsule and not just to the surface. The diffusion of oxygen through biomaterials such as alginate is between 100 and 150 μm . Therefore, the capsule size may be important to prevent hypoxia in the core of the capsule and hence, cell death.

More recently, some other extrusion methods that allow fabricating smaller beads have been reported. The vibrating nozzle technique is one of these new encapsulation tools based on a vibration, which creates a jet that is broken down into smaller and regular droplets. There are two varieties of this technology depending on how the vibration is applied. Applying the sinusoidal force by vibrating the nozzle and pulsating the alginate in a chamber before passing through the nozzle is called vibrating nozzle technique whereas applying the sinusoidal force by periodic changes of the nozzle/orifice diameter during extrusion is called vibrating chamber technique [28]. Several parameters may affect characteristics of the resultant capsules including the nozzle diameter, the flow rate of the laminar jet, the size of the frequency at defined amplitude, and the viscosity of the extruded alginate solution [29].

This technique requires a relatively low viscosity of alginate (<0.2 Pa/s) [30].

The jet cutter technology involves mechanical forces to break up the alginate laminar jet. As a consequence alginate solutions at high concentration (2–5 %) can be used to fabricate the droplets [31]. In this approach, a rotating cutting tool cuts the jet and, due to the surface tension of the solution the cylindrical segments take the form of drop during the fall. Both the vibrating technology and JetCutter® technology are able to produce large alginate bead batches and are easy to scale-up.

Another possibility is to generate an electrostatic potential between the tip of the nozzle and the gelation bath. In this case, the alginate solution viscosity, electrostatic voltage, the flow rate, the nozzle diameter, and the distance between the needle and the gelation bath are important factors to control the size of the beads.

Although most of these systems provide successful grades of reproducibility and some of them can be scale-up, none of them are able to generate capsules with a size less than 0.2–0.3 mm. Recently, a new encapsulation technology known as flow focusing has gained the attentions of scientist in the field as it provides the opportunity to fabricate capsules of less than 100 μm [32, 33] and to scale-up this fabrication by using an array structure.

1.4 Fabricating Cell-Loaded Alginate Capsules with Flow Focusing

This technology involves the formation of a micro jet of a fluid within a highly accelerated laminar flow of another immiscible fluid. This second fluid can be a gas so this process is based on the principle of aerodynamic focusing. The monodispersity of droplets depends on the Weber number, which in turn depends on the gas pressure, the gas velocity at the nozzle, the diameter of the jet, and the surface tension of the jet.

The Weber formula consists of:

$$We = \frac{P_g v_g^2 d_j}{\gamma}$$

where P_g is gas pressure

V_g is gas velocity at the nozzle

d_j is the jet and surface tension of the jet

This value must be between 1 and 40. If the gas pressure is too high, the weber number increases too much and the resulting spray shows polydispersity [34]. On the other hand, if that value is too small, the forces are not strong enough to break the surface tension of the fluid and will not form the droplets.

1.4.1 A Practical Example

The present sections deals with the preparation of cell-loaded alginate capsules using the flow focusing technology. As it was mentioned before, the selection of the alginate type is outstanding to ensure the final alginate bead properties and functionality.

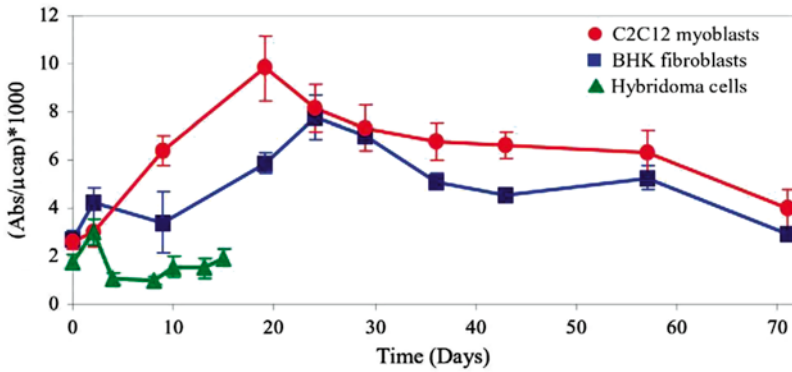


Fig. 4 Metabolic activity of C2C12 myoblast (*red circle*), BHK fibroblast (*blue square*), and hybridoma cells (*green triangle*) microencapsulated in solid alginate–agarose beads. Results are expressed as mean \pm SD from at least three separate sets of experiments [35]

In addition, the type of cell to be immobilized merits also some attention. There is a plenty of cells that have been enclosed within these types of capsules ranging from tumor-like cells to primary cells, genetically modified cells and even stem cells. Independently of the type of cell source it should be taken into account that it is convenient that the enclosed cells do not show a very active cell division capacity. If cells proliferate too fast, they may break the capsules, leading to the destruction of the living medicine and the activation of the host's immune response. After a careful analysis, we have observed that C2C12 myoblasts is a perfect candidate for cell immobilization purposes, not only because of its slow rate division capacity but also due to its differentiating properties, the relatively easy gene manipulation and long-term survival (Fig. 4).

To prepare a batch of cell-loaded alginate beads with the flow focusing, first it is necessary to prepare a 1.5 % (w/v) ultrapure low-viscosity glucuronic acid alginate in Milli-Q water with 1 % (w/v) of mannitol under stirring. It is important to use mannitol to make the solution isosmotic.

Once the alginate is dissolved in mannitol, is filtered with a 0.22 μm pore size filter and it is let stand overnight at 4 $^{\circ}\text{C}$ to remove air bubbles. Then, cells are put in alginate solution (cell density is variable) and mix gently to avoid forming bubbles. Before that, cells must be filtered through pores of 40 μm to remove cell aggregates. This is critical for successful encapsulation because if cell clumps are present there is a high risk for blocking the nozzle tip.

The alginate–cell suspension should be homogeneous and free of bubbles. Some of them may be adhered to the edge of the surface. If this happens, it is possible to eliminate them using a micropipette of 100–1,000 μL . Then the alginate–cell suspension will be

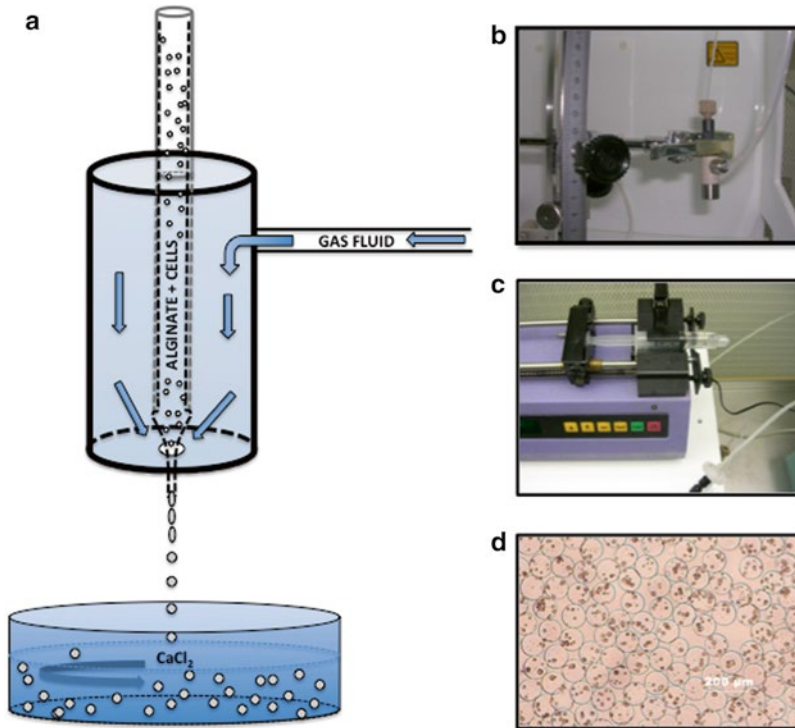


Fig. 5 (a) Flow Focusing technology involves the formation of a micro jet of a fluid within a highly accelerated laminar flow of a gas. The extruded droplets are collected in a CaCl_2 bath under stirring. (b) Flow Focusing system. (c) Peristaltic pump. (d) Alginate–PLL–alginate microcapsules with C2C12 myoblasts

transferred in a sterile syringe and connected to the peristaltic pump (Fig. 5). The suspension will be extruded through a 0.24 mm nozzle tip at a flow rate of 2 mL/h and focused with sterile air at 90–120 mbar pressure. Drops will be collected in a shaker containing 55 mM CaCl_2 solution and the cell-loaded beads will be maintained in the calcium chloride solution for 10 min to obtain the total polymerization of the alginate. Then, it is necessary to filter the beads with 40 μm cell strainer to eliminate the satellite peaks and wash filtered microcapsules with mannitol solution. Beads will be transferred into a 50 mL centrifuge tube and incubate them with 10 mL of 0.05 % PLL solution for 10 min. The concentration and incubation time of the polycation is variable assuming that the increase of both the concentration and the coating time will provoke a reduction in the size of the capsules and a thicker membrane with reduced permeability properties.

After coating the cell-loaded beads with PLL, and therefore creating the microcapsules, it is necessary to filter and wash them again with mannitol solution. Last but not least, the batch of microcapsules will be transferred into a 50 mL centrifuge tube and incubate them with 0.1 % (w/v) alginate solution for 10 min to

coat the positive PLL charge with a negatively charged alginate layer. This step will lead to the generation of alginate–PLL–alginate (APA) microcapsules. Before finishing, APA capsules will be filtered and washed with mannitol solution and then with complete culture medium. Cell loaded microcapsules can then be implanted or just maintained in culture medium at 37 °C in a humidified 5 % CO₂–95 % air atmosphere.

2 Materials

- Ultrapure low-viscosity glucuronic acid alginate (UPLVG) (FMC Biopolymer, Norway).
- Poly-L-Lysine (PLL hydrobromide M_w 15,000–30,000 Da; Sigma Aldrich, St. Louis, MO, USA).
- Calcium chloride solution (0.6 %).
- C2C12 myoblast cells derived from the skeletal muscle of an adult C3H mouse.
- Culture mediums: DMEM medium was supplemented with 10 % fetal bovine serum (FBS) and 1 % antibiotic/antimycotic solution for the myoblast cells.
- Differentiation media: DMEM medium supplemented with 2 % horse serum and 1 % antibiotic/antimycotic solution.
- Cells were cultured at 37 °C in a humidified 5 % CO₂–95 % air atmosphere.
- All materials must be sterile.

3 Methods

3.1 Preparation of the Reagents

1. Prepare a 1.5 % (w/v) Ultrapure low-viscosity glucuronic acid alginate in Milli-Q water with 1 % (w/v) of mannitol. This solution will be extruded to form alginate droplets.
2. Prepare a 0.05 % (w/v) PLL solution in Milli-Q water with 1 % (w/v) of mannitol. Ten milliliters of this solution is needed to create outer layer in 2 mL of alginate droplets.
3. Prepare a 0.1 % (w/v) Ultrapure low-viscosity glucuronic acid alginate in Milli-Q water with 1 % (w/v) of mannitol. Ten milliliters of this solution is needed to create outer layer in 2 mL of alginate droplets.
4. Prepare 55 mM calcium chloride solution in Milli-Q water with 1 % (w/v) of mannitol. Eighty milliliters of this solution is needed per capsule batch.
5. Sterilize all the solutions with a 0.22 µm filter.

3.2 Preparation of the Cell Pellet

1. Remove cell culture from the flask.
2. Wash cells attached to flask three times with PBS solution, pH 7.4.
3. Add 4 mL of trypsin–EDTA (Invitrogen) and wait between 5 and 8 min until cells detach from the flask.
4. Add 6 mL of complete medium to deactivate the action of the trypsin.
5. Filter the cell suspension through pores of 40 μm to remove cell aggregates.
6. Determine the cell concentration using coulter counter.
7. Transfer the necessary volume into a 50 mL falcon and centrifuge 5 min at 1,500 rpm.
8. Remove the supernatant and break the cell pellet.
9. Add the desired volume of alginate (LVG) 1.5 % at one time and resuspend the cells with extreme softness and care with the aid of a spatula.

3.3 Elaboration of Cell-Loaded APA Microcapsules

1. Mix the cell pellet with the corresponding volume of alginate solution to obtain the desired cell density.
2. Transfer the alginate–cell suspension in a sterile syringe and connect the latter to the peristaltic pump.
3. Extruded the suspension through a 0.24 mm nozzle tip at a flow rate of 2 mL/h and focused with sterile air at 90–120 mbar pressure.
4. Collect drops in a 55 mM CaCl_2 solution in a shaker.
5. Leave the cell-loaded microcapsules in the calcium chloride solution for 10 min to obtain the total polymerization of the alginate.
6. Filter microcapsules with 40 μm cell strainer to eliminate the satellite peaks.
7. Wash filtered microcapsules with mannitol solution.
8. Transfer the microcapsules to a 50 mL centrifuge tube and incubate them with 10 mL of 0.05 % PLL solution for 10 min.
9. Filter the cell-loaded capsules and wash again with mannitol solution.
10. Transfer the microcapsules to a 50 mL centrifuge tube and incubate them with 0.1 % (w/v) alginate solution for 10 min.
11. Filter and wash the APA capsules with mannitol solution and then with complete culture medium.
12. Culture the APA capsules in culture medium at 37 °C in a humidified 5 % CO_2 –95 % air atmosphere.
13. All the process is carried out at room temperature and aseptic conditions.

References

1. Chang TM (1964) Semipermeable microcapsules. *Science* 146:524–525
2. Lim F, Sun AM (1980) Microencapsulated islets as a bioartificial endocrine pancreas. *Science* 210:908–910
3. Orive G, Hernández RM, Gascón AR, Calafiore R, Chang TM, De Vos P, Hortelano G, Hunkeler D, Lacik I, James Shapiro AM, Pedráz JL (2003) Cell encapsulation: promise and progress. *Nat Med* 9:104–107
4. Remminghorst U, Rehm BHA (2006) Bacterial alginates: from biosynthesis to applications. *Biotechnol Lett* 28:1701–1712
5. Smidsrod O, Skjak-Bræk G (1990) Alginate as immobilization matrix for cells. *Trend Biotechnol* 8:71–78
6. Clark DE, Green HC (1936) Alginic acid and process of making same. US Patent 2036922
7. Orive G, Ponce S, Hernandez RM, Gascon AR, Igartua M, Pedraz JL (2002) Biocompatibility of microcapsules for cell immobilization elaborated with different type of alginates. *Biomaterials* 23:3825–3831
8. Orive G, Tamb SK, Pedraz JL, Halle JP (2006) Biocompatibility of alginate-poly-L-lysine microcapsules for cell therapy. *Biomaterials* 27:3691–3700
9. LeRoux MA, Guilak F, Setton LA (1999) Compressive and shear properties of alginate gel: effects of sodium ions and alginate concentration. *J Biomed Mater Res* 47:46–53
10. Kong HJ, Lee KY, Mooney DJ (2002) Decoupling the dependence of rheological/mechanical properties of hydrogels from solids concentration. *Polymer* 43:6239–6246
11. McHugh DJ (1987) Production and utilization of products from commercial seaweeds. Food and Agriculture Organization of the United Nations, Rome
12. Grant GT, Morris ER, Rees DA, Smith PJC, Thom D (1973) Biological interactions between polysaccharides and divalent cations: the egg-box model. *FEBS Lett* 32:195–198
13. Donati I, Holtan S, Morch YA et al (2005) New hypothesis on the role of alternating sequences in calcium-alginate gels. *Biomacromolecules* 6:1031–1040
14. Morch YA, Donati I, Strand BL et al (2006) Effect of Ca²⁺, Ba²⁺, and Sr²⁺ on alginate microbeads. *Biomacromolecules* 7:1471–1480
15. Augst AD, Kong HJ, Mooney DJ (2006) Alginate hydrogels as biomaterials. *Macromol Biosci* 6:623–633
16. Lee KY, Mooney DJ (2001) Hydrogels for tissue engineering. *Chem Rev* 101:1869–1879
17. Acarregui A, Murua A, Pedráz JL, Orive G, Hernández RM (2012) A perspective on bioactive cell microencapsulation. *BioDrugs* 26(5):283–301. doi:10.2165/11632640-000000000-00000
18. Kong HJ, Boonthekul T, Mooney DJ (2006) Quantifying the relation between adhesion ligand-receptor bond formation and cell phenotype. *Proc Natl Acad Sci USA* 103:18534–18539
19. Huebsch ND, Mooney DJ (2007) Fluorescent resonance energy transfer: a tool for probing molecular cell-biomaterial interactions in three dimensions. *Biomaterials* 28:2424–2437
20. Rowley JA et al (1999) Alginate hydrogels as synthetic extracellular matrix materials. *Biomaterials* 20:45–53
21. Orive G, De Castro M, Kong HJ, Hernández RM, Ponce S, Mooney DJ, Pedráz JL (2009) Bioactive cell-hydrogel microcapsules for cell-based drug delivery. *J Control Release* 135:203–210
22. Alsberg E, Anderson KW, Albeiruti A et al (2001) Cell-interactive alginate hydrogels for bone tissue engineering. *J Dent Res* 80:2025–2029
23. Dhoot NO, Tobias CA, Fischer I et al (2004) Peptide-modified alginate surfaces as a growth permissive substrate for neurite outgrowth. *J Biomed Mater Res A* 71:191–200
24. Koo LY et al (2002) Co-regulation of cell adhesion by nanoscale RGD organization and mechanical stimulus. *J Cell Sci* 115:1423–1433
25. Chen CS et al (1997) Geometric control of cell life and death. *Science* 276:1425–1428
26. De Vos P, Andersson A, Tam SK, Faas MM, Hallé JP (2006) Advances and barriers in mammalian cell encapsulation for treatment of diabetes. *Immunol Endocr Metabol Agents Med Chem* 6:139–153
27. Zhou H, Xu HH (2011) The fast release of stem cells from alginate-fibrin microbeads in injectable scaffolds for bone tissue engineering. *Biomaterials* 32:7503–7513
28. Whelehan M, Marison IW (2011) Microencapsulation using vibrating technology. *J Microencapsul* 28(8):669–688
29. Serp D, Cantana E, Heinzen C, Von Stockar U, Marison IW (2000) Characterization of an encapsulation device for the production of mono-disperse alginate beads for cell immobilization. *Biotechnol Bioeng* 70:41–53
30. Koch S, Schwinger C, Kressler J, Heinzen CH, Rainov NG (2003) Alginate encapsulation of genetically engineered mammalian cells: comparison of production devices, methods and microcapsule characteristics. *J Microencapsul* 20(3):303–316
31. Prusse U, Dalluhn J, Breford J, Vorlop KD (2000) Production of spherical particles by jet

- cutting. *Chemic Ingenieur Technik* 72:852–858
32. Gañan-Calvo AM, Gordillo JM (2001) Perfectly monodisperse microbubbling by capillary flow focusing. *Phys Rev Lett* 87:274501
 33. Santos E, Orive G, Calvo A, Catena R, Fernández-Robredo P, García Layana A, Hernández RM, Pedráz JL (2012) Optimization of 100 μm alginate-poly-L-lysine-alginate capsules for intravitreal administration. *J Control Release* 158:443–450
 34. Gañan-Calvo AM (1998) Generation of steady liquid microthreads and micron-sized monodisperse sprays in Gas streams. *Phys Rev Lett* 80:285
 35. Orive G, Hernández RM, Gascón AR, Igartua M, Pedraz JL (2003) Survival of different cell lines in alginate-agarose microcapsules. *Eur J Pharm Sci* 18(1):23–30

Microalgal Immobilization Methods

Ignacio Moreno-Garrido

Abstract

In this review, methods for the most common microalgal immobilization procedures are gathered and described. Passive (due to natural adherence of cells to surfaces) and active immobilization methods should be distinguished. Among active immobilization methods, calcium alginate entrapment is the most widely used method if living cells are intended to be immobilized, due to the chemical, optical, and mechanical characteristics of this substance. Immobilization in synthetic foams, immobilization in agar and carrageenan as well as immobilization in silica-based matrix or filters are also discussed and described. Finally, some considerations on the use of flocculation for microalgae are mentioned.

Key words Microalgae, Phytoplankton, Immobilization methods, Biotechnology

1 Introduction

Small size of microalgae (most of species used in biotechnology are smaller than 50 μm) imply serious difficulties when bioreactor designs are intended. On the one hand, loss of biomass could happen when a continuous flow system is stated. On the other hand, harvesting of suspended cell biomass is an expensive and often inefficient process. In order to solve both problems, biotechnology has resorted to immobilization techniques. Most of immobilization techniques designed for microorganisms in general can be used for microalgae in particular, taking into account light limitation if living cells immobilization is intended.

Current biotechnology involving microorganism is increasingly focusing on microalgae. Immobilization of those photosynthetic unicellular organisms are nowadays used in pharmaceutical, aquaculture, food, and cosmetic industries [1, 2], depuration processes [3–7], pre-concentration of trace substances [8], energy production, as biodiesel or biogas [9–11] as well as molecular hydrogen bio-production [12], toxicity testing [13–15], culturing techniques for handling culture collections [16] or even in research on gas exchange

systems for space travelling [1]. Current uses and potential biotechnology for immobilized microalgae have been previously reviewed by Robinson et al. [3], Cassidy and Trevors [17], Mallick [18], Abdel Hameed and Ebrahim [19], and Moreno-Garrido [20]. Olguín [21] and De-Bashan and Bashan [7] reviewed these techniques focusing on nutrient or pollutant removal.

Most of immobilization techniques are expensive if an industrial scale is attempted. Thus, products obtained should cover the immobilization expenses, and this is not always achieved [11, 22, 23].

Two groups of immobilization techniques can be distinguished: passive and active techniques.

Passive immobilization refers to the natural tendency of some microorganisms and plant cells [24], including microalgal species, to attach and growth on different submerged surfaces [25]. To this respect, immobilization on natural sponges from different species of the genus *Luffa* will be briefly revised, as well as passive colonization on different materials.

Active immobilization techniques imply deliberate entrapment of pre-cultured microalgal populations, not dependent on cellular ability to attach surfaces. Those techniques will be more extensively discussed, paying special attention to alginate gel immobilization techniques.

2 Microalgal Immobilization Methods

2.1 *Passive Methods*

Immobilizing passive methods exploit the ability of some microalgal cells to attach surfaces. In this section attachment to or colonization on loofa sponges and other materials will be discussed. Although some immobilization techniques for already polymerized synthetic foams can be considered “passive,” they will be discussed in the following for text structure reasons.

2.1.1 *Loofa Sponges*

The reticulated loofa sponge is obtained by the removal of hard pericarp tissue of the dried fruit of *Loofa cylindrica* (Cucurbitaceae) [26]. This material has a high porosity degree, stable physical properties, and it is biodegradable, nontoxic, and cheap [27]. A significant problem for the use of loofa sponges in fine experimentation is the variability among natural structures: some sponges could present more pore proportions in function of the growth condition of the plants. Some researchers tried to solve this problem by choosing similar sections [27], by cutting sections [26, 28, 29] in order to get pieces easy to handle and statistically more representative, or even disintegrate in fibers [30]. Even when repeatability could not be very high, loofa immobilization for microorganisms should not be discarded as a good solution in order to minimize costs in biotechnological devices.

In any case, for immobilization research, loofa sponge sections use to be washed, sometimes boiled, and then dried. Following a typical protocol for loofa sponges [26], sections of near 2.5 cm diameter are cut (2–3 mm thick), soaked in boiling water for 30 min, washed with tap water and left 24 h in distilled water, changing this washing water three or four times. Then, disks are oven dried at 70 °C, sterilized in autoclave for 20 min and soaked in culture medium for around 10 min under aseptic conditions. Disks are then transferred to flasks with microalgal cultures. In this concrete case, old cultures (3–4 weeks, stationary growth phase) were used. After incubation, loofa pieces are washed in order to remove free cells. Please note that loofa pieces could be pre-weighed before studies in order to check dry weight increase.

Duration of incubation for immobilization can vary in function of the organisms which is intended to be immobilized: Iqbal and Edivean [28], as well as Saeed et al. [31], immobilizing a fungus (*Phanaerochaete* or *Trichoderma*), incubated for 7 days; Ogbonna et al. [30] immobilized yeasts and incubated cells for just 24 h; Nagase et al. [32] immobilizing a microorganism consortium and Liu et al. [27] immobilizing plant cells incubated for 3 days. For *Chlorella sorokiniana*, Nasreen et al. [33] incubated for 24 days. Saeed and Iqbal [31] immobilized cyanophytes (*Synechococcus*) and incubated the loofa sponges with the algal culture for 2 weeks.

2.1.2 Passive Adherence to Glass, Plastic, or Wood

Some microalgal species have the ability of stick to submerged surfaces, acting as periphyton or epiphytes. This characteristic has been exploited in ecology studies and biotechnology.

For ecology and ecotoxicology studies, Gosh and Gaur [34] disposed typical glass slides (7.5 × 2.5 × 1.5 mm) glued to glass rods and placed the devices into a stream for 4 or 5 weeks, obtaining more attaches biomass in low-current locations. Nayar et al. [35, 36] also used glass slides, but for their locations (Ponggol, a tropical estuary located on the northeastern coast of Singapore) just 3–5 days are enough for collecting periphyton at the glass slides surfaces. Aadmiral et al. [25] used 1.5 cm² etched glass disks submerged for 10–20 days at the Dommel, a small lowland river at northern Belgium. Danilov and Ekelund [37] compare different substrata submerged in lakes of different trophic status. They conclude that, at experimental conditions (9 weeks exposition), glass tubes were the better substratum for periphytes attachment, as wood did not support the same diversity and abundance as glass did. Plastics were only covered by bacteria, but not by algae.

For biotechnology studies, natural tendency to attach certain surfaces is not enough, and etching agents are used in order to enhance attachment (thus, a semi-passive technique could also be considered). Franke and Franke [38] used microalgae attached to 3 mm diameter glass beads, etched with hydrofluoric acid for better

adhesion, in order to check photocatalyst capacity of attached biomass for persistent chemicals, such as TIO_2 . This etching technique has not been widely used for phytoplankton and could be promising if non-easily attaching cells are intended to be used. Laurinavichene et al. [39] use a technique for immobilizing *Chlamydomonas* in glass fiber, previously developed by Tsygankov et al. [40] for photosynthetic bacteria (*Rhodobacter*). In order to improve cellular attachment to the glass surfaces, they use a silane coupling reagent (3-(2-aminoethylaminopropyl)-trimethoxysilane) (LS-2480, Shinetsu Silicone Co. Ltd., Tokyo). Glass materials were washed in 5 % $\text{K}_2\text{Cr}_2\text{O}_7$ solution in 50 % H_2SO_4 at 80 °C for 1 h, and then soaked in a 15 % solution of LS-2480 in dichloromethane at room temperature for 2 h. After the modification, the glass material should be washed four times by sonication in dichloromethane. Those two authors use the attached biomass in order to produce hydrogen.

2.2 Active Methods

In contrast to passive methods, active immobilization methods do not depend on the ability of cells to attach surfaces: specific techniques are, thus, developed to trap or encapsulate living or dead microalgal cells. Immobilization in synthetic or natural polymers, silica gel or filters will be discussed in this section.

2.2.1 Synthetic Polymers

Most of prepolymers to be mixed in order to form synthetic polymeric foams are quite toxic for living cells. Thus, dead cells are commonly used as immobilized biomass. In other occasions, few surviving cells after immobilization are able to grow after polymerization and thus establish an immobilized population. Porous characteristics of already formed synthetic foams also permit embedding of microalgal cultures (a type of “passive” immobilization), but interior of the foam, even split into small pieces, uses to be light limiting for living photosynthetic populations at long time terms.

Polyurethane

Travieso et al. [41, 42] employed polyurethane 1 cm³ foam cubes as support media for *Scenedesmus quadricauda* in order to remove nutrients for cattle manure. For microalgae immobilization, those authors submerged the cut foam cubes in bubbled microalgae cultures for 10 days. Travieso et al. [43] advance one more step and design a reactor with a rotary drum with polyurethane foam in order to remove metals from effluents. Yamaguchi et al. [44] immobilized non-photosynthetic alga *Prototheca* in 8 mm³ polyurethane foams cubes in order to check degradation capacity for *n*-alkanes. For polyurethane colonization, those authors submerged the cubes in microalgal cultures for 10 days. Suzuki and Yamaguchi [45] also use *Prototheca* in a reactor containing the similar immobilizing material (10 mm³ polyurethane foams cubes) in order to check degradation of *n*-alkanes too.

Macroalgal pulverized biomass has been immobilized in polyurethane foams by Alhakawati and Banks [46] in order to remove copper from aqueous solutions. Those authors mixed, for each experiment, 30 g of Hypol (a prepolymer of the polyurethane foam), 15 g of seaweed biomass, and 0.978 g NaHCO₃. After that, 0.6 g Pluronic-85 dissolved in 45 mL of distilled water and acidified with 0.702 g of glacial acetic acid was mixed with the prepolymer and biomass mixture and then vigorously mixed with a mechanical mixer at 2,400 rpm. A foam with entrapped biomass resulted, and after 2–3 min it can be cut into slices. Material should be kept 24 h in a fume cupboard to promote solvent loss.

Polysulfone

Blanco et al. [47] used dead cyanophyte cells immobilized in a polysulfone matrix: after grounding biomass, it was mixed with polysulfone dissolved in *N,N*-dimethylformamide at 100 g/L. The mixture was then stirred for 1 h at room temperature, and then, dripped through a nozzle into 50 % (v:v) ethanol. By this procedure, spherical and durable beads containing 50 % biomass by weight were quickly formed by a phase inversion process. Toxicity of components probably does not permit to immobilize living cells.

Polyvinyl Alcohol and Polyvinyl Foams

Urrutia et al. [48] used urethane prepolymer (Hypol FHP 2002) to immobilize *Scenedesmus* cells in order to check nitrate uptake rates from water. Cultures were pre-concentrated by centrifugation and added in few milliliters to 10 g of prepolymer in an ice bath for 1 min, and then polymerized. After discarding the hard, impermeable outer layer of the foam, it was cut into 4–5-mm-side cubes and washed several times in fresh growth medium to remove the remaining toxic products. Foam pieces were suspended in the same medium to allow continued growth of algae into the pores of the support. Quite better survival rates were obtained if foams were previously polymerized and, after washing, mixed with cultures in order to let the cells adsorb to the foam material.

Hashim et al. [49] used dried biomass of *Sargassum baccularia* immobilized in polyvinyl alcohol. Algal (macroalgal, in this case) biomass was mixed with a 15 % polyvinyl alcohol (PVA) aqueous solution to a solid–liquid ratio of approximately 150 mg/mL. The mixture was dropped into a stirred saturated boric acid solution to form spherical gel beads. Gel beads formed were then transferred to a sodium phosphate solution and adjusted to pH 5.5 for hardening. Finally, the beads were washed with distilled water to remove any chemical residue. Jeon et al. [50] propose a mixture of techniques involving alginic acid and polyvinyl alcohol in order to metal removal from aqueous solutions (although no cells, even dead, are immobilized by this technique, till the data): 8.8 g of PVA is added to 100 mL of distilled water and mixed for 3 h. Then, 14 g of alginic acid is mixed thoroughly with PVA solution. In order to reduce the viscosity of this mixed solution,

temperature of the reactor must be controlled at 120 °C. This mixture is then pumped by peristaltic pump at 10 mL/min, dropped on a stirred mixed solution including 6 g of boric acid and 10 mL of glutaraldehyde (25 % solution) in 100 mL water, in order to get spherical beads. In order to complete gelation inside beads, these beads must be kept in a saturated boric acid and glutaraldehyde solution for 24 h under gentle stirring. Both the chemical components and temperature of this process do not permit to immobilize living microalgal cells.

Epoxy Resin

Blanco et al. [47] entrapped cells of *Phormidium laminosum* in epoxy resin, following this procedure: 4 g of distilled water, 1 g of Epikote 255, and 1 g of Epikure 3660 are mixed. After a precondensation time of ca 10 min, 3 g of 8 % (w/v) Na-alginate solution is added. When the mixture is homogeneous, 1 g of dried and ground microalgal biomass is added. Viscosity is regulated by addition of 2 mL of distilled water. The mixture is then dropped into a 2 % (w/v) calcium chloride solution, in order to get spherical beads. After a hardening period of 40 min, the beads are collected and dried at 55 °C in an oven for 24 h (size of the beads then diminished by desiccation). Then, alginate is dissolved by soaking the beads in 0.1 M phosphate buffer (pH 6.0) for 1 h to introduce porosity to the matrix. The beads are then washed for 15 min in distilled water and stored at 4 °C in ultrapure water until further use.

2.2.2 Natural Gel-Forming Substances

Natural gel-forming substances use to have a clear advantage on synthetic polymers: low toxicity of the components uses to permit the immobilization of living cells. This is not true for proteins which need to be cross-linked in order to form an immobilizing matrix, as cross-linking is usually performed by very toxic substances, such as glutaraldehyde. Apart from proteins, some natural products obtained from algae (agar, carrageenates, and alginates, especially the latter), are the most widely used substances in microalgal immobilization.

Proteins

Proteins mixed with cross-linking substances can be used in order to immobilize microalgal cells. Chouteau et al. [51, 52] used bovine serum albumin (BSA) cross-linked with glutaraldehyde, in order to immobilize *Chlorella* cells, following the procedure established by Babu and Panda [53] for *E. coli*. Adjusting the pH solution to 4.25, 2 mg/mL of BSA is optimally cross-linked with glutaraldehyde, 1.5 % after 2 h. Kubal and D'souza [54] used egg white also cross-linked with glutaraldehyde in order to immobilize yeast cells: 10 mL of egg white obtained from fresh eggs is mixed with 2 g of cells and then the mix is treated with glutaraldehyde (2 %). The mixture is well stirred and allowed to stand for 2 h at 4 °C. The hard gel obtained is shattered by passing through a syringe, and then washed with water to remove excess of

glutaraldehyde and stored till use. This technique could be used for microalgal cells as well. Seki and Suzuki [55] use casein instead BSA or egg white in order to immobilize the microalga *Heterosigma akashiwo*. In this case, cross-linking is also performed with glutaraldehyde: A suspension containing 20 g/L (dw) microalgal biomass and 10 g/L (dw) casein is stirred and pH of the suspension adjusted to pH 3 by HNO₃ in order to flocculate the microorganism with the casein. After 20 min for sedimentation, the flocs are collected by filtration and immersed in an excess stirred glutaraldehyde solution (10 %) overnight. After that period, the floc, cross-linked with glutaraldehyde, are collected by filtration and washed repeatedly with distilled water.

Glutaraldehyde being involved in all the above-mentioned protein immobilization methods implies that no living cells can survive to this procedure.

Agar

Agarose (predominant component of the agar) is a not-branched polysaccharide obtained from the cell wall of some algae among Rhodophyceae, mainly from the genus *Gelidium* and *Gracilaria*. Chemically, is a linear polymer formed by repeated monomers of a disaccharide conformed by D-galactose and 3,6-anhydro-L-galactopyranose. This substance has been used for decades as a component of solid cultures for microorganisms. This substance per se is able to adsorb metals in dilution [56]. Gelation and degelation of the gel is determined by temperature. Thus, if living cells are intended to be immobilized, temperature of the process should be carefully controlled. Vilchez et al. [57] immobilized *Chlamydomonas* cells in agar and studied the photosynthetic and respiratory activity of the entrapped organisms. After harvesting the microalgal cells, they are washed and resuspended (0.5–1 % w/v) in 20 mM Tricine–NaOH-buffered culture medium adjusted at pH 7.5. Then, they are mixed with an equal volume of an agar suspension (3 % w/v), at 35 °C. When the preparation became solid, the agar is cut into small cubes (8 mm³) and rinsed with fresh culture medium before use. Aksu et al. [58] used a special agarose type with gel properties at low temperature (Type VII, provided by Sigma). Beads are prepared by dropping 2.5 % (w/w) agarose solution into edible oil at 40 °C using a peristaltic pump. If cells are mixed, the proportion of agarose/microbial biomass is around 4. After dropping, temperature should be lowered to 15 °C using an ice bath. Then, phosphate buffer solution (pH 7.0) is added to the oil phase and thus particles move to aqueous phase. The oil phase is then removed from the medium and the particles stored in phosphate buffer solution of pH 7.0 at 4 °C till use. Khattar et al. [59] consider that their immobilized material (cyanophytes) can stand till 45 °C before cooling, and they simply use agar 2 % at this temperature mixed with concentrate microalgal culture before immediately pour the material into molds and cool it. Schreiter

et al. [60] gets temperatures of 39 °C at the moment of mixing 100 µL of concentrated microalgal culture of *Synechococcus* with 125 µL of agar.

Limitation of the use of agar for immobilizing living cells seems to be the agar temperature when mixed with algal inoculum to be entrapped. Cyanophyte in culture use to stand more temperature than eukaryotic algae, but temperatures near 50 °C could irreversibly damage any non-thermophilic species.

Carrageenan

Carrageenan is a mixture of linear, sulfated galactans. They are composed of alternating α -D-galactopyranose and β -D-galactopyranose or 3,6-anhydrogalactose. As in the case of Agarose, they are extracted from red seaweeds (Rhodophyceae), over all from the genera *Gigartina*, *Chondrus*, or *Eucheuma*. Molecules forming carrageenan present a varying degree of sulfation (15–40 %). Carrageenans are used in a variety of commercial applications as stabilizing agents or thickeners.

Cassidy et al. [61] successfully immobilized bacterial cells in carrageenan by mixing 1 g of κ -carrageenan with 90 mL of 0.05 M Na_2HPO_4 (pH 7.2) in a 500 mL Erlenmeyer flask. The solution is then heated to 70 °C and stirred for 30 min. After this time, 5 g of montmorillonite K10 clay are added and the solution mixed for another 15 min. 1 g skim milk powder is then added and mixing continued for an additional 1 h. The solution is then autoclaved for 10 min at 121 °C, and then maintained at 30 °C and stirred at 100 rpm for 1 h. Resuspended cells are added aseptically to the mixture at 30 °C and mixed into the κ -carrageenan solution for 15 min. The mixture is then extruded through a needle into a stirred solution of 0.3 M KCl maintained at 10 °C. Resulting beads are left in the KCl solution for 2 h at 10 °C, washed and stored till used.

Lau et al. [62] performed a complete study about the effects of carrageenan immobilization in *Chlorella vulgaris*. In this case, κ -carrageenan Type III extracted from *Eucheuma cottonii* is used. After preparing 20 mL of 5 % (w/v) carrageenan, it is autoclaved at 121 °C for 15 min. Microalgal cells are resuspended in 20 mL of deionized water and mixed with the 20 mL carrageenan, giving a final gel concentration of 2.5 % (w/v). The mixture is kept at 38 ± 1 °C in a temperature-controlled water bath. The algal-carrageenan sol is then extruded through a needle into a 2 % KCl solution. The beads are cured in this solution overnight, washed, and stored till used.

Travieso et al. [42] used immobilized cells of three microalgal species (*Chlorella vulgaris*, *Chlorella kessleri*, and *Scenedesmus quadricauda*) in order to check nutrient removal when immobilized by different methods, including alginate immobilization. For carrageenane immobilization these authors refer to the technique described in Lem and Glick [63], but in that paper no mention of

immobilization techniques is made. It is supposed that the technique is similar to that previously described for the experiments of Lau et al. [62], i.e., dropping carrageenan sol mixture with algae on 0.3 M KCl by a peristaltic pump.

Alginate

Calcium alginate is, by far, the most wide used technique for immobilizing freshwater or marine microalgae. Immobilization in calcium alginate beads do not restrict in a great way the light intensity needed to grow photosynthetic organisms [64], and low toxicity of the components, added to the fact of independence of temperature in the gelation process confers indubitable advantages to this technique, as metabolism of immobilized cells can stand active for long times [45, 65–68]. The same property of alginate permits the reuse of immobilized biomass obtained [69, 70] as a resource for improving fertility of deserted soils [71]. As one of the most adequate immobilization techniques for microalgal cells, special attention will be paid to it and a step-by-step procedure for marine and freshwater microalgal species will be described.

General Considerations About Alginate

Alginates are linear unbranched polymers containing β -(1→4)-linked D-mannuronic acid and α -(1→4)-linked L-guluronic acid residues. They are structural components of evolved brown algae (Phaeophyceae), and they are extracted overall from the genera *Macrocystis* and *Laminaria*. Alginates from different species show different percentages of each polymer component, and this has implications in the gel physical properties.

Alginates can be also found in bacteria. *Pseudomonas aeruginosa* increase the production of this substance in the present of copper, as it has a remarkable chemical affinity for these metal and other divalent cations [72, 73]. For complete information about biosynthesis and uses of alginate, included cell or enzyme immobilization, an exhaustive revision made by Ertesvåg and Valla [74] can be consulted. Lately, due to the low toxicity, this material has been also used for peritoneal animal implantations [75].

Alginate is usually provided as a sodium salt. When dissolved in water, and if dropped on a solution enriched with a divalent cation, the latter substitutes sodium and gelation occurs. Typically, sodium alginate dissolved in water around 1.5–3 % (w/v), mixed with a suspension of living or dead cells, is dropped into an aqueous solution of up to 4 % of CaCl₂ [76–81]. External gelation of the beads is instantaneous, but 30–40 min hardening use to be performed in order to ensure gelation to the inner part of the formed beads. When alginate is solved in water, many bubbles use to be formed. In order to avoid this, which could imply undesired flotation of beads, sodium alginate sol can be submitted to vacuum conditions (i.e., in a Kitasato flask) before addition of cells [82]. Other authors [83] just let the sol resting for 1 h to ensure deaeration.

Solution of sodium alginate in marine media has been a problem till the application of the protocols described by Hertzberg and Jensen [84], as sodium alginate does not dissolve well in saline media. These authors recommend to divide the desired volume of dissolving water into two aliquots, then sodium alginate is dissolved in one of them (i.e., 60–70 % of final volume) and sodium chloride (enough to ensure osmotic level of the final volume) in the other aliquot (30–40 % of final volume). These two parts can be mixed afterwards with no problems, when sodium alginate and salt are separately and previously dissolved. When recultures of immobilized cells are needed, known volumes of beads can be redissolved on known volumes of tri-sodium citrate [85, 86].

Immobilized cells can be successfully used for in situ tests [13, 86–88]. When used for measuring toxicity, two main problems must be taken into account if calcium alginate immobilized microalgal cells are intended to be used. First, if batch methods are used, adsorption of potential toxicants to alginate (mainly metals) can imply a fast, dramatic decrease of free dissolved toxicants: measurements of actual concentrations should be performed for a valid test [82]. Second, diffusion of toxicants into beads can be a slow process [89], and thus cells can be protected against xenobiotics and toxicity undervalued.

On the other hand, not all species are susceptible to be immobilized. Moreno-Garrido et al. [15] immobilized 11 marine microalgal species from different taxonomic groups: *Nannochloropsis gaditana* (Eustigmatophyceae); *Heterocapsa* sp. (Dinophyceae); *Rhodomonas salina* (Cryptophyceae); *Isochrysis* aff. *galbana* (Prymnesiophyceae); *Thalassiosira pseudonana*, *Chaetoceros gracilis*, *Phaeodactylum tricornerutum* and *Skeletonema costatum* (Bacillariophyceae); *Tetraselmis chui* (Prasinophyceae); *Porphyridium cruentum* (Rhodophyceae); and *Dunaliella salina* (Chlorophyceae). Some of the diatoms (*P. tricornerutum*, *C. gracilis*, *S. costatum*) and *I. galbana* demonstrated to grow for more than 2 weeks inside the alginate beads. Dinoflagellates do not seem to be good targets for calcium alginate immobilization techniques.

In this paper, 1.25 % alginate from *Macrocystis pyrifera* in 36 salinity media (see above for marine sodium alginate preparation) was dropped on 4 % calcium chloride and then hardened for 30 min. But when agitation is performed in marine cultures or in situ marine or estuarine expositions are intended, calcium can be replaced again by the excess of sodium and beads can lose stability [82].

In order to solve this problem, Widerøe and Danielsen [90] proposed the use of Ba and, overall, Sr instead Ca as hardening cation. Following these authors, Divalent cations that will cross-bind alginate threads listed according to affinity for alginate, are Pb > Cu > Cd > Ba > Sr > Ca > Co, Ni, Zn > Mn. Moreira et al. [86] also

studied alternative cations and alginate compositions in order to enhance bead hardness and durability for in situ marine or estuarine studies. These authors concluded that beads formed after dropping 4.9 % sodium alginate from *Laminaria hyperborea* on 4 % SrCl_2 solution demonstrated to be quite resistant on marine conditions and thus suitable for field experiments. Vilchez et al. [91] assayed 14 different divalent cations in order to harden sodium alginate solutions Ba^{2+} ; Ca^{2+} ; Cd^{2+} ; Co^{2+} ; Cu^{2+} ; Fe^{3+} ; Mn^{2+} ; Ni^{3+} ; Pb^{2+} ; Sr^{2+} ; and Zn^{2+} , and they found significant nitrate uptake activity only for Ca^{2+} and Ba^{2+} (no data of nitrate uptake of the rest of cations are shown in this paper).

Cheong et al. [92] provided an alternative use of alginate in order to microencapsulate cells: cells are suspended in 1 % CaCl_2 solution, and Xanthan gum is also added in order to form spherical capsules. A surfactant (Nonoxynol) is used to improve permeability of the membrane capsule wall. Then, this cellular suspension is dropped by a syringe into a 0.5 % sodium alginate stirred solution. The capsules formed are then washed with distilled water and shrunk for 10 min in 0.1 M HEPES pH 7.4 buffer solution and stored till use. In this case, when counts are needed, capsules are dissolved in 0.1 M citric acid—0.2 M Na_2HPO_4 pH 5 buffer.

Poncelet et al. [83] also proposed a calcium-alginate based emulsification method: after mixing sodium alginate with water (1–4 %) and adjust the pH value by a buffer to 8.0, alginate is mixed with a suspension of insoluble calcium salt (500 mM Ca_2 , added to reach 25 mM final concentration). The alginate–calcium salt mixture is then dispersed with canola oil (other authors use olive oil [93]) containing 80 mM glacial acetic acid, which liberates calcium which pre-gel the beads. After this, the oil–bead suspension is dropped into a typical 50 mM calcium chloride solution. Beads pass to the water fraction, oil is discarded and beads washed with 1 % Tween 80, sieved and stored till use.

Chan et al. [94] propose a modification of this method and investigate the influence of the concentration of calcium carbonate (0.5–1 g) incorporated to a typical sodium alginate 2 % solution. This mixture of sodium alginate–calcium carbonate is dispersed in isooctane containing Span 85, an after stirring for 10 min, a solution of Tween 85 is added. As in the protocol described above, glacial acetic acid is then added to the mixture in order to provoke the release of Ca^{2+} ions and microspheres are formed.

Calcium alginate beads containing immobilized microalgal cells can be used in removal of metals by different purposes [95]. The use of packed-bed reactors with beads seems to be more efficient in metal removal than other models, such as air-lift reactors [58, 96–98].

Alginate immobilizing microalgal cells can be also prepared in films instead of beads [99–101]. For this technique, typical sodium alginate sol are embedded on nets of different mesh sizes and

submerged in calcium alginate solutions. Alginate sols can be also embedded on filters, and this technique has been widely used in the design of biosensors: Frense et al. [102] simply used paper disks embedded in sodium alginate solution.

On other occasions, filters are not even needed to design a biosensor: Shitanda et al. [103] use poly-L-lysine in order to fix alginate layers directly on the surface of a transparent indium tin oxide electrode.

*Immobilization Method
Involving Alginate*

A general procedure for creating alginate beads immobilizing microalgae will be described. Materials will be listed (reagents, glassware and laboratory facilities), as well as a step-by-step procedure for marine and freshwater species. Procedure is based on that described by Hertzberg and Jensen in 1989 [84].

Materials

Reagents: Sodium alginate, sodium chloride (NaCl), calcium chloride (CaCl₂), distilled (or deionized) water, 2 L of sterile marine water (for marine species) or 2 L of sterile tap water (for freshwater species), new culture medium for microalgae (marine or freshwater), sodium hydroxide (NaOH) and chlorhydric acid (HCl) for pH adjusting.

Glassware and laboratory facilities: Microalgal culture, pH electrode, centrifuge and centrifuge vials, Kitasato-type vacuum flask (500 mL capacity) with hermetic top, vacuum pump, balance accurate to 0.01 g (minimum), weighting spatulas and trays, beakers (2 or 3 of 100 mL, at least 1 of 1 L), magnetic stirrer and magnetic bars, 50 mL syringe with needle, nylon sieve (smaller than 1 mm mesh).

Methods

Procedure (for making around 80 mL of hardened beads)

- Weight 1.50 g of sodium alginate.
- If freshwater cells are intended to be immobilized, mix the 1.50 sodium alginate powder with 100 mL of distilled water in a beaker.
- If marine cells are intended to be immobilized, mix the same weight in 60 mL of distilled water; then weight 3.50 g of sodium chloride and solve them in 40 mL of distilled water *in a different beaker*. Only when both reagents are completely solved the two solutions can be mixed. This is important.
[*Note*: sodium alginate is slow to dissolve. It takes some time and handling of a spatula is highly recommended. It is considered that sodium alginate is completely dissolved when formed sol is homogeneous and no lumps are visible. Sodium alginate solution must present a consistency like fluid honey].

- Measure the pH of the solution and adjust the value (by the use of HCl or NaOH) to the same pH value of the microalgal culture, mixing frequently with a spatula.
- Pour the sodium alginate solution into a Kitasato flask and submit it to vacuum. All bubbles will expand and explode. This process can be stopped when no more bubbles are observed in the solution.

[*Note:* this step is carried out in order to eliminate internal bubbles in the future beads which increase their flotation capacity. If researchers intend to maintain as much beads floating at the medium surface as possible, this step can be avoided].

- Gently pour the vacuumed sodium alginate solution to a clean beaker.

[*Note:* part of the solution will be difficult to recover from the flask. This, joined to the fact that alginate lost volume when hardened with calcium (see below) will imply near a 20 % of final volume respect to the original solution volume].

- Weight 16 g of CaCl_2 and dissolve it in 400 mL of sterile tap water or sterile marine water (in function of the type of microalgal species which is intended to be immobilized). Use a 1 L beaker to dissolve it with a magnetic stirrer.

[*Note:* higher concentrations than 4 % w/v could be used if harder beads are intended to be formed].

- Centrifuge an aliquot of the microalgal culture.

[*Note:* microalgal cells could be damaged by high speed or long time centrifugations. Centrifugation times, speeds, and temperatures should be selected in function of the chosen species and survival at the selected conditions assayed before, if living, unharmed cells are intended to be used].

- When the culture is centrifuged, discard the supernatant and concentrate the cells as much as possible (for an original solution of 100 mL, no more than 0.5 mL of concentrated cells medium should be used).
- Drop the concentrated cells on the dissolved sodium alginate and mix very gently (using a spatula) the cells with the solution till it presents a homogeneous color.

[*Note:* please take care of not to produce bubbles while mixing].

- Pour the mixture of sodium alginate plus cells into a syringe and drop it over the stirred 400 mL of calcium chloride solution.

[*Note:* stirring of the hardening media can continue during all the process. Bead shapes will not be altered. For homogeneous beads sizes, dropping speed should be maintained as possible.

Bead size can be selected by slowing or accelerating solution extrusion].

- After all desired alginate solution has been extruded keep the beads stirred for 30 min in the hardening calcium chloride solution.
- Then, drop the beads into a nylon sieve and wash them with at least 1 L of marine or tap water (in function of the species selected) in order to remove the calcium excess.
- Transfer the beads to a fresh microalgal culture medium (marine or freshwater). Beads are ready to be used.

Notes

Cell density estimation inside the beads can be performed by dissolving a known bead volume into a known phosphate or citrate buffer. After a vigorous shaking, the beads will dissolve and cells could be counted. Mixed sodium alginate could be sterilized in autoclave before mixing with concentrated microalgae, but sodium alginate solutions treated in this way lost gelation properties, and higher initial proportion than 1.50 % (w/v) are recommended.

2.2.3 Silica Gel and Polysilicate

Silica gel is a porous, vitreous form of SiO_2 synthetically produced from Na_3SiO_2 (sodium silicate). Porosity and high adsorption capacity can be exploited in microalgal biotechnology. Singh and Prasad [104] designed a cationic polyelectrolyte [poly (*N*-xylene-*N,N'*-dicyclohexyl ethylenediamine dibromide)], immobilized in silica, capable of electrostatic binding with *Spirogyra* sp. biofilm. The aim of this study was to pre-concentrate metals in order to better measurement by differential pulse anodic stripping voltammetry. This procedure implies two steps: first, polymer-modified silica gel needed to be prepared by mixing with C_2EXBr_2 polyelectrolyte via DMSO, which should evaporated and silica dried and stored in a dryer chamber. Then, algal biomass in powder is stirred in dimethylformamide, added to the modified silica and shaken for 2 h. Residual DMF is removed by slightly heat.

Stark and Rayson [105] used polysilicate to immobilize ten different biogenic materials (including *Chlorella* cells) in order to bind metal ions. Basically, the immobilization procedure consist on the addition of each material to a 6 % solution of $\text{Na}_2\text{SiO}_4 \cdot 5\text{H}_2\text{O}$ at pH 2.0 followed by the increasing addition of $\text{Na}_2\text{SiO}_4 \cdot 5\text{H}_2\text{O}$ solution till pH values of the mixture of 7.0. The resulting gel is washed with deionized water and then baked overnight at 80 °C.

Carrilho et al. [8] also used silica in order to immobilize algal biomass from the brown alga *Pilayella littoralis*. Powdered algae and silica gel (w/w ratio of 2:5) are separately dried at 80 °C for 10 min, and then mixed. The algae–silica paste is formed by the addition of few drops of deionized water and blending. The paste is then dried at 80 °C for 20 min. This wetting–drying process is repeated three to five times in order to get a better immobilization

of the alga on the silica. Then, the resulting oven-dried silica–algae matrix is sieved in a plastic strained to discard non-immobilized biomass. Godlewska-Żyłkiewicz, [106] performed a similar technique using *Chlorella vulgaris*, but the author heated the paste till 60 °C and w/w ratio for algae and silica gel here is 1.5:5.

A different approach for immobilizing in silica gel is provided from Rangasayatorn et al. [95]. In this case, 1 g of dry weight equivalent biomass of the cyanophyte *Spirulina platensis* is mixed with 25 mL of 6 % sodium silicate (Na_2SiO_3) solution and 25 mL of deionized water. Then 20 mL of 18 % HCl is added to form the gel. Resulting particles are washed, dried at 80 °C, and sieved in order to discard particles smaller than 150 μm .

Of course, as all these techniques imply heating of the biological material, no living cells are susceptible to be immobilized.

2.2.4 Immobilization on Filters

Immobilization on filters of different types has been used in order to design biosensors involving living microalgae, generally with the aim of measuring toxicity of volatile compounds. Naessens and Tran-Minh [107, 108], Naessens et al. [109], and Durrieu and Tran-Minh [110] immobilized *Chlorella vulgaris* cells on glass microfiber filters (GF/C Whatman, 45.7-mm filter diameter, 1.2-mm pore diameter) with the aim to design microalgal biosensors. Nowak et al. [111] immobilized several species in membrane filters (0.22 μm) in order to facilitate culturing and media renewal in 96 well plates. Podola et al. [112] used membrane filters (type ME28, Schleicher and Schuell, Dassel, Germany) to membrane-immobilize algal strains of genus *Klebsormidium* and *Chlorella*. Sanders et al. [113] used Millipore APHD fiber glass filter disks (Bedford, MA) in order to immobilize *Chlorella vulgaris* and the cyanophyte *Nostoc commune*. Finally, Védrine et al. [114] used Whatman quartz microfiber filter QMA in order to immobilize *Chlorella* cells.

2.3 Flocculation

Although it is commonly used to recovering of microalgae biomass, flocculation can be also considered as an immobilization method *sensu lato*. Flocculation techniques were developed in order to avoid time-consuming and expensive harvesting methods such as centrifugation or filtering. Theoretically, alkaline flocculants neutralize the negative surface charges of the microalgae and then allow them to coalesce into a floc [115, 116]. Some of the flocculants, such as anionic aluminum, can present toxicity and can limit the biomass recovered [117]. Thus, natural alternative flocculant agents, such as chitosan, have been used.

Chitosan is a lineal polysaccharide formed of β -(1-4)-linked D-glucosamine and N-acetyl-D-glucosamine, distributed randomly. It is a structural component of the crustacean exoskeleton [118]. Composition of each particular chitosan has an influence on the flocculation capacity [119]. This substance has been more or less successfully used to flocculate marine, brackish water, and freshwater

microalgal species [120, 121], although ionic strength (i.e., salinity of the media) also diminishes the flocculation capacity of this substance.

Kaya and Picard [122] described a specific procedure for immobilizing (and not just flocculate) viable cells of the freshwater green alga *Scenedesmus bicellularis* by the use of chitosan: 2 % (w/v) chitosan is dissolved in 99 mL of distilled water and 0.8 mL acetic acid, stirred and heated to 50 °C, with a pH value between 5.5 and 6. Then, an 1:1 ratio of microalgal cells suspension (8.2 g/L dry mass) and chitosan solution is dropped into 200 mL of stirred 1.5 % (m/v) Na₄P₂O₇ or K₄P₂O₇ solution (pH 6.0) for chelation. After 50 min for curation, chitosan gel beads are washed with 0.1 M phosphate buffer (pH 7.5). The same authors also assayed a variation for the described immobilization technique using konjac gel as a copolymer of chitosan, directly including the microalgal cells in the mixture of chitosan and konjac at various ratios. Finally, immobilization is carried out by introducing the mixture suspension of algae and gels into a mold consisting of two flat plexiglass slabs.

Aluminum or ferric chloride has been also used in order to flocculate marine microalgae, but concentrations of flocculants to be used were ten times higher than those used for freshwater species [123].

Schlesinger et al. [117] made a critical analysis of the state of the art about appropriate and inappropriate flocculant agents and found some contradictions about the stoichiometric ratios of flocculant–algae to be used. Freshwater algae are more efficiently flocculated by pH increase than marine species [116] and the topic is currently in the limelight due to the recent interest in the biotechnology production of biofuels by microalgae [124]. Polyelectrolytes has been also used in order to promote flocculation by Uduman et al. [125] and Zheng et al. [126], the latter by the use of poly-gamma-glutamic acid.

References

1. Borowitzka MA (1999) Commercial production of microalgae: ponds, tanks, tubes and fermenters. *J Biotechnol* 70:313–321
2. Spolaore P, Joannis-Cassan C, Duran E, Isambert A (2006) Commercial applications of microalgae. *J Biosci Bioeng* 101(2):87–96
3. Robinson PK, Mak AL, Trevan MD (1986) Immobilized algae: a review. *Process Biochem* 122–126
4. Greene B, Bedell GW (1990) Algal gels or immobilized algae for metal recovery. In: Akatsuka I (ed) *Introduction to applied phycology*. SPB Academic Publishing bv, The Hage, pp 137–149
5. Maeda S, Sakaguchi T (1990) Accumulation and detoxification of toxic elements by algae. In: Akatsuka I (ed) *Introduction to applied phycology*. SPB Academic Publishing bv, The Hage
6. Wilde EW, Benemann JR (1993) Bioremoval of heavy metals by the use of microalgae. *Biotechnol Adv* 11:781–812
7. De-Bashan L, Bashan Y (2010) Immobilized microalgae for removing pollutants: review of practical aspects. *Bioresour Technol* 101:1611–1627
8. Carrilho ENVM, Nóbrega JA, Gilbert TR (2003) The use of silica-immobilized brown

- alga (*Pilayella littoralis*) for metal preconcentration and determination by inductively coupled plasma optical emission spectrometry. *Talanta* 60:1131–1140
9. Harun R, Davidson M, Doyle M, Gopiraj R, Danquah M, Forde G (2011) Technoeconomic analysis of an integrated microalgae photobioreactor, biodiesel and biogas production facility. *Biomass Energy* 35:741–747
 10. Ahmad AL, Mat Yasin NH, Derek CJC, Lim JK (2011) Microalgae as a sustainable energy source for biodiesel production: a review. *Renew Sustain Energy Rev* 15:584–593
 11. Lam MK, Lee KT (2012) Microalgae biofuels: a critical review of issues, problems and the way forward. *Biotechnol Adv* 30:673–690
 12. Chader S, Mahmah B, Chetehouna K, Amrouche F, Abdeladim K (2011) Biohydrogen production using green microalgae as an approach to operate a small proton exchange membrane fuel cell. *Int J Hydrogen Energy* 36:4089–4093
 13. Moreira dos Santos M, Moreno-Garrido I, Gonçalves F, Soares AMVM, Ribeiro R (2002) An in situ bioassay with microalgae for estuarine environments. *Environ Toxicol Chem* 21(3):567–574
 14. Moreira dos Santos M, Soares AMVM, Ribeiro R (2004) An in situ bioassay for freshwater environments with the microalga *Pseudokirchneriella subcapitata*. *Ecotoxicol Environ Saf* 59:164–173
 15. Moreno-Garrido I, Campana O, Lubián LM, Blasco J (2005) Calcium alginate immobilized marine microalgae: experiments on growth and short-term heavy metal accumulation. *Mar Pollut Bull* 51:823–929
 16. Lukavsky J (1988) Long-term preservation of algal strains by immobilization. *Arch Protistenkd* 135:65–68
 17. Cassidy MB, Lee H, Trevors JT (1996) Environmental applications of immobilized microbial cells: a review. *J Ind Microbiol* 16:79–101
 18. Mallik N (2002) Biotechnological potential of immobilized algae for wastewater N, P and metal removal: a review. *Biometals* 15:377–390
 19. Abdel Hameed MS, Ebrahim OH (2007) Biotechnological potential uses of immobilized algae. *Int J Agricul Biol* 9(1):183–192
 20. Moreno-Garrido I (2008) Immobilized microalgae: current techniques and uses (review). *Bioresour Technol* 99:3949–3964
 21. Olgúin EJ (2003) Phycoremediation: key issues for cost-effective nutrient removal processes. *Biotechnol Adv* 22:81–91
 22. Huang G, Chen F, Wei D, Zhang X, Chen G (2010) Biodiesel production by microalgal biotechnology. *Appl Energy* 87:38–46
 23. Christenson L, Sims R (2011) Production and harvesting of microalgae for wastewater treatment, biofuels and bioproducts. *Biotechnol Adv* 29:686–702
 24. Archambault J, Volesky B, Kurz WGW (1990) Development of bioreactors for the culture of surface immobilized plant cells. *Biotechnol Bioeng* 35:702–711
 25. Admiraal W, Blanck H, Buckert-de Jong M, Guasch H, Ivorra N, Lehmann V, Nyström BAH, Paulsson M, Sabater S (1999) Short-term toxicity of zinc to microbenthic algae and bacteria in a metal polluted stream. *Water Res* 33(9):1989–1996
 26. Akhtar N, Iqbal J, Iqbal M (2004) Removal and recovery of nickel(II) from aqueous solution by loofa sponge immobilized biomass of *Chlorella sorokiniana*: characterization studies. *J Hazard Mater B* 108:85–94
 27. Liu YK, Seki M, Tanaka H, Furusaki S (1998) Characteristics of loofa (*Luffa cylindrica*) sponge as a carrier for plant cell immobilization. *J Ferment Bioeng* 85(4):416–421
 28. Iqbal M, Edyvean RGJ (2004) Biosorption of lead, copper and zinc ions on loofa sponge immobilized biomass of *Phanaerochaete chrysosporium*. *Minerals Eng* 17:217–223
 29. Ahmadi M, Vahabzadeh F, Bonakdarpour B, Mehranian M (2006) Empirical modeling of olive oil mill wastewater treatment using loofa-immobilized *Phanaerochaete chrysosporium*. *Process Biochem* 41:1148–1154
 30. Ogbonna JC, Tomiyama S, Tanaka H (1996) Development of a method for immobilization of non-flocculating cells in loofa (*Luffa cylindrica*) sponge. *Process Biochem* 31(8):737–744
 31. Saeed A, Iqbal M, Zafar SI (2009) Immobilization of *trichoderma viride* for enhanced methylene blue biosorption: batch and column studies. *J Hazard Mater* 168:406–415
 32. Nagase H, Pattanasupong A, Sugimoto E, Tani K, Nasu M, Hirata K, Miyamoto K (2006) Effect of environmental factors on performance of immobilized consortium system for degradation of carbedazim and 2,4-dichlorophenoxyacetic acid in continuous culture. *Biochem Eng J* 29:163–168
 33. Nasreen A, Iqbal M, Zafar SI, Iqbal J (2008) Biosorption characteristics of unicellular green alga *Chlorella Sorokiniana* immobilized in loofa sponge for removal of Cr(III). *J Environ Sci* 20:231–239
 34. Gosh M, Gaur JP (1998) Current velocity and the establishment of stream algal periphyton communities. *Aquat Botany* 60:1–10

35. Nayar S, Goh BPL, Chou LM, Reddy S (2003) In situ microcosms to study the impact of heavy metals resuspended by dredging on periphyton in a tropical estuary. *Aquat Toxicol* 64:293–306
36. Nayar S, Goh BPL, Chou LM (2005) Settlement of marine periphytic algae in a tropical estuary. *Estuarine Coastal Shelf Sci* 64:241–248
37. Danilov R, Ekelund NGA (2001) Comparison of usefulness of three types of artificial substrata (glass, wood and plastic) when studying settlement patterns of periphyton in lakes of different trophic status. *J Microbiol Methods* 45:167–170
38. Franke R, Franke C (1999) Model reactor for photocatalytic degradation of persistent chemicals in ponds and waste water. *Chemosphere* 39(15):2651–2659
39. Laurinavichene TV, Fedorov AS, Ghirardi ML, Seibert M, Tsygankov AA (2006) Demonstration of sustained photoproduction by immobilized, sulphur deprived *Chlamydomonas reinhardtii* cells. *Int J Hydrogen Energy* 31:569–667
40. Tsygankov AA, Hirata Y, Miyake M, Asada Y, Miyake J (1994) Photobioreactor with photosynthetic bacteria immobilized on porous glass for hydrogen photoproduction. *J Ferment Bioeng* 77(5):575–578
41. Travieso L, Sánchez Hernández E, Weiland P (1995) Final treatment for cattle manure using immobilized microalgae. I. Study of the support media. *Res Conserv Recycling* 13:167–175
42. Travieso L, Benítez F, Weiland P, Sánchez E, Dupeyrón R, Domínguez AR (1996) Experiments on immobilization of microalgae for nutrient removal in wastewater treatments. *Bioresour Technol* 55:181–186
43. Travieso L, Pellón A, Benítez F, Sánchez E, Borja R, O'Farrill NO, Weiland P (2002) BIOALGA reactor: preliminary studies for heavy metals removal. *Biochem Eng J* 12:87–91
44. Yamaguchi T, Ishida M, Suzuki T (1999) An immobilized cell system in polyurethane foam for the lipophilic micro-alga *Prototheca zopfii*. *Process Biochem* 34:167–171
45. Suzuki T, Yamaguchi T, Ishida M (1998) Immobilization of *Prototheca zopfii* in calcium alginate beads for the degradation of hydrocarbons. *Process Biochem* 33(5):541–546
46. Alhakawati MS, Banks CJ (2004) Removal of copper from aqueous solution by *Ascophyllum nodosum* immobilised in hydrophilic polyurethane foam. *J Environ Manage* 72:195–204
47. Blanco A, Sanz B, Llama MJ, Serra JL (1999) Biosorption of heavy metals to immobilized *Phormidium laminosum* biomass. *J Biotechnol* 69:227–240
48. Urrutia I, Serra JL, Llama MJ (1995) Nitrate removal from water by *Scenedesmus obliquus* immobilized in polymeric foams. *Enzyme Microb Technol* 17:200–205
49. Hashim MA, Tan HN, Chu KH (2000) Immobilized marine algal biomass for multiple cycles of copper adsorption and desorption. *Sep Purif Technol* 19:39–42
50. Jeon C, Park JY, Yoo YJ (2002) Novel immobilization of alginate acid for heavy metal removal. *Biochem Eng J* 11:159–166
51. Chouteau C, Dzyadevych S, Chovelon JM, Durrieu C (2004) Development of novel conductometric biosensors based on immobilised whole cell *Chlorella vulgaris* microalgae. *Biosens Bioelectron* 19:1089–1096
52. Chouteau C, Dzyadevych S, Durrieu C, Chovelon JM (2005) A bi-enzymatic whole cell conductometric biosensor for heavy metal ions and pesticides detection in water samples. *Biosens Bioelectron* 21:273–281
53. Babu PSR, Panda T (1991) Studies on improved techniques for immobilizing and stabilizing penicillin amidase associated with *E. coli* cells. *Enzyme Microb Technol* 13:676–682
54. Kubal BS, D'Souza SF (2004) Immobilization of catalase by entrapment of permeabilized yeast cells in hen egg white using glutaraldehyde. *J Biochem Biophys Methods* 59:61–64
55. Seki H, Suzuki A (2002) Adsorption of heavy metal ions to floc-type biosorbents. *J Colloid Interface Sci* 249:295–300
56. Burdin KS, Bird KT (1994) Heavy metal accumulation by carrageenan and agar producing algae. *Botanica Marina* 37:467–470
57. Vilchez MJ, Vígara J, Garbayo I, Vilchez C (1997) Electron microscopic studies on immobilized growing *Chlamydomonas reinhardtii* cells. *Enzyme Microb Technol* 21:45–47
58. Aksu Z, Eğretli G, Kutsal T (1998) A comparative study of copper(II) biosorption on Ca-alginate, agarose and immobilized *C. vulgaris* in a packed-bed column. *Process Biochem* 33(4):393–400
59. Khattar JIS, Sarma TA, Singh DP (1999) Removal of chromium ions by agar immobilized cells of the cyanobacterium *Anacystis nidulans* in a continuous flow bioreactor. *Enzyme Microb Technol* 25:564–568
60. Schreiter PP-Y, Gillor O, Post A, Belkin S, Schmid R, Bachmann TT (2001) Monitoring of phosphorus bioavailability in water by an immobilized luminescent cyanobacterial reporter strain. *Biosens Bioelectron* 16: 811–818
61. Cassidy MB, Lee H, Trevors JT (1997) Survival and activity of lac-lux marked *Pseudomonas aeruginosa* UG2Lr cells encap-

- sulated in κ -carrageenan over four years at 4°C. *J Microbiol Methods* 30:167–170
62. Lau PS, Tam NFY, Wong YS (1998) Effect of carrageenan immobilization on the physiological activities of *Chlorella vulgaris*. *Bioresour Technol* 63:115–121
 63. Lem NW, Glick BR (1985) Biotechnological uses of cyanobacteria. *Biotechnol Adv* 3:195–208
 64. Hatanaka Y, Kudo T, Miyataka M, Kobayashi O, Higashihara M, Hiyama K (1999) Asymmetric reduction of hydroxyacetone to propanediol in immobilized halotolerant microalga *Dunaliella Parva*. *J Biosci Bioeng* 88(3):281–286
 65. Chen Y-C (2001) Immobilized microalga *Scenedesmus quadricauda* (Chlorophyta, Chlorococcales) for long-term storage and for application for water quality control in fish culture. *Aquaculture* 195:71–80
 66. Chen Y-C (2003) Immobilized *Isochrysis galbana* (Haptophyta) for long-term storage and applications for feed and water quality control in clam (*Meretrix lusoria*) cultures. *J Appl Phycol* 15:439–444
 67. Tripathi U, Ramachandra RS, Ravishankar GA (2002) Biotransformation of phenylpropanoid compounds to vanilla flavor metabolites in cultures of *Haematococcus pluvialis*. *Process Biochem* 38:419–426
 68. Leino H, Kosourov SN, Saari L, Sivonen K, Tsygankov AA, Aro E-M, Allahverdiyeva Y (2012) Extended H₂ photoproduction by N₂-fixing cyanobacteria immobilized in thin alginate films. *Int J Hydrogen Energy* 37:151–161
 69. Tam NFY, Wong YS (2000) Effect of immobilized microalgal bead concentrations on wastewater nutrient removal. *Environ Pollut* 107:145–151
 70. Jiménez-Pérez MV, Sánchez-Castillo P, Romera O, Fernández-Moreno D, Pérez-Martínez C (2004) Growth and nutrient removal in free and immobilized planktonic green algae isolated from pig manure. *Enzyme Microb Technol* 34:392–398
 71. Trejo A, de-Bashan LE, Hartmann A, Hernandez J-P, Rothballer M, Schmid M, Bashan Y (2012) Recycling waste debris of immobilized microalgae and plant growth-promoting bacteria from wastewater treatment as a resource to improve fertility of eroded desert soil. *Environ Exp Botany* 75:65–73
 72. Boyd A, Chakrabarty AM (1995) *Pseudomonas aeruginosa* biofilms: role of the alginate exopolysaccharide. *J Ind Microbiol* 15:162–168
 73. Jang LK, Nguyen D, Geesey GG (1995) Selectivity of alginate gel for Cu vs. Co. *Water Res* 29(1):307–313
 74. Ertesvåg H, Valla S (1998) Biosynthesis and applications of alginates. *Polym Degrad Stab* 59:85–91
 75. Sakai S, Ono T, Ijima H, Kaekami K (2004) Behavior of enclosed sol- and gel-alginates in vivo. *Biochem Eng J* 22:19–24
 76. Hertzberg S, Kvittingen L, Anthonson T, Skjåk-Bræk G (1992) Alginate as immobilization matrix and stabilizing agent in a two-phase liquid system: Application in lipase-catalysed reactions. *Enzyme Microbiol Technol* 14:42–47
 77. Pane L, Feletti M, Bertino C, Carli A (1998) Viability of the marine microalga *Tetraselmis suecica* grown free and immobilized in alginate beads. *Aquaculture Int* 6:411–420
 78. Garbayo I, Vigarà AJ, Conchon V, Martins Dos Santos VAP, Vilchez C (2000) Nitrate consumption alterations induced by alginate-entrapment of *Chlamydomonas reinhardtii* cells. *Process Biochem* 36:459–466
 79. Metha SK, Gaur JP (2001) Removal of Ni and Cu from single and binary metal solutions by free and immobilized *Chlorella vulgaris*. *Eur J Protistol* 37:261–271
 80. Abu Al-Rub FA, El-Naas MH, Benyahia F, Ashour I (2004) Biosorption of nickel on blank alginate beads, free and immobilized algal cells. *Process Biochem* 39:1767–1773
 81. Katircioğlu H, Aslim B, Türker AR, Atici T, Beyatli Y (2008) Removal of cadmium(II) ion from aqueous system by dry biomass, immobilized live and heat-inactivated *Oscillatoria* sp. H1 isolated from freshwater (Mogan Lake). *Bioresour Technol* 99:4185–4191
 82. Moreno-Garrido I, Lubián LM, Blasco J (2007) Sediment toxicity tests involving immobilized microalgae (*Phaeodactylum tricornerutum* Bohlin). *Environ Int* 33:481–495
 83. Poncelet D, Babak V, Dulieu C, Picot A (1999) A physico-chemical approach to production of alginate beads by emulsification-internal ionotropic gelation. *Colloid Surface A: Physicochem Eng Aspects* 155:171–176
 84. Hertzberg S, Jensen A (1989) Studies of alginate-immobilized marine microalgae. *Botanica Marina* 32:267–273
 85. Moreira SM, Guilhermino L, Ribeiro R (2006) An in situ bioassay with the microalga *Phaeodactylum tricornerutum* for sediment-overlying water toxicity evaluations in estuaries. *Environ Toxicol Chem* 25(9):2272–2279
 86. Moreira SM, Moreira-Santos M, Guilhermino L, Ribeiro R (2006) Immobilization of the marine microalga *Phaeodactylum tricornerutum* in alginate for in situ experiments: Bead stability and suitability. *Enzyme Microb Technol* 38:135–141

87. Faafeng BA, van Donk E, Källqvist T (1994) In situ measurement of algal growth potential in aquatic ecosystems by immobilized algae. *J Appl Phycol* 6:301–308
88. Bozeman J, Koopman B, Bitton G (1989) Toxicity testing using immobilized microalgae. *Aquat Toxicol* 14:345–352
89. Aksu Z, Bülbül G (1999) Detgermination of effective diffusion coefficient of phenol in Ca-alginate-immobilized *P. putida* cells. *Enzyme Microb Technol* 25:344–348
90. Widerøe H, Danielsen S (2001) Evaluation of the use of Sr²⁺ in alginate immobilization of cells. *Naturwissenschaften* 88:224–228
91. Vílchez C, Garbayo I, Markvicheva E, Galván F, León R (2001) Studies on the suitability of alginate-entrapped *Chlamydomonas reinhardtii* cells for sustaining nitrate consumption processes. *Bioresour Technol* 78:55–61
92. Cheong SW, Park JK, Kim BS, Chang HN (1993) Microencapsulation of yeast cells in the calcium alginate membrane. *Biotechnol Techniq* 7(12):879–884
93. Espinosa EP, Barillé L, Bassem A (2007) Use of encapsulated live microalgae to investigate pre-ingestive selection in the oyster *Crassostrea gigas*. *J Exp Marine Biol Ecol* 343:118–126
94. Chan LW, Lee HY, Heng PWS (2002) Production of alginate microspheres by internal gelation using an emulsification method. *Int J Pharm* 242:259–262
95. Rangasayatorn N, Pokethitiyook P, Upatahm ES, Lanza GR (2004) Cadmium biosorption by cells of *Spirulina platensis* TISTR 8217 immobilized in alginate and silica gel. *Environ Int* 30:57–63
96. Vilchez C, Vega JM (1995) Nitrite uptake by immobilized *Chlamydomonas reinhardtii* cells growing in airlift reactors. *Enzyme Microb Technol* 17:386–390
97. Aksu Z, Kutsal T (1998) Determination of kinetic parameters in the biosorption of copper(II) on *Cladophora* sp., in a packed bed column reactor. *Process Biochem* 33(1):7–13
98. Moreno-Garrido I, Codd GA, Gadd GM, Lubián LM (2002) Cu and Zn accumulation by calcium alginate immobilized marine microalgal cells of *Nannochloropsis gaditana* (EUSTIGMATOPHYCEAE). *Ciencias Marinas* 28(1):107–119
99. Twist H, Edwards AC, Codd GA (1998) Algal growth responses to waters of contrasting tributaries of the River Dee, North-East Scotland. *Water Res* 32(8):2471–2479
100. Twist H, Edwards AC, Codd GA (1997) A novel In situ biomonitor using alginate immobilised algae (*Scenedesmus subspicatus*) for the assessment of eutrophication in flowing surface waters. *Water Res* 31(8):2066–2067
101. Kosourov SN, Seibat M (2008) Hydrogen photoproduction by nutrient-deprived *Chlamydomonas reinhardtii* cells immobilized within thin alginate films under aerobic and anaerobic conditions. *Biotechnol Bioeng* 102:50–58
102. Frense D, Müller A, Beckmann D (1998) Detection of environmental pollutants using optical biosensor with immobilized algae cells. *Sensors Accumulators B* 51:256–260
103. Shitanda I, Takada K, Sakai Y, Tatsuma T (2005) Compact amperometric algal biosensors for the evaluation of water toxicity. *Anal Chim Acta* 530:191–197
104. Singh R, Prasad BB (2000) Trace metal analysis: selective sample (copper II) enrichment on an AlgaSORB column. *Process Biochem* 35:897–905
105. Stark PC, Rayson GD (2000) Comparisons of metal-ion binding to immobilized biogenic materials in a flowing system. *Adv Environ Res* 4:113–122
106. Godlewska-Zyłkiewicz B (2003) Biosorption of platinum and palladium for their separation/preconcentration prior to graphite furnace atomic absorption spectrometric determination. *Spectrochimica Acta part B* 58:1531–1540
107. Naessens M, Tran-Minh C (1998) Whole-cell biosensor for determination of volatile organic compounds in the form of aerosols. *Anal Chim Acta* 364:153–158
108. Naessens M, Tran-Minh C (1999) Biosensor using immobilized *Chlorella* microalgae for determination of volatile organic compounds. *Sensord and Actuators B* 59:100–102
109. Naessens M, Leclerc JC, Tran-Minh C (2000) Fiber optic biosensors using *Chlorella vulgaris* for determination of toxic compounds. *Ecotoxicol Environ Saf* 46:181–185
110. Durrieu C, Tran-Minh C (2002) Optical algal biosensor using alkaline phosphatase for determination of heavy metals. *Ecotoxicol Environ Saf* 51:206–209
111. Nowak ECM, Podola B, Melkonian M (2005) The 96-well twin-layer system: a novel approach in the cultivation of microalgae. *Protist* 156:239–251
112. Podola B, Nowack ECM, Melkonian M (2004) The use of multiple-strain algal sensor chips for the detection and identification of volatile organic compounds. *Biosens Bioelectron* 19:1253–1260
113. Sanders CA, Rodríguez M Jr, Greenbaun E (2001) Stand-off tissue-based biosensors for the detection of chemical warfare agents using photosynthetic fluorescence induction. *Biosens Bioelectron* 16:439–446
114. Védrine C, Leclerc J-C, Durrieu C, Tran-Minh C (2003) Optical whole-cell biosensor

- using *Chlorella vulgaris* designed for monitoring herbicides. *Biosens Bioelectron* 18:457–463
115. Vandamme D, Foubert I, Fraeye I, Meeschaert B, Muylaert K (2012) Flocculation of *Chlorella vulgaris* induced by high pH: Role of magnesium and calcium and practical implications. *Bioresour Technol* 105:114–119
 116. Wu Z, Zhu Y, Huang W, Zhang C, Li T, Zhang Y, Li A (2012) Evaluation of flocculation induced by pH increase for harvesting microalgae and reuse of flocculated medium. *Bioresour Technol* 110:496–502
 117. Schlesinger A, Eisenstadt D, Bar-Gil A, Carmely H, Einbinder S, Gressel J (2012) Inexpensive non-toxic flocculation of microalgae contradicts theories; overcoming a major hurdle to bulk algal production. *Biotechnol Adv* 30(5):1023–1030
 118. Van Toan N (2009) Production of chitin and chitosan from partially autolyzed shrimp shell. *The Open Biomat J* 1:21–24
 119. Cheng Y-S, Zheng Y, Labavitch JM, Van der Gheynst JS (2011) The impact of cell wall carbohydrate composition on the chitosan flocculation of *Chlorella*. *Process Biochem* 46:1927–1933
 120. Morales J, de la Noüe J, Picard G (1985) Harvesting marine microalgae species by chitosan flocculation. *Aquacultural Eng* 4:257–270
 121. Bilanovic D, Shelef G, Sukenik A (1988) Flocculation of microalgae with cationic polymers—effects of medium salinity. *Biomass* 17:65–76
 122. Kaya VM, Picard G (1996) Stability of chitosan gel as entrapment matrix of viable *Scenedesmus bicellularis* cells immobilized on screens for tertiary treatment of wastewater. *Bioresour Technol* 56:147–155
 123. Sukenik A, Bilanovic D, Shelef G (1988) Flocculation of microalgae in brackish and Sea waters. *Biomass* 15:187–199
 124. Lee AK, Lewis DM, Ashman PJ (2010) Energy requirements and economic analysis of a full-scale microbial flocculation system for microalgal harvesting. *Chem Eng Res Design* 88:988–996
 125. Uduman N, Qi Y, Danquah MK, Hoadley AFA (2010) Marine microalgae flocculation and focused beam reflectance measurement. *Chem Eng J* 162:935–940
 126. Zheng H, Gao Z, Yin J, Tang X, Ji X, Huang H (2012) Harvesting of microalgae by flocculation with poly (γ -glutamic acid). *Bioresour Technol* 112:212–220

Therapeutic Applications of Encapsulated Cells

Argia Acarregui, Gorka Orive, José Luis Pedraz,
and Rosa María Hernández

Abstract

The synergy of some promising advances in the fields of cell therapy and biomaterials together with improvements in the fabrication of more refined and tailored microcapsules for drug delivery have triggered the progress of cell encapsulation technology. Cell microencapsulation involves immobilizing the transplanted cells within a biocompatible scaffold surrounded by a membrane in attempt to isolate the cells from the host immune attack and enhance or prolong their function *in vivo*. This technology represents one strategy which aims to overcome the present difficulties related to local and systemic controlled release of drugs and growth factors as well as to organ graft rejection and thus the requirements for use of immunomodulatory protocols or immunosuppressive drugs. This chapter gives an overview of the current situation of cell encapsulation technology as a controlled drug delivery system, and the essential requirements of the technology, some of the therapeutic applications, the challenges, and the future directions under investigation are highlighted.

Key words Alginate, Cell encapsulation, Drug delivery, Immobilization, Microcapsules, Therapeutic applications

1 Introduction

The aim of drug delivery systems is to maintain local and controlled delivery of therapeutic products with minimal side effects at specific locations in the body in order to restore lost function caused by disease or degeneration. To reach a better control of drug's delivery, numerous technologies using biomaterials in the form of fibers, capsules, three-dimensional porous scaffolds and injectable gels have been investigated [1]. During the last few years, the transplantation of encapsulated living cells pumping out active therapeutic molecules directly at the target tissue has proven to be an emergent technology [2]. Since the pioneering study by TMS Chang [3], the immobilization of cells has been developed based on the promise of its therapeutic usefulness in tissue transplantation and nowadays represents an evolving branch of biotechnology and regenerative medicine with numerous applications.

2 Cell Encapsulation Technology

Cell encapsulation technology is based on the entrapment of cells that secrete active therapeutic agents, in structures made from different biomaterials and surrounded by a semipermeable membrane. The purpose of this membrane is to control the influx rate of molecules essential for cell survival (oxygen and nutrients) and the efflux rate of therapeutic factors, metabolites and waste products, while completely excluding the harmful components of the host immune system (antibodies and immune cells) (Fig. 1). Thus, the long-term therapies of immunosuppressant drugs could be eliminated or at least reduced. In this application, cells may be considered “biological factories” or “living cell medicines” that can continuously produce and release therapeutic molecules in a biosafe way. The use of this technology provides important advantages because it allows a sustained and controlled delivery of therapeutic factors synthesized *de novo* by the encapsulated cells, which ensures the bioactivity of the product and attends to obtain physiological concentrations while reducing the risk of toxicity in case of microcapsule’s rupture. Furthermore, the use of an inducible genetic system (through genetic modification of the entrapped cells) enables to control drug or protein release, without altering the genome of the host [4, 5]. Finally, the microcapsules can be injected directly or transplanted during minimally invasive surgery into implantation sites such as the peritoneal cavity [6] and subcutaneous tissue [7], avoiding the repeated administrations and thus improving patient comfort. An ideal system would be one that achieves an effective concentration of the desired therapeutic product in the specific physiological site, while minimizing systemic exposure.

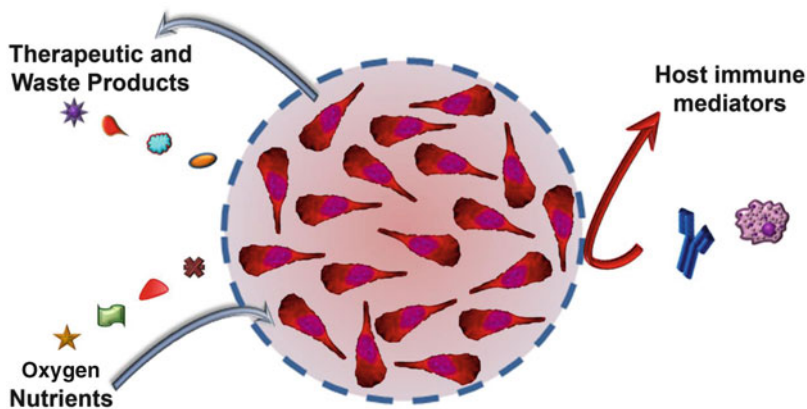


Fig. 1 A schematic illustration of a semipermeable membrane (*dashed line*) protecting transplanted cells by microencapsules. Nutrients, oxygen as well as therapeutic products diffuse across the membrane, whereas host immune mediators (antibodies and immune cells) are excluded

Alginate-poly-L-lysine-alginate (APA) or alginate-poly-L-ornithine-alginate (PLO) microcapsules, originally developed by Lim and Sun [8], which are based on an alginate core surrounded by a polycation layer membrane have been the most widely employed microcapsules. Apart from these polycations, other polymers such as chitosan [9], lactose-modified chitosan [10], oligochitosans [11], poly (methylene-*co*-guanidine) [12], and sodium silicate [13] have also been employed to cover the alginate beads. The applicability of cell encapsulation technology has been assessed for the treatment of a wide variety of diseases, including hypoparathyroidism [14], hemophilia B [15], anemia [16], liver failure [17], central nervous system (CNS) diseases [18], diabetes mellitus [19], cancer [20], and cardiovascular diseases [21].

3 Biomaterials

The biomaterial employed in the development of encapsulated cells is increasingly important and play key roles in overcoming the inherent insufficiency of tailored therapies. Biomaterials provide the three-dimensional and synthetic extracellular environments that mimic certain beneficial properties of the extracellular matrix (ECM), controlling cell attachment, viability, proliferation, and differentiation and improving immune protection by isolating entrapped cells from the host tissue [22, 23]. A variety of natural polymers, including collagen [24], hyaluronic acid (HA) [25], and cellulose sulfate [26] or alginate in combination with agarose [27], gelatin [28], and tyramine [29] have been used in the field of cell encapsulation; however alginate, which allows gel formation in minimally harmful conditions, has been the most employed biomaterial [30].

Alginate is a natural polysaccharide extracted from brown seaweeds and bacterium and is composed of unbranched binary copolymers of (1, 4)-linked β -D-mannuronic acid (M) and α -L-guluronic acid (G), of widely varying compositions and sequential structures. Alginate isolated from different sources differs in composition (M and G contents) as well as in the length of each block and thus can vary significantly some properties of alginate gels such as biocompatibility, stability, mechanical strength, biodegradability, or permeability [22]. As natural polymer, alginate performance is to be largely contaminated with impurities including endotoxins, heavy metals, proteins, and polyphenols which are directly associated with lower biocompatibility [31]. Therefore, it is indispensable to carry out an efficient purification process before the use of alginates and always choose clinical grade ones [5].

To provide control over the cell fate, the functionalization and modification of alginates with various peptides and proteins such as RGD (arginine-glycine-aspartate) or YIGSR (tyrosine-isoleucine-glycine-serine-arginine) are promising approaches. These functional

groups activate the intracellular signaling cascades through the focal contacts that provide tight control over the cell–matrix interactions [32]. As a result of such a coupling, the alginate adhesive interactions with various cell types as well as cell survival and functionality is enhanced [33, 34]. In this regard, biomimetic microcapsules using RGD-alginate provided the cell adhesion for the enclosed cells and prolonged their long-term functionality and drug release for more than 300 days, promoting the *in vivo* long-term functionality of the enclosed cells and improving the mechanical stability of the capsules [35].

4 The Requirements of the Technology

Several important requirements of the microcapsules, including permeability, mechanical resistance, size and morphology, and biocompatibility, play a major role on the overall performance of polymer microcapsules in biomedical applications [36].

The important advances in the technological properties achieved in the field of cell microencapsulation have provided high levels of permselectivity and structural stability that lasts through the desired lifetime of the graft [37, 38]. The type of biomaterial employed for the formation of the matrix and membrane, the type of gelling ion, and the encapsulation technology are some of the main parameters that control the mechanical resistance of the microcapsules [39]. The uniformity of the size and the spherical shape of microcapsules are important characteristics because they could affect the *in vivo* immune response to the microcapsules. Additionally, the size of the capsule should tailor to the implantation site; thus, a smaller capsule size may be more appropriate in implantation into the CNS or intravitreal administration [40].

Biocompatibility is the ability of a biomaterial to result in an appropriate host response in a specific application and involves many characteristics such as material composition, and microcapsules' structure, morphology, mechanical properties, and degradation [41]. The biomaterials must be totally biocompatible to avoid any inflammatory reaction, which can lead to the formation of cellular overgrowth surrounding the capsule, thus hindering diffusion of molecules through the semipermeable membrane and triggering the graft failure [30]. There have been different technologies and approaches for the evaluation and measurement of biocompatibility of microcapsules including scanning electron microscopy analysis, colorimetric assays, and histological analysis, among others [38]. In a recent study, micro-Fourier transform infrared spectroscopy was employed to investigate the physicochemical changes after the exposure of alginate beads and alginate-PLL capsules prepared to human peritoneal fluid [42].

The choice of cells depends on the intended therapeutic application such as the secretion of a naturally bioactive substance, the metabolism of a toxic agent or the release of an immunizing

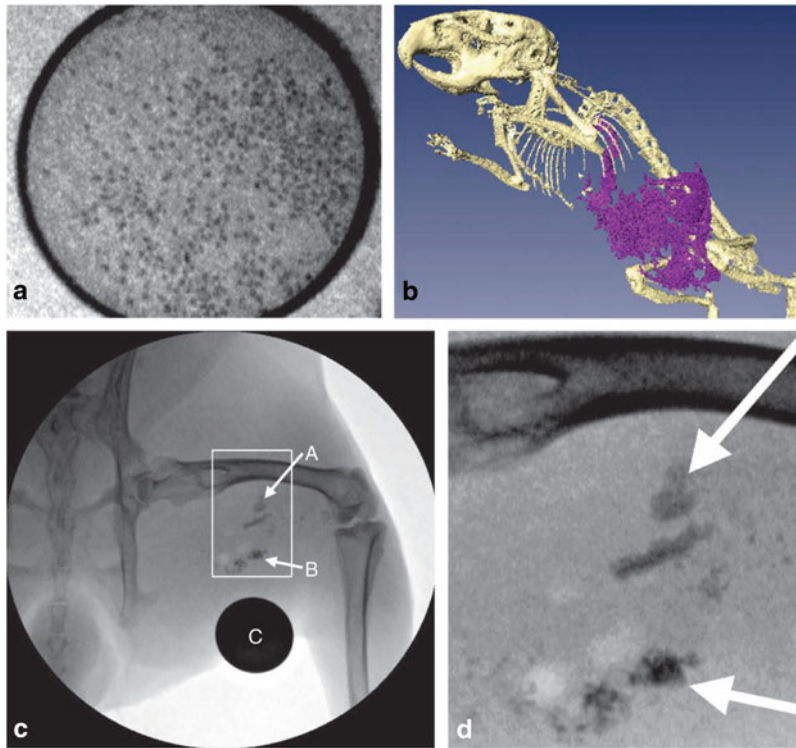


Fig. 2 Barium and bismuth X-Caps. **(a)** Fluoroscopic images of Ba X-Caps. Single capsules can be clearly identified. **(b)** In vivo imaging of X-Caps, as seen on high-resolution CT (XSPEC, Gamma-Medica) after transplantation in the peritoneal cavity of a mouse. **(c)** In vivo imaging of X-Caps immediately after intramuscular transplantation into a rabbit hind limb. A=2,000 Ba X-Caps; B=2,000 Bi X-Caps; C=quarter for reference of size and opacity. **(d)** Magnification of the fluoroscopic image shown in *boxed area* of **c**. Reproduced, with permission, from ref. 45 © 2011 Nature publishing group

agent [5]. Cell encapsulation technology has in part failed to reach clinical approval due to the immunogenicity of the encapsulated nonautologous cells, which eventually could initiate a host immune response and lead to fibrotic tissue around the microcapsules. Consequently, to overcome this difficulty in the last few years the use of mesenchymal stem cells (MSCs) has gaining attention. MSCs are well known for their hypoimmunogenic properties and moreover can be modified genetically to express a variety of genes, emerging as a promising cell source for cell-based microencapsulation and for continuous long-term delivery of therapeutic factors [43, 44].

Noninvasive imaging techniques, including X-ray [45] (Fig. 2), magnetic resonance [46], and bioluminescent imaging [47] have been employed to track and monitor the cell-containing microcapsules in vivo. In a recent study, Catena et al. performed luminometry assays to control the location and viability of microencapsulated cells transfected with the triple reporter gene TGL and they were able to interrupt the therapy by the administration of ganciclovir. This system may represent an appropriate tool to tightly control microencapsulated cells and, moreover, to improve the biosafety of this type of drug delivery system [47].

5 Therapeutic Applications and Clinical Trials

The application of cell encapsulation technology is obtaining promising results in different studies being conducted both *in vitro* and *in vivo*. Table 1 summarized some of the most important clinical trials already carried out or ongoing using alginate microcapsules as well as other cell encapsulation systems such as gelatin-microcarriers, cellulose sulfate or hollow fibers for the treatment of different diseases [48–62].

5.1 Endocrinological Disorders (Diabetes and Anemia)

Diabetes is a metabolic disease characterized by hyperglycemia resulting from defects in insulin secretion, insulin action or both. The drawbacks related to the cell-based treatments, by means of the

Table 1
Clinical trials already carried out or ongoing in the field of cell encapsulation

Therapeutic application	Cell encapsulation approach	References
Type 1 diabetes	Alginate-PLL encapsulated islets. Low dose immunosuppression	[48] [49, 50]
	Alginate-PLO-Alginate encapsulated islets. No immunosuppression	[51, 52] [53]
	Diabecell® device (Living Cell Technologies)	[54] (NCT00790257)
	Alginate encapsulated islets. Low dose immunosuppression	[54] (NCT01379729) [54] (NCT00260234)
	Alginate monolayer islet device	
	Alginate encapsulated β cells Viacyte (Novocell®)	
Parkinson disease	hRPE cells within gelatin microcarriers (Spheramine®)	[54, 55] (NCT00761436) (NCT00206687)
Alzheimer disease	NGF-secreting cells encapsulated in hollow fiber. NsG0202 implants (EC Delivery/NsGene)	[54] (NCT01163825)
Huntington's disease	BHK cells that secrete CNTF encapsulated in hollow fiber	[56]
Pancreatic carcinoma	Cellulose sulfate encapsulated cells that secretes the enzyme cytochrome P-450	[57, 58]
Hypoparathyroidism	Alginate encapsulated parathyroid tissue	[59]
Amyotrophic lateral sclerosis	BHK cells that secrete CNTF encapsulated in hollow fiber	[60]
Retinitis pigmentosa	Neurotech (NT-501)	[61, 62]
Intracerebral hemorrhage	Alginate encapsulated mesenchymal cells that secrete GLP-1 (GLP-1 CellBeads®)	[54] (NCT01298830)

PLL poly-L-lysine, PLO, poly-L-ornithine, PEG poly(ethylene glycol), hRPE cells human retinal pigment epithelial cells, BHK cells Baby Hamster Kidney cells, CNTF Ciliary Neurotrophic Factor, CSF cerebrospinal fluid, GLP-1 glucagon-like peptide 1

replacement of the damaged islets of Langerhans, such as the required immunosuppression treatments and the limited and irregular supply of cadaveric donors [63] have promoted the development of alternative therapeutic approaches. Several research groups have employed cell microencapsulation technology to create a living cell-based replacement system or a bioartificial pancreas to achieve insulin levels and control plasma glucose. Luca et al. have immobilized Sertoli cells (SCs) in alginate-based microcapsules and transplanted in non-obese diabetic mice, showing the reversal of spontaneous diabetes by creating newly formed functional islets β -cells [64]. In a recent study, islets were co-encapsulated with angiogenic proteins in permselective multilayer alginate microcapsules with the purpose of creating a new design of a bioartificial pancreas [65]. Currently, several studies have reported that MSCs, stem cells like embryonic stem cells (ESCs) or induced pluripotent stem cells (IPSCs) can differentiate into insulin producing cells and can therefore be considered potentially useful for the treatment of diabetes [66–71]. Tuch et al., have proposed to replace the pancreatic β -cells of diabetic recipients using pancreatic progenitors (PP) derived from hESC. In this project, the hESC will be differentiated into PP, which will then be encapsulated in alginate microcapsules before being transplanted into diabetic recipients with the aim of obtaining mature insulin producing cells in vivo while preventing their rejection by the immune system and the formation of teratomas (Fig. 3) [69].

Anemia associated with various chronic conditions, including end stage renal disease, malignancy and human immunodeficiency virus (HIV) infection has been treated with erythropoietin (Epo). However, regarding clinical setting, a major disadvantage of this treatment is the requirement of repeated injections [72]. With consideration of that fact, our research group has developed alginate-based microcapsules in which myoblasts genetically engineered to secrete Epo have been successfully entrapped and implanted in allogeneic and syngeneic mice [73–75] as well as in xenogeneic rats [16]. In a recent in vivo study, we have designed a composite delivery system combining Epo-secreting myoblasts entrapped in APA microcapsules and dexamethasone releasing poly (lactic-co-glycolic acid) (PLGA) microspheres to avoid or at least diminish the fibrotic layer caused by inflammation [76]. All of these studies included a single dose of microcapsules, which achieved high and constant hematocrit levels.

5.2 Central Nervous System (CNS) Diseases

Cell encapsulation technology enables the delivery of different molecules such as neurotrophic factors or growth factors by encapsulated cells with the aim of neuroprotecting or neuroregenerating cellular damage associated with most of the CNS diseases.

Parkinson's disease (PD) is a neurodegenerative disorder characterized by the extensive loss of the dopamine neurons of the substantia nigra pars compacta and their terminals in the striatum.

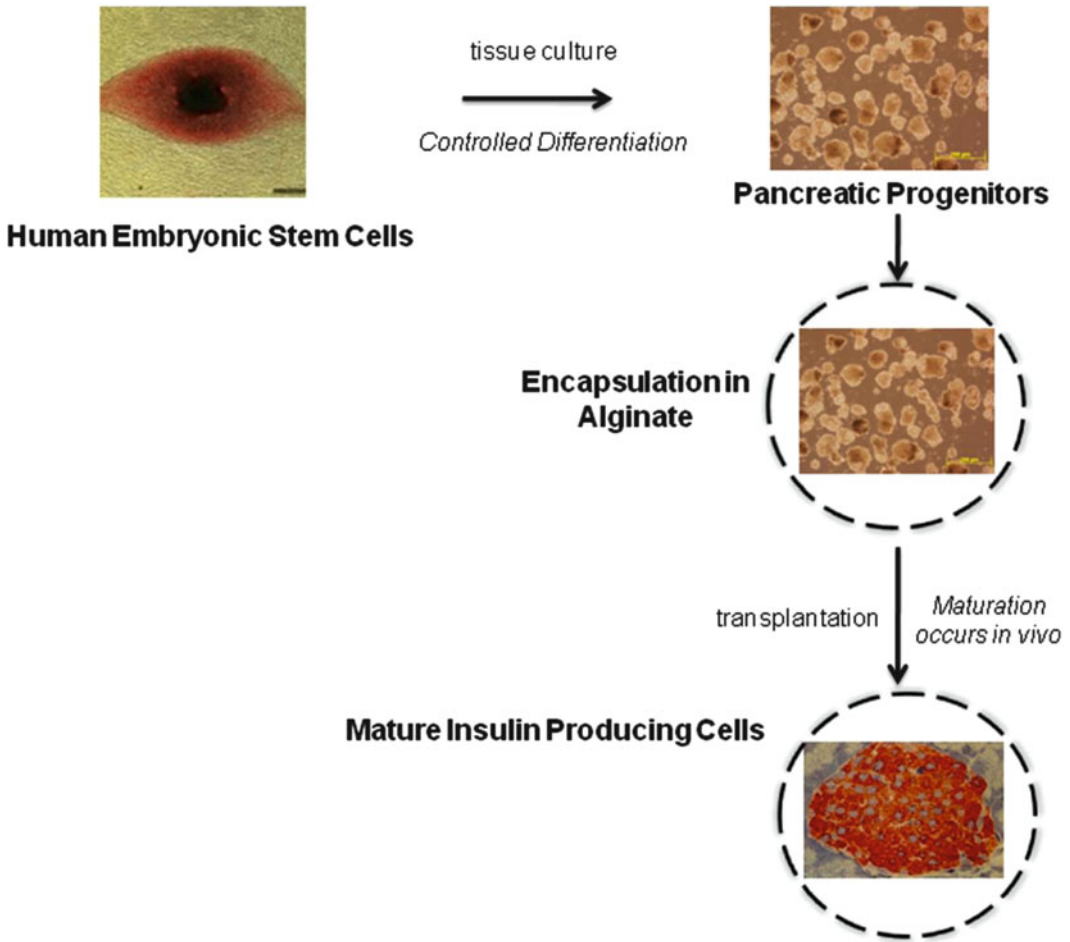


Fig. 3 Human embryonic stem cells will be differentiated into pancreatic progenitors, which will then be encapsulated before being transplanted into diabetic recipients. Reproduced, with permission, from ref. 69 © 2011 Wiley Online Library

The most widely employed approaches for the treatment of PD have been based in the administration of encapsulated choroid plexus (CP) cells as well as glial cell-derived neurotrophic factor (GDNF) or vascular endothelial growth factor (VEGF) secreting cells [77–82]. One of these studies reported that, GDNF-secreting fibroblasts within APA microcapsules were able to deliver continuous levels of GDNF for at least 6 months and resulted in substantial behavioral improvement and good biotolerance in a model of PD [78]. To improve and increase the survival of unencapsulated cells after transplantation another approaches have studied the co-implantation of unencapsulated cells that induced functional recovery and regeneration of the injured area combined with encapsulated cells that release various types of growth factors [83, 84].

Alzheimer's disease (AD) is a progressive neurodegenerative disorder characterized by the accumulation of amyloid β -peptide

(A β) in both the parenchyma and the cerebral vasculature and it is associated with neuronal and vascular toxicity. The immobilization of genetically engineered cells to produce VEGF, ciliary neurotrophic factor (CNTF) or glucagon-like peptide-1 (GLP-1) have been employed for the treatment of AD [85–88]. Recently, Spuch et al. implanted microencapsulated fibroblast cells releasing VEGF into a transgenic (APP/PS1) mouse model of AD with degenerative alterations in the microvasculature. The study reported increased angiogenesis, decreased presence of A β and tau protein, less apoptosis and protection of the cognitive behavior in the APP/PS1 mice after the implantation of the microcapsules [85].

Huntington's disease (HD) is characterized by the death of GABAergic neurons in the striatum and includes an array of different psychiatric manifestations and progressive motor abnormalities. CP cells, which secrete several neurotrophic factors affecting the production of the cerebrospinal fluid and the maintenance of the extracellular fluid concentrations in the brain [89] have been immobilized in alginate microcapsules to achieve an appropriate release of neurotrophic factors into the brain in rodent [82, 90–92] and primate [93] models of HD. These studies reported that the CP cells encapsulated in the alginate microcapsules prevented the degeneration of the striatal neurons.

5.3 Cardiovascular Diseases

Cardiovascular diseases (CVDs) are major causes of morbidity and mortality related to extensive loss of cardiac cells. In the recent years, due to the lack of donor organs for transplantation, cardiac cell replacement therapy has emerged as a novel and promising therapeutic approach to sustain the endogenous regenerative mechanisms in myocardial infarction (MI) [94, 95]. However, the heart is constantly contracting and thus large proportions of the injected cells are lost from the myocardium within the first few minutes after their injection [96, 97]. Not more than 0.1–15 % of all the injected cells is retained within the myocardium [21, 98]. To overcome the massive loss of the cells and improve cell retention and survival, one outstanding strategy could be the immobilization of the cells within microcapsules. Due to microcapsules are larger than the blood vessel diameter the heart's contractile forces are unable to eliminate the microcapsules into the bloodstream, significantly increasing the amount of retained microcapsules and thus the amount of cells [21, 99]. Yu et al. encapsulated MSCs in alginate microcapsules modified with RGD and implanted them in a rat model of MI. The results reported an improvement in cell attachment, cell growth and an increase in the expression of angiogenic growth factors. In addition, they showed successful maintenance of the shape of the left ventricle, induction of angiogenesis and prevention of the left ventricle remodeling after a MI [100]. These microencapsulated cells may have a much greater potential for heart regeneration compared with the unencapsulated cells [100, 101].

5.4 Cancer

There are a number of strategies using microcapsules containing cells that secrete various therapeutic products for the treatment of a variety of solid tumors. Some of these approaches are based in the idea that without angiogenesis, most solid tumors cannot grow past a critical size because of inadequate tissue oxygenation and nutrient supply and involved the encapsulation of cells that secrete antiangiogenic proteins such as endostatin, angiostatin [102–106] or the combination of endostatin, soluble neuropilin-1, and thrombospondin-2 [107]. In order to stimulate an immune response against tumors other groups have employed encapsulated cells genetically modified to produce tumor necrosis factor α (TNF α) [108] or interleukin-6 (IL-6) [109]. The capacity of tumor cells to evolve and escape from a given treatment may require a combination of therapies, in which multiple pathways are targeted in order to attack the tumor and improve treatment efficacy [110]. Finally, encapsulated cells have also been used for the long term production of antibodies [111–113] or retrovirus [114]. Dubrot et al. encapsulated hybridoma cells that secrete immunostimulatory antibodies (anti-CD137 and anti-OX40 mAb). The microcapsules were implanted in mice with induced tumors showing that the immunostimulatory monoclonal antibodies secreted by the implanted encapsulated hybridoma cells enhance tumor-specific cellular immunity (Fig. 4) [113].

Currently, several research groups are investigating the possibilities that MSCs encapsulation presents in the treatment of different types of cancer [43, 115]. In one of these works, Goren et al. showed that encapsulated genetically engineered MSCs to secrete hemopexin like protein (PEX), in alginate-PLL microcapsules maintain their proliferation and differentiation potential and long-lasting stability. These microcapsules were implanted in a model of human glioblastoma, reporting a reduction in tumor growth, in blood vessel formation, and tumor cell proliferation as well as an increase in tumor cell apoptosis [43].

6 Concluding Remarks and Future Directions and Challenges

Encapsulated cell technology offers a means for overcoming limitations of cell sourcing and immunosuppressant therapies. The therapeutic applications mentioned above represent only some examples, but authors believe that this technology may see exciting improvement in the next few decades. The key to the success of cell encapsulation is the focus on determining the effects of the encapsulation process and the appropriate deployment location, achieving biocompatibility, increasing immunoprotection, eliminating hypoxia, and preventing pericapsular fibrotic overgrowth and post-transplant inflammation. To triumph over these challenges a multidisciplinary collaboration of scientists and researchers

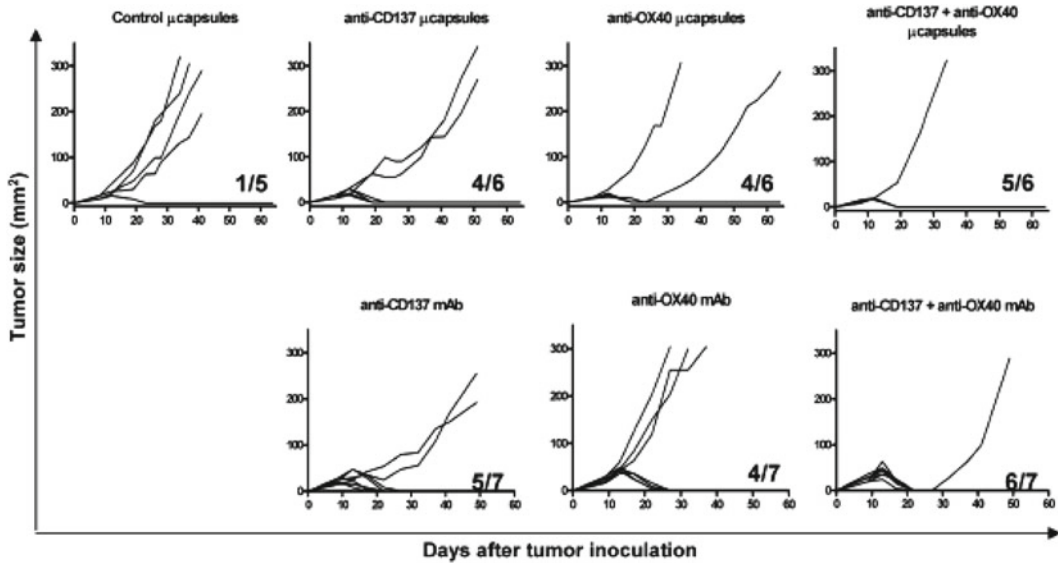


Fig. 4 Anti-CD137 and anti-OX40-producing microcapsules can be employed concomitantly. Mice with established CT26 tumors for 8 days were treated with the indicated subcutaneous microcapsules or purified monoclonal antibodies given as single doses. Individual follow-up of tumor sizes and the fraction of mice in each group that underwent complete rejection are given. Reproduced, with permission, from ref. 113 © 2010 SpringerLink

from the biomedical, physical, and chemical areas is necessary, giving a boost to cell encapsulation technology closer to a realistic approach for clinical applications.

References

- Balmayor ER, Azevedo HS, Reis RL (2011) Controlled delivery systems: From pharmaceuticals to cells and genes. *Pharm Res* 28:1241–1258
- Nafea EH, Poole-Warren AM, Martens PJ (2011) Immunisolating semi-permeable membranes for cell encapsulation: Focus on hydrogels. *J Control Release* 154:110–122
- Chang T (1964) Semipermeable microcapsules. *Science* 146:524–525
- Orive G, Hernandez RM, Gascon AR, Calafiore R, Chang TM, De Vos P, Hortelano G, Hunkeler D, Lacic I, Shapiro AM (2003) Cell encapsulation: Promise and progress. *Nat Med* 9:104–107
- Hernandez RM, Orive G, Murua A, Pedraz JL (2010) Microcapsules and microcarriers for in situ cell delivery. *Adv Drug Deliv Rev* 62:711–730
- McQuilling JP, Arenas-Herrera J, Childers C, Pareta RA, Khanna O, Jiang B, Brey EM, Farney AC, Opara EC (2011) New alginate microcapsule system for angiogenic protein delivery and immunoisolation of islets for transplantation in the rat omentum pouch. *Transplant Proc* 43:3262–3264
- Murua A, Orive G, Hernandez RM, Pedraz JL (2009) Cryopreservation based on freezing protocols for the long-term storage of microencapsulated myoblasts. *Biomaterials* 30:3495–3501
- Lim F, Sun AM (1980) Microencapsulated islets as bioartificial endocrine pancreas. *Science* 210:908–910
- Paul A, Cantor A, Shum-Tim D, Prakash S (2011) Superior cell delivery features of genipin crosslinked polymeric microcapsules: Preparation, in vitro characterization and pro-angiogenic applications using human adipose stem cells. *Mol Biotechnol* 48:116–127
- Donati I, Haug IJ, Scarpa T, Borgogna M, Draget KI, Skjak-Braek G, Paoletti S (2007) Synergistic effects in semidilute mixed solutions of alginate and lactose-modified chitosan (chitlac). *Biomacromolecules* 8:957–962
- De Castro M, Orive G, Hernandez RM, Bartkowiak A, Brylak W, Pedraz JL (2009) Biocompatibility and in vivo evaluation of

- oligochitosans as cationic modifiers of alginate/Ca microcapsules. *J Biomed Mater Res A* 91:1119–1130
12. Rokstad AM, Brekke OL, Steinkjer B, Ryan L, Kollarikova G, Strand BL, Skjak-Braek G, Lacik I, Espevik T, Mollnes TE (2011) Alginate microbeads are complement compatible, in contrast to polycation containing microcapsules, as revealed in a human whole blood model. *Acta Biomater* 7:2566–2578
 13. Dandoy P, Meunier CF, Michiels C, Su BL (2011) Hybrid shell engineering of animal cells for immune protections and regulation of drug delivery: Towards the design of “artificial organs”. *PLoS One* 6:e20983
 14. Moskalenko V, Ulrichs K, Kerscher A, Blind E, Otto C, Hamelmann W, Demidchik Y, Timm S (2007) Preoperative evaluation of microencapsulated human parathyroid tissue aids selection of the optimal bioartificial graft for human parathyroid allotransplantation. *Transpl Int* 20:688–696
 15. Wen J, Xu N, Li A, Bourgeois J, Ofosu FA, Hortelano G (2007) Encapsulated human primary myoblasts deliver functional hFIX in hemophilic mice. *J Gene Med* 9:1002–1010
 16. Murua A, Orive G, Hernandez RM, Pedraz JL (2009) Xenogeneic transplantation of erythropoietin-secreting cells immobilized in microcapsules using transient immunosuppression. *J Control Release* 137:174–178
 17. Mei J, Sgroi A, Mai G, Baertschiger R, Gonelle-Gispert C, Serre-Beinier V, Morel P, Buhler LH (2009) Improved survival of fulminant liver failure by transplantation of microencapsulated cryopreserved porcine hepatocytes in mice. *Cell Transplant* 18:101–110
 18. Zanin MP, Pettingill LN, Harvey AR, Emerich DF, Thanos CG, Shepherd RK (2012) The development of encapsulated cell technologies as therapies for neurological and sensory diseases. *J Control Release* 160:3–13
 19. Vaithilingam V, Tuch BE (2011) Islet transplantation and encapsulation: An update on recent developments. *Rev Diabet Stud* 8:51–67
 20. Salmons B, Brandtner EM, Hettrich K, Wagenknecht W, Volkert B, Fischer S, Dangerfield JA, Gunzburg WH (2010) Encapsulated cells to focus the metabolic activation of anticancer drugs. *Curr Opin Mol Ther* 12:450–460
 21. Paul A, Ge Y, Prakash S, Shum-Tim D (2009) Microencapsulated stem cells for tissue repairing: Implications in cell-based myocardial therapy. *Regen Med* 4:733–745
 22. Lee KY, Mooney DJ (2012) Alginate: Properties and biomedical applications. *Prog Polym Sci* 37:106–126
 23. Ye Z, Mahato RI (2008) Emerging trends in cell-based therapies. preface. *Adv Drug Deliv Rev* 60:89–90
 24. Ananta M, Brown RA, Mudera V (2012) A rapid fabricated living dermal equivalent for skin tissue engineering: An in vivo evaluation in an acute wound model. *Tissue Eng Part A* 18:353–361
 25. Burdick JA, Prestwich GD (2011) Hyaluronic acid hydrogels for biomedical applications. *Adv Mater* 23:H41–56
 26. Stiegler P, Matzi V, Pierer E, Hauser O, Schaffellner S, Renner H, Greilberger J, Aigner R, Maier A, Lackner C (2010) Creation of a prevascularized site for cell transplantation in rats. *Xenotransplantation* 17:379–390
 27. Sakai S, Hashimoto I, Tanaka S, Salmons B, Kawakami K (2009) Small agarose microcapsules with cell-enclosing hollow core for cell therapy: Transplantation of ifosfamide-activating cells to the mice with preestablished subcutaneous tumor. *Cell Transplant* 18:933–939
 28. Sakai S, Ito S, Kawakami K (2010) Calcium alginate microcapsules with spherical liquid cores templated by gelatin microparticles for mass production of multicellular spheroids. *Acta Biomater* 6:3132–3137
 29. Sakai S, Kawakami K (2008) Both ionically and enzymatically crosslinkable alginate-tyramine conjugate as materials for cell encapsulation. *J Biomed Mater Res A* 85:345–351
 30. Santos E, Zarate J, Orive G, Hernández RM, Pedraz JL (2010) Biomaterials in cell microencapsulation. *Adv Exp Med Biol* 670:5–21
 31. Heiligenstein S, Cucchiari M, Laschke MW, Bohle RM, Kohn D, Menger MD, Madry H (2011) Evaluation of nonbiomedical and biomedical grade alginates for the transplantation of genetically modified articular chondrocytes to cartilage defects in a large animal model in vivo. *J Gene Med* 13:230–242
 32. Chan G, Mooney DJ (2008) New materials for tissue engineering: Towards greater control over the biological response. *Trends Biotechnol* 26:382–392
 33. Vacharathit V, Silva EA, Mooney DJ (2011) Viability and functionality of cells delivered from peptide conjugated scaffolds. *Biomaterials* 32:3721–3728
 34. Comisar WA, Mooney DJ, Linderman JJ (2011) Integrin organization: Linking adhesion ligand nanopatterns with altered cell responses. *J Theor Biol* 274:120–130
 35. Orive G, De Castro M, Kong HJ, Hernandez RM, Ponce S, Mooney DJ, Pedraz JL (2009) Bioactive cell-hydrogel microcapsules for

- cell-based drug delivery. *J Control Release* 135:203–210
36. Brun-Graepi AK, Richard C, Bessodes M, Scherman D, Merten OW (2011) Cell microcarriers and microcapsules of stimuli-responsive polymers. *J Control Release* 149:209–224
 37. Leung A, Nielsen LK, Trau M, Timmins NE (2010) Tissue transplantation by stealth—Coherent alginate microcapsules for immunoisolation. *Biochem Eng J* 48:337–347
 38. de Vos P, Bucko M, Gemeiner P, Navratil M, Svitel J, Faas M, Strand BL, Skjak-Braek G, Morch YA, Vikartovska A (2009) Multiscale requirements for bioencapsulation in medicine and biotechnology. *Biomaterials* 30:2559–2570
 39. Schmidt JJ, Rowley J, Kong HJ (2008) Hydrogels used for cell-based drug delivery. *J Biomed Mater Res A* 87:1113–1122
 40. Santos E, Orive G, Calvo A, Catena R, Fernandez-Robredo P, Layana AG, Hernandez RM, Pedraz JL (2012) Optimization of 100 μ m alginate-poly-L-lysine-alginate capsules for intravitreal administration. *J Control Release* 158:443–450
 41. Orive G, Tam SK, Pedraz JL, Halle JP (2006) Biocompatibility of alginate-poly-L-lysine microcapsules for cell therapy. *Biomaterials* 27:3691–3700
 42. de Haan BJ, Rossi A, Faas MM, Smelt MJ, Sonvico F, Colombo P, de Vos P (2011) Structural surface changes and inflammatory responses against alginate-based microcapsules after exposure to human peritoneal fluid. *J Biomed Mater Res A* 98:394–403
 43. Goren A, Dahan N, Goren E, Baruch L, Machluf M (2010) Encapsulated human mesenchymal stem cells: A unique hypoinnogenic platform for long-term cellular therapy. *FASEB J* 24:22–31
 44. Houtgraaf JH, Dejong R, Monkhorst K, Tempel D, Dendekker W, Kazemil K, Hoefler I, Pasterkamp G, Lewis AL, Stratford PW (2013) Feasibility of intracoronary GLP-1 eluting Cell Bead infusion in acute myocardial infarction. *Cell Transplant* 22:535–543
 45. Barnett BP, Arepally A, Stuber M, Arifin DR, Kraitchman DL, Bulte JW (2011) Synthesis of magnetic resonance-, X-ray- and ultrasound-visible alginate microcapsules for immunoisolation and noninvasive imaging of cellular therapeutics. *Nat Protoc* 6:1142–1151
 46. Link TW, Woodrum D, Gilson WD, Pan L, Qian D, Kraitchman DL, Bulte JW, Arepally A, Weiss CR (2011) MR-guided portal vein delivery and monitoring of magnetocapsules: Assessment of physiologic effects on the liver. *J Vasc Interv Radiol* 22:1335–1340
 47. Catena R, Santos E, Orive G, Hernandez RM, Pedraz JL, Calvo A (2010) Improvement of the monitoring and biosafety of encapsulated cells using the SFGNESTGL triple reporter system. *J Control Release* 146:93–98
 48. Soon-Shiong P, Heintz RE, Merideth N, Yao QX, Yao Z, Zheng T, Murphy M, Moloney MK, Schmehl M, Harris M (1994) Insulin independence in a type 1 diabetic patient after encapsulated islet transplantation. *Lancet* 343:950–951
 49. Calafiore R, Basta G, Luca G, Lemmi A, Montanucci MP, Calabrese G, Racanicchi L, Mancuso F, Brunetti P (2006) Microencapsulated pancreatic islet allografts into nonimmunosuppressed patients with type 1 diabetes: First two cases. *Diabetes Care* 29:137–138
 50. Calafiore R, Basta G, Luca G, Lemmi A, Racanicchi L, Mancuso F, Montanucci MP, Brunetti P (2006) Standard technical procedures for microencapsulation of human islets for graft into nonimmunosuppressed patients with type 1 diabetes mellitus. *Transplant Proc* 38:1156–1157
 51. Elliott RB, Escobar L, Tan PL, Muzina M, Zwain S, Buchanan C (2007) Live encapsulated porcine islets from a type 1 diabetic patient 9.5 year after xenotransplantation. *Xenotransplantation* 14:157–161
 52. Wynyard S, Garkavenko O, Elliot R (2011) Multiplex high resolution melting assay for estimation of porcine endogenous retrovirus (PERV) relative gene dosage in pigs and detection of PERV infection in xenograft recipients. *J Virol Methods* 175:95–100
 53. Tuch BE, Keogh GW, Williams LJ, Wu W, Foster JL, Vaithilingam V, Philips R (2009) Safety and viability of microencapsulated human islets transplanted into diabetic humans. *Diabetes Care* 32:1887–1889
 54. US National Institutes of Health. ClinicalTrials.gov [online]. Available from URL: <http://www.clinicaltrials.gov> [Accessed 2012 July]
 55. Stover NP, Watts RL (2008) Spheramine for treatment of parkinson's disease. *Neurotherapeutics* 5:252–259
 56. Bloch J, Bachoud-Levi AC, Deglon N, Lefaucheur JP, Winkel L, Palfi S, Nguyen JP, Bourdet C, Gaura V, Remy P (2004) Neuroprotective gene therapy for huntington's disease, using polymer-encapsulated cells engineered to secrete human ciliary neurotrophic factor: Results of a phase I study. *Hum Gene Ther* 15:968–975

57. Lohr M, Hoffmeyer A, Kroger J, Freund M, Hain J, Holle A, Karle P, Knofel WT, Liebe S, Muller P (2001) Microencapsulated cell-mediated treatment of inoperable pancreatic carcinoma. *Lancet* 357:1591–1592
58. Salmons B, Lohr M, Gunzburg WH (2003) Treatment of inoperable pancreatic carcinoma using a cell-based local chemotherapy: Results of a phase I/II clinical trial. *J Gastroenterol* 38(Suppl 15):78–84
59. Hasse C, Klock G, Schlosser A, Zimmermann U, Rothmund M (1997) Parathyroid allotransplantation without immunosuppression. *Lancet* 350:1296–1297
60. Aebischer P, Schluep M, Deglon N, Joseph JM, Hirt L, Heyd B, Goddard M, Hammang JP, Zurn AD, Kato AC (1996) Intrathecal delivery of CNTF using encapsulated genetically modified xenogeneic cells in amyotrophic lateral sclerosis patients. *Nat Med* 2:696–699
61. Sieving PA, Caruso RC, Tao W, Coleman HR, Thompson DJ, Fullmer KR, Bush RA (2006) Ciliary neurotrophic factor (CNTF) for human retinal degeneration: Phase I trial of CNTF delivered by encapsulated cell intraocular implants. *Proc Natl Acad Sci USA* 103:3896–3901
62. Talcott KE, Ratnam K, Sundquist SM, Lucero AS, Lujan BJ, Tao W, Porco TC, Roorda A, Duncan JL (2011) Longitudinal study of cone photoreceptors during retinal degeneration and in response to ciliary neurotrophic factor treatment. *Invest Ophthalmol Vis Sci* 52:2219–2226
63. Shapiro AM (2011) Strategies toward single-donor islets of langerhans transplantation. *Curr Opin Organ Transplant* 16:627–631
64. Luca G, Fallarino F, Calvitti M, Mancuso F, Nastruzzi C, Arato I, Falabella G, Grohmann U, Becchetti E, Puccetti P (2010) Xenograft of microencapsulated sertoli cells reverses T1DM in NOD mice by inducing neogenesis of beta-cells. *Transplantation* 90:1352–1357
65. Opara EC, Mirmalek-Sani SH, Khanna O, Moya ML, Brey EM (2010) Design of a bio-artificial pancreas(+). *J Investig Med* 58:831–837
66. Godfrey KJ, Mathew B, Bulman JC, Shah O, Clement S, Gallicano GI (2012) Stem cell-based treatments for type 1 diabetes mellitus: Bone marrow, embryonic, hepatic, pancreatic and induced pluripotent stem cells. *Diabet Med* 29:14–23
67. Ngoc PK, Phuc PV, Nhung TH, Thuy DT, Nguyet NT (2011) Improving the efficacy of type 1 diabetes therapy by transplantation of immunoisolated insulin-producing cells. *Hum Cell* 24:86–95
68. Wang N, Adams G, BATTERY L, Falcone FH, Stolnik S (2009) Alginate encapsulation technology supports embryonic stem cells differentiation into insulin-producing cells. *J Biotechnol* 144:304–312
69. Tuch BE, Hughes TC, Evans MD (2011) Encapsulated pancreatic progenitors derived from human embryonic stem cells as a therapy for insulin-dependent diabetes. *Diabetes Metab Res Rev* 27:928–932
70. Montanucci P, Pennoni I, Pescara T, Blasi P, Bistoni G, Basta G, Calafiore R (2011) The functional performance of microencapsulated human pancreatic islet-derived precursor cells. *Biomaterials* 32:9254–9262
71. Shao S, Gao Y, Xie B, Xie F, Lim SK, Li G (2011) Correction of hyperglycemia in type 1 diabetic models by transplantation of encapsulated insulin-producing cells derived from mouse embryo progenitor. *J Endocrinol* 208:245–255
72. Murua A, Orive G, Hernandez RM, Pedraz JL (2011) Emerging technologies in the delivery of erythropoietin for therapeutics. *Med Res Rev* 31:284–309
73. Orive G, De Castro M, Ponce S, Hernandez RM, Gascon AR, Bosch M, Alberch J, Pedraz JL (2005) Long-term expression of erythropoietin from myoblasts immobilized in biocompatible and neovascularized microcapsules. *Mol Ther* 12:283–289
74. Murua A, de Castro M, Orive G, Hernandez RM, Pedraz JL (2007) In vitro characterization and in vivo functionality of erythropoietin-secreting cells immobilized in alginate-poly-L-lysine-alginate microcapsules. *Biomacromolecules* 8:3302–3307
75. Ponce S, Orive G, Hernandez RM, Gascon AR, Canals JM, Munoz MT, Pedraz JL (2006) In vivo evaluation of EPO-secreting cells immobilized in different alginate-PLL microcapsules. *J Control Release* 116:28–34
76. Murua A, Herran E, Orive G, Igartua M, Blanco FJ, Pedraz JL, Hernandez RM (2011) Design of a composite drug delivery system to prolong functionality of cell-based scaffolds. *Int J Pharm* 407:142–150
77. Sajadi A, Bensadoun JC, Schneider BL, Lo Bianco C, Aebischer P (2006) Transient striatal delivery of GDNF via encapsulated cells leads to sustained behavioral improvement in a bilateral model of parkinson disease. *Neurobiol Dis* 22:119–129
78. Grandoso L, Ponce S, Manuel I, Arrue A, Ruiz-Ortega JA, Ulibarri I, Orive G, Hernandez RM, Rodriguez A, Rodriguez-Puertas R (2007) Long-term survival of encapsulated GDNF secreting cells implanted within the striatum of parkinsonized rats. *Int J Pharm* 343:69–78

79. Kishima H, Poyot T, Bloch J, Dauguet J, Conde F, Dolle F, Hinnen F, Pralong W, Palfi S, Deglon N (2004) Encapsulated GDNF-producing C2C12 cells for parkinson's disease: A pre-clinical study in chronic MPTP-treated baboons. *Neurobiol Dis* 16:428–439
80. Yasuhara T, Shingo T, Kobayashi K, Takeuchi A, Yano A, Muraoka K, Matsui T, Miyoshi Y, Hamada H, Date I (2004) Neuroprotective effects of vascular endothelial growth factor (VEGF) upon dopaminergic neurons in a rat model of parkinson's disease. *Eur J Neurosci* 19:1494–1504
81. Yasuhara T, Shingo T, Muraoka K, wen Ji Y, Kameda M, Takeuchi A, Yano A, Nishio S, Matsui T, Miyoshi Y (2005) The differences between high and low-dose administration of VEGF to dopaminergic neurons of in vitro and in vivo parkinson's disease model. *Brain Res* 1038:1–10
82. Skinner SJ, Geaney MS, Lin H, Muzina M, Anal AK, Elliott RB, Tan PL (2009) Encapsulated living choroid plexus cells: Potential long-term treatments for central nervous system disease and trauma. *J Neural Eng* 6:065001
83. Ahn YH, Bensadoun JC, Aebischer P, Zurn AD, Seiger A, Bjorklund A, Lindvall O, Wahlberg L, Brundin P, Kaminski Schierle GS (2005) Increased fiber outgrowth from xenotransplanted human embryonic dopaminergic neurons with co-implants of polymer-encapsulated genetically modified cells releasing glial cell line-derived neurotrophic factor. *Brain Res Bull* 66:135–142
84. Shanbhag MS, Lathia JD, Mughal MR, Francis NL, Pashos N, Mattson MP, Wheatley MA (2010) Neural progenitor cells grown on hydrogel surfaces respond to the product of the transgene of encapsulated genetically engineered fibroblasts. *Biomacromolecules* 11:2936–2943
85. Spuch C, Antequera D, Portero A, Orive G, Hernandez RM, Molina JA, Bermejo-Pareja F, Pedraz JL, Carro E (2010) The effect of encapsulated VEGF-secreting cells on brain amyloid load and behavioral impairment in a mouse model of alzheimer's disease. *Biomaterials* 31:5608–5618
86. Garcia P, Youssef I, Utvik JK, Florent-Bechard S, Barthelemy V, Malaplate-Armand C, Kriem B, Stenger C, Koziel V, Olivier JL (2010) Ciliary neurotrophic factor cell-based delivery prevents synaptic impairment and improves memory in mouse models of alzheimer's disease. *J Neurosci* 30:7516–7527
87. Klinge PM, Harmening K, Miller MC, Heile A, Wallrapp C, Geigle P, Brinker T (2011) Encapsulated native and glucagon-like peptide-1 transfected human mesenchymal stem cells in a transgenic mouse model of alzheimer's disease. *Neurosci Lett* 497:6–10
88. Antequera D, Portero A, Bolos M, Orive G, Hernandez RM, Pedraz JL, Carro E (2012) Encapsulated VEGF-secreting cells enhance proliferation of neuronal progenitors in the hippocampus of AbetaPP/Ps1 mice. *J Alzheimers Dis* 29:187–200
89. Emerich DF, Skinner SJ, Borlongan CV, Vasconcellos AV, Thanos CG (2005) The choroid plexus in the rise, fall and repair of the brain. *Bioessays* 27:262–274
90. Borlongan CV, Skinner SJ, Geaney M, Vasconcellos AV, Elliott RB, Emerich DF (2004) Neuroprotection by encapsulated choroid plexus in a rodent model of huntington's disease. *Neuroreport* 15:2521–2525
91. Borlongan CV, Thanos CG, Skinner SJ, Geaney M, Emerich DF (2008) Transplants of encapsulated rat choroid plexus cells exert neuroprotection in a rodent model of huntington's disease. *Cell Transplant* 16:987–992
92. Emerich DF, Schneider P, Bintz B, Hudak J, Thanos CG (2007) Aging reduces the neuroprotective capacity, VEGF secretion, and metabolic activity of rat choroid plexus epithelial cells. *Cell Transplant* 16:697–705
93. Emerich DF, Thanos CG, Goddard M, Skinner SJ, Geany MS, Bell WJ, Bintz B, Schneider P, Chu Y, Babu RS (2006) Extensive neuroprotection by choroid plexus transplants in excitotoxin lesioned monkeys. *Neurobiol Dis* 23:471–480
94. Wang F, Guan J (2010) Cellular cardiomyoplasty and cardiac tissue engineering for myocardial therapy. *Adv Drug Deliv Rev* 62:784–797
95. Malliaras K, Kreke M, Marban E (2011) The stuttering progress of cell therapy for heart disease. *Clin Pharmacol Ther* 90:532–541
96. Yasuda T, Weisel RD, Kiani C, Mickle DA, Maganti M, Li RK (2005) Quantitative analysis of survival of transplanted smooth muscle cells with real-time polymerase chain reaction. *J Thorac Cardiovasc Surg* 129:904–911
97. Teng CJ, Luo J, Chiu RC, Shum-Tim D (2006) Massive mechanical loss of microspheres with direct intramyocardial injection in the beating heart: Implications for cellular cardiomyoplasty. *J Thorac Cardiovasc Surg* 132:628–632
98. Mazo M, Gavira JJ, Pelacho B, Prosper F (2011) Adipose-derived stem cells for myocardial infarction. *J Cardiovasc Transl Res* 4:145–153
99. Al Kindi AH, Asenjo JF, Ge Y, Chen GY, Bhatena J, Chiu RC, Prakash S, Shum-Tim D

- (2010) Microencapsulation to reduce mechanical loss of microspheres: Implications in myocardial cell therapy. *Eur J Cardiothorac Surg* 39:241–247
100. Yu J, Du KT, Fang Q, Gu Y, Mihardja SS, Sievers RE, Wu JC, Lee RJ (2010) The use of human mesenchymal stem cells encapsulated in RGD modified alginate microspheres in the repair of myocardial infarction in the rat. *Biomaterials* 31:7012–7020
 101. Zhang H, Zhu SJ, Wang W, Wei YJ, Hu SS (2008) Transplantation of microencapsulated genetically modified xenogeneic cells augments angiogenesis and improves heart function. *Gene Ther* 15:40–48
 102. Teng H, Zhang Y, Wang W, Ma X, Fei J (2007) Inhibition of tumor growth in mice by endostatin derived from abdominal transplanted encapsulated cells. *Acta Biochim Biophys Sin (Shanghai)* 39:278–284
 103. Zhang Y, Wang W, Xie Y, Yu W, Teng H, Liu X, Zhang X, Guo X, Fei J, Ma X (2007) In vivo culture of encapsulated endostatin-secreting chinese hamster ovary cells for systemic tumor inhibition. *Hum Gene Ther* 18:474–481
 104. Schuch G, Oliveira-Ferrer L, Loges S, Laack E, Bokemeyer C, Hossfeld DK, Fiedler W, Ergun S (2005) Antiangiogenic treatment with endostatin inhibits progression of AML in vivo. *Leukemia* 19:1312–1317
 105. Cirone P, Bourgeois JM, Chang PL (2003) Antiangiogenic cancer therapy with microencapsulated cells. *Hum Gene Ther* 14:1065–1077
 106. Li AA, Shen F, Zhang T, Cirone P, Potter M, Chang PL (2006) Enhancement of myoblast microencapsulation for gene therapy. *J Biomed Mater Res B Appl Biomater* 77:296–306
 107. Bartsch G Jr, Eggert K, Soker S, Bokemeyer C, Hautmann R, Schuch G (2008) Combined antiangiogenic therapy is superior to single inhibitors in a model of renal cell carcinoma. *J Urol* 179:326–332
 108. Hao S, Su L, Guo X, Moyana T, Xiang J (2005) A novel approach to tumor suppression using microencapsulated engineered J558/TNF-alpha cells. *Exp Oncol* 27:56–60
 109. Moran DM, Koniaris LG, Jablonski EM, Cahill PA, Halberstadt CR, McKillop IH (2006) Microencapsulation of engineered cells to deliver sustained high circulating levels of interleukin-6 to study hepatocellular carcinoma progression. *Cell Transplant* 15:785–798
 110. Cirone P, Shen F, Chang PL (2005) A multi-prong approach to cancer gene therapy by coencapsulated cells. *Cancer Gene Ther* 12:369–380
 111. Shi M, Hao S, Quereshi M, Guo X, Zheng C, Xiang J (2005) Significant tumor regression induced by microencapsulation of recombinant tumor cells secreting fusion protein. *Cancer Biother Radiopharm* 20:260–266
 112. Kuijlen JM, de Haan BJ, Helfrich W, de Boer JF, Samplonius D, Mooij JJ, de Vos P (2006) The efficacy of alginate encapsulated CHO-K1 single chain-TRAIL producer cells in the treatment of brain tumors. *J Neurooncol* 78:31–39
 113. Dubrot J, Portero A, Orive G, Hernandez RM, Palazon A, Rouzaut A, Perez-Gracia JL, Hervas-Stubbs S, Pedraz JL, Melero I (2010) Delivery of immunostimulatory monoclonal antibodies by encapsulated hybridoma cells. *Cancer Immunol Immunother* 59:1621–1631
 114. Dvir-Ginzberg M, Konson A, Cohen S, Agbaria R (2007) Entrapment of retroviral vector producer cells in three-dimensional alginate scaffolds for potential use in cancer gene therapy. *J Biomed Mater Res B Appl Biomater* 80:59–66
 115. Kleinschmidt K, Klinge PM, Stopa E, Wallrapp C, Glage S, Geigle P, Brinker T (2011) Alginate encapsulated human mesenchymal stem cells suppress syngeneic glioma growth in the immunocompetent rat. *J Microencapsul* 28:621–627

Whole Cell Entrapment Techniques

Jorge A. Trelles and Cintia W. Rivero

Abstract

Microbial whole cells are efficient, ecological, and low-cost catalysts that have been successfully applied in the pharmaceutical, environmental, and alimentary industries, among others.

Microorganism immobilization is a good way to carry out the bioprocess under preparative conditions. The main advantages of this methodology lie in their high operational stability, easy upstream separation and bioprocess scale-up feasibility.

Cell entrapment is the most widely used technique for whole cell immobilization. This technique—in which the cells are included within a rigid network—is porous enough to allow the diffusion of substrates and products, protects the selected microorganism from the reaction medium, and has high immobilization efficiency (100 % in most cases).

Key words Entrapment immobilization, Whole cells, Alginate, Agar, Agarose, Polyacrylamide, Post-immobilization, Stability, Reusability

1 Introduction

The reactions catalyzed by microorganisms are widely used in the pharmaceutical, environmental, and alimentary industries. The main operational advantages presented by microorganisms are low production cost and stereo-, regio-, and chemo-selective reactions in mild conditions.

Immobilization can improve the properties of a selected microorganism, because it increases its stability and allows its reuse, making the scale-up bioprocess possible [1, 2].

This technique has been widely used for many extremophiles, mesophiles, gram-positive and gram-negative microorganisms [3–5]. Besides, immobilization allows for easy product separation, reduces processing costs, and enables biocatalyst recycling.

Immobilized whole cells depend on the biocatalyst properties and matrix characteristics. The specific interaction among them results in an immobilized derivative with different physical, chemical, mechanical, and kinetic properties (Fig. 1).

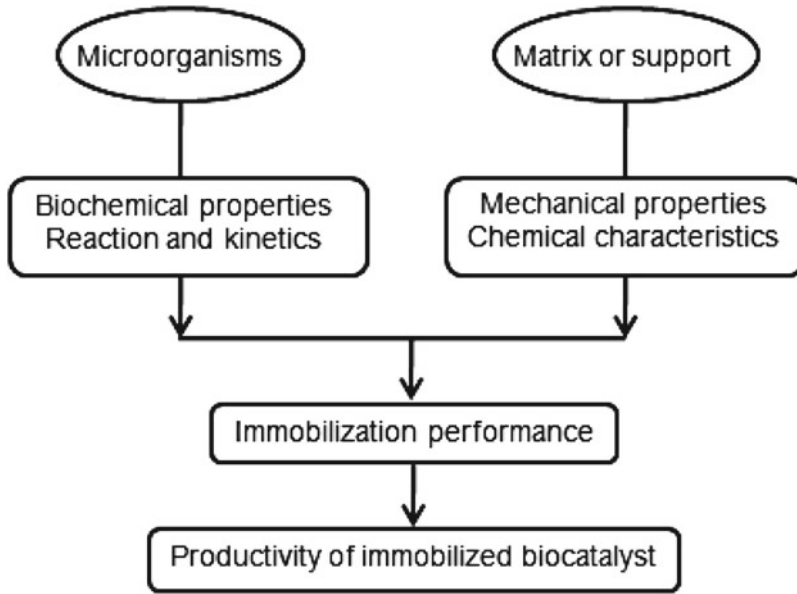


Fig. 1 Design of an immobilized biocatalyst

Table 1
Experimental parameters to be taken into account for microorganism immobilization

General description	Reaction scheme Type of reaction Reactions conditions Microorganism selection Selection of appropriate matrix
Immobilization methodology	Immobilization parameters Immobilization efficiency Processing time
Physicochemical characterization	Biocatalyst configuration Compressibility degree Abrasion resistance Operational stability
Kinetic parameters	Deactivation time Conversion values Reaction velocity Productivity Diffusional restrictions

However, the best way to immobilize whole cells must be found experimentally. Therefore, some parameters such as microorganism stability during the immobilization procedure, mechanical resistance, operational stability, and reusability should be considered among other variables (Table 1).

The entrapment techniques, in which microorganisms are enclosed in a rigid network to prevent cell release into the surrounding medium, are the most widely used for whole cell immobilization. This network is produced by a physical or chemical polymerization process and is porous enough to allow the diffusion of substrates and products [6].

This method is very simple and requires a small amount of biocatalyst to obtain active derivatives. The immobilization process begins with the suspension of a microorganism in a solution of the selected matrix. Subsequently, the biocatalyst formation begins with a temperature change or polymerization (using a chemical reagent). Depending on the type of reactor, the immobilized microorganism may be used in different forms such as spheres, films fibers or cylinders.

There are some disadvantages that should be considered in whole cell entrapment, such as diffusional problems between substrates and products and microorganism activity decrease due to the process of matrix formation. For these reasons, immobilization by entrapment should be optimized for each microorganism.

The matrices used in this method could be divided into hydrogels (alginate, κ -carrageenan, chitosan), thermogels (agar, agarose, cellulose), and synthetic polymers (polyacrylamide, polyvinyl alcohol, polyurethane) [7–9].

One of the best known methods and a very simple one is the entrapment in sodium alginate, a natural polysaccharide. The water-soluble alginate is mixed with the whole cells and dropped into a calcium chloride solution in which water-insoluble alginate beads are formed (Fig. 2). Currently, there are new alginate entrapment protocols which describe modifications for improving this method [10, 11].

Another widely used method is agarose or agar entrapment. In a similar manner to that of the alginate method, a mixture of agarose and whole cells is dropped into a stirred oil solution where beads are formed (Fig. 3).

Finally, a commonly used synthetic immobilization method employs polyacrylamide gel. Whole cells, a monomer (acrylamide) and a cross-linker reagent (e.g., bis-acrylamide) are mixed and polymerized by starting the reaction with an initiator (e.g., ammonium persulfate) in the presence of a catalytic enhancer (e.g., N,N,N',N' -tetramethylethylenediamine) (Fig. 4).

In summary, the immobilized microorganisms fulfill the requirements of low cost production in terms of industrial application due to their high yield, their long half-life, and their high stereo-, regio-, and chemo-selectivity [12, 13].

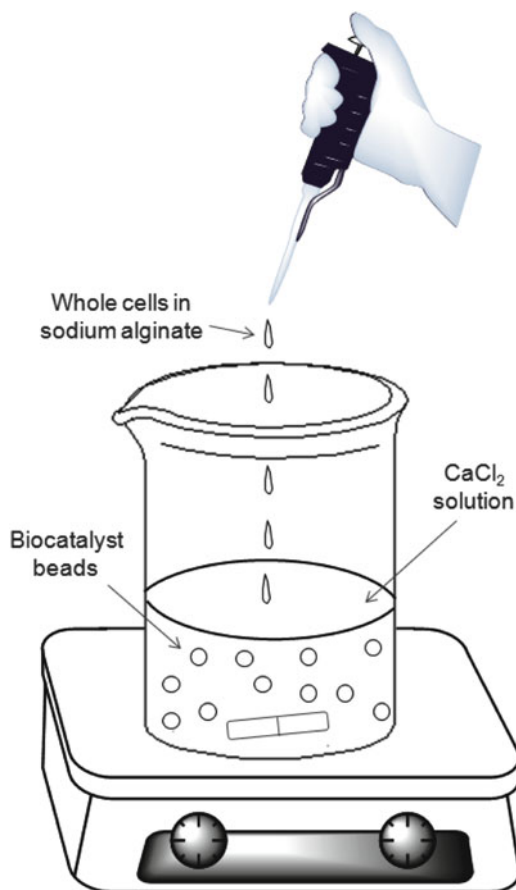


Fig. 2 Schematic drawing of the alginate immobilization procedure

2 Materials

Prepare all the solutions using ultrapure water and analytical grade reagents. Prepare and store all reagents at room temperature (unless otherwise indicated).

2.1 Alginate Immobilization Components

1. Tris-HCl: 50 mM Tris-HCl solution, pH 7. Weigh 6.06 g Tris base and dissolve in 800 mL of water, adjust to desired pH with concentrated HCl. Add water up to 1 L and start autoclaving procedure.
2. Sodium alginate: 1 % (w/v) solution (*see Note 1*). Add 20 mL water to 0.2 g alginic acid, mix well and start autoclaving procedure (*see Note 2*).
3. Calcium chloride: 10 % CaCl₂ solution. Add 100 mL water to a 1 L graduated cylinder. Weigh 10 g CaCl₂ and dissolve with a magnetic stirrer. Make up to 1 L with water and start autoclaving procedure (*see Note 3*).

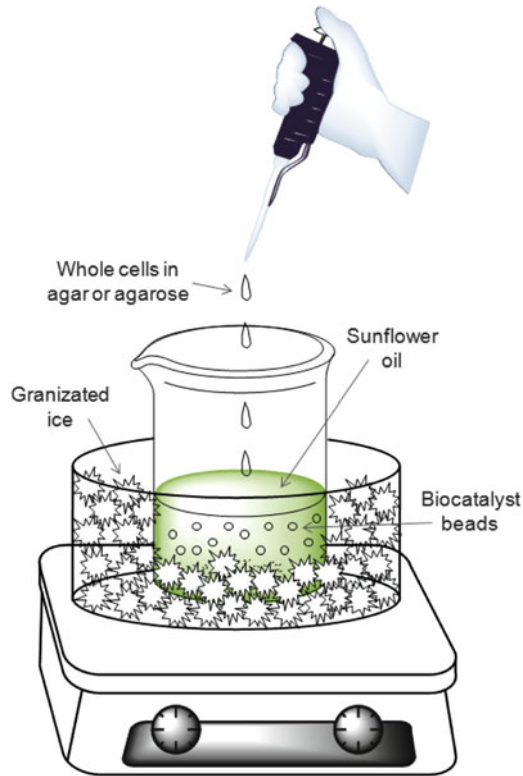


Fig. 3 Schematic drawing of the agar or agarose immobilization procedure

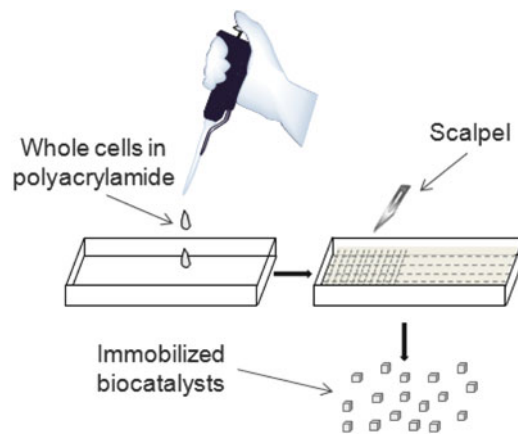


Fig. 4 Schematic drawing of the polyacrylamide immobilization procedure

4. Chitosan solution: 1 % (w/v) solution. Add 100 mL water to a 1 L graduated cylinder. Weigh 1 g chitosan and dissolve with a magnetic stirrer. Make up to 1 L with water and start autoclaving procedure (*see Note 4*).
5. Peptone solution: 0.1 % (w/v) solution. Weigh 0.1 g peptone and prepare 1 L solution as in previous steps. Store at 4 °C.

6. Polyethylenimine solution: 1 % (w/v) solution, pH 5. Add 100 mL water to a 1 L graduated cylinder. Add 1 mL polyethylenimine and make up to 1 L with water (*see Note 5*).

2.2 Agar or Agarose Immobilization Components

1. Agar or agarose: 1 % (w/v) solution. Add 3 mL water to 0.03 g agar or agarose, mix well and gently heat up in microwave oven until the matrix is completely dissolved (*see Note 6*).
2. Sunflower oil. Nonvolatile oil expressed from sunflower (*Helianthus annuus*) seeds, which is commonly used in food.
3. Hexane. Reagent of analytical grade.

2.3 Polyacrylamide Immobilization Components

1. Acrylamide mixture: 30 % acrylamide/Bis solution (29.2/0.8). Weigh 29.2 g of acrylamide and 0.8 g Bis-acrylamide and transfer to a graduated cylinder containing about 40 mL of distilled water. Mix during 30 min with a magnetic stirrer. Make up to 100 mL with distilled water and filter through a 0.45 μm filter (*see Note 7*). Store at 4 °C, in a bottle wrapped in aluminum foil.
2. Ammonium persulfate: 10 % (w/v) APS solution in distilled water. Store at 4 °C (*see Note 8*).
3. *N,N,N',N'*-Tetramethylethylenediamine: TEMED solution. Store at -20 °C in a bottle wrapped in aluminum foil.
4. Plastic box (3.5 \times 1 \times 0.5 cm).
5. Scalpel. Small and sharp bladed instrument used for surgery.

2.4 General Reagents

1. Saline solution: 0.9 % (w/v) solution. Add 100 mL distilled water to a 1 L graduated cylinder; weigh 0.9 g NaCl and dissolve with a magnetic stirrer. Make up to 1 L with distilled water and start autoclaving procedure.
2. Potassium phosphate buffer: 30 mM buffer solution, pH 7. Add 100 mL distilled water to a graduated cylinder; weigh 3.24 g K_2HPO_4 and 1.55 g KH_2PO_4 and dissolve in 800 mL of distilled water. Adjust to desired pH, add distilled water up to 1 L and start autoclaving procedure.

3 Methods

Carry out all the procedures at room temperature unless otherwise specified.

3.1 Alginate Entrapment

1. Grow the microorganisms until exponential or stationary phase (*see Note 9*) in the corresponding medium.
2. Harvest the cells from the culture broth by centrifugation at 17,500 $\times g$ during 10 min.

3. Wash the pellet once with Tris–HCl buffer and recentrifuge for 10 min at $17,500 \times g$.
4. Mix the pellet with 20 mL of alginic acid solution.
5. Add the mixture drop-wise to a stirred solution of 0.1 M CaCl_2 (*see Note 10*). Shake during 30 min to 2 h (*see Note 11*).
6. Filter the resulting gel beads and wash the biocatalysts twice with saline solution.
7. Store the biocatalyst in sterile water at 4 °C until use.

3.2 Alginate-Chitosan Entrapment (*See Note 12*)

1. Immerse the resulting beads from the previous item in 100 mL chitosan solution. Stir during 40 min at 100 rpm.
2. Filter and wash the biocatalysts twice with peptone solution.
3. Store the biocatalyst in sterile water at 4 °C until use.

3.3 Alginate-Polyethylenimine (PEI) Entrapment (*See Note 13*)

1. Mix the obtained gel beads (Subheading 3.1) in 100 mL PEI solution. Stir during 5 min at 100 rpm.
2. Filter and wash the biocatalysts twice with enough water to remove the polymer solution.
3. Store the biocatalyst in sterile water at 4 °C until use.

3.4 Agar or Agarose Entrapment

1. Grow the microorganisms until stationary phase in the corresponding medium (*see Note 9*).
2. Harvest the cells from the culture broth by centrifugation at $17,500 \times g$ during 10 min.
3. Wash the pellet once with phosphate buffer and recentrifuge for 10 min at $17,500 \times g$.
4. Remove the supernatant and mix the pellet with 3 mL of agar or agarose solution (*see Note 14*).
5. Add the homogeneous mixture dropwise to 10 mL of stirred sunflower oil at 25 °C (*see Note 15*).
6. Cool the oil bath with ice and filter the resulting gel beads (mean diameter: 4 mm).
7. Wash the biocatalysts once with hexane (*see Note 16*) and then wash twice with saline solution to obtain free solvent beads.
8. The beads can be used directly as biocatalyst or stored in phosphate buffer at 4 °C (*see Note 17*).

3.5 Polyacrylamide Entrapment

1. Grow the microorganisms until stationary phase in the corresponding medium (*see Note 9*).
2. Harvest the cells from the culture broth by centrifugation at $17,500 \times g$ during 10 min.

3. Wash the pellet once with phosphate buffer and recentrifuge for 10 min at $17,500 \times g$.
4. Remove the supernatant and mix the pellet with: 7.3 mL phosphate buffer, 2.7 mL acrylamide mixture, 14 μL TEMED and 50 μL of ammonium persulfate, in that order.
5. Mix the resulting solution and place into a plastic box.
6. Cut the gel into small cubic pieces (1.0 cm \times 1.0 cm \times 0.2 cm, approximately).
7. Store the biocatalyst in phosphate buffer at 4 °C until use.

4 Notes

1. The concentration used for alginate immobilization must be assayed for each microorganism. Generally, the tested range is 2–5 % w/v because release of microorganisms in the surrounding medium is observed at lower matrix rates whereas at higher concentrations the immobilization process becomes more complex due to the high viscosity of the alginate solution. We have performed microorganism immobilization trials with calcium alginate 4 % w/v [14]. There are some articles in the literature reporting the use of different immobilized microorganisms in alginate gel [15, 16].
2. Alginate is a generic term used for the salts and derivatives of alginic acid. This polysaccharide consists of varying proportions of d-mannuronic acid and l-guluronic acid, the variation in the proportions of both acids being dependent mainly on the source seaweed species [13]. Alginate from *Laminaria hyperborea* and *Macrocystis pyrifera* (high or low guluronic acid content, respectively) are the most frequently used for microorganism immobilization.
3. These cross-linking solutions can contain different cations such as calcium, barium, strontium or a combination thereof (1–20 %). Barium and strontium are added when high rigidity is required [11, 17].
4. Use low molecular weight chitosan (80 % deacetylated).
5. Branched polyethyleneimine (PEI), M.W. 70000 is recommended, but PEIs with different molecular weight should be assayed.
6. The concentration used for agar or agarose immobilization should be assayed for each immobilization. Generally, the tested range is 1–4 % w/v, but matrix disintegration was observed at concentrations of 1 %. On the other hand, working at concentrations higher than 4 % is very difficult due to the high viscosity of the solution.

7. Wear a mask when weighing acrylamide. Unpolymerized acrylamide is a neurotoxin and care should be exercised to avoid skin contact.
8. This reagent can also be stored at $-20\text{ }^{\circ}\text{C}$ to increase its half-life.
9. Depending on the enzymes involved in the route of interest, the stages of microorganism growth should be evaluated.
10. The magnetic stirrer size should not exceed 2/3 parts of the beaker surface. Shaking speed should be gentle and controlled to avoid sphere breaking and deformation, respectively.
11. Shaking time depends on the desired stiffness. Therefore, this is another variable to be tested for each microorganism.
12. Cationic chitosan can form gels with nontoxic multivalent anionic counterions such as sodium alginate by ionic cross-linking. Microencapsulation with sodium alginate-chitosan protects the microorganisms against adverse conditions such as high pH values.
13. This method has been mainly used for enzyme immobilization. The gel beads coated with PEI have shown higher resistance to phosphate ions. Partially quaternized polyethyleneimine (QPEI) was a better stabilizer than unmodified PEI.
14. The temperature of the agar or agarose solutions is very important because it can affect the viability of microorganisms (at high temperatures) or the matrix can begin to polymerize (at low temperatures).
15. The kind of oil used is very important because the degree of unsaturation of triglycerides affects its viscosity and consequently the immobilization process. Therefore, unsaturated oils should be used since their aggregation state is liquid at room temperature.
16. Hexane can be replaced by another nonpolar solvent.
17. Some microorganisms have been immobilized by agarose entrapment. Immobilized biocatalysts were stable for more than 4 months in storage conditions ($4\text{ }^{\circ}\text{C}$) [18].

Acknowledgments

This work was supported by Agencia Nacional de Promoción Científica y Tecnológica, Universidad Nacional de Quilmes and CONICET.

References

- Guisan JM (2006) Immobilization of enzymes and cells. Humana Press, Totowa, NJ
- Nedovic V, Willaert R (2004) Fundamentals of cell immobilisation, vol 1. Kluwer Academic, Dordrecht
- Trelles JA, Valino AL, Runza V, Lewkowicz ES, Iribarren AM (2005) Screening of catalytically active microorganisms for the synthesis of 6-modified purine nucleosides. *Biotechnol Lett* 27:759–763
- Trelles JA, Fernández-Lucas J, Condezo LA, Sinisterra JV (2004) Nucleoside synthesis by immobilised bacterial whole cells. *J Mol Catal B: Enzym* 30:219–227
- Fernández-Lucas J, Condezo LA, Martínez-Lagos F, Sinisterra JV (2007) Synthesis of 2'-deoxyribosynucleosides using new 2'-deoxyribosyltransferase microorganism producers. *Enzyme Microb Technol* 40:1147–1155
- Park JK, Chang HN (2000) Microencapsulation of microbial cells. *Biotechnol Adv* 18:303–319
- van der Sluis C, Mulder AN, Grolle KC, Engbers GH, ter Schure EG, Tramper J, Wijffels RH (2000) Immobilized soy-sauce yeasts: development and characterization of a new polyethylene-oxide support. *J Biotechnol* 80:179–188
- Hung CP, Lo H-F, Hsu WH, Chen SC, Lin LL (2008) Immobilization of *Escherichia coli* novablue γ -glutamyltranspeptidase in Ca-alginate- κ -carrageenan beads. *Appl Biochem Biotechnol* 150:157–170
- Hae S (2012) Agarose-gel-immobilized recombinant bacterial biosensors for simple and disposable on-site detection of phenolic compounds. *Appl Microbiol Biotechnol* 93:1895–1904
- Yujian W, Xiaojuan Y, Wei T, Hongyu L (2007) High-rate ferrous iron oxidation by immobilized *Acidithiobacillus ferrooxidans* with complex of PVA and sodium alginate. *J Microbiol Methods* 68:212–217
- Moreno-Garrido I (2008) Microalgae immobilization: current techniques and uses. *Bioresour Technol* 99:3949–3964
- Hulst AC, Tramper J, Van't Riet K, Westerbeek JM (1985) A new technique for the production of immobilized biocatalyst in large quantities. *Biotechnol Bioeng* 27:870–876
- Arvizu-Higuera DL, Hernández-Carmona G, Rodríguez-Montesinos YE (2002) Parameters affecting the conversion of alginic acid to sodium alginate. *Ciencias Marinas* 28:27–36
- Britos CN, Cappa VA, Rivero CW, Sambeth JE, Lozano ME, Trelles J A (2012) Biotransformation of halogenated 2'-deoxyribosides by immobilized lactic acid bacteria. *J Mol Catal B Enzym* 79:49–53
- Ha J, Engler CR, Wild JR (2009) Biodegradation of coumaphos, chlorferon, and diethylthiophosphate using bacteria immobilized in Ca-alginate gel beads. *Bioresour Technol* 100:1138–1142
- Yujian W, Xiaojuan Y, Hongyu L, Wei T (2006) Immobilization of *Acidithiobacillus ferrooxidans* with complex of PVA and sodium alginate. *Polym Degrad Stabil* 91:2408–2414
- Jeon C, Park JY, Yoo YJ (2002) Characteristics of metal removal using carboxylated alginic acid. *Water Res* 36:1814–1824
- Rivero CW, Britos CN, Lozano ME, Sinisterra JV, Trelles JA (2012) Green biosynthesis of floxuridine by immobilized microorganisms. *FEMS Microbiol Lett* 331:31–36

INDEX

A

- Acinetobacter venetianus*.....302, 303, 307–309
- Adsorption
- affinity binding.....25
 - hydrophobic adsorption.....7, 10, 24, 25, 44, 244, 256
 - ionic adsorption.....38, 84, 152, 154, 155, 159, 161, 162
- Agarose, enzyme immobilization
- matrix.....107, 130, 229
- Aldehyde-dextran crosslinking.....6
- Alginate
- application.....335, 354
 - microcapsule preparation.....321, 354, 355, 357
- Amino-epoxy sepabeads
- heterofunctional epoxy supports.....46, 48, 49, 52
 - multipoint covalent attachment.....46, 52
 - support for enzyme immobilization.....46, 48, 49
- Amino-glyoxyl agarose
- heterofunctional glyoxyl supports.....82–86
 - multipoint covalent attachment.....84
 - support for enzyme immobilization.....67
- Antibodies immobilization
- anti-HRP.....156, 159–162
 - biosensors.....150
 - magnetic nanoparticles.....10
 - oriented immobilization.....152, 153

B

- Bioaffinity immobilization
- biotin-streptavidin.....140–141
 - Concanavalin A.....129–136
- Biomedical applications
- immobilized enzymes.....285–297
- Biosensors
- enzyme electrodes.....144, 338
 - immobilized antibodies.....150
- Biotin-streptavidin bioaffinity
- immobilization.....140–141
- Boronate-epoxy-supports.....53
- heterofunctional epoxy supports.....43–56

C

- Carbon nanotubes.....27, 167, 217–227
- immobilization on.....27, 219, 227
- Carboxyl-glyoxyl agarose.....82, 86
- heterofunctional supports.....82, 86
- Cell immobilization
- entrapment.....301
 - microalgae.....327, 330, 335
- Chelate-glyoxyl agarose.....83, 84
- heterofunctional agarose supports.....83–84
- Chymotrypsin.....65, 76, 78, 84, 85, 286
- immobilization on epoxy-supports.....78–79, 84, 85
- CLEAs. *See* Crosslinked enzyme aggregates (CLEAs)
- CLECs. *See* Crosslinked enzyme crystals (CLECs)
- Clinical applications
- of immobilized enzymes.....18
- Concanavalin A.....129–136, 142
- affinity immobilization.....129–131, 134, 142
- Covalent coupling, enzymes to supports.....22, 23
- Crosslinked enzyme aggregates
- (CLEAs).....6, 24, 248, 256, 276, 287
- Crosslinked enzyme crystals (CLECs).....6, 248, 276, 287
- Crosslinking
- enzymes adsorbed on aminated supports.....34, 37, 40
 - glutaraldehyde.....34, 35, 40
- Cyclodextrin glucantransferase from
- Thermoanaerobacter sp.*.....96, 99, 100, 113, 114

D

- Disulfide bonds.....23, 26, 89–115, 149, 152
- reversible enzyme immobilization.....89–115

E

- Electrodes.....141, 142, 144, 147, 182, 209–215, 217–227, 230, 231, 234–236, 303, 304, 310, 311, 338
- enzyme electrodes.....209

Encapsulation	
alginate gels	313–323
cell immobilization	313, 316, 320
Entrapment	21, 22, 24, 139,
209, 229–237, 242, 246, 250, 287,	
301, 315, 316, 328, 350, 365–373	
cell immobilization	301
Enzyme electrodes.....	209
Enzyme immobilization	
crosslinked enzyme aggregates.....	24
entrapment	21, 22, 139,
209, 229–237	
immobilization on electrodes.....	209–215
immobilization on nanoparticles	123
irreversible covalent immobilization	162
physical adsorption	5, 8, 20,
24, 45, 74, 209	
reversible covalent immobilization.....	89–115
sol–gel immobilization	209, 234, 241–251
Enzyme stabilization	
heterofunctional epoxy supports	43, 44, 51
heterofunctional glyoxyl agarose.....	75, 86
monofunctional epoxy supports	43, 44, 51
monofunctional glyoxyl agarose.....	82
sol–gel immobilization	209, 246
Epoxy supports	
enzyme immobilization	43–56
enzyme stabilization	44
heterofunctional supports	43–56
monofunctional supports	43–56
multipoint covalent attachment	44, 46, 50
F	
Fructosyltransferase	38
G	
β -Galactosidase from <i>A. oryzae</i>	49, 55
β -Galactosidase from <i>Escherichia coli</i>	26, 50, 95,
98, 103, 108	
β -Galactosidase from <i>Kluyveromyces lactis</i>	95, 99,
104, 109	
β -Galactosidase from <i>Thermus sp.</i>	49, 50, 55
β -Glucosylase from <i>A. niger</i>	49, 52, 55
Glutaraldehyde	
activation of aminated supports	34, 37, 40
crosslinking agent	34, 35, 37, 40
immobilization of enzymes.....	37
stabilization of enzymes.....	34, 39, 40
Glutaryl acylase	49, 52, 55
Glyoxyl-agarose	
enzyme stabilization	60, 64
enzyme immobilization	67
heterofunctional supports	82
monofunctional supports	82, 85
multipoint covalent attachment	68–69
H	
Horseradish peroxidase (HRP).....	24, 130, 132,
135–136, 140, 142, 156, 157, 159,	
160, 210, 211, 215	
Hyperactivation of lipases.....	7, 256,
264–266, 268, 270	
immobilization techniques.....	256, 264–266, 268, 270
L	
<i>Laminaria hyperborea</i>	314, 337, 372
Lecitase Ultra (LECI)	259
Lipase	
hyperactivation	7, 256, 264–266,
268, 270	
immobilization	83, 84, 119, 121–123,
241–251, 255–271	
ionic liquids	248, 251, 258,
266, 267, 275–283	
organic solvents	241, 242, 275–283
stabilization	257
Lipase from <i>Alcaligenes sp. (QL)</i>	259
Lipase from <i>Burkholderia cepacia</i>	249
Lipase from <i>Candida antarctica</i> (fraction A)	
(CAL-A)	259
Lipase from <i>Candida antarctica</i> (fraction B)	
(CAL-B).....	259
Lipase from <i>Candida rugosa</i>	117–125
Lipase 2 from <i>Geobacillus thermocatenulatus</i>	76
Lipase from <i>Mucor Javanicus</i> (MJL).....	259
Lipase from <i>Penicillium roqueforti</i> (PrL)	249
Lipase from <i>Pseudomonas fluorescens</i>	
(PFL).....	248, 249, 259
Lipase from <i>Rhizomucor miehei</i> (RML).....	256
Lipase from <i>Rhizopus niveus</i> (RNL).....	259
Lipase from <i>Thermomyces lanuginose</i> (TLL)	259
Lipase from <i>Thermus thermophilus</i> (TTL)	259
M	
<i>Macrocystis pyrifera</i>	314, 315, 336, 372
Magnetic nanoparticles	10, 20, 117,
122, 156, 158, 159	
physical and chemical properties	177
Metal chelate supports	
agarose gels	77
epoxy supports	45, 46
Microalgae immobilization.....	327, 328, 330, 335, 338
Multipoint covalent immobilization	
chymotrypsin	65
enzyme stabilization	5–6, 59–70

epoxy supports 44, 45, 52
 glutaraldehyde..... 35, 37, 38
 glyoxyl supports 59–70, 73–87
 Penicillin G acylase..... 24, 65, 67–69
 Myoblast cells 320, 322

P

Penicillin G Acylase from *E. coli*..... 50, 52, 65, 67, 96
 Protein A 153

S

Shewanella oneidensis 303, 305–308, 310
 Silica 19, 25, 35, 167,
 229, 233–235, 242, 247, 292,
 301–311, 330, 340–341
 cell immobilization 301–311
 Sol-gel encapsulation
 lipases
 activity assay 259–261, 263–264
 entrapment reaction 24, 229, 235,
 242, 246, 250
 hydrophobic modifications 7, 8, 242,
 243, 249, 256, 266
 optimization 243
 recycling 242, 244

structure and morphology
 of immobilizates 7, 244
 materials 156–157, 243,
 244, 249, 250, 301
 technique 241–251

Supports

 classification 19
 selection 27

T

Tannase from *Lactobacillus plantarum* 76, 80–81
 Thiol group immobilization
 β -galactosidase from *Escherichia coli* 95, 98,
 103–104, 108
 β -galactosidase from *K. lactis* 99, 104–105
 commercial adsorbents 91
 disulfide oxides 90, 91
 materials 26, 94, 97, 98, 102
 preparation 50, 98
 2-pyridyldisulfide agarose gels 90–91
 titration 97, 101
 Tomato pectinase 129, 131–134

Y

Yeast invertase 142, 143, 146